NASA CONTRACTOR REPORT

NASA CR-73258

POTENTIAL STRUCTURAL MATERIALS AND DESIGN CONCEPTS FOR LIGHT AIRPLANES

By L. Pazmany, H. Prentice, C. Waterman and F. Tietge

October 1968

FINAL REPORT

Distribution of this report is provided in the interest of information exchange. Responsibility for the contents resides in the author or organization that prepared it.

Prepared under Contract No. NAS 2-4423 by
SAN DIEGO AIRCRAFT ENGINEERING, INC.
San Diego, California 92101

For THE MISSION ANALYSIS DIVISION
OFFICE OF ADVANCED RESEARCH AND TECHNOLOGY
NATIONAL AERONAUTICS AND SPACE ADMINISTRATION
AMES RESEARCH CENTER
MOFFETT FIELD, CALIFORNIA

PRECEDING PAGE BLANK NOT FILMED.

PREFACE

San Diego Aircraft Engineering, Inc. was responsible for executing the NASA study of potential structural materials and design concepts for light aircraft, as well as for the preparation of this report which describes the evaluation and application of several of these materials to the conceptual design of a single-engine, four-place airplane of the 1980's.

NASA contract NAS 2-4423 authorized these tasks which were performed for the Mission Analysis Division, Office of Advanced Research and Technology at the Ames Research Center of National Aeronautics and Space Administration, Moffett Field, California.

Ladislao Pazmany, Chief Design Engineer of San Diego Aircraft Engineering, managed the study program. He reported directly to Mr. G. D. McVicker, Chief Engineer and Executive Vice President of San Diego Aircraft Engineering, and to Mr. Frank Fink, President of the company. Assisting him were the following staff members:

Aerodynamics:	Larry Frohlich & Gary Johnson
Design & Weights:	Charles Waterman
Costs & Statistics:	Fred Tietge
Fatigue:	Fred Jones
Fasteners:	John O'Husky
Structures:	Hillyer Prentice

T. L. Galloway of NASA served as project monitor, coordinating the many objectives of this study in all its phases, as well as providing effective liaison between personnel of the Mission Analysis Division of NASA and San Diego Aircraft Engineering, Inc.

Acknowledgment is extended to the many people in the fields of education, government, and industry who gave freely of their time and supplied much valuable information. I.e.:

Aircraft Owners and Pilots Association
Aluminum Company of America
American Aviation Corporation
Beech Aircraft Corporation
Bell Helicopter Company
Bellanca Aircraft Engineering Corp.
Boeing Aircraft Company
Bölkow GMBH
Brantley Helicopter Corporation
Cessna Aircraft Company
General Dynamics Corporation/Convair
Crescent Mold Engineering Corporation
Department of Transportation(FAA&CAB)
McDonnell-Douglas Aircraft Company
E.I. DuPont de Nemours & Company
Experimental Aircraft Association
Fiberite Corporation
Flight Safety Foundation
Gibbs Flying Service
Goodyear Aerospace Corporation
Haveg Industries, Inc.
Heath Tecna Corporation
HITCO
Hughes Tool Company, Aircraft Division
Leach Industries
Lockheed California Company
M.C.W., Inc.
North American/Rockwell-Columbus Div.
Owens-Corning Fiberglas Corporation
Piper Aircraft Corporation
Pixie Mold and Tool Corporation
Ryan Aeronautical Company
Swedlow, Incorporated
Union Carbide Corporation
Whittaker Corporation, Narmco Research and Development Division

PRECEDING PAGE BLANK NOT FILMED.

CONTENTS

	PAGE
PREFACE	iii
Acknowledgments	iii
INTRODUCTION	1
SYMBOLS, ABREVIATIONS, AND CONVERSION FACTORS	2
PHASE I - INVESTIGATION	4
Evolution of the Post WW II Light Aircraft Industry	4
Safety	4
Overall Safety	4
Safety Associated with Design	7
Conclusion	11
Utilization	12
Industry Survey	14
Cost	20
Dollar Value and Price Trends	20
Cost as a Function of Speed and Empty Weight	23
Life	24
Performance	24
Aircraft Production	26
Design Considerations	28
Airplane Weights	28
Wing Configuration	32
Planform	32
Cantilevered	32
Strut Braced	48
Wing Area vs High Lift Devices	52
Helicopter Weights	54
Crashworthiness	55
Design-Induced Pilot Error	56
Cost Considerations	78
Operating Costs	78
Fixed vs Retractable Landing Gear	81
Reciprocating vs Turbo-Prop Engine Airplane	87
Fixed Pitch vs Constant Speed Propeller	88
Strut-Braced vs Cantilevered Wings	90
Airframe Cost	90
Value of a Pound Saved	93
Consumer Price Breakdown	95
Effect of Labor Savings/Mass Production	99
Performance Considerations	103
Airplane	103
Configuration Constants	103
Determination of Critical Performance Requirements	108
Airplane Configuration	118
Airplane Performance Summary	120
Helicopter	120
Power Required to Hover	123
Final Weight Analysis	124

PAGE

Potential Structural Materials 132
Initial Selection 132
Material Costs 133
Promising Candidate Materials 133
Metallic Materials 136
Non Metallic Materials 142
Evaluation of Promising Candidate Materials 145
Tension Members 148
Single Columns 149
Compression Structure 151
Shear Panels 159
Compression Flanges 159
Installation Costs 162
Material/Concept Feasability 166
Fatigue Evaluation 167
Establishing a Fatigue Load Spectrum 167
Estimation of Fatigue Life 169
Pressurization Considerations 170
Material Fatigue Properties 171
Fastening Devices and Methods 178
Riveting 178
Electric Welding 183
Brazing 195
Bonding 199
PHASE II - APPLICATION OF MATERIALS AND CONCEPTS 208
Airplane Configuration 208
Study Guidelines 208
Design Justifications 208
Weight and Balance Study 211
Application of Selected Materials and Structural Concepts 211
Component Design 212
Vertical Tail 212
Horizontal Tail 215
Wing 219
Fuselage 223
Component Technical Analysis 226
Wing Geometry 232
Wing Loads Criteria 232
Wing Design, Symmetrical Flight Condition 233
Wing Deflections 238
Design Unsymmetrical Flight Condition 239
Design Landing Conditions 240
Parameters 240
Basic Conditions 241
Wing Control Surface Loading Conditions 241
Aileron Loading 241
Flap Loading (Primary) 243

PAGE

Flap Loading (Secondary) 245
Net Ultimate Flap Loads 246
Flap Torsional Wind-Up 246
Wing Material/Concepts 248
Wing Material/Concept I 249
Stress Analysis of Skins and Stiffeners 249
Stress Analysis of Main Spar 258
Stress Analysis Closing Spar 265
Wing-Fuselage Main Attachment 266
Wing Material/Concept II 267
Stress Analysis of Skins and Stiffeners 267
Stress Analysis of Main Spar 268
Wing Material/Concept III 272
Stress Analysis of Skins and Stiffeners 272
Stress Analysis of Main Spar 272
Horizontal Tail Stress Analysis 277
Geometry 277
Loads Criteria 277
Horizontal Tail Material/Concept 280
Stress Analysis, Skins and Stiffeners 280
Stress Analysis, Main Spar 282
Stress Analysis, Closing Spar 284
Stress Analysis, Fuselage Attachment 286
Stress Analysis, Anti-Servo Tab 288
Vertical Tail Stress Analysis 290
Loads Criteria 291
Stress Analysis of Fin Skins and Stiffeners 293
Stress Analysis, Main Spar 296
Stress Analysis of Rudder 300
Component Cost and Manufacturing Considerations 301
Vertical Tail 301
Horizontal Tail 309
Wing 309
Fuselage 316
CONCLUSIONS 317
General 317
Recommendations for Future R & D Programs 319
Category I, Structural Materials and Concepts 320
Category II, Other Design Areas 321
APPENDIX A - Accident Rates U.S.General Aviation 1938-1966. 323
APPENDIX B - General Aviation Accidents, Casualties and Damage for 1963 (Typical) 324
APPENDIX C - Accidents per Eligible Aircraft by State for 1965. 325
APPENDIX D - Type of Accident vs Phase of Operation for Small Fixed-Wing Aircraft in 1963 & 1964 326
APPENDIX E - Type of Accident vs Kind of Flying for Small Fixed-Wing Aircraft in 1963 & 1964 327

APPENDIX F - Type of Accident vs Kind of Flying for Helicopters in 1963 and 1964 328
APPENDIX G - Analysis, In-Flight Airframe Failure in U.S. General Aviation, 1963 329
APPENDIX H - Operating Costs Analysis 330
APPENDIX J - Vehicle Price Per Lb. of Useful Load 331
APPENDIX K - Operating Cost Analysis (Fixed Gear vs Retractable Gear Airplanes) 332
APPENDIX L - Typical Operating Costs for Reciprocating and Turbo-Prop Airplanes 335
APPENDIX M - Aircraft Guidelines 336
APPENDIX N - Parametric Study of Factors Affecting Maximum Speed . . . 337
APPENDIX P - Parasite Drag of Current Airplanes 343
APPENDIX Q - Static Stability Computations 347
APPENDIX R - Weight and Balance Calculations (Far Term Airplane) . . . 348
APPENDIX S - Consumer Price Breakdown of Far Term Airplane (Estimated). 351
APPENDIX T - Estimated Cost of Conventional Sheetmetal Airplane at 100,000 Unit 354
REFERENCES 355

ILLUSTRATIONS

FIGURE		PAGE
1	Statistical History of General Aviation	5
2	General Aviation Accident and Injury Index for 1963 (Typical)	6
3	Number of Accidents vs Causes (1963 & 1964) for Small Fixed Wing Aircraft	7
4	Number of Accidents vs Causes for Helicopters in 1965	8
5	Number and Utilization of General Aviation Aircraft by Aircraft Type	12
6	Number and Utilization of General Aviation Aircraft by Type of Flying	13
7	Questionnaire (Responses) Geographical Distribution	14
8	Price Index vs Calendar Year	20
9	General Aviation Aircraft Consumer Price Trends	21
10	Price Weight Ratio	22
11	Price per Pound of Useful Load vs Speed	23
12	Gross Weight Trend	25
13	Empty/Gross Weight Trend	25
14	Installed Power Trend	25
15	Maximum Speed^3/Power Trends	26
16	Maximum Speed Trends	27
17	Landing Speed Trends	27
18	Number of Aircraft Shipped	27
19	Typical Contemporary Light Airplane Empty Weight Breakdown	28
20	Wing Configurations	33
21	V-n Diagram, 3.8g	34
22	V-n Diagram, 6.0g	35
23	Equations and Diagrams for Running Load, Shear, and Moment	36
24	Wing Chord vs Wing Station	36
25	Ultimate Shear vs Wing Station	37
26	Ultimate Bending Moment vs Wing Station	38
27	Wing Section Airload Components	39
28	Wing Section Force Coefficients	39
29	Design Ultimate Wing Torque vs Wing Station	42
30	Cap Loads due to Chordwise Bending	43
31	Axial Load Diagram (n = 5.7g)	43
32	Axial Load Diagram (n = 9.0g)	44
33	Spar Cap Geometry	44
34	Lower Spar Cap Thickness Diagram (n = 5.7g)	45
35	Upper Spar Cap Thickness Diagram (n = 5.7g)	45
36	Spar Cap Thickness Diagram (n = 9.0g)	46
37	Spar Web Geometry	46
38	Configuration I - Spar Web Shear Flow Diagram	47
39	Skin Gages for Torque Box	48
40	Single Spar Metal Covered Wing with External Strut Brace	49
41	Configuration I - Strut Braced Wing, Vertical Shear Diagram	49
42	Configuration I - Strut Braced Wing, Bending Moment Diagram	50
43	Upper and Lower Spar Cap Thickness Diagram (n = 9.0)	50
44	Upper and Lower Spar Cap Thickness Diagram (n = 5.7)	51

FIGURE		PAGE
45	Configuration I - Strut Braced Wing Spar Web Shear Flow Diagram	51
46	Wing Area vs High Lift Device Trade Off	53
47	Contemporary Helicopter, Empty Weight Breakdown (Turbine Engine)	54
48	Contemporary Helicopter, Empty Weight Breakdown (Piston Engine)	54
49-50-51-52	Fuel Selector Valve Configurations	59
53	Upsetting Couple on Tail-Wheel Airplanes	61
54	Restoring Couple on Tricycle-Gear Airplanes	61
55	Ratio of Track Width to C.G.Height for Low and High Wing Aircraft	63
56	Effect of Moment of Inertia on Swerve Tendency	63
57	Effect of Center of Lateral Area on Swerve Tendency	64
58	CAR Part 3. Control Knobs	66
59	Cost of Owning and Operating vs Amount of Flying	78
60	Operating Cost Breakdown for Typical Light 4-Place Airplane	79
61	Helicopter Operating Costs - Reciprocating vs Turbine	80
62	Helicopter Operating Costs - Reciprocating vs Turbine	80
63	Operating Cost vs Utilization Rate for Airplane Pair A	83
64	Operating Cost vs Utilization Rate for Airplane Pair B	84
65	Operating Cost vs Utilization Rate for Airplane Pair C	85
66	Operating Cost vs Utilization Rate When Considering the Value of a Man's Time	86
67	Typical Operating Costs vs Utilization for Reciprocating and Turbine Airplanes	87
68	Consumer Price per Pound (Empty) vs Empty Weight (1967 General Aviation Helicopters)	90
69	Consumer Price per Pound of Empty Weight vs Empty Weight (Light Airplanes)	91
70	Consumer Price per Pound of Empty Weight vs Maximum Speed	91
71	Unit Airframe Cost vs Weight Empty (Light-Single Engine Airplanes - 1967)	92
72	Unit Airframe Cost vs Air Speed (Light-Single Engine Airplanes - 1967)	92
73	Typical Cost of Structure	93
74	Worth in Dollars per Pound of Weight Saved (Light Airplane)	96
75	Worth in Dollars per Pound of Weight Saved (Piston-Helicopter).	96
76	Worth in Dollare per Pound of Weight Saved (Turbine-Helicopter)	97
77	Typical Consumer Price Percentage Breakdown of a Four-Place Single-Engine Airpiane	98
78	Typical Consumer Price Percentage Breakdown of a Four-Place Reciprocating Engine Helicopter.	100
79	Price Effect of Labor Saving	101
80	Factors Affecting Maximum Speed	104
81	Engine Specific Weight	107

FIGURE

		PAGE
82	Performance Boundaries For Retractable Landing Gear Configurations	108
83	Performance Boundaries for Fixed Landing Gear Configurations	109
84	Take-Off Performance Chart	110
85	Graphic Derivation for Empirical Solution of Take-Off Distance	111
86	Preliminary Gross Weight vs Power Loading	116
87	Minimum Design Weight vs Specific Wing Weight	119
88	Profile Drag - Lift Ratio vs Thrust Coefficient	121
89	Profile Drag - Lift Ratio vs Thrust Coefficient/Solidity	122
90	Rotor Power at Hover vs Disc Area, W=2000 lbs	124
91	Rotor Power at Hover vs Disc Area, W=2400 lbs	125
92	Rotor Power at Hover vs Disc Area, W=2800 lbs	126
93	Mapping of Rotor Power Required to Hover	127
94	Hover Power and Forward Flight Power, W=2000 lbs.	128
95	Hover Power and Forward Flight Power, W=2400 lbs.	129
96	Hover Power and Forward Flight Power, W=2800 lbs.	130
97	Solution of Helicopter Gross Weight Equation	131
98	Gross Weight and Power vs Rotor Diameter	131
99	Comparative Shear Crippling Efficiencies	139
100	Comparative Column Efficiencies	140
101	Comparative Tension Efficiencies	141
102	Skin Panel Fiber Orientation	145
103	Strength vs Angle of Stress in Tension for Undirectional and Multidirectional Layups of Equivalent Material and Thickness	146
104	Compression Modulus vs Percent Filament in 0^0 Direction	146
105	Relation Between Direction of Laminations and Direction of Load Application	147
106	Weight/in. vs Tension Load	148
107	Round Tube Column Optimum (D/t) Ratios	149
108	Optimum (Maximum) Stress Round Tube Columns	150
109	Minimum Weight Round Tube Columns	151
110	Minimum Area Curves - Wide Column Concept	153
111	Minimum Area Curves - Compression Panel Concept	153
112	Sandwich Panels	154
113	Theoretical vs Optimum Wide Column Weights Graphite and S-Glass Filament Sandwich Construction	155
114	Theoretical vs Optimum Compression Panel Weights Graphite and S-Glass Filament Sandwich Construction	155
115	Theoretical vs Optimum Thicknesses, Graphite and S-Glass Filament Sandwich Construction	156
116	Optimum Weight, Wide Column Concept	156
117	Minimum Weight, Wide Column Concept	157
118	Minimum Weight, Compression Panel Concept	157

FIGURE		PAGE
119	Optimum (Max.) Stess, Wide Columns, Aluminum Sheet, Stringer Type	158
120	Minimum (Opt.) Weight, Wide Columns, Aluminum Sheet, Stringer Type	158
121	Minimum Thickness, Shear Panel Buckling	160
122	Shear Buckling Coefficients - Flat Plates	160
123	Minimum Weight Shear Panel Buckling	161
124	Compression Flange Structural (Crippling) Efficiencies	161
125	Composite VG Records - Five Type of Operations	168
126	S-N Comparison Curves for Axially Loaded Aluminum Alloys Notched Specimens	172
127	S-N Comparison Curves for Various Materials - Notched Specimens	172
128	S-N Comparison Curves for Axially Loaded Aluminum Alloys Smooth Specimens	173
129	S-N Comparison Curves for Various Materials - Smooth Specimens	174
130	S-N Comparison Curves for Axially Loaded 4130 and 4340 Steel Alloys - Notched Specimens	175
131	S-N Comparison Curves for Axially Loaded 4130 and 4340 Steel Alloys - Notched Specimens	176
132	S-N Curves of Laminates Made of Scotchply 1002 Resin and Unwoven Glass Fibers, All Oriented Parallel to the Principal Axis	176
133	S-N Curves of Laminates Made of Scotchply Resins and Unwoven Glass Fibers Having Alternate Plies at 0° and 90° to the Principal Axis	177
134	S-N Curves of Laminates Made of Scotchply Resins and Unwoven Glass Fibers Having Alternate Plies Oriented at $\pm 5^{\circ}$ to Principal Axis	177
135	Standard Automatic Riveting Machine	179
136	Riveting Equipment	181
137	Current Light Aircraft Spot Welded Fuselage Construction	185
138	Current Light Aircraft Spot Welded Flap Construction	186
139	Design Practices for Welded Tubular Joints	190
140	Typical Examples of Brazing	196
141	Comparison of Crippling Strength of Bonded and Riveted Built-Up Compression Elements	201
142	Effect of Width of Skin to Stringer Bond on Fatigue Strength of Compression Panels	202
143	Comparison of Fatigue Strength of Bonded Single and Double-lap Joints with Riveted Joint	203
144	Comparison of Riveted, Bonded and Integrally Stiffened Aluminum Alloy Box Beams	203
145	Comparison of Fatigue Strength of a Simple Lap Joint and a Scarf Joint	204
146	Three-View of Far Term Light Airplane	209

FIGURE		PAGE
147	Vertical Stabilizer, Far Term Light Airplane	213
148	Rudder, Far Term Light Airplane	214
149	Horizontal Stabilizer, Far Term Light Airplane	217
150	Wing Planform, Far Term Light Airplane	220
151	Wing Sections, Far Term Light Airplane	221
152	Wing/Landing Gear Interface, Far Term Light Airplane	222
153	Wing Spar Configurations	224
154	Fuselage, Far Term Light Airplane	225
155	Continuous Filament Graphite/Epoxy Allowables vs % of Unidirectional Fibers	228
156	Continuous Filament S-Glass/Epoxy Allowables vs % of Unidirectional Fibers	229
157	Continuous Filament Graphite/Epoxy Allowables vs Load Angle to Fibers.	230
158	Continuous Filament S-Glass/Epoxy Allowables vs Load Angle to Fibers	231
159	Wing Planform	232
160	Wing Chord vs Y_{sta}	233
161	Wing Cell Areas	236
162	Wing Thickness	236
163	Ultimate Shear, Moment, And Torque Symmetrical Flight Condition	237
164	Wing Deflections Relative to Airplane ℄	238
165	Unsymmetrical Wing Loading	239
166	Landing Loads Geometry	240
167	Aileron Geometry	241
168	Flap Geometry and Loads	243
169	Ult. Wing Skin Shear Flow, q_t, Due to Max. Torque Flight Condition	250
170	Wing Torque Box Geometry	250
171	Flat Plate Shear Buckling Coeficients	252
172	Ult. Wing Skin Shear Stress vs Shear Buckling Allowable	253
173	Wing Pressure Distribution	254
174	NACA 63_2 - 215 Airfoil Idealized Normal Chordwise Pressure Distribution	255
175	Skin Fiber Orientation	255
176	Wing Skin Stiffeners	256
177	Leading Edge Loads	256
178	Leading Edge Geometry	257
179	Leading Edge Fiber Orientation	257
180	Spar Web Fiber Orientation	259
181	Spar Web Geometry	259
182	Wing Spar Web, Net Ultimate Shear Flow	260
183	Wing Spar Web Thickness - Material/Concept I	260
184	Skin Element Fiber Orientation	261
185	Spar Web Element Fiber Orientation	261
186	Skin Splice Fiber Orientation	262

FIGURE		PAGE
187	Composite Section @ Sta. 24	262
188	Composite Section Sta. 24 Fiber Orientation	264
189	Wing Spar Cap Thickness	254
190	Closing Spar Geometry	265
191	Effective Section Closing Spar	265
192	Wing-Fuselage Attachment	266
193	Spar Cap Splice	266
194	Spar Web Splice	267
195	Skin Fiber Orientation	267
196	Leading Edge Fiber Orientation	268
197	Skin Fiber Orientation	269
198	Skin Splice Fiber Orientation	269
199	Web Fiber Orientation	269
200	Composite Section @ Sta 24	270
201	Wing Spar Cap Thickness-Material/Concept II	271
202	Wing Spar Web Thickness-Material/Concept II	271
203	Leading Edge Fiber Orientation	272
204	Skin Fiber Orientation	273
205	Web Fiber Orientation	273
206	Composite Section @ Sta. 24	273
207	Wing Spar Cap Thickness - Material/Concept III	275
208	Wing Spar Web Thickness - Material/Concept III	275
209	Horizontal Tail Planform	277
210	Horizontal Tail Ultimate Shear and Moment, @ 25% Chord, Maneuver/Gust Condition	278
211	Loading Distribution on Anti-Servo Tab	278
212	Horizontal Tail Ult. Shear & Torque @ 25% Chord Anti-Servo Tab Loading Cond. (Per Side)	279
213	Horizontal Tail Unsymmetrical Load Distribution	280
214	Horizontal Tail Torque Box Shear Flow	280
215	Horizontal Tail Skin Stiffener Loading	281
216	Horizontal Tail Main Spar Cross Section	283
217	Horizontal Tail - Closing Spar Loads	284
218	Horizontal Tail Closing Spar Ultimate Beam Shear and Bending Moment	285
219	Horizontal Tail Closing Spar Cross Section	285
220	Horizontal Tail - Fuselage Hinge Loads	286
221	Horizontal Tail Main Spar Lug	287
222	Horizontal Tail Anti-Servo Tab Spar Loads	288
223	Anti-Servo Tab Chordwise Load Distribution	289
224	Vertical Tail Geometry	290
225	Vertical Tail Chordwise Load Distribution	291
226	Rudder Loads Spanwise Distribution	291
227	Vertical Tail-Fin Gust Load Condition Shear, Torque and Bending	292
228	Vertical Tail-Rudder Ult. Shear, Moment and Torque	294
230	Vertical Tail Single Cell Area of Section Normal to Hinge	295

FIGURE		PAGE
231	Vertical Tail Sking Shear Stress vs Buckling Allowable	295
232	Loading Distribution on Fin Stiffener	296
233	Fin Stiffener Cross-Section	296
234	Fin-Spar Cross-Section	297
235	Fin-Required Spar Web Thickness vs $f_s \leq T_{cr}$	298
236	Fin-Fuselage Attachment Loads	299
237	Fin Main Spar, Attachment to Fuselage	300
238	Two-Piece Concept Vertical Stabilizer	303
239	Vertical Stabilizer Molding Die Arrangement	304
240	Vertical Stabilizer Unit Cost vs Production Rate	308
241	Horizontal Tail, Exploded View	310
242	Wing, Exploded View	311
243	Far Term Light Airplane Wing Unit Manufacturing Costs	313
244	Manufacturing Cost of Wing vs Graphite Cost	314
245	Fuselage, Exploded View	315
246	Induced Drag Factor	339
247	Wing Transition Point Effect on Drag	341
248	Parasite Drag Area, Cessna 182 and Skylane	344
249	Parasite Drag Area, Piper Cherokee "C"	344
250	Parasite Drag Area, Cessna 210 Centurion	345
251	Parasite Drag Area, Piper Comanche "260"	345
252	Parasite Drag Area, Beechcraft Debonair	346
253	Parasite Drag Area, Piper, PA-28R-180, Cherokee "Arrow"	346
254	Far Term Airplane Empty Weight Breakdown (Piston Engine)	350
255	Consumer Price Breakdown of Far Term Airplane (Estimated)	351

TABLES

TABLE		PAGE
I	Airframe Failures by Manufacturer (1963 thru 1965)	9
II	In-Flight Airframe Failures, 1963, 1964 and 1965	10
III	Contemporary Airplane Weight Statistics	29
IV	Wing Configuration I (for n = +3.8 and -1.9g)	40
V	Wing Configuration I (for n = +6.0 and -3.0g)	41
VI	Spar Web Shear Allowables	46
VII	Wing Structure Weight Summary	52
VIII	Fixed vs Retractable Landing Gear, Performance Comparisons for Three Airplane Pairs	81
IX	Typical Operating Costs for Airplanes with Fixed Pitch and Constant Speed Propellers	88
X	Typical Operating Costs for Cantilevered and Strut-Braced Wing Airplanes	89
XI	Value of a Pound Saved	94
XII	Cost Breakdown of a typical Light Airplane	97
XIII	Cost Breakdown of a Typical Light Helicopter	99
XIV	Aerodynamic Parameters for Configuration Optimization	105
XV	Value of Reducing the Helicopter Fixed Weight by 100 lbs	130
XVI	Initial Selection of Metallic Materials and Comparative Structural Efficiencies	134
XVII	Initial Selection of Non-Metallic Materials and Comparative Structural Efficiencies	135
XVIII	Promising Candidate Materials - Metallic	137
XIX	Promising Candidate Materials - Non-Metallic	143
XX	Minimum Area Equations for Optimized Wide Columns and Compression Panels	152
XXI	Break-Even vs Actual Fabrication & Installation Costs	164
XXII	Break-Even vs Actual Fabrication & Installation Costs With Net Savings for Feasable Materials	165
XXIII	Aluminum - Satisfactory Combinations of Structural and Rivet Alloys	180
XXIV	Aluminum Rivet Ultimate Shear Strength	182
XXV	Allowable Ultimate Shear Strengths of Single Spotwelds (Aluminum Alloys)	186
XXVI	Allowable Ultimate Tensile Stresses Near Fusion Welds in 4130, 4140, 4340, or 8630 Steels	188
XXVII	Weld Metal Strengths for Welded Joints	188
XXVIII	Effect of Brazing on Allowable strength	197
XXIX	Advantages and Limitation of Bonding	207
XXX	Far Term Airplane Guidelines	208
XXXI	Far Term Airplane General Data	210
XXXII	Far Term Airplane Empennage Weights	218
XXXIII	Wing Weights	224
XXXIV	Composite Allowables - Non-Continuous Filament	227
XXXV	Ultimate Landing Loads	241
XXXVI	Moments per Moment Distribution Method Using Ave. ω Between Supports	244

TABLE		PAGE
XXXVII	Net Ultimate Flap Loading	246
XXXVIII	Wing Material Concepts	248
XXXIX	Ultimate Wing Skin Shear Stress	249
XL	Effectiveness Factors, n	262
XLI	Main Spar Margins of Safety	263
XLII	Effectiveness Factors, n	269
XLIII	Main Spar Margins of Safety	270
XLIV	Effectiveness Factors, n	274
XLV	Main Spar Margins of Safety	274
XLVI	Wing Margin of Safety Summary	276
XLVII	Horizontal Tail Margin of Safety Summary	289
XLVIII	Vertical Tail Panel Dimensions	290
XLVIX	Vertical Tail Margin of Safety	300
L	Industry Estimates of Vertical Stabilizer Tooling Costs (Dollars)	302
LI	Cost Analysis to Produce 100,000 Vertical Stabilizers Per Year	306
LII	Fabrication Sequences and Estimated Times	307
LIII	Equivalent Parasite Areas for Several Current Airplanes	343

INTRODUCTION

The expansion and competitive position of general aviation in the field of transportation depends upon improving the safety and utility of light aircraft while reducing their cost. Toward this end, the Mission Analysis Division of NASA is investigating various areas associated with the design of light aircraft and has sponsored this study on structural materials and concepts.

The primary objectives of the study were

(1) To make a comparative evaluation of a wide variety of materials and structural concepts, presently and potentially available for application to light aircraft, by investigating the effect of design, manufacturing, operational, and material requirements on the cost of this class of aircraft.

(2) To apply the more promising materials and structural concepts to the conceptual design of light aircraft

(3) To identify key problem areas where additional research may increase the potential of promising materials or concepts.

In pursuing these objectives the contractor was to consider two levels of technology and two types of light aircraft, fixed and rotary wing. The levels of technology were classified as "near term," 5 years hence, and "far term," 15 years hence. The conceptual designs were to meet the contract guidelines listed in Appendix M.

The study was performed in two phases. Phase I was concerned with researching, correlating, and evaluating available information on (a) operational characteristics; (b) material properties; (c) structural concepts and capabilities; (d) manufacturing and cost considerations; as they apply to light four-place airplanes and helicopters. The intent of Phase II was to select the more promising structural materials and concepts and apply them to the two conceptual designs for the two levels of technology. However, upon completion of Phase I, the results indicated (a) that the economic gains associated with improved light aircraft structural design would be more significant for "far term" aircraft; (b) that light fixed wing and light helicopters structures are similar; (c) the need for a more definitive analysis of the fabrication cost of the selected materials and concepts.

Thus, it was decided (with the agreement of NASA) to eliminate from consideration in Phase II the "near term" airplane and helicopter, and the "far term" helicopter. Phase II concentrated on establishing detailed structural design, cost, and fabrication analyses for those materials and concepts that showed the most promise of reducing labor hours and facilitating mass production as applied to the "far term" light airplane conceptual design.

A major aim of the study was to identify key problem areas where additional research would increase the potential of the more promising materials and concepts and lead to safer and more economical light aircraft.

SYMBOLS, ABBREVIATIONS, AND CONVERSION FACTORS

A = Area, in^2, ft^2
A_d = Disk area
AMPR = Aeronautical Manufacturers Planning Report
AR = Aspect ratio
a = Area of individual element
b = Width, in. or span, ft.
C = Restraint coefficient
CAA = Civil Aeronautics Admin.
CAB = Civil Aeronautics Board
C_c = Chordwise force
C_{D_i} = Induced drag coefficient
C_{D_o} = Drag coefficient
C_{D_w} = Wing parasite drag coefficient
C_e = Specific engine weight
C_f = Fabrication cost/lb. , $/lb.
C_{fb} = Baseline material fabrication cost/lb. , $/lb.
C_{fn} = Candidate material fabrication cost/lb. , $/lb.
C_i = Installation cost/lb., $/lb.
C_L = Lift coeficient
$C_{L_{50}}$ = Lift coeficient at 50 feet, take off
C_m = Material cost/lb., $/lb.
C_{mb} = Baseline material cost/lb., $/lb.
C_{mn} = Candidate material cost/lb. $/lb.
C_N = Normal force coefficient
C_Q = Torque coefficient
C_T = Torque coefficient
C_T = Thrust coefficient
C_{TO} = Take-off parameter
C_w = Specific wing weight
C_w = Dollars worth of a pound of material saved
C_d = Section drag coefficient
c.g. = Center of gravity
$c_{m_{a.c.}}$ = Section-Moment coefficient about the aerodynamic center
c_r = Root chord
c_t = Tip chord
ct/cr = Taper ratio
c_ℓ = Section lift coefficient
D = Diameter, in.
D_c = Drag force
D.O.C. = Direct Operating Cost
E = Modulus of elasticity in tension, psi
E_c = Modulus of elasticity in compression, psi
E_t = Tangent modulus, psi
e = Elongation in percent
F = Allowable stress or fahrenheit
FAA = Federal Aviation Agency
FAR = Federal Air Regulations
F_b = Allowable bending stress, psi
F_c = Allowable compressive primary buckling stress, psi
F_{cc} = Ultimate allowable crippling strength, psi
F_{cr} = Allowable compressive crippling stress, psi
F_{cu} = Ultimate allowable compressive stress, psi
F_{cy} = Yield allowable compressive stress, psi
F_{su} = Ultimate allowable shear stress psi
F_{tu} = Ultimate allowable tensile stress, psi
F_{ty} = Yield allowable tensile stress, psi
f = Internal (calculated) stress, psi
f = Equivalent parasite drag area
f_{cc} = Ultimate crippling stess of element, psi
G.A.G. = Ground-Air-Ground fatigue spectrum
G.W. = Gross Weight
gt = Shear flow
HP = Horsepower
h_e = Spar cap centrord
I.O.C. = Indirect Operating Cost
J_n = Inertia relief factor
K = Factor
K_d = 33% markup factor for distributor/dealer
K_p = 10% profit factor for manufacturer
K_t = Theoretical stress-concentration factor
ksi = One thousand pounds per sq.in.

L = Length, in.
MAC = Mean Aerodynamic Chord
MIL-HDBK-5 = Military Handbook - Metallic Materials and Elements for Aerospace Vehicle Structures
M_x = Bending moment
N = Normal force
N = Cycles to failure, fatigue
N_x = Compressive load per unit width, lb/in
N_{xy} = Shear flow, lb/in
n = Load factor
n = Exponent, subscript
n_{ult} = Ultimate load factor
P = Applied load, lb. or power
P_f = Fabrication cost, $.
P_i = Installation cost, $.
P_{ib} = Baseline material installation cost, $.
P_{in} = Candidate material installation cost, $.
P_m = Material cost, $.
q = Shear flow, lb/in.
R = Ratio of minimum to maximum stress fatigue
R/C = Rate of climb
S = Structural efficiency or wing area
S_{50} = Take-off distance to clear 50 ft.
$\$_{Savings}$ = Net overall savings realized $
S_b = Baseline material structural efficiency
S_{ht} = Horizontal tail area
S.L. = Sea Level
S-N = Stress vs cycles to failure, fatigue
S_n = Candidate material structural efficiency
STOL = Short Take-Off and Landing
S_{vt} = Vertical tail area
S_w = Wing area
S_z = Shear load
T = Torque
T.O.C. = Total Operating Cost
t = Thickness in. Also indicates tension when subscript
$\bar{t}$ = Cross-sectional area per unit width
t_c = Core thickness, in.
t/cr = Airfoil thickness ratio
V = Speed
V_A = Design maneuvering speed (knots)
V_C = Design cruise speed (knots)
V_{cr} = Cruise speed
V_D = Design dive speed (knots)
V_F = Flap speed
VG = Positive and negative accelerations vs air speed
V_{max} = Maximum speed
V_{NE} = Design never-exceed speed (knots)
V-n = Refers to diagram plotting limit load factor vs indicated airspeed
V_T = Tip speed
W = Weight, lb.
W_b = Baseline material weight, lb.
W_{ht} = Horizontal tail weight
W_n = Candidate material weight, lb.
W_o = Initial weight
W/P = Power loading
W/S = Wing loading
W_{vt} = Vertical tail weight
W_w = Wing weight
w = Density, lb/in^3
$\bar{w}$ = Running load
$x_{a.c.}$ = Aerodynamic center ordinate
$x_{e.a}$ = Elastic axis ordinate
$y_{a.c.}$ = Aerodynamic center abscissa
$y_{e.a}$ = Elastic axis abscissa
α = Thermal coefficient of expansion, in/in/°F.
Γ = Dihedral
ΔP = Difference in installation cost, $.
$\Delta\$_{oc}$ = Difference in operating cost,$.
$\Delta\$_{pp}$ = Change in purchase price of airplane
ΔW = Difference in weight, lb.
ε = Efficiency factor (materials)

Λ	= Sweep	τ_{cr}	= Allowable shear buckling stress
λ	= Taper ratio	η_p	= Propulsive efficiency
$\bar{\eta}$	= Plasticity reduction factor	δ	= Mass density of air
T_{cr}	= Shear buckling stress, psi	σ	= Solidity ratio
ω_{D_c}	= Chordwise running load	μ	= Poison ratio
ω	= Running load	θ	= Angle of twist

CONVERSION FACTORS FOR INTERNATIONAL SYSTEM OF UNITS
(Ref. 47)

w	g/cm^3 = .03613 lb/in^3	$\frac{WC}{L^3}$, $\frac{W}{bL^2}$, $\frac{W}{b^2L}$, $\frac{WK^{1/3}}{b^2a}$	kg/cm^3 = 36.13 lb/in^3
P	kg = 2.205 lb		
$\frac{K_{eff}\,W}{L}$	kg/cm = 5.602 lb/in		
E_c	kg/cm^2 = 14.22 psi		
F, f, $\frac{P}{L^2}$	kg/cm^2 = 14.22 psi	α	cm/cm/°c = .555 in/in/°F
$\frac{N_x}{L}$, $\frac{N_x}{b}$, $\frac{N_{xy}}{b}$	kg/cm^2 = 14.22(10^3) ksi	km/hr	= 0.6214 mph = 0.5396 knots

This page intentionally left blank

PHASE I - INVESTIGATION

The first phase of this study researched, compiled, and correlated the available data on and related to structural materials and concepts. The data is sub-divided and is discussed in the following order.

Evolution of the Post WW II Light Aircraft Industry
Design Considerations
Performance Considerations
Contemporary-to-Advanced Materials and Concepts

Evolution of the Post WW II Light Aircraft Industry

Although the history of General Aviation light aircraft began with the Wright Brothers' No. 3 Flyer of 1905, this report will concern itself only with the industry since the end of World War II. This was the beginning of the most significant period of growth, with the exception of war-time production quantities that were on the decline in 1947. General Aviation did not recover from this decline until 1952, after which the industry has experienced a fairly constant growth to date. In the paragraphs to follow, the historical aspects of the following items will be discussed:

Safety
Utilization
Cost
Life
Performance
Production

Safety.-The overall aspects of safety in General Aviation and particularly light aircraft, and safety as associated with the aircraft structure, will be discussed in this sub-section.

Overall safety: Several quantitative measures are commonly used to describe air travel safety. The most common measures used to describe General Aviation safety are in terms of accidents per hour or per plane-mile.
The General Aviation safety record has been constantly improving since the end of World War II. Referring to Figure 1, this fact is evident both in terms of accidents per hour and per plane-mile. The post World War II accident rate has declined from 79 accidents per 100,000 hours to about 31 in 1967. In terms of accidents per million plane-miles, the rate has declined from 8.8 in 1946 to 2.0 in 1967. This is commendable in the face of a near doubling of eligible aircraft between 1954 and 1966. The data from which Figure 1 is plotted is presented in Appendix A.

Figure 2 graphically illustrates that small single-engine airplanes comprise the bulk (87%) of all General Aviation accidents. The remainder of the accidents are made up of 4% by rotorcraft and 9% by all other type and size of General Aviation aircraft. The pie in Figure 2 is also divided into zones, the area of which is proportionate to the number of fatal, serious

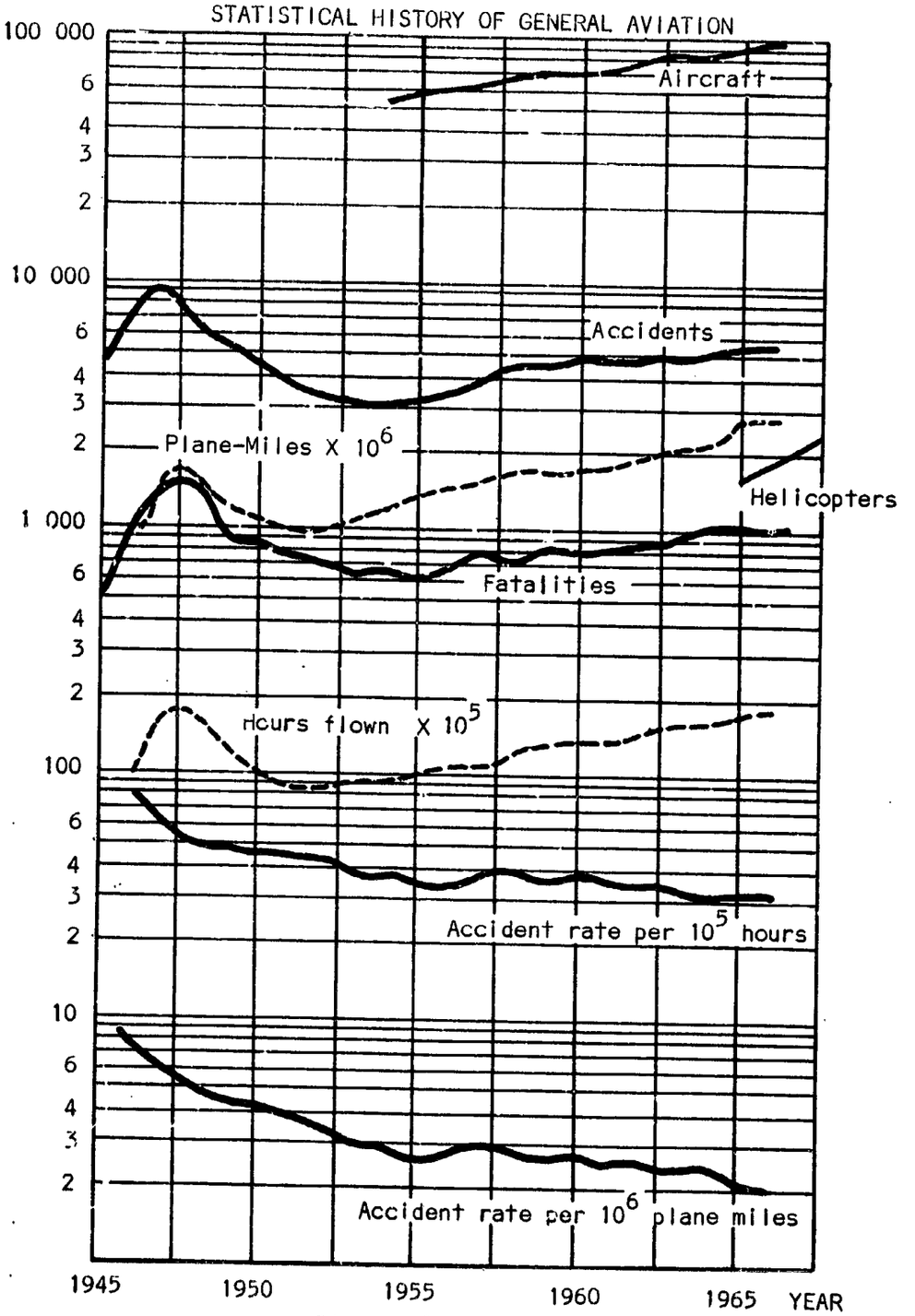

STATISTICAL HISTORY OF GENERAL AVIATION
100 000
6
4
3
2
10 000
6
4
3
2
1 000
6
4
3
2
100
6
4
3
2
10
6
4
3
2
Aircraft
Accidents
Plane-Miles X 10^6
Helicopters
Fatalities
Hours flown X 10^5
Accident rate per 10^5 hours
Accident rate per 10^6 plane miles
1945
1950
1955
1960
1965
YEAR

Figure 1

GENERAL AVIATION ACCIDENT & INJURY INDEX FOR 1963 (TYPICAL)

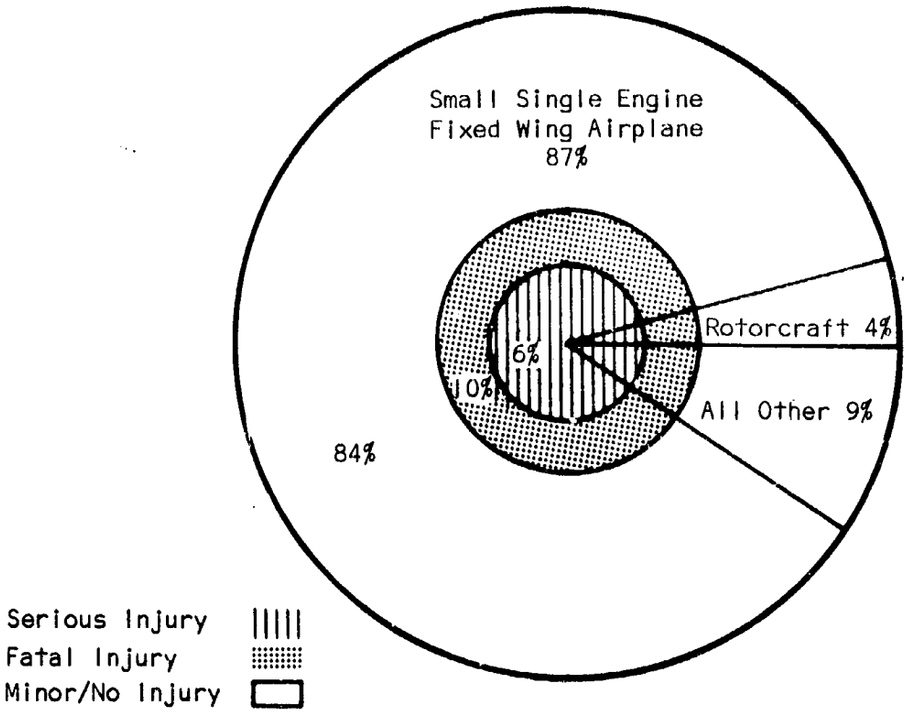


Figure 2

injury, and minor no injury accidents. I.e. 10% of all accidents are fatal, 6% involve serious injury and 84% involve minor to no injury. Although this illustration is plotted from 1963 data, it is typical and representative of today's statistics. Figure 2 is plotted from data in Appendix B.

When the accident statistics are analyzed from a geographical viewpoint, no clear cut patterns are apparent. On the average, 5.3 of every 100 eligible aircraft in the United States are involved in an accident each year (assuming that 1965 is representative of any recent year). Delaware and the District of Columbia have a low record of less than one per hundred aircraft. Nevada and Hawaii have a high record of 10 or more per hundred aircraft. Appendix C provides accident data for each state.

Analysis of accidents versus phase of operation for small fixed-wing aircraft (in 1963 and 1964) reveals that:

(1) 7% of the accidents occur during taxi.
(2) 16% of the accidents occur during takeoff.
(3) 8% of the accidents occur during cruise.
(4) 67% of the accidents occur during landing.
(5) 2%, phase of operation-static or unknown.

The number of accidents versus phase of operation is tabulated in Appendix D.

Safety as associated with design: This part of the discussion on safety is concerned with that portion of the statistics that are improvable by better design.

Analysis of all the accidents in 1963-64 versus their causes, is illustrated graphically in Figure 3 and 4. It is apparent in Figure 3 that for small fixed-wing aircraft, 68% of the accidents have causes associated with improvable design considerations. Sixty-two percent of this improvable 68%, or approximately 42% of all the accidents, are associated with the landing gear (i.e., gear collapsed, retracted, wheels-up landing, nose over/down, hard landing and ground/waterloop). It should be recalled, from two paragraphs back, that 67% of all accidents in small fixed-wing aircraft occur during the landing operation. It should be noted that airframe failures are associated with just slightly over 1% of all the accidents in 1963. The accidents not associated with, or improvable by design considerations are those such as collisions, weather associated, etc. Figure 3 is based on data in Appendix E.

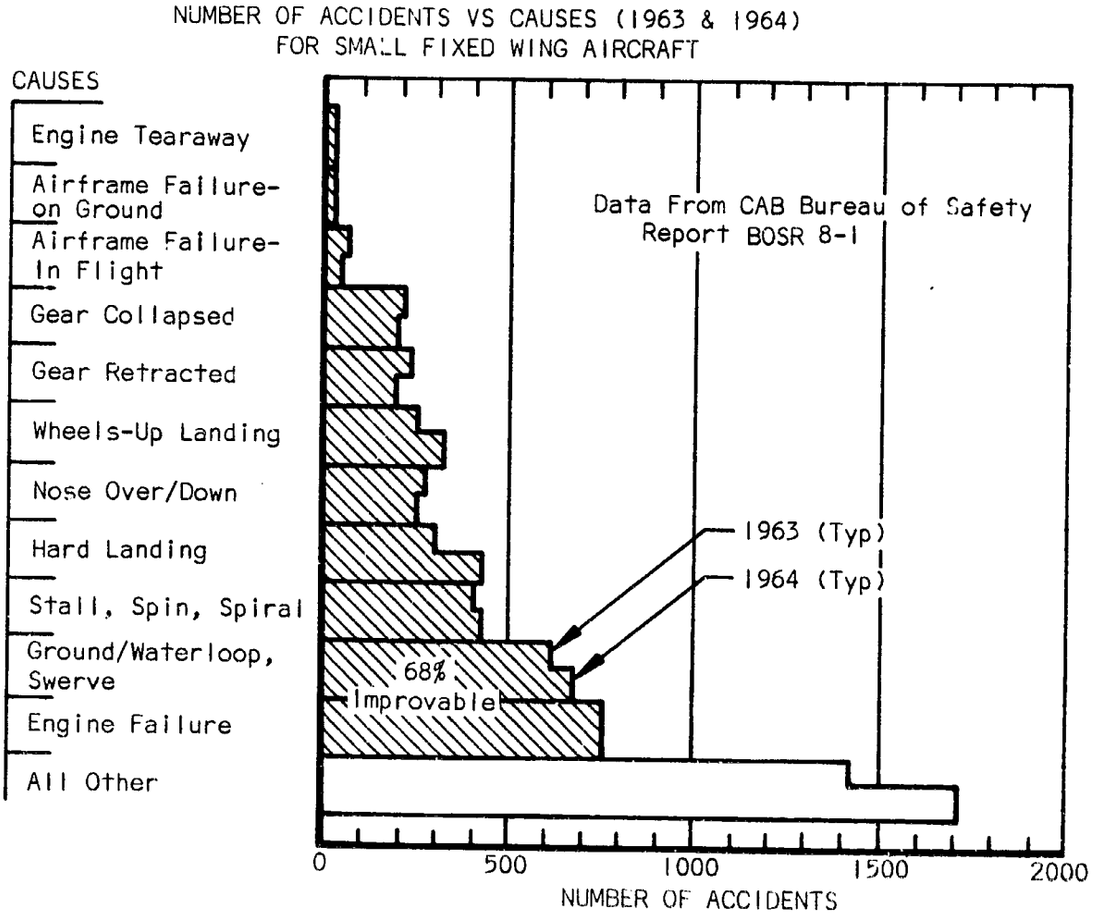
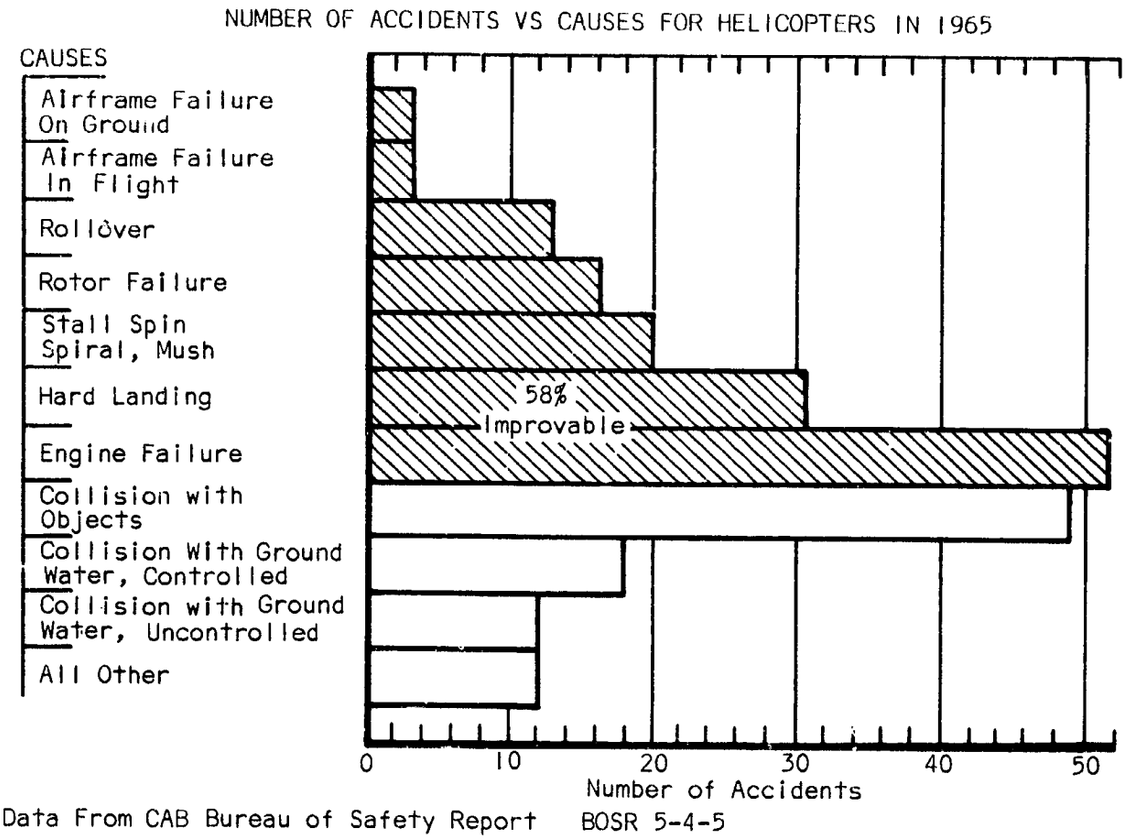


Figure 3

Analysis of helicopter accidents versus cause reveals a similar situation, where 58% of the accidents have causes associated with improvable design considerations (see Figure 4). Figure 4 is based on data in Appendix F.



Data From CAB Bureau of Safety Report BOSR 5-4-5

Figure 4

Even though airframe failures are the cause of only 1% of the accidents in 1963 thru 1965, they bear some scrutiny. These accidents and their severity are arranged by manufacturer in Table I. It is readily apparent that the aerodynamically clean and high performance airplanes have a relatively high incidence of airframe failure. It is interesting to note that the Mooney group, with their stability augmentation devices, have a very low incidence of airframe failure. The respective numbers of airplanes active in 1965 (included in the last column in Table I) must be considered when comparing the data for each airplane.

TABLE I

AIRFRAME FAILURES BY MANUFACTURER*
(1963 THRU 1965)

AIRCRAFT	FATAL	SERIOUS	MINOR TO NONE	ACTIVE AIRCRAFT IN 1965
Aero Commander 520, 560F, 580P	3	-	1	75, 213, X
Aeronca 11AC, C2, 7AC	1	1	1	755, 3, X
Alon Ercoupe 415C	-	-	1	71
Beech, D18, G18S, SNB5	1	-	1	3, X, X
Beech 23	2	-	-	662
Beech 35 Bonanza	20	-	2	6286
Bellanca 14-13, 14-19	3	-	-	227, X
Cessna 120, 140, 150	4	-	1	6749
Cessna 172, 180, 182	3	-	4	15 146
Cessna 195A, 195B	1	-	-	491
Cessna 210	-	-	1	1287
Cessna 310B, 320	2	-	1	1827
Globe-Swift	-	-	1	X
Helio	1	-	-	76
Luscombe 8A, 8C	-	1	1	22
Mooney 18C	2	-	1	2491
Mooney 20C, M20A, M20E	3	-	-	
Navion G NAVA, NAVB, NAV4	4	1	-	1170
Piper J4, PA12, PA16, PA18	3	-	3	4168
Piper PA20 PA22	2	-	4	449, 5726
Piper PA23, PA30	2	-	-	2483, 657
Piper PA24 Comanche	14	-	3	3025
Piper PA25	-	-	2	1072
Piper PA28	3	-	-	3573
Stinson 180	1	2	1	X
Taylorcraft BCS12D, BC-12D	-	-	2	1525
Hiller UH12E4	1	-	1	113
Hughes 269	-	-	1	259
Bell 47G2, 47H1	1	-	2	473

*Tabulated from CAB Summary Reports of Accidents - X Unknown

Referring to Table II, the cause, location of failure, and severity of the accident are tabulated for two of the airplanes listed in Table I. It is readily apparent that eight of the eleven Bonanza failures were associated with weather, subsequent disorientation and/or loss of control, resulting in wing and/or tail failure. One of the eleven Bonanza failures was due to fatigue of the wing center section, and one was due to inadequate inspection and maintenance. Four of the five Comanche airframe failures were associated with weather, subsequent disorientation and/or loss of control, resulting in wing and/or tail failure. One of the five was the result of instrument failure. In almost all these airframe failure accidents, the pilot disregarded the threat of weather conditions. See Appendix G for a tabulation of all the in-flight airframe failures in 1963.

TABLE II- IN-FLIGHT AIRFRAME FAILURES, 1963, 1964, and 1965 *

		BEECHCRAFT BONANZA												TOTALS			PIPER COMANCHE							TOTALS		
AIRCRAFT														1963	1964	1965								1963	1964	1965
% of total														18.7	6.5	16.4								10.	19.4	9.1
CASUALTY	Minor/None	X			X									2								I				3
	Serious																					I				
	Fatal		X	X		X	X	X	X	X	X	X		9	2	9	X	X	X	X	X	I	5	6	2	
LOCATION	Total Aircraft		D_a	D_i	S	D_a	D_i	D_a	D_a	D_i	D_i	D_i					D_a	D_a	D_i	D_i	D_i	S_a	6			
	Systems																									
	Controls																			S_a			I			
	Landing Gear																									
	Propeller																									
	Powerplant	S												I												
	Horizontal			D_a		D_a		D_a		D_a		D_a		5				D_a	D_a		D_a		3			
	Vertical			D_a		D_a		D_a				D_a		4				D_a	D_a		D_a		3			
	Fuselage	S												I												
	Wing	S	D_a			D_a	D_a	D_a	D_a	D_a	D_a	D_a		9				D_a	D_a	D_a	D_a		4			
CAUSE	Lack of Respect for Nature		X		X			X			X	X		5			X	X	X		X		4			
	Foolishness																									
	Horseplay																									
	General Lack of Proficiency																					X	I			
	Collision (e.g. bird)			X										I												
	WEATHER: Ice, Snow, etc.					X		X			X			3			X	X	X	X			4			
	WEATHER: Loss of Control Disorientation	X	X		X	X		X	X		X	X		8			X	?	?	X	X		5			
	WEATHER: Turbulence				X									I			?						I			
	WEATHER: Gust																									
	Inadequate Material						X							I						X			I			
	Inadequate Design																									
	Inadequate Inspection & Maintenance									X				I												

*Tabulated from CAB Summary Reports of Accidents

D = destroyed
S = substantial
a = in air
i = at impact
X = associated with

Conclusion: It has been shown that approximately 60%-70% of all accidents are improvable, i.e., they have causes associated with design, material selection, configuration, etc., which can be affected by the designer. For example, 80% of these "improvable" accidents are associated with the landing operation (i.e., gear collapsing, retracting, wheels-up, nose-over, etc.). The designer cannot pass the responsibility through the instructor, to the pilot. The handling characteristics of an aircraft should require a minimum of proficiency from the pilot. A good example of this is the pilot-proof retractable landing gear system recently introduced by one of the light airplane manufacturers which will extend the gear automatically when approaching landing conditions.

A very small percentage (1%) of the accidents were/are caused by structural failure. Most of these structural failures are the result of an unqualified pilot venturing into bad weather (instrument conditions), becoming disoriented, losing control and finally resulting in overload and failure of the structure.

A partial solution is to increase the design limit load factors, possibly from 3.8 to 6.0 g's. This might possibly save some airplanes attempting a pull-out after emerging from a dive, and would help a few aircraft encountering turbulence (clear air turbulence and gust). The cost of additional structure has been estimated to be 60 pounds at $7.00 per pound (or a total of $420.00). This solution treats only the "symptom" and does nothing to treat the "cause" of most of these accidents -- spiral divergence.

Another solution, is to provide inherent (built-in) aerodynamic stability. This approach has been investigated for the past fifteen years, with no practical results as yet.

A third solution, and probably the best, would seem to be the industry-wide adoption of "black box" stability augmentation systems. These devices are presently available for just about any aircraft on the market. They almost eliminate the possibility of spiral divergence, regardless of how the aircraft gets into such a maneuver. Whether from turbulence or from deliberate intention of the pilot, the device will recover the aircraft to straight and level flight. They have been designed for full or part-time use and even when activated can be over-powered by the pilot.

There are only two manufacturers with certified wing-leveling devices on the market at present. Such a device is already provided as standard equipment by one of the leading light airplane manufacturers, and is offered optionally by most of the other large manufacturers. These devices are available as an accesory to individual airplane owners for $500.00 to $800.00.

It is safe to assume that these devices could be sold for a fraction of today's price if they were mass produced. Since the public is now to pay hard cash for safety, it would seem that the industry should follow the lead of that one manufacturer, by mandate if necessary, and bury the cost of the device in

the overall price of the aircraft. Stability augmentation could thus be acquired with these gyro-referenced devices, far more economically in terms of dollars and weight (even at today's prices), than with structural and/or aerodynamic modifications. They also are nearly universal in their ease of retrofit.

Utilization.-The number of eligible General Aviation aircraft has been growing at the rate of 4-3/4% per year since at least 1954. Eighty-seven percent (87%) of these,are small fixed-wing single-engine airplanes and four percent (4%) are helicopters. See Figure 5a. One- to three-place single-engine airplanes have been replaced by four-plus-place airplanes as the more popular aircraft. Referring to Figure 5b, it can be seen that the contemporary single-engine airplane is utilized at an average of 175 hours per year and is representative of the utilization rate for General Aviation as a whole. Turbine-powered aircraft, as a type, are operated at a greater rate (450 hours per year) than any other type of General Aviation aircraft.

NUMBER & UTILIZATION OF GENERAL AVIATION AIRCRAFT BY AIRCRAFT TYPE

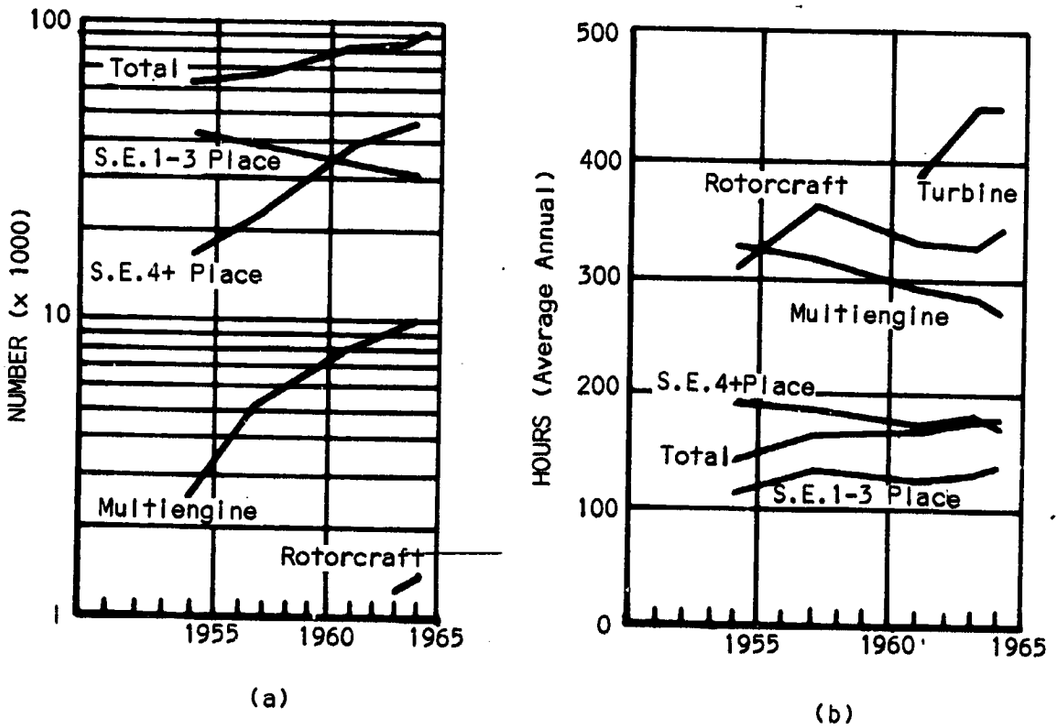


Figure 5

In observing the General Aviation fleet from a type of flying point-of-view (see Figure 6a), it can be seen that personal-type aircraft make up 50% of the fleet and business-type aircraft make up 25%. The remainder of the fleet is comprised of instructional, aerial application, air taxi, and industrial-type aircraft. Air taxi-type aircraft are by far the fastest growing category in the fleet. Referring to Figure 6b, it can be seen that personal-type flying logs, on the average, only 80 hours per year. All other types of flying log more than the industry average of 175 hours per year. The highest rates (375 hours per year) are logged by instructional flying.

Finally, in considering both the number of each type of aircraft and the utilization rate of each, the total hours logged per year for each type and/or kind of flying can be ranked thus:

1)	Business	38 %
2)	Personal	24 %
3)	Instructional	17 %
4)	Air Taxi	11 %
5)	Aerial Application	6 %
6)	Industrial	4 %

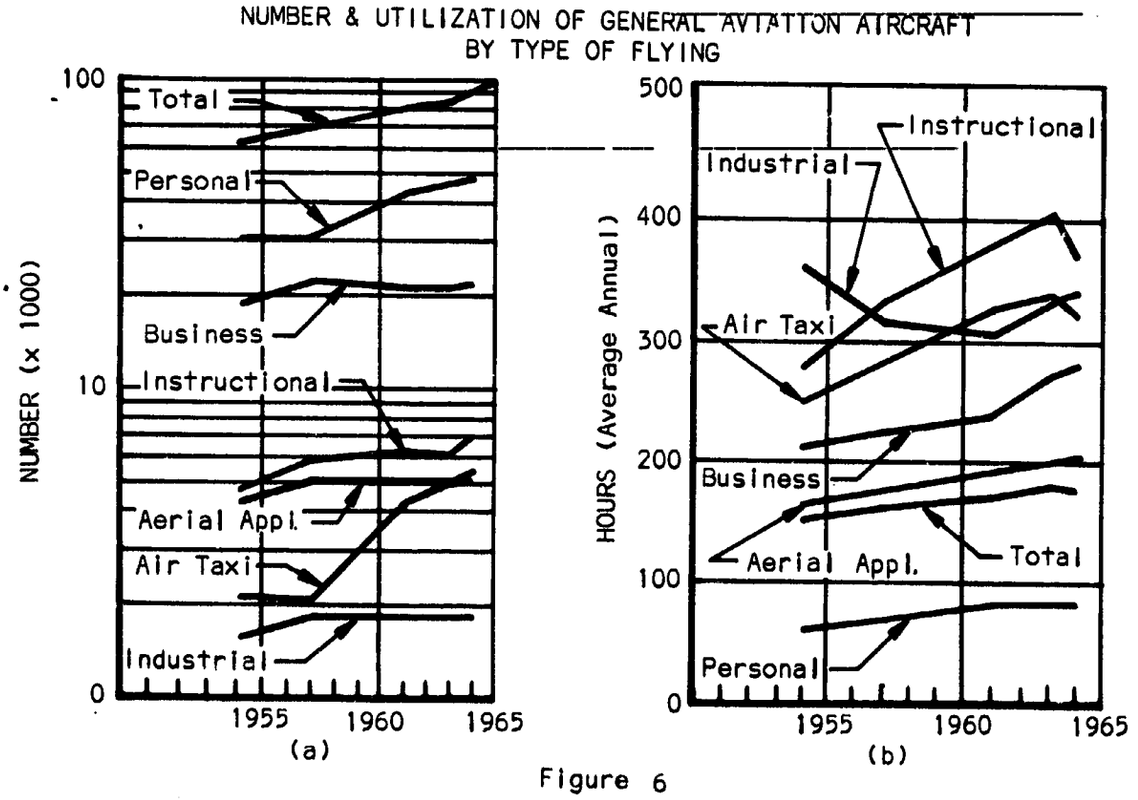


Figure 6

Industry Survey: A field survey of the Light Aircraft Industry, from the operators and maintenance station viewpoint was conducted by the contractor. This survey was accomplished by sending out approximately one thousand (1000) questionnaires to people presently operating and servicing light aircraft. Seven hundred (700) questionnaires were sent to individuals and companies in all fifty states of the United States, and the District of Columbia. Three hundred (300) questionnaires were sent to the national headquarters of the Experimental Aircraft Association (E.A.A.), Hales Corners, Wisconsin. These questionnaires were then distributed to the E.A.A. designees in various regions of the country.

The questionnaires were in two (2) different formats. One was specifically prepared for aircraft owners and operators, and one for ground service maintenance stations. The objective of the survey was to determine present-day light aircraft utilization, problem areas, and recommendations for corrective measures and improvements as observed by individuals in the field. Approximately 5% of the questionnaires were returned with a surprisingly good geographical distribution (see Figure 7).

QUESTIONNAIRE (RESPONSES)
GEOGRAPHICAL DISTRIBUTION

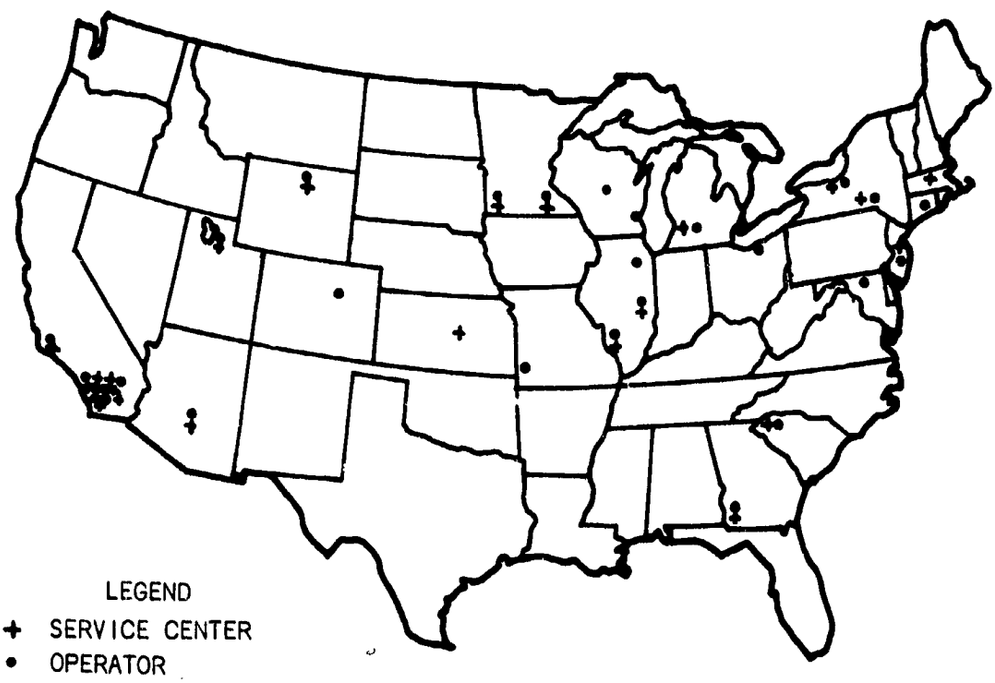


Figure 7

Most of the responding contacts were unanimous in the need for the following items:

Simplicity in design to reduce excessive maintenance costs.

Improved safety features.

Improved flight characteristics.

Improved Pilot training procedures.

The above listed items are not in any special order or preference as they all share equal importance. See Appendix H, a summary of the operating cost questionnaires.

It should be noted that most of the questionnaires were sent to Operators and Service Stations, and very few to private owners. Therefore, the answers reflect, in general, a higher utilization and a more professional point of view than that of the total General Aviation fleet.

While conducting this survey the contractor came across two excellent Government publications:

Aircraft Design-Induced Pilot Error, a study conducted by the Bureau of Safety, Civil Aeronautics Board, Washington, D.C.

General Aviation Inspection Aids, publication No. AC 20-7, controlled by the Department of Transportation FAA Flight Standards Service.

The information presented in these two documents is intended to alert the General Aviation community to data gained from operating and service experience. Therefore, data in these publications should be of value and interest to everyone associated with the light aircraft industry. A later sub-section in this report paraphrases the above-mentioned study on design-induced pilot error.

Response to the Operator and Service Station Questionnaires is listed on the following pages. It should be noted that these responses apply to the aircraft and aircraft-operators in the group polled and do not necessarily apply to the entire industry. All answers are listed in order of importance.

(Operators Questionnaire - Response)

A) Polled aircraft are used for:
(1) Flight training
(2) Flying clubs
(3) Charter service
(4) Rental

B) Most commonly used aircraft in polled group are:
(1) Cessna (all models)
(2) Piper (all models)
(3) Beech (all models)
Vintage - most aircraft 1966

Average basic cost of polled aircraft:
(1) Cessna $ 10,000
(2) Piper $ 10,250
(3) Beech $ 47,000

Cost of radios and navigational aids on polled aircraft:
(1) Cessna $ 1,500
(2) Piper $ 2,000
(3) Beech $ 5,000

C) Average yearly hours flown by polled aircraft:
(1) Cessna 485
(2) Piper 495
(3) Beech 485
(4) Champion 505

Average down time (days/year)
(1) Cessna 21
(2) Piper 16
(3) Beech 14
(4) Champion 12

D) Average cruise altitude:
5,000 ft.

E) Omitted

F) Most significant areas of maintenance:
(1) Inspection
(2) Repair
(3) Replacement

G) Most causes for inspection:
(1) Manufactures and FAA bulletins
(2) Looking for cracks
(3) Wear

Most causes for repair:
(1) Accident due to pilot error or act of God.
(2) Corrosion
(3) Wear

Most causes for replacement:
(1) Wear
(2) Deterioration
(3) Cracks

H) Most structural difficulties have been found:
(1) Cessna
(2) Piper
(3) Beech

Type of trouble:
(1) Corrosion*
(2) Cracks
(3) Deterioration
(4) Structural failure

* The emphasis on corrosion may not be justified as the most common type of trouble, because over 50% of the questionnaires returned were from areas with close proximity to large bodies of water.

I) Most common reason for selecting present aircraft:
(1) Initial cost
(2) Cost of operation
(3) Size

Average duration of ownership:
2-3 years

Reason for replacement:
(1) Upgrading
(2) Cost of maintenance

J) Most common cause of accidents:
(1) Pilot aptitude showing negligence and poor judgment (more so in professional people)
(2) Age or sex showed no special bearing

K) Most desirable features for future aircraft:
(1) Improved safety
(2) Retractable landing gear
(3) Lower initial and operating cost at the expense of greater performance
(4) STOL capability
(5) Oxygen system
(6) Cabin pressurization

L) Future aircraft safety improvements:
(1) Cockpit standardization
(2) STOL capabilities
(3) Better radio and instruments
(4) Fire resistant materials

M) Future aircraft improvements other than safety:
(1) Design for reduced cost of maintenance
(2) Better performance
(3) Create a good two-place aircraft in the $3,000 to $5,000 class
(4) Reduce cockpit noise

N) About 50% of the operators have made operating cost and maintenance analyses.

O) Most operators would submit analysis if they were available.

P) No response. Lack of helicopter experience.

(Aircraft Service Questionnaire - Findings)

A) Most common component subjected to maintenance:
(1) Powerplant and propeller
(2) Landing gear
(3) Exterior finish
(4) Doors, hatches, cowling, windshield

Most common component subjected to repair:
(1) Powerplant and propeller
(2) Doors, hatches, cowling, windshield
(3) Landing gear
(4) Exterior finish

Most common component subjected to replacement
(1) Landing gear
(2) Powerplant, propeller
(3) Exterior finish
(4) Doors, windshields, cowls

B) Most expensive maintenance services performed are:
(1) Engine overhaul
(2) Radio repair
(3) Fabric replacement
(4) Inspections

C) Most expensive structural maintenance are:
(1) Damage repair
(2) Inspections
(3) Fabric replacement
(4) Surface preservation

D) Type of construction most maintenance free is:
(1) Sheet metal
(2) Reinforced plastics
(3) Tube and fabric
(4) Wood

E) Effect of maintenance and repair costs:
(1) Sheet metal (advantages):
a. Ease of repair
b. Lower rate of deterioration
c. Fewer replacements (most items can be repaired)
d. Cheaper labor cost
(2) Sheet metal (disadvantages):
a. Cracking
b. Riveting can increase the cost of some repairs
(3) Tube and fabric (advantages):
a. Cheaper repair if extensively damaged

F) Most service stations charge for their services by parts and labor rate.

G) Labor rates seldom vary from aircraft to aircraft or from component to component.

H) Typical maintenance, repair and replacement job costs are:

Engine	
50 hr. inspection	$ 45.00
100 hr. inspection	105.00
"Top" overhaul	475.00
Major overhaul	1,725.00
Propeller	250.00
Structure	700.00
Control System	100.00
Hydraulic System	(no replies)
Electric Systems	75.00
Air Conditioning	(no replies)
Annual Inspection	185.00
Other,	
Instruments and Radio	100.00

I) Most work was performed on the following types of aircraft:
(1) Cessna
(2) All aircraft
(3) Piper
(4) Beechcraft

J) The causes for repair and replacement work are:
(1) Wear of engines, systems, brakes, tires
(2) Damage due to accident
(3) Cracks of cowling, hinges, sheet metal
(4) FAA and manufacturers' bulletins
(5) Deterioration

K) Pressurization in aircraft increases structural maintenance by approximately 50%.

L) Hangar space required:

Airplanes	900 square feet
Helicopters	400 square feet

M) Tie-down space required:

Airplanes	1000 square feet
Helicopters	1500 square feet

N) Cost for items "L" and "M":

Hangar airplane	$ 37.50 per month
Hangar helicopter	35.00 per month
Tie-down airplane	15.00 per month
Tie-down helicopter	17.50 per month

O) Helicopter operations and services caused the following maintenance problems different from airplanes:
(1) Higher maintenance
(2) Harder to park or move around
(3) Components - higher wear and short service life
(4) High operating costs

P) How would you handle a tenfold increase in operations?

The magnitude of this question must have surprised many of the service centers. Most were so overwhelmed with the idea of a tenfold increase in business that they could not conceive all the problems that would arise.

Q),U),V), Suggestions for future light aircraft improvements are: (These three questions were very similar in nature. The listed answers are a composite analysis)
(1)Pilot training
(2)Improved design
(3)STOL capabilities
(4)Low cost
(5)Improved subsystems
(6)Better engines

R) What is the range in types of aircraft that you provide services for:

The response to this question indicated a misunderstanding of it, as the replies were aquantitative rather than a qualitative nature.

S) Frequency and type of accident does not seem to be related to sex, age, or occupation.

T) Increased demand for the following items were listed:
(1)Improved safety
(2)STOL capabilities
(3)Oxygen systems
(4)Lower initial and operational cost

W) Most service centers do not make operational analyses of their operating costs.

X) Mostly no response.

In summary, two outstanding areas of interest have emerged from the response to these questionnaires.

(1) Inspection and Maintenance - present airplanes are poorly designed to facilitate inspection and maintenance.

a) Performance of proper inspection and maintenance is very costly. In one airplane the engine must be removed to inspect a fuel strainer. Another very popular design requires removal of the seats, rugs, floor panels to inspect a control pulley.

b) As stated above, the inspection of some items can be very difficult, causing mechanics to neglect them, resulting in failures and accidents.

c) There are no standardized inspection procedures, or check lists, which ensure that the critical parts or systems are inspected at the right time or frequency.

d) Comprehensive inspection procedures should be instigated, in order to cut down the frequency of inspections on items which historically have proven to be trouble free.

e) It is recommended that the aircraft manufacturers, in conjunction with FAA, provide inspection procedures for each type and model, and that these procedures should be periodically updated, based on experience.

f) An industry-wide program to indoctrinate the designers with regard to inspection and maintenance problems should be instituted. This program should reach everyone directly concerned with the airplane design.

(2) Standardization - present airplane cockpits are designed with no standardization in mind. The instrument panels and secondary controls should be standardized.

The Light Aircraft Industry, coordinated by FAA, and with the inputs of NASA, AOPA, and other concerned organizations should establish the location, shape, size, and function of instruments and controls.

Cost.-Evaluation of any material or structural concept is ultimately, if not initially, performed in terms of price or cost. This section discusses several parameters that are associated with or influenced by cost, i.e.:

Dollar value and price trends.
Consumer price trends (total and per pound empty).
Cost as a function of speed.

Dollar value and price trends: When comparing or evaluating anything in terms of dollars (or any currency) over a period of time, the effects of currency value fluctuation must always be considered. Otherwise, a change in price or cost due to some technical reason could be artificially magnified, diminished, or compensated by dollar value fluctuation, thus camouflaging the particular cost or price effect being evaluated. This currency value fluctuation (usually inflation) is measured and described in terms of a consumer price index and is compared to any convenient point in time. The U.S. Government publishes a running tabulation of this index (based on price of representative goods, products, and services) in the Statistical Abstract of the United States (ref. 2) which is published yearly. These price index values are plotted versus calendar year in Figure 8 for the period 1937 to 1985. The data from reference 2

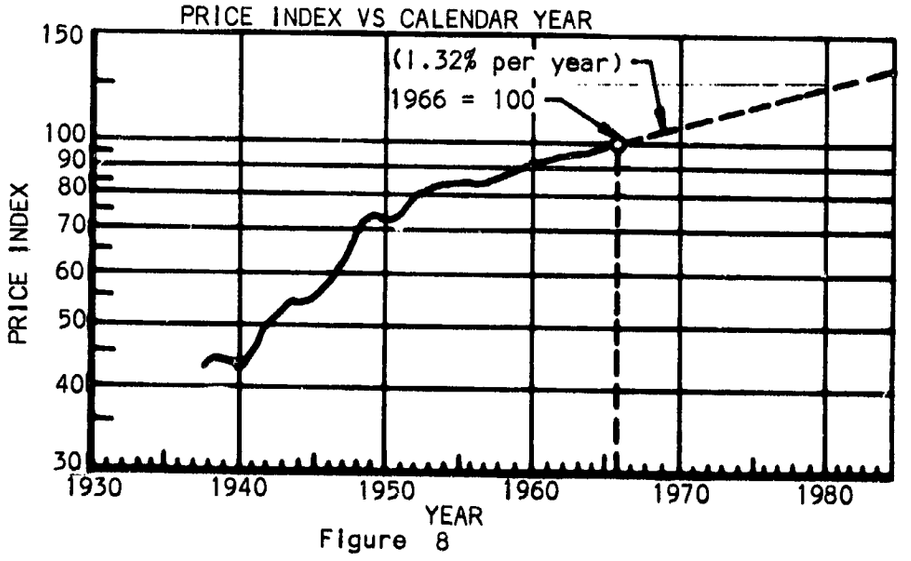


Figure 8

is based on 1958 equalling 100. The plot in Figure 8 is adjusted so that 1966 equals 100. So that any constant rate of inflation (i.e., a constant percentage increase per year) could be depicted as a straight line, the data is plotted on a semi-logarithmic graph. The constant inflation rate of 1.32% per year, apparent since about 1951, is extended to 1985. Therefore, in order to eliminate the effect of dollar value fluctuation, all dollars discussed hereafter will be 1966 dollars. Dollars of any particular year on the graph are converted to 1966 dollars by dividing the dollar value in question by the price index for that year.

The price trends of several typical General Aviation aircraft are illustrated in Figure 9. From the graph, three price categories are apparent. The low-price category includes those aircraft priced below $12,500.00 and are characterized by fixed landing gear, four-cylinder engines (180 hp max.) and a fixed pitch propeller. The middle-price category aircraft are priced approximately between $12,500 and $20,000 and are characterized by six-cylinder engines (up to 300 hp) and include some with retractable landing gear. The high-price category aircraft are priced above $20,000.00 and are characterized by six-cylinder engines (up to 400 HP),retractable landing gear, and constant speed propeller. The very high-price aircraft, i.e. twins, executive, and air taxi type, are not included since they are beyond the scope of the study.

GENERAL AVIATION AIRCRAFT CONSUMER PRICE TRENDS
(in 1966 dollars)

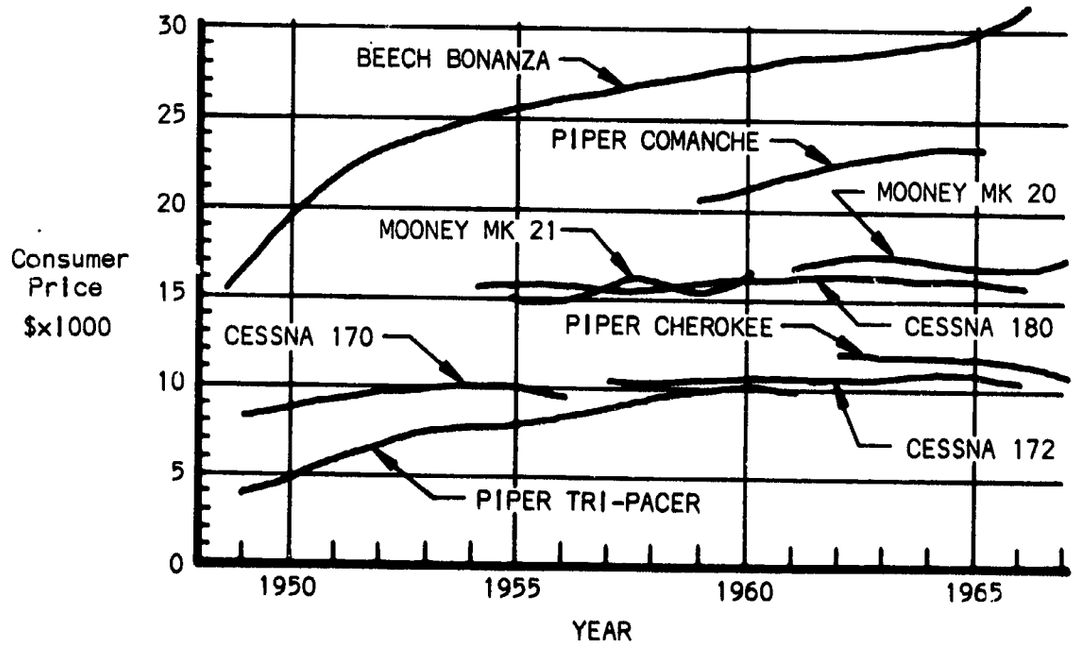


Figure 9

The following observations have been made from these price trends:

(1) Price of low-price aircraft in this decade is fairly constant to declining.

(2) Price of middle-price aircraft is fairly constant to rising.

(3) Price of high-price aircraft is generally rising.

The price per pound (empty) of aircraft is plotted in Figure 10 and illustrates, with only three exceptions, that not only is the price of airplanes rising, but consumers are paying a little more for each pound of aircraft.

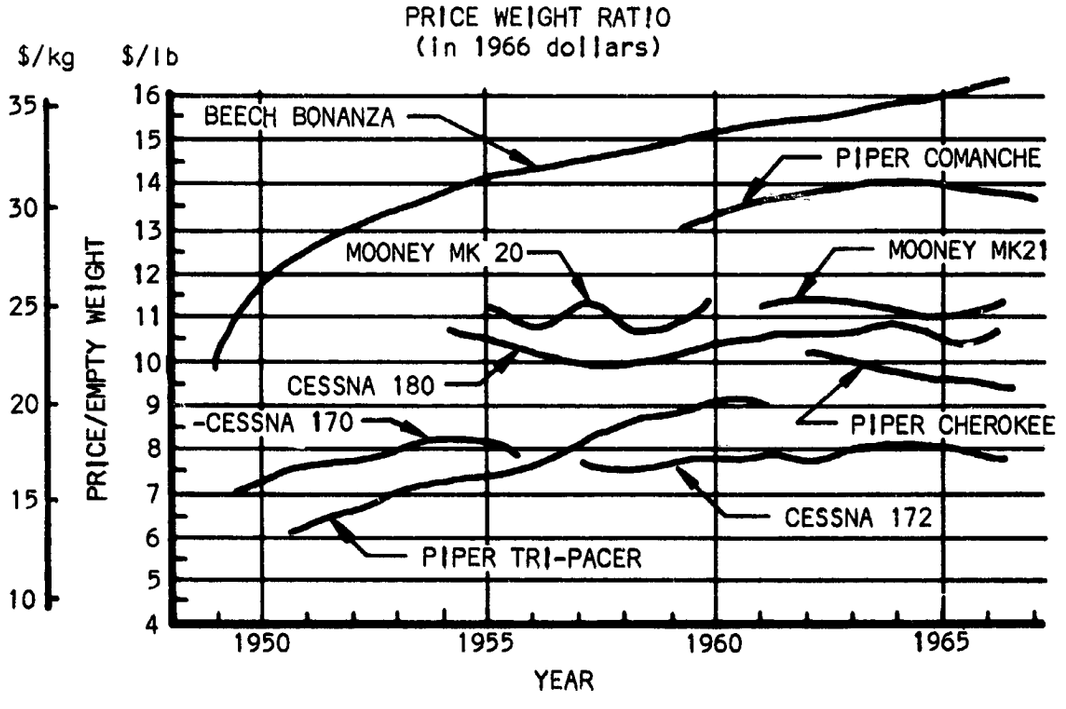


Figure 10

The increase of cost per pound is probably due to the 6% per year increase of U.S. aluminum and aircraft industry wages. No doubt, the following enhancements are contributory to the higher consumer prices:

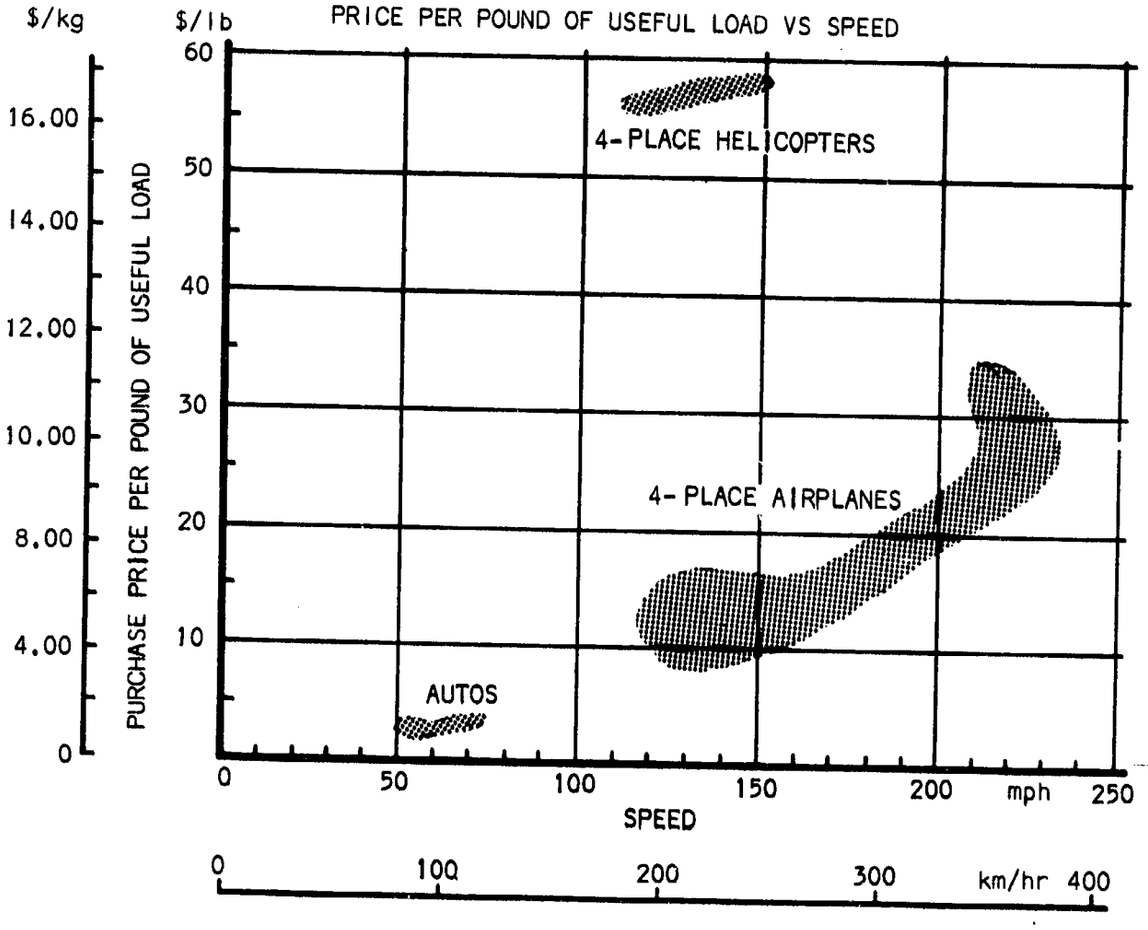
Aerodynamic cleanness - More sophisticated instruments
Safety features - Comfort items - Luxurious interiors
Style changes - Engine refinements - Propeller advancements
Accommodations for accessories and non-standard equipment

Cost as a function of speed and empty weight: As a comparative measure of the capital outlay required to transport a pound of payload (people) in four-place (minimum) vehicles at various speeds, Figure 11 (plotted from data in Appendix J) shows that:

(1) It costs from $2.50 to $4.00 per pound to travel at 50 - 70 miles per hour in an automobile.

(2) It costs from $8.50 to $34.50 per pound to travel at 115 - 230 miles per hour in a General Aviation light, four-place airplane.

(3) It costs from $56.00 to $58.00 per pound to travel at 110 - 145 miles per hour in a four-place helicopter.



NOTE: Useful load includes all persons on board, fuel, oil and baggage.

Figure 11

Life. - Based on the limited "experience" data available, the life of General Aviation aircraft would seem to be almost indefinite, with only a few exceptions. The mechanisms by which the life of an aircraft are shortened are deterioration (wear, weathering, and corrosion) and fatigue. The rate at which these mechanisms work are directly affected by the following factors:

(1) Utilization rate (hours per year)
(2) Use (instruction, pleasure, sport, business, etc.)
(3) Geographical location of base
(4) Storage (hangared or outside tiedown)
(5) Maintenance quality
(6) Design and material selection

Examples of how geographical location can affect life are:

(1) Aircraft based at seaside airports have had to have their skins replaced within two years due to corrosion.

(2) The soil on which an aircraft is tied down can "dust" the aircraft and combine with condensation drops clinging to underside surfaces. The corrosiveness of these drops is dependent on the make-up of soil in that particular geographical location.

It would seem, then, that deterioration is a significant "life" mechanism for an aircraft.

Fatigue, which is affected by utilization rate, use, and original design and material selection, is a mechanism to be considered in the life of an aircraft. It will be discussed in detail in a following main section of this report.

Performance. - Several parameters describing the general performance trends of representative airplanes are discussed in this sub-section. The "representative" airplanes are designated as follows:

(A) Piper Tripacer/Cherokee
(B) Mooney Mark 20/21
(C) Cessna 180
(D) Piper Comanche
(E) Beechcraft Bonanza

Figure 12 indicates nothing more than a continuing gradual increase in gross weight of all the representative airplanes. Figure 13 plots the trend of empty weight to gross weight, which is a measure of structural efficiency and aerodynamic capability. The whole group of airplanes have remained at or near a ratio of 0.6 indicating no change or improvement in structural concept or aerodynamic capability. Figure 14 indicates no more than a gradual trend to greater installed power, in response to customer demand for higher performance.

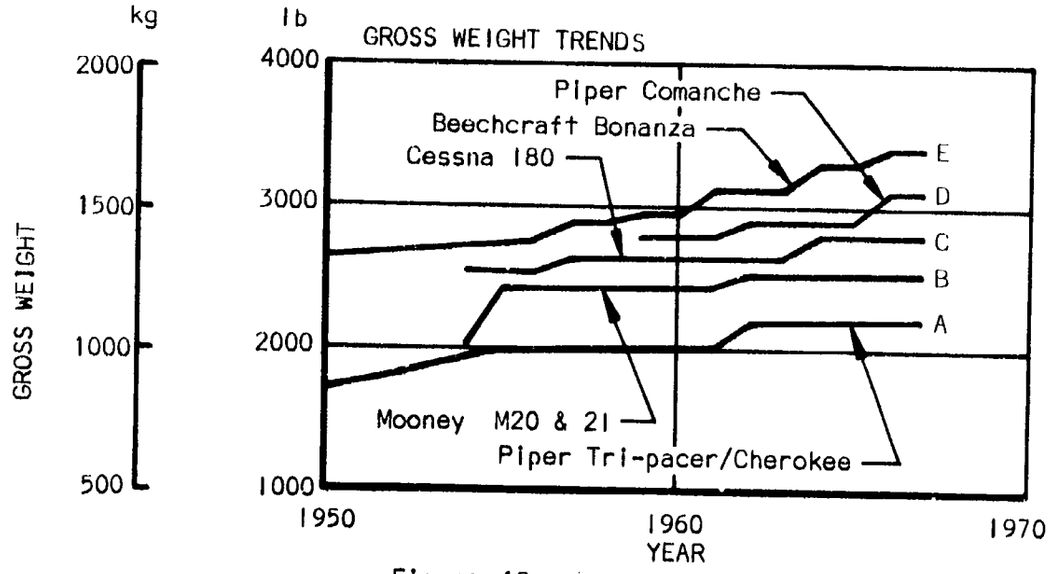


Figure 12

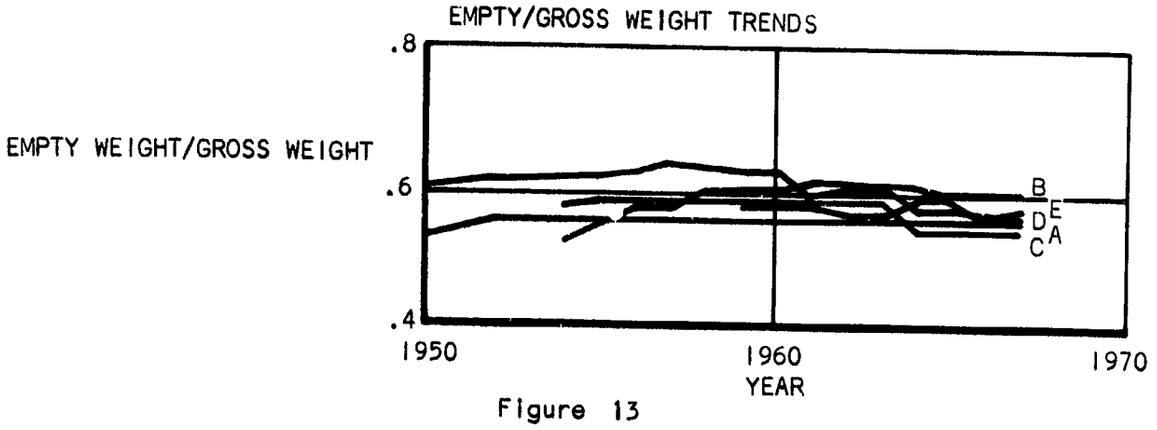


Figure 13

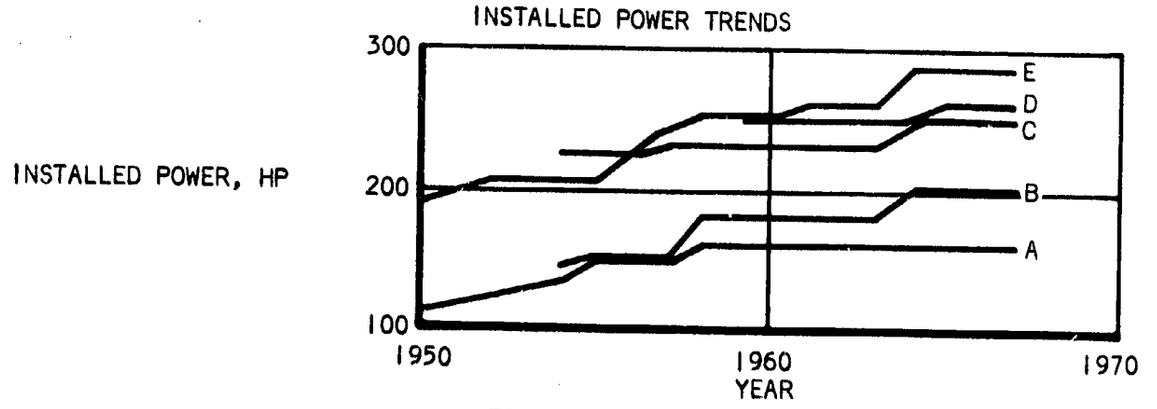


Figure 14

Figure 15 plots ratios of maximum speed (cubed) to installed power and is an approximate measure of aerodynamic efficiency. It is apparent that there has been no significant change in the ratio since the introduction of each airplane. The variations shown for some of the airplanes are not necessarily real, since cubing the speed makes it very sensitive to the accuracy of the data used.

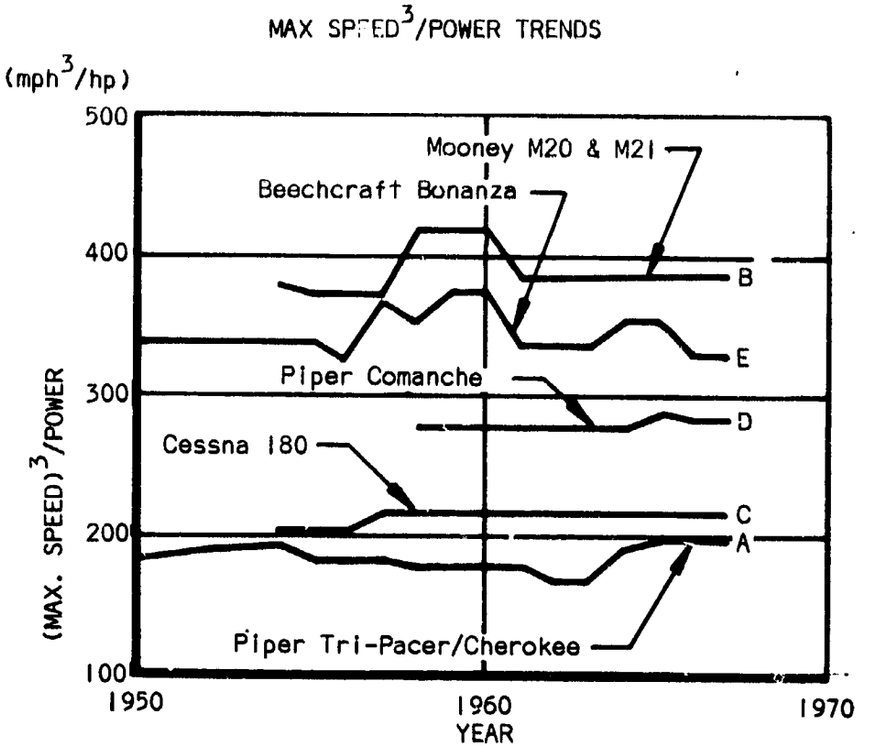


Figure 15

Figure 16 shows a general increase in maximum speed capability of the representative airplane, in response no doubt, to customer demand. Figure 17 shows this same general increase in landing speed, which is a direct result of increasing the airplane's maximum speed. The acquisition of efficient high cruise and maximum speed is accomplished in part at the expense of low-speed capability.

Aircraft Production. - Figure 18 illustrates the history of General Aviation production quantities since the end of World War II. It has been characterized by an initial high level of >15,000 aircraft shipped in 1947; to a low of 3,058 near the end of the Korean War; and back to the post World War II level of >15,000.

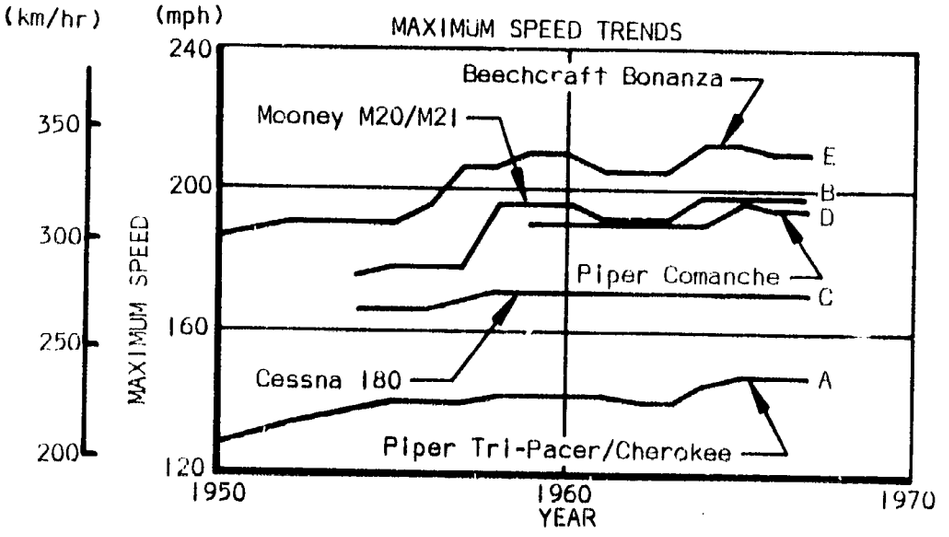


Figure 16

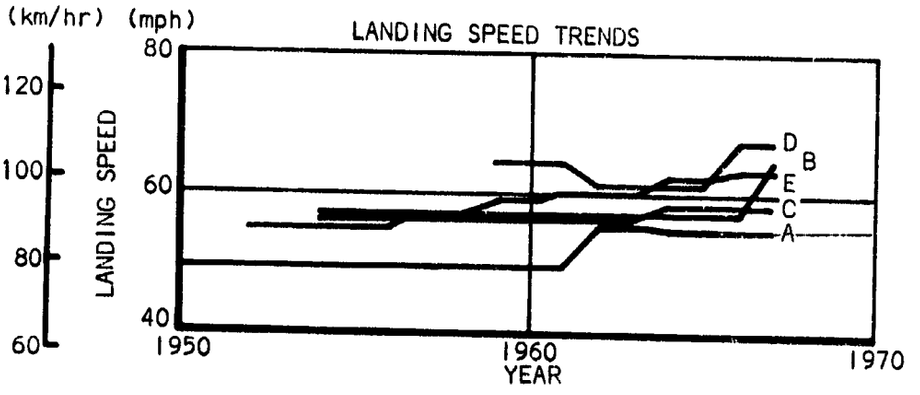


Figure 17

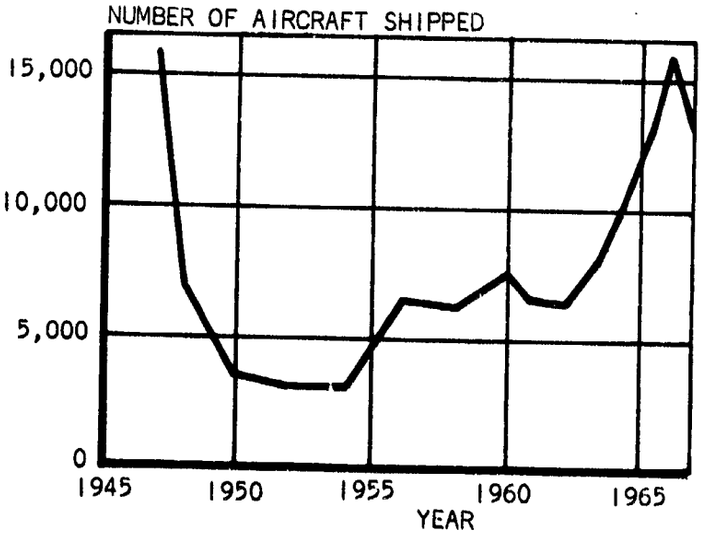


Figure 18

Design Considerations

Before the aircraft configuration was selected, several areas were investigated. I.e., the wing configuration in particular and, in general, crashworthiness and design-induced pilot error. These topics are discussed in the order listed:

Airplane weights
Wing configuration (including high-lift devices)
Helicopter weights
Crashworthiness
Design-induced pilot error

Airplane weights.- To estimate the empty and gross weights of the conceptual airplane, an analysis of seventeen contemporaty light airplanes was conducted. See Table III.

A weight breakdown of a typical contemporary light airplane, which approximates the contract guidelines, is illustrated in Figure 19.

TYPICAL CONTEMPORARY LIGHT AIRPLANE EMPTY WEIGHT BREAKDOWN

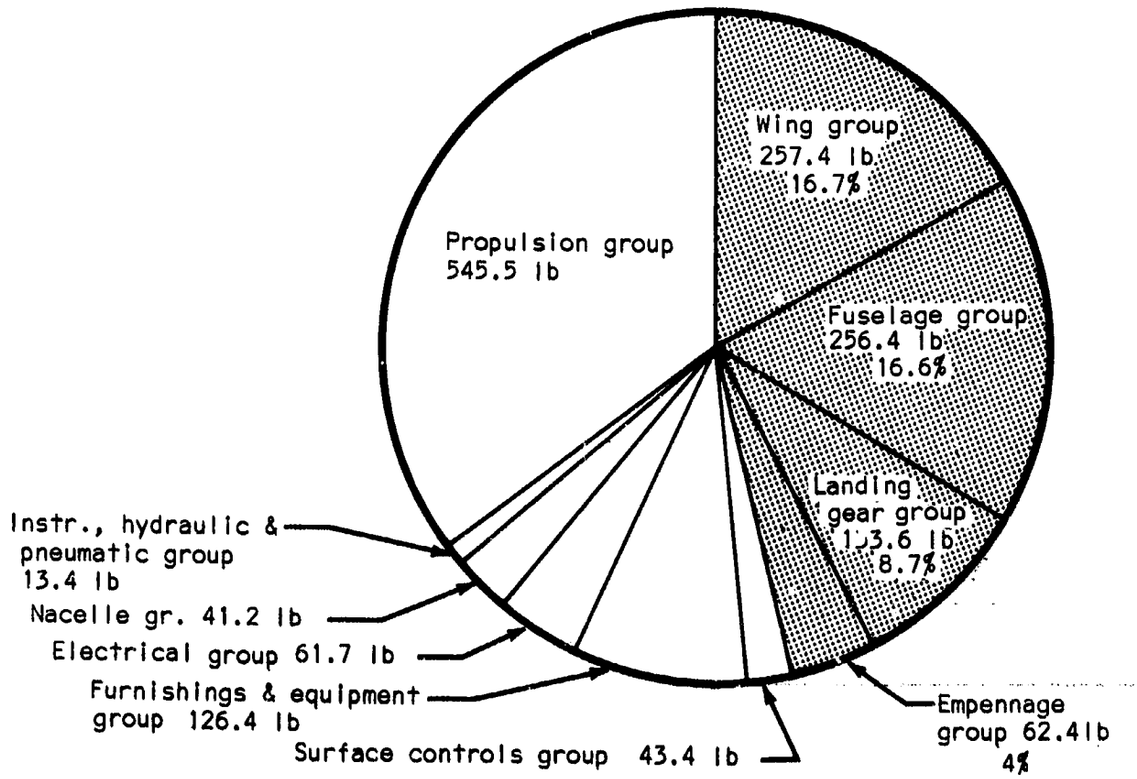


Figure 19

TABLE III - CONTEMPORARY AIRPLANE WEIGHT STATISTICS

DESIGNATION	W_{useful} (lb)	W_{gross} (lb)	$\frac{Wu}{Wg}$
Cessna 182	1,240	2,800	.443
Beech Musketeer	1,140	2,550	.447
Cessna 180	1,285	2,800	.459
Cessna Skylane	1,180	2,800	.421
Mooney Super 21	1,000	2,575	.389
Mooney Exec. 21	1,118	2,740	.408
Waco S220	1,100	2,753	.400
Found FBA-2C	1,300	3,000	.434
Bellanca 260C	1,200	3,050	.394
Waco TS250-4	1,078	2,753	.391
Piper Comanche B	1,372	3,100	.443
Cessna 210	1,435	3,300	.435
Beech Debonair C33	1,270	3,050	.416
Aero Comm. 200	1,060	3,000	.353
Navion H	1,350	3,315	.407
Beech Deb. C33A	1,450	3,300	.440
Beech Bonanza V35	1,485	3,400	.437
		17	7.117
		$\frac{Wu}{Wg}$ (avg) =	.419

Estimated Useful Load

Pilot and 3 passengers	680 lb	(per Appendix M)
Fuel (estimated)	360	
Oil (estimated)	23	
Baggage	200 lb	(per Appendix M)
Useful load =	1,263	

Estimated gross weight = $\frac{1,263}{0.419}$ = 3,020 lb

Estimated empty weight = 3,020-1,263 = 1,757 lb

The following more comprehensive weight analysis was conducted to determine the detail and group weight breakdown of the prospective light airplane.

Wing group: S_w x Unitary Wt. = 175 sq.ft. x 1.43 lb/sq.ft. = 250.0 lb

Empennage group: = 51.0 lb

(Horizontal tail) Calculate factor A: (reference 3 , Fig. 52)

$$A = \frac{G.W.(lbs) \times n_{ult} \times S_{ht}^2 \times AR_h}{S_w \times t/c_r \ (\%)}$$

Where: G.W. = 3,020 lbs (from previous page)
n_{ult} = 5.7 g
S_{ht} = 36 sq.ft. (est.)
AR_h = 4 (est.)
S_w = 175 sq.ft. (est.)
t/c_r = 9% (est.)

Then:

$$A = \frac{3,020 \times 5.7 \times 36^2 \times 4}{175 \times 9} = 56,600$$

at A = 56,600, W_{ht} = 36 lb

(Vertical tail) The weight of the vertical tail is estimated based on the horizonatal tail weight previously found.

W_{ht} = 36 lb
S_{ht} = 36 sq.ft.
Unitary weight = 1 lb/sq.ft.
S_{vt} = 15 sq.ft.
W_{vt} = 15 sq.ft. x 1 lb/sq.ft. = 15 lb

Fuselage group: (ref.3 - Fig.51 - extrapolated) = 300.0 lb

Landing gear group: = 166.0 lb

The weight of the landing gear is estimated as being 5.5% of the gross weight. (ref.3 - page 64)

$$3,020 \times \frac{5.5}{100} = 166 \text{ lb}$$

Assume 70% of this weight for the main gear and 30% for the nose gear. Then:

Main gear = $\frac{70}{0}$ x 166 = 116.2 lb

Nose gear = $\frac{30}{100} \times 166$ = 49.8 lb

Surface controls group:			= 35.5 lb
Nacelle group:			= 41.0 lb
Cowl assy.	= 25.0 lb		
Engine Mount assy	= 16.0 lb		
Propulsion group:			= 513.6 lb
Basic engine	= 380.0 (per appendix M)		
Air induction system	= 4.0 lb		
Exhaust system	= 16.0 lb		
Cooling system	= 5.0 lb		
Fuel system	= 19.0 lb		
Oil-cooler	= 5.5 lb		
Engine controls	= 3.1 lb		
Starting system	= 17.0 lb		
Propeller installation	= 64.0 lb		
Instruments and navigational equip. group:			= 14.8 lb
Navigational Equip.:	= 0.6 lb		
Compass	= 0.6 lb		
Instruments			
Gauge panel (incl. oil temp. & pressure and fuel quantity gauges	= 1.5 lb		
Fuel quan. transmitters	= 0.6 lb		
Airspeed indicator	= 0.8 lb		
Pitot system	= 1.0 lb		
Tachometer and Drive	= 1.7 lb		
Altimeter, sensitive	= 1.4 lb		
Stall warning horn and actuator	= 0.6 lb		
Manifold pressure gauge & system	= 1.2 lb		
Cylinder head temp. gauge and system	= 0.8 lb		
Position indicator-wing flap	= 0.4 lb		
Clock	= 0.4 lb		
Rate of climb	= 1.0 lb		
Turn and bank-elec.	= 2.2 lb		
Hydraulic an pneumatic group:			= 3.3 lb
Brake system	= 3.3 lb		
Electrical group			= 61.7 lb
Power supply equip.			
Generator	= 16.2 lb		
Battery	= 28.0 lb		
Battery box & mount	= 2.5 lb		

Power disdribution and control	=	12.3 lb
Starter contactor	=	1.1 lb
Battery contactor	=	1.1 lb
Battery cables	=	3.9 lb
Generator regulator	=	1.7 lb
Switches, rheostats and circuit breakers	=	1.5 lb
Wiring	=	3.0 lb
Lights		
Navigation	=	0.4 lb
Panel and cabin	=	0.3 lb
Dome	=	0.4 lb
Landing	=	2.4 lb

Furnishings and equipment group: = 120.0 lb

Air conditioning and anti-icing equipment group: = 6.0 lb

Total - Airplane (empty and dry) = 1,562.7 lb

Gross = Empty + Useful = 1562.7 + 1263 = 2,825.7 lb

Wing configuration.- Analysis of the wing was broken-down into four separate analyses ~~which are discussed in the fol~~lowing order:

Planform
Cantilevered
Strut-braced
Area vs high-lift device

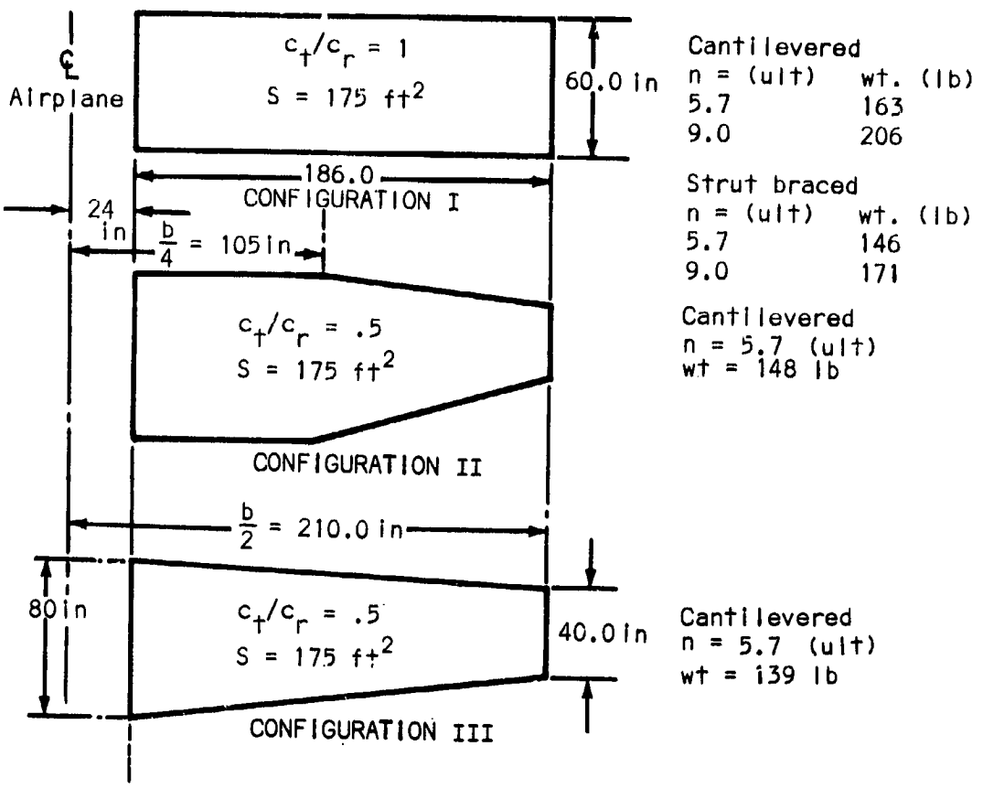
Planform: Three wing planforms were investigated; i.e., rectangular, rectangular/taper and tapered. See Figure 20.

A rectangular planform was analyzed to determine the weight increase of a 9 g wing over a 5.7 g design ultimate load factor wing, for both cantilevered and strut-braced wings.

All three wings were assumed to have a single spar at 35% of chord and a closing channel at 75% chord. The span, area, and airfoil were assumed the same for each configuration. The primary structural components investigated were the spar caps, spar web, and torque box skins. This analysis demonstrated that the tapered wing planform could be designed lighter than the other configurations.

Cantilevered: Analysis of cantilevered wings considered rectangular wings at 5.7 and 9 g's; a rectangular taper wing and a tapered wing at only 5.7 g's.

WING CONFIGURATIONS



NOTE: Weights include Spar Caps, Spar Webs, Skins, and Struts if applicable.

Figure 20

These analyses are further sub-divided into the following categories:

Design loads
Member sizing
Weights

(Design loads) Design maneuvering wing load is as follows:

$$n_1 \frac{W}{S} = 3.8 \frac{(3020)}{175} = 65.5 \text{ psf.}$$

where: Limit n_1 = 3.8 g
W = 3020 lb
S = 175 ft²

The following trade-off calculations are based on the preliminary gross weight estimate, W = 3020 lb on page 29.

Minimum design airspeeds and limit flight load factors are listed in the two tables below:

(based on ref. 4, Appendix A, Fig. 3 and Table I)

Flap speed	V_F = 102 mph
Maneuver speed	V_A = 140 mph
Cruise speed	V_C = 160 mph
Dive speed	V_D = 222 mph

Item		Normal Category
Flaps up	n_1	3.8
	n_2	- 1.9
	n_3	3.8
	n_4	- 1.9
Flaps down	n_{flap}	1.9
	n_{flap}	0

Two V-n diagrams, where S = 175 ft^2 and W = 3020 lbs, were developed. C_N values were calculated based on data from ref. 6 for the NACA 63_2215 airfoil. For the positive maneuver envelope to n = 3.8, and C_N = 1.408. See Figure 28.

$$n = C_N \frac{\rho S V^2}{2W} = \frac{1.408\ (.00512)(175)\ V^2}{2\ (3020)} = .000209\ V^2$$, See Figure 21

For the negative maneuver envelope to n =-1.9g, and C_N =-1.138: $n = -.000169V^2$

V-n DIAGRAM, 3.8 g

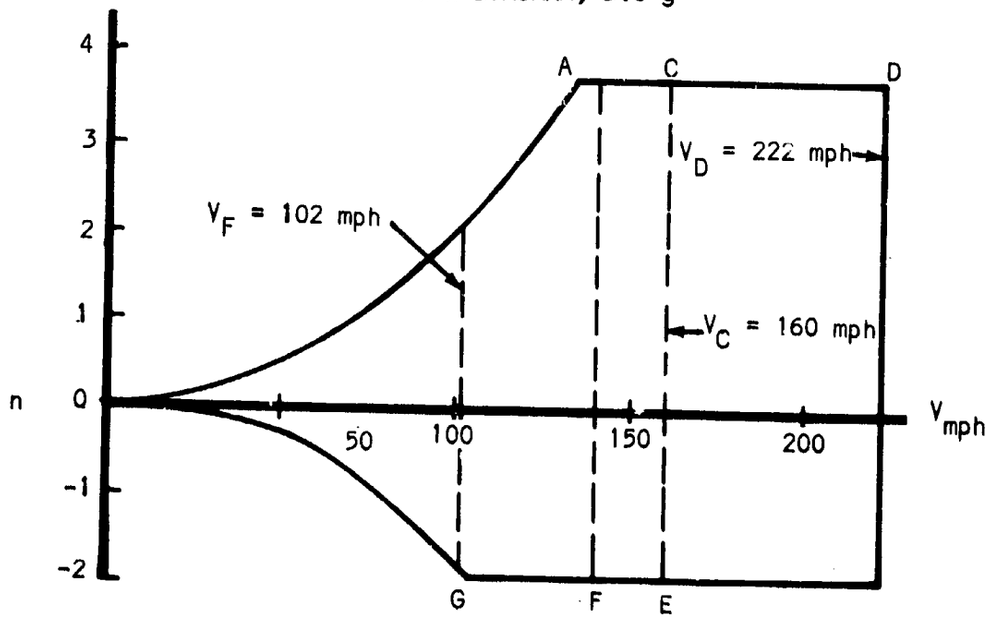


Figure 21

The V-n diagram for a 6 g limit load factor was developed by maintaining the normal category design airspeeds. The equations on page 34 were used along with a 6 g cutoff to construct the V-n Diagram in Figure 22

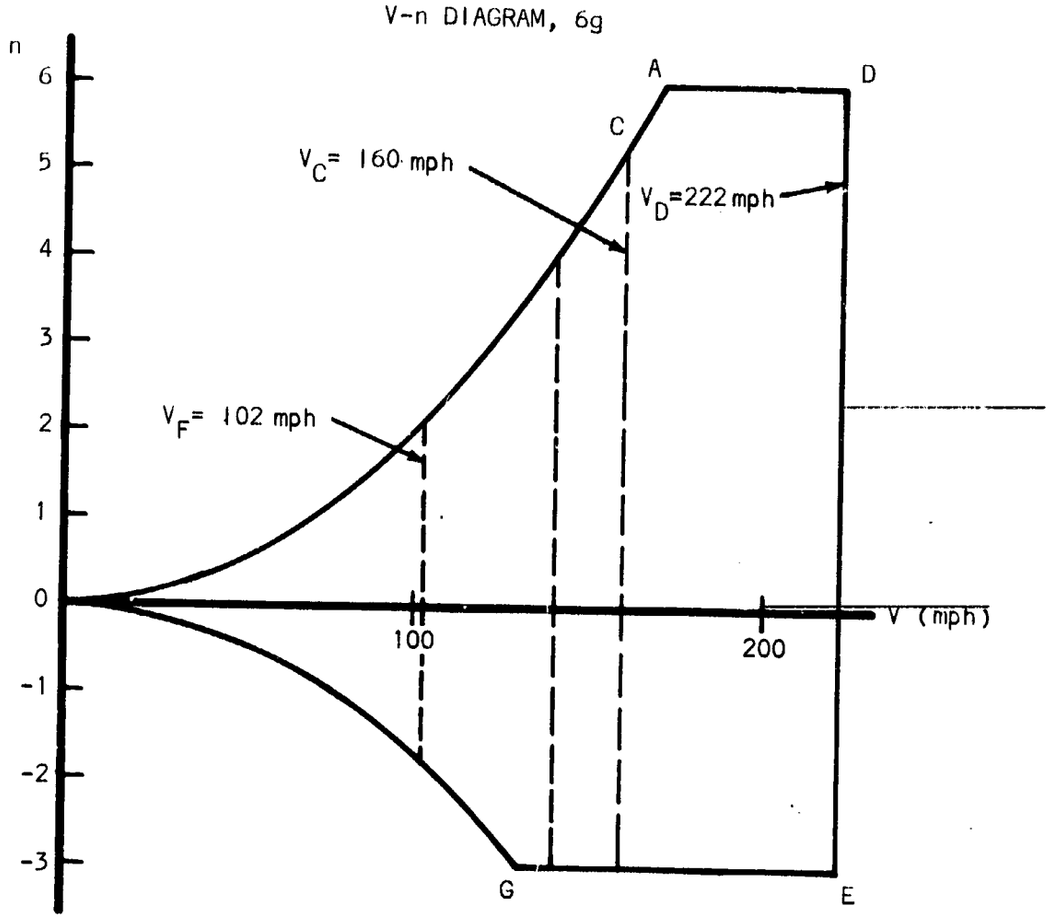


Figure 22

On the following page in Figure 23, are the equations and diagrams used for determining:

(1) running load
(2) shear
(3) moment

Figure 24 plots the length of the wing chord versus wing station Y.

EQUATIONS AND DIAGRAMS FOR RUNNING LOAD, SHEAR, AND MOMENT

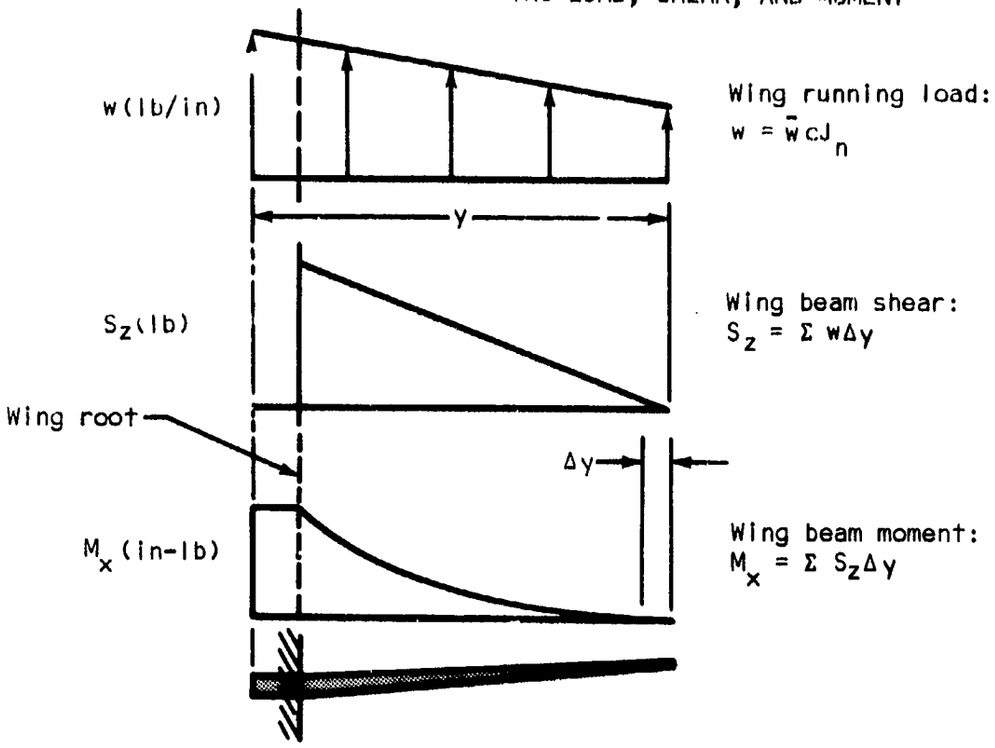


Figure 23

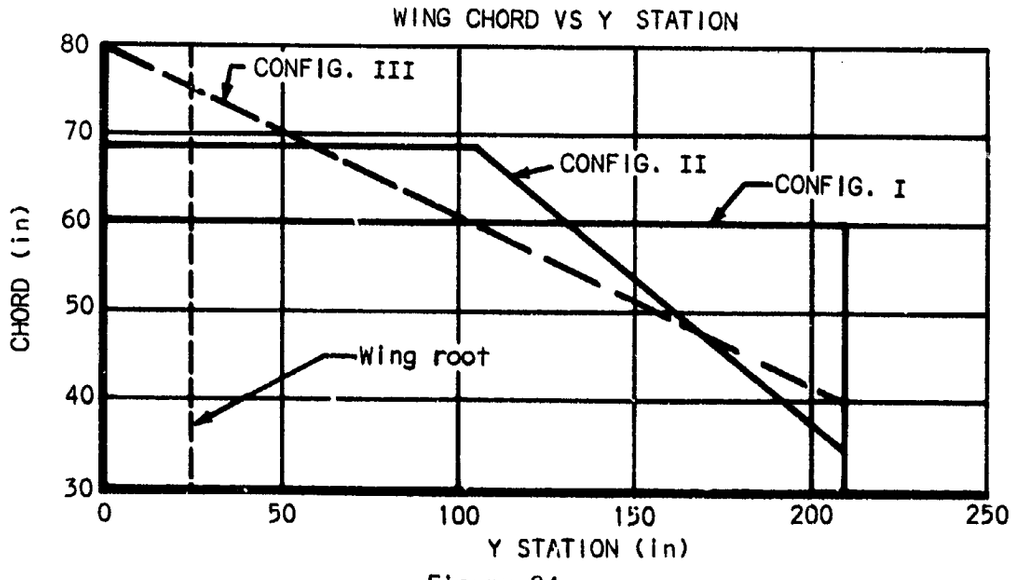


Figure 24

The average wing load and relief factor were determined as follows:

Average wing load $\bar{w} = \frac{W}{S}$

$$\bar{w} = \frac{3,020}{175} = 17.25 \text{ psf}$$

$$\text{Limit } \bar{w} = n_1 \frac{W}{S} = 3.8\ (17.25) = 65.5 \text{ psf} \quad (\text{limit } n_1 = +3.8 \text{ g})$$

$$\text{Ultimate } \bar{w} = 65.5 \times 1.5 = 98.3 \text{ psf}$$

Assuming that the inertia distribution is similar to the airloading, the inertia relief factor $J_n = \frac{W - W_W}{W}$, where: W = aircraft gross weight = 3020 lb
W_W = wing weight = 308 lb

$$J_n = \frac{3020-308}{3020} = .90$$

Based on the above, the design ultimate shears and design ultimate moments are plotted in Figures 25 and 26

ULTIMATE SHEAR VERSUS WING STATION

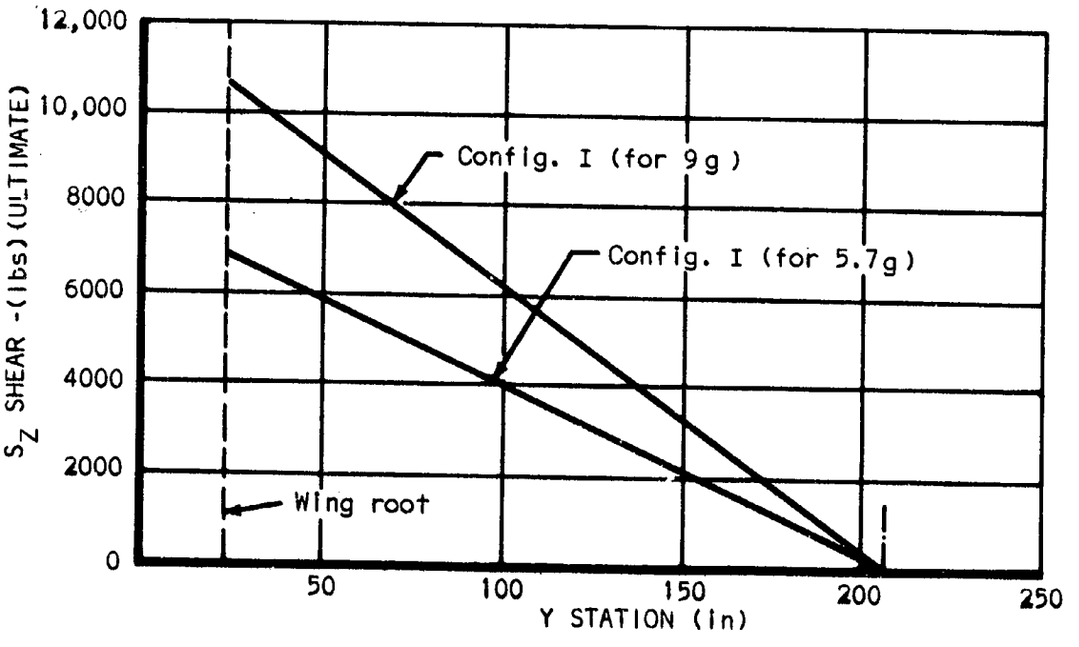


Figure 25

ULTIMATE BENDING MOMENT VERSUS WING STATION

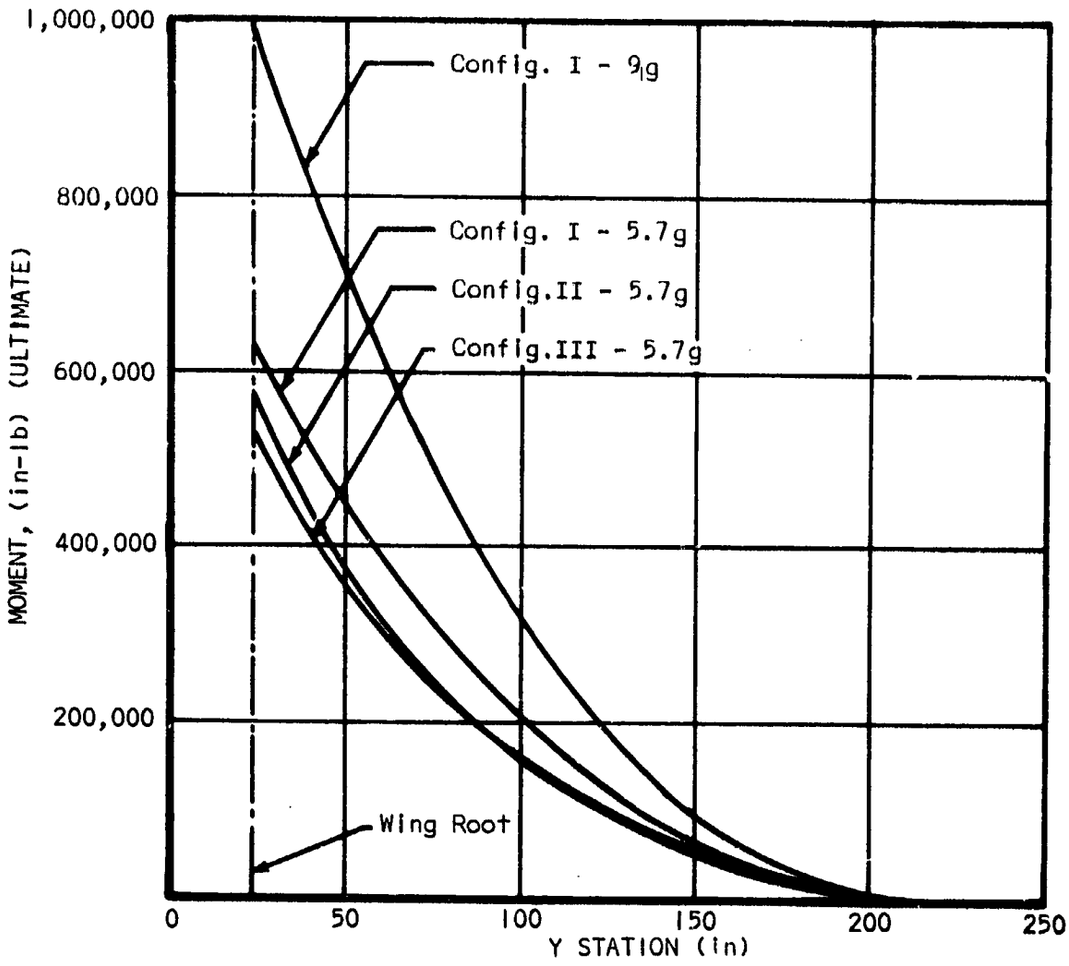


Figure 26

Wing aerodynamic center and elastic axis coordinates at the wing/fuselage intersection are listed in the following table.

Operation	Wing Config. I	II	III
c	60	68.57	75.425
$x_{a.c.} = .267c$	16	18.3	20.1
$y_{a.c.} = .020c$	1.20	1.37	1.51
$x_{e.a.}$ = scaled	21.0	24.0	26.4
$y_{e.a.}$ = scaled	.6	.6857	.754

Translation of airloads from a.c. (aerodynamic center) to e.a. (elastic axis). Inertia loads are assumed negligible for affecting torque and are omitted.

WING SECTION AIRLOAD COMPONENTS

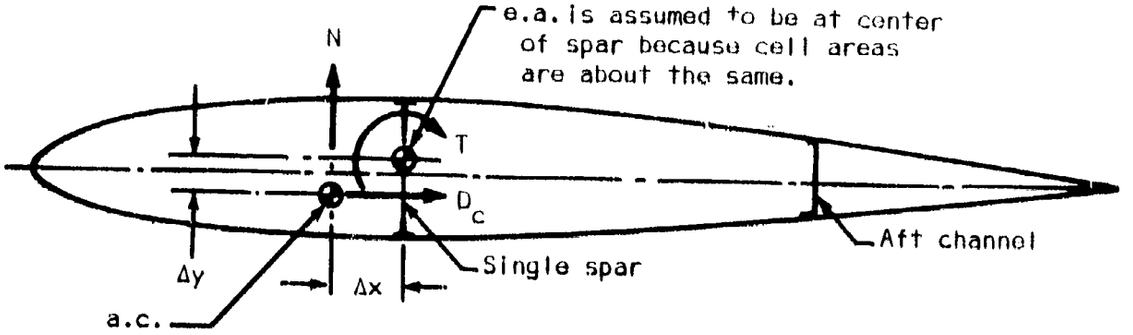


Figure 27

Where $S_w = 175\ ft^2$,

$$N = C_N \left(\frac{1}{2}\rho\frac{S}{2}\right) V^2 = C_N\,(0.00256)\left(\frac{175}{2}\right) V^2 = C_N\,(.224)\,V^2$$

$$D_c = C_c \left(\frac{1}{2}\rho\frac{S}{2}\right) V^2 = C_c\,(0.224)\,V^2$$

$$T = C_T \left(\frac{1}{2}\rho\frac{S}{2}\right) V^2 = C_T\,(0.224)\,V^2$$

$$C_T = c\,C_{m_{a.c.}} + \Delta x C_N - \Delta y C_c$$

$\Delta x = x_{e.a.} - x_{a.c.}$

$\Delta y = y_{e.a.} - y_{a.c.}$

where:

$n = 3.8$

$W = 3020$ lb

$S = 175\ ft^2$

$$C_N = \frac{n(W/S)}{\rho/2\,V^2} = \frac{25{,}600}{V^2} \qquad \text{for } n = -1.9\ , \quad C_N = \frac{-12{,}800}{V^2}$$

WING SECTION FORCE COEFFICIENTS

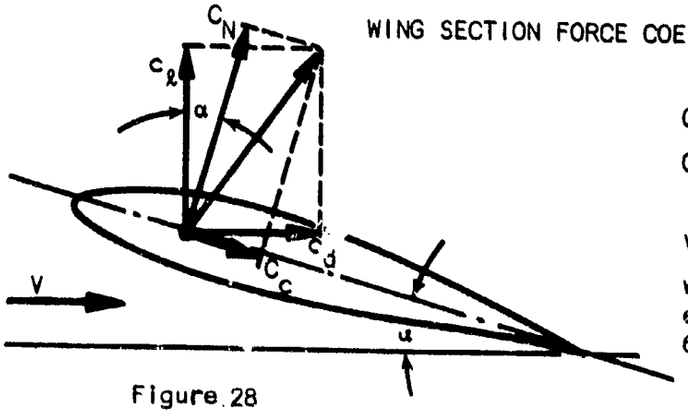


Figure 28

$C_N = c_\ell \cos\alpha + c_d \sin\alpha$

$C_c = c_d \cos\alpha - c_\ell \sin\alpha$

Values of c_ℓ and c_d were obtained from reference 6, for the NACA 63_2215 airfoil.

Airload Coordinates From Aerodynamic Center To Elastic Axis			
Operation	Wing Configuration		
	I	II	III
c	60	68.57	75.43
$C_{m_{a.c.}}$	-.03	-.03	-.03
$c\ C_{m_{a.c.}}$	-1.80	-2.06	-2.26
$\Delta x = x_{e.a.} - x_{a.c.}$	5	5.7	6.3
$\Delta y = y_{e.a.} + y_{a.c.}$	1.8	2.06	2.26

Wing torques at 3.8 and -1.9 g's, at the wing/fuselage intersection, about the elastic axis, are tabulated in Table IV.

Table TABLE IV - WING CONFIGURATION I (for n = +3.8 and -1.9g)

n	3.8			-1.9		
V-n diagram points	A	C	D	E	F	G
① V	134	160	222	222	160	102
② V^2	17950	25600	49300	49300	25600	10400
③ C_N ref.Figure 28	1.43	1.00	.52	-.26	-.50	-1.23
④ Δx ref.Figure 27	5	5	5	5	5	5
⑤ $\Delta x\ C_N$	7.15	5.0	2.60	-1.50	-2.5	-6.15
⑥ C_c ref.Figure 28	-.248	-.116	-.02	-.005	-.04	-.235
⑦ Δy ref.Figure 27	1.8	1.8	1.8	1.8	1.8	1.8
⑧ $\Delta y\ C_c$	-.446	-.209	-.036	-.009	-.072	-.423
⑨ $c\ C_{m_{c.g.}}$	-1.80	-1.80	-1.80	-1.80	-1.80	-1.80
⑩ $C_T = ⑤ - ⑧ + ⑨$	5.796	3.41	.84	-3.29	-4.23	-7.53
⑪ $.224\ V^2$	4030	5750	11050	11050	5750	2330
⑫ $N = C_N\ (.224)\ V^2$	5760	5750	5750	-2875	-2875	-2870
⑬ $D_c = C_c (.224)\ V^2$	-1000	-668	-221	-55	-230	-548
⑭ $T_{limit} = C_T (.224) V^2$	23400	19600	9300	-36400	-24300	-17500

Wing torsional shear flow @ wing-fuselage intersection ∿ Cond. E critical:

$A = 317.36\ in^2$ total Double cell as calc. from full size layout

$$\text{Ult. } q_t = \frac{T}{2A} = \frac{1.5\ (-36,400)}{2\ (317.36)} = 86.2\ \text{lb/in.}$$

The normal coefficient for load factors of + 6g and - 3g is as follows:

(for n = 6.0) $C_N = \frac{n(W/S)}{\rho/2\ V^2} = \frac{40,400}{V^2}$

(for n = -3.0) $C_N = \frac{-20,200}{V^2}$

where $\begin{cases} W = 3020 \text{ lb} \\ S = 175 \text{ ft}^2 \end{cases}$

TABLE V - WING CONFIGURATION I (for n = + 6 g to - 3 g)

n		6	5.4	6	-3.0		
V-n diag. pts.		A	C	D	E	F	G
①	V	169	160	222	222	160	130
②	V^2	28600	25600	49300	49300	25600	16900
③	C_N ref. Figure 28	1.42	1.42	.82	-.41	-.79	-1.14
④	Δx ref. Figure 27	5	5	5	5	5	5
⑤	$\Delta x C_n$	7.10	7.10	4.10	-2.05	-3.95	-5.70
⑥	C_c ref. Figure 28	-.248	-.248	-.069	-.025	-.098	-.205
⑦	Δy ref. Figure 27	1.8	1.8	1.8	1.8	1.8	1.8
⑧	$\Delta y C_c$	-.446	-.446	-.124	-.045	-.178	-.369
⑨	$c\ C_{m_{a.c.}}$	-1.8	-1.8	-1.8	-1.8	-1.8	-1.8
⑩	$C_T = ⑤ - ⑧ + ⑨$	5.746	5.746	2.424	-3.85	-5.57	-7.13
⑪	$.224\ V^2$	6410	5740	11050	11050	5740	3790
⑫	$N = C_N\ (.224)\ V^2$	9100	8150	9060	-4530	-4530	-4320
⑬	$D_c = C\ (.224)\ V^2$	-1590	-1425	-763	-276	-563	-777
⑭	$T_{lim} = C_T(.224)\ V^2$	36800	33000	26800	-42600	-32000	-27000

Wing torsional shear flow @ wing-fuselage intersection ∿ Cond. E. Critical

$A = 317.36\ in^2$ Double cell

Ult. $q_t = \frac{1.5T}{2A} = \frac{1.5\ (-42\ 600)}{2\ (317.36)} = -100.8$ lb/in

The wing torsional shear flow at wing-fuselage intersection (condition E critical) for configuration II and III is as follows:

Assume: $A = \left(\frac{c_{conf.}}{c_I}\right)^2 A_I$, and $T = \left(\frac{c_{conf.}}{c_I}\right) T_I$

Therefore: $q_t = \frac{(c_{conf.}/c_I)\, T_I}{2(c_{conf.}/c_I)^2 A_I} = \left(\frac{c_I}{c_{conf}}\right)\left(q_{t_I}\right)$

For configuration II, $q_t = \left(\frac{60}{68.57}\right)(-86) = -75.3$ lb/in

For configuration III, $q_t = \left(\frac{60}{80}\right)(-86) = -64.5$ lb/in

Design ultimate torque: Figure 29, below, plots the design ultimate torque versus wing station. It is based on the general equations and data presented thus far.

DESIGN ULTIMATE WING TORQUE VERSUS WING STATION

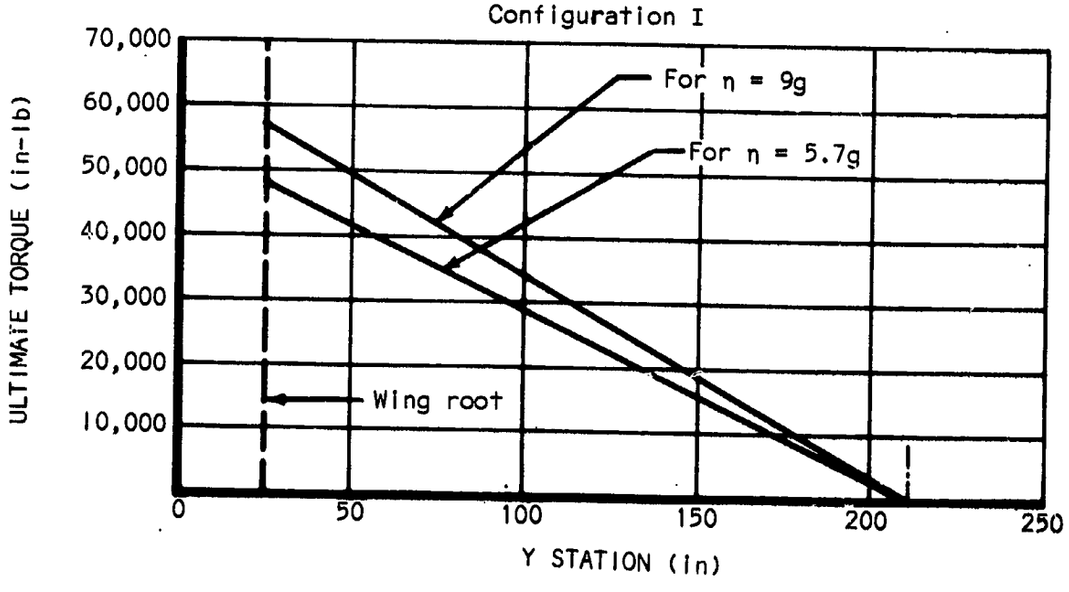


Figure 29

Axial load due to chordwise bending:

CAP LOADS DUE TO CHORDWISE BENDING

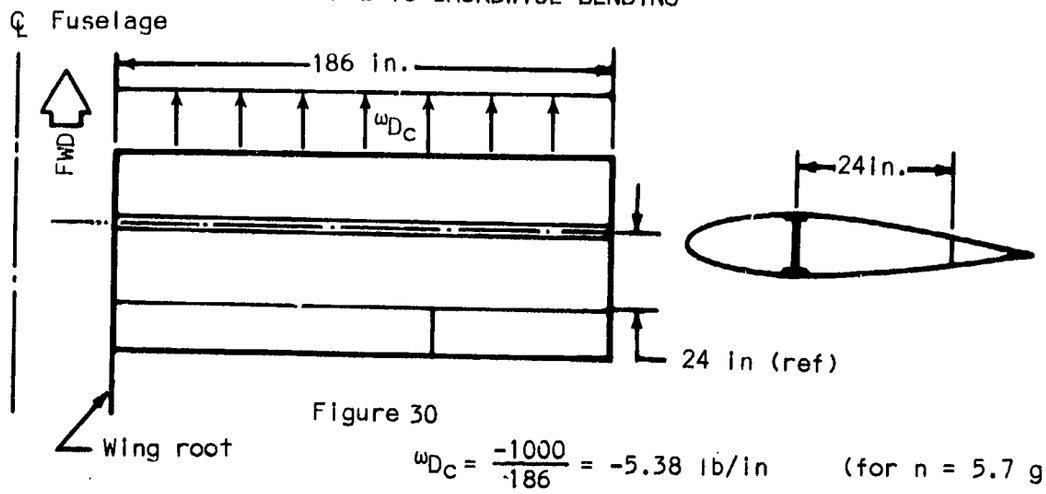


Figure 30

$$\omega_{D_C} = \frac{-1000}{186} = -5.38 \text{ lb/in} \qquad \text{(for n = 5.7 g)}$$

$$\omega_{D_C} = \frac{-1590}{186} = -8.55 \text{ lb/in} \qquad \text{(for n = 9 g)}$$

The axial loads due to chordwise bending (compression in spar and tension in aft closing member) versus wing station have been calculated and are plotted in Figures 31 and 32, for n = 5.7 g and 9 g, respectively.

AXIAL LOAD DIAGRAM (n = 5.7g)
(DUE TO CHORDWISE BENDING)

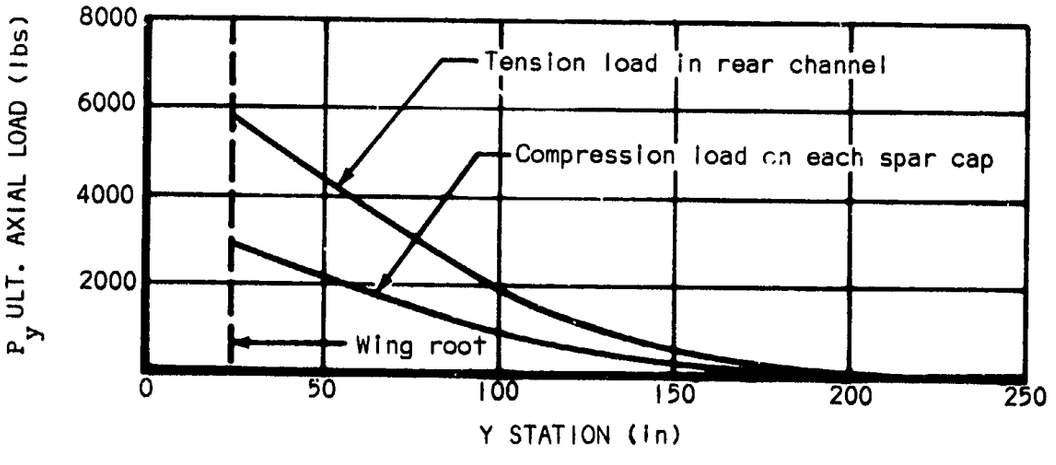


Figure 31

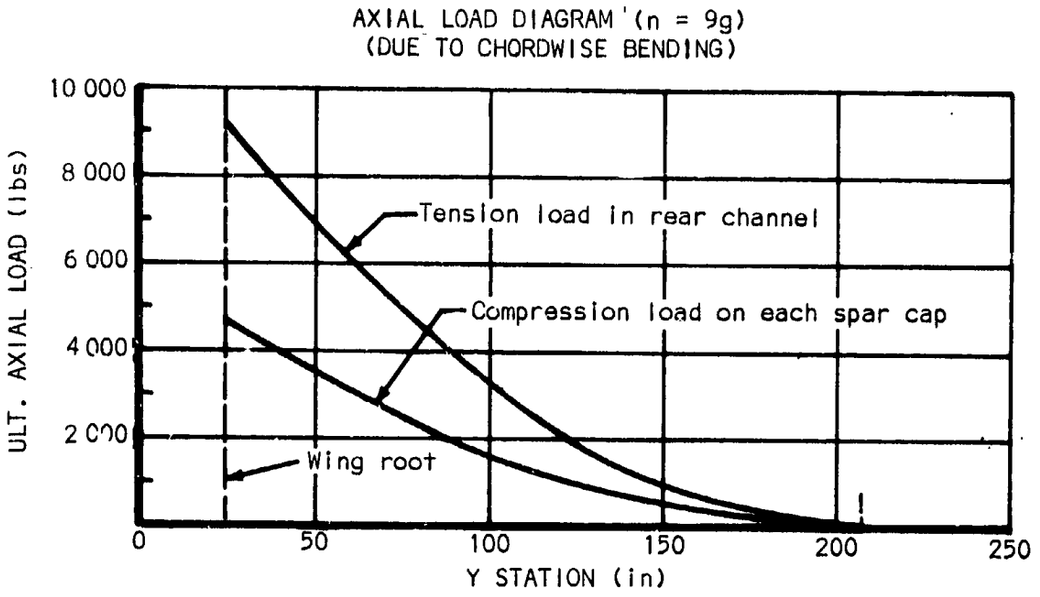


Figure 32

(Determination of member sizes). The spar caps are assumed to be made from 2024-T4 aluminum extrusion, material specification QQ-A-200/3. Material allowables per reference 7 are:

$$F_{tu} = 57 \text{ ksi}, \quad F_{cy} = 38 \text{ ksi}, \quad F_{ty} = 42 \text{ ksi}, \quad F_s = 30 \text{ ksi}$$

Spar cap thickness general equations are:

$$f = \frac{P}{A} = \frac{M_x/h_e}{b\,t} \pm \frac{P_y}{bt}$$

solving for "t":

$$t = \frac{1}{fb}\left(\frac{M_x}{h_e} \pm P_y\right)$$

let $f = F_{tu}$ or F_{ty}

$h_e = .9\,h$

SPAR CAP GEOMETRY

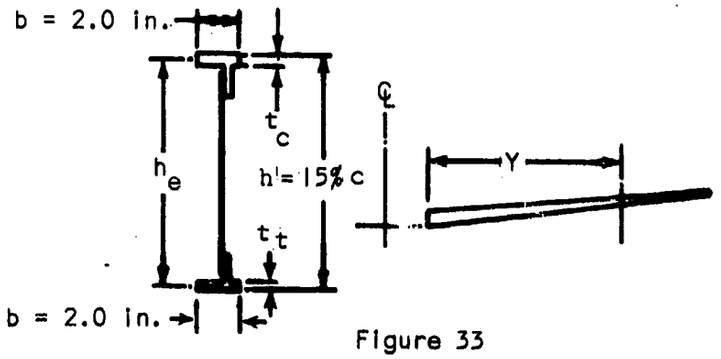


Figure 33

Applying the general equations and Figures 26 and 31, the theoretical thickness curves were computed and plotted in Figures 34, 35, and 36. For practical purposes the spar caps were considered to be linearly tapered or constant section over their length.

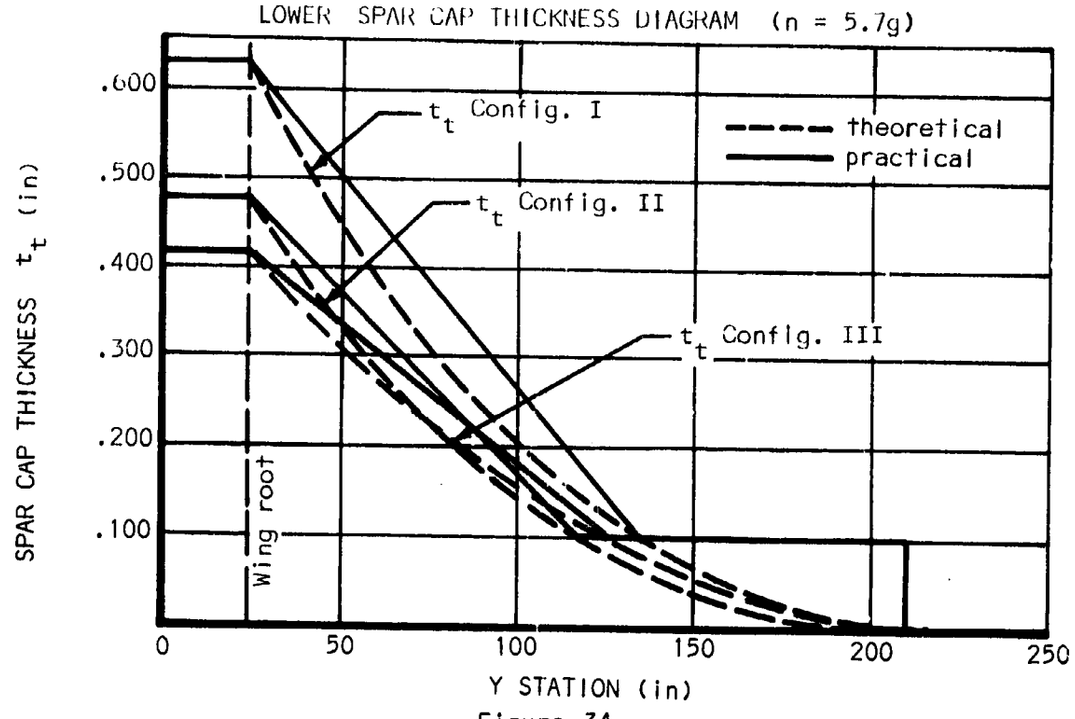


Figure 34

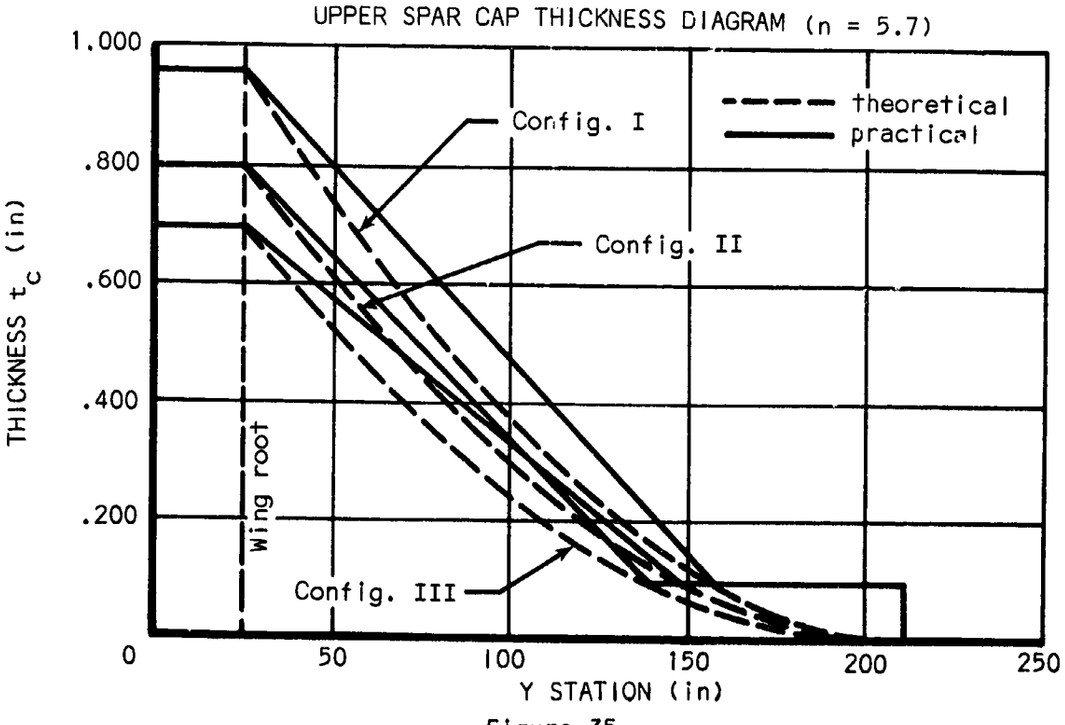


Figure 35

SPAR CAP THICKNESS DIAGRAM (n = 9g)

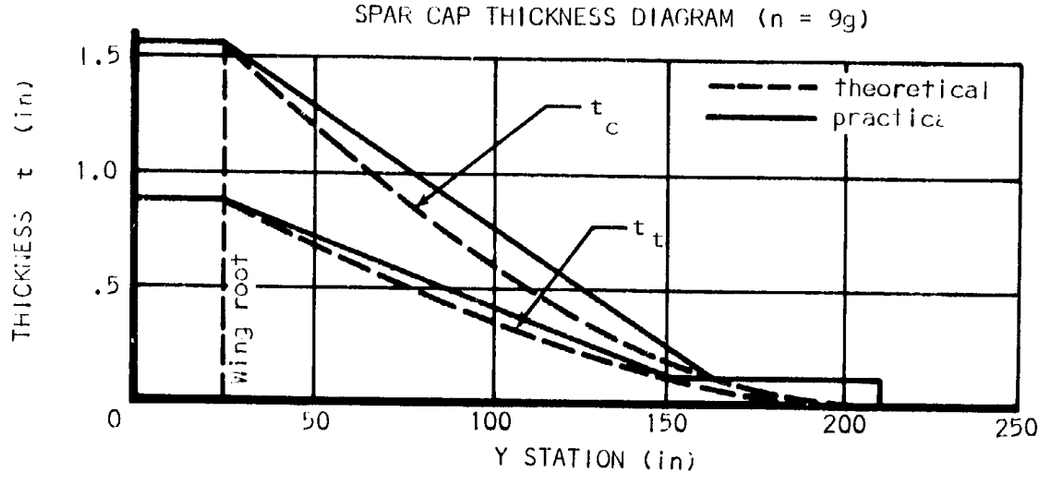


Figure 36

SPAR WEB GEOMETRY

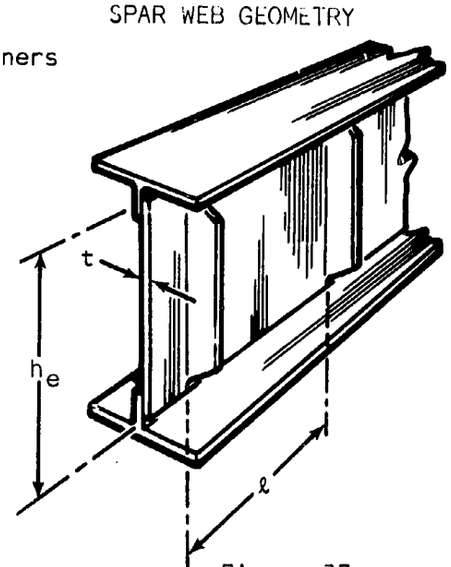


Figure 37

Spar web sizing: The spar web will have stiffeners as shown in Figure 37.

The panel dimensions are:

h_e = 8.1 in $\quad \frac{h_e}{\ell} = 1.35$

ℓ = 6.0 in

The spar web thicknessess were determined with the following equations:

$$F_s = .8F_{s_u} = .8 \times 30000 = 24000 \text{ psi}$$

$$\tau_{s_{cr}} = \frac{K_s E_c t^2}{b^2}, \text{ were } K_s = 4.8,$$

(simple supported, four sides)

$$\left.\begin{aligned} q_{all} &= 5\,\tau_{s_{cr}}\, t \\ q_{all} &= F_s\, t \end{aligned}\right\} \text{ whichever is smaller,}$$

$$q = \frac{V}{h_e}$$

For Configuration I:

(n=5.7); $\quad q = \frac{7330}{8.1} = 905$ lb/in

(n=9.0); $\quad q = \frac{12047}{8.1} = 1490$ lb/in

TABLE VI - SPAR WEB SHEAR ALLOWABLES

t	.032	.040	.050	.063
F_s	24000	24000	24000	24000
$\tau_{s_{cr}}$	2000	3100	5200	8400
$5\tau_{s_{cr}}$	10000	15500	26000	42000
q_{all}	320	620	1200	1512

CONFIGURATION I - SPAR WEB SHEAR FLOW DIAGRAM

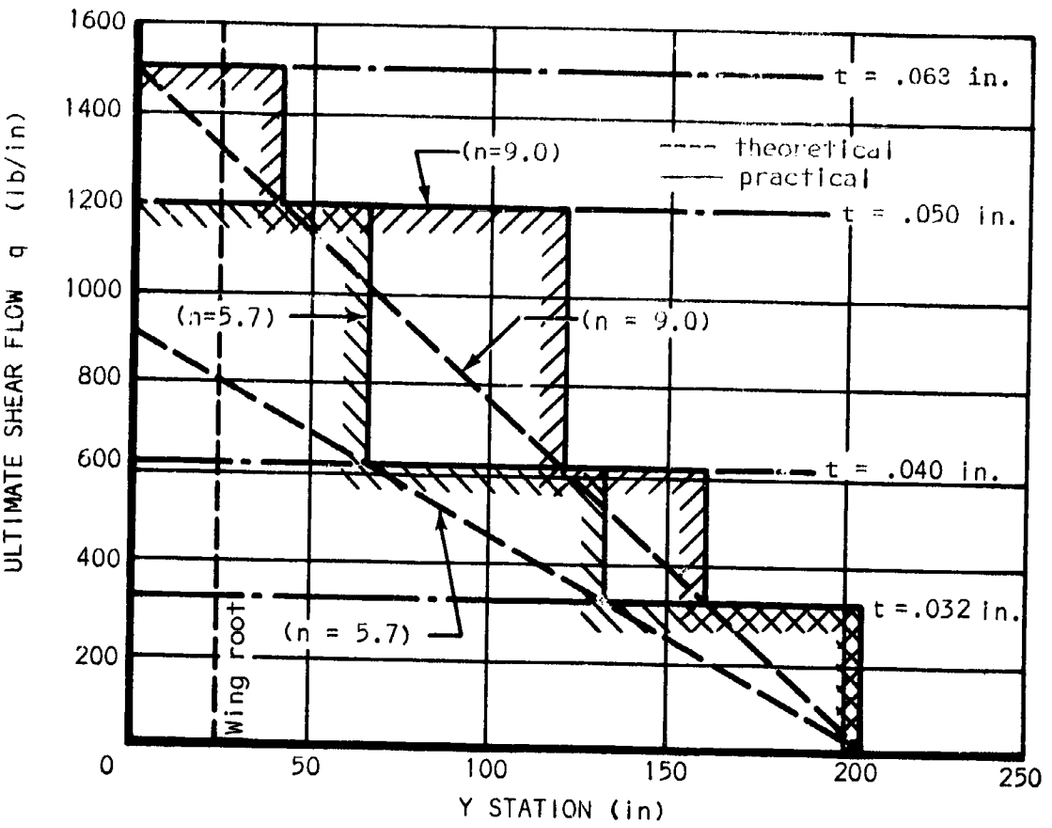


Figure 38

Wing skin sizing: The wing skins were critical for tension field permanent buckling at ultimate load. The proper skin gages for each wing configuration were determined by superimposing the allowable permanent shear buckling curves on the shear flow diagrams for each configuration (Figure 39).

The ultimate shear flow at the wing root was first plotted for each configuration, using values from pages 40, 41 and 42. A straight line function was assumed to complete the shape of each diagram.

The permanent shear buckling allowables were obtained from Reference 19, page C11.54. They are a function of the following:

F_{cy} = 38.000 psi

E_c = 10×10^6 psi

τ_{cr} = Obtained in similar manner as the values for the spar shear web (Ref. page 46).

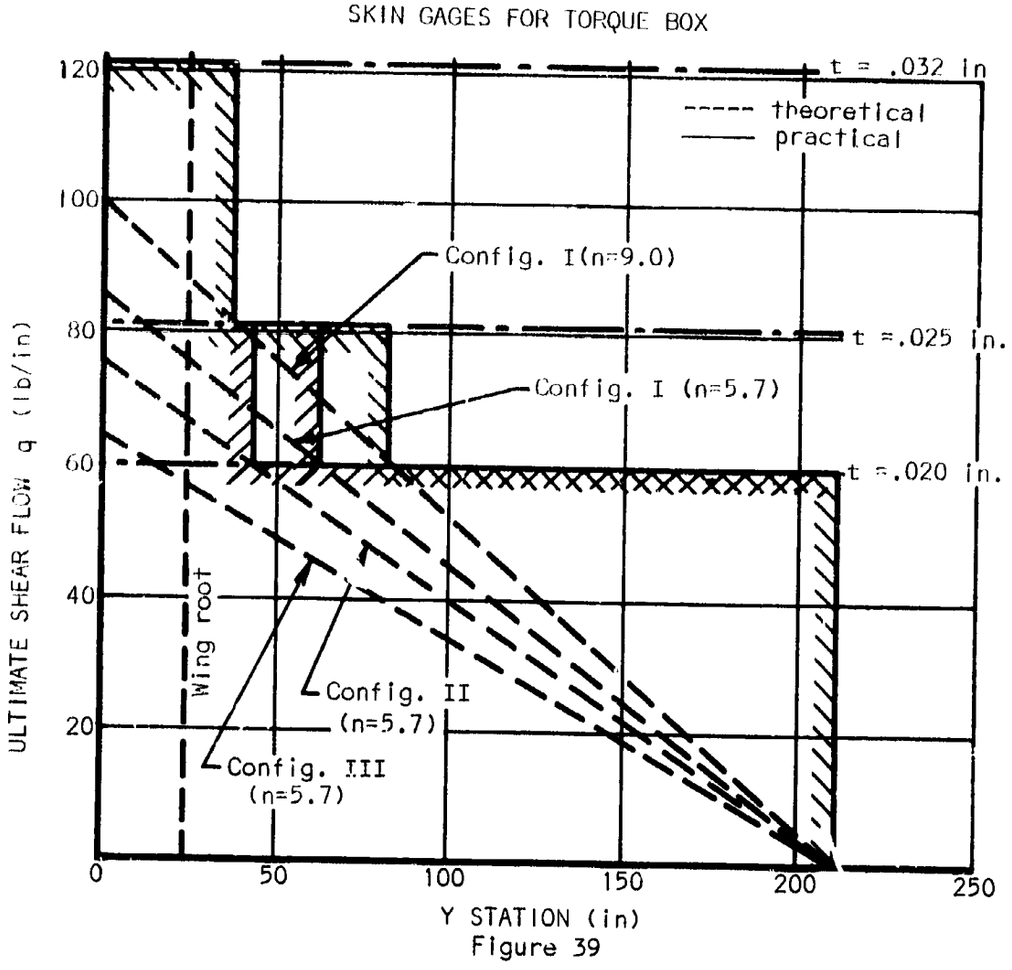


Figure 39

(Determination of weights). Spar cap weights are calculated on the basis of the thicknesses presented in Figure 34, 35 & 36 using the density of aluminum as .100 lbs/cu.in. These weights are listed in Table VII.

(Spar web and wing skins) Similarly, the spar web and wing skin weights calculations are based on Figures 38 and 39, respectively. These weights are also included in Table VII at the end of this section on wing configurations.

Strut braced: The following analysis is for wing Configuration I with single external strut brace and applied ultimate load factors of n=5.7 and n=9.0. This analysis is subdivided into the following categories:

Design loads
Member sizing
Weights

Figure 40 illustrates the basic geometry used in determining loads:

SINGLE SPAR METAL COVERED WING WITH SINGLE EXTERNAL STRUT BRACE

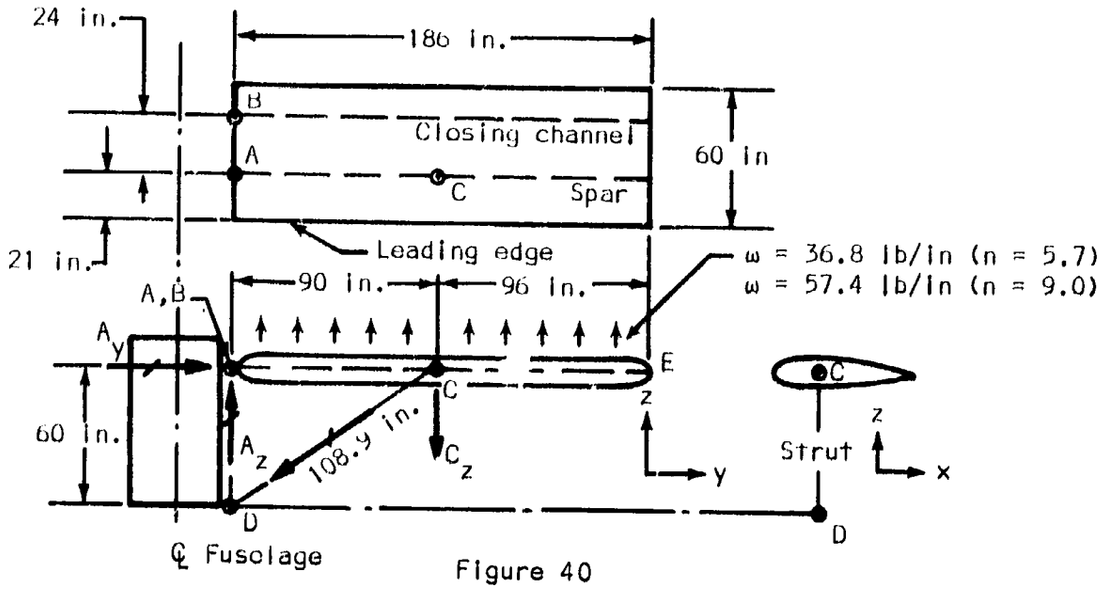


Figure 40

Using conventional stress analysis equations, shear, bending and axial loads were determined, including the effect of chordwise bending due to drag loads. Figure 41 shows the wing spar shear diagrams and Figure 42 shows the spar bending moments.

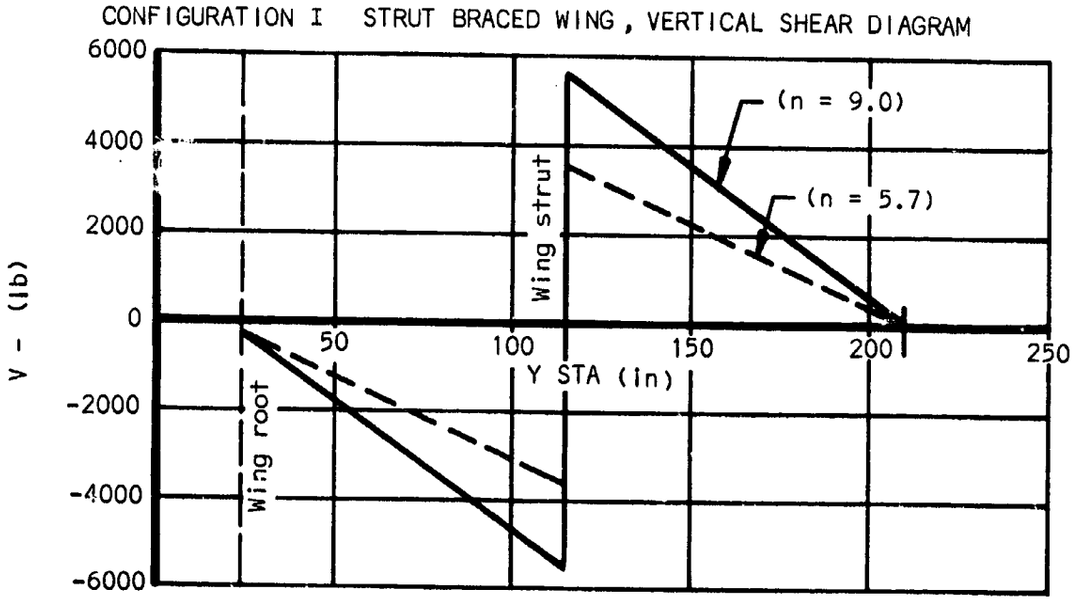


Figure 41

Spar cap sizing was based on equations given on page 44 and Figure 42. The results are shown on Figure 43 for n = 5.7 and in Figure 44 for n = 9.0.

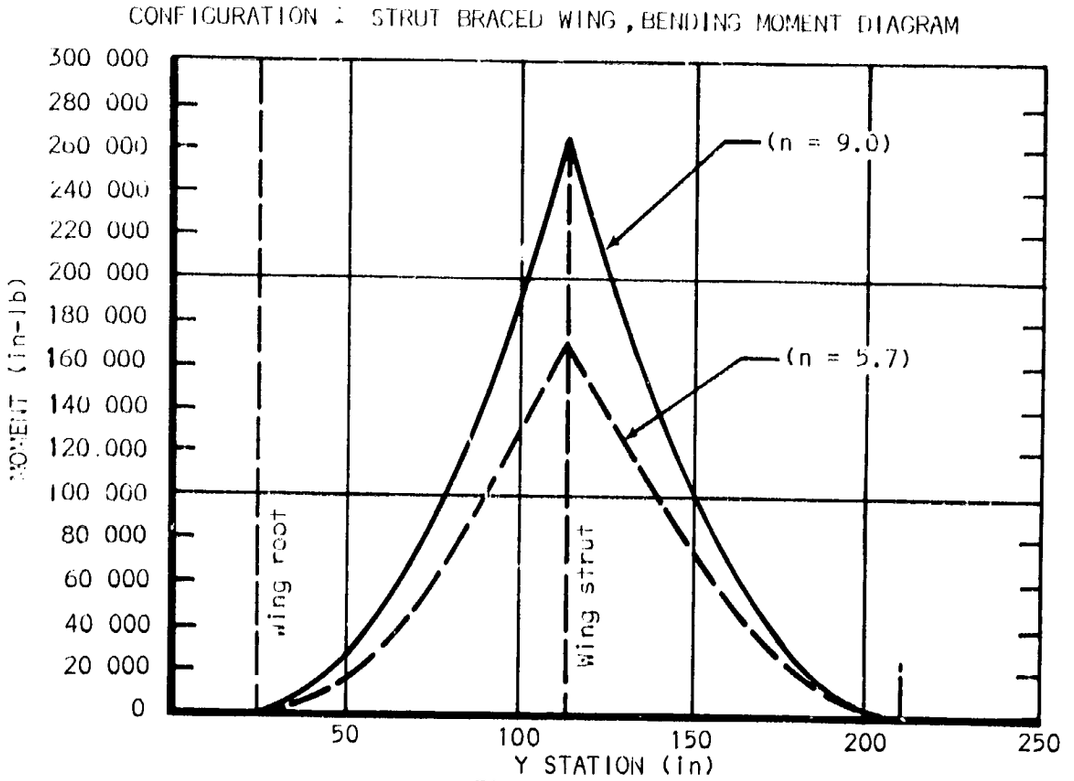


Figure 42

Spar cap sizing was based on equations given on page 44 and Figure 42. The results are shown on Figure 43 for n = 9.0 and in Figure 44 for n = 5.7 .

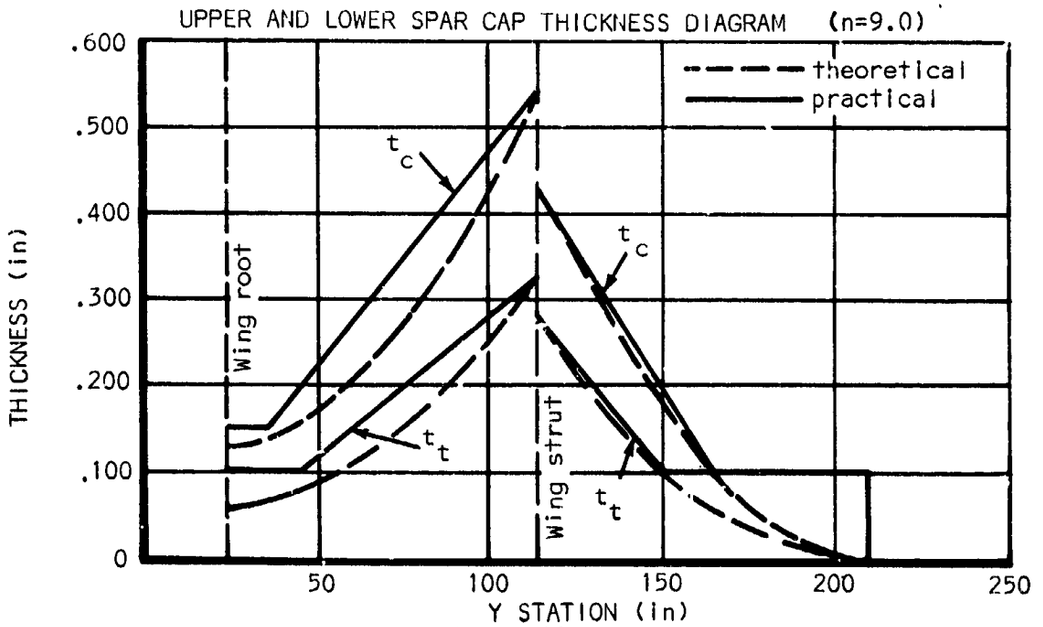


Figure 43

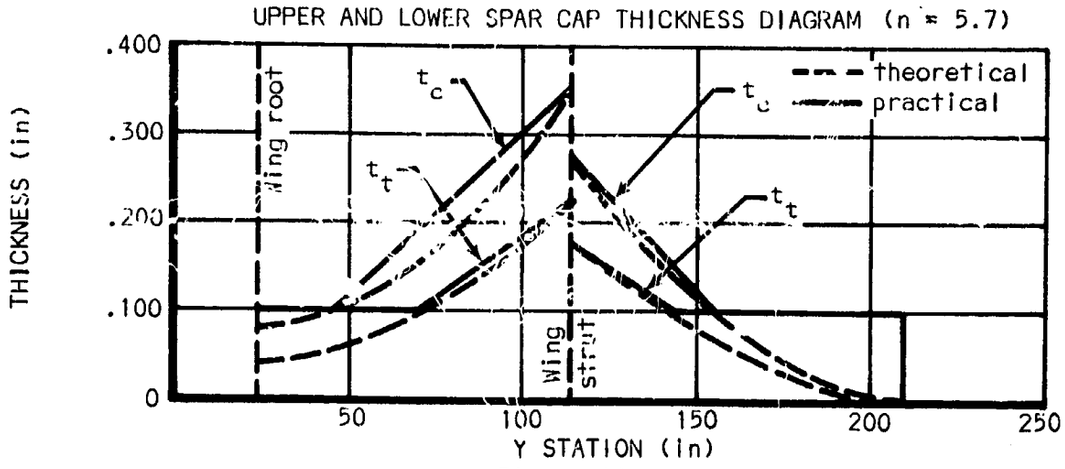


Figure 44

Spar web sizing was based on equations given on page 46 and Figure 41. The results are shown on Figure 45.

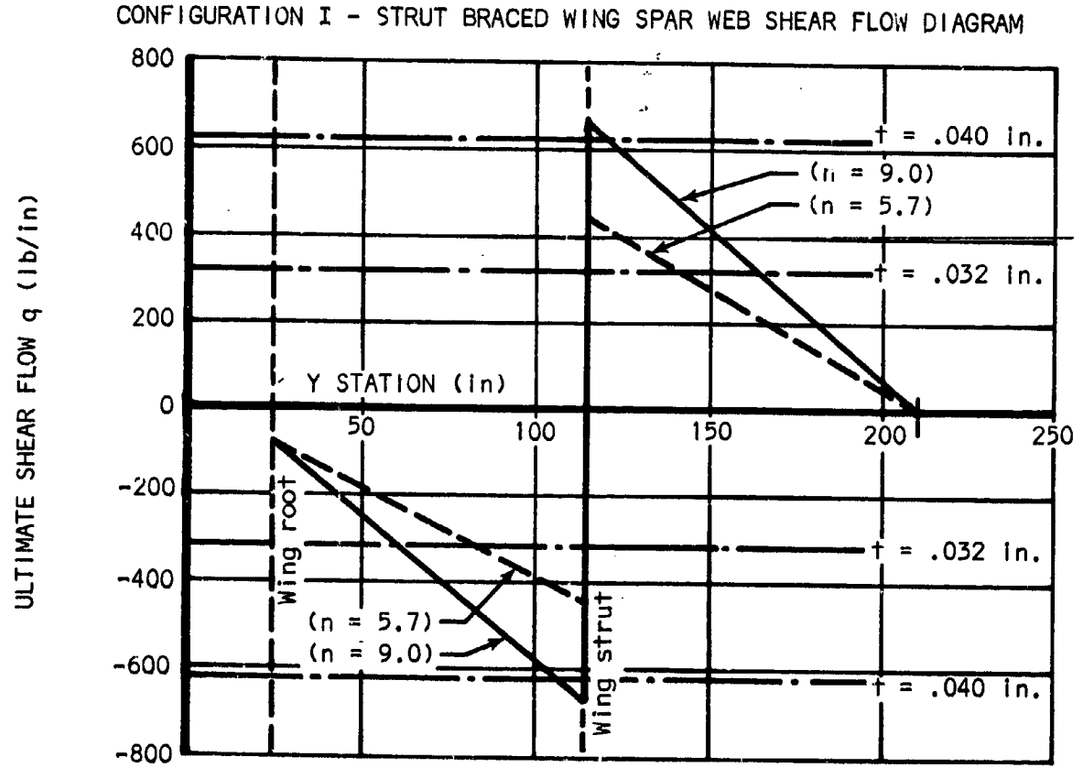


Figure 45

(Weights). Spar cap weights were calculated on the basis of the thicknesses presented in Figures 34, 35, 36, 43, and 44, using the density of aluminum as .100 lbs/cu.in. Similarly, the spar web calculations are based on Figures 38, 39, and 45. These weights are all summarized in Table VII.

TABLE VII - WING STRUCTURE WEIGHT SUMMARY

(Weight of ribs, ailerons, flaps and mechanisms are not included in total)

Configuration	Strut install.	Spar cap lower	Spar cap upper	Spar web	Torque box skins	Total lb
I n = 9.0	---	37.2	63.2	17.65	88.4	206.45
I n = 9.0 (strut braced)	30 est.	16.66	23.68	12.47	88.4	171.21
I n = 5.7	---	25.68	39.37	15.24	83.1	163.39
I n = 5.7 (strut braced)	24 est.	11.43	16.88	11.46	83.1	146.87
II n = 5.7	---	19.9	32.3	16 est	80.1	148.3
III n = 5.7	--	18.51	29.2	16 est	75.6	139.31

est. = estimated

Wing area versus high-lift devices: Wing area is a function of the type of high-lift device employed. In addition to the plain wing, the following high-lift device configurations were considered: All of these configurations must demonstrate a maximum stall speed of 48 knots (@ S.L.).

Plain flap
Split flap
Single-slotted flap
Double-slotted flap
Double-slotted flap plus leading edge slat

These configurations and their associated parameters are illustrated and compared in Figure 46.

The plain wing with its obviously greater area is too heavy. The plain flap, which most contemporary light airplanes have, provides considerable less area and therfore less weight. The split flap and the single-slotted flap provide only a small improvement over the plain flap. The double slotted flap is the lightest and second smallest in area. It has a fixed vane and is relatively simple in construction. The double slotted, fixed vane flap is currently used on the Mooney Mustang. The double slotted flap plus leading edge slat adds unnecessary complexity and weight.

Preliminary selection of wing configuration: Analysis of the rectangular strut-braced wing has demonstrated that it can be as much as 17% lighter than the rectangular contilevered wing. Strut drag on a high wing affects performance by only two or three miles per hour.

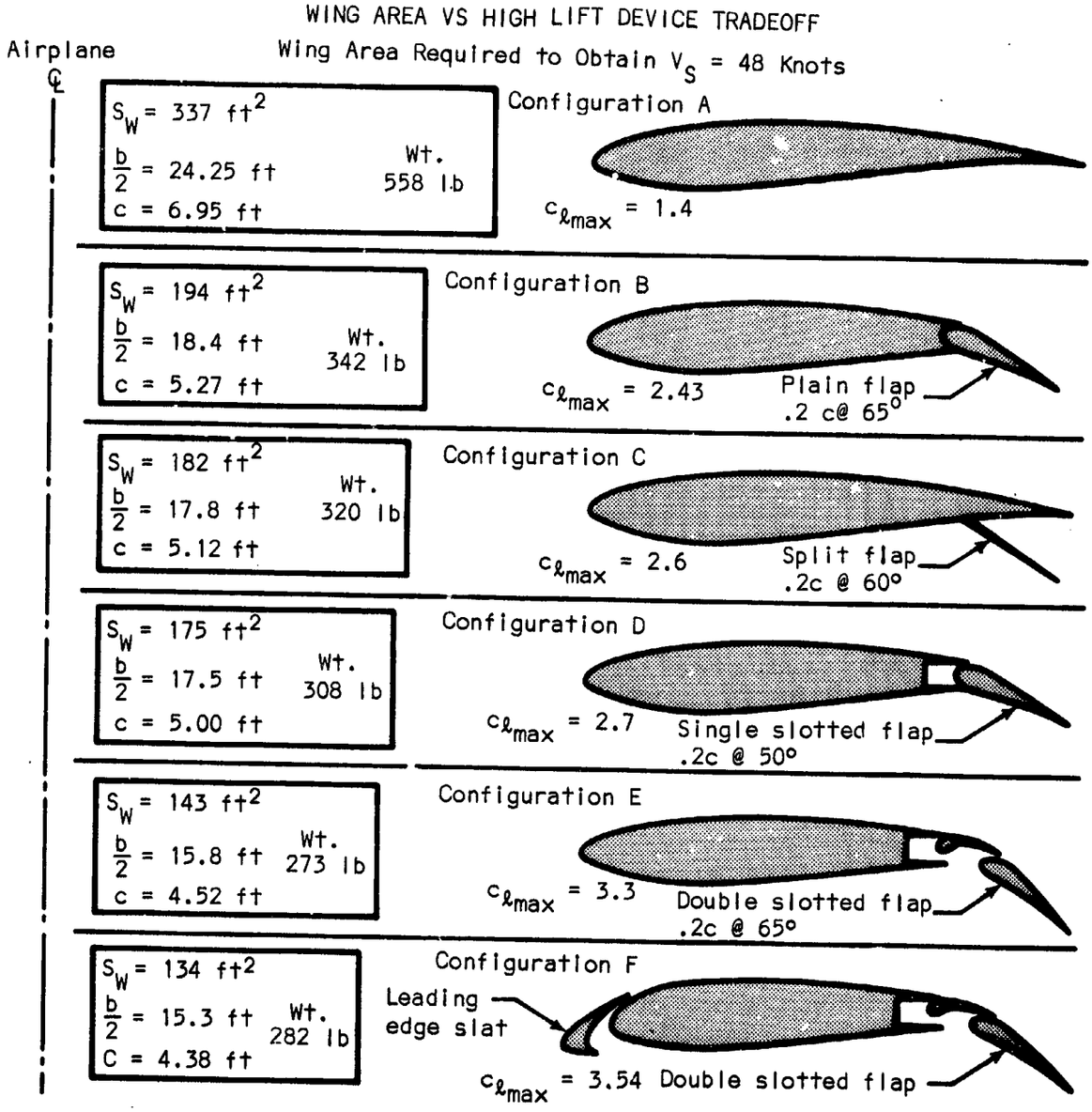


Figure 46

A strut used on the upper side of a wing creates more drag than the same strut on the lower side, because it is in higher speed air, resulting in higher interferance drag. It also causes flow separation, hence reducing wing efficiency. The great majority of low wing light airplanes have cantilevered wings, with few exceptions (e.g., the Piper PA-25-235 Pawnee).

The rectangular/taper wing is approximately 9% lighter than the rectangular wing, and the tapered wing is approximately 15% lighter than the rectangular wing. Therefore, based on its minimum weight and small area, the tapered wing with double-slotted flaps (fixed vane) high lift device was selected for application (in Phase II of the Study) to the Far Term light airplane.

Helicopter weights.- The group weight breakdown of two contemporary helicopters, which are representative of the helicopter guidelines, are illustrated in Figures 47 and 48.

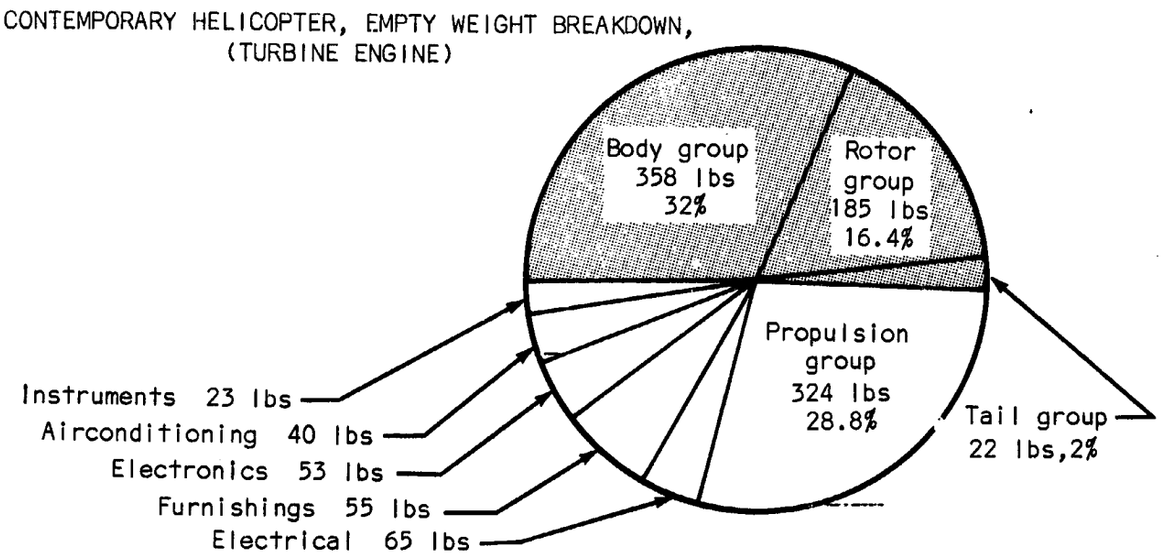


Figure 47

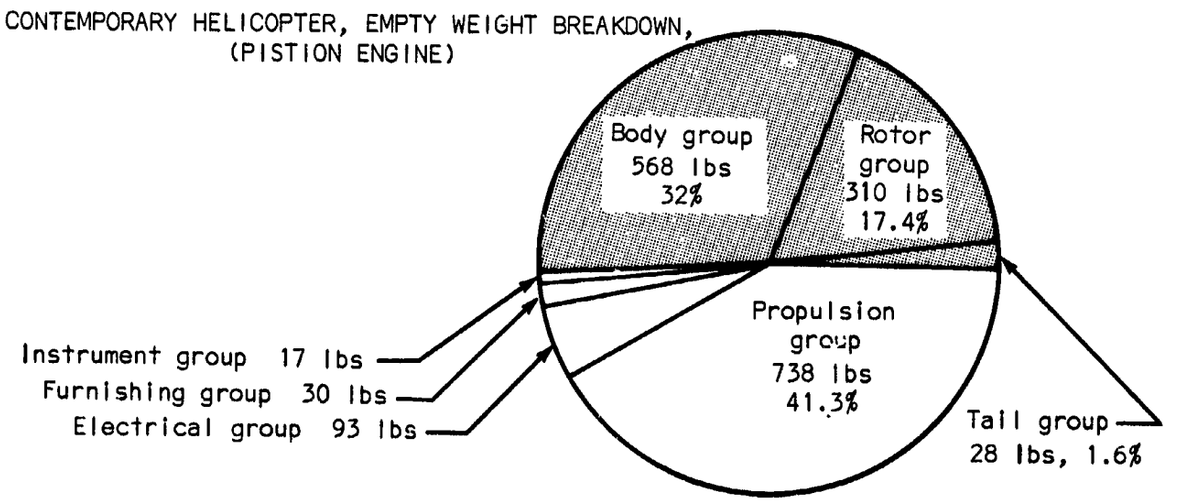


Figure 48

Crashworthiness.- During the course of this study, the subject of crashworthiness and its relation to aircraft design was considered on many occasions and from every possible view point. Recent CAB and FAA studies and statistical data provides excellent guidelines and background data which indicated the need to reevaluate present regulations.

The manufacturers indicate some degree of scepticisum. Some of them pointed out"shoulder harnesses are optional equipment in all our models, but we very seldom sell a kit". Also "crashworthiness is based very much on emotions; we would like more facts and figures".

The users recognize the need of improved safety. This was the most desirable feature listed for future aircraft as a result of the poll conducted during this study. Nevertheless, the operator very seldom is willing to pay for the additional safety.

Perhaps, as the Department of Transpoaration recently defined areas of improvement in the automotive industry, similar improvements will be outlined for future airplanes.

A brief bibliography of technical reports applicable to light aircraft crashworthiness design is as follows:

"Crash Survival Design Guide", Technical Report 67-22, U.S. Army Aviation Material Laboratories, Fort Eustis, Virginia - July 1967

Swearingen, J.J.,"Injury Potentials of Light Aircraft Instrument Panels", Federal Aviation Agency, Office of Aviation Medicine - April 1966

Hasbrook, A.H., "General Design Requirements for Crashworthiness and Delethalization of Passenger Transport Aircraft", Av-CIR-0-45(67), Cornell University, issued under Office of Naval Research Contract No.Nonr-401(21) - August 1956

Hasbrook, A.H., "Recommendations for Crash Safety Design Criteria for General Aviation Aircraft", THE FLYING PHYSICIAN - 1965

Robertson, Harry S., "Aircraft Fuel Tank Design Criteria", Technical Report Av-SER-65-17, Flight Safety Foundation, Inc - March 1966

Nissley, P.M., "Structural Design For Fuel Containment Under Survivable Crash Conditions", Technical Report ADS-19, Federal Aviation Angency - August 1964

Greer, D.L., "Crashworthy Design Principles", Technical Report ADS-24 Federal Aviation Agency - September 1964

Design-induced pilot error.-Because of the startling number of accidents involving the pilot as a causal element, the Federal Aviation Agency established a flight research program entitled "Aircraft Design-Induced Pilot Error." The first phase of this two-phase design compatibility program was to assess the influence of airplane design factors or configurations in General Aviation accidents wherein the pilot was determined to be a causal element. After learning of the FAA interest and intent to develop such a program, the Civil Aeronautics Board offered to conduct this first-phase study because of its role and responsibility for the investigation of aircraft accidents and the promotion of air safety. In addition, this provided an opportunity to relate the Board's wealth of accident statistics and related data to a dynamic safety function: the prevention of accidents. The study was subsequently conducted by the Board's Bureau of Safety with financial assistance from the FAA.

In July 1967, the National Transportation Safety Board published a report (PB 175 629) with the results and conclusions of the study. The report highlights were summarized by the contractor and are reproduced in the following pages.

The Aircraft Design-Induced Pilot Error Project is an evaluation and comparison of the accident records of 35 makes and models of General Aviation airplanes during 1964. Rotorcraft, agricultural airplanes, or those airplanes whose active number was less than 500 were excluded.

Reason for the study stems from the fact that most of the General Aviation accidents (83%) were attributed to "pilot error" (total of 3,732 in 1964).

Typical "pilot errors" appear more influenced by some airplane designs than others. In other cases, the aircraft owner's manual contains information which induces the pilot to err. The study showed that many of the accidents were design-induced, and, therefore, probably could have been prevented. The study was not intended to serve as an evaluation of the safety of the various models or as criticism of any particular manufacturer.

Airplane makes and models were grouped by type of utilization to provide a common exposure index and by design parameters related to specific accident types. Distributions were prepared based on flight hours, total number of accidents, and number of active aircraft. It was concluded that type of flying and pilot rating or proficiency were significant variables in defining accident risk.

It was found that certain types of accidents were related primarily to detail design, particularly those involving retractable landing gear and fuel systems mismanagement. In these cases improper sensing of controls, inadequate identification of controls, inadequate pilot warning, and lack of standardization were the major design factors.

In other cases, the design factors were less clearly identifiable. For instance, in many takeoff and landing accidents the information available in

the flight manual is inadequate, or provides little margin for error, such as: lack of data on takeoff with cross winds, runway surface, takeoff and landing distances, margins between stall and approach speeds. All these factors require a level of skill beyond that of many General Aviation pilots.

It was found also that certain aircraft configurations definitely have an influence on the accident rates. For instance, low-wing tricycle-gear airplanes are less prone to nose-over or groundloop than tail-wheel airplanes.

Another interesting finding was that airplanes certified under the relatively new CAR 3 and FAR 23 regulations have significantly less stall accidents than other aircraft certified under the old CAR 4a regulation. This indicates that the requirements governing stall warning in the new regulations have had an appreciable effect. Most of these accidents occur during takeoff or go-around resulting in stalls, spins, spirals, or mushing into the ground.

In hard landings of airplanes with tricycle-type landing gear, it was found that in most cases they resulted in failure or collapse of the nose gear, but no damage to the main gear. This would indicate nose wheel first contact, rather than contact at a high rate of sink in a nose-high attitude.

A detailed analysis of the most significant type of accidents is described next:

Accidents involving engine failure: For the purpose of the study, only those accidents were considered in which the power plant failure was induced by pilot error. A relatively large number of such accidents involved mismanagement of the fuel system (98 accidents during year 1964). Fuel starvation occurred while:

(1) There was ample fuel on board.

(2) The fuel system was capable of normal operation.

(3) There was no evidence of fuel contamination.

From the 35 different airplanes studied, 9 had no accidents. Among the other 26 airplanes, some had one accident each, to a maximum of 19 accidents for one particular model.

For twin-engine airplanes, the frequency of this type of accident was negligible (less than one accident per 200,000 hours of flying).

For single-engine airplanes, the following type of accident was most common:

(Fuel quantity gauges) In these airplanes, a single fuel quantity gauge is used to indicate the amount of fuel in two or more tanks. The selector switch for the gauge is independent from the Fuel Selector Valve, which was not

repositioned following engine failure because the pilot believed that the fuel selector and gauge were on the same tank. In this mistaken belief, and with fuel showing on the gauge, the pilot in each instance judged the engine failure to be for other than fuel starvation reasons.

Solution: Use independent gauges for each tank or combine gauge switching with selector valve.

(Poor location of fuel selector valve) Four accidents (all with the same airplane) during 1964 were attributed to the poor location of selector valve. A small pilot, or one with short legs, has to move the seat far forward to a position from where he cannot see or reach the valve.

Solution: Better Selector Valve location.

(Failure of the engine to respond when the Selector was repositioned to a tank with fuel) Present regulations specify that if the engine of a single-engine airplane can be supplied with fuel from more than one tank, it must be possible, in level flight, to regain full power and fuel pressure in not more than 10 seconds after switching to any full tank, after engine malfunction due to fuel depletion becomes apparent, while the engine is being supplied from another tank.

This requirement is very seldom met with fuel injection engines, even using boost pumps. Without boost pumps it often takes 30-35 seconds to restart the engine. With carburetor-engines the recovery was well within 10 seconds with or without the use of boost pumps.

This is not a problem with high-wing airplanes (with wing tanks); all accidents occurred with low-wing airplanes.

The present regulations do not contain a prohibition against running one tank dry until engine failure .To the contrary, this often is a recommended practice in the owner's handbook. However, the handbook generally does not give information on the time required to recovery and the use of boost pumps.

Solution: In low-wing airplanes, where "head" of fuel pressure does not exist, and purging of the fuel lines is dependent on the pump, it is recommended that the power-recovery-time test without the use of boost pumps be made. If it results in excess of 10 seconds, the appropriate information should be provided to the pilot by means of the owner's handbook. An alternate solution would be the installation of "low-level warning lights."

(Fuel Selector Valve mispositioned) There is a lack of standardization on the design of Fuel Selector Valves. There is no uniformity in General Aviation airplanes in the manner in which the fuel selector portrays the tank in use.

FUEL SELECTOR VALVE CONFIGURATIONS

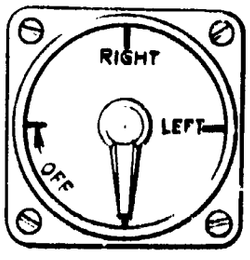


Figure 49

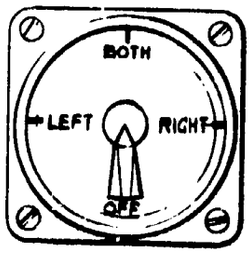


Figure 50

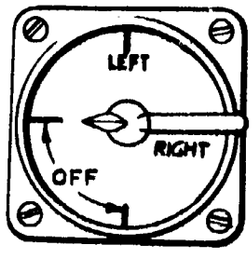


Figure 51

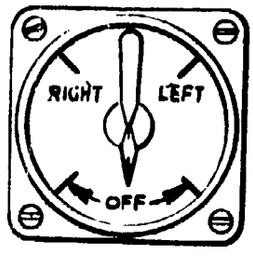


Figure 52

Selectors in Figures 49 and 50 utilize the handle as an indicator but the tanks are reversed. Selectors in Figures 51 and 52 have a small pointer opposite to the handle to indicate the tank. In addition, some other types of Selector Valves are combined with an auxiliary pump handle, which has to be depressed properly before it will engage with the valve. When this is not done properly, the handle could be rotated without really making a change in the valve, with subsequent engine failure which will be unexpected and masked to the pilot.

Solution: Standardization on a rational design.

Accidents involving stalls, spins, spiral, mush: To begin, airplanes certified under the new CAR 3 or FAR 23 regulations have a much lower frequency of accidents than the older airplanes certified under CAR 4a. The later requirements, including adequate stall warning, indicate a step in the right direction.

62% of all stall accidents occurred during initial climb or go-around. Stall accidents during the landing phase were in the order of 10% of the total number, and stalls during in-flight phase accounted for 28% of the total.

The large number of in-flight stalls are related to the lack of pilot proficiency and judgment rather than airplane design. The commonly held opinion that stall accidents are related to poor aerodynamic characteristics, spiral stability, and/or inattention to airspeed during landing or in-flight maneuvers is not valid. The major problem in stalls is related to initial climb on takeoff at full engine power.

A very interesting comparison between two models of an airplane, one with a tail wheel and the other with a nose wheel, showed that the first model had 10 times more stall accidents per hour of flying than the second. With the exception of the landing gear, both airplanes are practically the same. Similar studies were made with other airplanes in order to detect any relationship between type of landing gear and stall frequency, but no correlation was found.

Takeoff instructions in owner's manuals were similar for both airplanes with the exception that for the model with nose wheel, there is a table giving airspeed corrections at speeds near stall, both for flaps up and flaps down. It

was noted that, for this model, the airspeed indicator reads low by 7-10 miles per hour in the takeoff range. It is therefore possible that large difference in stall frequency between these two airplanes stems from the fact that pilots are unknowingly taking off at higher speeds relative to stall in the model with nose wheel, because they do not realize that the speeds given in the manual are calibrated rather than indicated.

Another study involving a very popular four-place airplane showed that this particular make had a rate appreciably higher than other competitive airplanes. Out of 27 stalls, 19 occurred on takeoff and two on go-around. It was found that cross winds were not a factor in any of the accidents. In several go-around and takeoff accidents, severe rolling tendency with flaps down was reported. It is possible that the rolling tendency of this airplane in power-on stall may be a significant factor in its stall accident history.

Another factor that may be related to the stall accidents on takeoff on these models is premature gear retraction because of a reduction in lift when the gear doors opened.

A review of the owner's manual of several airplanes was made, and it was found that data on altitude and temperature effects were minimal in many cases, although complete charts were provided in a few cases; takeoff speed was often not clearly specified, and in other cases the speeds given provided no margin from stalling speed. No data on takeoff from other than hard surface runways were included in any manuals; and few considered cross wind or gave maximum safe values. It was therefore recommended that the various manufacturers critically review the adequacy of such data as are now presented in owners' manuals.

Groundloop accidents: The groundloop-type accident is defined as one resulting from a loss of directional control or a sudden swerve while taxiing, taking off, or landing. The main factors attributed to the pilot were:

(1) Improper operation of brakes and/or flight controls (loss of directional control results from "over control" during takeoff or landing).

(2) Improper compensation for wind conditions (cross wind picks up the upwind wing and airplane veers to one side of the runway. Nose wheel often collapses after cross wind gust picks up a wing).

(3) Loss of traction on slippery runways.

(4) Failure to initiate a go-around or abort the takeoff at the proper time.

(5) Veering or fishtailing on takeoff or "long landing."

(6) Wrong type of approach or landing for existing wind conditions, i.e., wheel landing vs. full-stall landing.

(7) Taxiing or turning too fast.

(Tail-wheel airplanes) The study discloses that tail-wheel type airplanes have a much higher relative frequency of groundloop accidents than nose-gear airplanes. The center of gravity is located behind the main wheels in the tail-wheel type airplanes. Inertia moments created in these airplanes, as a result of curvilinear motion, tend to cause the airplane to swerve or veer since the effect is to increase the curvature by decreasing the radius of curvature. Also, in tail-wheel type airplanes, it is desirable to keep the center of gravity as close to the main landing gear as possible in order to minimize the airplane's ground yaw inertia characteristics. However, its maximum forward position is restrained by the airplane's tendency to nose over.

UPSETING COUPLE ON TAIL-WHEEL AIRPLANES

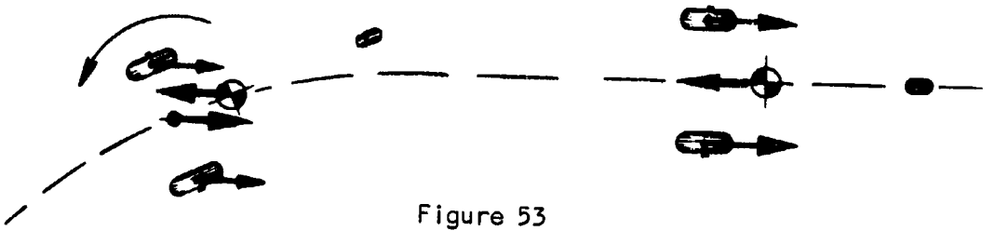


Figure 53

The swivel-type tail wheel does not provide appreciably large yaw restoring moments; its contribution to prevent groundloop is very small. Anyway, in order to provide any significant contribution, the tail wheel should be firmly on the ground, but braking during landing tends to unload the wheel and thereby further reduce its correcting or lateral force capability.

A dramatic example on the effect of c.g. position with respect to main-landing gear on groundloop accidents is pointed up in a comparison of four models made by the same manufacturer. Models "A" and "B" are tail-wheel versions; Models "C" and "D" are nose-wheel versions. The groundloop records for the tail-wheel versions were significantly worse than the tricycle-gear versions.

(Nose-wheel airplanes) The tricycle-gear airplane is basically ground stable with respect to adverse yaw inertia moments. With the center of gravity

RESTORING COUPLE ON TRICYCLE-GEAR AIRPLANES

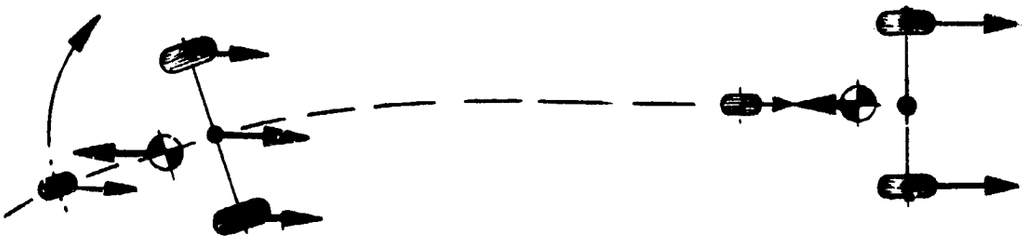


Figure 54

ahead of the main landing gear, the inertia effect tends to align the airplane along a tangent to its particular ground path at any given time. The farther forward the center of gravity is located, the greater the ground roll stability of the airplane and more rapid the convergence in crabbed landing.

A statistical evaluation to determine the differences in the groundloop records of tail-wheel airplanes and tricycle-gear airplanes discloses that this latter group is far superior to its tail-wheel counterpart. That is, chances of having a groundloop in a tricycle-gear airplane are much less than in tail-wheel airplanes.

Although not directly related to the kinematics of the airplane, the enhanced visibility during takeoff and landing of a nose-wheel equipped airplane can be a decided advantage in preventing a swerve or groundloop, especially so during landing or takeoff on relatively narrow runways in adverse wind conditions.

A nose wheel that is free to caster will permit the inertia moments to stabilize the aircraft. Most present airplanes have more or less restrained nose wheels. To reduce ground loops, the caster restraint should be minimized. The design generally represents a compromise. For instance, the desirable characteristic to avoid groundloop during landing is maximum freedom to caster. On the other hand, the same nose wheel during takeoff phase should be irreversible (no caster) so the pilot can steer the airplane. While landing in a crabbed attitude, the inertia forces tend to align the airplane with its initial path of flight, and the nose wheel casters as it contacts the runway. The airplane straightens out and continues traveling in a straight line. Should the nose wheel fail to caster, the airplane will tend to swerve and groundloop.

In the statistical comparison of all single-engine, tricycle-gear airplanes, two particular models have shown a much higher rate of groundloop accidents than the statistical average. After evaluating every possible factor which might have had an influence on this high rate, it was found that both airplanes have rigid connections between the nose-wheel steering and the rudder pedals. Also the ground steering forces were high, resulting in very reduced amount of free castering.

(Groundloop initiation) Many groundloops are initiated as a result of a wing tip contacting the ground due to a gust. An important parameter related to this groundloop initiation mode is the ratio of the lateral wheel base to the height of the center of gravity. See Figure 55.

The larger this ratio, the smaller the tendency of adverse external forces to tip the airplane sideways. Thus, it would appear that low-wing aircraft might be naturally less susceptible to groundloops precipitated by gust upset than their high-wing counterparts, since low-wing configurations provide for a large lateral wheel base and a relatively low center of gravity.

A comparison of the rates of accidents of high-wing and low-wing airplanes with tricycle-type landing gears showed that the low-wing airplanes had

RATIO OF TRACK WIDTH TO C.G. HEIGHT FOR LOW AND HIGH WING AIRCRAFT

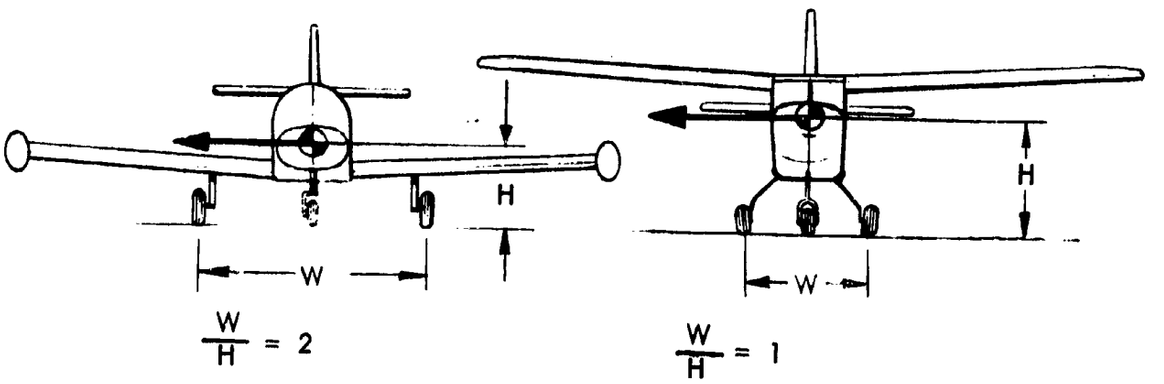


Figure 55

a significantly lower rate on an accident basis, but when compared on a flight-time basis shows no significant difference.

When the groundloop was initiated without wing tip touching the ground, it was found that the frequency of accidents had a relation to the location of the center of gravity with respect to the main gear, and the radius of gyration about the vertical axis through the main landing gear.

In tail-wheel airplanes, a relatively large radius of gyration about a vertical axis through the main landing gear reduces the swerve tendency.

EFFECT OF MOMENT OF INERTIA ON SWERVE TENDENCY

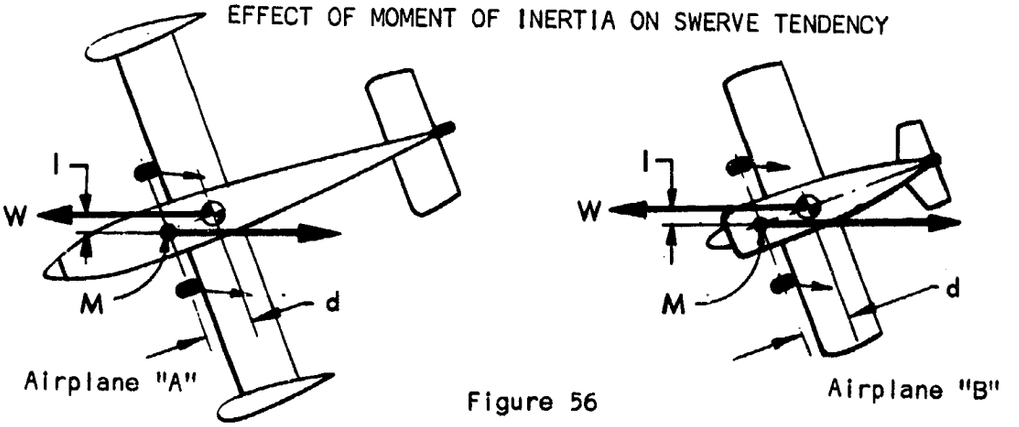


Figure 56

Figure 56 illustrate this concept. Assume both airplanes, "A" and "B", to have the same weight "W", and the c.g. located at the same distance "d" behind the main gear. Airplane "A" has a large moment of inertia about the vertical axis due to wing tip tanks, great span and long fuselage, while Airplane "B" has a small moment of inertia, with most of the mass concentrated near the c.g.

E.g., a spinning ice skater, with arms extended, accelerates his rotation by folding his arms and reducing his moment of inertia.

(Other design parameters affecting the groundloop) Torsional flexibility of both the landing-gear structure and tires can markedly affect the capability of developing lateral or cornering forces. The softer the main landing gear tire, the less tendency to develop lateral loads which cause groundloops. It is interesting to note that a very popular light airplane which utilizes relatively large soft balloon-type tires (8.00 x 4 @ 12 psi) was considered to have a much lower than average groundloop frequency as compared to all other high-wing, tail-wheel airplanes in the study.

The location of the fuselage center of pressure determines the relative swerve of veering reaction of the airplane to crosswinds. A center of pressure location close to the main landing gear axis, as might be conceivable in some tricycle configuration, reduces this swerve tendency. Figure 57 illustrate this concept.

EFFECT OF CENTER OF LATERAL AREA ON SWERVE TENDENCY

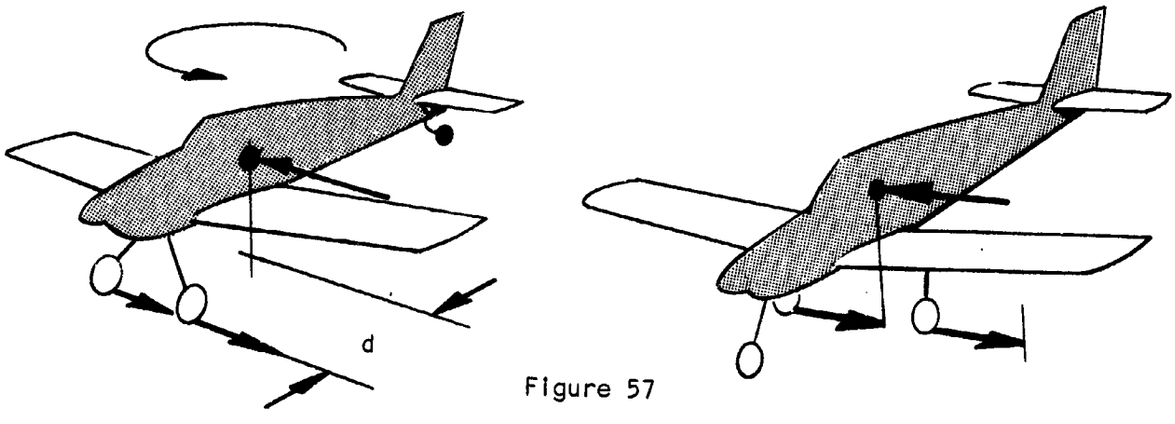


Figure 57

Accidents involving retractable landing gear: The accidents in this group involved landing gear retraction while the airplane was on the ground, and landings made with the wheels in the up position. There were 311 "wheels-up" landings and 154 "gear retracted" accident reports reviewed in this study.

Only those accidents in which pilot error was evident were included. Other accidents due to mechanical failure of the extension/retraction mechanism or those which were associated with engine failure or forced landing were not included. They were eliminated since factors other than system design played a significant part in the pilot's actions, or failure to act with respect to actuating the landing gear extension mechanism.

(Premature retraction) In this category are the accidents that occurred during takeoff and which were initiated by the pilot's attempt to retract the landing gear before flying speed was obtained. Also in this category are those

accidents occurring during landing in which the gear collapsed during the landing roll because of damage on the extension/retraction mechanism in the course of the previous takeoff. This damage occurred when the pilot placed the landing gear selector switch or lever to the "up" position during takeoff while most of the weight of the airplane was still supported by the landing gear. The takeoff in these instances was accomplished successfully despite damage to the landing gear mechanism.

There were 30 of these accidents in the 1964 records reviewed. However, these accidents are not considered as "design-induced" since they occurred at a time, or flight phase, when there was no intent to operate some other systems; e.g., flaps. Unusual conditions, obstructions, or emergency circumstances were not present to influence the pilot to retract the landing gear as quickly as possible.

(Inadvertent retraction) Accidents in this classification are those in which the pilots placed the landing gear lever to the "up" position unintentionally while the airplane was on the ground. Most of these accidents occurred at a time when the pilots intended to actuate some other system such as flaps or landing lights. The total number of these errors could not be determined because the accident reports often did not identify the pilot's intention at the time of the inadvertent retraction. There was, however, enough information in many of the pilots' statements to lead to certain conclusions concerning the landing actuating levers or switches, their placement in the cockpit, and similarity to other switches or levers.

Thirteen different airplanes were involved in 80 inadvertent retractions. In connection with this subject, CAA Technical Manual No. 103 - September 1953, title: Aircraft Design Through Service Experience, stated in part: "Service reports show numerous cases of confusion of the retractable landing gear controls with other controls .....".

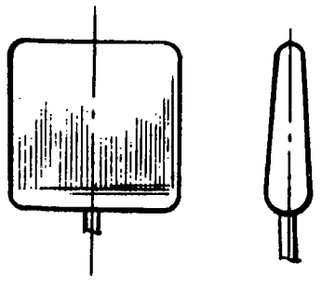
On October 1, 1959, Amendment 3-5 to CAR Part 3 became effective. The preamble to this amendment states "Accident records have shown that approximately one-sixth of all accidents with airplanes certificated under Part 3 have involved the misuse of the landing gear control. Incorrect operation of this control has been attributed to its proximity and similarity to the wing flap control. Therefore, Section 3.384 is being amended to specify the location and shape of the landing gear and wing flap controls to reduce the possibility of confusion." The amendment reads as follows:

> The wing flaps or auxiliary lift device control shall be located centrally or to the right of the pedestal centerline or of the powerplant throttle centerline and shall be sufficiently displaced from the landing gear control to avoid confusion.
>
> The landing gear control shall be located to the left of the throttle centerline or of the control pedestal centerline.

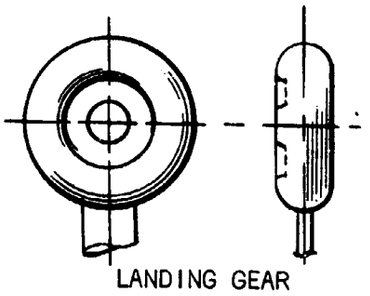
The control knobs shall be shaped in accordance with Figure 13 (Flap control shaped like an airfoil, landing gear control shaped like a wheel).

Note: The official report analyzed in great detail each airplane and their accidents. In this summary only the conclusions are reproduced, which were as follows:

CAR PART 3
CONTROL KNOBS



FLAP



LANDING GEAR

Figure 58

The great majority of these accidents involved qualified pilots; training activities are not considered as a significant causal factor.

Nearly all accidents occurred during daylight hours when light conditions within the cockpit were sufficient for proper identification of all controls.

In 66 inadvertent retraction of the landing gear accidents in which qualified pilots were involved, t. ere were 53 instances where the landing gear control was operated by mistake for the wing-flap control.

In the aircraft involved in 37 of these 66 accidents, the landing-gear control and wing-flap control switches were nearly identical in appearance and opposite to the location specified in CAR Part 3. While these airplanes accounted for 57.5% of the non-student, non-passenger involved inadvertent landing gear retractions, they flew only 21.7% of the hours accomplished by all retractable landing gear airplanes selected for review in this study.

In the remaining 29 cases in this group, there were six instances where the wing-flap landing-gear control levers or switches did not conform to either the configuration or location specified in CAR Part 3. There were 16 cases in which the configuration was in conformance to CAR Part 3, but the location was not. <u>There were only seven of the 66 instances in airplanes that conformed to Part 3 in both configuration and location</u>.

From an overall standpoint, the airplanes having the landing-gear and wing-flap control arrangement specified in CAR Part 3 were involved in only 18.7% of the total number of inadvertent landing gear retraction accidents reviewed in this study. These airplanes, however, accomplished 33.7% of the total 1964 flight hours for the 15 retractable landing-gear airplanes in this study.

From the foregoing, it is concluded that the majority of the inadvertent retractions were caused by airplane design factors. It is also concluded that the wisdom of Amendment 3-5 to CAR Part 3 has been demonstrated.

All but two airplanes have safety-limiting switches or hydraulic valves, as appropriate to the system. Accordingly, it is likely that the same error has been made many times without causing an accident. It is noted that these safety switches or valves are located on one main landing gear leg only, and in these accidents failed to perform their intended function. In this respect it is noted that the pilot's handbooks sometimes note that the safety switch is to prevent inadvertent retractions on the ground when the airplane is not in motion. Accordingly, the protection afforded by this device is very limited and confined to periods of low hazard. Earlier handbooks do not make this distinction, and the pilots may be placing more reliance on this device than is warranted.

In some of these accidents, the safety devices did not provide protection for the airplane while taxiing, or while on the landing roll, because of high strut pressure or because of rough or rolling ground that caused a rocking motion of the aircraft and subsequent irregular extension of the shock struts. Only one instance involved a faulty microswitch. It is likely that had there been at least two or more switches, one on each main landing gear and operating in series, these accidents could have been avoided. It is recognized that such protection as does exist has been provided by the manufacturer voluntarily since there is no requirement for such safety devices in CAR Part 3 or FAR Part 23. It is recommended that the question of the need for devices to prevent inadvertent retraction of the landing gear on aircraft certificated under Part 23 be included on the agenda for discussion at the next Annual Airworthiness Review.

(Failure to assure landing gear locked down) Accidents in this classification are those in which the landing gear lever or switch was moved to the "down" position by the pilot, but for various reasons the landing gear extended only partially and the gear collapsed upon touchdown. In most instances the pilots were unaware of the unsafe landing gear and took no action to extend it by use of the emergency landing gear extension system. However, this classification also includes accidents in which the pilot was aware of the unsafe condition of the landing gear and used the emergency system, but used it incorrectly. Because of the incorrect use, the landing gears did not go into the down locks, and collapsed during the landing roll.

There were 97 accidents in this classification.

Approximately 75% of these accidents occurred in daylight. However, there was only one instance in which sunlight striking the down-position light-indicator caused the pilot to believe the landing gear was locked in the "down" position.

In this regard, CAA Technical Manual No. 103, Aircraft Design Through Service Experience, states:

Red warning lights are often used as the means to indicate if the gear is not secured in its extreme position. However, in actual operation, due to the effects of direct sunlight, it is often difficult to observe if the light is on. Accordingly, it is desirable to shield the lamp from the direct rays of the sun. In the past numerous wheels-up landings can be attributed to failure to observe the lamp being on due to the adverse effects of direct sunlight.

Since there was only one accident in 1964 in this classification in which sunlight was a factor, it can be concluded that this problem has in great measure been solved.

The automatic dimming of the landing gear position light has been demonstrated as a cause of pilot error. The airplane handbooks for all the airplanes having this feature emphasize the fact that the lights will be dimmed when the navigation lights are turned on. However, in the cases studied there were comments by the pilots that they were not aware of this device. In the case of rental aircraft, it is doubtful that the renter will be very familiar with information in the handbook. In the two twin-engine aircraft with this device, there is a secondary feature which tends to reduce the possibility of error because of the dimmed light. This is the flashing red light in the landing gear control handle in one airplane, and the flashing of the "UP" position light in the other.

There were 10 accidents in which the landing gear position lights were not functioning. However, in six instances, it was because of electrical-system failure, or because the generators were not turned on. Accordingly, there does not appear to be any appreciable problem with the operation of the landing gear position lights. However, of particular interest is the number of comments from the pilots indicating that they did not use the position lights to determine if the landing gear was locked in the "down" position. It is apparent that many pilots are relying on the aural warning signal rather than the lights to tell them if the gear is in an unsafe condition.

There were 34 instances in which the landing-gear-warning horn, for various reasons, did not function, and five instances where power-on approaches prevented the horn from being heard until too late to prevent the wheels-up landing. When reliance is placed primarily on the aural signal for indication of an unsafe landing gear situation, as the accident reports indicate, then malfunctions of this device contribute materially to pilot error.

Reliance on the aural signal is not confined to General Aviation pilots. On April 15, 1964, the Federal Aviation Agency issued Amendment 40-41 to Part 40, Scheduled Interstate Air Carrier, Certification and Operation Rules, which provided that landplanes of over 12 500 pounds maximum weight must have a wing-flap actuated aural warning signal in addition to the other position indicating and warning devices related to the landing gear.

The Study group believes that if the warning system, position lights, and checklists are inadequate in air carrier aircraft operated by two professional pilots, the problems must be equally as acute, if not more so, in General Aviation aircraft operated by a single pilot. Accordingly, in view of the number of wheels-up landings during 1964, the Board on May 20, 1966, forwarded to the Administrator a letter recommending that a wing-flap-actuated aural warning signal be required on all landplanes certificated under Part 23 of the Federal Aviation Regulations.

In view of the large number of warning-horn failures, we conclude that these accidents fall in the design-induced category.

There were 22 instances of tripped circuit breakers. When the tripped circuit breaker is combined with malfunctioning landing gear position lights, or malfunctioning aural warning systems, pilot error by virtue of a lack of information is likely.

On June 7, 1966 the Board forwarded to the Administrator a letter recommending studies to determine the cause of the large number of tripped circuit breakers associated with accidents in which the pilots failed to assure that the landing gear was locked in the down position, or failed to extend the landing gear.

(Failure to extend) Accidents in this classification are those in which the pilot did not operate the landing gear lever or switch to the "down" position, and as a result, the aircraft was landed with the wheels in the retracted position. There were 121 accidents in this classification.

In a few instances the auto-dim feature, or sunlight conditions were factors in the pilots' failure to observe the landing gear position lights. However, these instances are so infrequent that cockpit lighting conditions do not appear to have a significant part in inducing pilot error with respect to the "failed" to extend the landing gear classification of accidents.

What is apparent with respect to the landing-gear position lights is that for various reasons many pilots simply are not using them. As in the previous classification of wheels-up landings, the principal device the pilot is using to determine that the landing gear is locked in the "down" position is the warning horn.

The 43 instances of landing-gear warning-horn failure in this classification, as in the 34 instances in the "failed" to assure the landing gear was locked in the "down" position, indicates a deficiency that certainly induces pilot error. However, because of lack of information in the accident reports, it was not possible to determine if the deficiency is in the design of the horn, the throttle actuated micro-switches, or other components of the aural warning system, or whether the problem is simply inadequate maintenance. In any event, it is likely that a significant reduction in the number of pilot-error, wheels-up landings can be made if the reliability of the aural warning system is improved.

In this regard it is believed that the wing-flaps-actuated device recommended in the Board's letter of June 7, 1966 would contribute substantially to a reduction in the number of wheels-up landings in general aviation aircraft.

As in the previous classification, tripped circuit breakers are considered to have been a factor in producing pilot error. Improvements in this regard would contribute materially to a reduction in pilot-error, wheels-up landing accidents.

Power-on approaches were involved in 33 of the wheels-up landings in this classification, and in five in the previous classification. It is believed that a wing-flaps-actuated aural warning device would contribute substantially to a reduction in wheels-up landings associated with power-on approaches. In this regard, it is interesting to note that at least one general aviation twin-engine aircraft handbook recommends that on the approach normally about 12" of manifold pressure should be maintained to provide a reasonable approach angle. Since the landing gear warning horn microswitches are typically set at 12 inches of manifold pressure, this recommended procedure very nearly defeats the intent of the regulations providing for the aural warning signal if the landing gear is not locked in the down position. If the airplane design is such that power must be used to achieve a "reasonable" descent angle, then this feature can influence the pilot to make a wheels-up landing; or, at the very least, will deprive him of the benefits of one of the devices considered necessary in the interests of safety.

It is recommended that for those aircraft requiring a power-on approach to avoid excessively steep descent angles, the throttle-actuator warning-horn microswitch be set at a manifold pressure high enough to provide adequate aural signal.

(Miscellaneous factors related to wheels-up landings) The problem of identical switches for the landing gear selector and flap selector was apparent in other areas in the course of this study. On a few occasions it was noted that battery master switches were turned off when the pilot intended to turn off the fuel-boost pump. The resulting complete electrical failure influenced wheels-up landings since there was insufficient current to operate the landing gear.

In comparing the selector switch locations in the early model airplanes in which this situation occurred with the selector switches in later models of the same airplane, it was noted that the battery master switch had been moved from its location immediately adjacent to the fuel boost pump switch, and relocated to another part of the panel. Confusion between the two was thus minimized and accidents attributable to this situation are practically eliminated.

While not related to this category of accidents there were other similar situations that came to the attention of the study group in the course of discussions with pilots. In two instances pilots reported that the ignition switches were inadvertently turned off instead of the fuel boost pumps. The

result was an immediate loss of power that could have been critical had it occurred to less experienced pilots. If an accident were to occur for this reason, it could be very difficult to determine the true position of the switches because of severe cockpit disintegration. Accordingly, it is recommended that consideration should be given to discussing at the next Annual Airworthiness Review a requirement for guards to be placed over critical switches that are normally turned on and off only once during a flight. These switches should include, but not necessarily be limited to, the battery master switch, and to toggle-type ignition switches.

Further, consideration should be given to a requirement that these switches should be located remotely with respect to other switches that are used frequently, or which may be turned off during a critical phase of flight, e.g., boost-pump switches which are often turned off during initial climb.

In a few accidents there were comments that the landing gear aural warning signal could not be distinguished from the stall warner. In another instance the stall warner sounded like a radio beacon code signal and was accordingly ignored.

Part of the problem lies in the fact that the same or identical warning horns are used for both purposes. In most instances the landing-gear aural warning is supposed to be identified by its regular, intermittent note generated by the flasher unit. The stall warner, conversely, has an intermittent, supposedly irregular signal which becomes steady when the stall is reached. In practice the intermittent regular landing-gear aural signal is difficult to distinguish from the intermittent, irregular stall warning which the pilot expects. Consequently the signal fails in its intended purpose.

At least one manufacturer has attempted to solve this problem by using separate horns and separate operating frequencies in order to distinguish clearly between the two signals. As a result, the frequency for the stall warner is set at 1000 cycles per second, the frequency of the landing gear warning horn is set at 500 cps. In addition, the landing gear warning horn is connected to a flasher.

It is believed that this is a step in the right direction. However, the situation would be still further improved if the stall warning device could not be mistaken for the landing gear aural signal. As, for example, the case with a stick-shaker for stall warning. A light signal for stall warning will do equally well as far as separating the signals. However, this in turn may be confused with other emergency warning lights.

It is noted that NASA pilots conducting an evaluation of the handling qualities of General Aviation aircraft considered the visual stall warning light to be unsatisfactory and, in some instances, totally inadequate as a result of glare from the sun.

It is recommended that the subject of providing separate non-conflicting distinct warnings for landing gear position and stalls, by devices which do not

require a great deal of discrimination by the pilot, be placed on the agenda for discussion at the next Annual Airworthiness Review.

Nose-over accidents: Many nose-over accidents occurred as a result of gear collapse or groundloop. Therefore, these accidents cannot be considered basically as design-induced pilot error. All other nose-over accidents, which occurred during takeoff or landing, involved hitting soft ground, snow, etc. with either the nose or main wheels, whereas the accidents which occurred during taxiing or static operation involved a quartering tail wind, frequently with gusts, as the pilot started to turn into the wind after taxiing downwind.

Considering the single-engine airplanes only, as would be expected, tail-wheel airplanes had a significantly higher frequency of nose-over accidents than did tricycle-gear airplanes.

Among the tricycle gear airplanes there was a highly significant difference between high-wing and low-wing airplanes. The overall nose-over accident frequency for low-wing airplanes was one such accident per 300 000 hours of flying. In fact, the frequency was too low to permit a statistically significant cmmparison among the different aircraft in this category.

For the high-wing tricycle airplanes, there was some variation depending on the type of airplane. Some had an accident rate as low as the low-wing airplanes, but one very popular model had a frequency above the mean for the group comparable to that of airplanes with tail wheel. The accident files for this particular airplane were thoroughly reviewed to determine the circumstances under which the nose-over accidents occurred. Also, they were compared to the statistics of other similar airplanes (also high-wing-tricycle gear), but with much lower accident rates. Every aspect was carefully investigated (e.g., landing gear geometry, tire sizes, c.g. location, pilots' experience, etc.) and it was concluded that there was no relationship between any of these factors and the frequency of the accidents.

Accidents resulting from hard landing: The hard-landing accident type is defined as one involving stalling or flying into the runway. In general, the primary cause was described as "improper level off", but many of the accidents were precipitated by the following environmental or operational factors:

Gusts, crosswinds, downdraft and turbulence.

"Level off" too high.

High rate of sink with improper flare.

Bouncing or porpoising with inadequate recovery.

Contacting the ground with nose wheel first.

Night landings.

Inadequate short field approach.

The hard-landing accident frequency of two very popular low-wing single-engine tricycle-gear airplanes was much higher than average. A substantial number were caused by the airplane contacting the ground nose-wheel first and/or bouncing or porpoising. In addition, there were several accidents in which the pilot may have landed with the nose wheel in a crabbed attitude. In most of the accidents the damage was confined to the nose gear, the propeller, the engine mount, the cowling, and the wing tips. Relatively few of these accidents resulted in damage to the main landing gear.

Most of these accidents involved students or relatively low-time pilots. It might be rationalized that a relatively low-experience level was the determining factor.

In comparison, a very popular high-wing, tricycle-gear airplane extensively used for instruction had a much lower rate of hard-landing accidents; therefore, "pilot experience" should not be solely responsible for these accidents.

(Relationship to "gear collapse") This type of accident is a structural failure (not a retraction mechanism failure) and it is closely related to hard landings.

Two of the airplanes investigated, both tricycle gear, one high-wing, the other low-wing, had a very high frequency of these accidents, compared with the remainder of the fleet, which suggests a relative weakness of the nose-gear itself, that can be improved by redesign.

It is also interesting to note that those airplanes which had a relatively low frequency of hard landings did not have "collapsed gear"-type accidents.

(Landing approach and flare) Two important factors influencing an airplane's landing approach and subsequent flare are the approach speed, and the lift-to-drag ratio (L/D) in the landing configuration.

The approach speed divided by the stalling speed (Va/Vs) is a measure of the excess airspeed that is required to flare the airplane. The lift-to-drag ratio (L/D) at a given approach speed determines the power setting required to maintain a fixed descent angle. The two ratios can be uniquely related, but in general the lower the lift-to-drag ratio, the higher the approach speed should be.

One of the airplanes investigated (low-wing, four-place) had a relatively high frequency of hard landings with nose-first contact and substantial damage to the nose gear. This was related to improper or inadequate flare, but the investigation did not disclose how the design influences this type of accident.

Another very popular low-wing, two-place aircraft, with a limited elevator control designed to preclude stalls, had a frequency of hard-landing accidents much higher than average. The limited elevator control does not provide the

necessary elevator power for landing flare resulting in hard impact. Since it may be impossible to avert the airplane's descent at relatively low approach speeds, the pilots maintained a large excess speed through the approach. This fast, flat approach increases the likelihood of nose-wheel-first contact.

It would appear that the pilot is faced with a dilemma: if the approach speed is too high, he risks a nose-first contact; if too low, it may be impossible to flare the airplane. To make things worse, some owners limited the full extension of the nose-wheel strut by attaching a cable between torque links to avoid nose-wheel first contacts.

Overshoot accidents: This does not seem to be a significant problem. Nevertheless, the study indicates that twin-engine airplanes have a lower rate of overshoot accidents than single-engine airplanes. The following factors may be involved:

(1) Improved glidepath control on power-on approaches.

(2) Utilization primarily from regular airports.

(3) Higher pilot experience and proficiency.

The wing location (high versus low) does not make a significant difference.

The overshoot accident frequency of two comparable airplanes, both modern design, four-place, low-wing, tricycle-gear type, show that one of them had a larger rate than the other. After analyzing all factors involved, it was found that most of the accidents were on grass or dirt strips, frequently wet or slippery. The airplane with a smaller rate of accidents has an Owner's Manual with charts showing approach speeds, touchdown speeds, and landing distances (based on rather low braking coefficients of 0.1 to 0.2).

On the other hand, the airplane with a higher rate of overshoot accidents has an Owner's Manual which does not spell out touchdown speeds, and the landing distances are based on a large braking coefficient (0.3), resulting in ground-rolls distances as much as three times shorter than the previous airplane. The manuals for both airplanes state that landing distances are for dry, hard-surface runways. Neither provides information on the increase in landing roll to be expected on grass or dirt, either dry or wet.

The ground-rolls based on the low braking coefficients can be achieved under most circumstances, but the ones based on the large (0.3) coefficient cannot be.

Furthermore, the longer distances given for the first airplane would tend to discourage pilots from utilizing short fields, whereas the shorter distances given for the second airplane would encourage such operation.

Based on the above analysis, it was recommended that published landing roll distances be reviewed based on a more conservative braking coefficient, and corrected also for landing on grass or dirt strips.

Undershoot: There was no significant variation among different airplanes. This type of accident is not a major problem, particularly with the twin-engine aircrafts.

One model of a certain line of airplanes had a higher rate than other models of the same line. It was found that this particular model had an increase in weight with no change in flap configuration, resulting in approximately 5% higher stall speed. The approach speed in the Owner's Manual, however, was not changed, resulting in a reduced margin above stall. Numerous pilot statements related the undershoot accidents to "down drafts or gusts" encountered on the final approach. It appears more probable that the pilot, instead, encountered a rapid increase in the rate of sink.

An improved flap was introduced in production in 1961; the statistics for the new models indicate a much lower rate of undershoot accidents. It is recommended that the approach speed for the earlier model be increased to compensate for the heavier weight.

Conclusions:

(Powerplant failure or malfunction) Separate selector switches for fuel tanks and fuel quantity gauges have resulted in the pilots selecting a tank other than that supplying the engine. Location of the fuel-selector valve lever in a position not readily accessible to the pilot has resulted in mispositioning and/or failure to reposition the selector lever.

Engine operation from one tank until the tank is completely empty, as recommended in some Owners Manuals, and failure of the engine to recover quickly after a tank with fuel is selected, have been factors in some accidents. It appears that the time required for recovery of full power in service operation is appreciably greater than that demonstrated in tests and required by FAR 23, especially on low-wing airplanes with fuel injection systems.

Lack of standardization of fuel selector controls, and especially the use of similar controls with opposite sensing is a factor in inducing mispositioning of the selector.

(Accidents Involving Stall, Spin, Spiral, Mush) The frequency of accidents of this type to airplanes certificated under CAR 4a is significantly higher than to airplanes certificated under CAR 3 and FAR 23

For single-engine airplanes certificated under CAR 3/FAR 23, 64% of all accidents of this type occurred during initial climb on take-off or go-around.

Cross-winds appeared to be a major factor in stalls on take-off and

go-around for at least one of the airplane types studied.

Take-off data in Owners Manuals were found to be inadequate in general, and this appears to be a factor in many stall accidents on take-off that are charged to pilot error.

In general, stall accidents are not a problem on twin-engine airplanes. One airplane model did have an accident frequency appreciably higher than the others, primarily involving inadvertent spins in single-engine operation.

(Ground-Loop Accidents) Tricycle gear airplanes in general had a significantly lower frequency of ground-loop accidents than airplanes with tail wheels.

Two airplanes with tricycle gear had a ground-loop accident frequency significantly higher than any other airplane of this configuration, and comparable to that of tail-wheel airplanes.

It appears that the relatively high ground-loop frequency of the above two airplanes may have been influenced by detail design of the nose-gear configuration.

(Accidents involving retractable landing gear). The majority of accidents related to inadvertent retraction involved qualified pilots who inadvertently operated the landing gear control instead of the wing-flap control.

Pilots may be placing considerably more reliance on landing gear safety switches than is warranted. In any event the degree of protection deserved to preclude inadvertent retraction and that actually afforded,should be reviewed, resolved, and clarified at the next Annual Airworthiness Review.

Automatic dimming of the landing gear position lights, when navigation lights are turned on, can induce pilot error under certain conditions of light.

Pilots are apparently relying more on the aural warning signal rather than lights to detect an unsafe gear condition. In many instances, however, the warning horns did not function for various reasons. In addition, power approaches have precluded the horn from being heard until too late to prevent a wheels-up landing.

Tripped landing-gear circuit breakers combined with malfunctioning landing-gear position lights or malfunctioning aural warning systems tend to induce pilot error.

In practice, pilots experience some difficulty in distinguishing the intermittent regular landing gear aural signal from the intermittent irregular stall warning.

(Nose-over accidents) First type nose-over accidents are not a problem

on the twin-engine airplanes or the single-engine, low-wing airplanes with tricycle landing gear studied in this report.

One high-wing tricycle gear airplane had a first type nose-over accident frequency that was significantly higher than that of any other airplane of this configuration, and comparable to the frequency of airplanes with tail wheels. Factors involved in the accidents to this one airplane are discussed in the report.

(Hard landings) A review of the accidents involving two airplanes having the highest frequency of hard landings (both tricycle configurations) discloses frequent occurrence of damage to the nose gear and related structure. Relatively few involved main landing gear damage such as might be sustained under severe vertical impact loads.

(Overshoot accidents) Some airplane Owners Manuals do not contain information or correction factors for landing distances on other than dry, hard surface runways, nor do they specify the touchdown speeds upon which such distances are based. In addition, the landing distances given in at least one manual do not appear compatible with the proficiency of General Aviation pilots as a whole and may influence the overshoot by encouraging landings in relatively short fields.

(Undershoot accidents) Only two of the airplanes in the study had a significant frequency of undershoots. The causes of those involving one of the airplanes appeared related to inadequate approach speeds which may have been based on information in the airplane flight manual.

Note: The preliminary design of a Far Term conceptual airplane was influenced by the findings of this report. The airplane illustrated in Figure 146 on page 209, features tricycle landing gear and a low wing configuration. Additionally, to minimize post-crash fire, the fuel is carried in the outboard wing panels.

Cost Considerations

Before initiating the actual predesign of the conceptual aircraft in Phase II, several cost analyses were undertaken to determine: (1) the operating cost sensitivity of such items as configuration, selection of structural concept, and saving a pound of weight; (2) the relationship of structural cost to the overall price; (3) the effect of labor savings and/or mass production. The above analyses are discussed in detail in the order listed:

Operating costs
Fixed versus retractable landing gear
Reciprocating versus turboprop engines
Fixed pitch versus constant speed propellers
Strut-braced versus cantilevered wings
Value of a pound saved
Airframe costs
Consumer price breakdown
Effect ~~of labor savings~~/mass production

Operating costs.- The operating cost of any airplane or helicopter is made up of: (1) indirect or fixed costs which accrue whether the aircraft is flown or not; and (2) direct operating costs which are strictly a function of flying time.

Referring to Figure 59, the fixed indirect operating costs (I.O.C) include

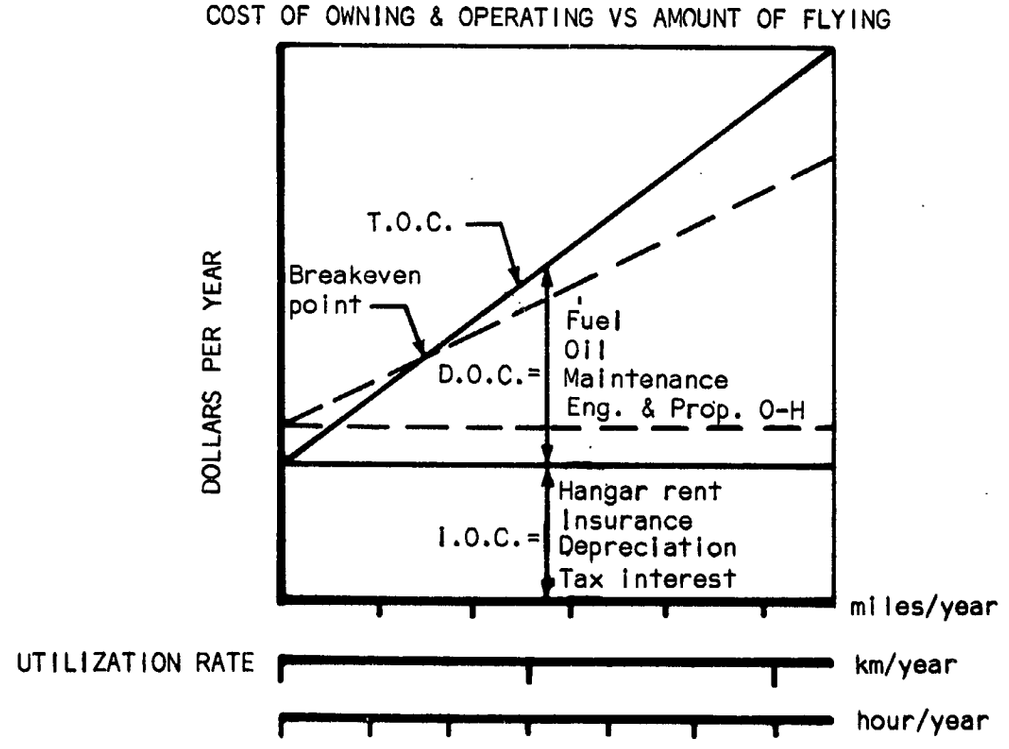


Figure 59

such items as hangar rent, insurance, depreciation, interest, and tax. The variable direct operating costs (D.O.C.) include such items as fuel, oil, maintenance, and engine and propeller overhaul. The total operating cost (T.O.C.), for any particular utilization rate, is the sum of the I.O.C. and the D.O.C.

Several configuration variations will be analyzed in the following paragraphs, on the basis of operating cost. When comparing the operating costs of two or more aircraft, it is convenient and of particular significance to determine if, and at what utilization rate, the respective T.O.C.'s are equal. If the D.O.C.'s are equal, there will never be a break-even point. Conversely, if the D.O.C.'s are unequal, there will be a break-even point, or point of equal total operating cost (T.O.C.). Referring to Figure 59, a second aircraft, with a different I.O.C. & D.O.C., is indicated in broken lines. The resulting "break-even point" is indicated.

Figures 60, 61, and 62 illustrate the relative magnitudes of the various operating costs for a typical light airplane, light piston powered helicopter and light turbine powered helicopter. Note that operating costs are presented in terms of both dollars per hour and dollars per mile.

OPERATING COST BREAKDOWN FOR TYPICAL LIGHT 4-PLACE AIRPLANE
(333 HRS/YR UTILIZATION)

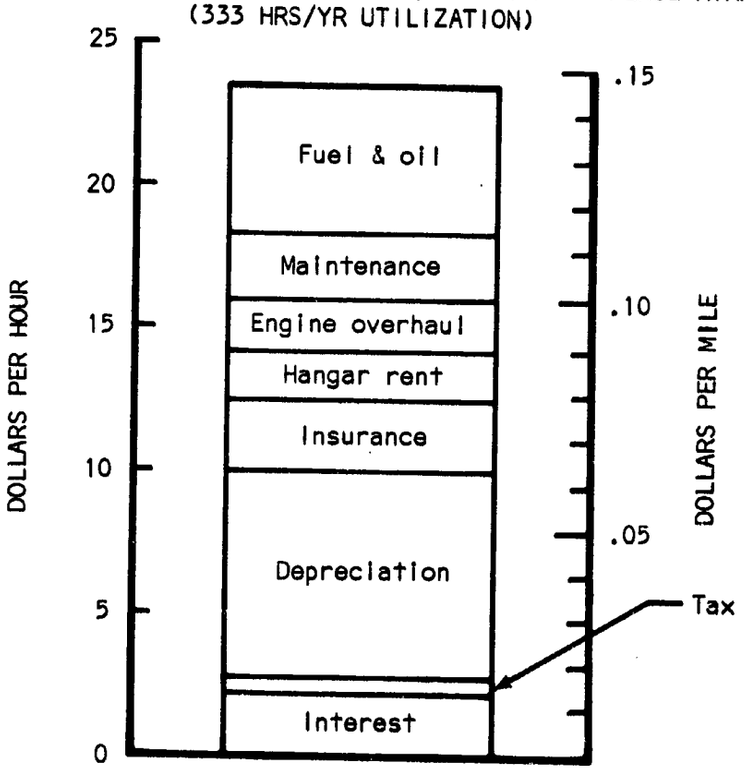


Figure 60

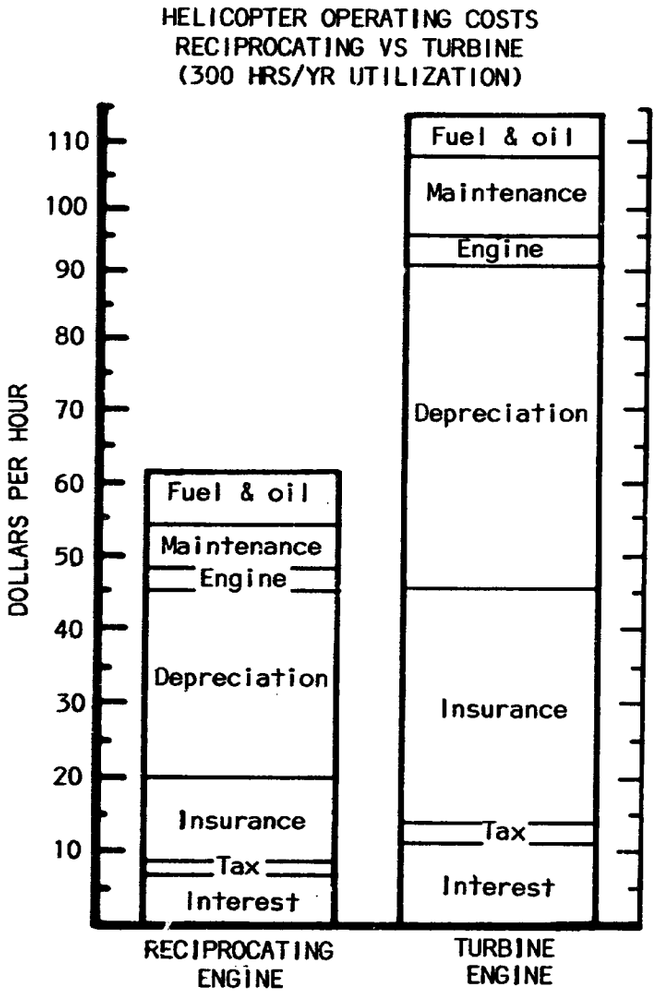


Figure 61

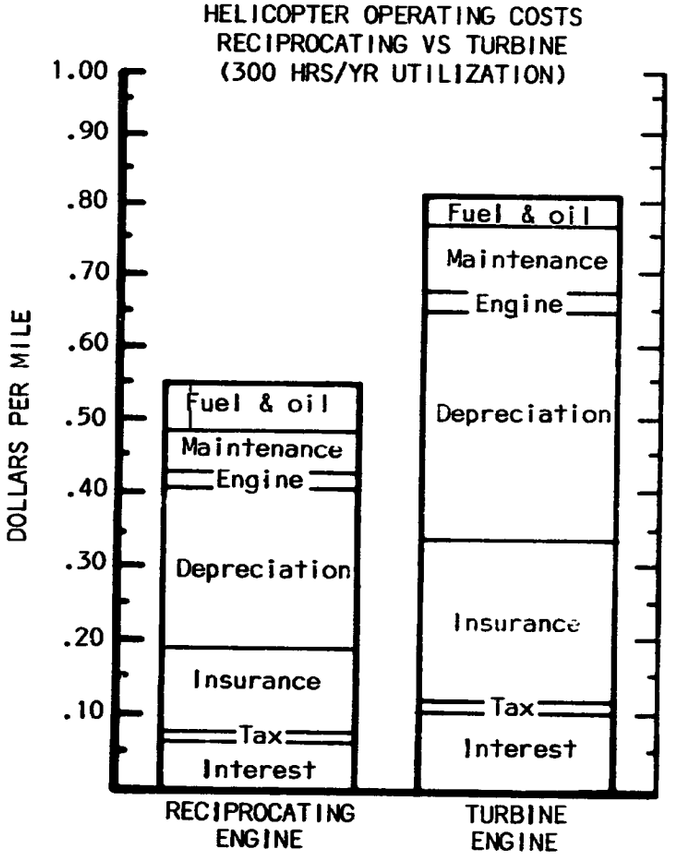


Figure 62

Fixed versus retractable landing gear.- To determine the relative economics associated with fixed and retractable landing gear light airplanes, three pairs of contemporary airplanes, designated A, B, and C, were compared. These airplane pairs are nearly identical, respectively.

TABLE VIII. - FIXED VS RETRACTABLE LANDING GEAR, PERFORMANCE COMPARISONS FOR THREE AIRPLANE PAIRS

ITEM	Fixed Gear	Retract. Gear	Difference
Designation	A_f	A_r	---
Basic price	$23,995	$25,975	$1,980
Top speed	174 mph	198 mph	24 mph
Cruise speed	163 mph	190 mph	27 mph
Range	910 s. mi.	1010 s. mi.	100 s.mi.
Empty weight	1785 lbs	1865 lbs	80 lbs
Useful load	1810 lbs	1435 lbs	375 lbs
Gross weight	3600 lbs	3300 lbs	300 lbs
Rate of climb	920 fpm	1115 fpm	195 fpm
Service ceiling	14,800 ft	18,300 ft	3500 ft
Engine	285 hp	285 hp	---
Propeller	Constant Speed	Constant Speed	---
Designation	B_f	B_r	---
Basic price	$14,995	$18,250	$3255
Top speed	147 mph	190 mph	43 mph
Cruise speed	139 mph	178 mph	39 mph
Range	800 s. mi.	920 s. mi.	120 s. mi.
Empty weight	1475 lbs	1525 lbs	50 lbs
Useful load	1100 lbs	1050 lbs	50 lbs
Rate of climb	780 fpm	800 fpm	20 fpm
Service ceiling	12,000 ft	17,200 ft	5,200 ft
Engine	180 hp	180 hp	---
Propeller	Constant Speed	Constant Speed	---
Designation	C_f	C_r	---
Basic price	$13,900	$16,900	$3,000
Top speed	152 mph	170 mph	18 mph
Cruise speed	143 mph	162 mph	19 mph
Range	760 s. mi.	995 s. mi.	235 s. mi.
Empty weight	1270 lbs	1380 lbs	110 lbs
Useful load	1130 lbs	1120 lbs	10 lbs
Gross weight	2400 lbs	2500 lbs	100 lbs
Rate of climb	750 fpm	875 fpm	125 fpm
Service ceiling	16,400 ft	15,000 ft	1400 ft
Engine	180 hp	180 hp	---
Propeller	Fixed Pitch	Constant Speed	---

In general, it can be concluded that: (1) The retractable gear airplanes have a greater rate of climb, range, service ceiling, and cruise speed, all due to the lower drag. (2) The fixed gear airplanes have in general a greater useful load, allowable gross weight, and a lower empty weight and price. (3) The reliability of the airplane is reduced when a hydraulic or mechanical

system is added and maintenance costs are increased. (4) The insurance rates are higher because the retractable gear costs more, and there is always a chance of gear-up landings. (5) With the trend away from tail wheel gear toward tricycle gear, retraction becomes more desirable in order to reduce drag.

The cost of owning and operating versus utilization rate was determined for these three airplane pairs. Direct and indirect operating costs (per year) were plotted against miles and hours per year to determine their break-even points. I.e., the utilization at which the sum of the lower indirect and higher direct operating costs on the fixed gear airplane equal the sum of the higher indirect and lower direct operating costs on the retractable gear airplane. See Figures 63, 64, and 65.

Due to the difference between the depreciation rate normally used during the first five years of ownership and that normally used thereafter (i.e., 12% and 5%, respectively), break-even points were determined for both of these conditions. For the first five years of ownership, the break-even points for the three airplane pairs are:

Pair	Miles/year	Hours/year (fixed)	Hours/year (retractable)
A	32,400	199	170
B	75,600	544	425
C	98,200	686	606

Similarly, the break-even points for ownership after the first five years are:

Pair	Miles/year	Hours/year (fixed)	Hours/year (retractable)
A	26,600	163	140
B	42,000	302	236
C	49,600	347	306

See appendix K

The preceding break-even points would be reduced if the value of a man's time saved is considered. Many methods of determining the value of his time could be used, but a generally accepted formula is:

VMH (or value per man-hour) = 2.5 x yearly ernings/2000 hours

Referring to Figure 66, and recognizing the value of a man's time, the resulting affect on airplanes B_r and B_f is an earlier break-even point from 75600 miles/year to 9070 miles/year. This new break-even point, converted to hours per year for each airplane is:

A_f = 9070 mi/yr ÷ 139 mi/hr = 65 hr/yr

A_r = 9070 mi/yr ÷ 178 mi/hr = 51 hr/yr

There can be no doubt then, of the economy provided by a retractable landing gear airplane.

OPERATING COST VS UTILIZATION RATE FOR AIRPLANE PAIR A
(with fixed and retractable landing gear)

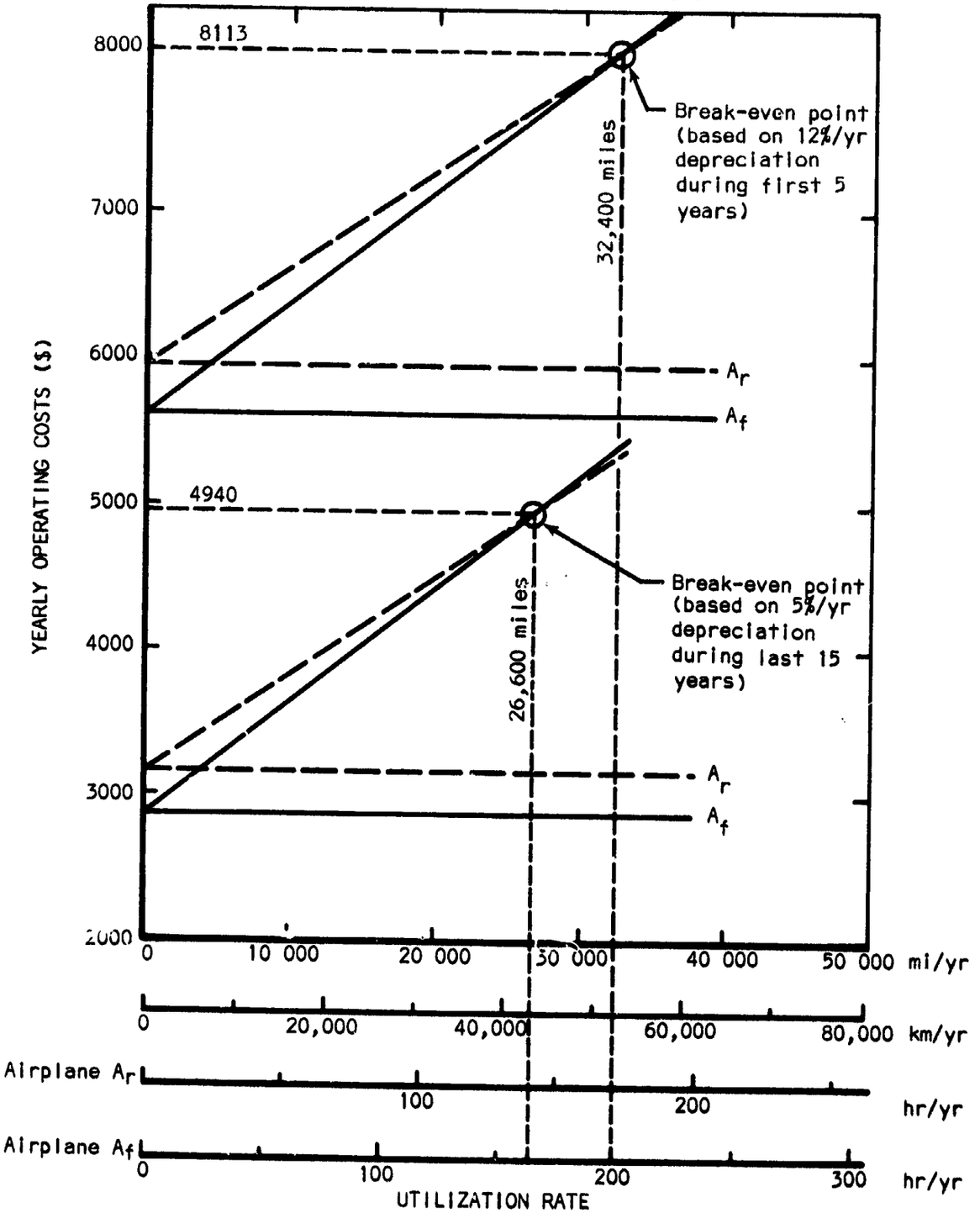


Figure 63

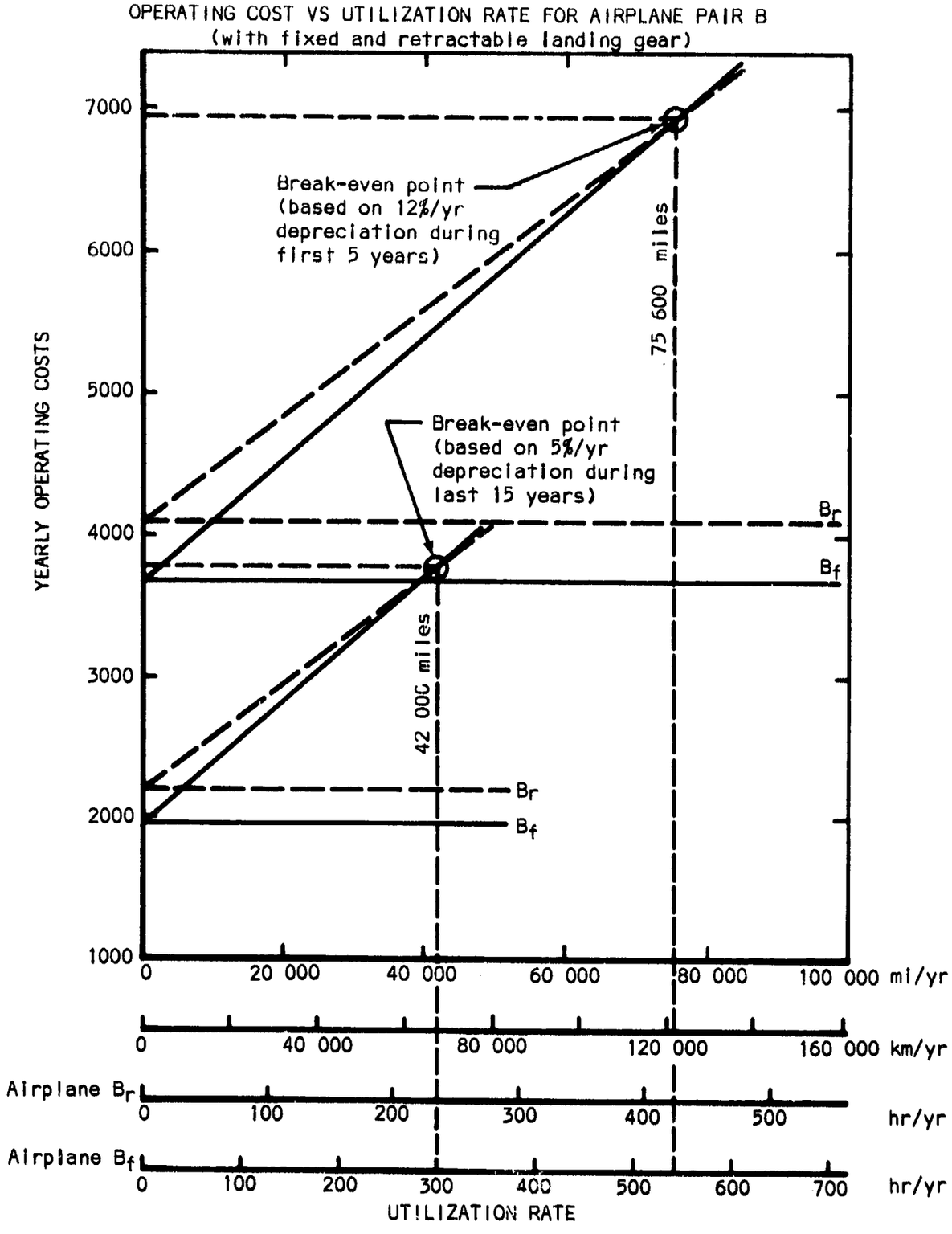

OPERATING COST VS UTILIZATION RATE FOR AIRPLANE PAIR B
(with fixed and retractable landing gear)
YEARLY OPERATING COSTS
7000
6000
5000
4000
3000
2000
1000
Break-even point
(based on 12%/yr
depreciation during
first 5 years)
75 600 miles
Break-even point
(based on 5%/yr
depreciation during
last 15 years)
Br
Bf
42 000 miles
Br
Bf
0
20 000
40 000
60 000
80 000
100 000 mi/yr
0
40 000
80 000
120 000
160 000 km/yr
Airplane Br
0
100
200
300
400
500
hr/yr
Airplane Bf
0
100
200
300
400
500
600
700
hr/yr
UTILIZATION RATE

Figure 64

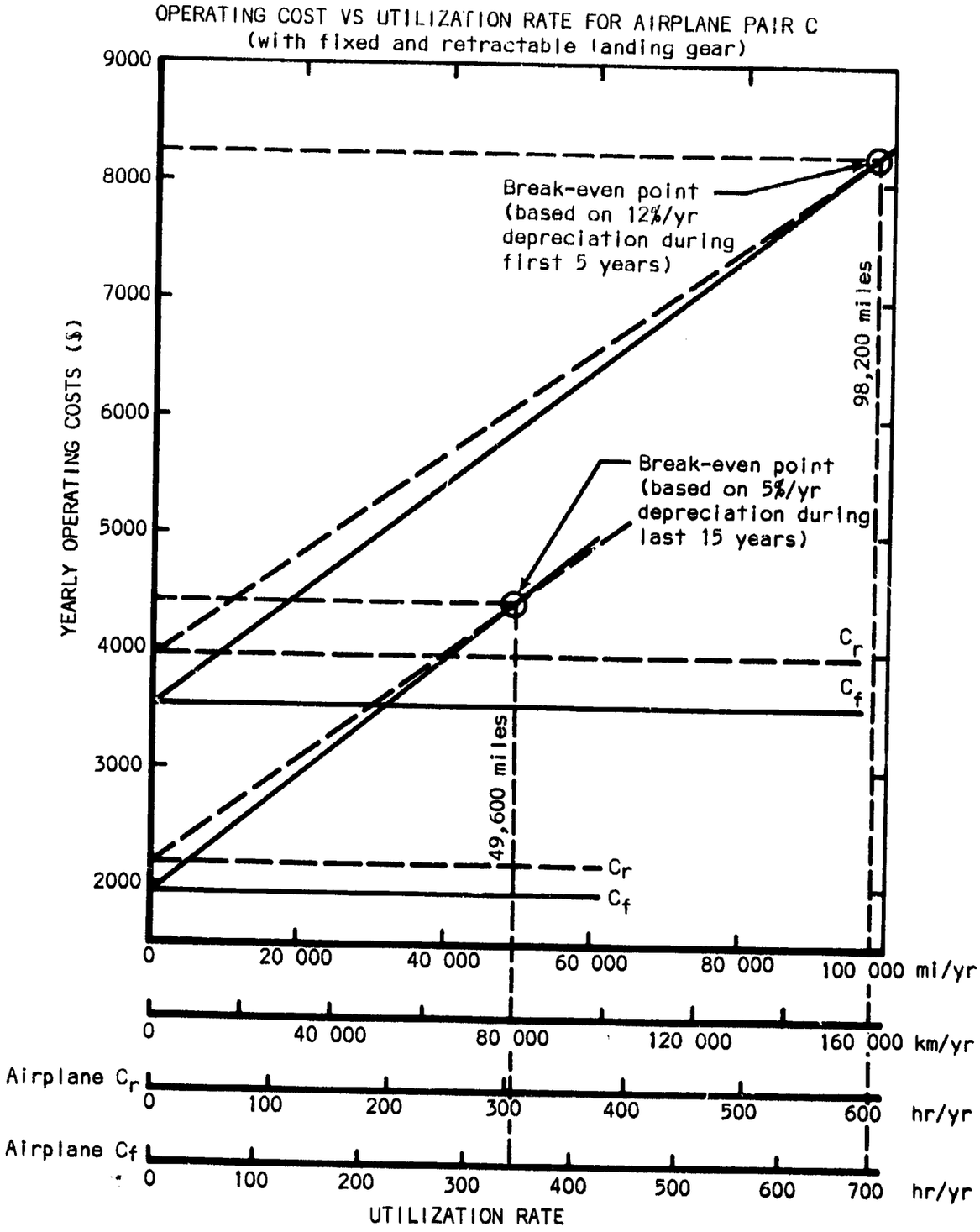

OPERATING COST VS UTILIZATION RATE FOR AIRPLANE PAIR C
(with fixed and retractable landing gear)
YEARLY OPERATING COSTS ($)
9000
8000
7000
6000
5000
4000
3000
2000
Break-even point
(based on 12%/yr
depreciation during
first 5 years)
98,200 miles
Break-even point
(based on 5%/yr
depreciation during
last 15 years)
C_r
C_f
49,600 miles
C_r
C_f
0
20 000
40 000
60 000
80 000
100 000 mi/yr
0
40 000
80 000
120 000
160 000 km/yr
Airplane C_r
0
100
200
300
400
500
600 hr/yr
Airplane C_f
0
100
200
300
400
500
600
700 hr/yr
UTILIZATION RATE

Figure 65

OPERATING COST VS UTILIZATION RATE WHEN CONSIDERING THE VALUE OF A MAN'S TIME
(for airplane pair B, with fixed and retractable landing gear)

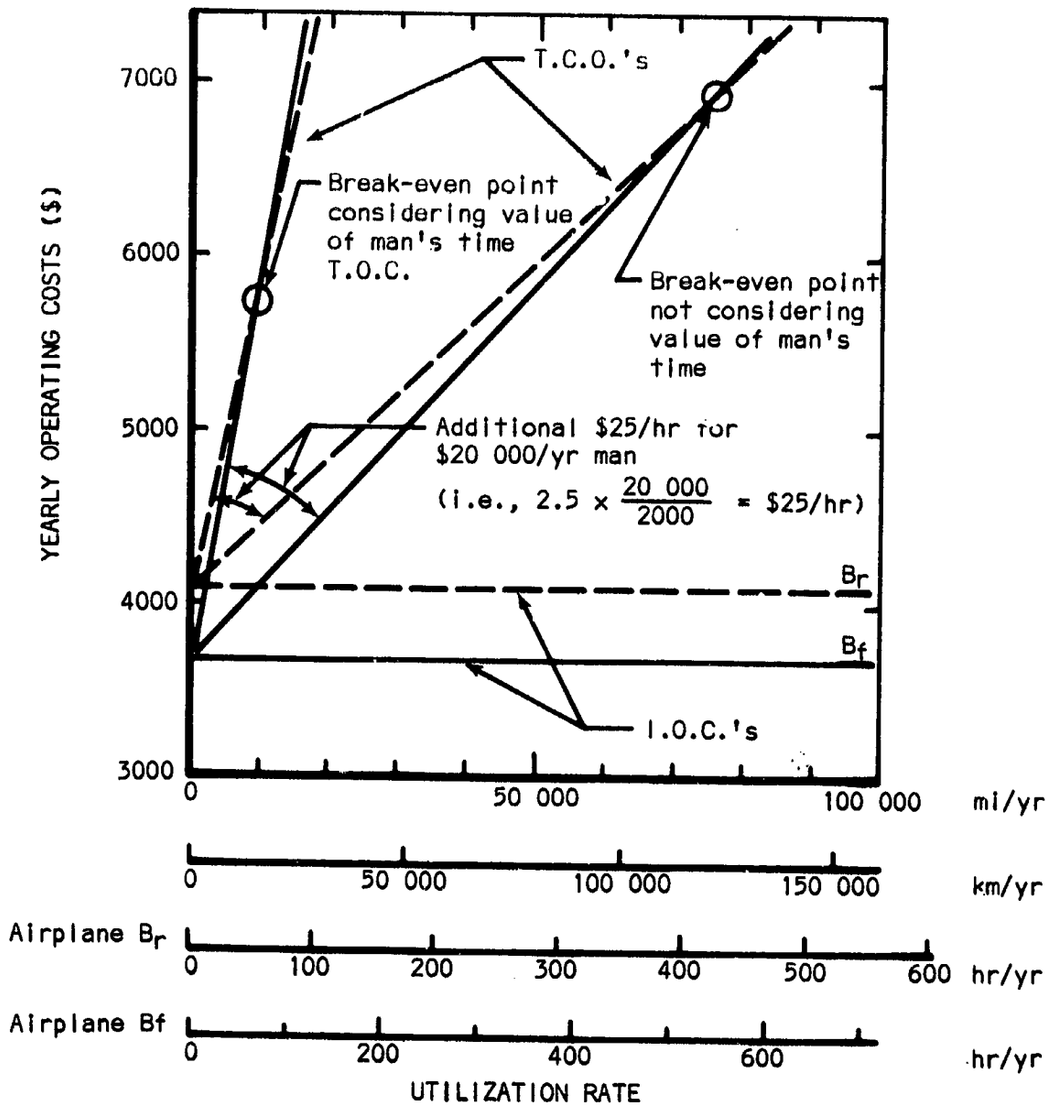


Figure 66

In conclusion, it appears that the retractable gear airplane A_r has the lowest breakeven point. This is due primarily to (1) the significant cruise speed differential between A_r and A_f; (2) The fact that a lower interest rate is available on the A_r airplane, which is in a higher price category than A_f, B_r, B_f, C_r, and C_f; and (3) the fact that the A airplanes have direct operating costs from one and one-half to twice that of the other airplane pairs.

Reciprocating versus turbo-prop engine airplane.- Figure 67 compares operating costs for turbo-prop versus reciprocating engine powered airplanes. The turbine engine costs are assumed to be the same as those used in contemporary helicopters.

TYPICAL OPERATING COSTS VS UTILIZATION FOR RECIPROCATING AND TURBINE AIRPLANES

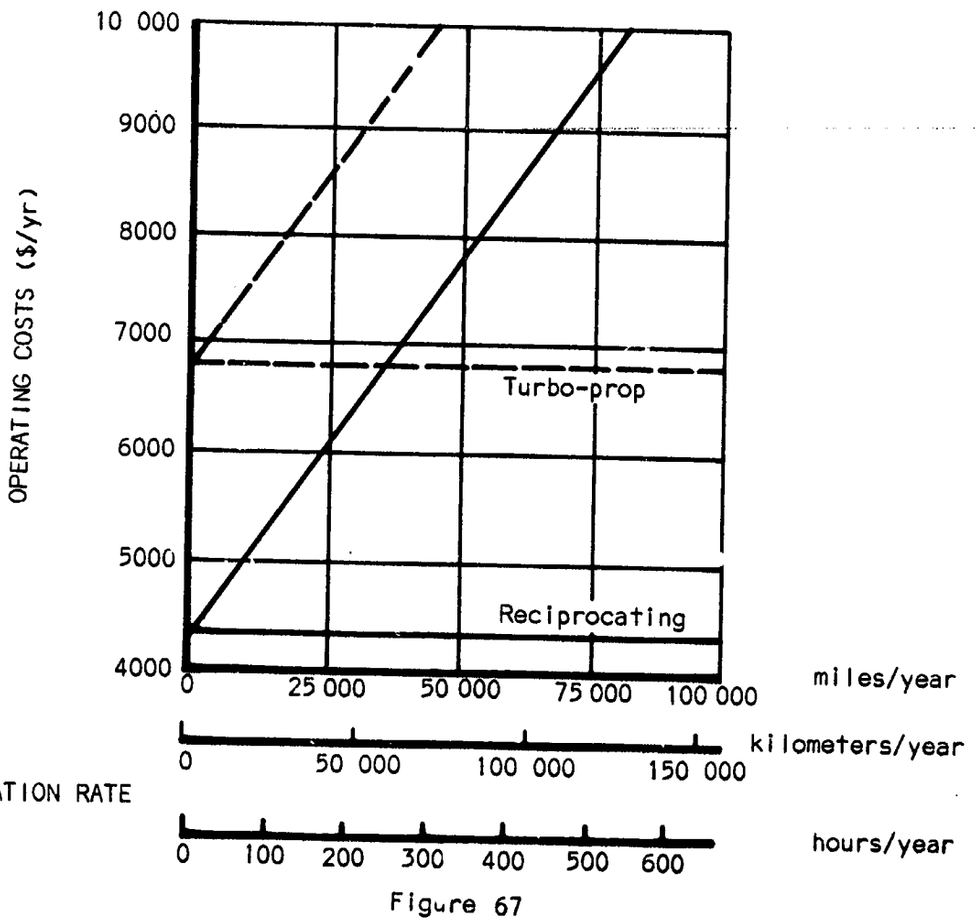


Figure 67

Inspection of the total operating cost for the reciprocating engine-powered airplane and the turbine-powered airplane in Figure 67 clearly indicates that the reciprocating engine airplane is the logical economic choice. See Appendix L .

The reasons for the turbine airplane's higher costs are as follows: (1) The initial cost of the turbine engine is approximately $13,000.00 more than for a reciprocating engine (250 hp); probably because of higher material costs and lower production rates. (2) The overhaul cost for the turbine engine (based on a 1500 hr TBO or time before overhaul) is higher than for a reciprocating engine.

Figures 67 illustrates that the total operating cost curves for the turboprop and reciprocating engine airplanes diverge. Therefore, at present day costs, it is always more expensive to own and operate a single-engine turbo - prop light airplane.

Fixed pitch versus constant speed propeller.— The cost of owning and operating airplanes with fixed pitch and/or constant speed propellers (and which approximate the airplane guidelines in Appendix M) was determined and the

TABLE IX - TYPICAL OPERATING COSTS FOR AIRPLANES WITH FIXED PITCH AND CONSTANT SPEED PROPELLERS

Item	Constant speed propeller		Fixed pitch propeller	
Consumer price	$17,000 *		$16,800 *	
Direct operating costs (hrly)				
Fuel (@43¢ per gallon)	11.47 gph	4.93	11.89 gph	5.11
Oil (3/4 pint/hr @60¢/qt)		.22		.22
Inspection & maint.		1.72		1.75
Engine & prop.overhaul (1200 hrs)		2.50		2.33
Total direct operating costs		9.37		9.41
Cruise speed	150 mph		150 mph	
Cost per mile				
Gross weight	3014 lbs		3100 lbs	
Horsepower	250 hp		250 hp	
Indirect operating cost (yrly)				
Hangar rent ($40/mo.)		$ 480		$ 480
Insurance (4% + $215)		895		855
Depreciation (12% x price)		2040		1920
Tax ($7.70/1000 valuation)		131		129
Interest (80% x price x 5.5%)		748		739
Total indirect operating costs		$4294		$4123
Wing area	208 ft^2		244 ft^2	

*The net difference in consumer prices includes propeller cost difference (for the constant prop. assy, governor and prop. controls = $600) and cost of additional wing area = $400. Assuming equal performance on both models.

results are listed in Table IX. The analysis indicates that a constant speed propeller is more desirable, for the following reasons:

(1) Lower direct operating costs.
(2) Smaller wing (less 36 ft^2).
(3) Lighter airplane (less 86 lbs).

In this analysis the performance was held constant and the configuration was varied. Takeoff and climb performance are the conditions which necessitate the configuration changes.

The constant speed propeller costs approximately $600 more, as an option, than fixed pitch; but the additional wing area and weight cost on the fixed pitch airplane costs approximately $400. Therefore, the initial cost differential is approximately $200 more for the constant speed propeller airplane.

TABLE X - TYPICAL OPERATING COSTS FOR CANTILEVERED AND STRUT-BRACED WING AIRPLANES

Item	1967 Model Cantilevered Wing	1966 Model Strut Braced Wing
Direct operating costs (hrly)		
Fuel (43¢/gal)	$ 6.71 15.6 gph	$ 6.79 15.8 gph
Oil (3/4 pt/hr at 60¢/qt)	.22	.22
Inspection & maint.	1.75	1.75
Engine & Prop. overhaul	3.83	3.83
Total direct operating costs	$12.51	$12.59
Consumer price	$ 26,864 *	$ 25,975
Indirect operating costs (yrly)		
Hangar rent ($40/mo.)	$ 480	$ 480
Insurance	1289	1254
Depreciation	3224	3110
Tax	207	200
Interest	1020	989
Total indirect operating costs	$6220	$6033
Cruise speed	192 mph	190 mph
Cost per mile	$.0651/mi	$.0663/mi

Break-even point

Cantilever: .0651 d + 6220 = Strut braced: .0663 d + 6033

d = 156,000 miles/yr or 813 hour/yr

*Reduced from $27,975 to exclude inflation and style changes.

Strut-braced versus cantilevered wings.- The analysis of strut-braced wings versus cantilevered wings resolves into two main considerations:

(1) Increased initial price for cantilevered wing.
(2) Direct operating cost savings realized by cantilevered wing.

Referring to Table X , the consumer price for a typical cantilevered model is $2,000.00 higher than the price for a comparable (earlier) strut-braced model. Twelve hundred twenty dollars of this difference were attributed to the cantilevered wing and styling changes. The remainder was attributed to inflation. To rationalize the increased expenditure, the owner of a cantilevered wing airplane would have to increase his flying time per year to 813 hours, which is 4.7 times more than the 175-hour average for U.S. General Aviation.

Referring again to Table X , the pure operating cost savings of $40.00 do not justify the indicated increase in consumer price, unless the airplane is utilized more than 813 hours per year.

Airframe cost.- The price per pound of empty weight for most of the light helicopters in U.S. production is plotted against empty weight in Figure 68. The only conclusions that can be drawn are: (1) That reciprocating engine powered helicopters cost between $23.00 and $33.00 per pound empty; (2) that turbine powered helicopters cost $60.75 and $75.75 per pound empty; and (3) that the price per pound empty of helicopters is apparently not a function of empty weight.

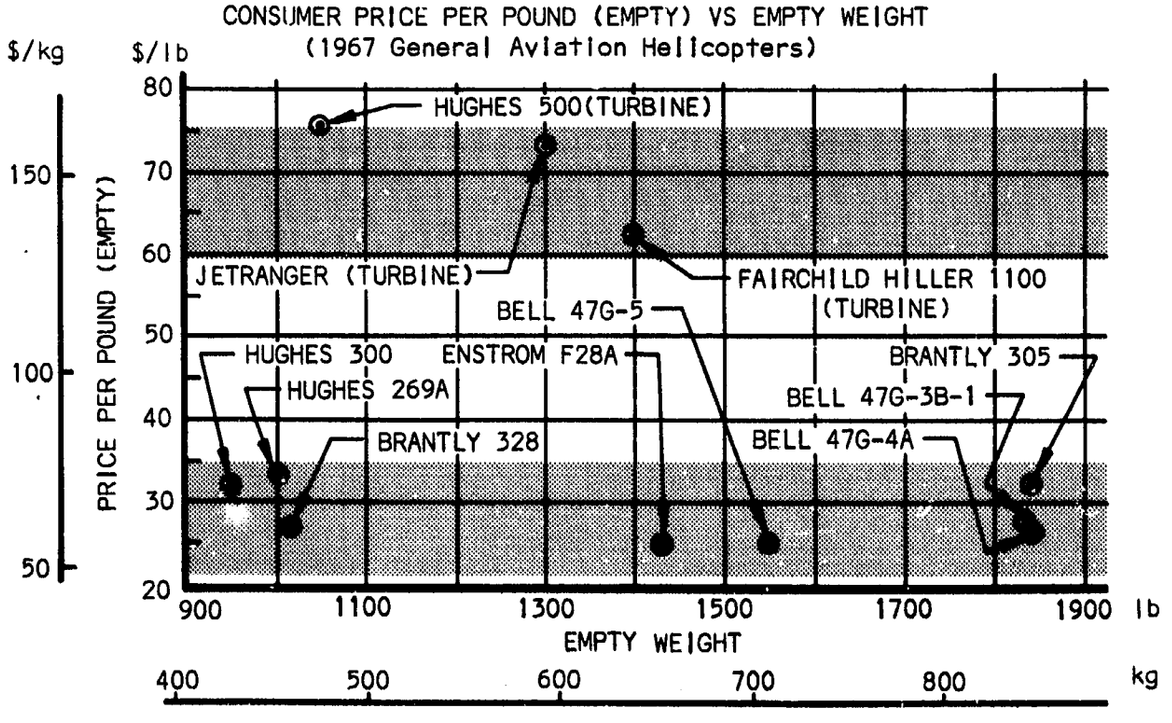


Figure 68

The price per pound of empty weight for most of the light airplanes in U.S. production is plotted against empty weight in Figure 69. It varies from about $8.00/lb to about $27.00/lb.

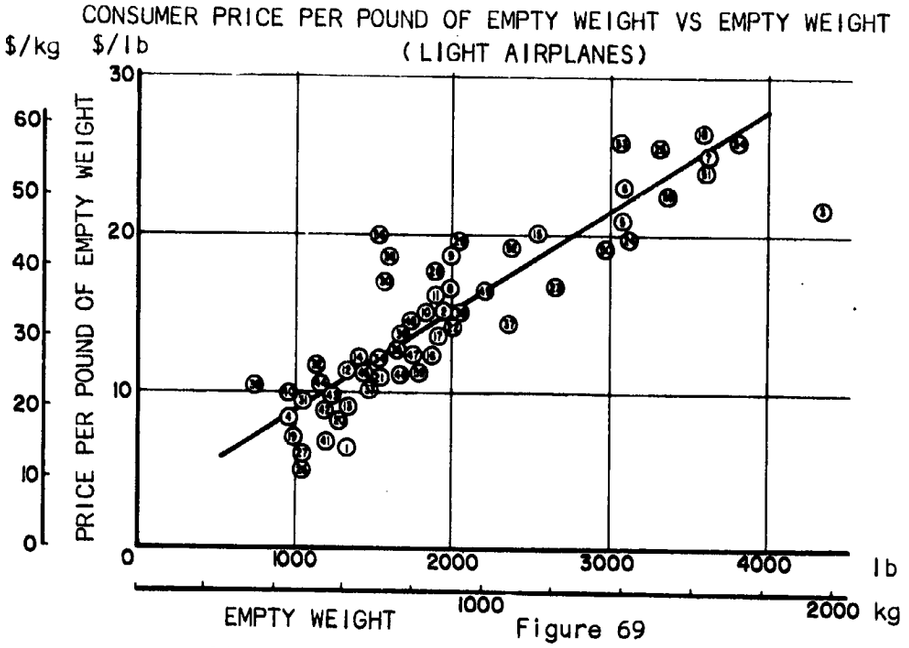


Figure 69

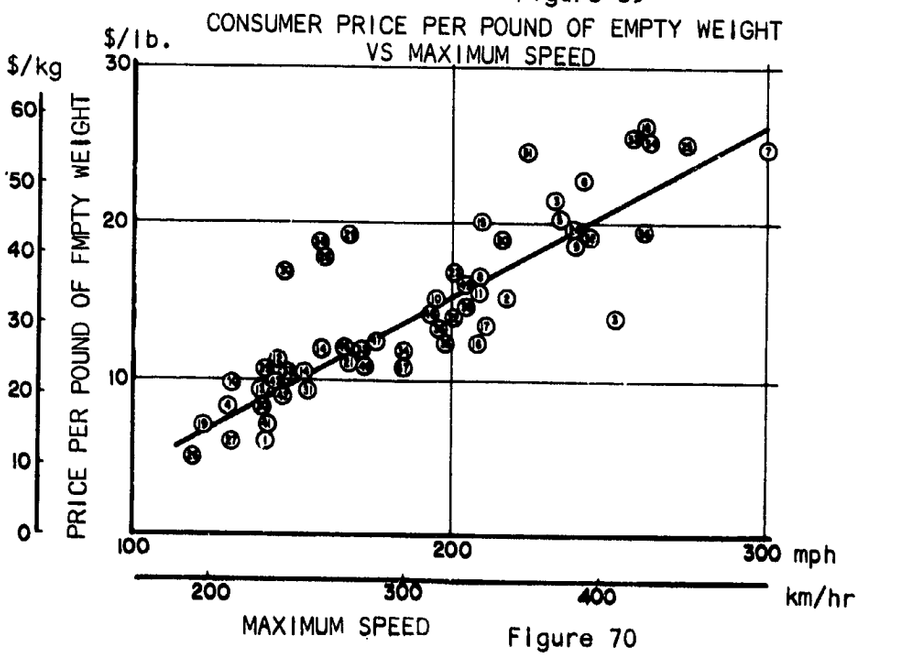


Figure 70

The price per pound of empty weight of most of the light airplanes in U.S. production is plotted against maximum speed, in Figure 70. The cost varies from about $6.00/lb at 115 mph. to $27.00/lb at 300 mph.

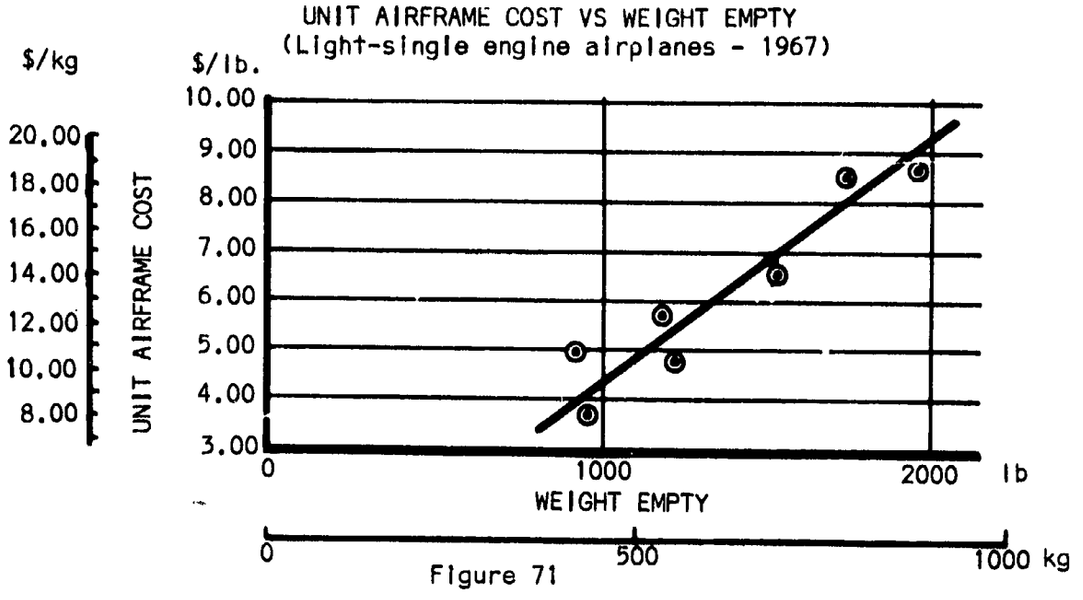


Figure 71

The cost per pound of airframe for some representative light airplanes in U.S. production is plotted against empty weight in Figure 71.

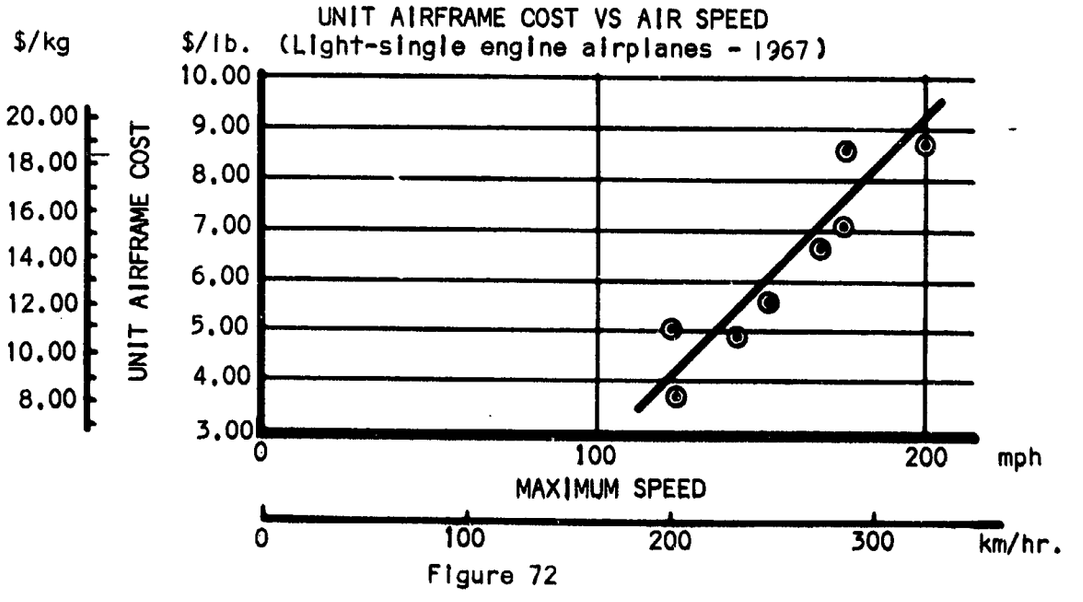


Figure 72

The cost per pound of airframe for some representative light airplanes in U.S. production is plotted against maximum speed in Figure 72. It varies from $3.90/lb to $9.25/lb.

Based on manufacturer's suggested retail prices and on catalog wholesale prices, the airframe (structure) cost of the various main components of typical light airplanes has been determined. Figure 73 illustrates the cost per pound of structure for: the wing, tail group, fuselage, and landing gear.

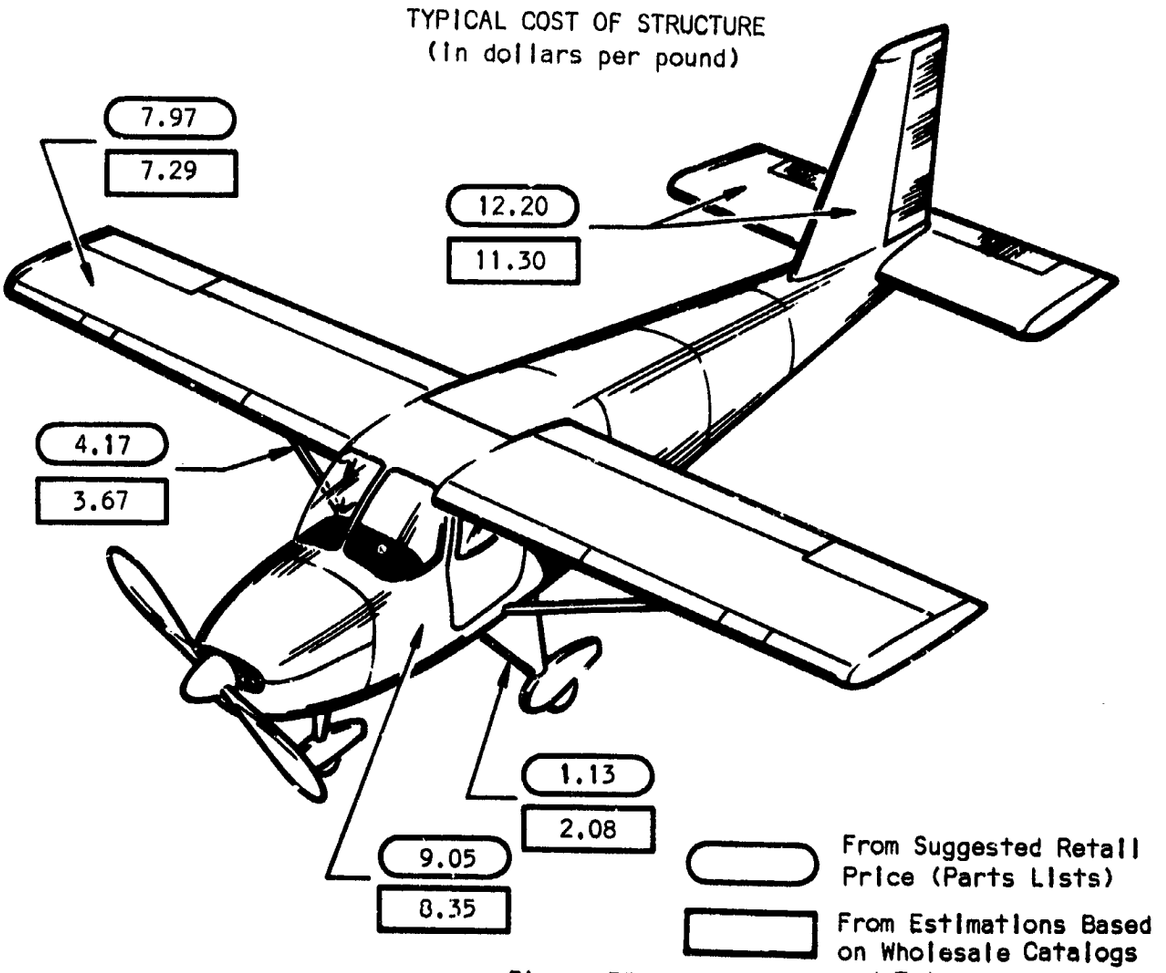


Figure 73

Value of a pound saved. - To determine the worth of a pound saved on a light airplane, two contemporary light airplanes, having identical powerplants and cruise speeds but different gross weights, were compared (for a twenty-year service life and a 333-hours-per-year utilization rate). See Table XI.

Airplane B is 140 pounds lighter than airplane A, by virtue of a greater design effort expended on a greater quantity of individually lighter detail

TABLE XI - VALUE OF A POUND SAVED (for a 20 year service life)

SPECIFICATIONS	AIRPLANE A (HEAVIER)	AIRPLANE B (LIGHTER)
Weight	3014 lb	2875 lb
Cruise speed	150 mph	150 mph
Engine hp	250 hp	250 hp
Fuel consumption	11.47 gph	11.25 gph
Consumer price	$17,000	$XX,XXX (see below)
DIRECT OPERATING COSTS (HOURLY)		
Fuel and oil	$5.34	$5.25
Maintenance	$2.35	$2.35
Engine overhaul	$1.88	$1.88
Total D.O.C	$9.57/hr	$9.48/hr
INDIRECT OPERATING COSTS (YEARLY)		
Hangar rent	$480	$480
Insurance(4% + $215)	.04 x $17000+$215 = $895	.04 x Price + $215 =
Depreciation(5yr,40% residual)		
First 5 years	.12 x $17000 = $2040	.12 x price =
Last 15 years	.35/15 x $17000 = $ 397	.35/15 x price =
Tax ($7.70/1000 value)	.0077 x $17000 = $ 131	.0077 x price =
Interest (first 5 years only @ 80% x 5.5%)	.044 x $17000 = $ 748	.044 x price =
Total I.O.C.		
First 5 years	.1717 x$17000+$695	.1717 x price+$695 =
Following 15 yrs	.3607 x$17000+$695	.3607 x price+$695 =

parts. Additionally, these parts are likely made from structurally more efficient, and more expensive, materials.

The direct operating cost of the heavier airplane A is $0.09 more than that of the lighter airplane B, due entirely to the greater fuel consumption of airplane A.

The indirect operating costs of the lighter airplane B are greater since they are identical respective functions of a higher consumer price.

The higher consumer price of the lighter airplane B is solved for by equating the total operating costs for the two airplanes, in terms of consumer price for airplane B. I.e.,

Assuming: No interest after 5 years and,
Depreciating to 5% (scrap value),

$$(T.O.C.)_A = (T.O.C.)_B$$

$$\left.\begin{array}{l} 20\text{yr}(333\text{hr} \times \frac{\$9.57}{\text{hr}} + .0477 \times \$17000 + \$695) \\ + 5\text{yr}(.12 \times \$17000 + .044 \times \$17000) \\ + 15\text{yr}(.35/15\text{yr} \times \$17000) \end{array}\right\} = \left\{\begin{array}{l} 20\text{yr}(333\text{Hr} \times \frac{\$9.48}{\text{hr}} + .0477 \times \text{price} + \$695) \\ + 5\text{yr}(.12 \times \text{price} + .044 \times \text{price}) \\ + 15\text{yr}(.35/15/\text{yr} \times \text{price}) \end{array}\right.$$

$$\left.\begin{array}{r} \$\ 93\ 854 \\ 13\ 940 \\ 5\ 950 \\ \hline \$113\ 744 \end{array}\right\} = \left\{\begin{array}{l} .954\ \text{price} + \$77\ 037 \\ .820\ \text{price} \\ .350\ \text{price} \\ \hline 2.124\ \text{price} + \$77\ 037 \end{array}\right.$$

$$2.124\ \text{price} = \$113\ 744 - \$77\ 037$$

$$\text{Price} = \$17\ 284$$

$$\frac{\$284}{140\ \text{lb}} = \$2.03/\text{lb}$$

The price differential for airplane B, at which the higher indirect operating costs exactly compensate the lower direct operatings costs, represents the dollar amount that can be spent for its 140 pounds of weight saved. I.e., \$17284 - \$17000 = \$284 for 140 pounds saved, or \$2.03 per pound.

Note that the \$2.03/pound is for a 333 hours/year utilization rate and a 20-year service life. The worth of a pound saved is directly proportional to service life and utilization rate. Refer to Figure 74 for dollar value per pound saved, for service lives and utilization rates, ranging from five to thirty years and from 100 to 900 hours per year, respectively.

The same process was repeated for both piston-powered and turbine-powered helicopters, the results of which are illustrated in Figures 75 and 76.

Consumer price breakdown.- The consumer price of a typical four-place airplane (approximately \$17,000) is broken down both by dollar and by percentage of total in Table XII. The airframe fabrication cost represents approximately 36% of the consumer price. Dividing the airframe fabrication cost by its AMPR, or airframe weight, yields a unit airframe cost of \$6.75 per pound.

WORTH IN DOLLARS PER POUND OF WEIGHT SAVED (LIGHT AIRPLANE)

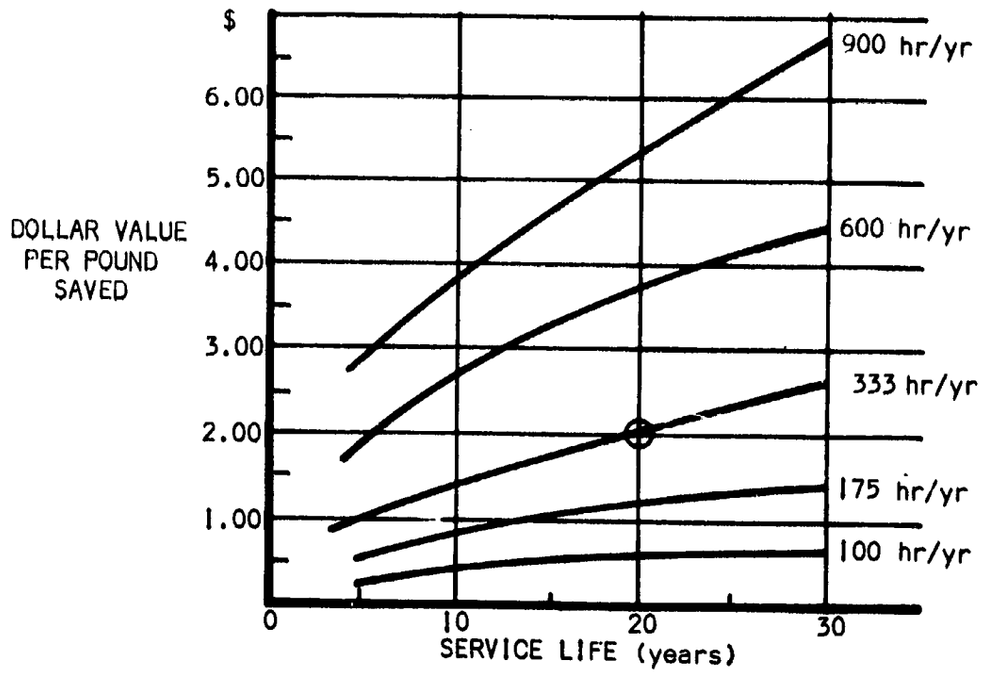


Figure 74

WORTH IN DOLLARS PER POUND OF WEIGHT SAVED (PISTON-HELICOPTER)

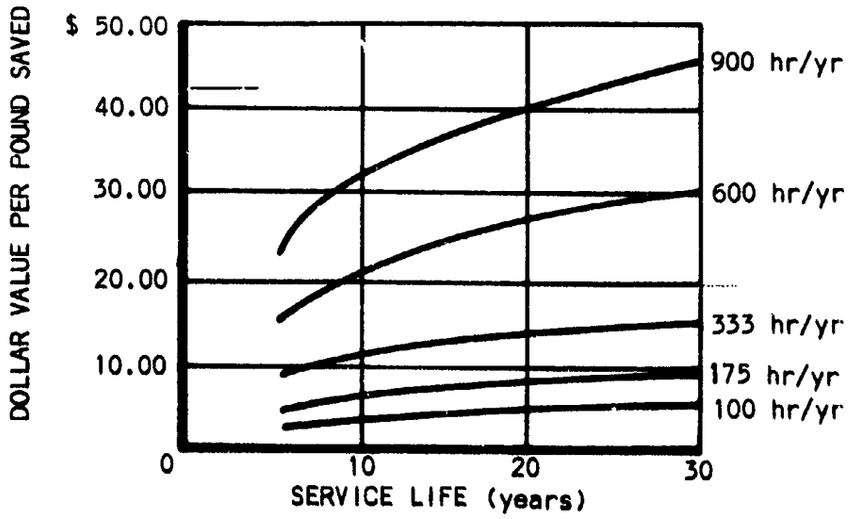


Figure 75

WORTH IN DOLLARS PER POUND OF WEIGHT SAVED (TURBINE-HELICOPTER)

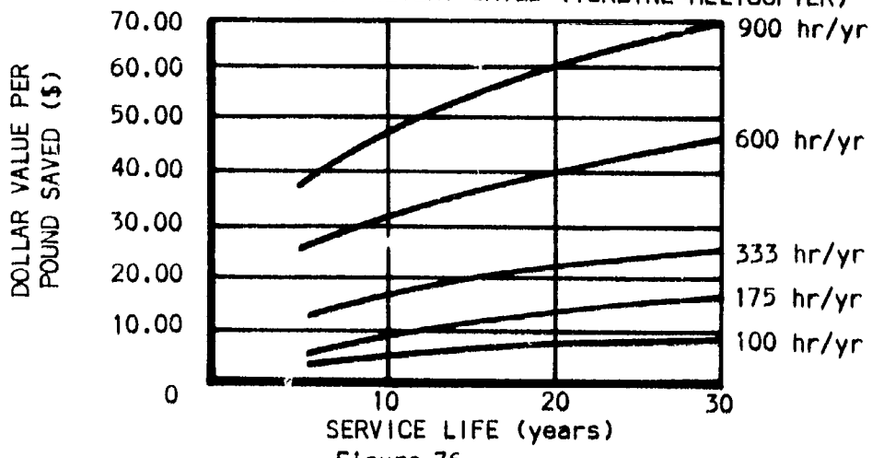


Figure 76

TABLE XII - COST BREAKDOWN OF A TYPICAL LIGHT AIRPLANE

Item	Dollars	Percent Total
Direct Labor - 630 hours (@ $2.70/hr)	$ 1,700.00	10.0
Overhead (130% of $1,700.00)	2,210.00	13.0
Material - Airframe	765.00	4.5
Equipment ($2420 Engine; $375 Prop.; $1305 Other)	4,100.00	24.2
Sub-Total	$ 8,775.00	51.7
Direct, Sales, and General Administrative Expenses (32% of $8,775.00)	2,810.00	16.5
Sub-Total (Manufacturing Cost)	$ 11,585.00	68.2
Factory Profit (10% of $11,585.00)	1,159.00	6.8
Total Dealer's Cost	$ 12,744.00	75.0
Distributor and Dealer Mark-up (33% of $12,744.00)	4,256.00	25.0
Total Cost to Customer	$ 17,000.00	100.0

AIRFRAME FABRICATION COST ANALYSIS

Airframe Labor (80% of Direct Labor)	$ 1,360.00
Airframe share of Overhead (80% of $2,210 + $2,810)	4,015.00
Raw Materials	765.00
Airframe Fabrication Cost	$ 6,140.00

* AMPR Weight is assumed to be 910 pounds.

Unit Airframe Cost: $\frac{\$\ 6,140.00}{910\ \text{lbs}} = \$\ 6.75/\text{lb}$

* AMPR weight includes Empty Weight less the following items: wheels, brakes and tires, engine (incl. carb. air box), starter, propeller and spinner, instruments, navigation equipment, battery and generator, electronics, cabin heat and vent.

Figure 77 illustrates this same breakdown. It should be noted that, although airframe labor and raw material represent only 12.5% of the consumer price of typical four-place, single-engine airplanes, this has a much farther-reaching effect on the total price of the airplane; i.e., dealer's markup, manufacturer's markup, and overall burden (the sum of which represents 61.3% of total price) are all functions of airframe cost. These effects are described quantitatively in Appendix S.

TYPICAL CONSUMER PRICE PERCENTAGE BREAKDOWN
OF A FOUR-PLACE SINGLE-ENGINE AIRPLANE

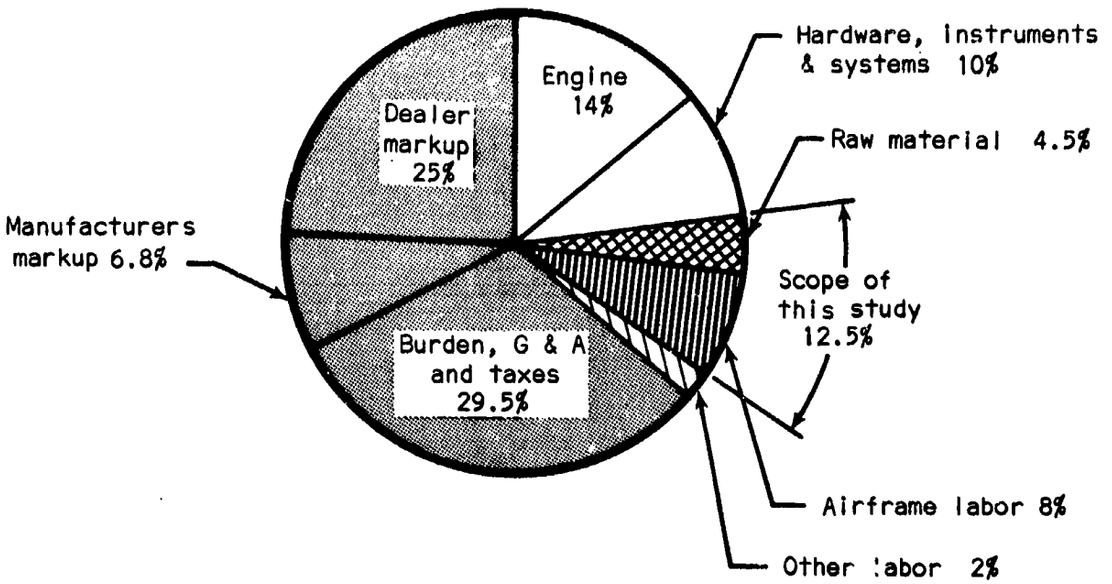


Figure 77

Similarly, the consumer price of a typical four-place light helicopter (approximately $60,000) is broken down by dollar and by percentage of total in Table XIII. The airframe fabrication cost represents approximately 38% of the consumer price. Dividing the airframe fabrication cost by its AMPR weight yields a unit airframe cost of $19.20 per pound.

Figure 78 graphically illustrates the breakdown in Table XIII. Here, as in the airplane pie-chart, the airframe labor and raw material represent only 17.6% of the consumer price of the typical light helicopter, but affect other constituents of the consumer price. These items, representing 48% of the consumer price, are: burden, G&A expenses, taxes, and markup.

TABLE XIII - COST BREAKDOWN OF A TYPICAL LIGHT HELICOPTER

Item	Dollars	Percent total
Direct labor 3050 hours at $2.85/hr	8690	14.6
Overhead at 130 percent	11300	19.0
Main rotor & tail rotor	1040	1.8
Material-airframe	3490	5.9
Equipment (engine, instr.,etc.) oil tanks, fuel system, electrical, power controls	10430	17.6
Subcontractor fabrication & assembly transmission & tail rotor gear boxes	7040	11.8
Sub-Total	41990	70.7
Indirect, sales, and general administrative expense at 10 percent	4200	7.1
Sub-Total	46190	77.8
Profit at 3.06 percent	1410	2.3
Total manufacturer's cost	47600	80.0
Distributor and dealer mark-up at 25%	11900	19.9
Total cost to customer	59500	100.0

AIRFRAME FABRICATION COST ANALYSIS

Airframe share of direct labor *80% x 8690	6952
Airframe share of overhead *80% x 11300	9050
Airframe share of indirect, sales, G&A expense(80% x 4200)*	3360
Airframe material	3490
Total airframe fabrication cost	22852

$$\text{Unit airframe cost} = \frac{\text{total airframe cost}}{\text{airframe (AMPR) weight}} = \frac{22852}{1190} = \$19.20/\text{lb}$$

* Estimate based on light airplane data.

Effect of labor savings/mass production.- As indicated previously, the cost of labor involved in manufacturing a light airplane (or any product for that matter) affects other portions of the total price. The change in consumer price, resulting from reductions in airframe fabrication labor, has been calculated and is illustrated in Figure 79. This plot was based on the following three assumptions:

(1) That manufacturer and dealer mark-ups would remain a constant percentage of consumer price (i.e., 6.8% + 25% = 31.8%).

(2) That raw materials and purchased hardware cost would remain constant regardless of labor savings.

(3) That overall burden (i.e., overhead, sales, and G&A expense) is 2.95 times labor.

TYPICAL CONSUMER PRICE PERCENTAGE BREAKDOWN
OF A FOUR-PLACE RECIPROCATING ENGINE HELICOPTER

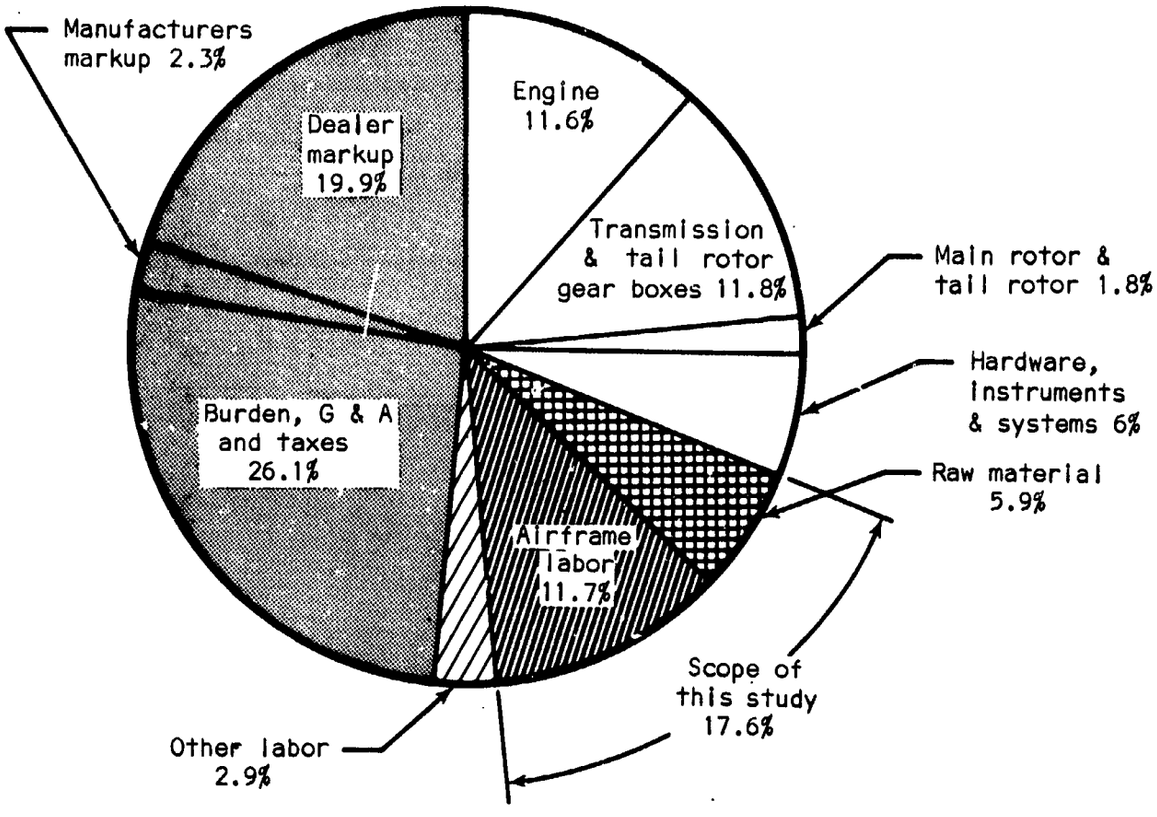


Figure 78

NOTES: a. The 2.95 is derived from data in Table XII, i.e.,

$$\frac{\$2,210 + \$2,810}{\$1,700} = 2.95$$

b. General formula used was:

$$CP_n = (L_n + 2.95\ L_n + M + E) + .318\ CP_n$$

Substituting:

$$CP_n = \frac{3.95\ L_n + 4865}{.682}$$

$$CP_n = 5.8\ L_n + 7140$$

Then converting to percentages:

$$\frac{CP_n}{CP_o} = \frac{5.8\ L_n}{CP_o} + \frac{7140}{CP_o}$$

$$\frac{CP_n}{CP_o} = \frac{5.8\ L_n}{10\ L_o} + \frac{7140}{CP_o}$$

Calling: $\frac{L_n}{L_o} = x$ and $\frac{CP_n}{CP_o} = y$

Then: $y = .58x + .42$

Where:

CP_n = Consumer Price - new

CP_o = Consumer Price - original
= $10\ L_o$ = \$17,000

L_n = Labor - new

L_o = Labor - original

M = Materials = \$765

E = Equipment = \$4,100

Thus, as labor approaches zero, the resulting consumer price approaches a limit of 42%. Obviously, the 100% savings in labor can only be approached through automation

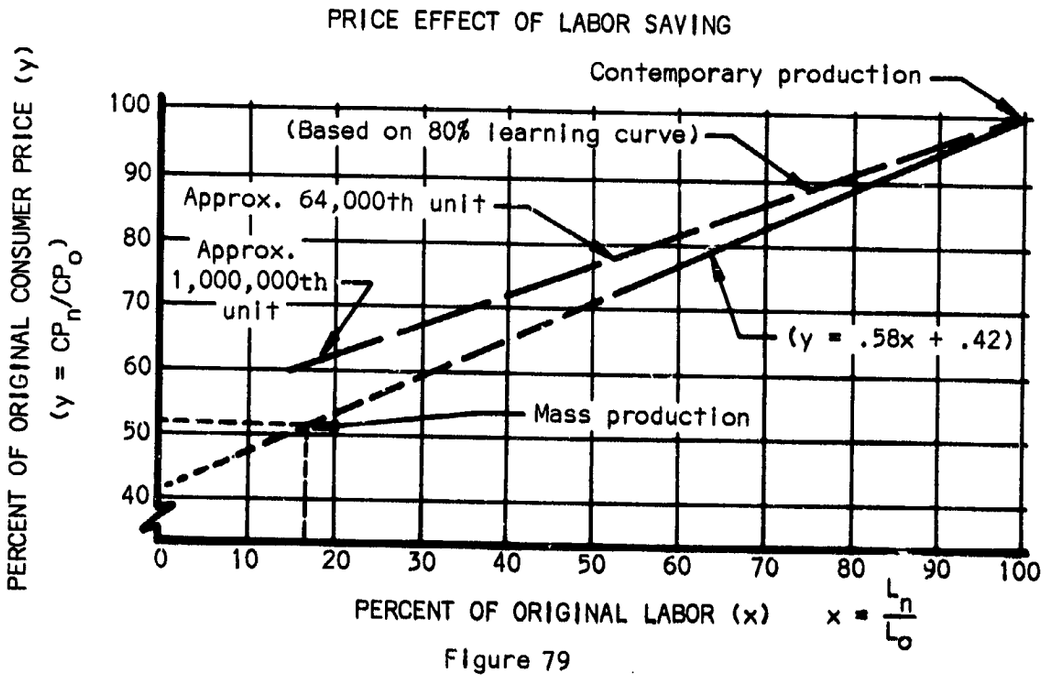


Figure 79

The following method of estimating potential price reductions resulting from very high labor savings (i.e., as the result of mass production), approximates the above estimate of 42%. The General Aviation single-engine, four-place light aircraft is really no more complicated or sophisticated than today's automobile. As an example, there is nothing on a light, General Aviation aircraft that is any more complicated than an automobile automatic transmission or a power brake unit. Some aircraft instruments are quite complicated and sophisticated, but mass production has proven itself in comparable sophisticated domestic products, such as remote control automatic tuning color television (e.g., consumer price of color television has been reduced by mass production from $1,500/$2,000 to less than $300.00).

Therefore, on the reasonable assumption that General Aviation light aircraft and automobiles are transportation vehicles of comparable complexity, the following dimensionless relationship has been generated to equate the two:

$$\frac{\$/lb_{auto}}{\$/lb_{steel}} \cong K \frac{\$/lb_{aircraft}}{\$/lb_{aluminum}}$$

This equation indicates that, for vehicles of comparable complexity, the ratio of raw material specific cost, (ingot), to finished product specific cost should be equal or similar for both vehicles, except as affected by production rate. This production rate or "mass production factor" is given as K in the equation.

The equation is solved for K with the following data:

$\$/lb_{auto}$ = $ .70 (from Reference 27)

$\$/lb_{aircraft}$ = $10.50 (from Figure 69)

$\$/lb_{steel}$ = $ .04 (from Reference 28)

$\$/lb_{aluminum}$ = $ .31 (from Reference 28)

solving: $\frac{.70}{.04} \cong K \frac{10.50}{.31}$

$K = \frac{17.5}{33.9} = .52$ or 52%

In other words, the cost per pound of a typical four-place, single-engine General Aviation aircraft could be expected to be reduced to 52% of today's cost if mass produced. This amounts to a practical consumer price reduction of 48%, which approximates the 58% limit price reduction determined in Figure 76. Obviously, the potential savings attainable through labor savings are well worth striving for. Consequently, relative fabrication costs should play a significant role when selecting candidate materials as is shown on page 162.

Performance Considerations

Airplane.- For the purpose of optimizing a configuration to meet the given set of guidelines, this study was limited to the parameters which would be affected by structural materials and at the same time have a major influence on the performance. In the final analysis, the basic parameters to be optimized were reduced to wing loading, W/S; and power loading, W/P. A method is presented which optimizes W/S and W/P for a minimum weight configuration to meet specific performance requirements.

It should be kept in mind that the aircraft guidelines set forth in Appendix M, which limit the scope of this study, are not far beyond the capabilities of present light aircraft. Because of this similarity in performance requirements, many aerodynamic parameters may be eliminated from the investigation of economically feasible means of improvement.

This point is best illustrated by Figure 80, which is the result of a parametric study of factors affecting maximum speed (see Appendix N). It can be seen that the sensitivity of maximum speed to parameters such as wing area, aspect ratio, wing thickness ratio, extent of laminar boundary layer, gross weight, and fuselage frontal area are rather small when compared to the effect of a retractable vs. fixed gear or a 10% change in power available.

It should be noted that although the effect of delaying the boundary layer transition does not justify a large expense to achieve abnormal surface smoothness on conventional wings, it may be an important consideration for new materials such as plastics where an extremely smooth surface may be achieved at no extra manufacturing cost.

Configuration constants: For the purpose of the optimization analysis in this study, the aerodynamic parameters presented in Table XIV were considered constant.

Wing planform geometry was determined from a design weight study on page 33, Figure 20. An aspect ratio of seven was used throughout the study. This is a very representative value for existing light aircraft, being a weight/performance trade-off which has evolved over many years of light aircraft experience.

Lift coefficient for climb at fifty feet ($C_{L_{50}}$) was assumed to be 1.5. This corresponds to a maximum lift coefficient ($C_{L_{max}}$) capability of 2.15, assuming a climb speed of 1.2 V_{stall}. These values are slightly higher than current production airplanes; however, they are within the present state of the art for a well-designed wing. The analysis has been kept flexible with respect to lift coefficient, however, and the optimization technique presented may be used for any $C_{L_{max}}$ and $C_{L_{50}}$ capability.

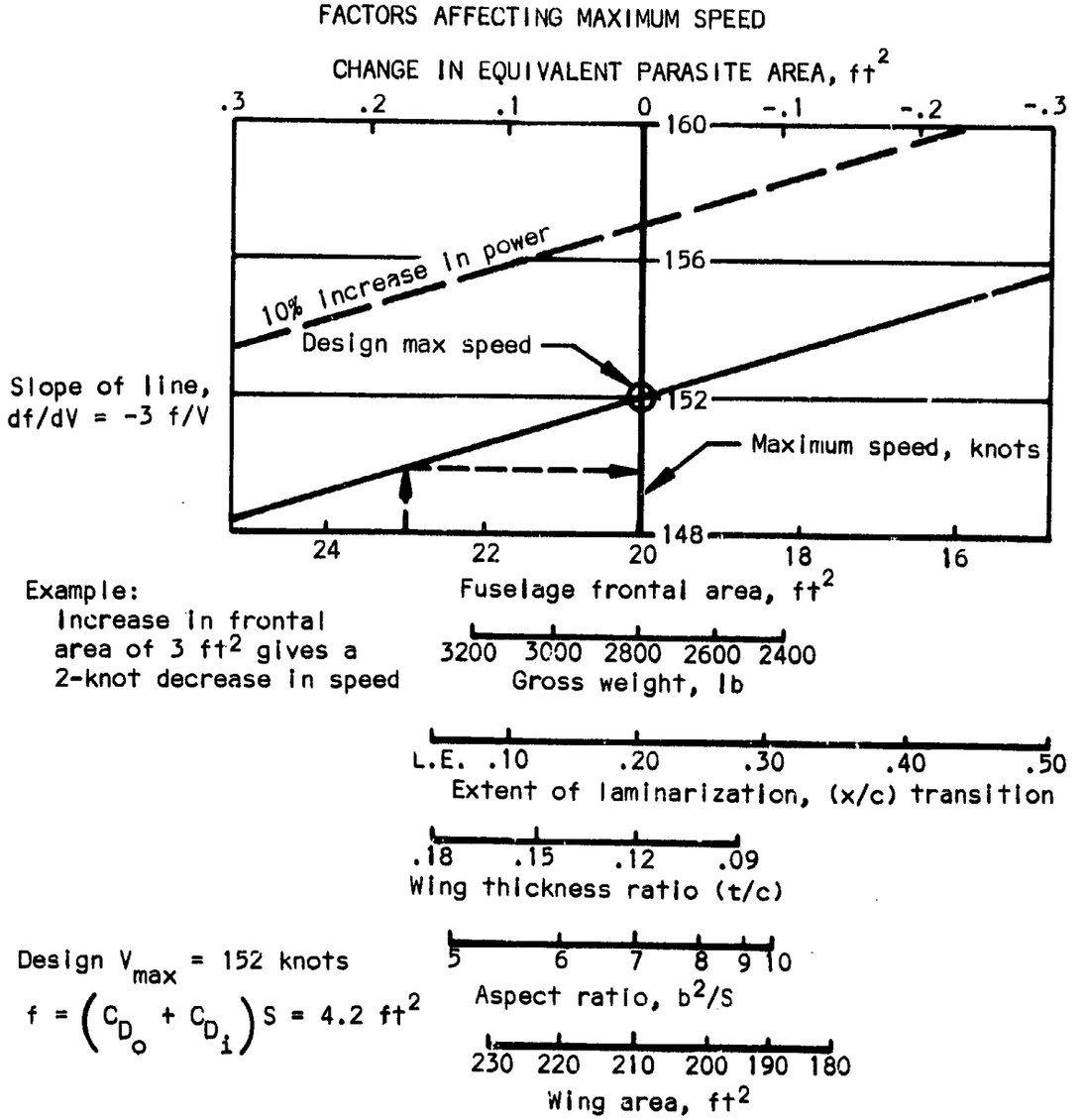


Figure 80

A study of typical engine-propeller combinations gave average propulsive efficiencies of $\eta_p = 0.85$ at maximum speed, 0.80 at cruise speed, and 0.75 at climb speed. These values were used both in the evaluation of equivalent parasite area of present airplanes (Appendix P) and in the performance analysis presented here. Since the equivalent parasite areas calculated in Appendix P were used in estimating the drag for new configurations, the assumption of equal propulsive efficiencies considerably reduced the amount of calculations without introducing more significant error.

TABLE XIV.—AERODYNAMIC PARAMETERS FOR CONFIGURATION OPTIMIZATION

WING:

Aspect Ratio	AR	=	7
Taper Ratio	λ	=	.6
Thickness Ratio	t/c	=	.15
Maximum Lift Coefficient	$C_{L_{max}}$	=	2.15
Takeoff Lift Coefficient	$C_{L_{50}}$	=	1.50
Induced Drag Factor	K	=	$\frac{1}{\pi AR e}$ .055

ENGINE:

Specific Fuel Consumption, Sfc, lb/bhp-hr

Reciprocating	=	0.51
Turbine	=	0.80

Propulsive Efficiency, η_p

Climb	=	0.75
Cruise	=	0.80
Max. Speed	=	0.85

WEIGHTS:

Specific Engine Weight, C_e, lb/bhp

	Present	Future
Reciprocating	1.6	1.4
Turbine	.65	.50

Specific Wing Weight, C_w, lb/ft^2

Present	=	1.76
Future	=	1.50

Initial Weight, W_o, lb [Gross weight - (engine + wing)]

Fixed gear configuration	2196
Retractable gear	2276

Equivalent Parasite Drag Area, f, ft^2

Fixed gear + fuselage + empennage	f_{oF}	= 3.99
Fuselage + empennage (retracted gear)	f_{oR}	= 2.84
Wing parasite area	f_w	= $C_{D_w} \cdot S$
	C_{D_w}	= 0.0075

Parasite drag of the fuselage, gear, and empennage is considered constant with respect to the analysis and is determined for both the fixed gear and the retractable gear configurations. From the parasite drag study presented in Appendix P, typical values of f representing a well-designed fixed gear and retractable gear configuration with 175 square feet of wing area are the following:

$$\bar{f}_F = 5.30 \text{ ft}^2 \text{ (fixed gear)}$$

$$\bar{f}_R = 4.15 \text{ ft}^2 \text{ (retractable gear)}$$

The variable part representing the wing is:

$$\bar{f}_w = C_{D_w} \cdot S$$
$$= 0.0075 \cdot 175$$
$$= 1.31 \text{ ft}^2$$

so that the fixed part for each is:

$$f_{o_F} = 3.99 \text{ ft}^2$$

$$f_{o_R} = 2.84 \text{ ft}^2$$

With the use of these constants, equivalent parasite area may be expressed as a function of wing area, i.e.,

$$\bar{f} = f_o + f_w \qquad (1)$$
$$= f_o + C_{D_w} \cdot S$$

Specific engine weight C_e and specific wing weight C_w were evaluated using current statistics of existing four-place airplanes.

Figure 81 shows the specific weights of reciprocating and turbine engines in the horsepower range under consideration. The maximum power and weight limits specified by the contract guidelines are shown here also. It can be noted that very few existing reciprocating engines fall within these boundaries; however, future improvements appear quite promising. The average values used for reciprocating and turbine engines, present and future, are indicated in Table XIV.

The wing weight parameter C_w was established at 1.76 lb/ft^2, based on statistical data for typical light airplane, with all metal cantilevered wings.

In order to analyze a configuration with respect to wing and powerplant size, a weight (W_o) is defined to be the gross weight of the airplane, minus the wing weight and engine weight, the two variables. Total weight may then be expressed as:

$$W = W_o + C_e P + C_w S \qquad (2)$$

Using an estimated fuel weight of 360 pounds, the W_o weight was found to be 2276 pounds for a typical retractable gear airplane, and 2196 pounds for a fixed gear airplane. These values are used only for the first estimate of weight. Once a particular configuration is selected, the actual mission fuel weight can be calculated using average specific fuel consumptions of 0.51 lb/bhp – hr for

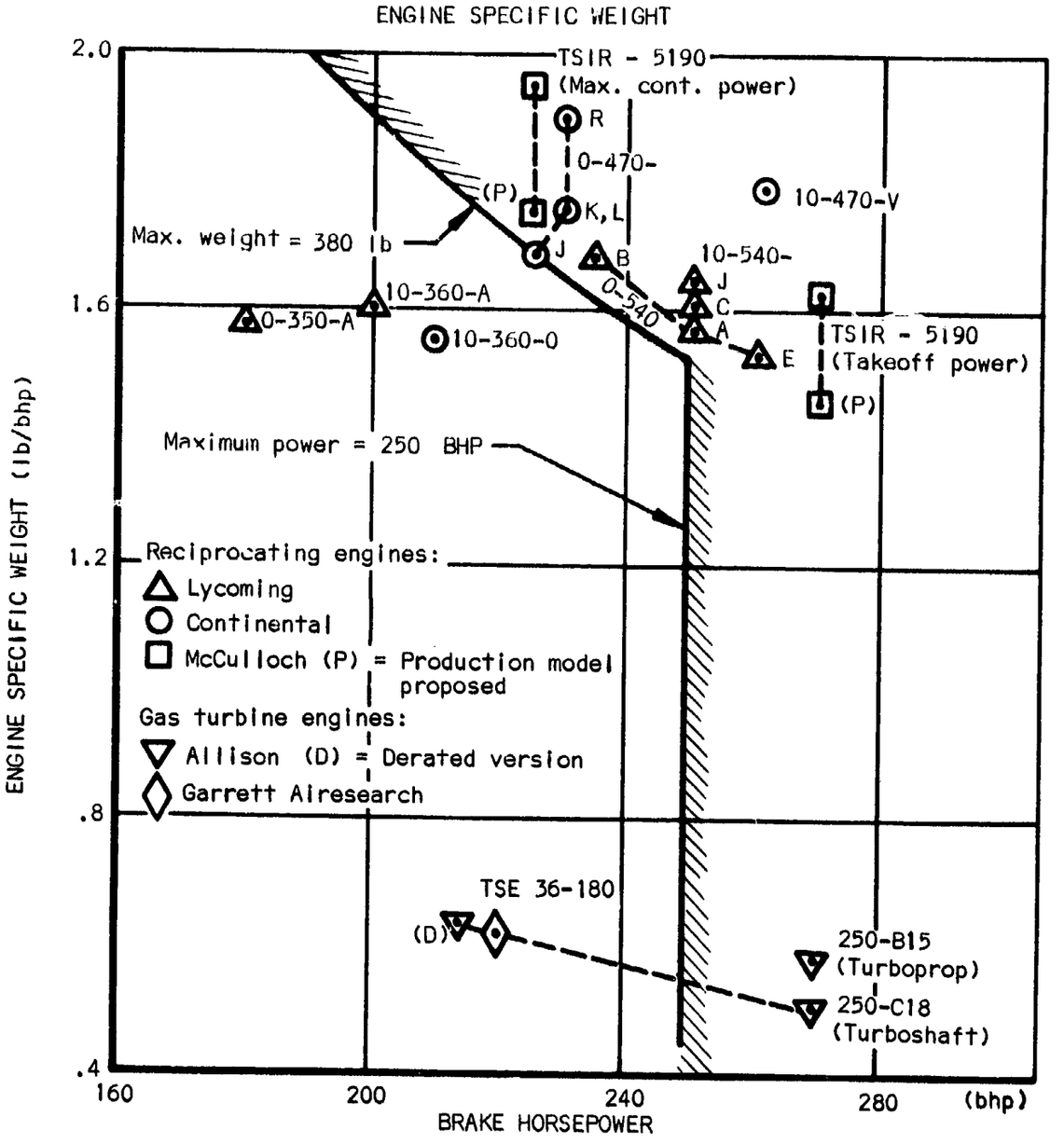


Figure 81

reciprocating engines and 0.8 lb/bhp - hr for turbine engines. Mission fuel is calculated for 4.5 hr endurance at cruise (130 knots at an altitude of 5000 feet). The initial fuel weight estimate of 360 lb, which included 10 lb for warm-up and taxi and 30 lb of unusable fuel, is then adjusted, and the final gross weight calculated.

Determination of critical performance requirements: Having restricted analysis to the optimization of wing loading and power loading, it is now possible to express all of the performance requirements in terms of W/S and W/P for various gross weights. This permits plotting of all the performance requirements as boundaries on a single graph as presented in Figures 82 and 83. The first is for a retractable gear configuration and the second is for a fixed

PERFORMANCE BOUNDARIES FOR RETRACTABLE LANDING GEAR CONFIGURATIONS

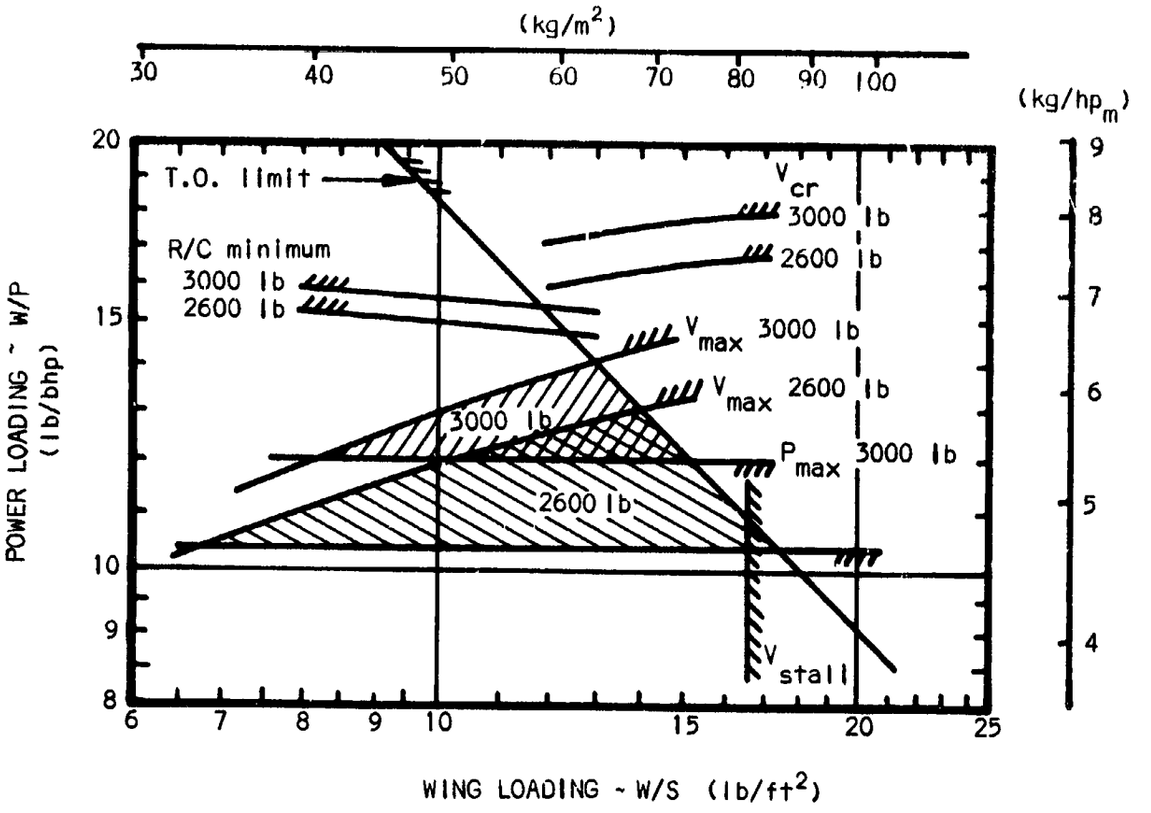


Figure 82

gear configuration. The necessity of having two plots is because of the different equivalent parasite areas for the two configurations. As can be seen, the three defining requirements are the takeoff distance, the maximum speed, and the maximum allowable installed horsepower. Depending on the gross weight and $C_{L_{max}}$, V_{stall} may or may not be a limiting factor. Each of the areas enclosed by these boundaries represents all of the possible configurations which will either meet or exceed the given requirements for a given gross weight.

The techniques used to establish the boundaries for the various performance criteria are presented in the following pages.

PERFORMANCE BOUNDARIES FOR FIXED LANDING GEAR CONFIGURATIONS

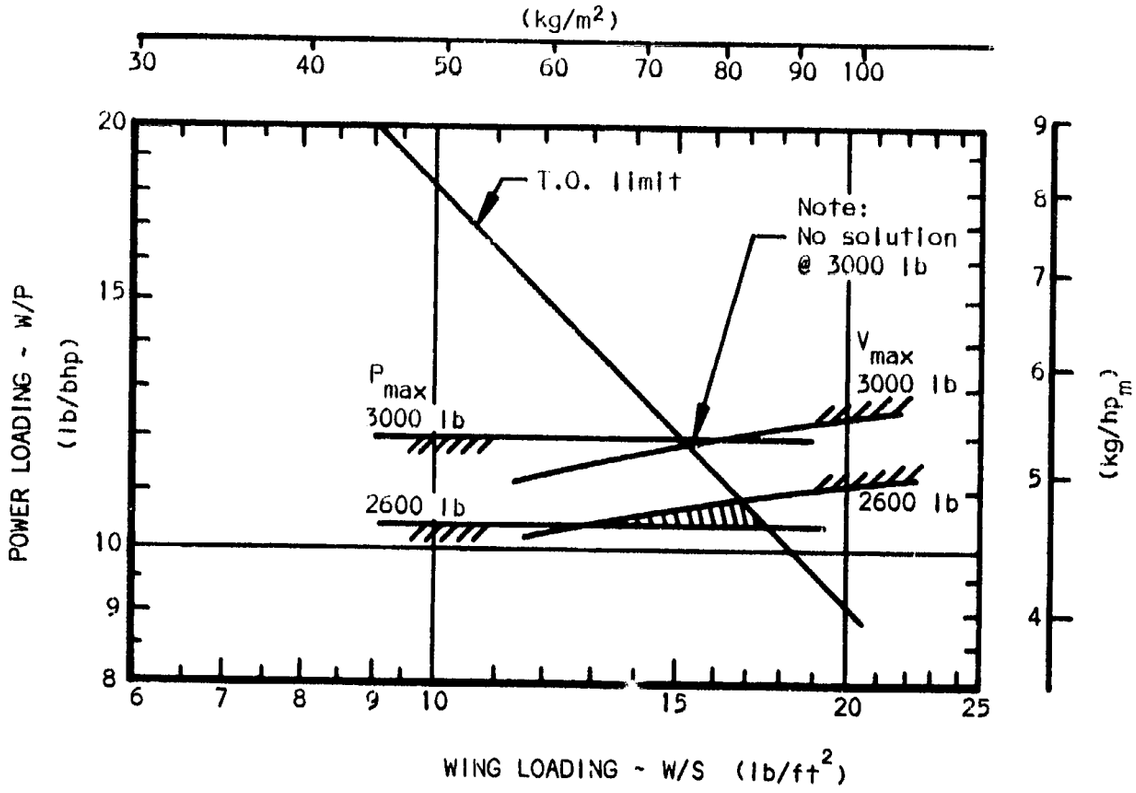


Figure 83

(Takeoff performance) For the analysis of takeoff performance, a semi-empirical method was devised. The basic concept is similar to an expression found in reference 8 , page 197, which suggests that the takeoff distance to clear a fifty-foot obstacle is some function of $\frac{(W/P)(W/S)}{C_{L_{50}}}$.

I.e., $$S_{50}' = F_{TO}\left[\left(\frac{W}{P}\right)\left(\frac{W}{S}\right)\right] 1/C_{L_{50}'} \qquad (3)$$

By constructing a logarithmic plot of the above variables, it is possible to determine the function directly from data on present airplanes with known takeoff performance. In Figure 84 , power loading W/P is plotted as the ordinate on a logarithmic scale, and wing loading W/S, takeoff lift coefficient $C_{L_{50}'}$ and takeoff distance S_{50} are all plotted on the abscissa. The procedure is to enter the power loading W/P and the wing loading W/S and locate their

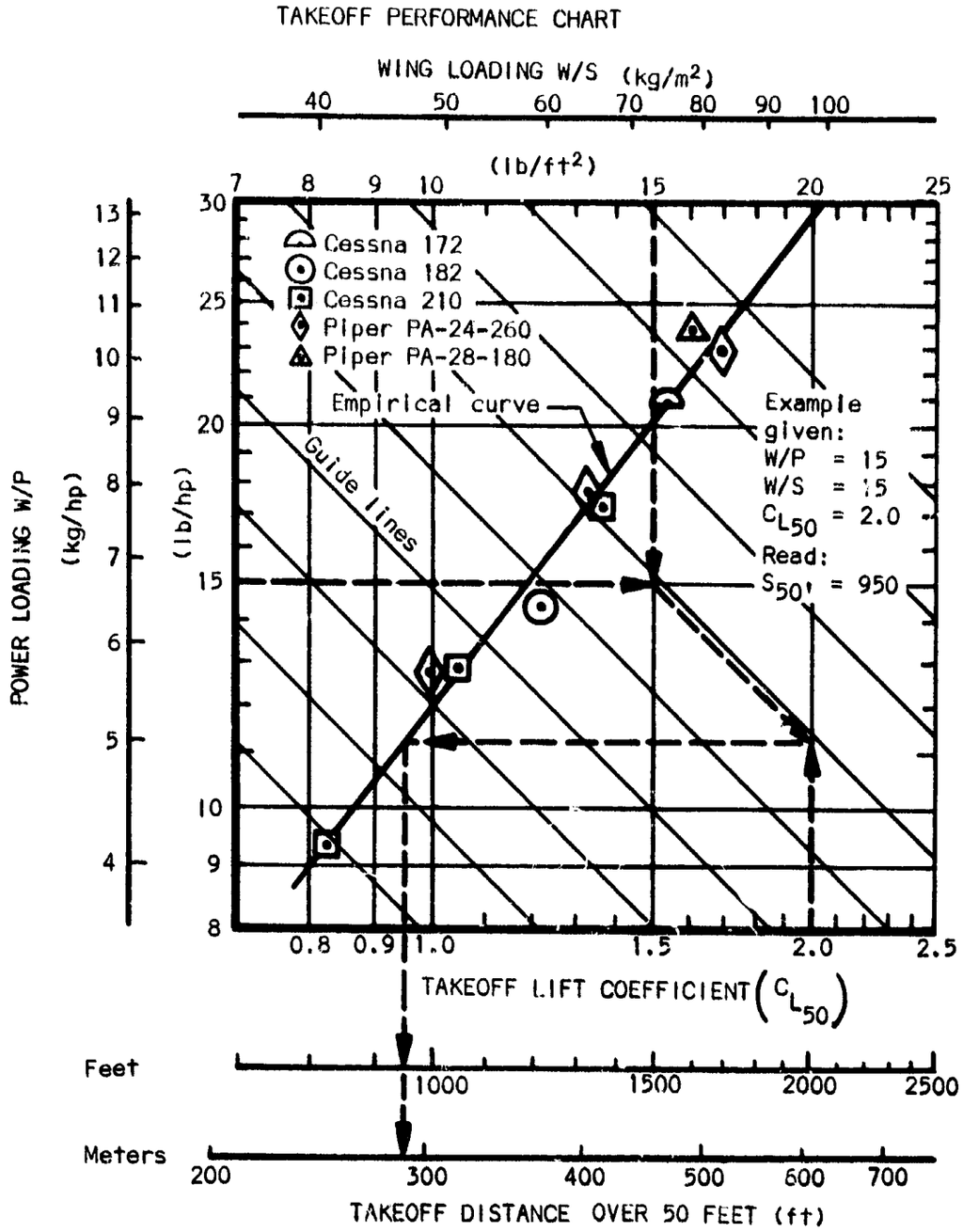


Figure 84

intersection. At this point, proceed along the 45° guide lines until the lift coefficient at 50', $C_{L_{50'}}$, has been reached. The ordinate of the point thus determined represents the parameter $\frac{W/P \cdot W/S}{C_{L_{50}}}$ as shown by the graphic deriva-

tion in Figure 85. This ordinate is then plotted against the known takeoff distance on the abscissa.

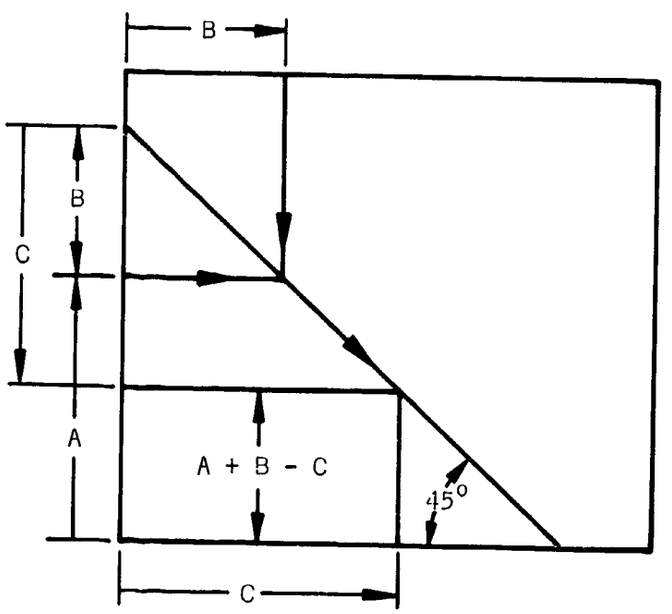
When enough data has been plotted, a curve is fitted to it. This is the empirical curve which defines F_{to}. To use the graph, enter W/P , W/S , and $C_{L_{50}}$, as above, then move horizontally to the empirical curve and read the takeoff distance from the lower scale.

To determine the restrictions imposed by a specific takeoff distance (the contract guideline is S_{50} = 1000 ft), enter Figure 81 at the required takeoff distance and proceed to the empirical curve, than move horizontal to the value of takeoff lift coefficient the wing is designed for. The 45-degree line through this point represents the maximum product of wing loading and power loading which will meet the takeoff requirements. This product defines a design constant which will represent the takeoff performance criteria:

$$C_{TO} = [(W/P)\ (W/S)]_{max} \qquad (4)$$

Note that the 45-degree lines in Figure 84 are lines of equal (W/P) (W/S) and that the 45-degree line located as above will be the graphic boundary for the takeoff performance criteria.

GRAPHIC DERIVATION FOR EMPIRICAL SOLUTION OF TAKEOFF DISTANCE



$A = \log W/P$
$B = \log W/S$
$C = \log C_{L_{50}}$
$A + B - C = \log\left(\frac{W/P \cdot W/S}{C_{L_{50}}}\right)$

Figure 85

(Maximum speed performance) In order to plot this boundary it was necessary to rearrange the equation for power required and select specific gross weights.

$$P \cdot 550 \cdot \eta_p = \frac{\rho V^3 f}{2} + \frac{2 K_1 W^2}{\rho V S}$$

$$\frac{P}{W} \; 550 \; \eta_p = \frac{\rho V^3}{2} \frac{f}{W} + \frac{2 K_1}{\rho V} \frac{W}{S}$$

Inverting,

$$\left(\frac{W}{P}\right) = \frac{\eta_p}{\frac{\rho V^3}{1100}\left(\frac{f}{W}\right) + \frac{K_1}{275 \rho V}\left(\frac{W}{S}\right)} \tag{3}$$

Now, it is desirable to express (f/W) in terms of W and (W/S). From equation (1),

$$f = f_o + C_{D_w} S$$

$$\therefore \frac{f}{W} = \frac{f_o'}{W} + \frac{C_{D_w}}{(W/S)} \tag{6}$$

Substituting,

$$\left(\frac{W}{P}\right) = \frac{\eta_p}{C_1\left(\frac{f_o'}{W} + \frac{C_{D_w}}{(W/S)}\right) + C_2\left(\frac{W}{S}\right)} \tag{7}$$

where:

$$C_1 = \frac{\rho V^3}{1100} \tag{8}$$

$$C_2 = \frac{K_1}{275 \rho V} \tag{9}$$

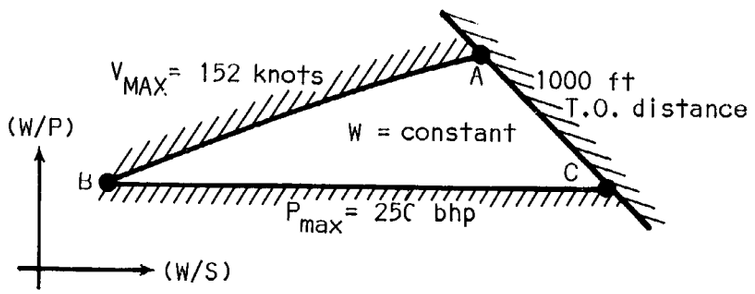
The constants C_1 and C_2 represent the design requirement, a given speed at a given altitude (or density) which in this case is 152 knots at sea level (note the V in the equation must be in feet/sec). The induced drag factor $K_1 = 1/(\pi AR_e)$ is fixed at a value corresponding to an aspect ratio of 7 and is not considered as a valable in this analysis.

With appropriate values for f_o, C_{D_w}, and η_p from Table XIV, there is an expression for W/P as a function of W/S and W. This is plotted in Figures 82 and 83 for a retractable gear and a fixed gear configuration at four different weights (2400, 2600, 2800, and 3000 lb).

The third boundary is the maximum allowable installed power limit of 250 bhp. For each weighr this is a horizontal line at the proper value of (W/P).

W, (lb)	$(W/P)_{min.}$ (lb/bhp)
2400	9.6
2600	10.4
2800	11.2
3000	12.0

The final plot of the three boundaries has the following form:



At any point within the boundaries of the triangle there is a combination of wing loading and power loading at the given weight which will equal or exceed the performance requirements. More specifically, point "A" represents the minimum value of installed power which will just achieve the maximum speed and takeoff requirements. Moving along the line from "A" to "B" maintains the maximum speed and improves the takeoff performance until at point "B" the maximum allowable installed power is reached. It is also the point of largest wing area. Another interesting condition is to assume that the takeoff performance is just adequate and look at the various configurations between points "A" and "C". This is a trade off between power and wing area. At point "C" is the condition of maximum power and minimum wing area.

With the retractable gear configuration it may be noted that there is much more freedom of choice in configuration than with the fixed gear. If a fixed-gear airplane weighed 3000 lbs, there would be no solution. Either the limit of maximum installed power would have to be relaxed or the high lift, $C_{L_{max}}$, capability would have to be increased. In other words, the fixed-gear airplane is much more defined by the performance requirements than is the retractable-gear airplane.

(Rate of climb performance) R/C = 1000 ft/min at sea level. Beginning with the power formula again and adding the power to climb,

$$P \cdot 550\,\eta_p = \frac{\rho V^3 f}{2} + \frac{2 K_1 W^2}{\rho V S} + \frac{W (R/C)}{60}$$

$$\frac{P}{W}\eta_p = \frac{\rho V^3}{1100}\frac{f}{W} + \frac{K_1}{275\,\rho V}\frac{W}{S} + \frac{(R/C)}{33\,000}$$

Substituting for (f/W) and using the definitions for C_1 and C_2 [eqs. (6), (8), and (9)],

$$\frac{W}{P} = \frac{\eta_p}{C_1\left(\frac{f_o'}{W} + \frac{C_{D_W}}{(W/S)}\right) + C_2(W/S) + \frac{(R/C)}{33\,000}} \qquad (10)$$

Using the appropriate configuration constants from Table XIV and the rate of climb performance requirement, eq. (10) will define the boundaries for climb performance as shown in Figures 82 and 83.

(Cruise speed performance) V_{cr} = 130 knots at 5000 feet. The boundaries imposed by this requirement were calculated in a manner similar to the maximum speed requirement except that 75% normal rated power was used. The results are plotted in Figures 82 and 83.

Optimization for minimum weight: Having determined the critical performance criteria by the preceding methods, the influence of these criteria on final gross weight must be determined, beginning with the expression for gross weight as given in eq. (2).

$$W = W_o + C_e P + C_w S$$

Dividing by W and rearranging:

$$\frac{W_o}{W} = 1 - \frac{C_e}{W/P} - \frac{C_s}{W/S}$$

and inverting,

$$W = \frac{W_o}{1 - \frac{C_e}{W/P} - \frac{C_w}{W/S}} \qquad (11)$$

From the takeoff criteria C_{TO} is determined where

$$C_{TO} = \left[\left(\frac{W}{P}\right)\left(\frac{W}{S}\right)\right]_{max} \qquad (12)$$

$$\therefore \quad C_{TO} > \left(\frac{W}{P}\right)\left(\frac{W}{S}\right) \qquad (13)$$

and

$$\frac{W}{S} \leq \frac{C_{TO}}{W/P} \tag{14}$$

From the rules for inequalities,

$$\frac{C_w}{W/S} \geq \frac{C_w}{C_{TO}} \left(\frac{W}{P}\right) \tag{15}$$

$$\therefore \quad \left(1 - \frac{C_e}{W/P}\right) - \frac{C_w}{W/S} \leq \left(1 - \frac{C_e}{W/P}\right) - \frac{C_w}{C_{TO}} \left(\frac{W}{P}\right) \tag{16}$$

Substituting for the denominator in eq. (11),

$$W \geq \frac{W_o}{1 - \frac{C_e}{W/P} - \frac{C_w}{C_{TO}} \frac{W}{P}} \tag{17}$$

The expression on the right of eq. (17) represents the minimum possible weight for an airplane which meets a specific takeoff criteria (C_{TO}). Using the predetermined values of W_o, C_e, and C_w from Table XIV, and the value of C_{TO} determined by Figure 84, the minimum weight may be plotted as a function of power loading (W/P). This is done for both the turbine and reciprocating power plants with fixed and retractable gear configurations in Figure 86.

It is also convenient to plot two other boundaries on this same graph, representing maximum and minimum power which will satisfy the requirements. The maximum allowable power has been limited to 250 bnp and is plotted in Figure 86 as a straight line passing through the origin. The minimum power (maximum power loading) boundary is obtained from Figures 82 and 83 by reading the maximum value of power loading for each weight which will satisfy all the performance requirements (i.e., the apex of each weight triangle). These combinations of weight and power are plotted in Figure 86 for both fixed- gear and retractable-gear configurations.

It is obvious from Figure 86 that the takeoff criteria is the limiting factor for minimum weight in this case. The minimum weight configuration may therefore be determined by differentiating eq. (17) with respect to (W/P). Substituting for clarity,

$$x = \frac{W}{P} \tag{18}$$

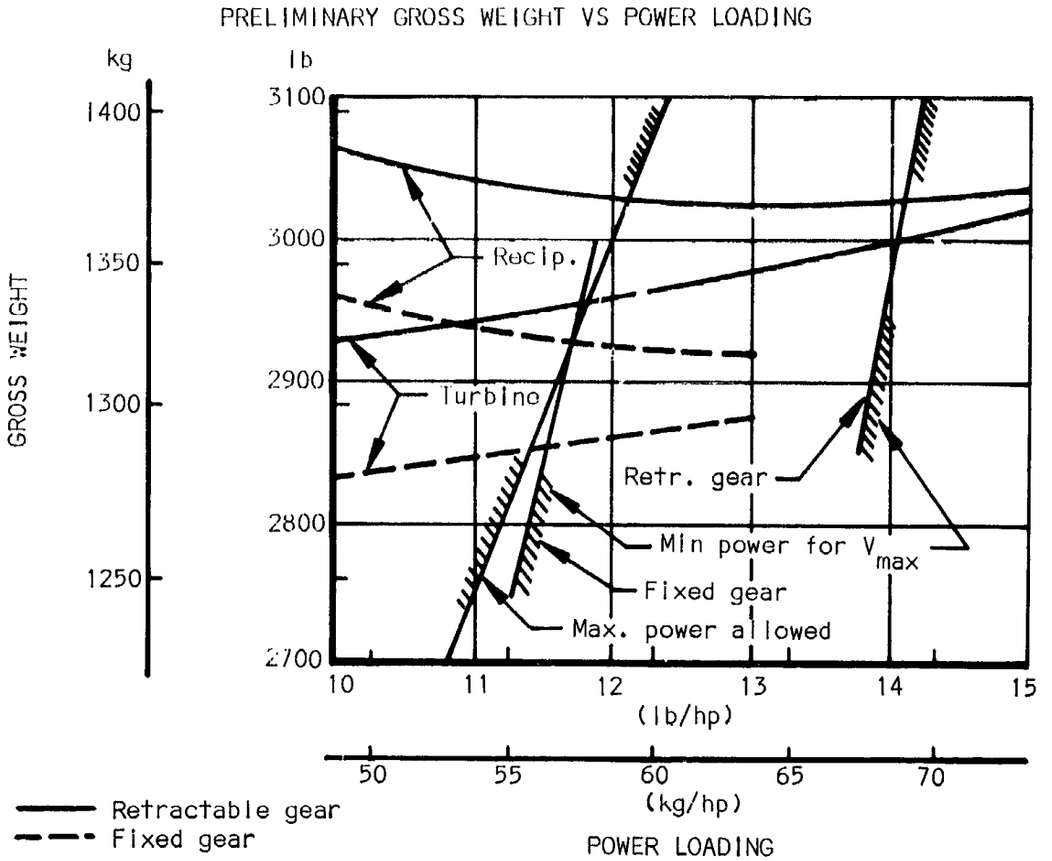


Figure 86

and rearranging eq. (17) gives

$$W\left(1 - \frac{C_e}{x} - \frac{C_w}{C_{TO}}\, x\right) = W_o$$

Differentiation yields

$$dW\left(1 - \frac{C_e}{x} - \frac{C_w}{C_{TO}}\, x\right) + W\left(\frac{C_e}{x^2} - \frac{C_w}{C_{TO}}\right) dx = 0$$

Solving for $\frac{dW}{dx}$ and setting it equal to zero,

$$\frac{dW}{dx} = \frac{-W\left(\frac{C_e}{x^2} - \frac{C_w}{C_{TO}}\right)}{1 - \frac{C_e}{x} - \frac{C_w}{C_{TO}} \times} = 0$$

$$\therefore \quad \frac{C_e}{x^2} - \frac{C_w}{C_{TO}} = 0$$

or,

$$x^2 = C_{TO} \frac{C_e}{C_w} \tag{19}$$

Substituting the equations for x and C_{TO},

$$\left(\frac{W}{P}\right)^2 = \left(\frac{W}{P}\right)\left(\frac{W}{S}\right)\frac{C_e}{C_w}$$

$$\therefore \quad \frac{W/P}{W/S} = \frac{C_e}{C_w} \tag{20}$$

Equation (20) represents the condition for a minimum weight configuration. It should be kept in mind that eq. (20) is valid only when the takeoff criteria defines the minimum weight boundary of Figure 86. The other performance boundaries must also be checked to insure that the takeoff boundary is valid at its minimum.

The boundary imposed by the stall speed criteria was not shown in Figure 86 since it was not limiting in this case. For an analysis where the stall speed requirement may be a critical factor, the boundary on Figure 86 may be found easily from the following relation:

$$\frac{W}{S} \leq C_{L_{max}} \, q \text{ stall} \tag{21}$$

Substituting this expression in eq. (11) yields

$$W \geq \frac{W_o}{1 - \frac{C_e}{W/P} - \frac{C_w}{C_{L_{max}} q_{stall}}} \quad , \qquad (22)$$

which is the desired equation for the stall speed boundary.

(Minimum weight in terms of specific weight constants) In order to generalize the results of the optimization analysis, the minimum weight is now expressed in terms of the specific weights.

When takeoff performance is the minimum weight criteria,

$$C_{TO} = \left(\frac{W}{S}\right)\left(\frac{W}{P}\right)$$

Substituting for (W/S) in the condition for minimum weight [eq. 20)] yields:

$$\frac{W}{P} = \sqrt{C_{TO}\,\frac{C_e}{C_w}} \qquad (23)$$

Substituting for (W/P),

$$\frac{W}{S} = \sqrt{C_{TO}\,\frac{C_w}{C_e}} \qquad (24)$$

With these values put in the basic weight expression, eq. (11),

$$W_{min} = \frac{W_o}{1 - \frac{C_e}{\sqrt{C_{TO}\,\frac{C_e}{C_w}}} - \frac{C_w}{\sqrt{C_{TO}\,\frac{C_w}{C_e}}}}$$

Simplifying,

$$\frac{W_o}{W_{min}} = 1 - 2\sqrt{\frac{C_e\,C_w}{C_{TO}}} \qquad (25)$$

or inverting,

$$\frac{W_{min}}{W_o} = \frac{1}{1 - 2\sqrt{\frac{C_e\,C_w}{C_{TO}}}} \qquad (26)$$

Equation (26) represents the minimum weight ratio (gross weight to gross weight minus engine and wing) in terms of the specific weights of the engine and wing and the takeoff performance parameter C_{TO}.

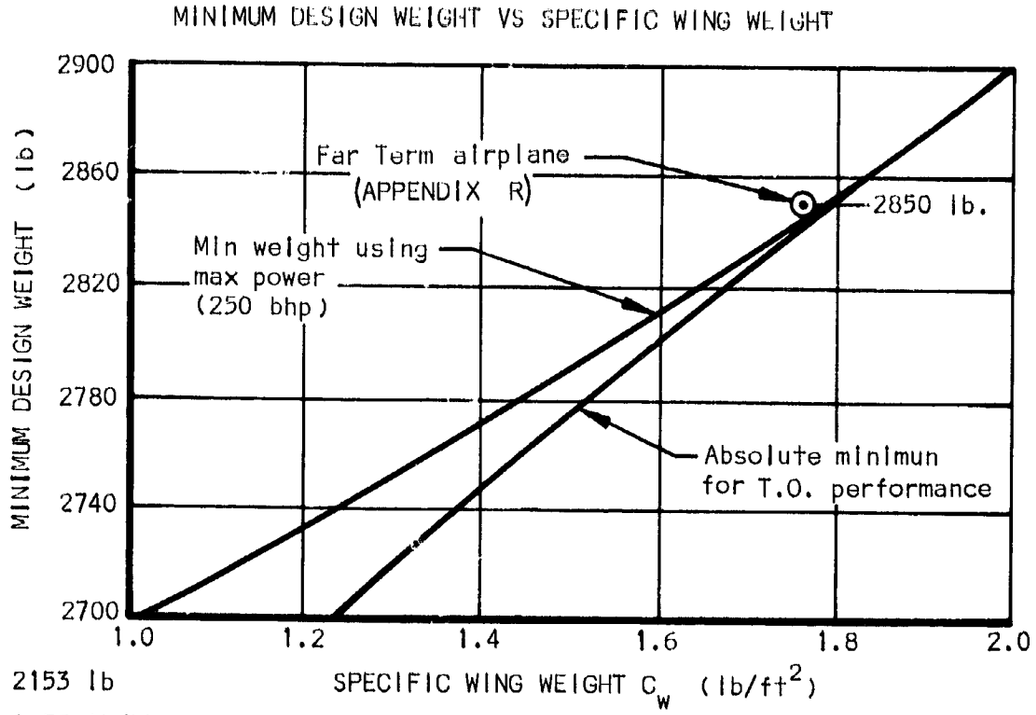
Airplane configuration: The more detailed weight analysis in Appendix R, revealed that the original estimate of W_o was conservative. It was determined that a retractable gear configuration could be designed with W_o = 2153 pounds. (This compares with the original estimate of 2276 lbs.).

Using this value of W_o in equation (26), the minimum design weight can be expressed as a function of specific wing weight C_w for particular values of C_e and C_{TO}. This function has been plotted in Figure 87.

The minimum weight using the maximum power allowed is determined by the intercept of the maximum power condition and the takeoff performance criteria. (This is illustrated in Figure 86). This function is found by solving the basic weight equation eq. (2) for the simultaneous conditions of maximum power and the takeoff criteria: $S = \frac{W^2}{C_{TO} P}$ from eq. (4). The resulting equation is:

$$W = W_o + C_e (250) + C_w \left[\frac{W^2}{C_{TO} (250)} \right] \qquad (27)$$

Equation (27) is also plotted in Figure 84 for the given values of C_{l_o} and C_e.



W_o = 2153 lb

C_e = 1.52 lb/bhp

C_{TO} = 182 lb^2/bhp-ft^2

Figure 87

It should be noted that the functions in Figure 87 are convergent as specific wing weight increases, which indicates that the maximum power condition is intercepting the takeoff criteria closer to its minimum. The distance between the two lines represents the possible savings in weight by optimizing the wing loading-power loading combination along the takeoff criteria, as compared to designing for the takeoff criteria with maximum allowable power.

The estimated specific wing weight for the Far Term airplane is estimated at 1.76 lb/ft^2. Entering Figure 87 at this value, it is seen that there is only 7 pounds difference between designing for maximum power and the absolute minimum weight. It was decided that the base airplane would be designed at maximum allowable power since this is already so close to the absolute minimum.

The configuration used as the Far Term airplane is also shown in Figure 87. The Far Term airplane is slightly heavier (61 lbs) than the minimum. This is because the takeoff design criteria for the Far Term airplane is slightly conservative, i.e., [C_{TO} (Far Term design) = 181 and $C_{TO_{max}}$ = 182].

Airplane Performance Summary: Since the Far Term airplane was designed to meet the most critical performance requirement, (1000 ft. take off distance), the other performance requirements of Appendix M are exceeded. A summary of the calculated performance for the Far Term airplane configuration, (2850 lb., retractable gear with 250 bhp. and 180 ft^2 wing.) are as follows:

Performance	Calculated	Guidelines
Max. Speed at Sea level	166 knots	152 knots
Normal Cruise at 5000 ft.	152 knots	130 knots
Rate of Climb at Sea Level	1650 fpm	1000 fpm
Stall Speed (Sea Level Power off)	46.6 knots	48 knots
Service Ceiling	20,000 ft.	14,000 ft.

Helicopter.- Finding an optimum configuration for a helicopter is a much more complex task than for an airplane because of the larger number of variables and the extremes of flight conditions. In this report, two flight conditions have been studied in some detail: hovering out-of-ground effect and sea level maximum speed.

For hovering, two generalized charts have been drawn up to calculate the rotor power required for any combination of disc area, density, tip speed, thrust required, and solidity. See Figures 88 and 89. The first four quantities are combined into the thrust coefficient, C_T.

$$C_T = \frac{T}{A_d \rho V_T^2}$$

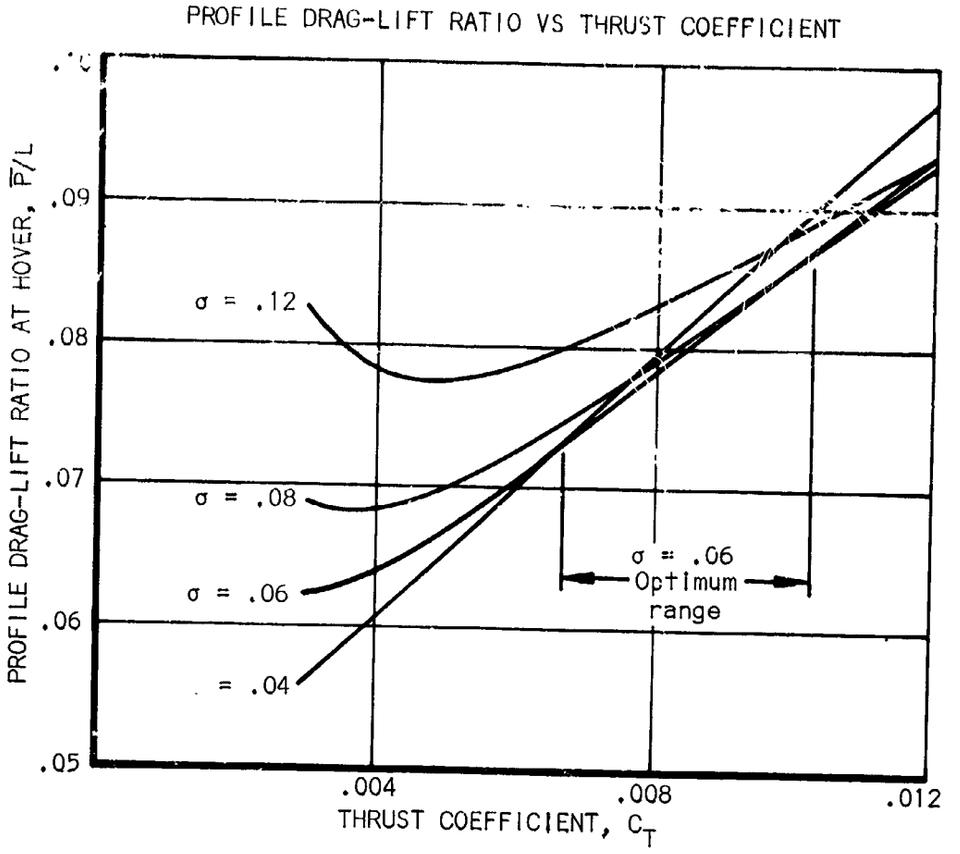


Figure 88

The power required is in the form of a drag-to-lift ratio ($\bar{P}/L$), where $\bar{P}$ is defined as the energy absorbed by the rotor at a rate equal to the tip speed. To obtain the actual horsepower required, we use the following relation:

$$P = \frac{\bar{P}}{L} \frac{W V_T}{550} \quad ,(hp)$$

Figure 88 shows that, over a large range of thrust coefficients, a solidity of 0.06 is optimum or near optimum and, in further analyses, this value will be used. Figure 89 is essentially the same information presented using C_T/σ as the parameter. This is useful when studying blade stall which is a function of C_T/σ.

The formula used is derived from the analysis given in reference 9 .

$$C_Q = \frac{C_T^{3/2}}{\sqrt{2}\,B} + \frac{\sigma\,\delta_o}{8} - \frac{2\,\delta_1}{3a}\frac{C_T}{B^2} + \frac{4\,\varepsilon_2}{a^2\sigma}\left(\frac{C_T}{B^2}\right)^2$$

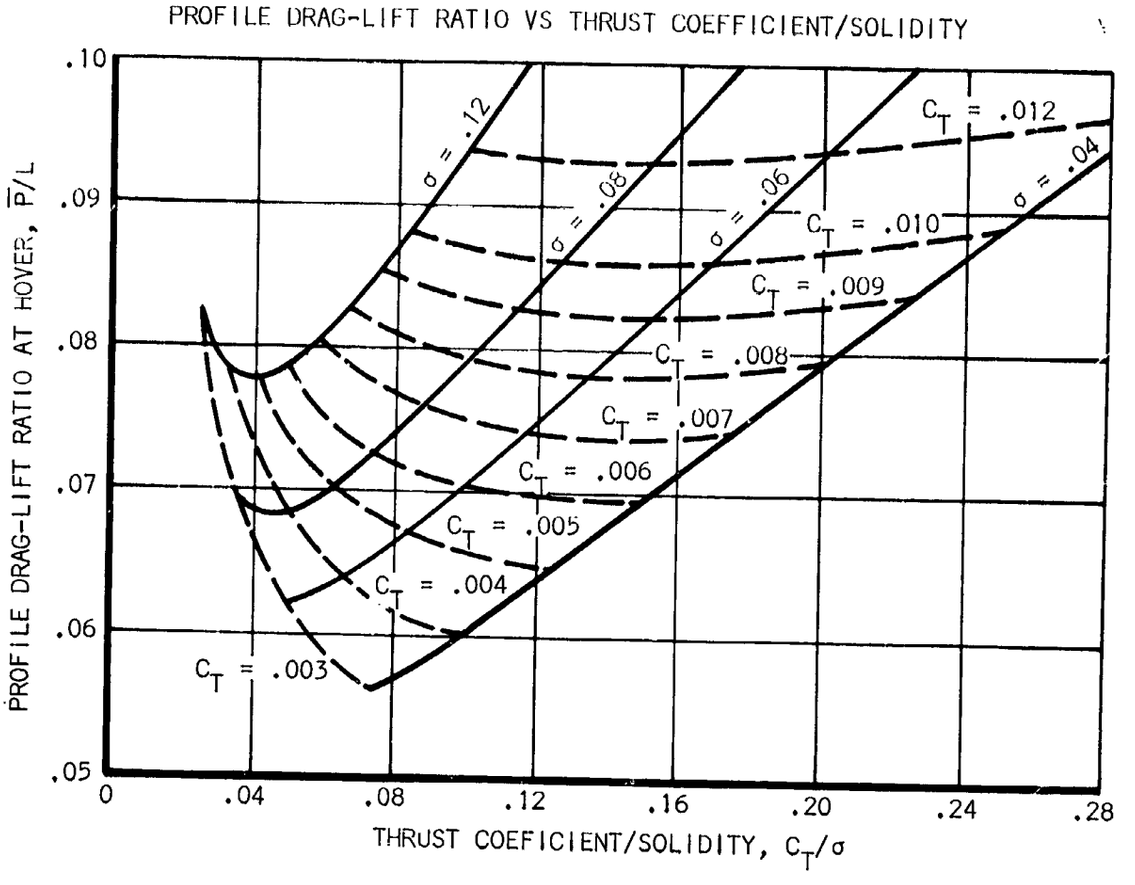


Figure 89

Dividing through by C_T yields:

$$\frac{C_Q}{C_T} = \sqrt{\frac{C_T}{2\,B^2}} + \frac{\delta_o \sigma}{8\,C_T} - \frac{2\,\delta_1}{3\,a\,B^2} + \frac{4\,\delta_2\,C_T}{a^2\,B^4\,\sigma}$$

$$C_Q = \frac{P}{A_d\,\rho\,V_T^3}$$

so that

$$\frac{C_Q}{C_T} = \frac{P}{A_d\,\rho\,V_T^3}\,\frac{A_d\,\rho\,V_T^2}{T} = \frac{P}{T\,V_T}$$

But, $T = L$ (Thrust = Lift)

and $P/V_T = \bar{P}$, so that C_Q/C_T

is the desired result of $(\bar{P}/L)$:

$$\left(\frac{\bar{P}}{L}\right) = \sqrt{\frac{C_T}{2B^2}} + \frac{\delta_o \sigma}{8 C_T} - \frac{2\delta_1}{3aB^2} + \frac{4\delta_2}{a^2 B^4}\frac{C_T}{\sigma}$$

For the purpose of visually showing the actual power required to hover over a range of variables, the following procedure was used:

Power required to hover:

To calculate the rotor power required to hover, the following formula was used:

$$C_Q = \frac{C_T^{3/2}}{\sqrt{2}B} + \sigma\left[\frac{\delta_o}{8} - \frac{2\varepsilon_1}{3a}\frac{C_T}{\sigma B^2} + \frac{4\delta_2}{a^2}\left(\frac{C_T}{\sigma B^2}\right)^2\right]$$

Substituting for C_T and C_Q,

$$\text{Power} = \frac{W^{3/2}}{B\sqrt{2\rho A_d}} + \frac{\sigma \delta_o \rho A_d V_T^3}{8} - \frac{2\delta_1 W V_T}{3\sigma B^2} + \frac{4\delta_2 W^2}{\sigma a^2 B^4 \rho A_d V_T}$$

For the purpose of calculation, three different weights were used: 2000, 2400, and 2800 pounds. For each weight, the power required was plotted against disc area and tip speed. The disc area is adjusted by multiplying it by the density ratio which eliminates density as a variable. The blade solidity was held constant at 0.06 for this study. This is a fairly typical value and, as can be seen in Figure 88, gives the minimum power requirement over a fair range of thrust coefficients.

The results for each of the weights are shown in Figures 90, 91, and 92. A composite mapping of all three weights is shown in Figure 93.

The forward flight performance was established, using methods presented in reference 9 .

In an effort to find the optimum disc areas and tip speed, the aircraft guidelines were introduced into the calculations. Hover out-of-ground effect must be maintained at 5000 feet of altitude and a sea level maximum speed of 105 knots. The hover power requirements (reduced to 5000 feet) and the power required to fly at 105 knots at sea level, for weights of 2000, 2400, and 2800 pounds, were cross-plotted in Figures 91, 92, and 93.

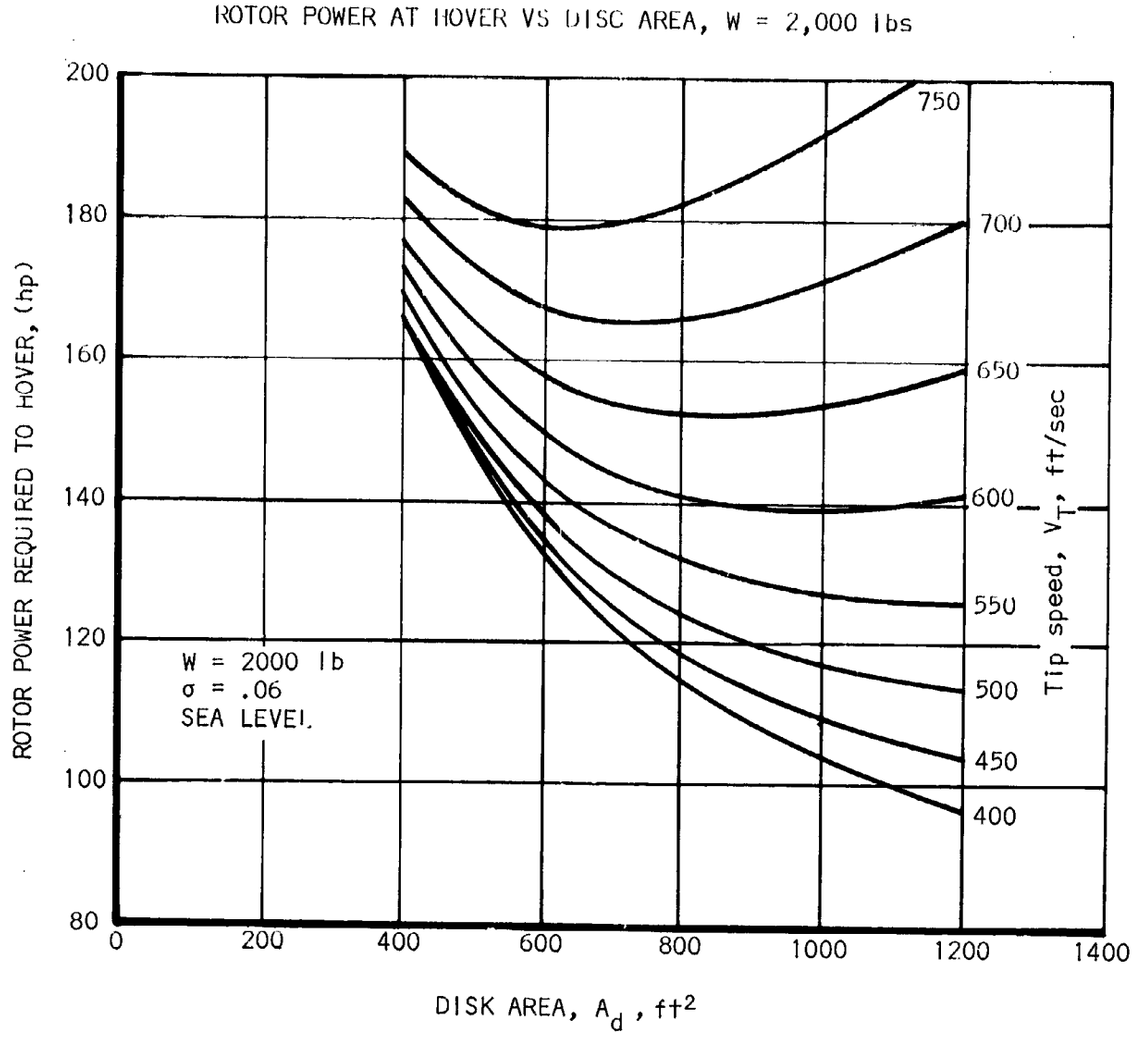


Figure 90

From these crossplots, a combination of tip speed and disc area can be selected, giving the minimum power requirements once the gross weight has been determined. In an actual application, some iteration will be necessary since, when a parameter such as disc area is changed, the gross weight is correspondingly changed.

Final weight analysis: A formula has been generated to determine what the gross weight will be as various parts of the configuration are varied. In particular, these variables are: rotor disc area, rotor tip speed, and the installed power.

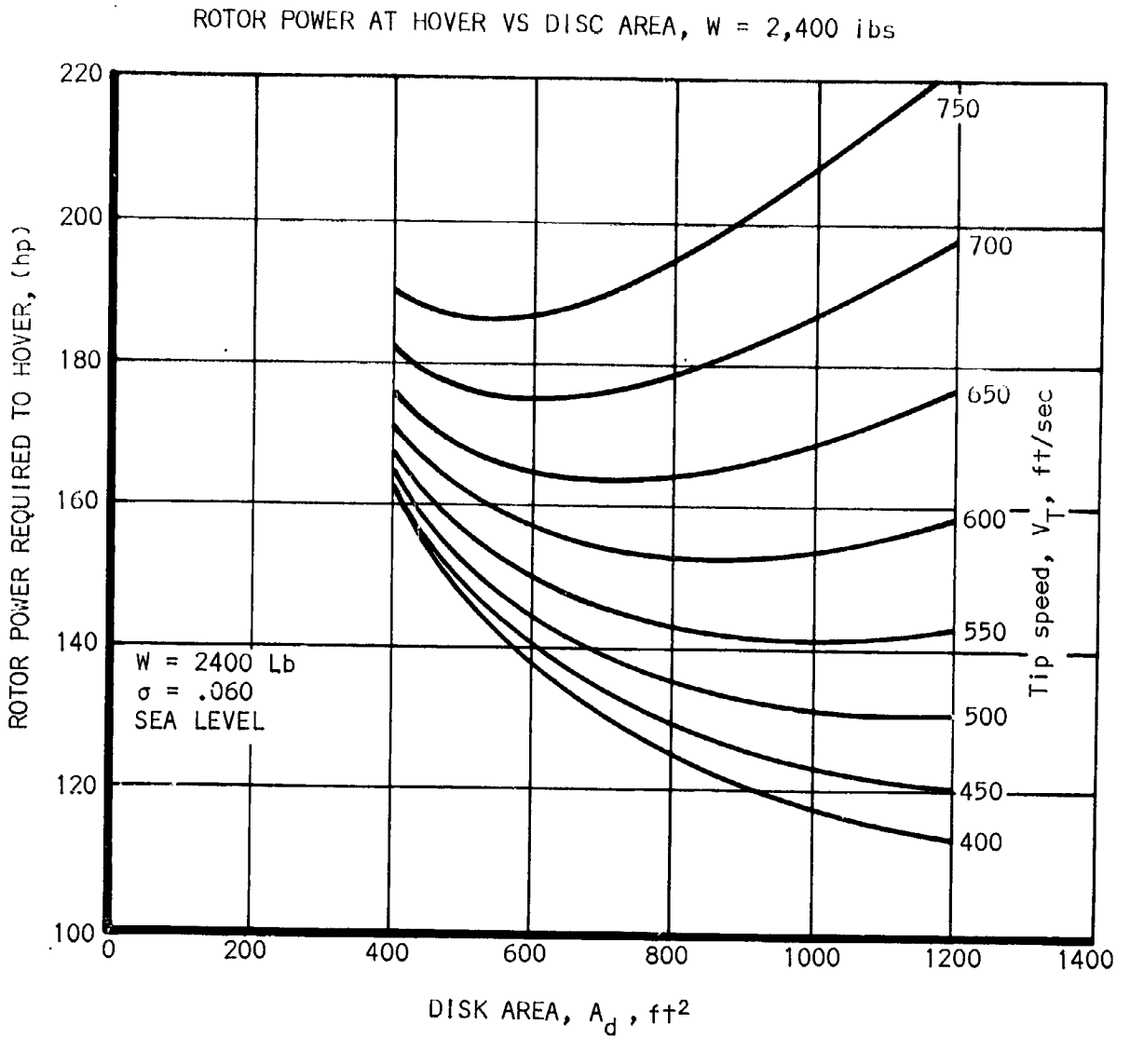


Figure 91

The component weights affected are the main rotor and hubs, the transmission, and the engine weight. A fixed weight, W_o, was assumed representing the remainder of the structure, payload, and fuel. Two values of this fixed part were assigned: one representative of a reciprocating engine configuration W_o = 1800 lb.; and one of a turbine engine configuration W_o=1900 lb. The difference was the mission fuel weight (note that the engine weight was not included in this term).

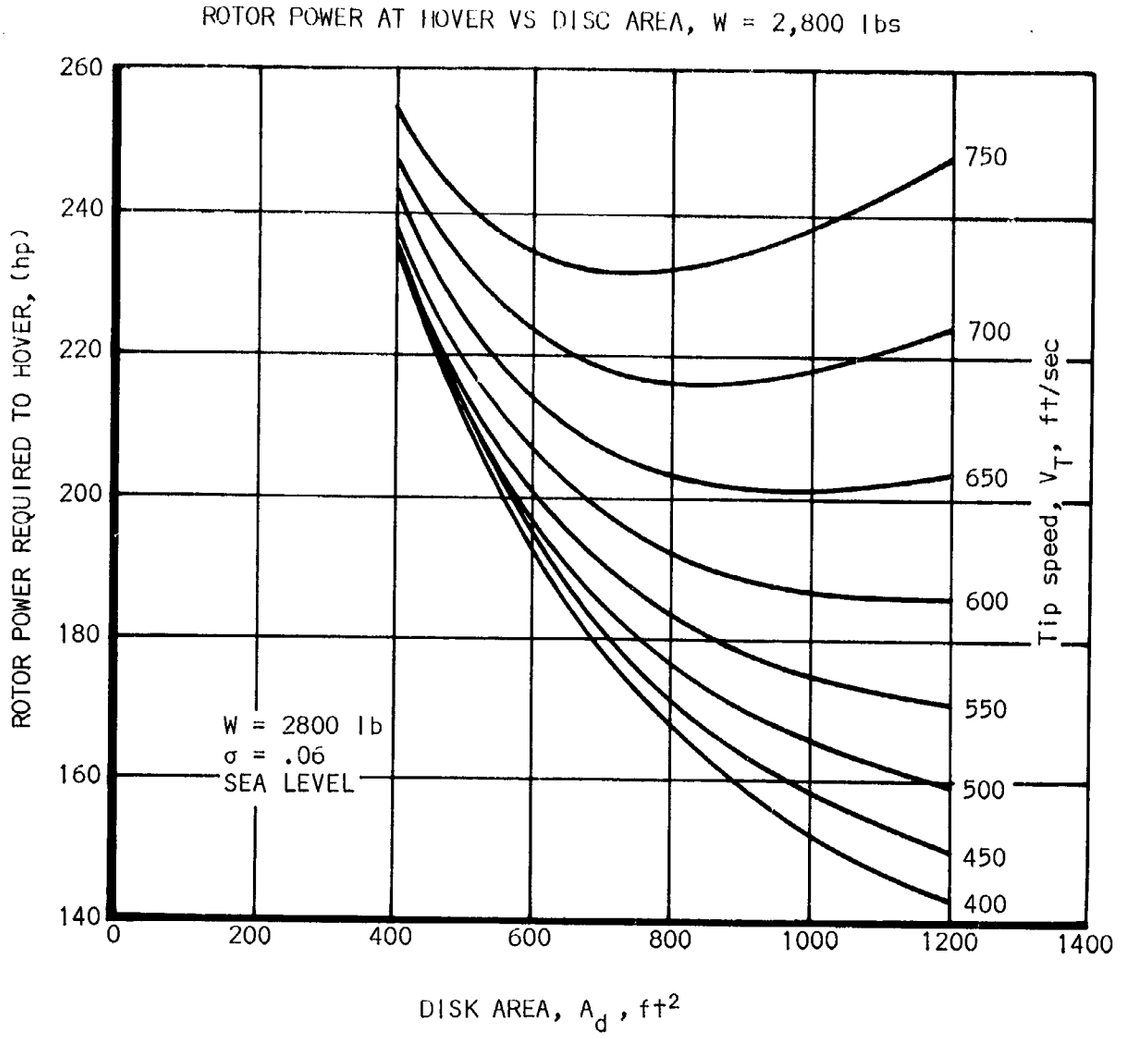


Figure 92

The engine weight was handled the same way as in the airplane analysis by assuming a value of specific weight, C_e~lb/bhp, for typical reciprocating and turbine engines. Terms for the rotor and hub weights and the transmission weight are empirical expressions developed by a helicopter manufacturer. The constants were altered slightly to better fit this category of helicopter. They give reasonable accuracy and are especially good in a comparative configuration study such as this.

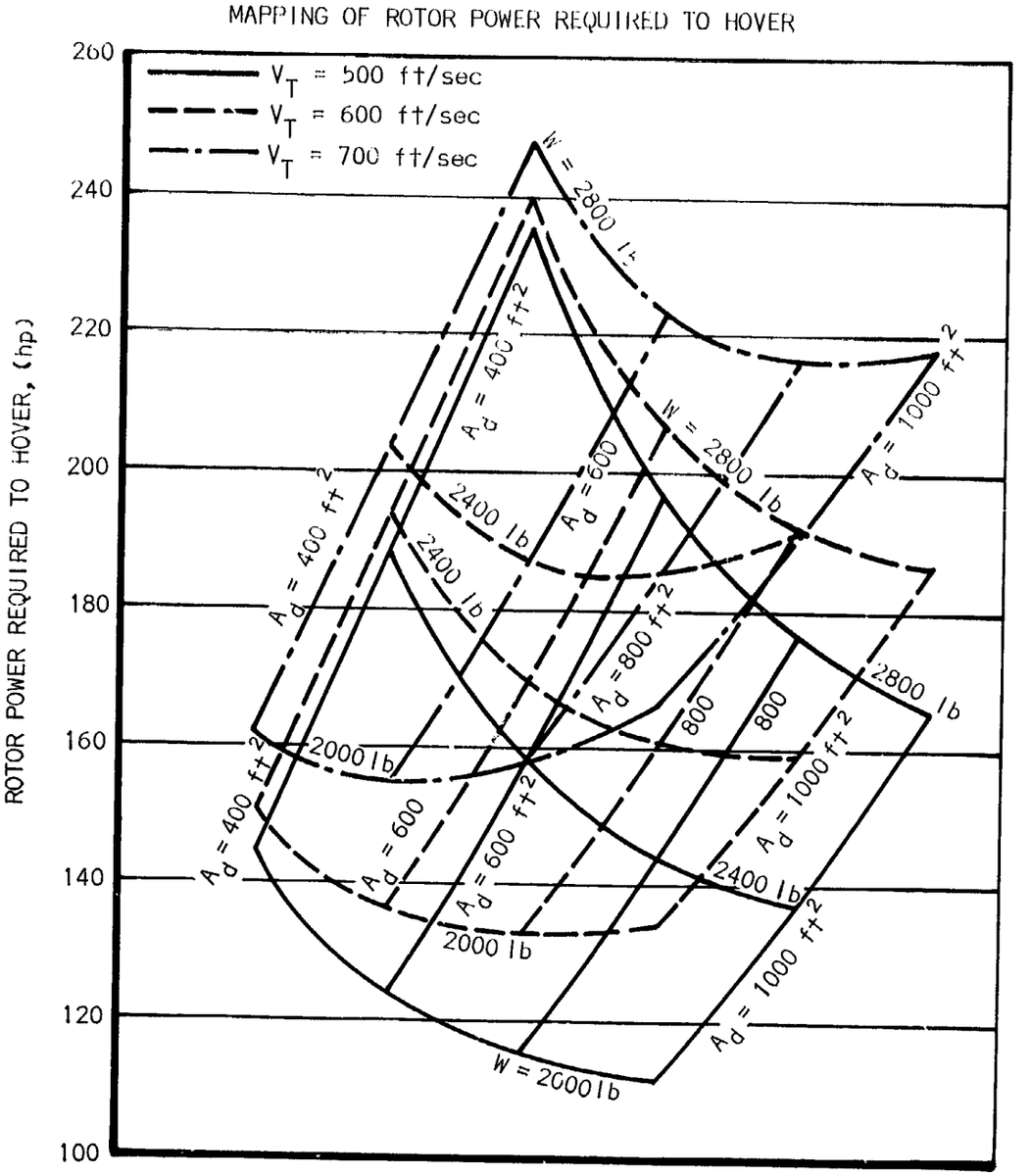


Figure 93

The resulting formula is the following:

$$W = W_o + W_{engine} + W_{transmission} + W_{rotor\ and\ hub}$$

$$W = W_o + C_e P + 42.4 \left(\frac{P R}{V_T}\right)^{.763} + 1.35W^{.342} R^{1.576} \sigma^{.630}$$

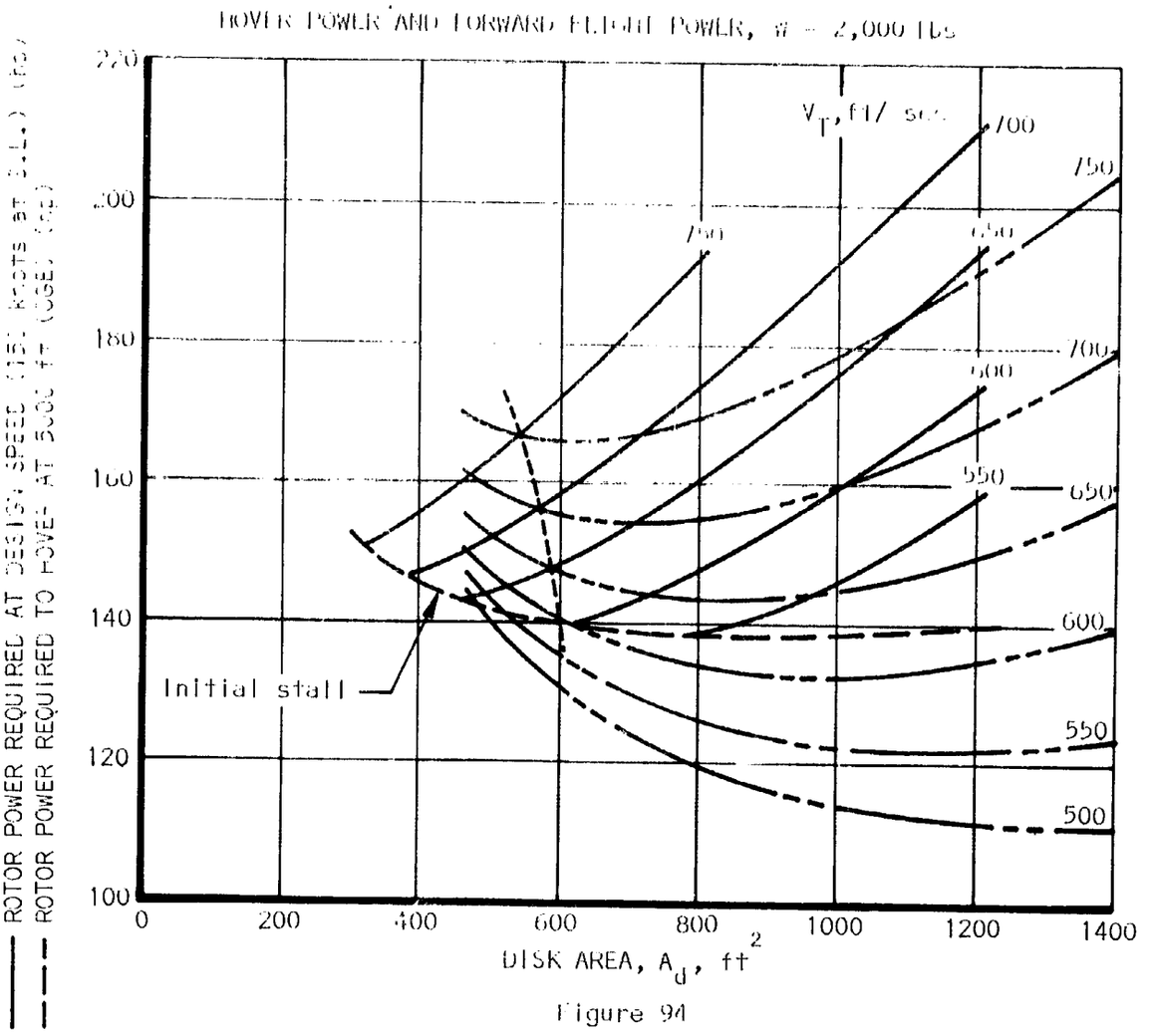


Figure 94

Previously, the rotor power requirements have been developed for three arbitrary gross weights (2000 lb, 2400 lb, and 2800 lb), at various tip speeds and disc areas. Figures 94, 95, and 96 show these power requirements for the design maximum speed of 105 knots at sea level and for the design hover out-of-ground effect (OGE) at 5000 ft. altitude.

A tip speed of 600 ft/sec was selected, which is a compromise between power and blade stall. For various arbitrary disc areas (or rotor diameters) the weight equation was applied. At a fixed diameter, the rotor power was found for each of the three arbitrary weights at V_t = 600 ft/sec. The rotor power has been assumed to be 80% of the total installed power. The remainder is for the tail rotor and transmission and cooling losses so that $P = 1.25\ P_{rotor}$ The rotor solidity in this study has been established previously to be $\sigma = 0.06$.

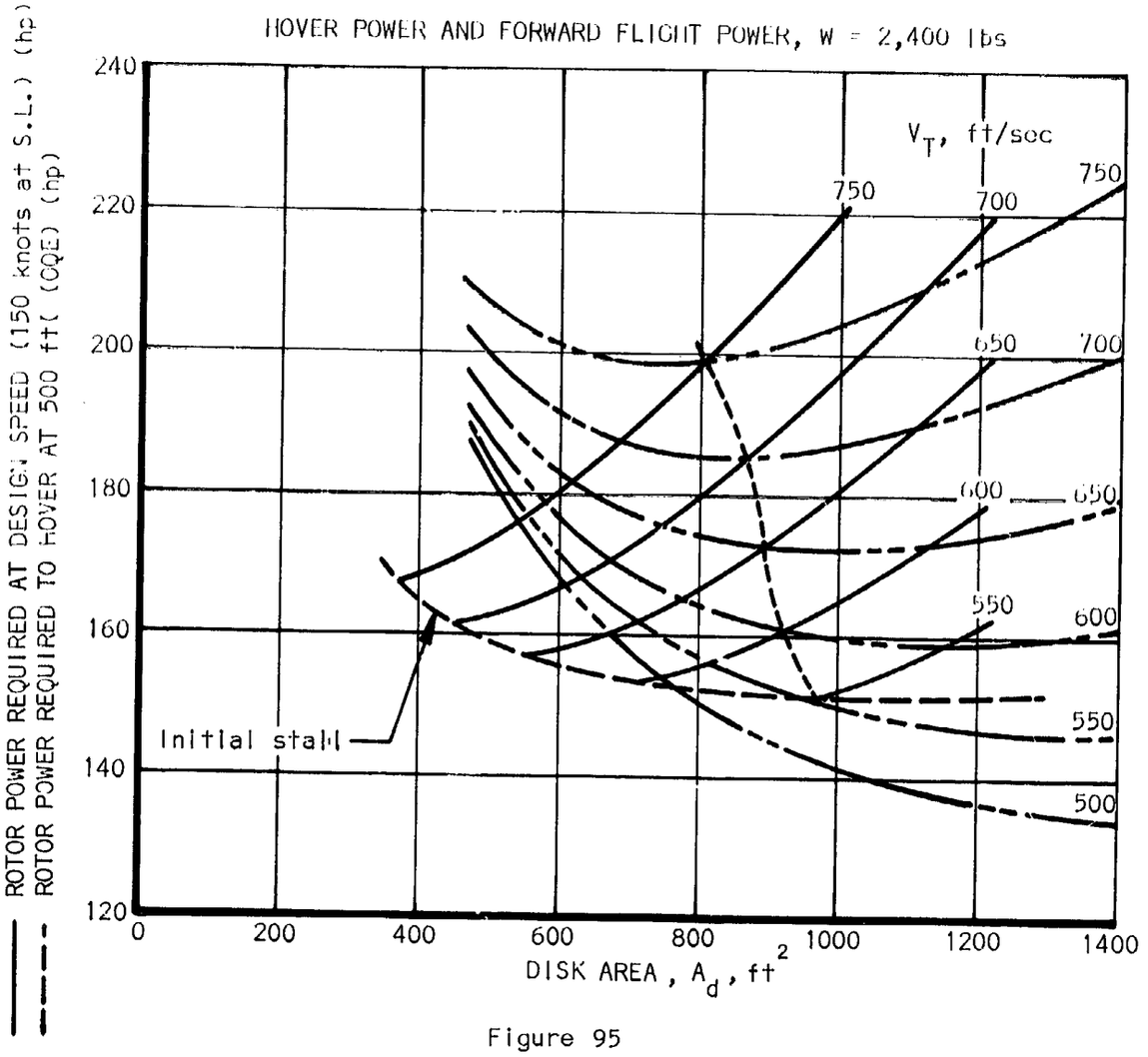


Figure 95

This is all the information needed to solve the weight equation. When the actual weight has been calculated. it is plotted against the arbitrary weights and the real solution can be found on a 45° line of agreement, such as in Figure 97. By plotting the power on this same graph, its value for the solution can also be found.

This has been done for several rotor diameters and the results plotted in Figure 98. Configurations with turbine and reciprocating engines are shown. The turbine versions, even with 100 lb. more fuel, have gross weights approximately 150 lb. less and require about 15 bhp less in installed power.

A turbine-powered helicopter with 218 bhp installed power, a rotor diameter of 28 ft., and a gross weight of 2400 lbs. was selected for further parametric study.

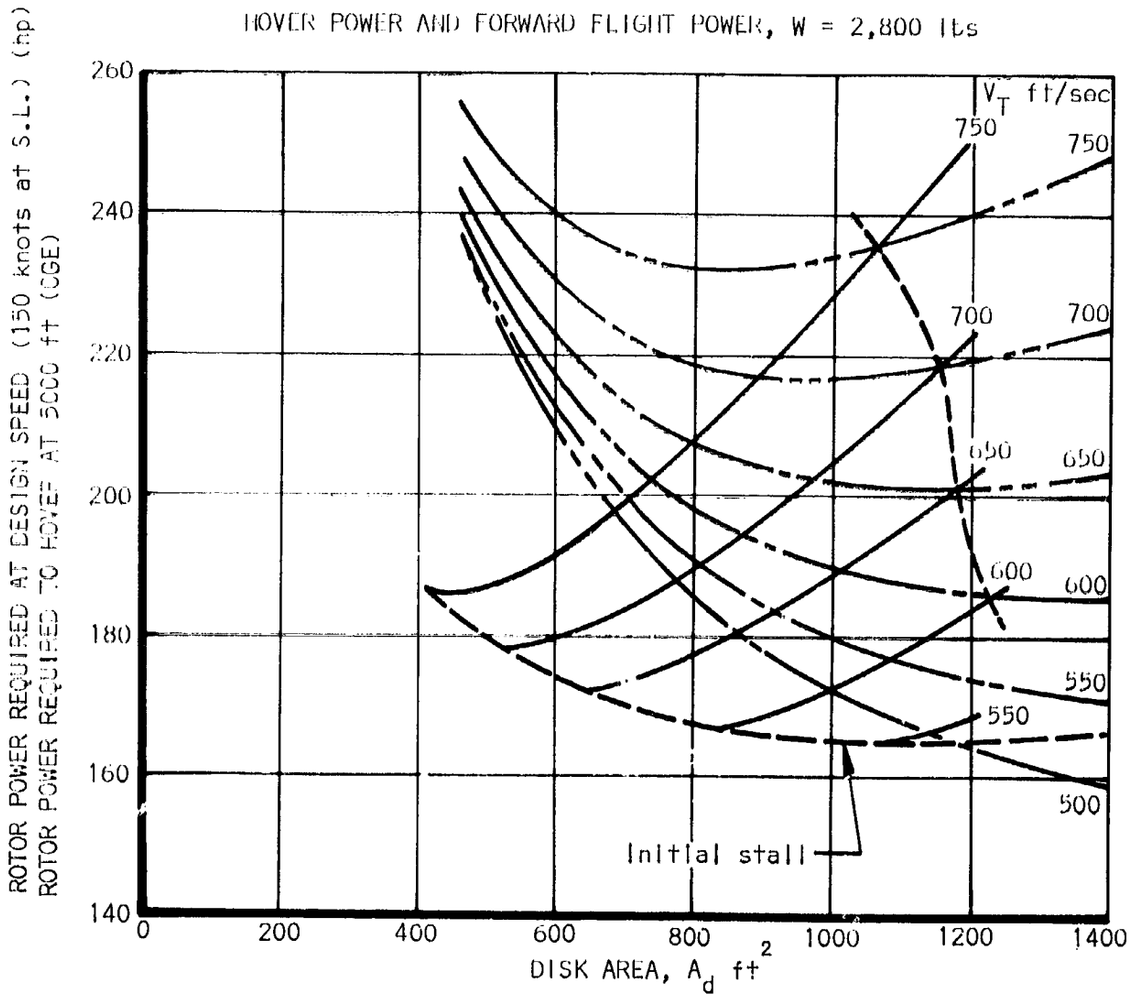


Figure 96

Using this configuration, the sensitivity to weight savings was investigated. For a savings of 100 lbs. of the fixed weight W_o, the savings in power, gross weight, and fuel consumption (maintaining the same rotor diameter) was determined. For comparison, the same was done for a similar configuration with a reciprocating engine. The results are presented in the following table.

TABLE XV. — VALUE OF REDUCING THE HELICOPTER FIXED WEIGHT BY 100 lb.

Type of Engine	W_o lb.	W lb.	ΔW lb.	P bhp	ΔP bhp	Fuel Cons. gal/hr	ΔF.C. gal/hr
Turbine	1900 1800	2400 2280	120	218 203	15	17.45 16.23	1.22
Recip.	1800 1700	2550 2410	140	235 218	17	13.23 12.28	0.95

	Recip. Config.	Turb. Config.
V_L fps	600	600
R, ft	15	15
P, bhp	228	212
W, lb	2570	2430

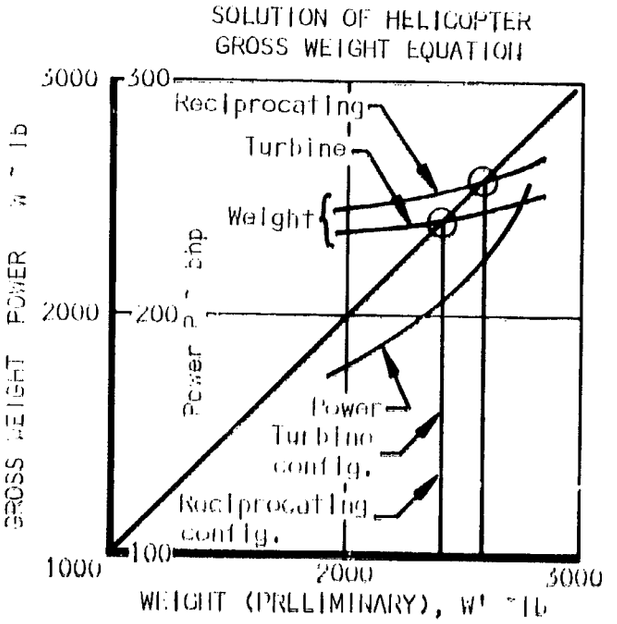


Figure 97

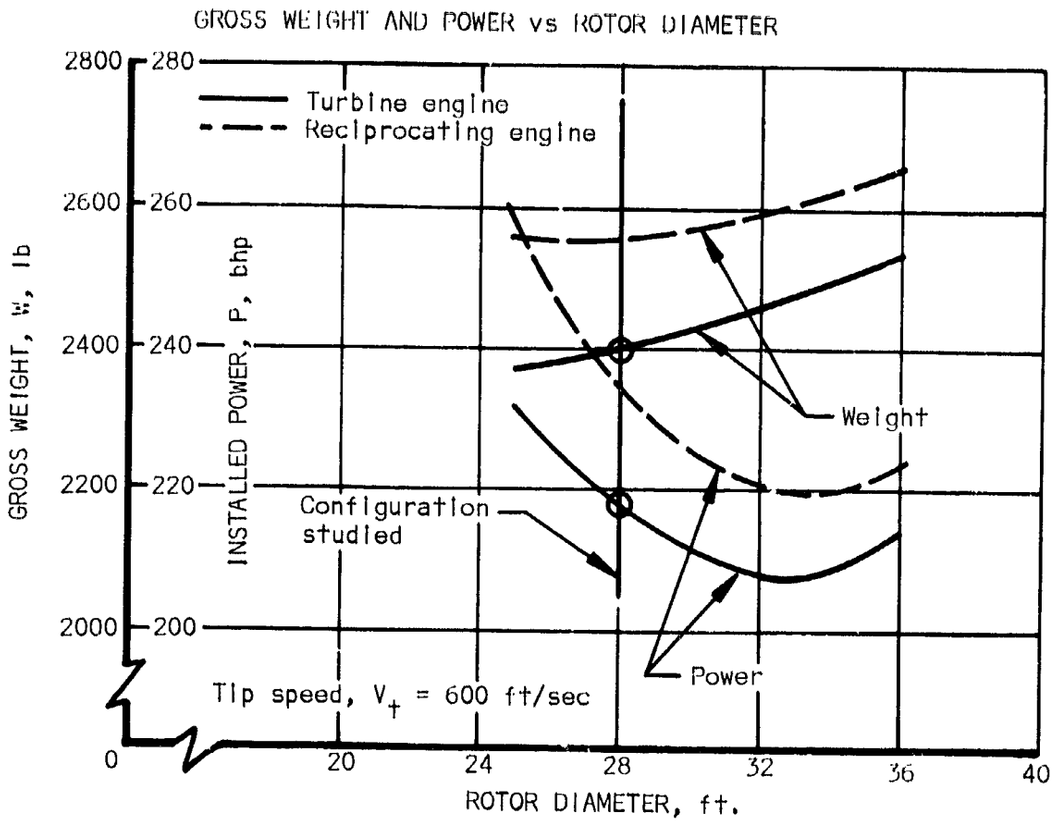


Figure 98

Potential Structural Materials

This chapter concerns the investigation of a wide variety of structural materials applicable in the design of light aircraft (including helicopters) during the next 5 to 15 years. Materials available in five years are classified near-term. Those available fifteen years from now are considered far-term. High-priced near-term materials are also considered as far-term, anticipating cost reductions during the next 15 years.

The objective of this investigation was to determine from the initial compilation, a list of promising candidate materials based on parameters involving strength, stiffness, weight, and raw material cost.

Candidate materials will be further evaluated in subsequent chapters against such parameters as design-concept compatibility, method of joining, fatigue, formability, and costs relating to fabrication.

Initial selection.- Materials were first selected from the broad spectrum of the various types available. In the beginning, an effort was made to pick representative examples from each type, basing the selection on one or more of the following characteristics:

(1) Accepted use in present-day aircraft construction
(2) Low density
(3) Low material cost

    Not always an important factor because fabrication costs can be far more significant.

(4) High stiffness

    Many areas of light aircraft and helicopter structures are designed for stiffness. This takes precedence over static strength requirements

(5) High strength

(6) Weldability, Brazability, Bondability

    Inasmuch as present-day fabrication methods such as riveting contribute considerably to the overall cost of the finished product, a number of potential materials lending themselves to welding, brazing, and or bonding were included

(7) Minimum maintenance

(8) Materials exhibiting good corrosion resistance to atmospheric environments were considered.

Tables XVI and XVII tabulate the initial selection of materials, together with their pertinent properties.

In evaluating the initial selection of materials, structural efficiencies were determined for comparison purposes. These structural efficiencies are:

$$\text{Tension} = \frac{F_{tu}}{w} \qquad \text{Column} = \frac{\sqrt{E_c}}{w} \qquad \text{Shear Buckling} = \frac{\sqrt[3]{E_c}}{w}$$

Each structural efficiency was also divided by the material cost to obtain additional comparisons. In the case of far-term materials (to be used 15 years from now), the projected cost 15 years from now will be used. Comparative structural efficiencies are also presented in Tables XVI and XVII

Material Costs.- Material costs, in dollars per pound, were determined by using price information obtained from the following companies:

Steel	- Ryerson & Sons, Los Angeles, California Republic Steel, Los Angeles, California
Aluminum	- Aluminum Company of America, San Diego, California
Magnesium	- The Dow Chemical Company, Los Angeles, California
Titanium	- Reactive Metals, Inc., Los Angeles, California
Beryllium	- Beryllium Metals & Chemicals Corp., New York, New York
Plastics (Reinforced)	- Whittaker Corp. (Narmco Division), San Diego, California Owens-Corning Fiberglas Corporation, New York, New York General Dynamics/Convair, San Diego, California Goodyear Aerospace Corporation, Akron, Ohio
Plastics (Unreinforced)	- Whittaker Corp. (Narmco Division), San Diego, California General Electric (Chemical Material Dept), Pittsfield, Mass. U.S. Rubber Company, Chicago, Illinois DuPont (Textile Fibers Dept), Wilmington, Delaware Borg-Warner (Marbon Chemical Div.), Washington, West Virginia Fibertite Corporation, Orange, California
Woods	- Niedermeyer-Martin Company, Portland, Oregon Gordon Plywood Company, Alhambra, California
Core Materials	- Hexcel Products, Inc., Los Angeles, California

Promising candidate materials.- The selection of promising candidate materials was based primarily on an evaluation of the comparative structural efficiencies listed in Tables XVI and XVII for all initially selected materials. Additional considerations, such as ability to absorb energy, formability, fatigue, stress corrosion and atmospheric corrosion, low-quench sensitivity,

TABLE XVI

INITIAL SELECTION OF METALLIC MATERIALS AND COMPARATIVE STRUCTURAL EFFICIENCIES

Material	Availability ⑤	F_{tu} KSI	F_{ty} KSI	F_{cy} KSI	E_c $\frac{PSI}{10^6}$	w $\frac{lb}{in^3}$	Material Cost $\frac{\$}{lb}$ ⑥	Characteristics	$\frac{F_{tu}}{w}$ $\times 10^{-5}$	$\frac{F_{tu}}{w\ \$/lb}$ $\times 10^{-5}$	$\frac{\sqrt{E_c}}{w}$ $\times 10^{-5}$	$\frac{\sqrt{E_c}}{w\ \$/lb}$ $\times 10^{-3}$	$\frac{\sqrt[3]{E_c}}{w}$ $\times 10^{-4}$	$\frac{\sqrt[3]{E_c}}{w\ \$/lb}$ $\times 10^{-2}$	Ref.
									Tension		Column		Shear Buckling		
Alloy Steels															
1025 Tube	N	55	36	56	29	.284	0.50 ①	Low Cost, Weldable	194	388	19	38	-	-	7
4130 Norm.Tube	N	95	75	95	29	.283	0.92 ①	High Strength, Weldable	336	365	19	21	-	-	7
4130 (180KHT) Bar	N	180	169	179	29	.283	6.13 ①	High Strength, Weldable	635	4900	19	146	-	-	7
4340 (260HT) Bar	N	260	217	242	29	.283	8.16 ①	Ultra High Strength, Weldable	919	5750	19	119	-	-	7
18Ni Maraging	N	319	284	-	24	.296	2.25 ①	Ultra High Strength, Weldable	1078	480	17	8	-	-	7
Stainless Steel															
301 (Full Hard)	N	185	140	129	28	.286	0.75	Corrosion Resistant, Weldable	645	860	18	24	11	15	7
PH15-7Mo (RH950)	N	225	200	210	30	.277	1.28	Ultra High Strength, Corrosion Resistant	813	635	20	16	11	9	7
Aluminum Alloys															
Sheet															
2024-T3	N	64	42	45	10.7	.100	0.65	Common use, Good Strength/Wgt.	640	985	33	50	22	34	7
2024-T3 (CLAD)	N	60	45	37	10.7	.100	0.66	Low Cost, High Energy Absorb.	600	910	32	48	22	34	7
2219-T87	N	62	56	50	10.8	.102	0.86	Weldable	610	710	32	37	22	25	7
5086-H32	N	40	28	26	10.4	.096	0.53	Weldable, Low Cost	417	787	34	64	23	43	7
5456-H343 ④	N	55	41	39	10.4	.096	0.60	High Welding Efficiency	552	920	34	57	23	38	7
6061-T6	N	42	36	35	10.1	.098	0.54	Low Cost, Corr.Resist, Weldable Formable, High Energy Absorb.	428	794	32	60	22	41	7
7005-T6	N	67	58	59	10.5	.101	0.65	Weldable, Low Distortion	465	716	32	49	22	33	29
7075-T6	N	76	66	67	10.5	.101	0.71	High Strength/Weight	752	1060	32	45	22	31	7
7178-T6	N	83	73	73	10.5	.102	0.75	High Strength/Weight	814	1145	32	45	21	30	7
Extrusions															
2014-T6	N	60	53	55	10.7	.101	0.97	Low Cost, Heavy Extrusions	590	608	32	33	-	-	7
2024-T4	N	60	44	39	10.7	.100	1.12	Common use, Good Str./Weight Low Cost, High Energy Absorb.	600	535	33	29	-	-	7
6061-T6	N	58	35	34	10.1	.098	0.44	Low Cost, Corr.Resist,Weldable Formable, High Energy Absorb.	388	1710	32	73	-	-	7
7075-T6	N	81	73	74	10.5	.101	1.39	High Strength/Weight	802	577	32	23	-	-	7
7075-T73	N	66	58	58	10.6	.101	1.42	Stress Corrosion Resistant	655	462	32	23	-	-	7
7178-T6	N	88	79	79	10.5	.102	1.49	High Strength/Weight	863	579	32	21	-	-	30
6061-T6 (Tube)	N	42	35	34	10.1	.098	0.70	Low Cost, Corr.Resist. Weldable Formable, High Energy Absorb.	428	612	32	46	-	-	7
Forgings															
2014-T6	N	65	55	55	10.7	.101	-	Common use	643	-	32	-	-	-	7
6151-T6	N	44	37	39	10.5	.098	-	High Forgeability, Low Cost	450	-	33	-	-	-	7
Castings															
356-T6	N	25	16.5	16.5	10.3	.097	-	Low Cost, Common use	258	-	33	-	-	-	7
A356-T61	N	38	28	28	10.5	.097	-	Premium Type	392	-	33	-	-	-	7
359-T61	N	45	34	34	10.7	.097	-	High strength	463	-	34	-	-	-	7
Magnesium Alloys															
Sheet															
AZ31B-H24	N	39	29	24	6.5	.064	1.10	High Stiff/Wt. Weld. Low Dens.	610	955	40	36	29	27	7
LA 141-T7	P	19	14	15	6.1	.048	25 (5) ②	Low Density	396	80	52	10	38	8	7, 31
Mg Yttrium-T5	P	55	50	50	6.5	.067	(6) ②	Good Strength/Weight, Weldable	820	137	38	6	28	5	32
Extrusions															
AZ31B-F	N	35	22	12	6.5	.064	1.20	High Stiff/Wt. Weld. Low Dens.	547	455	40	33	-	-	7
ZK60A-T5	N	45	36	30	6.5	.066	3.06	Good Strength/Weight & Stiffness/Weight	682	223	39	13	-	-	7
Castings															
ZK61A-T6	N	34	23	-	6.5	.065	-	Good Strength/Weight	523	-	39	-	-	-	33
ZE63A-T6	N	38	24	-	6.5	.065	-	Good Strength/Weight, Weldable	585	-	39	-	-	-	33
AZ91C-T6	N	27	14	14	6.5	.065	-	Ductile, Sound Castings	416	-	39	-	-	-	7
Titanium Alloys															
Bars															
Ti-6Al-4V ⑧	N	160	150	-	16.4	.160	4.33	High Strength, Weldable Corrosion Resistant	1000	231	25	6	-	-	7
Ti-13V-11Cr-3Al	N	170	160	162	15.5	.174	5.73		977	170	23	4	-	-	
Ti-6Al-4V Sheet ⑧	N	157	143	152	16.4	.160	13.65		980	72	25	2	16	1	7
Beryllium Alloys															
Sheet															
Unalloyed (Hot Pressed)	P	40	27	27	42.5	.067	-		597	-	97	-	-	-	7
Powder Sheet	P	70	50	50 ②	42.5	.067	275 (70) ②	High Stiffness/Weight Excellent for Compression	1045	15	97	1	52	1	34
Lockalloy ⑦	P	44	31	28	28	.076	290 (70) ②		580	8	70	1	40	1	34
Extrusions															
Unalloyed	P	95	45	45	42.5	.067	-		1390	-	97	-	-	-	34
Lockalloy ⑦	P	56.5	44.5	40 ②	28	.076	-		743	-	70	-	-	-	34

NOTES: ① Bar ② 3/4" Diameter x .065" Wall ⑤ N = Near Term P = Potential ⑥ Costs: t = .032" for Sheet t = .125" for Extrusion ( ) = 1982 Estimate ⑦ 62% Be - 38% Al

② Estimated ④ t = .050" Minimum Thickness ⑧ Solution Heat Treated and Aged

TABLE XVII

INITIAL SELECTION OF NON-METALLIC MATERIALS AND COMPARATIVE STRUCTURAL EFFICIENCIES

MATERIAL	AVAILABILITY ②	F_{tu} PSI	F_{ty} PSI	F_{cu} PSI	E_c $\frac{PSI}{10^6}$	w $\frac{LB}{in^3}$	MATERIAL COST $/LB	CHARACTERISTICS	$\frac{F_{tu}}{w}$ × 10^{-3}	$\frac{F_{tu}}{w\ \$/LB}$ × 10^{-3} ①	$\frac{\sqrt{E}}{w}$ × 10^{-3}	$\frac{\sqrt{E_c}}{w\ \$/LB}$ × 10^{-3} ④	$\frac{\sqrt[3]{E_c}}{w}$ × 10^{-2}	$\frac{\sqrt[3]{E_c}}{w\ \$/LB}$ × 10^{-2} ①	REF.
GLASS REINFORCED PLASTICS															
Chopped Fiber															
E-Glass/Polyester	N	20	-	26	1.99	.070	0.65	Corrosion Resistant, Formable	286	494	70	52	18	29	44
E-Glass/Nylon Copolymer	N	20	-	18	1.6	.048	1.64(0.66)	Low Density, Formable	418	261 (643)	71	15 (37)	4.1	15 (37)	44
18% S-Glass/Epoxy	N	45	-	62	7.8	.060	4.00(2.00)	High Strength & Stiff/Weight	750	190 (380)	46	12 (24)	3.3	8 (16)	44
Continuous Fiber							①								
181 Cloth E-glass/Epoxy	N	45	-	45	3.3	.070	2.00(1.00)		643	321 (643)	26	13 (26)	3.1	11 (22)	44
143 Cloth E-glass/Epoxy	N	60	-	60	6.1	.070	2.00(1.00)	Corrosion Resistant Formable	1210	605(1210)	32	16 (32)	3.5	14 (28)	44
181 Cloth S-glass/Epoxy	N	98	-	66	4.2	.070	4.00(2.00)	High Strength/Weight	1540	535 (770)	29	7 (14)	2.5	6 (12)	44
143 Cloth S-glass/Epoxy	N	139	-	76	5.9	.070	4.00(2.00)		1980	495 (990)	35	9 (18)	3.0	8 (15)	44
Glycol Phthalate (Fragrex)	N	49 ①	-	-	2.6	.070	3.15 ①	Low Curing Temp., Formable	700	223	23	7	2.8	9	44
FILAMENT REINFORCED PLASTICS/EPOXY MATRIX															
Unidirectional															
Boron	P	140	-	175	33	.071	700(10.00)		1970	(197)	81	(8)	45	(5)	16,45
Graphite	P	95.9	-	96.5	15.4	.051	600 (1.00)	High Strength/Weight	1870	(1870)	77	(77)	49	(49)	16,45
E-Glass	P	150	-	85	6.9	.076	2.00(1.00)	Low Density	1970	(1970)	35	(35)	25	(25)	16
S-Glass	P	210	-	120	7.6	.073	4.00(2.00)	Corrosion Resistant	2880	(1440)	38	(19)	27	(14)	16
Hollow Glass	P	80	-	80	4.5	.065	-		1230	-	33	-	25	-	16
Hi-Modulus Glass	P	210	-	120	9.2	.073	-		2880	-	42	-	29	-	16
Laminate (t=.016 in) ±45° Layers															
Boron	P	19.8	-	37.7	4.18	.071	700(10.00)		279	-	-	-	-	-	16,45
Graphite	P	5.8	-	31.6	2.10	.051	600 (1.00)		114	-	-	-	-	-	16,45
E-Glass	P	17.5	-	29.8	2.19	.076	2.00(1.00)	High Strength/Weight	230	-	-	-	-	-	16
S-Glass	P	17.7	-	37.3	2.49	.073	4.00(2.00)	Low Density	243	-	-	-	-	-	16
Hollow Glass	P	17.6	-	28.8	1.53	.065	-	Corrosion Resistant	271	-	-	-	-	-	16
Hi-Modulus Glass	P	17.7	-	37.3	2.98	.073	-		243	-	-	-	-	-	16
Laminate (t=.040 in) ±45°, 0°, 0°, 0° Layers															
Boron	P	91.9	-	120.1	21.9	.071	700(10.00)		1295	-	-	-	-	-	16,45
Graphite	P	29.5	-	46.5	10.2	.051	600 (1.00)		1175	-	-	-	-	-	16,45
E-Glass	P	97.0	-	62.9	5.0	.076	2.00(1.00)	High Strength/Weight	1275	-	-	-	-	-	16
S-Glass	P	133.1	-	86.9	5.6	.073	4.00(2.00)	Low Density	1825	-	-	-	-	-	16
Hollow Glass	P	55	-	59.5	3.3	.065	-	Corrosion Resistant	847	-	-	-	-	-	16
Hi-Modulus Glass	P	133.1	-	86.9	6.8	.073	-		1825	-	-	-	-	-	16
UNREINFORCED THERMOPLASTICS															
ABS (Sheet)	N	5.8	-	5.0	.190	.040	0.90		95	105	11	12	14	16	59
ABS (High Strength)	N	7.3	-	10.4	.180	.039	0.46 ⑥	Low Density	187	407	11	24	14	31	40
Polycarbonate	N	9.5	8.5	-	.345	.043	1.90	Formable	221	116	14	7	16	9	41
Nylon Yarn	N	22	-	-	.640	.049	5.10		450	88	16	3	18	3	42
Whittaker PBI-R	N	20	-	30	.700	.043	5.00		465	93	20	4	21	4	-
WOOD				F_{cy}											
Hardwoods ④															
White Ash	N	15.2	7.2	4.3	1.4	.022	5.80		600	104	54	9	-	-	45
Yellow Birch	N	15.1	7.6	4.6	1.85	.025	6.60		603	92	54	8	-	-	45
Softwoods ④								Low Density							
White Cedar	N	10.2	6.7	4.1	1.4	.016	2.10		638	303	74	35	-	-	45
Douglas Fir	N	10.9	5.9	4.2	1.5	.018	0.52	Presently used in	606	1170	68	131	-	-	45
Sitka Spruce	N	9.4	5.3	3.5	1.4	.015	0.67	some light aircraft	626	955	79	118	-	-	45
Plywoods, 3-ply (.070 in thick) parallel to face grain															
Birch-Birch	N	8.6	-	2.7	1.2	.028	2.06		307	149	39	19	38	18	43
Poplar-Poplar	N	4.6	-	1.6	.8	.020	2.12		230	109	45	21	46	22	43
Mahogany-Poplar	N	6.7	-	2.6	.9	.020	2.05		340	166	48	23	48	23	43
Modified Woods, Staypak (parallel laminated)															
Birch, t=0.46	P	44.1	18.9	8.0	4.4	.049	-	Good Strength/Weight	900	-	43	-	-	-	43
Spruce, t=0.32	P	55.8	25.9	4.3	4.7	.047	-	Stabilized Wood	760	-	46	-	-	-	43

CORE MATERIALS	AVAILABILITY ②	F_{su} (min) PSI	F_{cu} (min) PSI	w LB/FT^3	MATERIAL COST $/LB	CHARACTERISTICS	REF.
Resin Coated Nylon 3/16 cell	N	45	140	2.0	22.90	Light Weight, Fireproof	44
5052 Aluminum 1/4 cell	N	44	92	2.3	4.17	Inexpensive, presently used in aircraft	44
5052 Aluminum 1/4 cell	N	52	112	2.3	4.84		44
2024 Aluminum 1/4 cell	N	138	300	2.8	11.62	High Strength/Weight	44
Nylon Phenolic 3/8 cell	N	56	160	2.5	14.10	Good Strength/Weight	44

NOTES: ① ESTIMATED ② N = NEAR TERM, P = POTENTIAL ③ ( ) = 1982 ESTIMATE ④ PARALLEL TO GRAIN ⑥ RESIN

⑤ MIL HDBK 17 material properties were used in this table if available. Otherwise, manufacturers published data were used.

loading intensity, and accepted usage in present-day aircraft, also influenced the choosing of candidates. Metallic material condidates are listed in Table IV, together with their structural efficiencies. Non-metallic material candidates are presented in Table V in a similar manner. Figures 99,100, and 101 list the comparative structural efficiency of materials by decreasing order of magnitude.

Metallic Materials: (Ref. Table XVIII)

TUBING - Two steels and one aluminum alloy were selected as tubing candidates. While the 6061-T6 aluminum alloy is superior from the standpoint of structural efficiencies, 1025 steel is still being used today in areas where low cost and ease of welding so dictate. The 4130 normalized steel tubing is used where column loading intensities are moderate-to-high and size limitations are present. The most likely areas of application for tubing are fuselage weldments and engine mounts.

BAR MATERIAL - Candidates are listed with the intent of showing materials of high strength for use in areas of landing-gear assemblies, rotor mechanisms, and primary structural fittings having space limitations. Although there are many types of high-strength materials available, the selection represents the lower and upper end of the chrome-alloy series (4130 and 4340), and also includes one of the newer types of maraging steels, 25 Ni. This steel, although 1.8 times as strong as 4130 (180 H.T.), is also seventeen times as costly ($2.25/lb vs. $0.13/lb). It is a high-quality steel with superior corrosion resistance and toughness over the commonly-used chrome-alloy series.

FORGINGS are occasionally used in helicopters and light aircraft. When used, 2014-T6 is the primary forging alloy, especially for miscellaneous low-stressed fittings where economy and increased corrosion performance predominate.

SHEET - A number of sheet materials are available for use in the construction of light aircraft and helicopters. Sheet stock is used mainly as a covering for the airframe. It is also bent and formed into frames, ribs, stringers, stiffeners, and various types of brackets.

The 2024-T3 alloy, especially the clad version, is by far the most commonly-used skin covering on present-day light aircraft. In addition to having high structural efficiencies, it is a good corrosion-resistant candidate, exhibiting superior qualities of fatigue, energy absorption, and formability when compared to most of the other sheet materials.

The 5XXX series aluminum sheet material is included because of its low-cost structural efficiencies. It also has good formability.

Type 6061-T6 is next in importance to 2024-T3 clad as a material candidate. Its low cost, coupled with its high corrosion resistance and high stress corrosion resistance, formability, and energy absorption characteristics, makes it extremely attractive.

TABLE XVIII
PROMISING CANDIDATE MATERIALS - METALIC

MATERIAL	AVAIL-ABILITY	F_{tu}	F_{ty}	F_{cy}	F_{su}	E_c	e	w	CORROSION RESISTANT	MATERIAL COST	WELD-ABILITY	THERMAL CO-EFF.	COMPARATIVE STRUCTURAL EFFICIENCIES						REF.
	⑥	KSI	KSI	KSI	KSI	$\frac{PSI}{10^6}$	%	$\frac{LB}{in^3}$		$ / LB		in/in/°F	$\frac{F_{tu}}{w}$	$\frac{F_{tu}}{w\ \$/LB}$	$\frac{\sqrt{E_c}}{w}$	$\frac{\sqrt{E_c}}{w\ \$/LB}$	$\frac{\sqrt[3]{E_c}}{w}$	$\frac{\sqrt[3]{E_c}}{w\ \$/LB}$	
TUBING																			
1025 Steel	N	55	36	36	35	29	8-13	.284	POOR	0.50 ①	EXCEL	.70	194	388	19	38	-	-	7
4130(Normalized)	N	95	75	75	55	29	12	.283	FAIR	0.92 ①	GOOD	.63	336	365	19	21	-	-	7
6061-T6	N	42	35	34	27	10.1	12	.098	EXCEL	0.70 ⑦	GOOD	1.30	429	613	32	46	-	-	7
BAR (t=1.00 in)																			
4130 (180HT)	N	180	163	179	109	29	12	.283	FAIR	0.13	GOOD	.63	635	4900	19	146	-	-	7
4340 (260HT)	N	260	217	242	149	29	10	.283	FAIR	0.16	FAIR	.63	919	5750	19	114	-	-	7
25 Ni (Maraging)	N	319	284	-	-	24	8	.296	GOOD	2.25	FAIR	.59 ⑤	1078	480	17	8	-	-	5
FORGING																			
6181-T6	N	44	37	39	28	10.3	10	.098	EXCEL	-	-	1.28	450	-	33	-	-	-	7
2014-T6	N	65	55	55	39	10.7	7	.101	POOR	-	-	1.25	643	-	32	-	-	-	7
SHEET (t=.032 in)																			
2024-T3	N	64	42	45	40	10.7	15	.100	POOR	0.65	GOOD	1.29	640	985	33	50	22	34	7
2024-T3 CLAD	N	60	45	37	38	10.2	15	.100	GOOD	0.65	GOOD	1.29	600	910	32	49	22	33	7
5086-H32	N	40	28	26	24	10.4	6	.096	GOOD	0.53	EXCEL	1.32	417	787	34	64	23	43	7
5456-H343 ④	N	53	41	39	31	10.4	6	.096	GOOD	0.60	EXCEL	1.32	552	920	34	57	23	38	7
6061-T6	N	42	36	35	27	10.1	10	.098	EXCEL	0.54	GOOD ②	1.30	429	794	32	60	22	41	7
X7005-T6	N	47	38	39	-	10.5	-	.101	GOOD	0.65	GOOD	1.30	465	716	32	49	22	33	29
7075-T6	N	76	66	67	46	10.5	7	.101	POOR	0.71	GOOD	1.29	750	1060	32	45	22	31	7
7178-T6	N	83	73	73	50	10.5	7	.102	POOR	0.71	GOOD	1.30	814	1145	32	45	21	30	7
AZ 31B-H24	N	39	29	24	18	6.5	6	.064	POOR	1.10	GOOD	1.40	610	555	40	36	29	27	7
EXTRUSION(t≤.250)																			
2014-T6	N	60	53	55	35	10.7	7	.101	POOR	0.97	GOOD	1.25	590	608	32	33	-	-	7
2024-T4	N	60	44	39	32	10.7	12	.100	POOR	1.12	GOOD	1.29	600	535	33	29	-	-	7
6061-T6	N	38	35	34	24	10.1	10	.098	EXCEL	0.44	GOOD	1.30	396	1710	32	73	-	-	7
7075-T6	N	81	73	74	45	10.5	7	.101	POOR	1.39	GOOD ②	1.29	802	577	32	23	-	-	7
7075-T73	N	66	58	58	-	10.6	-	.101	GOOD	1.42	GOOD	1.29	655	460	32	23	-	-	30
7178-T6	N	88	79	79	47	10.5	5	.102	POOR	1.49	GOOD	1.30	868	579	32	21	-	-	7
Mg Yttrium-T5	P	55	50	50	30	6.5	4	.067	POOR	(6.00) ③	GOOD	1.40 ⑤	520	1177	39	(b)	-	-	7
CASTING																			
A356-T61	N	38	28	28	27	10.5	5	.097	GOOD	-	-	1.19	596	-	33	-	-	-	7
356-T6	N	25	16.5	16.5	25	10.3	3	.097	GOOD	-	-	1.19	392	-	33	-	-	-	7
359-T61	N	45	34	34	31	10.7	4	.097	GOOD	-	-	1.16	464	-	34	-	-	-	7
ZK 61A-T6	N	34	23	-	-	6.5	2	.065	FAIR	-	-	1.40 ⑤	523	-	39	-	-	-	30
ZE 63A-T6	N	38	24	-	-	6.5	4	.065	FAIR	-	-	1.40 ⑤	584	-	39	-	-	-	30
AZ 91C-T6	N	27	14	14	-	6.5	2	.065	FAIR	-	-	1.40	415	-	39	-	-	-	7

① 3/4 x .065 WALL ② RESISTANCE WELDABILITY ③ ( ) = 1980 ESTIMATE ④ t = .051 ⑤ ESTIMATED
⑥ N = NEAR TERM, P = POTENTIAL

Type X7005 aluminum alloy is one of the more recently developed materials. It can be easily brazed, soldered, or welded and still maintain its high properties without requiring solution heat treating afterwards. Its low-quench sensitivity, eliminating severe distortion during cooling after heat treatment, makes this alloy a material candidate.

Types 7075-T6 and 7178-T6 are included as they represent the highest strength aluminum alloys available today. While their corrosion and stress-corrosion resistance, formability, energy absorption, and quench sensitivity characteristics are inferior to some of the other aluminum alloys, they exhibit superior tensile structural efficiencies and will outperform other aluminum alloys when used in areas of high-load intensity.

AZ 31B-H24 magnesium alloy has superior column and shear buckling structural efficiencies and is, therefore, listed with the aluminum sheet material. Its higher cost and lower corrosion resistance make it a less likely candidate.

EXTRUSIONS are used mainly as flange material in beams and major bulkheads, stringer material in wide columns (fuselage semi-monocoque, wing-plate stringer), and stiffeners in high-loading intensity areas.

Type 2014-T6 is generally used for sections greater than 0.125-inch thick where its low cost, together with its high-yield strength, makes it a desirable candidate.

Type 2024-T4 extrusions are commonly found in light aircraft for sections under 0.125-inch thick. This alloy, in addition to having good structural efficiencies, exhibits superior fatigue and energy-absorption qualities.

Type 6061-T6 shows considerable promise for extrusions requiring thin sections and high corrosion resistance. The low cost, high energy absorption, and stress-corrosion resistance of this alloy make it an excellent candidate.

The 7075 and 7178 extrusions have the highest mechanical properties of the aluminum alloys. While the T6 tempers are relatively low in stress-corrosion resistance and energy-absorption capabilities, the T73 temper of 7075 is excellent in both respects and warrants consideration in the final selection of candidate materials.

Mg Yttrium-T5 is a new high-strength magnesium alloy. Its high compression yield strength (improving the compressive tangent modulus), coupled with its low density, makes it the most efficient of all the metallic candidates when used in compression critical structures. However, the projected cost of $6.00 per pound fifteen years from now reduces its chances of becoming a prime candidate.

CASTINGS are used mainly for rotor mechanisms, wheel hubs, pulleys, brackets, bellcranks, and various fittings.

A356-T61 and 359-T61 are premium-quality composite mold castings. Although they are in general use today, anticipated high production rates for light aircraft/helicopters make these alloys less likely candidates than a permanent mold or die-cast material.

Type 356-T6 is a permanent mold casting alloy in general use today, and it appears it will remain a likely candidate in the future.

AZ 91C-T6, available as a permanent mold casting, is one of the most common magnesium castings in use today.

CORE MATERIAL (Ref. Table XVII) is used in honeycomb-sandwich constructions. Type 3003 1/4-inch cell, 2.3 pounds per cubic foot aluminum honeycomb core is considered to be the most promising candidate. It is of adequate strength for light aircraft construction and is only a fraction of the cost of the expensive reinforced plastic honeycomb.

COMPARATIVE SHEAR CRIPPLING EFFICIENCIES

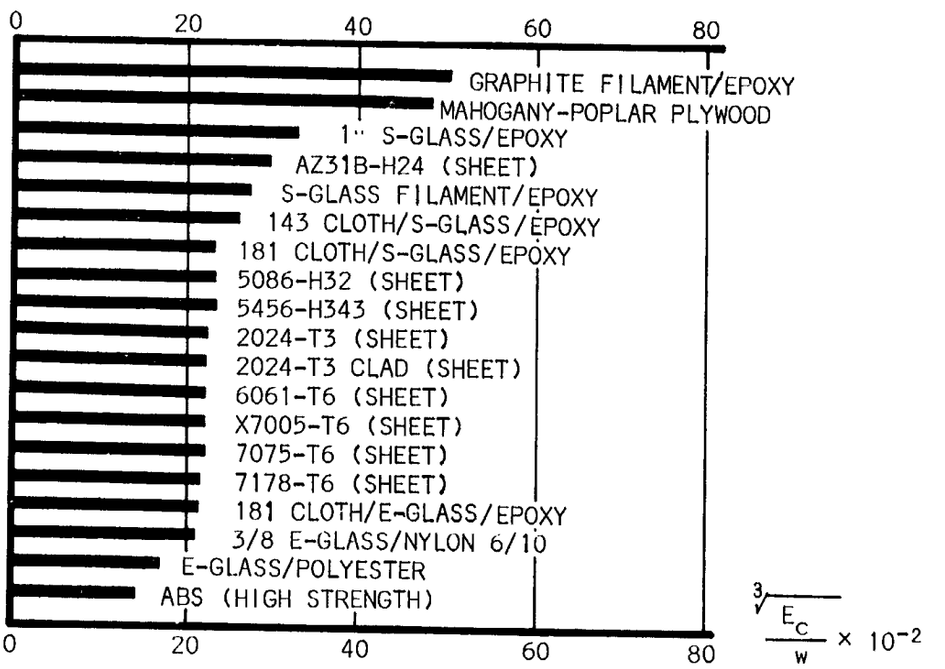


Figure 99

COMPARATIVE COLUMN EFFICIENCIES

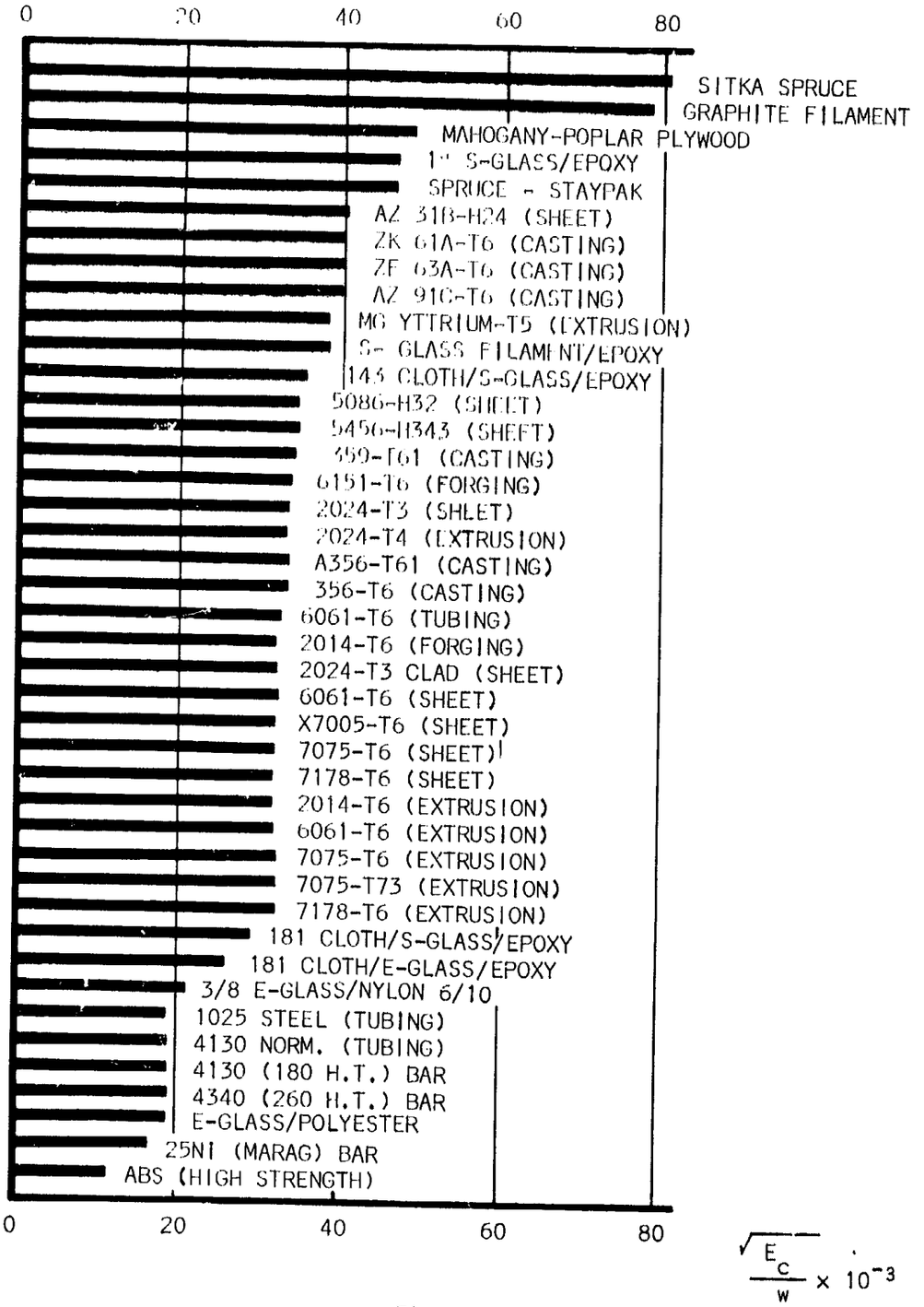


Figure 100

COMPARATIVE TENSION EFFICIENCIES

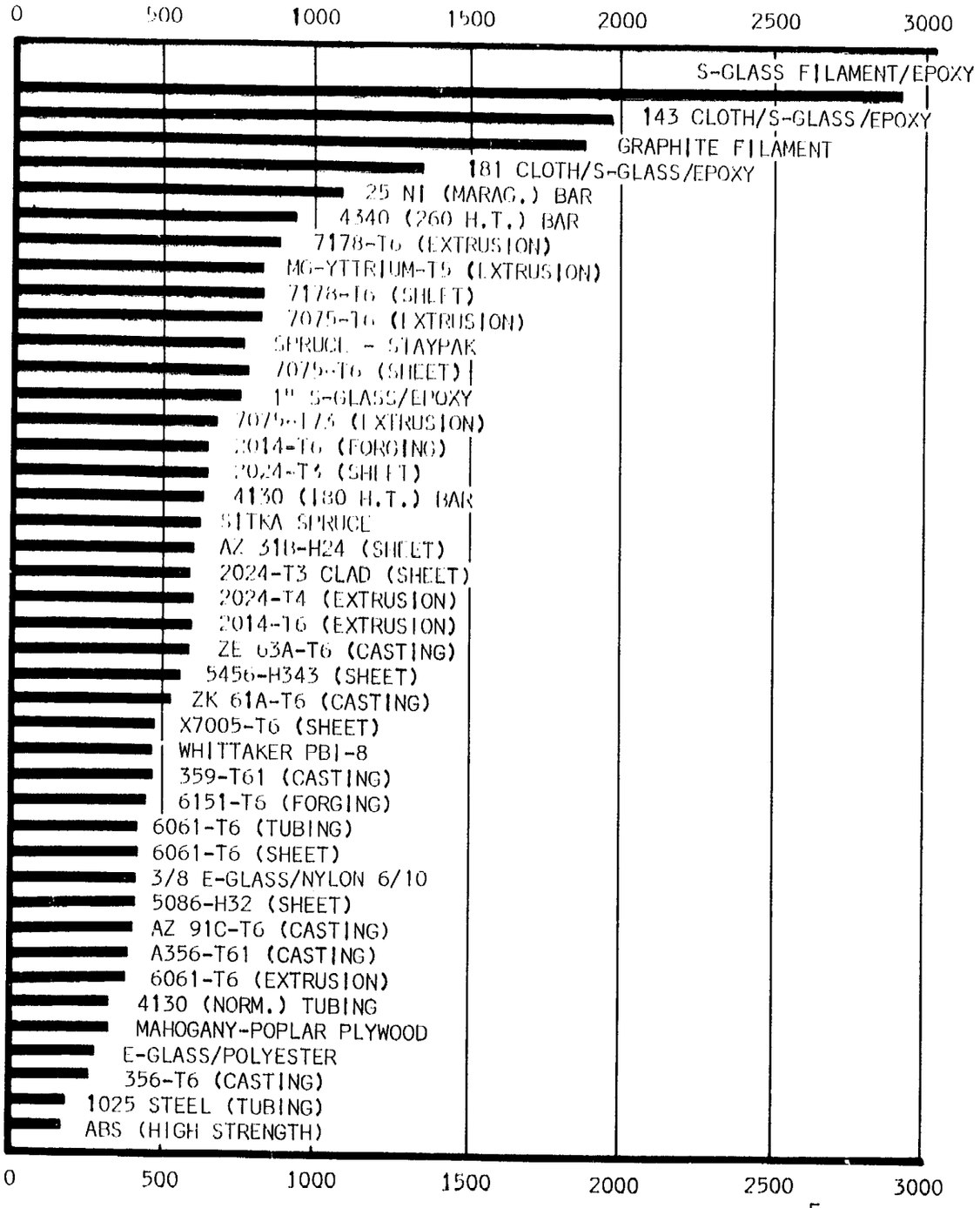


Figure 101

Non-Metallic Materials : (Ref. Table XIX)

NON-REINFORCED THERMOPLASTICS are used for fairings and for low-stressed skin.

ABS (High Modulus) is low in cost and can be molded to shapes. This material, although not highly flammable, will support combustion.

CHOPPED FIBER-REINFORCED PLASTICS are best adapted for areas of low - loading intensity such as secondary fittings, fairings, and low-stressed skin.

3/8 E-Glass/Nylon 6/10, is a medium-cost injection moldable thermoplastic reinforced with 1/4-inch to 3/8-inch long glass fibers (30% by weight). It is finding use in the design of next-generation commercial transports in such areas as access covers for wing fuel tanks. Nylon 6/10 is a self-extinguishing material from the standpoint of flammability.

E-Glass/Polyester is a low-cost discontinuous glass fiber, reinforced polyester-type sheet molding compound. Fairings, low-stressed skins, and fittings are possible areas of application for this material. It is also a flame-retardant (non-burning) material.

1-inch S-Glass/Epoxy, a one-inch chopped fiber system with an epoxy matrix, is a high-strength, high-cost material used in helicopter wheels.

CLOTH REINFORCED THERMOSETS may be used for all types of structures by providing the optimum fiber orientation for each type of loading. They are best used in multi-layer combinations in laminates or in sandwich construction.

Type 143 Cloth/E-Glass in an epoxy matrix is used in laminate and sandwich form in light aircraft and helicopters. Its use is restricted, as a rule, to secondary structure. However, the advancing state of the art of fiberglass composites and resin systems indicates that this material is a candidate for primary structure.

Type 143 Cloth/S-Glass and epoxy matrix system is a higher-strength and higher-cost composite than the E-Glass system. It is a candidate material when structural efficiencies outweigh material cost, or can be shown cost effective.

UNIDIRECTIONAL FILAMENT-REINFORCED COMPOSITES are in their infancy at present. Most of the composites are extremely expensive and are being used only in isolated cases. However, their superior structural efficiencies indicate that, projected ahead fifteen years from now, these composites, with reduced costs, will be potential candidates. They should be laminated in various fiber orientations, depending on the loading conditions.

TABLE XIX
PROMISING CANDIDATE MATERIALS – NON-METALLIC

MATERIAL	APPLI-CATION ③	F_{tu} KSI	F_{ty} KSI	F_{cu} KSI	F_{su} KSI	E_c PSI / 10^6	e %	ρ LB/IN.³	WEATHER-ABILITY	MATERIAL COST ② $/LB	THERMAL COEFFICIENT OF EXPANSION IN/IN-°F	COMPARATIVE STRUCTURAL EFFICIENCIES: F_{cu}/ρ	F_{tu}/ρ $/LB	$\sqrt{E_c}/\rho$	$\sqrt{E_c}/\rho$ $/LB	$\sqrt[3]{E_c}/\rho$	$\sqrt[3]{E_c}/\rho$ $/LB	REF
NON-REINFORCED																		
ABS (High Strength)	NT-FT	7.3	–	10.4	–	.180	20	.039	EXCEL	1.40	6.00	180	470	11	24	14	31	5,40
NON-CONTINUOUS FIBER REINFORCED																		
3/8 E-Glass/Nylon 6/10	FT	20	–	18	11	1.0	5–6	.048	EXCEL	1.54 (10.00)	0.60	375	415	2	(30)	21	(30)	25
1" S-Glass/Epoxy	FT	45	–	62	8	7.8	–	.060	EXCEL	4.00 (10.00)	–	750	750	2	(30)	27	(30)	26
E-Glass/Polyester	NT	20	–	26	–	1.99	–	.070	EXCEL	0.40	1.00	370	410	10	22	15	29	35
CLOTH REINFORCED																		
DAP Prepreg	NT-FT	49 ①	–	–	–	2.6 ①	–	.070 ①	EXCEL	5.15 (11.00)	–	700	480	23	(14)	20	(12)	37,38
181 Cloth/E-Glass	NT-FT	45	–	45	–	3.3	–	.073	EXCEL	(8.00)	–	642	(342)	11	(6)	21	(21)	14
181 Cloth/S-Glass	NT-FT	94	–	65	–	4.2	–	.073	EXCEL	(8.00)	–	890	(475)	24	(14)	23	(12)	36
FILAMENT REINFORCED (EPOXY MATRIX)																		
Unidirectional																		
Graphite	FT	95.9	–	56.5	5.2	15.4	–	.051	EXCEL	(11.00)	–	1870	(1870)	77	(77)	49	(49)	1c
S-Glass	FT	210	–	120	13.6	7.6	–	.073	EXCEL	(2.00)	–	2980	(1490)	38	(19)	27	(13)	1b
±45° Layers (t=.016 in)																		
Graphite	FT	5.8	–	31.6	24.8	2.1	–	.051	EXCEL	(11.00)	–	774	(114)	28	(28)	25	(25)	1b
S-Glass	FT	17.7	–	37.3	50.0	2.6	–	.073	EXCEL	(2.00)	–	849	(170)	22	(11)	19	(10)	16
±45°,0° Layers (t=.024 in)																		
Graphite	FT	35.8	–	39.9	20.4	6.6	–	.051	EXCEL	(11.00)	–	781	(781)	60	(60)	37	(37)	1b
S-Glass	FT	81.8	–	64.9	39.5	4.2	–	.073	EXCEL	(2.00)	–	1100	660	28	(14)	22	(11)	16
±45°,0°,0° Layers (t=.032 in)																		
Graphite	FT	50.8	–	44.0	17.8	8.8	–	.051	EXCEL	(11.00)	–	1100	(1100)	68	(68)	41	(20)	1b
S-Glass	FT	113.8	–	78.7	34.0	5.1	–	.073	EXCEL	(2.00)	–	1560	780	31	(15)	24	(12)	16
±45°,0°,0°,0° Layers (t=.040 in)																		
Graphite	FT	59.8	–	46.5	15.9	10.2	–	.051	EXCEL	(11.00)	–	1450	(1170)	67	(63)	43	(43)	16
S-Glass	FT	133.1	–	86.9	30.5	5.6	–	.073	EXCEL	(2.00)	–	1824	(912)	30	(76)	24	(12)	16
WOOD				F_{cy}														
Sitka Spruce	NT	9.4	5.3	3.5	1.0	1.4	–	.015	POOR	0.40	–	420	935	79	118	–	–	43
Mahogany/Poplar Plywd	NT	6.7	–	2.6	1.9	.9	–	.020	POOR	0.25	–	325	167	48	23	48	23	43
Spruce – Staypak	NT	35.8	25.9	4.3	1.3	4.7	.75	.047	FAIR	③	–	760	②	46	④	–	–	43

NOTES: ① ESTIMATED ② ( ) = 1982 ESTIMATE ③ NT – NEAR TERM; FT – FAR TERM ④ EXPERIMENTAL, NO PRICE AVAILABLE

Graphite filament/epoxy matrix composite exhibits exceptional structural efficiencies due to low density and high modulus.

S-Glass/epoxy matrix composites show superior tension efficiencies and modulus as compared with Graphite; however, they do not compare with the column and shear buckling efficiency of the Graphite system.

WOOD has been used as primary and secondary structure in light aircraft for many years. Although aluminum alloys have predominated the light aircraft field for the past decade, there are still a few airplanes being constructed of wood. Generally speaking, a wooden structure (such as a wing) is aerodynamically smoother and lighter than its metal counterpart. However, it is also more expensive to build. Another disadvantage to wood construction is its higher maintenance cost due to weathering and moisture absorption.

Sitka-Spruce is probably the most common wood used in light aircraft. It has a column efficiency more than twice that of the aluminum alloys.

Mahogany (poplar core) plywood is one of the more common woods used for skins. Its shear buckling efficiency is twice that of the aluminum alloys.

Spruce-Staypak is a compressed wood with greatly increased mechanical properties and higher density.

Evaluation of promising candidate materials.- The promising candidates are now compared on the basis of types of members and concepts. Composites, which are anisotropic, require some mention being made as to allowables versus fiber orientation. When these materials in single-laminate configuration are loaded at an angle to the direction of the fibers, their strength is reduced considerably. The reduction in allowable is a function of the angle. Figure 103 illustrates the effect due to the low shear transfer capability of the resin matrix. For this reason, composite systems are normally found in various combinations of fiber-oriented layers. As an example, a wing skin panel carrying torsion might require three layers with the following orientation (see Figure102):

SKIN PANEL FIBER ORIENTATION

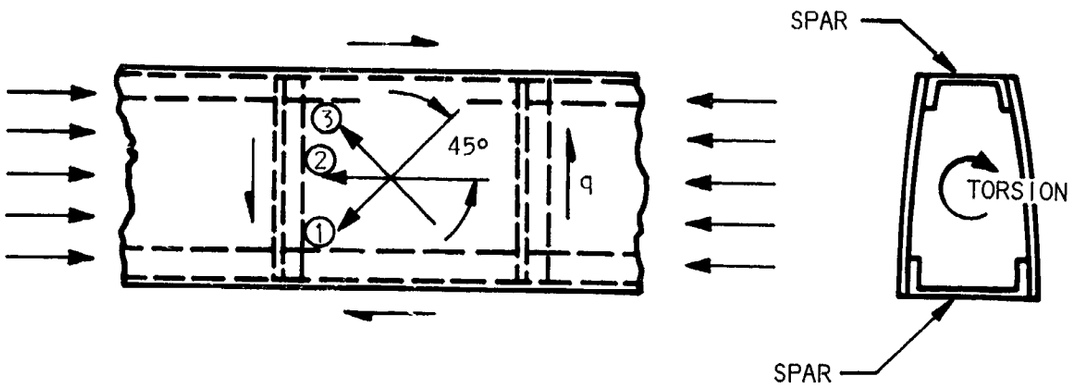
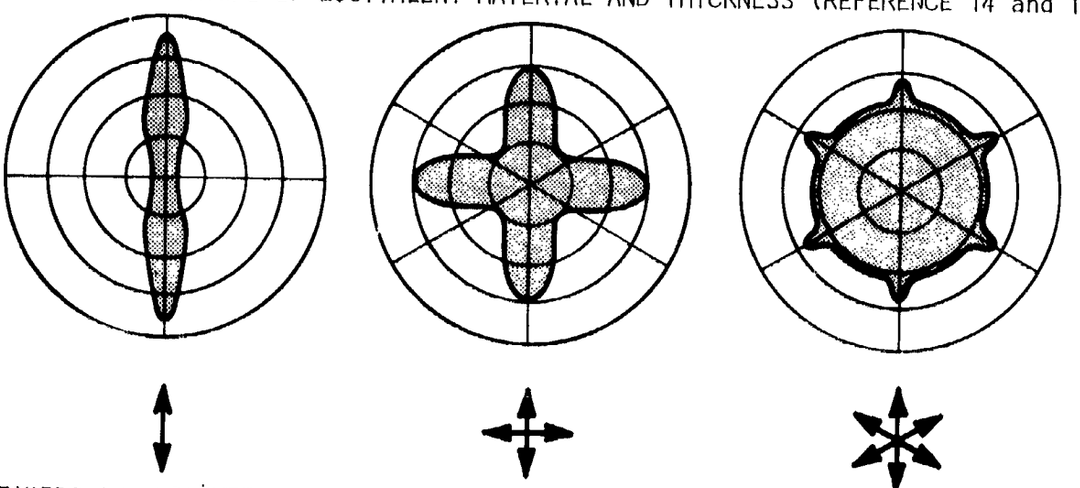


Figure 102

Layers (1) and (3) stabilize the panel against shear buckling; while layer (2) resists the direct shear and axial loading in the panel skin. Figure 103 also shows variation in strength with several combinations of fiber orientations. Figure 104 indicates variation in compression modulus with change of filament direction. Basic good design practices, when using laminated structure, are presented in Figure 105. Fiber-to-resin matrix proportion is another important relationship, strengthwise. A resin-rich composite is weakened by the influence of the lower strength matrix, while a resin-starved composite is unsatisfactory because of insufficient bonding between each fiber. In filament-wound structures, 70-to-85 percent by volume is considered normal for fiber content. Included in the comparisons, where appropriate, are several composite laminate combinations. A summary of the basic properties of candidates is presented in Table XIX. For more detailed or added information see Ref. 14

STRENGTH VS ANGLE OF STRESS IN TENSION FOR UNIDIRECTIONAL AND MULTI-DIRECTIONAL LAYUPS OF EQUIVALENT MATERIAL AND THICKNESS (REFERENCE 14 and 15)



FIBERS ARE ORIENTED AT 0° TO EACH OTHER, GIVING MAXIMUM STRENGTH PARALLEL TO WARP

NINETY-DEGREE ORIENTATION GIVES LESS MAXIMUM STRENGTH, BUT EQUAL STRENGTH FOR PARALLEL AND PERPENDICULAR LOADING

THIS FABRIC ORIENTATION YIELDS STILL LESS MAXIMUM STRENGTH, BUT EQUAL STRENGTH IN EACH DIRECTION OF FIBER WARP

Figure 103

COMPRESSION MODULUS VS PERCENT FILAMENT IN 0° DIRECTION (REFERENCE 16)

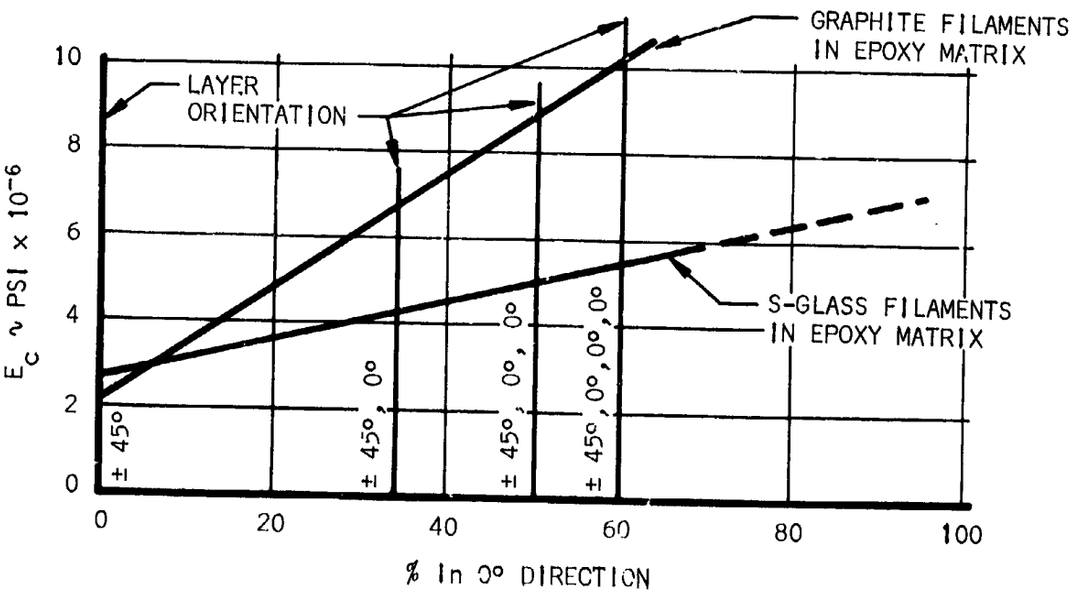
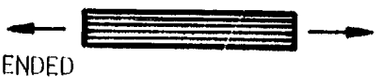


Figure 104

RELATION BETWEEN DIRECTION OF LAMINATIONS
AND DIRECTION OF LOAD APPLICATION

TENSION



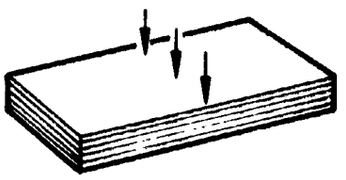
RECOMMENDED



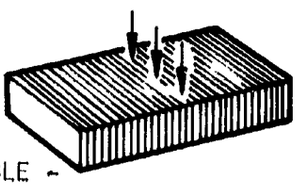
UNDESIRABLE

TENSILE STRESSES SHOULD BE SUSTAINED BY LAMINATIONS, NOT ACROSS BONDING PLANE

COMPRESSION



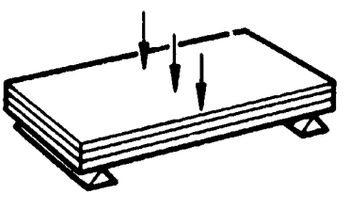
RECOMMENDED -
FLATWISE AT RIGHT ANGLE TO LAMINATIONS



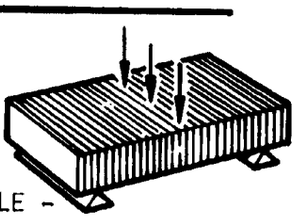
UNDESIRABLE -
EDGEWISE PARALLEL TO LAMINATIONS

COMPRESSION STRENGTH OF LAMINATES IS GREATER FLATWISE THAN EDGEWISE

FLEXURE



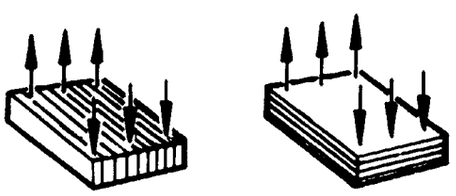
RECOMMENDED -
FLATWISE AT RIGHT ANGLE TO SPAN



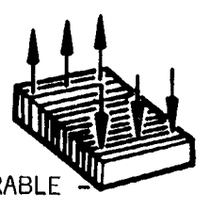
UNDESIRABLE -
LAMINATIONS AT RIGHT ANGLE TO SPAN

BENDING STRESSES SHOULD BE SUSTAINED BY LAMINATIONS, NOT ACROSS BONDING PLANE

SHEAR



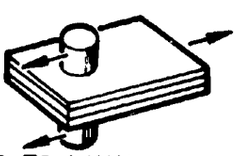
RECOMMENDED -
FLATWISE AT RIGHT ANGLES TO LAMINATIONS



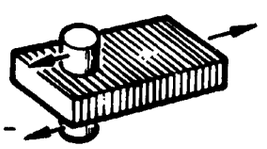
UNDESIRABLE -
EDGEWISE PARALLEL TO LAMINATIONS

SHEARING STRESSES SHOULD OCCUR IN A PLANE NORMAL TO LAMINATIONS
TO PREVENT CLEAVAGE ACROSS BONDING PLANES

BEARING



RECOMMENDED -
LOAD DISTRIBUTED TO LAMINATIONS



UNDESIRABLE -
LOAD CARRIED THRU BOND

BEARING STRESSES SHOULD BE APPLIED THRU LAMINATIONS
RATHER THAN ACROSS BONDING PLANES

Figure 105

Tension Members:

AXIALLY LOADED MEMBER

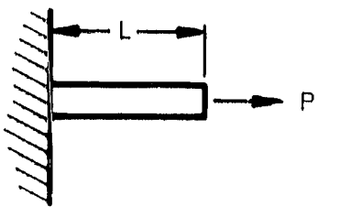


Figure 106 shows weight per inch versus axial load (4,000 pounds maximum) for the various materials. The ordinate provides for the use of an efficiency factor which might be encountered under conditions of riveting or welding.

Derivations: $f = \frac{P}{A}$, $W = A\,L\,w$, $A = \frac{W}{L\,w}$ and $f = K_{eff}\,F$

To develop curves of $\frac{WK}{L}$ efficiency versus Tension Load P , let:

$$K_{eff}\,F = \frac{P}{W/L\,w}$$

$$K_{eff}\,\frac{W}{L} = \frac{P}{F/w} \quad \text{(Figure 106)}$$

SYMBOLS:

f	=	Stress
A	=	Cross section area
W	=	Weight
w	=	Density
K_{eff}	=	Efficiency factor
F	=	Smaller of F_{tu} or: 1.5 F_{ty}

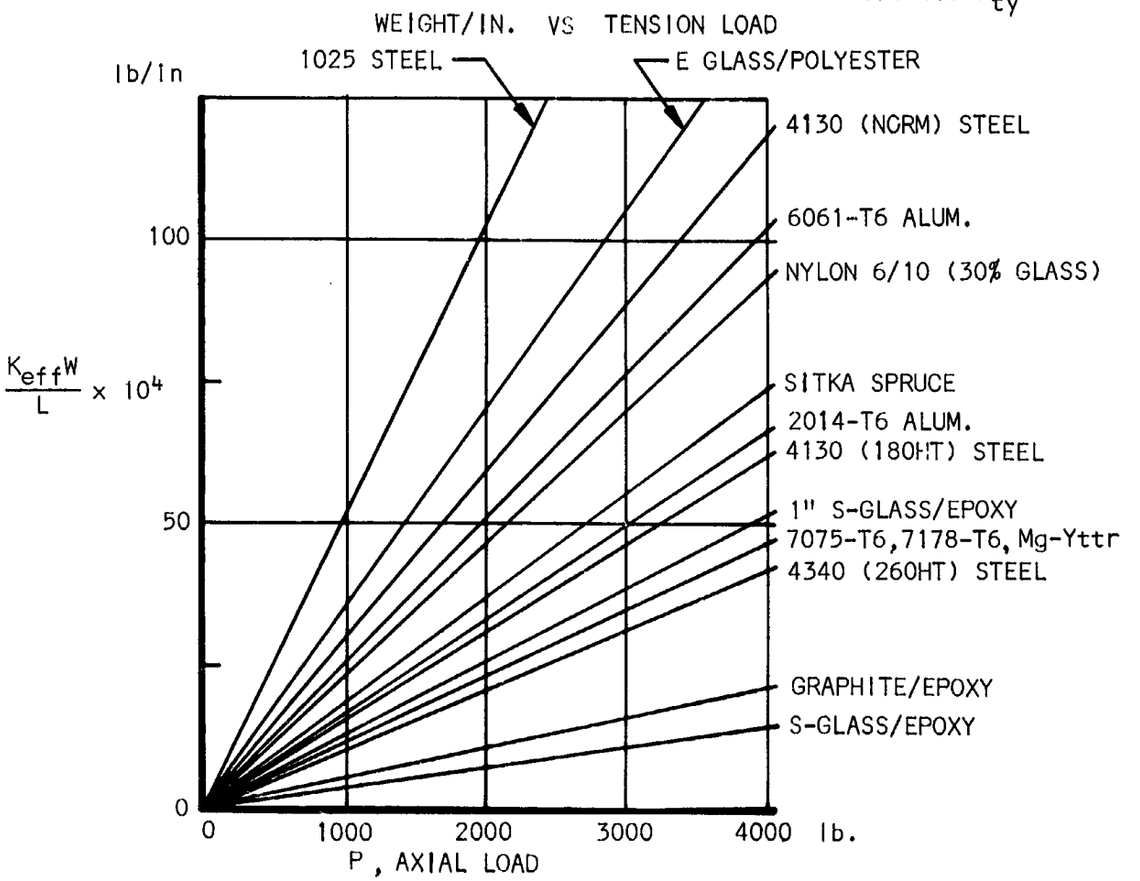


Figure 106

Simple Columns:(assume round tubes)

Structural indexes were used to assist in the evaluation of promising candidate materials when applied as simple columns. As defined in reference 17, a structural index is a measure of loading intensity and has the advantage of eliminating the effect of size in dealing with allowable stresses. For a simple column, the structural index becomes P/L^2. Derivations:

Primary buckling $$F_c = \pi \left(\sqrt{E_t}\right)\left(\sqrt{\frac{D}{8rt}}\right)\left(\sqrt{\frac{P}{L^2}}\right)$$

and rippling $$F_{cr} = K_2 \frac{\sqrt{EE_t}}{D/t}$$

Equating the two equations gives optimum value of D/t

$$\left(D/t\right)_{opt} = 2\left(\frac{K_2^2\, E}{\pi P/L^2}\right)^{1/3} = .742\left(\frac{E}{P/L^2}\right)^{1/3} \qquad [K_2 = .40 \text{ (Reference 17)}]$$

Figure 107 plots D/t ratios versus structural index for the materials under consideration.

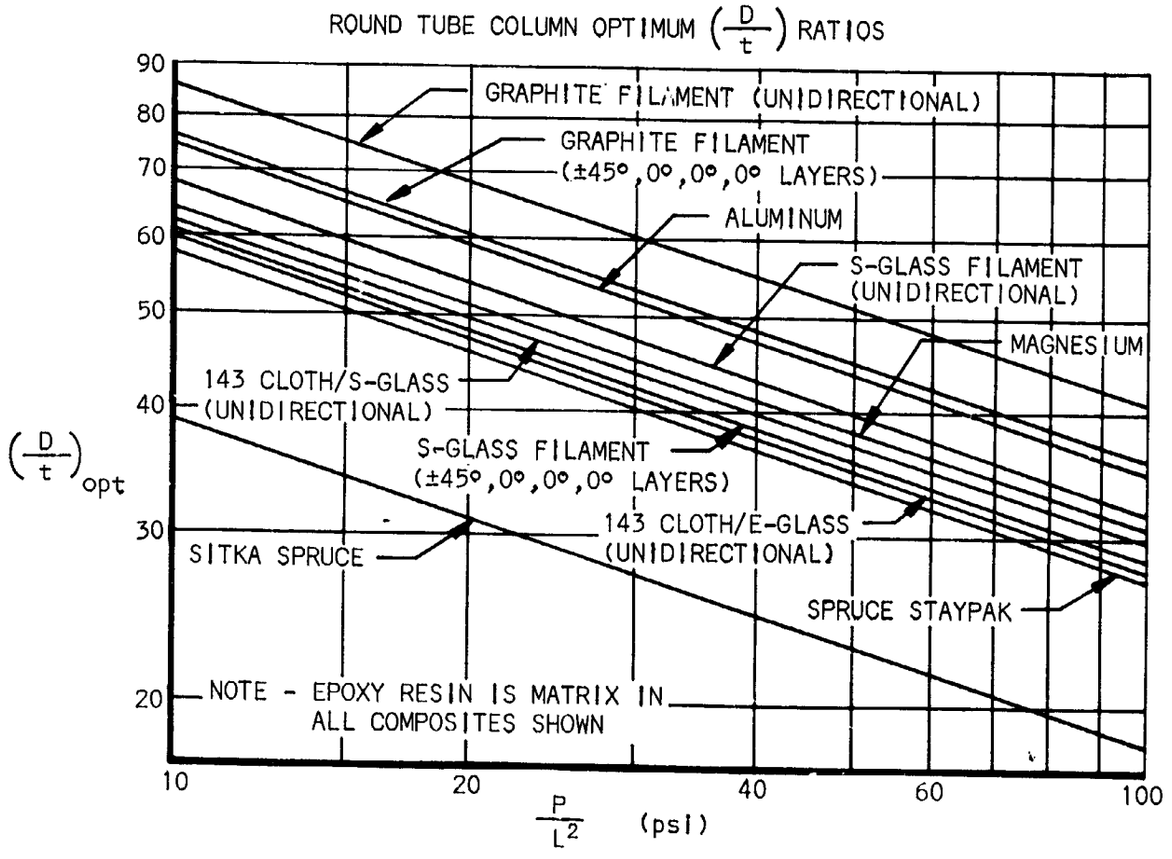


Figure 107

To obtain allowable compression stresses for optimum round tube columns, substitute the value for optimum D/t in the primary buckling equation:

$$P/L^2 = \frac{8f^3}{\pi K_2 E^{1/2} E_t^{3/2}} = \frac{6.37 f^3}{E^{1/2} E_t^{3/2}}$$

For study purposes, limit f to $.80F_{cy}$.

The allowable F_c may then be calculated and plotted for various materials, as shown in Figure 108.

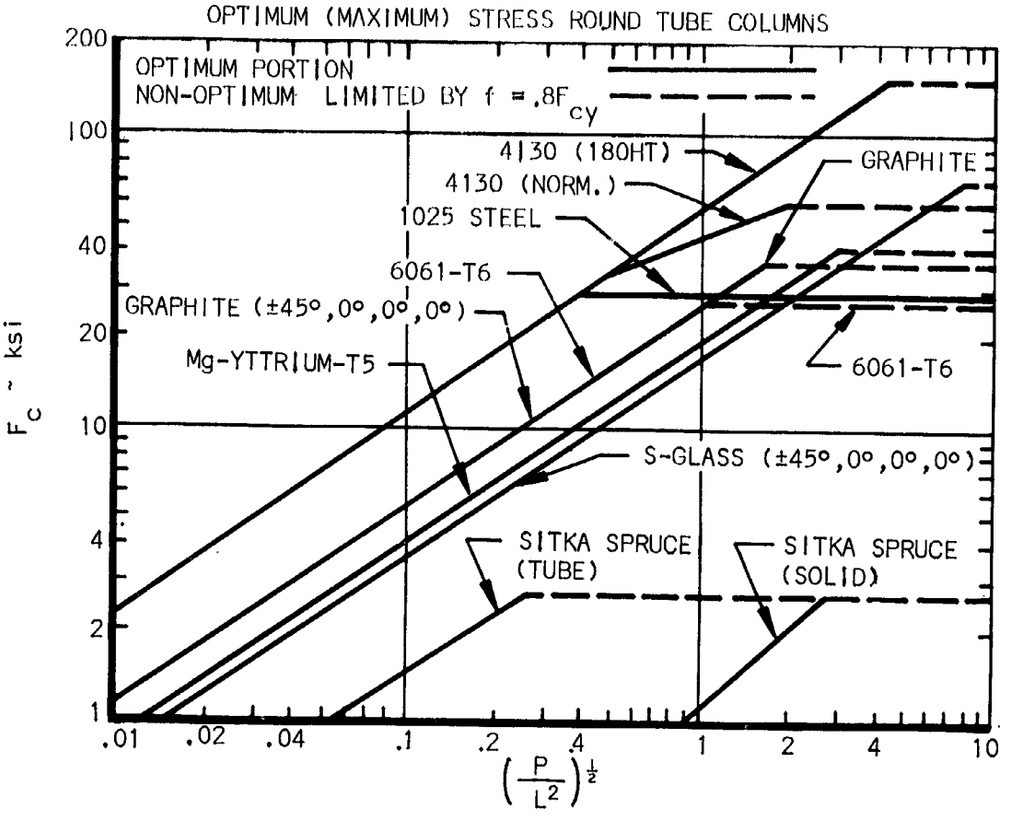


Figure 108

It is now possible to develop a formula for minimum weight, as follows:

(1) Divide structural index by allowable F_c and multiply by density of material: $\frac{P(w)/L^2}{F_c}$

(2) By substituting $\frac{P}{F_c} = A$ & $w = \frac{W}{AL}$, the following identity is obtained: $WC/L^3 = \frac{F/L^2}{F_{c/w}}$, where C is restraint coefficient.

Values for WC/L^3 versus P/L^2 may now be determined and plotted for a number of materials (see Figure 109).

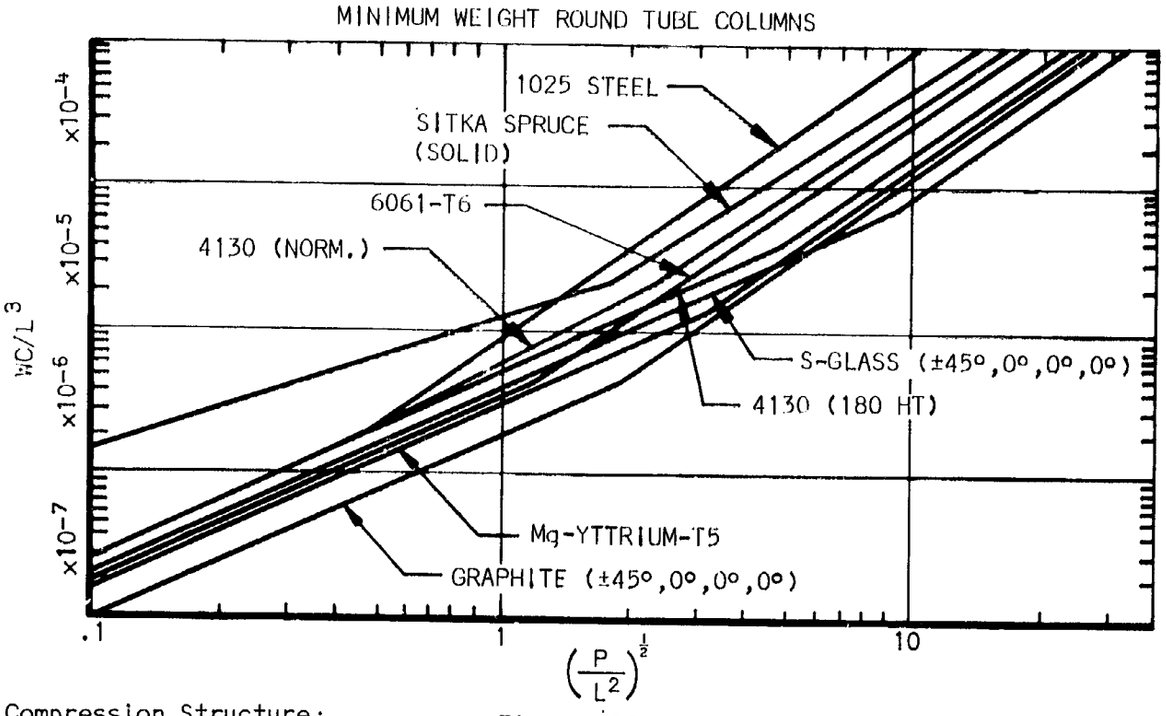


Figure 109

Compression Structure:

Probably the most detailed and extensive evaluation of structure occurs during the design of compression critical sections of the airframe. The section under compression is generally treated either as a wide column or a compression panel. The wide-column approach is used when the length of the panel is short compared to its width, as in a multi-rib wing box. A compression panel concept is assumed when the length of the panel is long compared to its width, as in a multi-spar wing box.

The wide-column analysis assumes primary buckling between the ribs, which provide simple supports for loaded edges of the column. The following equation, taken from reference 18, is a result of equating general and local instability formulas:

$$\frac{N_x}{L\bar{\eta}E} = \varepsilon \left(\bar{t}/L\right)^2$$

Where: N_x = compressive load in pound/inch
L = length of column in inches
$\bar{\eta}$ = plasticity reduction factor
E = modulus of elasticity, psi
$\bar{t}$ = cross-sectional area per unit width
ε = efficiency factor, a function of buckling coefficient & shape factor

The analysis of compression panels is based upon all edges of the panel being simply supported, while plate theory expressions for local and general stability are equated to obtain the following equation:

$$\frac{N_x}{b\bar{\eta}E} = \varepsilon \left(\bar{t}/b\right)^n$$

Where: b = width of plate
n = an exponent which is a function of configuration

In the evaluation of wide-column and compression panel concepts, truss core sandwich, honeycomb sandwich, flat plate, and zee-stiffened plate construction will be considered for each case.

Minimum area equations for optimized wide columns and compression panels of zee-stiffened plate, flat plate, and truss core sandwich construction are presented in Table XX. Efficiency factors, ε , were obtained from reference 18, while the plasticity reduction factor, $\bar{\eta}$, was taken as unity for all cases.

TABLE XX
MINIMUM AREA EQUATIONS FOR OPTIMIZED WIDE COLUMNS AND COMPRESSION PANELS (Reference 18)

TYPE OF CONSTRUCTION	WIDE COLUMN	COMPRESSION PANEL
Zee-Stiffened Plate	$\frac{N_x}{LE} = 0.911\ (\bar{t}/L)^2$	$\frac{N_x}{bE} = 1.030\ (\bar{t}/b)^{2.36}$
Truss Core Sandwich	$\frac{N_x}{LE} = 0.605\ (\bar{t}/L)^2$	$\frac{N_x}{bE} = 1.108\ (\bar{t}/b)^2$
Flat (unstiffened) Plate	$\frac{N_x}{LE} = 0.823\ (\bar{t}/L)^3$	$\frac{N_x}{bE} = 3.62\ (\bar{t}/b)^3$

Minimum area curves for truss core sandwich, honeycomb sandwich, flat plate, and zee-stiffened plate of wide column and compression panel construction are shown in Figures 110 and 111.

The zee-stiffened plate, flat plate, and truss core curves were developed from the data in Table XX. Minimum area curves for honeycomb sandwich were obtained from reference 18. Curves were generated by calculating typical weights and strengths, and algebraically converting the results to the general form of the other configurations. As stated in reference 18, the high efficiency of honeycomb sandwich construction is attributed to the fact that the full compressive strength of face sheets can be utilized by reducing the cell size of the honeycomb core.

A panel optimization computer program was used in reference 16 for evaluating numerous filament-wound materials in truss core and honeycomb sandwich construction. These configurations, in their optimum proportions of unidirectional to cross-ply fibers are pictured in Figure 112. By utilizing data from reference 16, optimum weight and corresponding core thickness versus structural index may be determined for graphite and S-Glass wide columns and compression panels.

MINIMUM AREA CURVES – WIDE COLUMN CONCEPT

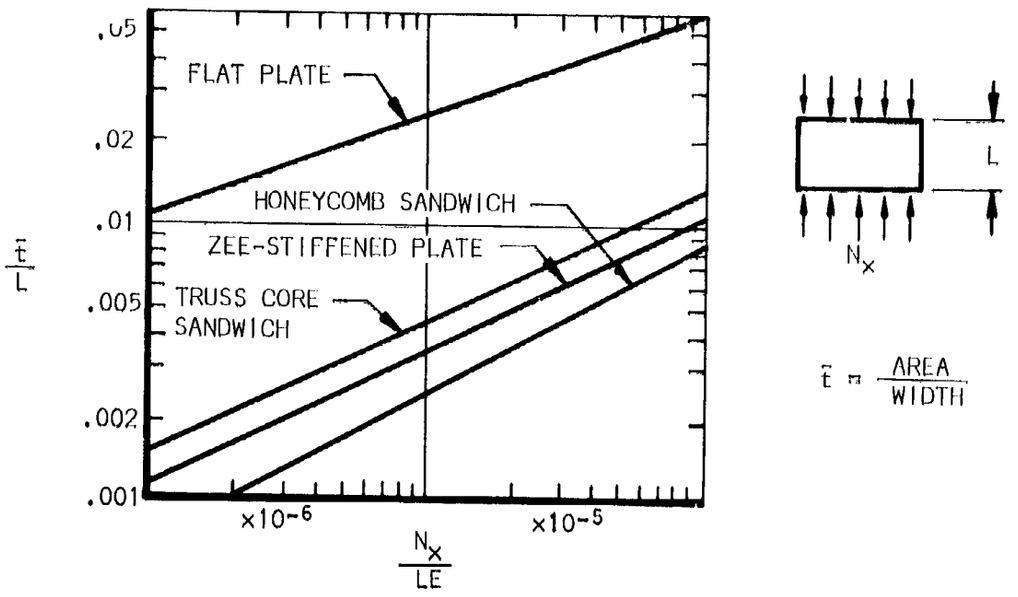


Figure 110

$\bar{t}$ = Equivalent cross sectional area/unit width of panel of all material effective in carrying axial load.

MINIMUM AREA CURVES - COMPRESSION PANEL CONCEPT

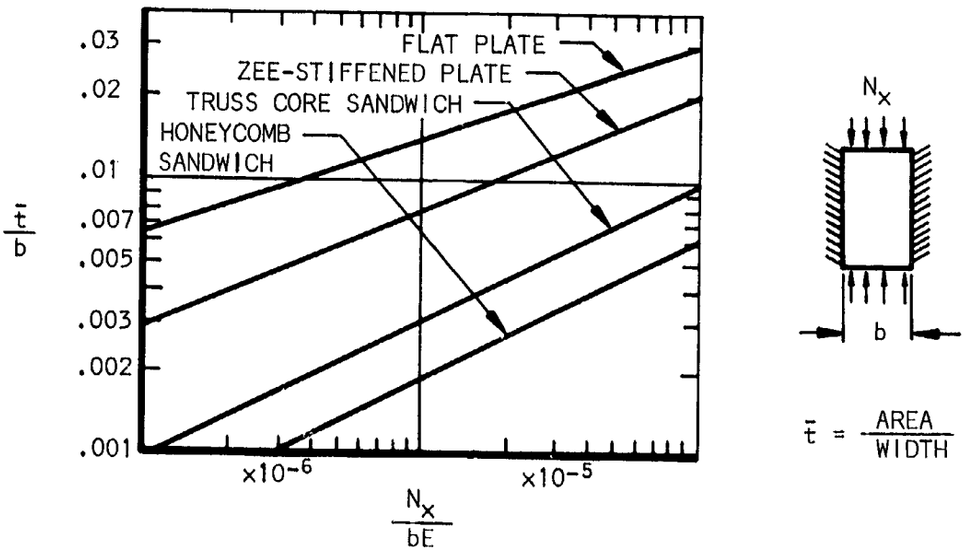
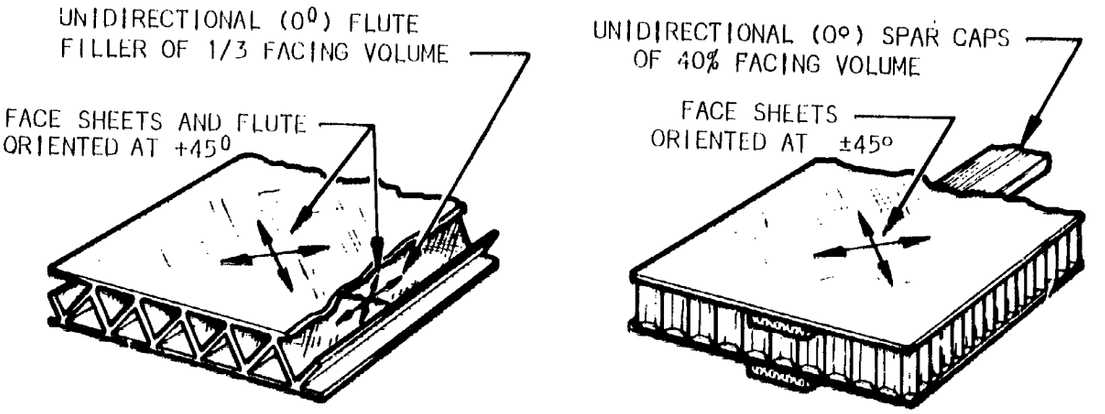


Figure 111

SANDWICH PANELS



CORRUGATION SANDWICH PANEL

HONEYCOMB SANDWICH PANEL

Figure 112

Resulting values are plotted in Figures 113 through 115. Optimized configuration weights reflect ±45° fiber orientation in the skins for the most efficient alignment to react torsional shear. Minimum skin gages are set at .020 inches. Four failure modes considered were: general buckling, face wrinkling, intercell buckling, and shear crimping.

Minimum weight diagrams can also be developed from minimum area curves in Figures 110 and 111, as follows:

(1) Multiply ordinate $\bar{t}/L$ by material density, w :

$w\bar{t}/L = W/bL^2$ because $W = bL\bar{t}w$, $w = W/bL\bar{t}$

(2) Multiply abscissa N_x/LE by material modulus, E :

$EN_x/LE = N_x/L$; the weight is thus presented as a function of the structural index: N_x/L (or q/L).

Minimum weights for various materials and concepts are shown in Figures 117 and 118.

In the discussion of sheet stringer-type wide columns, mention should be made of extruded Y stringers developed by NACA (NACA TN 1389) for increasing allowable stresses in compression structures. Figure 119 compares allowable stress versus structural index of sheet stringer wide columns constructed of 2024 and 7075 Y-stringers against a 2024 conventional stringer envelope.

These same constructions are compared on a weight basis in Figure 120 which was derived from optimum stress curves by dividing N_x/L by F_c and then multiplying by w to obtain:

$$\left(N_x/L\right)\left(1/F_c\right)\left(w\right) = \bar{t}w/L = W/bL^2$$

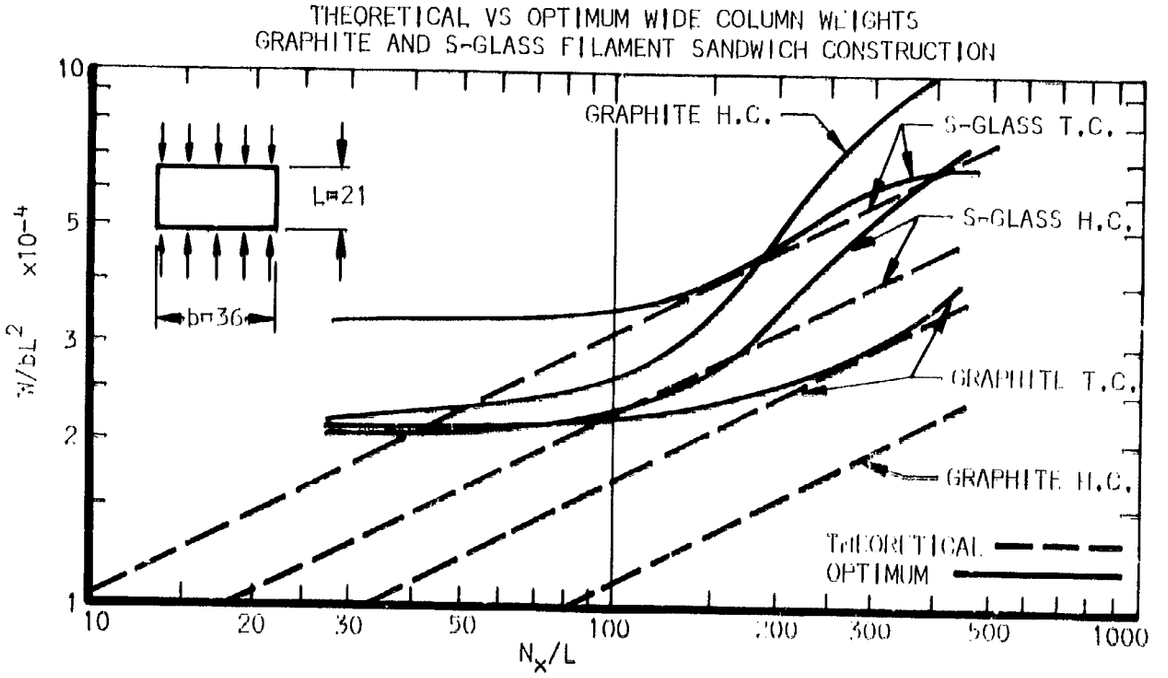


Figure 113

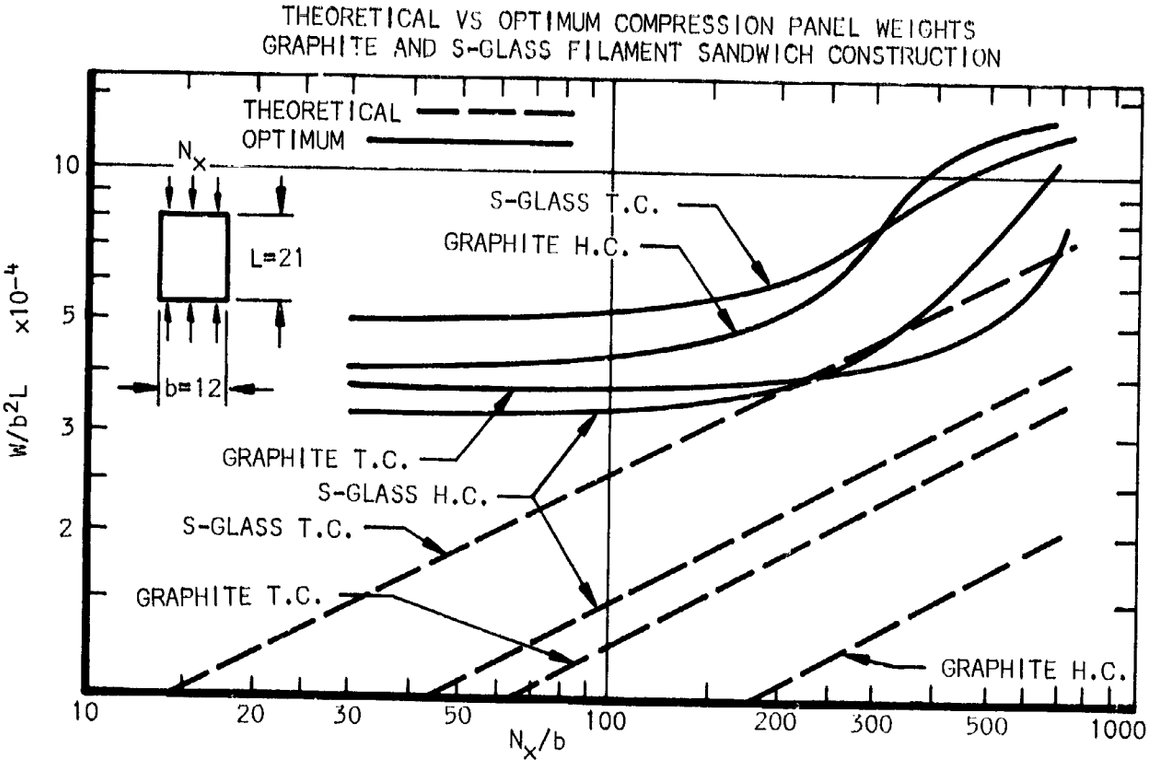


Figure 114

THEORETICAL VS OPTIMUM CORE THICKNESSES
GRAPHITE AND S-GLASS FILAMENT SANDWICH CONSTRUCTION

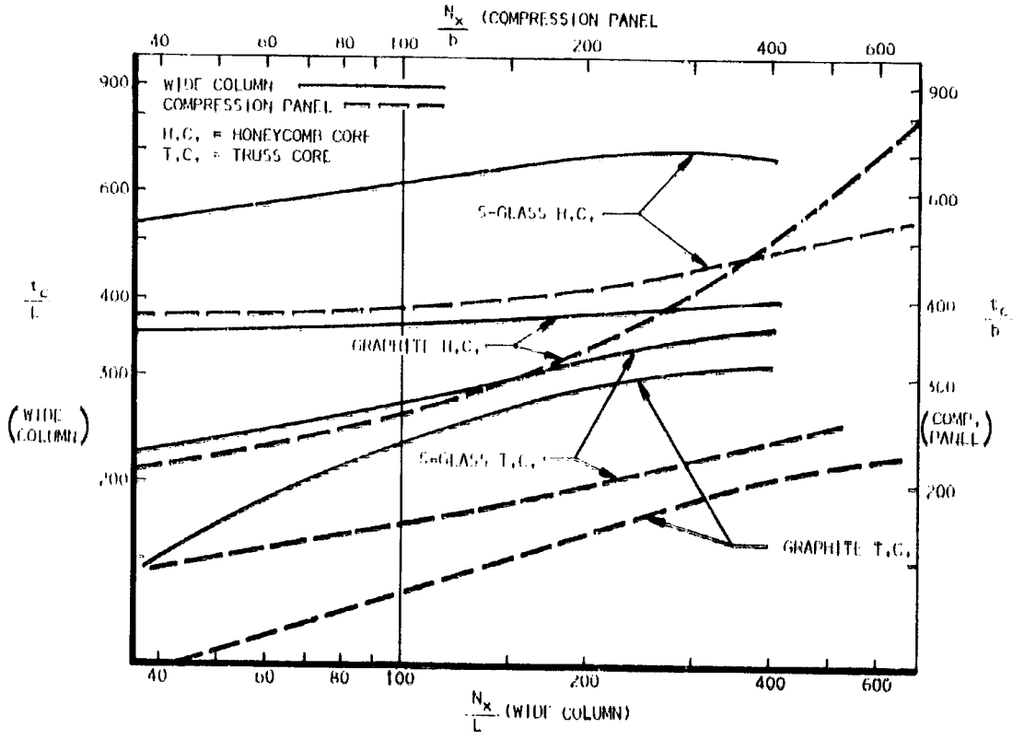


Figure 115

OPTIMUM WEIGHT - WIDE-COLUMN CONCEPT

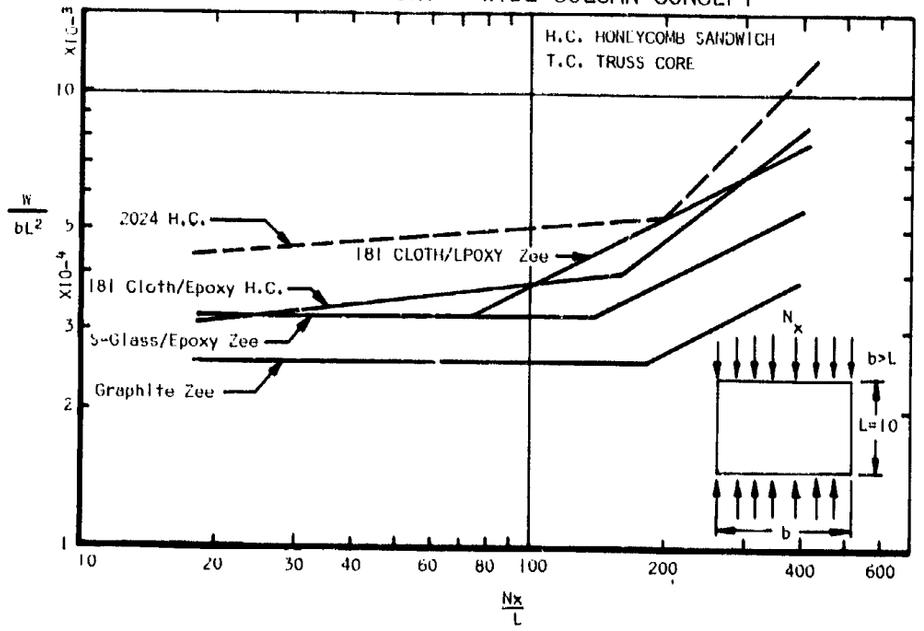


Figure 116

MINIMUM WEIGHT - WIDE-COLUMN CONCEPT

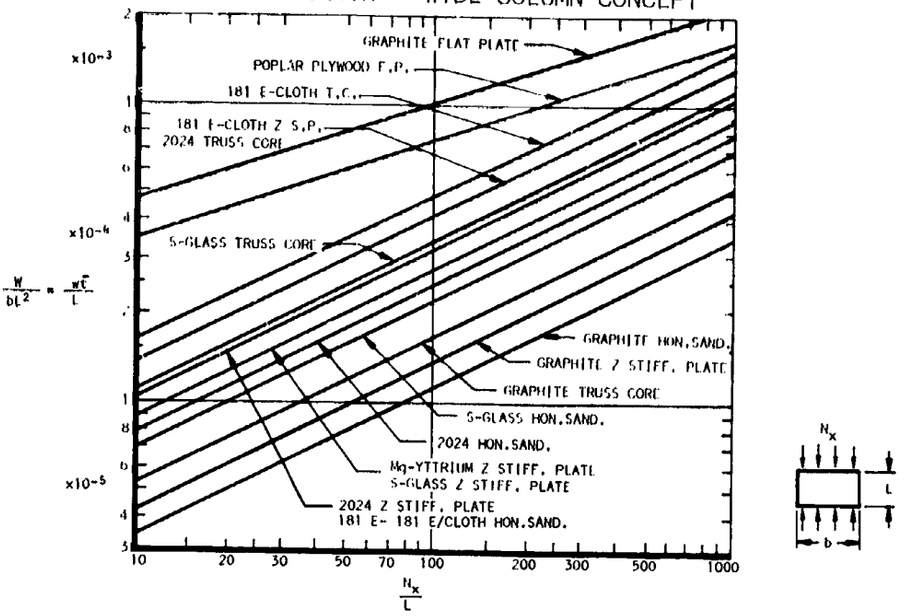


FIGURE 117

MINIMUM WEIGHT - COMPRESSION PANEL CONCEPT

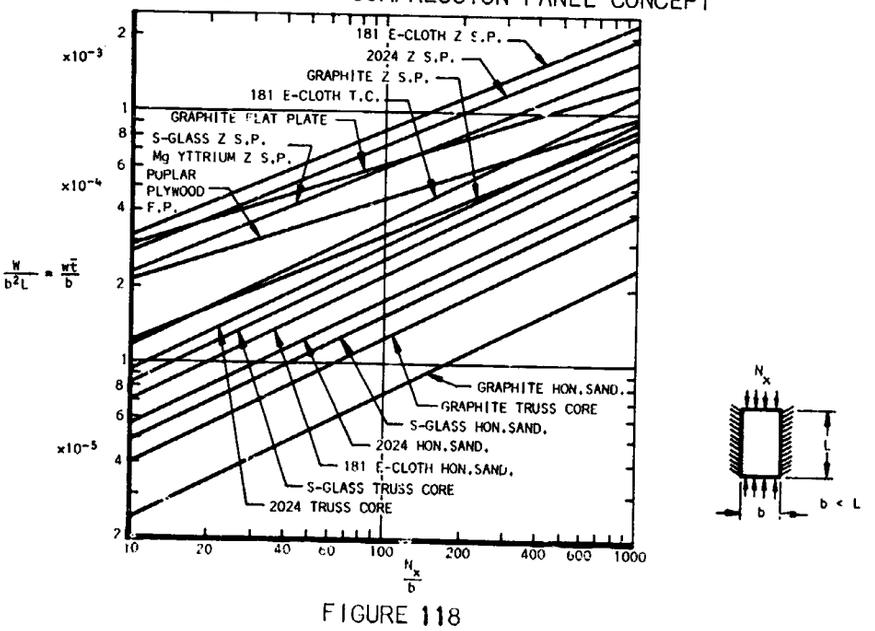


FIGURE 118

S.P. = STIFFENED PLATE
F.P. = FLAT PLATE

H.C. = HONEYCOMB SANDWICH = HONEYCOMB CORE
T.C. = TRUSS CORE

OPTIMUM (MAX.) STRESS - WIDE COLUMNS
ALUMINUM SHEET - STRINGER TYPE

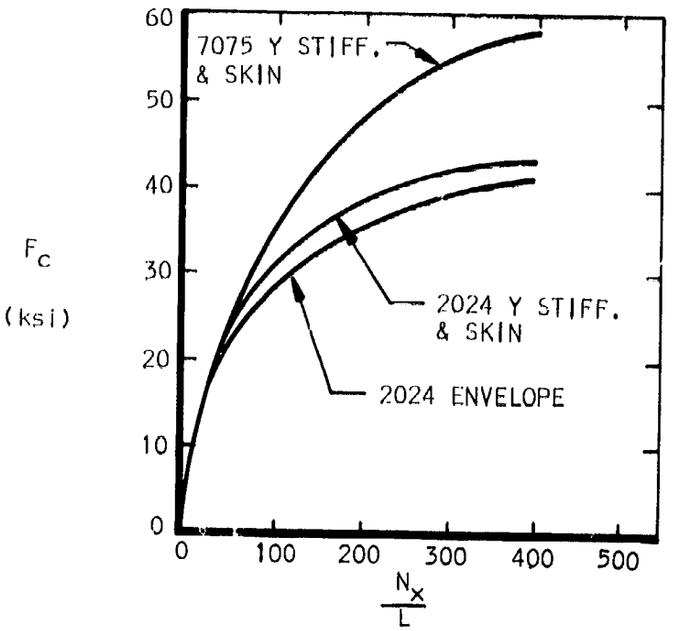


Figure 119

MINIMUM (OPT.) WEIGHT - WIDE COLUMNS
ALUMINUM SHEET - STRINGER TYPE

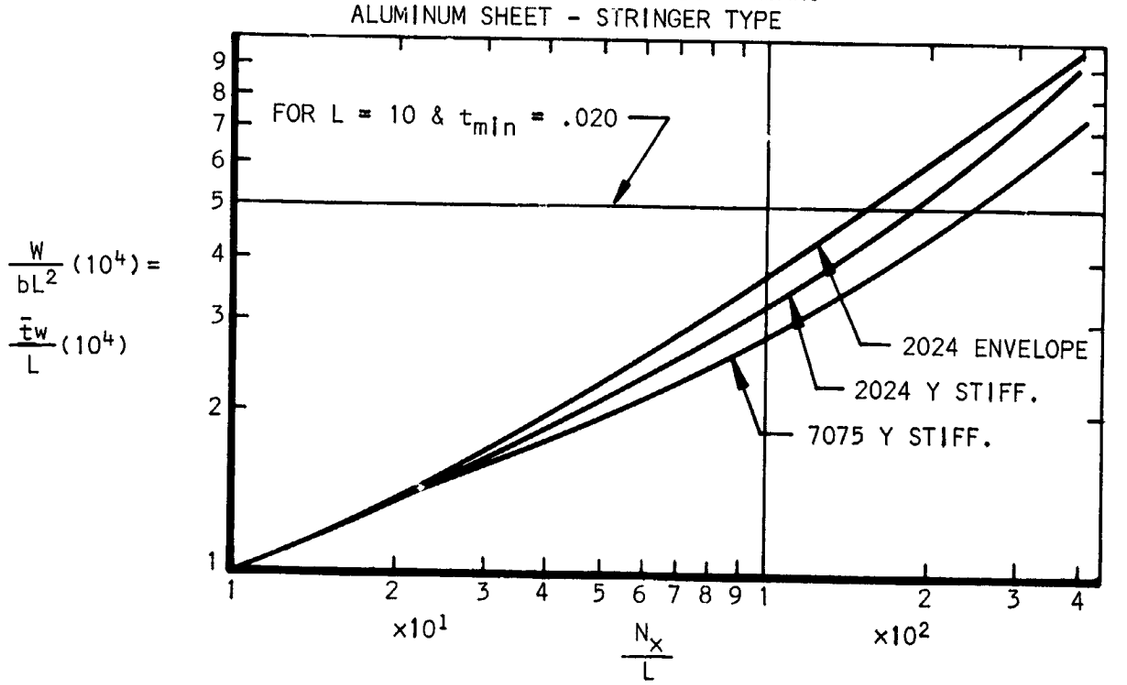


Figure 120

Shear Panels: Wing, fuselage, and empennage skins on small aircraft (including helicopters) are of light-gage construction. Loading intensities due to torsional shear are low level; therefore, the panels are normally designed for shear buckling at the 1 to 1.2 g level. This requirement is established for appearance purposes since the panel itself has ample strength to carry the ultimate torsional shear flow as a tension field member.

Materials for shear panel application are compared on a thickness basis in Figure 121. The curves were obtained through a substitution and division process of the shear buckling equation for flat plates.

Shear buckling: $\tau_{cr} = \dfrac{K_s E_c t^2}{b^2}$

Where: τ_{cr} = shear stress at which panel will buckle
K_s = shear buckling coefficient dependent upon edge conditions around panel (Ref. Fig. 122)
b = short side dimension of panel
t = panel thickness
E_c = compression modulus of elasticity

$\tau_{cr} = N_{xy}/t$,

$N_{xy} = q$ = torsional shear flow;

Therefore:

$$N_{xy}/t = \frac{K_s E_c t^2}{b^2} \quad , \quad N_{xy} = \frac{K_s E_c t^3}{b^2}$$

Obtain structural index (abscissa): $N_{xy}/b = \dfrac{K_s E_c t^3}{b^3} = K_s E_c (t/b)^3$

Calculate ordinate: $t/b \sqrt[3]{K_s} = (N_{xy}/bE)^{1/3}$

Minimum weights versus structural indexes for flat plate shear panel materials are presented in Figure 123. Curves were derived by multiplying shear buckling equations, as modified for minimum thickness form, by material density, w :

$$wt/b \sqrt[3]{K_s} = w (N_{xy}/bE)^{1/3}$$

But: $W = wabt$, $w = W/abt$

Where: W = panel weight
a = long side of panel

Therefore: $W/b^2 a \sqrt[3]{K_s} = w (N_{xy}/bE)^{1/3}$

Shear buckling coefficients, K_s , for various edge conditions are shown in Figure 122.

Compression Flanges: In reviewing candidate materials for use as compression flanges on spars and similar bending members, the following structural index will be applied to represent crippling efficiency:

$$S = \frac{\sqrt{F_{cy} E_c}}{w}$$

This relationship is in general agreement with Needham's equation for crippling in reference 19 and assumes b/t , flange width to thickness ratio, to remain constant.

Crippling structural efficiencies for candidate materials are illustrated in Figure 124.

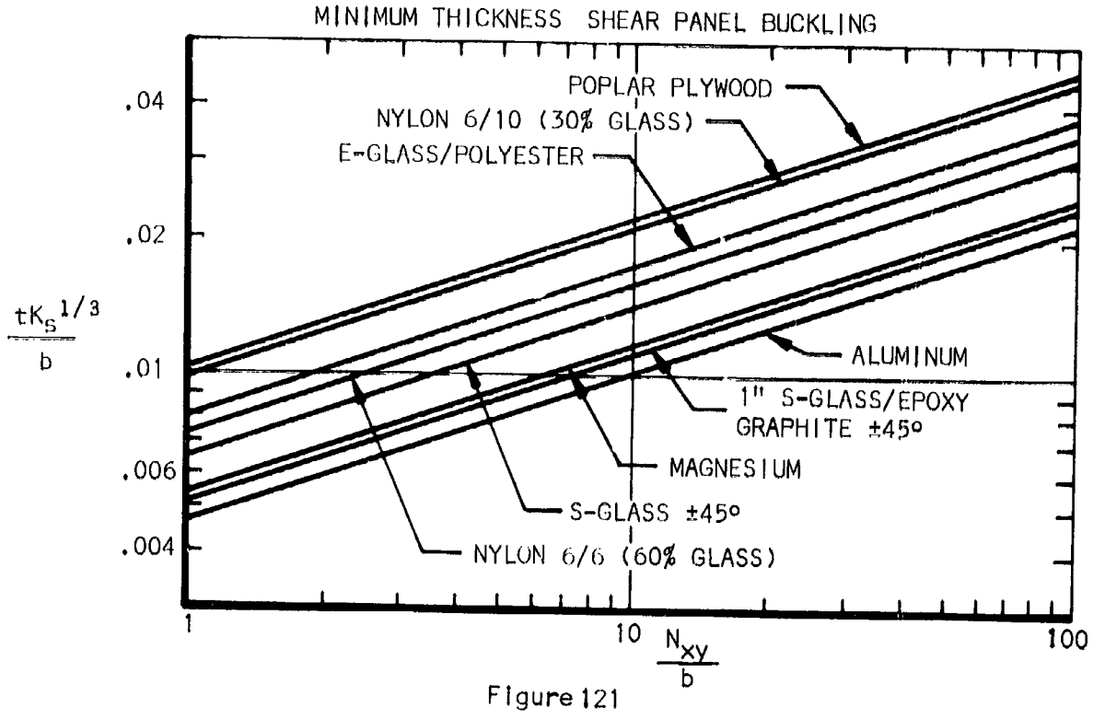


Figure 121

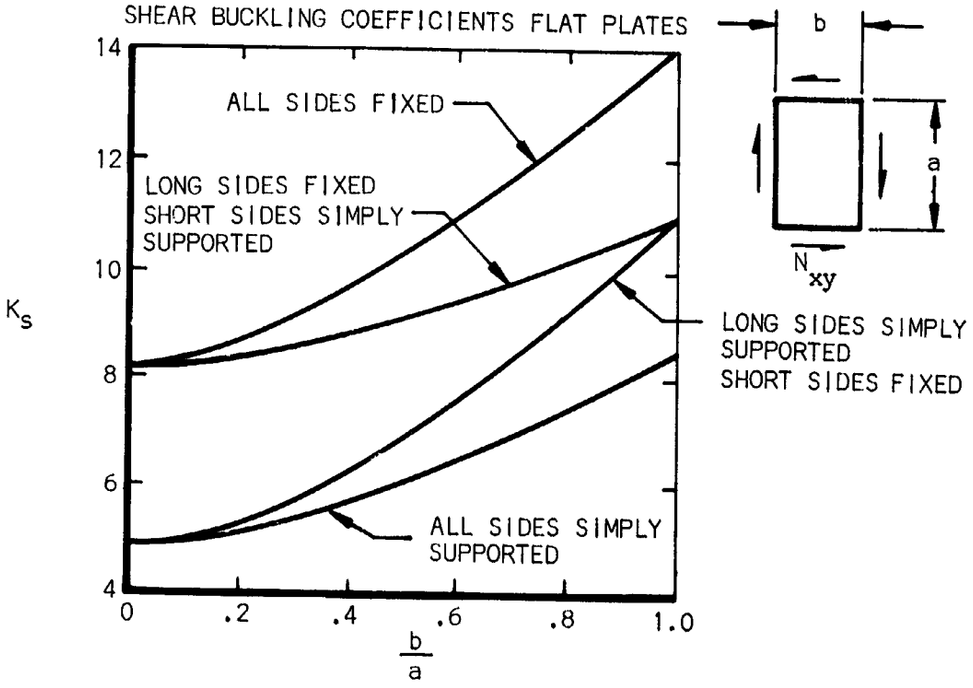


Figure 122

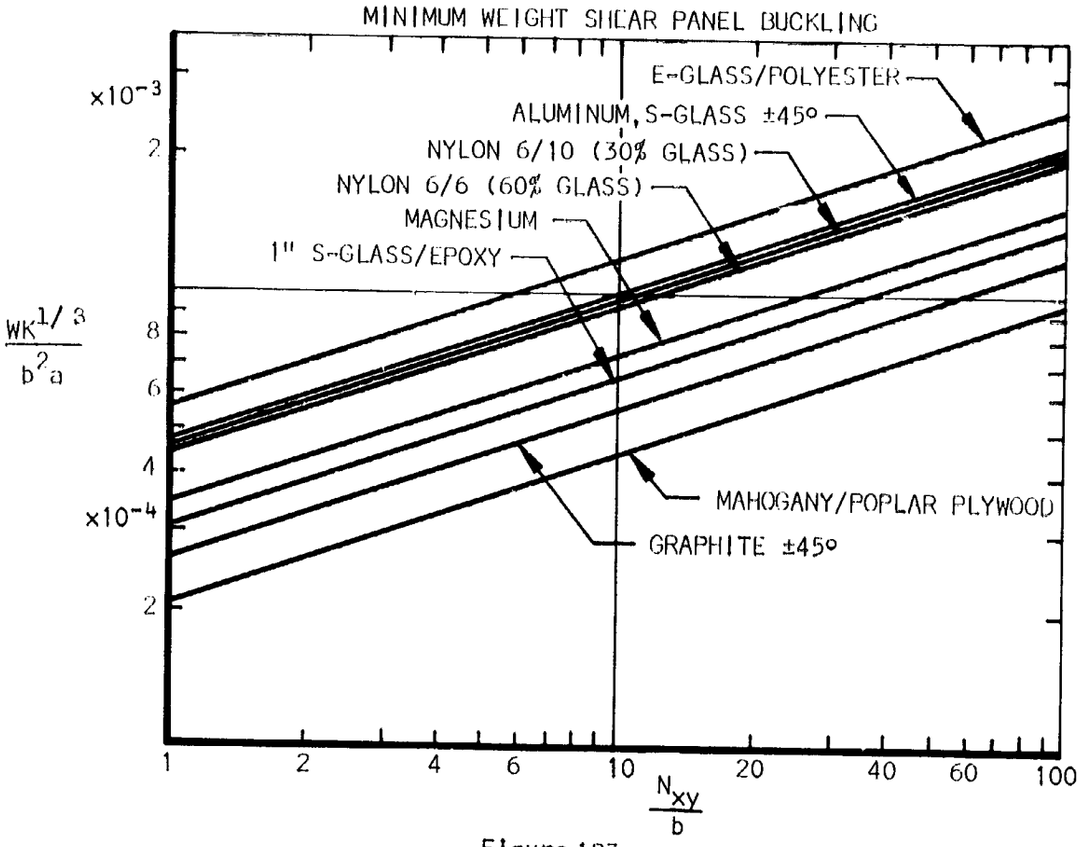


Figure 123

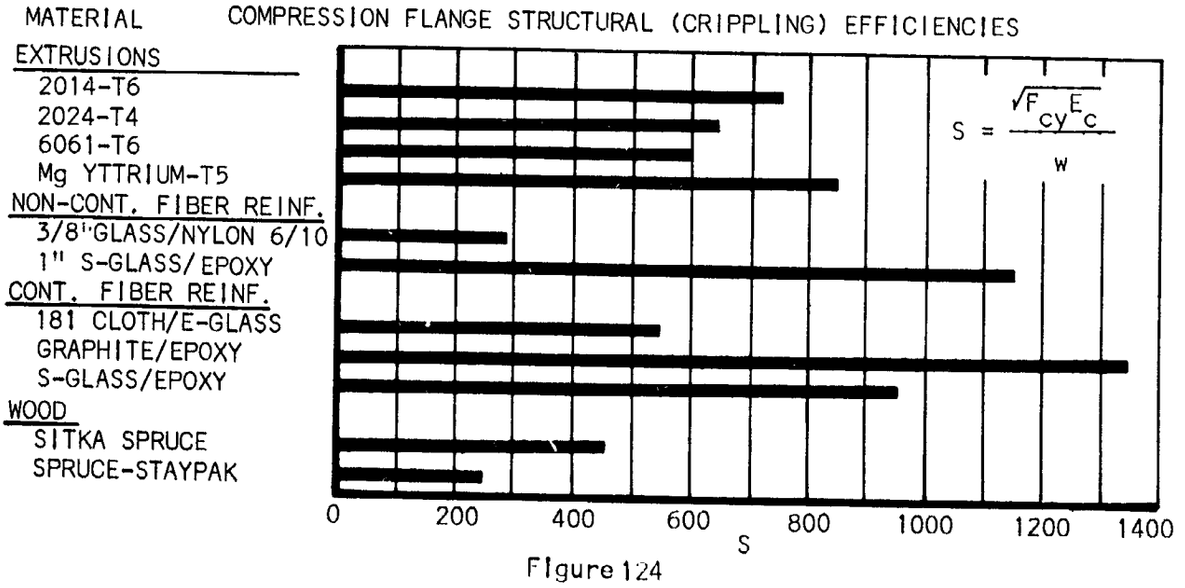


Figure 124

Installation Costs: In determining the feasibility of various structural material concepts, the total cost of the installation must be compared against the dollar's worth value of a pound of material saved. The installation cost includes material cost plus fabrication cost. In order to justify a material/concept change, one of the following conditions must be satisfied:

(1) significant weight savings with no increase in total installation cost

(2) significant decrease in installation cost with no appreciable increase in weight

(3) significant weight savings with significant cost savings

The dollar's worth value of a pound of weight saved for the typical four-place light airplane, which will be discussed in the following main section, has been calculated versus service life. See Figure 74.

In the following evaluation of required break-even costs versus material/concept, a $2.00 per pound value for a pound of weight saved will be used for the light aircraft, based on a 333 hr/yr utilization rate with an original single-owner expectancy of 20 years. See TABLE XI for a detailed discussion.

A typical light aircraft will be used as a baseline against which weights and costs will be compared. This airplane utilizes aluminum sheet metal stringer-stiffened construction, with a two-spar wing. Its installation cost per pound, C_{lb}, is $7.00 for an empty weight of 1500 lbs. (ref.Fig.71).

To determine the required break-even fabrication cost per pound for candidate materials/concepts, the following derivation is performed, noting that the letters n and b in the subscripts indicate new candidate and base line materials, respectively:

Installation Cost = Material Cost + Fabrication Cost; $P_I = P_m + P_f$

* Where: P_m = Mat'l Cost/lb x Weight = $C_m W$, And: P_f = Fab'n Cost/lb x Weight = $C_f W$

* Therefore: $P_I = W\left(C_m + C_f\right)$. Substituting candidate mat'l for base line mat'l:

$\frac{\text{Price Increase}}{\text{Weight Decrease}} \leq$ Dollar's worth of a pound of material saved, or $\frac{\Delta P}{\Delta W} \leq C_w$

Where: $\Delta P = P_{In} - P_{Ib} = W_n\left(C_{mn} + C_{fn}\right) - W_b\left(C_{mb} + C_{fb}\right)$, and $\Delta W = W_b - W_n$

Therefore, $C_w = \dfrac{W_n\left(C_{mn} + C_{fn}\right) - W_b\left(C_{mb} + C_{fb}\right)}{W_b - W_n}$, but: $W_n = W_b\left(S_b/S_n\right)$

* Mat'l = Materials; Fab' = Fabrication

Where: S_b = structural efficiency of baseline material

S_n = structural efficiency of new candidate material

So: $$C_w = \frac{W_b\left(S_b/S_n\right)\left(C_{mn} + C_{fn}\right) - W_b\left(C_{mb} + C_{fb}\right)}{W_b - W_b\left(S_b/S_n\right)} = \frac{\left(S_b/S_n\right)\left(C_{mn} + C_{fn}\right) - \left(C_{mb} + C_{fb}\right)}{1 - S_b/S_n}$$

Re-arrange, in terms of new candidate fabrication cost required to break even on material change:

$\left(1 - S_b/S_n\right)\left(C_w\right) + \left(C_{mb} + C_{fb}\right) = \left(S_b/S_n\right)\left(C_{mn} + C_{fn}\right)$. Finally, the required fabrication cost is:

$$C_{fn} = \frac{\left(1 - S_b/S_n\right)\left(C_w\right) + \left(C_{mb} + C_{fb}\right)}{S_b/S_n} - C_{mn}$$

From which the required installation cost is: $C_{in} = C_{fn} + C_{mn}$

The maximum breakeven fabrication and installation costs for material/concepts used as tension members, shear panels, simple columns and wide columns and compression flanges are calculated in Tables XXI and XXII. In the case of wide columns, non-optimum factors due to practical stringer spacing and joint reinforcement are accounted for in calculating breakeven costs (ref. Table XXII).

TABLE XXI

BREAK-EVEN VS ACTUAL FABRICATION & INSTALLATION COSTS

MATERIAL	C_{mn}	S_b	$\frac{E}{\rho}$	BREAK-EVEN C_{fn} FABR.	BREAK-EVEN C_{in} INSTL.	ACTUAL C_{fn} FABR.	ACTUAL C_{in} INSTL.	FEASIBILITY
	(1)	(2)		(3)(4)	(3)(4)	(5)		BRKEVN ? ACT.
SHEAR PANELS								
Baseline Material = 2024-T3 Clad, $S_b = \sqrt[3]{E^2/w} = 22$								
$C_{ib} = C_{mb} + C_{fb} = 0.56 + 5.90 = 6.46$								
AZ31B-H24	1.10	29	.74	8.48	9.58	5.90	7.00	Yes
Graphite (±45°)	(1.00)	39	.96	12.50	13.30	8.85	9.85	Yes
Mahogany/Poplar Plywood	2.05	48	.45	14.95	17.00	11.80	13.85	Yes
1" S-Glass/Epoxy	(2.00)	44	.69	9.20	11.20	5.90	7.90	Yes
3/8" L-Glass/Nylon	(0.65)	23	.96	6.27	6.92	5.90	6.55	Yes
S-Glass (±45°)	(2.00)	22	.98	4.74	6.74	8.85	10.85	No
TENSION MEMBERS								
Baseline Material = 2014-T6 Extr., $S_b = F_{tu}/w = 590$								
$C_{ib} = C_{mb} + C_{fb} = 0.97 + 5.90 = 6.87$								
MG Yttrium-T5	(6.00)	870	.72	3.90	9.90	5.90	11.90	No
Graphite (0°)	(1.00)	1870	.32	23.80	24.80	8.85	9.85	Yes
S-Glass (0°)	(2.00)	2880	.20	38.80	40.80	8.85	10.85	Yes
1" S-Glass/Epoxy	(2.00)	750	.79	6.84	8.84	5.90	7.90	Yes
Sitka Spruce	0.67	626	.94	6.45	7.12	11.80	12.47	No
Spruce-Staypak	(1.34)	760	.78	7.66	9.00	11.80	13.14	No
ZK60A-T5	3.06	682	.86	4.89	7.95	5.90	8.96	No
COMPRESSION FLANGES								
Baseline Material = 6061-T6, $S_b = \sqrt{F_{cy} Ec/w} = 599$								
$C_{ib} = C_{mb} + C_{fb} = 0.44 + 5.90 = 6.34$								
2014-T6 Extr.	0.97	760	.79	7.60	8.57	5.90	6.87	Yes
1" S-Glass/Epoxy	(2.00)	1160	.52	12.00	14.00	5.90	7.90	Yes
MG Yttrium T-5	(6.00)	852	.70	3.90	9.90	5.90	11.90	No
Graphite (6)	(1.00)	1350	.44	15.95	16.95	8.85	9.85	Yes
S-Glass (6)	(2.00)	955	.63	9.25	11.25	8.85	10.85	Yes

(1) ( ) indicates 1982 estimate
(2) Ref. Table XVIII and XIX
(3) C_w = $2.00/Lb. ref p. 162
(4) Formulas on p. 163
(5) Ref. p. 166 & estimated
(6) ±45°, 0°, 0°, 0° layers

TABLE XXII

BREAK-EVEN VS FABRICATION AND INSTALLATION COSTS WITH NET SAVINGS FOR FEASIBLE MATERIALS

MATERIAL / CONCEPT	C_{mn}	$\frac{W_n}{bL^2(10^{-4})}$	NON-OPTIMUM: Z SPACING K_1	NON-OPTIMUM: JOINTS K_2	K_n	$\frac{K_n W_n}{K_b W_b}$	BREAK-EVEN: C_{fr} FABR.	BREAK-EVEN: C_{in} INSTL.	ACTUAL: C_{fa} FABR.	ACTUAL: C_{ia} INSTL.	FEASIBILITY	$\Delta\$_{pp}$	$\Delta\$_{oc}$	$\$_{Savings}$
	(2)	Figs.113&116			$K_1 K_2$		(3)(4)	(3)(4)	(5)		BRK-EVN ≥ ACT.	(6)	(7)	(8)
Baseline Material = 2024-T4 Zee, $K_b = K_1 (K_2) = 1.20 (1.1) = 1.32$												+ INCREASE	+ SAVINGS	
$C_{ib} = C_{mb} + C_{fb} = 1.10 + 5.90 = 7.00$														
@Nx/L = 30, $W_b/b_L 2 = (10^{-4}) = 5.0$														
2024 Honeycomb	0.93	4.6	1.0	1.4	1.4	.977	6.29	7.00	19.00	20.15	No			
181 Cloth Zee (1)	1.00	3.2	1.2	1.1	1.32	.64	10.95	12.05	8.85	9.85	Yes	-1.02	0.72	1.84
181 Cloth Honeycomb	1.45	3.3	1.0	1.4	1.4	.70	9.45	10.85	19.00	20.65	No			
Graphite Zee z(1)	1.00	2.55	1.2	1.1	1.32	.51	14.65	15.65	8.85	9.85	Yes	-2.87	0.98	3.85
Graphite Honeycomb	1.45	2.12	1.0	1.4	1.4	.446	16.75	18.00	19.00	20.65	No			
Graphite Truss Core	1.20	2.2	1.0	1.4	1.4	.467	16.10	17.30	5.00	14.00	Yes	0.90	1.06	0.16
S-Glass Zee	2.00	3.2	1.2	1.1	1.32	.64	10.05	12.05	8.85	10.86	Yes	-0.07	0.72	0.79
S-Glass Honeycomb	2.23	2.14	1.0	1.4	1.4	.457	15.47	17.70	19.00	21.45	No			
S-Glass Truss Core	2.40	3.3	1.0	1.4	1.4	.70	8.47	10.67	15.00	7.40	No			
@Nx/L = 400, $W_b/b_L 2 (10^{-4}) = 9.8$														
2024 Honeycomb	0.93	11.0	1.0	1.4	1.4	1.19					No			
181 Cloth Zee	1.00	7.6	1.2	1.1	1.32	.78	8.55	9.55	8.85	9.85	No			
181 Cloth Honeycomb	1.45	8.2	1.0	1.4	1.4	.89	6.67	8.12	19.00	20.65	No			
Graphite Zee (1)	1.00	3.8	1.2	1.1	1.32	.38	20.70	21.70	8.85	9.85	Yes	-4.76	1.24	6.00
Graphite Honeycomb	1.45	10.0	1.0	1.4	1.4	1.08					No			
Graphite Truss Core	1.20	3.6	1.0	1.4	1.4	.39	19.80	21.00	15.00	16.22	Yes	-0.99	1.22	2.21
S-Glass Zee	2.00	5.5	1.2	1.1	1.32	.56	12.10	14.10	8.85	10.85	Yes	-1.34	0.88	2.22
S-Glass Honeycomb	2.23	6.4	1.0	1.4	1.4	.69	8.87	11.10	19.00	21.45	No			
S-Glass Truss Core	2.40	6.4	1.0	1.4	1.4	.69	8.70	11.10	15.00	17.40	No			

NOTES

(1) E-Glass

(2) Based on values from Tables XVI and XVII with some modification where core materials are concerned.

(3) C_w = $2.00/Lb. Ref. Pg. 162

(4) Formulas on Pg. 163

(5) Ref. Pg 166 and estimated

(6) $\Delta\$_{pp}$ = Change in Purchase Price/Lb. of Baseline wt. of component

(7) $\Delta\$_{oc}$ = Change in Operating Cost/Lb. of Baseline wt. of component Ref. Pg.166

(8) $Savings = Net Dollars Saved/Lb. of Baseline wt. of component

Material/Concept Feasibility: The feasibility of the various material/concepts is evaluated by comparing the maximum allowable break-even fabrication costs with the actual fabrication costs.

The actual fabrication costs are as follows:

Material/Concept	C_{fn} ($/Lb.)
Truss Core	15.00
Honeycomb sandwich	19.20
Aluminum zee stringer	5.90
Reinforced plastic zee stringers	8.85
Wood construction	11.80

Tables XXI and XXII also compare the break-even fabrication costs with the actual fabrication costs for the various types of members.

In the final analysis, those material/concepts deemed feasible are reviewed from the standpoint of change in purchase price of airplane, change in operating costs over 20 year (6667 hr.) period, and the net overall savings realized.

The wide column concept for two different structural index levels is shown as an example in Table XXII. The change in purchase price of the airplane is determined as follows:

$$\Delta\$_{PP} = \left(W_n C_{ln} - W_b C_{lb}\right)\left(K_p\right)\left(K_d\right), \text{ where:}$$

W_n, C_{ln}, W_b, C_{lb}, } defined on p. 162

K_p = 1.10 (based on 10% profit)

K_d = 1.33 (based on 33% markup for (distributor and dealer)

Therefore:

$$\Delta\$_{PP} = W_b\left[\left(S_b/S_n\right)\left(C_{ln}\right) - C_{lb}\right]K_pK_d$$

$K_pK_d = 1.10 \times 1.33 = 1.46$

$W_n = W_b\left(S_b/S_n\right)$ (ref. p.162)

The change in operating costs over 20 years (6667 hrs.) is based on the worth of a pound of material saved being equal to C_w=$2.00 (ref. Fig.74).

Therefore: $\Delta\$_{oc} = \left(W_b - W_n\right)\left(C_w\right) = W_b\left(1 - S_b/S_n\right)\left(C_w\right)$

The net overall savings realized is equal to:

$$\$_{savings} = \$_s = \Delta\$_{oc} - \Delta\$_{PP}$$

Fatigue Evaluation.- Existing requirements for the strength of light airplane structures are based largely on the concept of "one-time" loading. For many years this appeared to be satisfactory but recently it has been recognized that the margin of safety provided against failure under "one-time" loading may no longer be adequate with respect to the repeated loads which occur during the lifetime of the aircraft. A survey of the 1963 General Aviation Accident Reports indicates evidence that some airframe failures could be attributed to fatigue.

Whether or not the failures involved were the result of inadequate pilot proficiency, lack of respect for adverse weather, or the result of inadequate inspection and maintenance is of secondary importance. The point is that the airplane involved encountered flying conditions which resulted in loads being applied to the airframe of sufficient magnitude and frequency to cause catastrophic failure of the primary airframe structure.

Establishing a Fatigue Load Spectrum: Up to the present time, light airplane manufacturers have designed their aircraft to FAA requirements per F.A.R. part 23. This document does not require proof by analysis or test of the "safe life" or "fail safe" characteristics of their aircraft. At the same time little data is available with regard to what load spectra should be used by operators of the various category airplanes.

An assessment of repeated loads on general aviation and transport aircraft is being conducted with the F.A.A. by NASA's Langley Research Center; the results to date are presented in references 48 and 20. They reveal a large amount of scatter in the repeated load history, due principally to the diverse nature of general aviation.

Composite VG records (positive and negative accelerations vs airspeed) from references 48 and 20 for different types of operations are presented in Figure 125 . These data are superimposed upon their respective V-n diagrams to indicate where the most severe areas might be in respect to possible exceedances of the design flight envelope. Design flight envelope exceedances in the low speed portions are probably due to landing shocks and are not considered significant.

A review of the instructional flying records, Figure 125, reveals a case where a particular aircraft exceeded the design dive speed as well as the positive and negative limit load factors at the design dive speed.

The twin-engine executive operations, Figure 125, show one case of exceeding the negative limit load factor at a speed slightly less than design cruise. Investigation revealed the incidence to be gust induced.

The following significant conclusions can be made after reviewing the composite VG records.

COMPOSITE VG RECORDS - FIVE TYPES OF OPERATIONS .

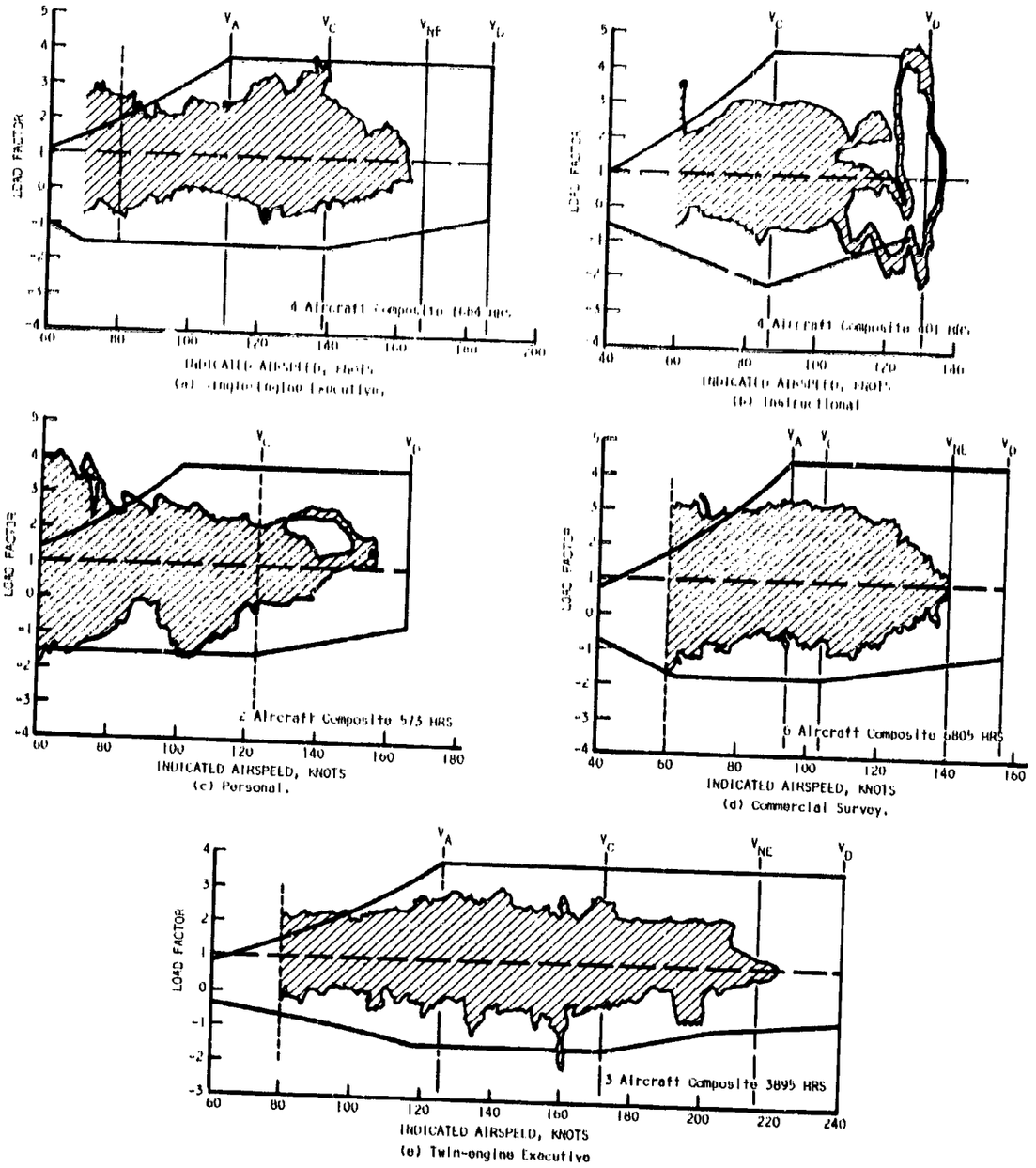


Figure 125

(1) Atmospheric-induced, as well as pilot-induced, loads in excess of the design flight envelope may be encountered during normal operation of the general aviation fleet.

(2) All types of operations are flown above the design cruising speed.

It is evident, therefore, that General Aviation should be classified into different roles. Needless to say, the fatigue load spectrum will be different for each role.

Estimation of Fatigue Life: The estimation of fatigue life using the "Miners" Cumulative Damage Rule involves the calculation of damage incurred on the airplane as a direct result of its operating environment.

Generally speaking the operating environment for a light airplane, regardless of its type of utilization such as executive, personal, instructional or commercial survey operation, can be defined as follows:

(1) Gust Environment - The airplane while in steady flight encounters a specified number of positive and negative gusts of varying intensities defined by the gust spectrum for the airplane.

(2) Maneuver Environment - The airplane is subject to a specified number of positive and negative maneuvering loads of varying intensity defined by the maneuvering spectrum for the airplane.

(3) Ground-Air-Ground Environment (G.A.G.).- At least once per flight the airplane is subject to loads associated with the following conditions.

a) Taxi condition at maximum take-off weight.
b) Steady 1g Flight Cruise Condition at minimum landing weight.
c) Landing impact loads at maximum landing weight.

From a structural design aspect it is apparent that before any design fatigue load spectrum can be developed and before any safe life prediction can be made, it is necessary to define not only in what roles that airplane is going to be utilized, but also for how long it is going to be utilized in one role before being used in another role. This is obvious when one is confronted by the following statements:

(1) Landing Impact Acceleration for instructional-type airplanes is more severe and more frequent, approximately 4 per 30-minute flight, than on any other category light airplane and will account for a considerable amount of damage in the fatigue life of the airplane.

(2) Commercial Survey Aircraft have the longest flight duration, therefore less G.A.G. damage is inflicted on the airplane. They have more

severe gust experience than other types of usage, since 97% of the time they are in rough air.

Pressurization Considerations: The effect of pressurization produces a stress configuration consisting of hoop stress and longitudinal stress in addition to the in-flight shear, bending moment, and torque loads on the fuselage structure. It then follows that the weight of the basic pressurized fuselage will be higher than that of an unpressurized fuselage. From a minimum weight standpoint, the optimum structure is cylindrical with the elimination of flat or slab panels.

Sealing requirements demand that careful consideration be given to the number and spacing of rivets, particularly at longitudinal and transverse skin splices and at the attachment of pressure bulkheads and canopy structure. Likewise, more care must be taken in the fabrication, inspection,and quality control of the fuselage structure, particularly in the region of cut outs in the structure for windows, entry doors and access doors, at the attachment of the floor structure to the frames of the fuselage,and at the intersection of the wing and fuselage.

Entry doors and their locking and operating mechanisms should be designed on the fail safe concept to insure that the door structure and the sealing qualities are adequate should a simple failure in one of the latches or shear pins occur.

The use of metal-to-metal adhesive bonding, particularly to reinforce areas where high stress concentrations are present, increases the fatigue life of the fuselage. It demands good quality control and considerable component testing. Materials exhibiting low crack progagation characteristics are important. As an example, it has been shown (ref. 21) that 7075-T6 aluminum alloy is more prone to explosive fracture than 2024-T3 alloy.

From a structural standpoint, it is highly probable that any fatigue crack, once started, will tend to run longitudinally along the fuselage. This is due to the fact that in a pressurized fuselage the stringers are fairly closely spaced and the hoop tensile stress is twice the longitudinal stress. For this reason, circumferential reinforcing rings are placed at intervals along the fuselage to arrest the crack propagation of a fatigue crack and to reduce the hoop stress in the skin.

The spacing and cross section of the reinforcing rings are important Williams (ref. 22) states that rings spaced more than 30" apart, while locally restricting the radial expansion of the skin, allow unrestricted expansion in the area midway between the rings; with a 10" spacing the radial expansion of the skin nowhere exceeds that of the rings by more than a small percentage, so that the maximum hoop stress in the skin is equally reduced by material added to the rings as by the weight added to the skin.

Material Fatigue Properties: Many mechanical devices are subjected to forces that vary in magnitude and, often, in direction. If this variation occurs a relatively small number of times and the stresses do not exceed the yield strength of the material, design studies can be made safely on the basis of the static properties of the material. Unfortunately, this is not true in the design of airplanes since the structure usually experiences many repeated loadings (magnitude and direction) in its service lifetime.

This section summarizes and compares the fatigue properties of some of the basic materials as previously selected for aircraft structural applications. This data has been compiled and evaluated to present a qualitative picture of the fatigue characteristics associated with the material.

For the most part, complete information was not available for the materials; therefore, various methods were utilized in extending the data to provide information which could not be obtained directly. All the fatigue data shown represents axial loading tests and is ultimately plotted as standard S-N curves whereby the points along the curve represent the number of loading cycles a material may endure at a particular max stress before failure.

S-N curves for notched and unnotched sheet specimens representing stress Ratios (R) of -1.0 and +0.25 are shown in Figures 126, 127, 128, and 129. For the most part, these curves are derived by means of averaging the results directly from several references as shown in the respective tables.

Where basic information in the reference did not provide data representing correct stress ratios from which comparisons could be made, the basic data is expanded through use of an approximate Modified Goodman diagram. This method is described in reference 23.

The reference literature (ref. 24) associated with the 4130 and 4340 materials provided fatigue data in terms of alternating and mean stress. With use of modified Goodman Diagrams it is possible to reconstruct S-N curves (Figures 130 & 131) as a function of maximum-stress and any stress ratio desired.

Figure 127 illustrates that the fatigue strength of the higher strength aluminum alloy (7075-T6) actually is inferior to the lower strength alloys. This would suggest that increases in static strength have been obtained at the expense of an actual reduction in fatigue strength.

This is not true in the comparison of 4340 and 4130 steels; however, the difference in the static strength of these two materials is much greater than the difference in the fatigue strengths (ref. Figures 130 and 131).

Comparison S-N curves for plastic laminates reinforced with unwoven glass filaments are presented in Figures 132,133 and 134. The curves represent three constructions: (1) all plies parallel, (2) alternate plies $\pm 5^{\circ}$ to the

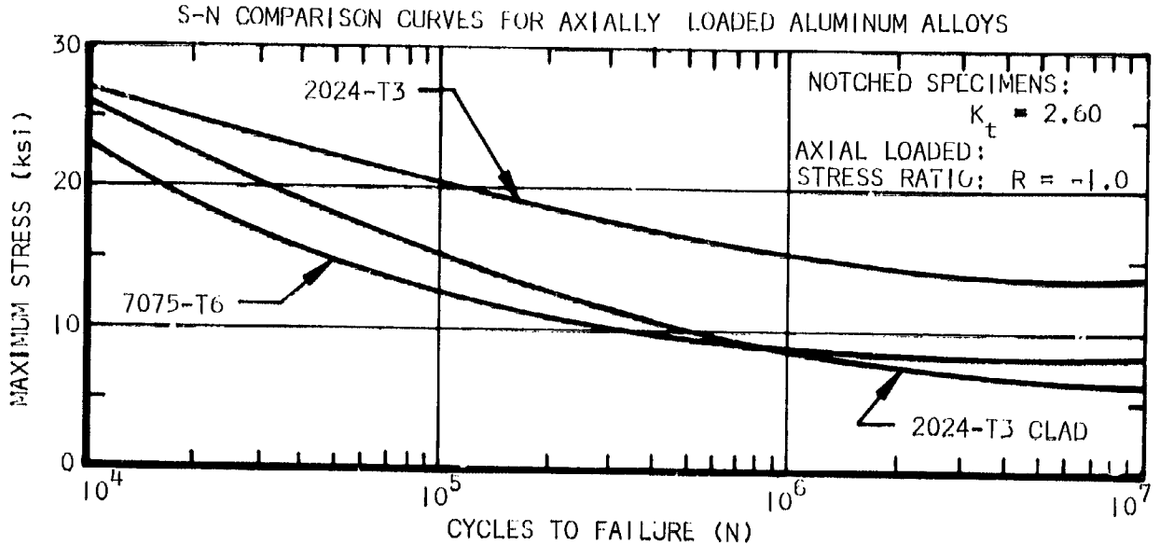


Figure 126

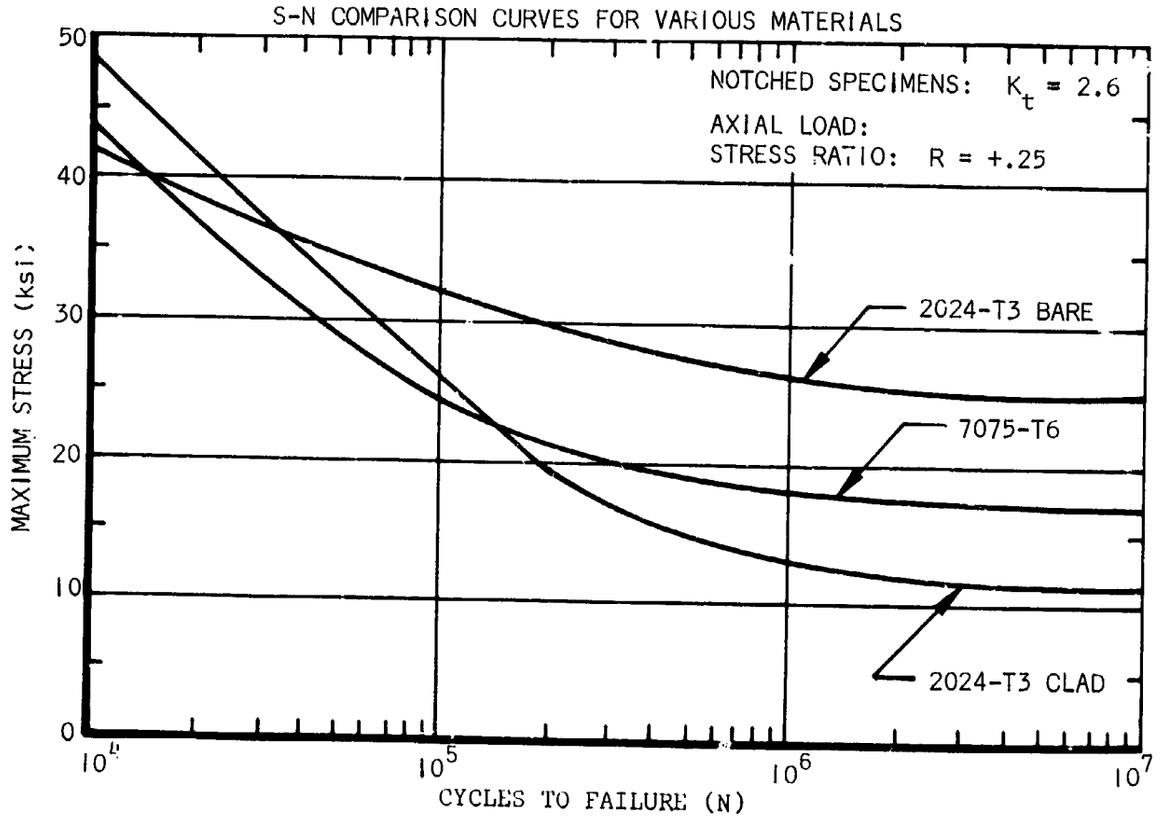


Figure 127

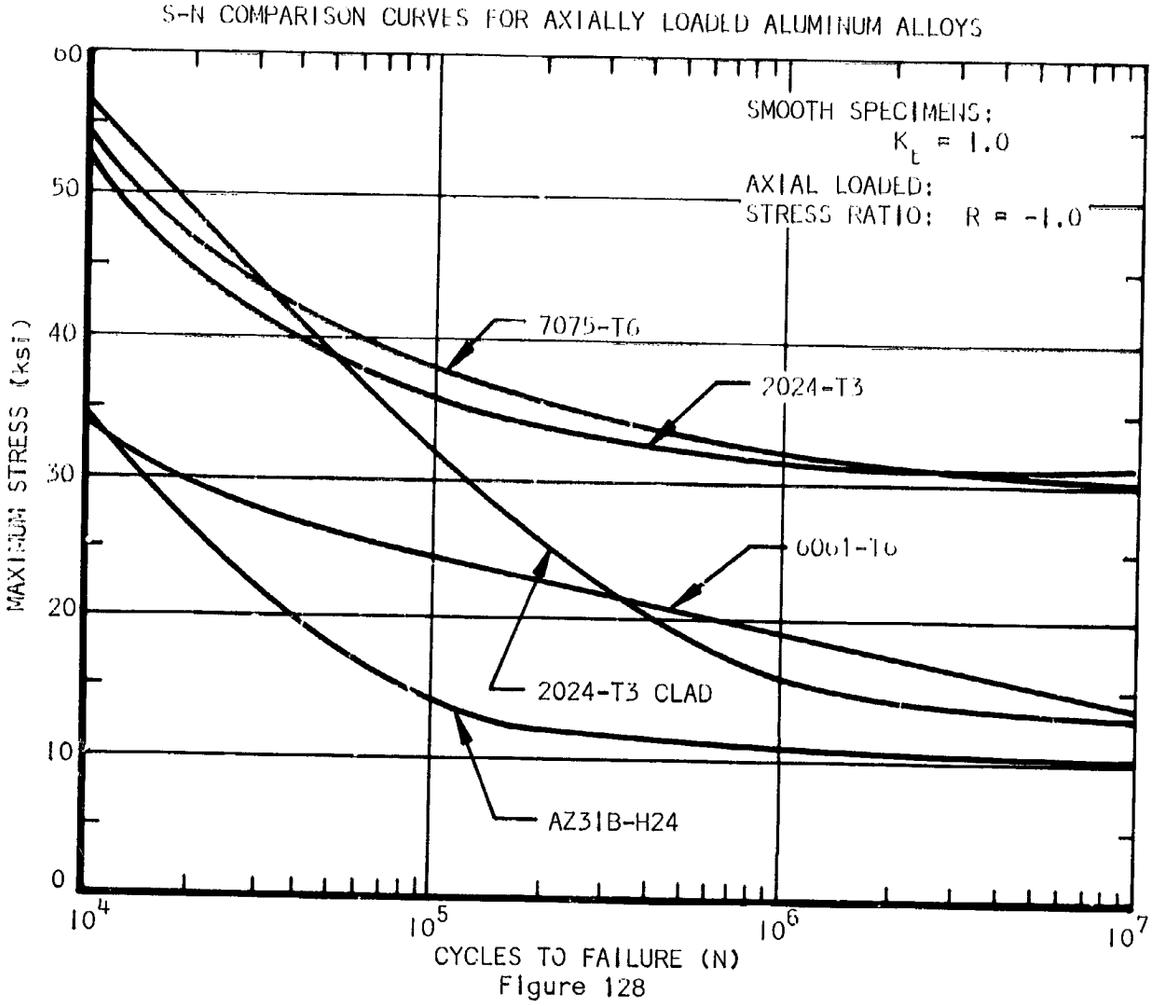


Figure 128

principal axis, (3) alternate plies 0° and 90° to the principal axis. All indicate the fatigue strength of the S-glass filaments to be superior to the E-glass type. It also appears (Figures 133 and 134) that the fatigue characteristics of the S-glass laminates may be even further improved with the use of different resins.

In recent years, more and more consideration is being directed toward the fracture characteristics of materials. Acceptance is given to the fact that fatigue failures could occur as a result of one or a combination of several loading environments. These environments include normal working loads, noise induced vibrations, and accidental damage. When a crack originally develops in a structure, it creates a point of high stress concentration, and subsequent application of normal service loads will cause further extension of

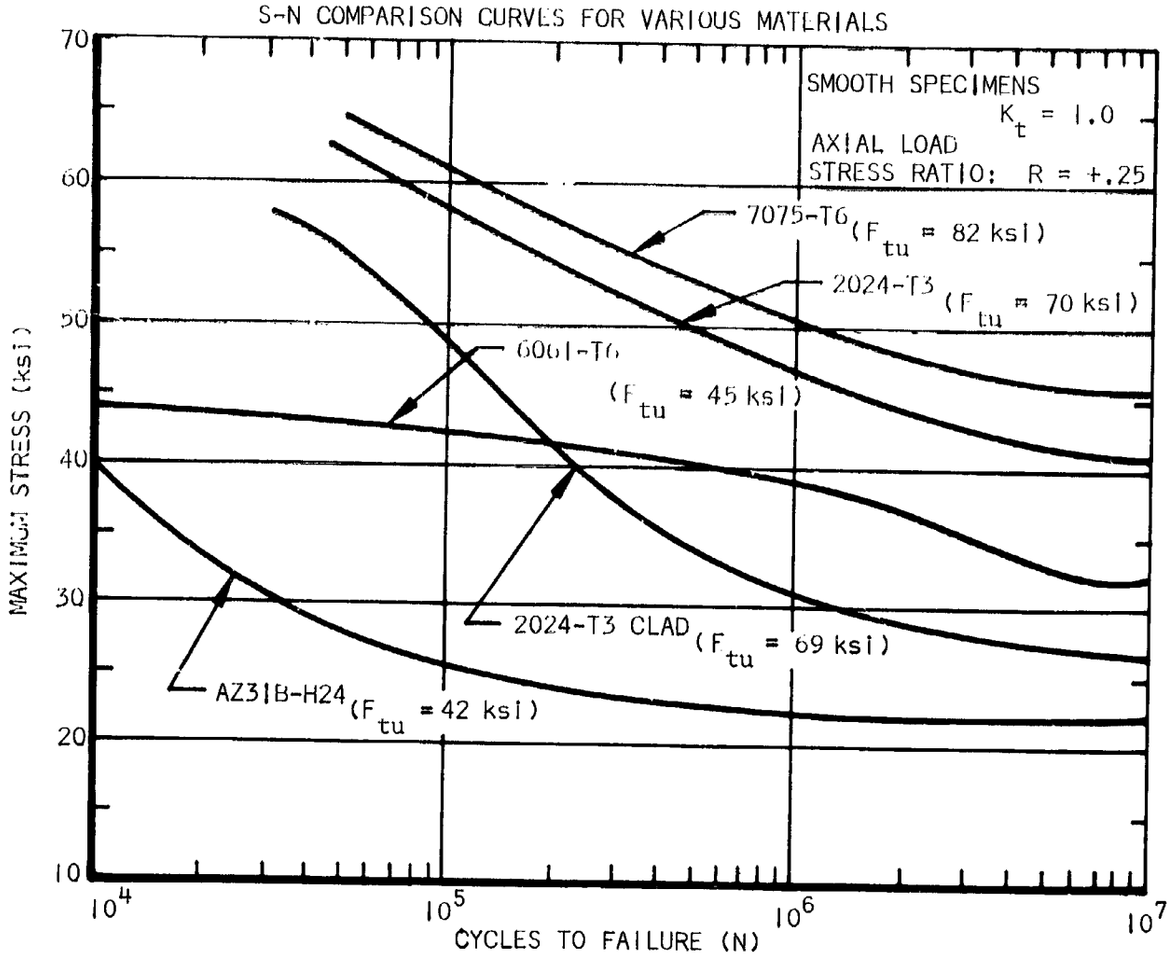


Figure 129

the crack. This extension, of course, largely depends upon the load/stress level and the inherent crack-propagation characteristic of the material. It is extremely important these cracks be detected before they can extend to a length which would cause a catastrophic failure. Structural inspections take place periodically, and consist of frequent visual examinations to detect any obvious defects, together with a detailed overhaul about once a year.

Two questions which still need answering are as follows:

(1) How long must a crack be before it can be detected?
(2) How long can it become before it leads to serious failure?

The ideal condition would be such that a defect which is approaching a detectable length would not become catastrophic prior to the next scheduled

S-N COMPARISON CURVES FOR AXIALLY LOADED 4130 & 4340 STL. ALLOYS

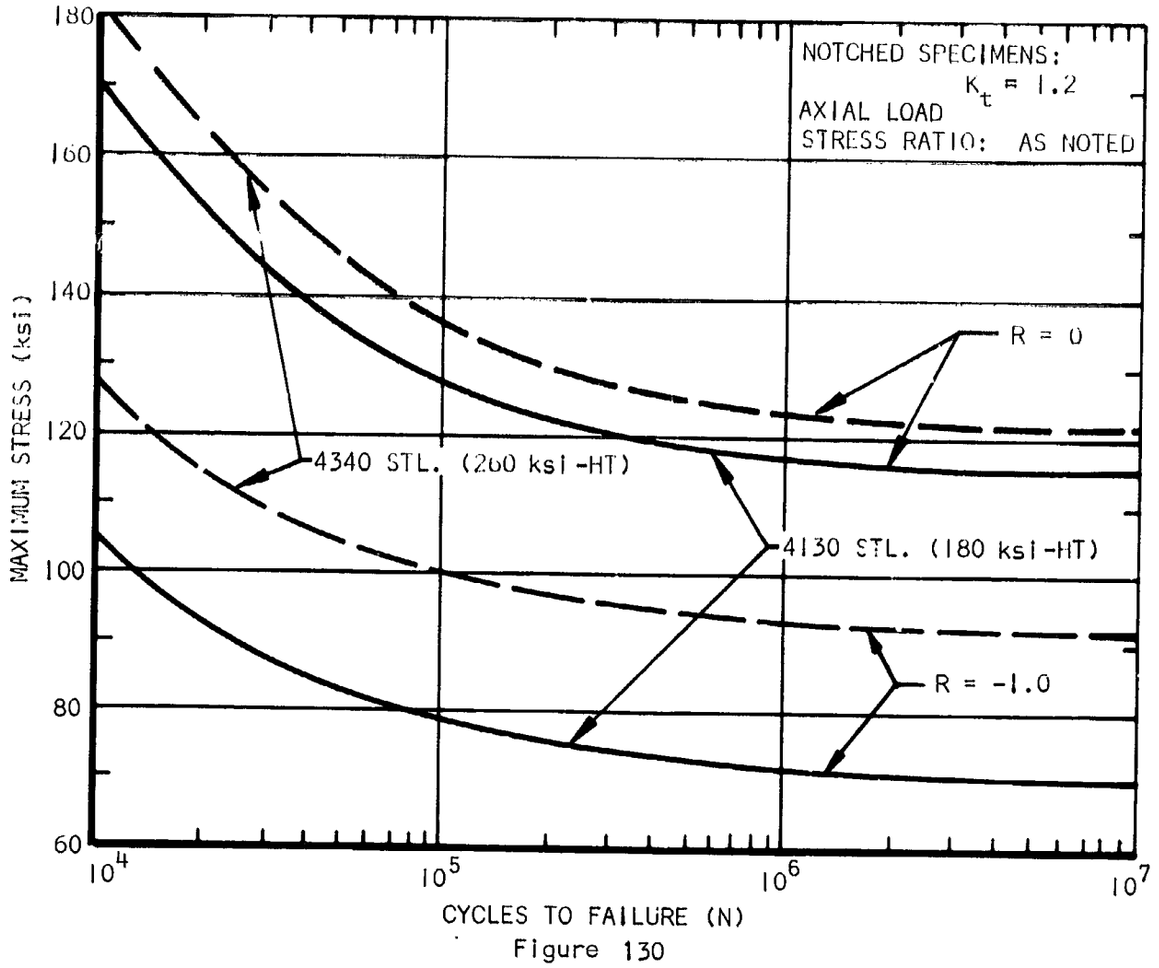


Figure 130

inspection. A good design would therefore consider a material which would satisfy these requirements; i.e., low crack-propagation rate to allow sufficient time for crack detection and high notch resistance to insure adequate strength at any crack location. These requirements actually have led to a return to the use of lower strength aluminum alloys, particularly in fatigue critical areas.

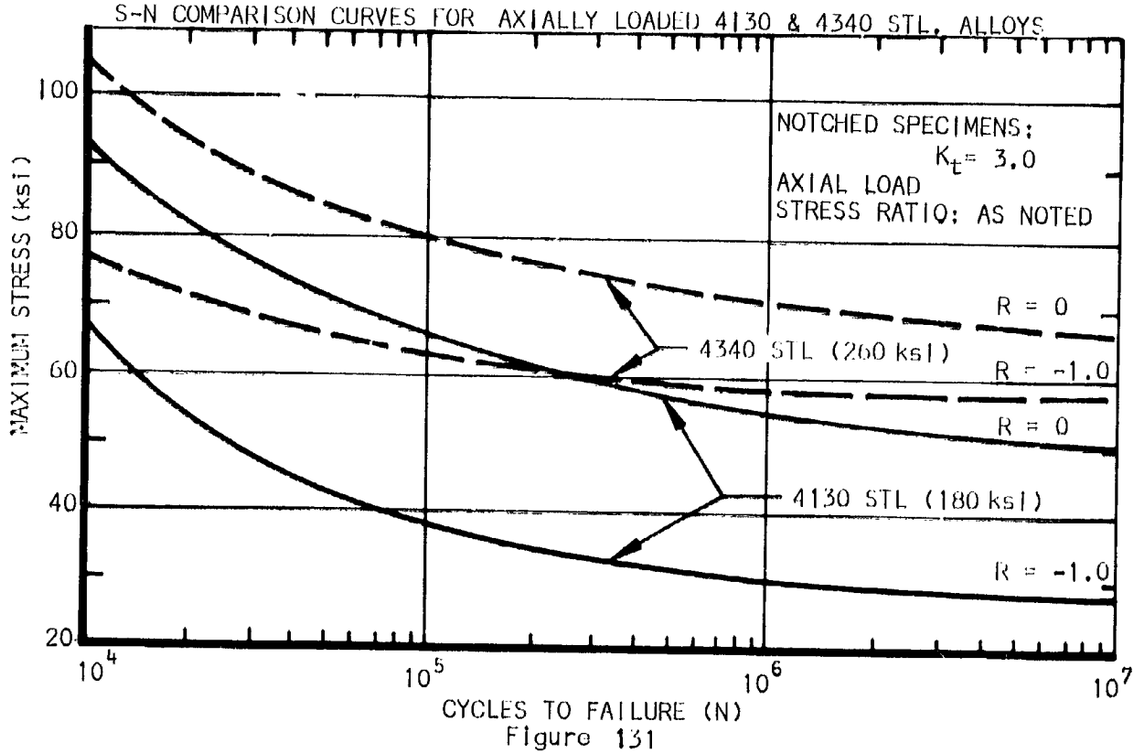


Figure 131

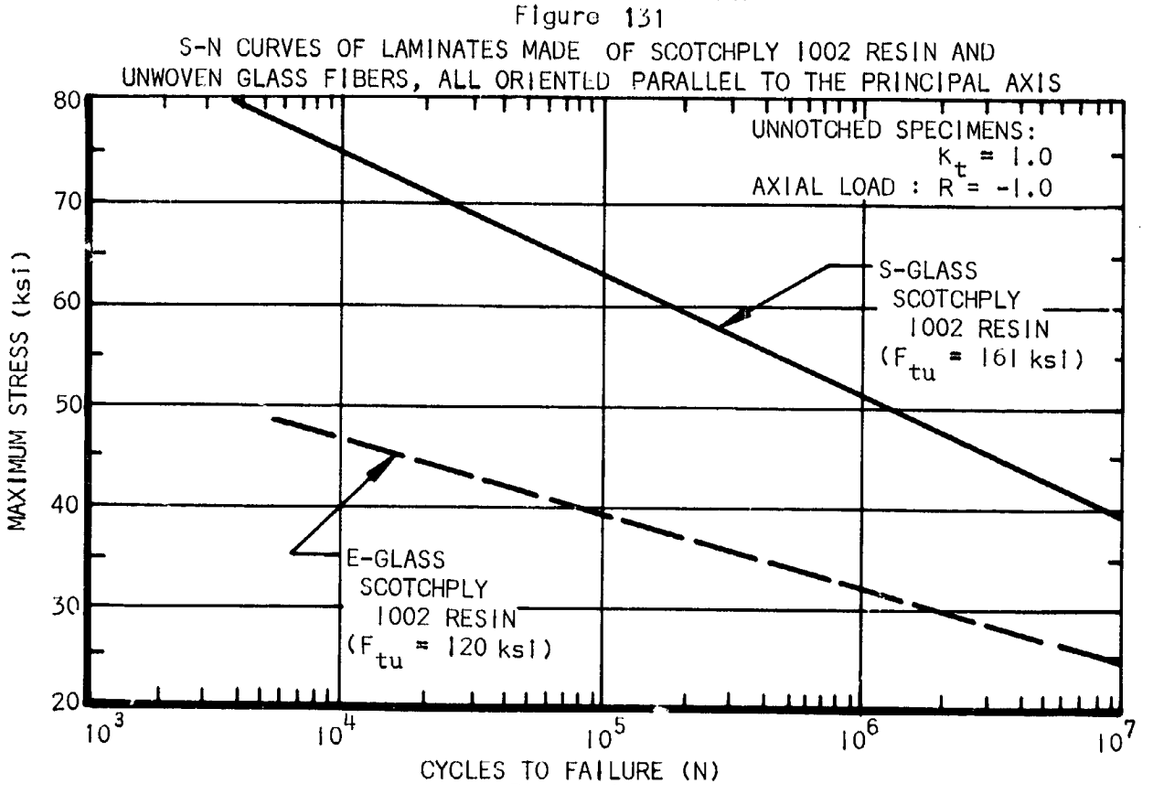


Figure 132

S-N CURVES OF LAMINATES MADE OF SCOTCHPLY RESINS AND UNWOVEN GLASS FIBERS HAVING ALTERNATE PLIES AT 0° and 90°TO THE PRINCIPAL AXIS

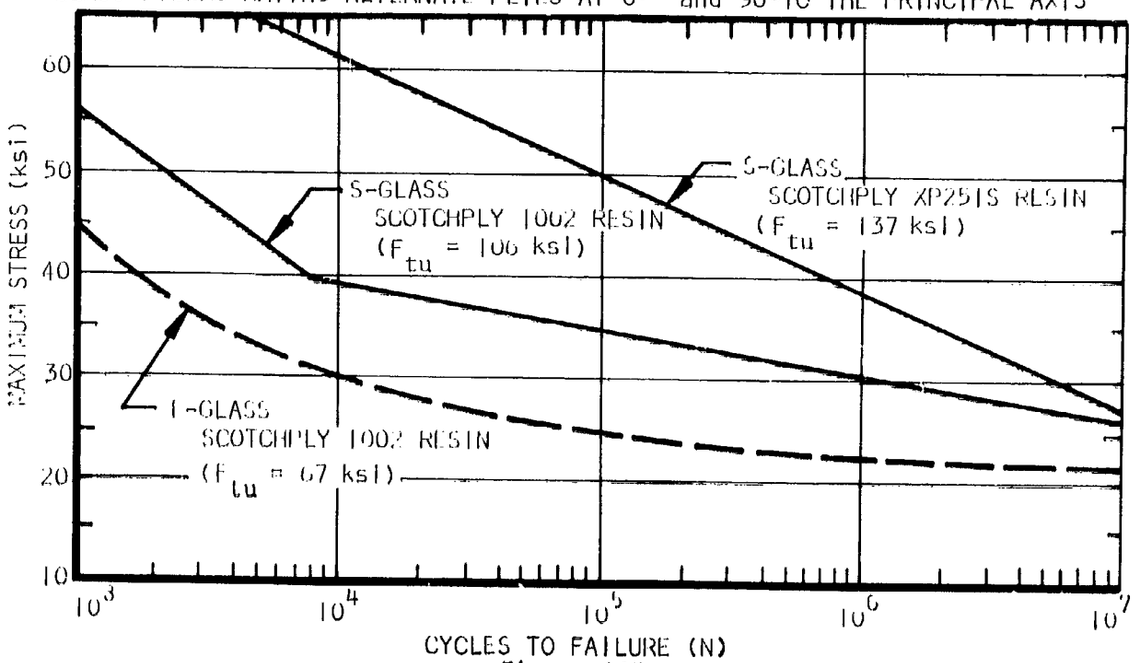


Figure 133

S-N CURVES OF LAMINATES MADE OF SCOTCHPLY RESINS AND UNWOVEN GLASS FIBERS HAVING ALTERNATE PLIES ORIENTED AT ±5° TO PRINCIPAL AXIS

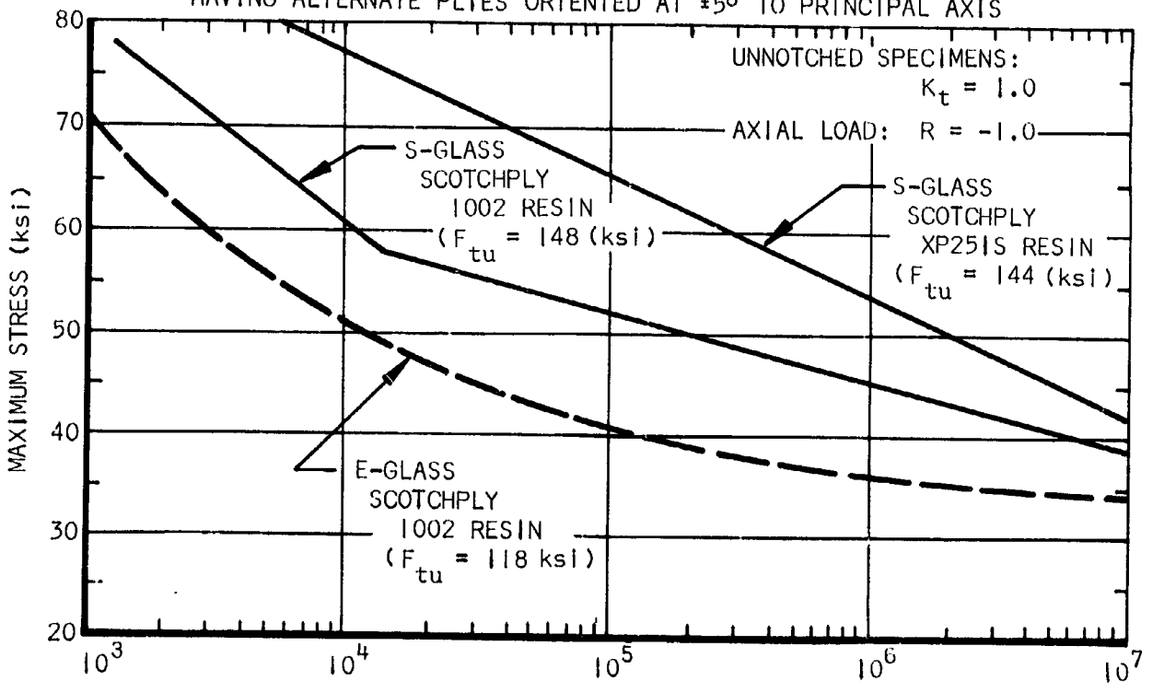


Figure 134

Fastening Devices and Methods.- Metals may be joined by either mechanical means (such as bolting) or by welding, brazing, soldering or adhesive bonding. All of these methods may be used to some degree in aircraft construction. Soldering is never used for structural purposes, but is frequently used in electrical work.

This section includes a discussion of the various joining processes adaptable to aircraft construction. Each method is presented in the following manner:

(1) A brief description.

(2) Illustrations are provided as necessary to clearly define the method of construction.

(3) Typical allowable strengths are given where applicable.

(4) Some comparisons (Fatigue and Static Strengths) are made between two or more of the techniques used.

(5) Advantages and disadvantages of each method are listed.

(6) Typical applications in aircraft manufacturing are given for each joining process.

Riveting: Rivets play an important role in the light aircraft industry. At the present it is the primary method of joining aluminum. Riveted construction is readily controlled and inspected, and it does not require the application of heat that might partially anneal or significantly impair the corrosion resistance of the heat-treated alloys used. The limited heating required in dimpling sheets of some alloys, and tempering before riveting does not impair essential properties. Sheets less than 0.050 inch thick generally are dimpled for countersunk head fasteners. Thicker material is machine countersunk.

Countersunk head rivets are used primarily for attaching outer skins whereas universal-head (modified round) rivets are used extensively in interior structures where protruding heads are not objectionable. Surface skin panels often are riveted by automatic machines (as illustrated in Figure 135) made to form one or both heads of the rivet. The machines are fed with rivets or slugs; and the heads are usually shaved flush with the exterior surface.

Rivet alloy 2117-T4 is the most popular for general use, especially for automatic riveting, because it retains good driving characteristics indefinitely after solution heat treatment. 2024-T4 alloy rivets are used occasionally where higher strength is required; however, these must be used within 30 minutes after heat treatment, or refrigerated until used.

STANDARD AUTOMATIC RIVETING MACHINE

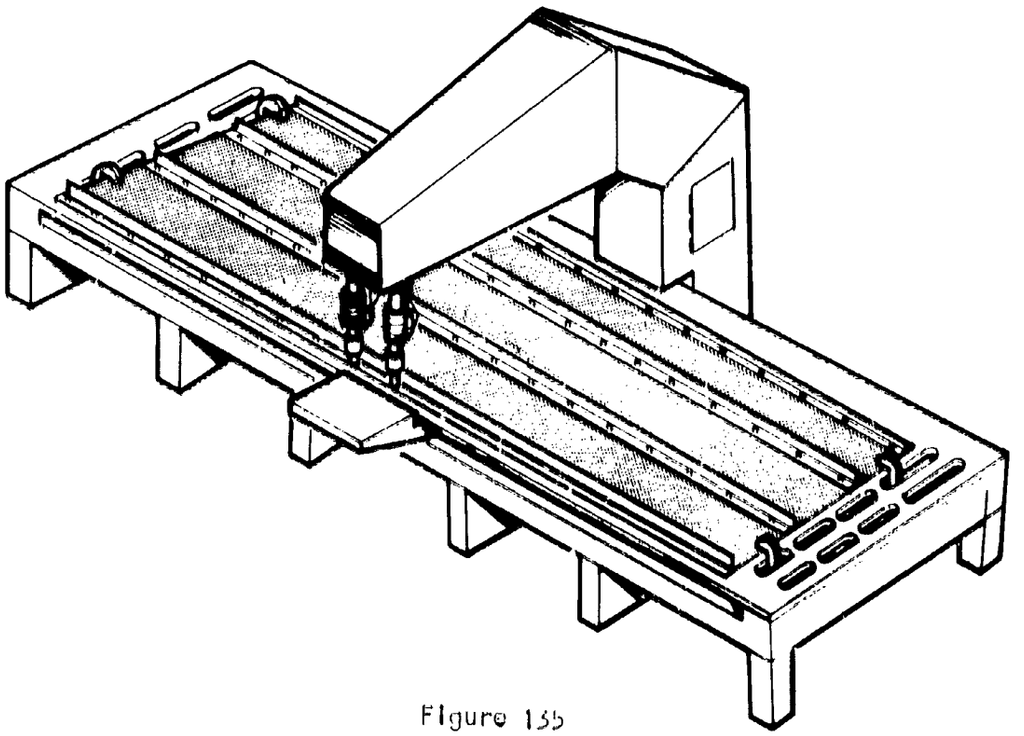


Figure 135

Specifications for the design of aluminum-alloy structures generally designate the rivet alloys to be used. Table XXIII lists some combinations of structural and rivet alloys that combine satisfactorily in many applications. Compatability from the standpoint of electrolytic corrosion could be one requirement. Alloy 2213 is generally specified where rivets are to be used at elevated temperatures; however, this probably would not apply in the light aircraft field.

It is considered poor practice to use a large rivet in relatively thin metal or a small rivet in thick metal. Furthermore, a loss in shear strength can result when a relatively soft rivet is driven in a hard, thin plate. Tests indicate reductions in shear strengths of approximately 30 percent when the rivet diameter is four times greater than the sheet being joined.

The type of rivet to be driven generally governs the selection of the driving method. All standard rivets require backing up, pressure, or impact, and a driving-set or head-forming fixture. Blind rivets require special tools. Common practice is to drive solid aluminum rivets with either squeeze riveters or pneumatic hammers. The cup in a rivet set must conform to the style of the manufactured rivet head. Bucking bars or pneumatic backups used in hammer riveting should have sufficient force to counteract the hammer blows.

TABLE XXIII
ALUMINUM - SATISFACTORY COMBINATIONS
OF STRUCTURAL AND RIVET ALLOYS

STRUCTURAL ALLOYS	RIVET ALLOYS
1 xxx SERIES	1100
3 xxx SERIES	6053,6061
5 xxx SERIES	5056,6053,6061
6 xxx SERIES	6053, 6061, 7277
2 xxx and 7 xxx SERIES	2017,2024,2117,2219 6061,7075,7277
Magnesium Base	5056

Flush-riveted joints require countersunk head rivets. Either the manufactured or the driven head can be countersunk; however, in most instances the manufactured countersunk head is used. Countersinking the metal for flush rivets is done by machine countersinking in heavy gages, or by predimpling or dimpling in thinner gages, as is common in aircraft construction. In a predimpling operation, dies are used to press countersink the metal, whereas in dimpling, the rivet is used with a die. For some alloys, heated dies must be used. Countersinking can also be accomplished by spinning rather than pressing. Either technique used is influenced by the thickness and strength of the alloy, rivet size, hole diameter, and countersink angle.

It is important that all driving sets have smooth polished surfaces, so the metal can flow easily while being formed. As a rule the diameter of the driven head should not be less than 1.3 times the diameter of the original shank. The rivet length should be sufficient to fill the hole and form a satisfactory head.

Tubular, semitubular, and split rivers are usually driven with high-speed automatic or semi-automatic riveting machines.

Driving equipment required for blind rivets depends on the rivet type. The drive-pin type can be driven with an ordinary hammer; the explosive type requires a heat source such as a soldering iron. Most manufacturers of blind rivets provide the driving equipment needed.

Careful attention to details in rivet design and fabrication pays big dividends in fatigue life. When a fatigue failure occurs in a structure, it is usually at a point of stress concentration which could have been improved with little or no added expense.

To meet the requirements of large volume production demands, automatic riveting machines must be used to insure high quality with reasonable costs. Commercial and Military aircraft manufacturers have been using automatic riveting for more than five years. It has been estimated fatigue life is increased

RIVETING EQUIPMENT

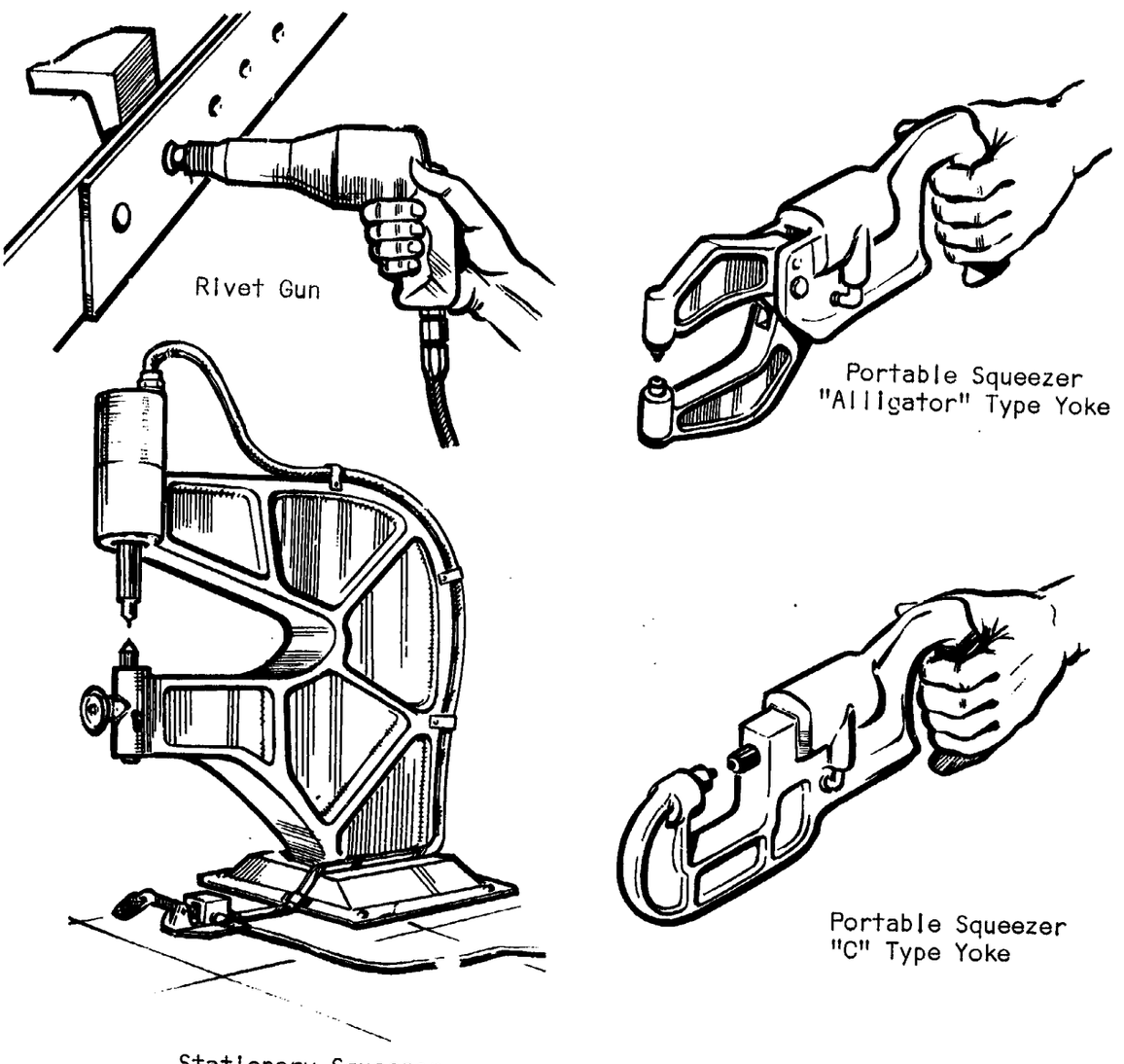


Figure 136

by approximately 200 percent over hand riveting. This increase is attributed to riveting uniformity, something impossible with hand riveting.

A large commercial aircraft manufacturer is installing one of the world's largest automatic riveting machines at its plant. Riveting will be performed at the rate of six seconds per rivet.

This machine is equipped with an automatic-sensing device, whereby riveting is performed to tolerances of 0.005 inch while maintaining consistent repeatability. Normality sensors automatically determine the contour of the wing surface; and guide the angle of the drill accordingly so all holes are exactly alike. All operations of this system are preplanned on perforated tape to automatically cycle from hole to hole while drilling, countersinking, pressure squeezing, impacting, and shaving the rivet to a smooth surface corresponding to the panel contour.

Automatic riveting machines can be set up to travel over the panel or remain stationary while the work, held in a fixture, moves past the machine.

The size and shape of the assemblies determine which method is more suitable. Tack rivets are used to temporarily fasten the sheets together, and later are replaced by permanent hand-driven types.

Design-allowable strengths: The strength of a riveted joint is governed by the shear strength of the individual rivets, the bearing strength of the sheet, and the efficiency of the sheet in tension. Some typical ultimate shear strengths of single rivets are given in Table XXIV based on values shown in MIL-HDBK-5 (Strength of Metal Aircraft Elements). Due to the light loadings anticipated, joint strengths will probably be based on the bearing strength of the sheet, or the shear strength of the rivets.

TABLE XXIV

ALUMINUM RIVET ULTIMATE SHEAR STRENGTH (single shear in lbs)

Rivet Size / Sheet Gage	Protruding Head		Dimpled Sheet 2024-T3,T42,T81		Countersunk Sheet 2024-T42 and higher Structural Aluminum	
	(3/32") AD3	(1/8") AD4	(3/32") AD3	(1/8") AD4	(3/32") AD3	(1/8") AD4
0.020	202		209	299	132	163
0.025	210		235	360	156	221
0.032	217	374	257	413	178	272
0.040		386	273	451	193	309
0.050		388		484	206	340

Sheet gage is thickness of thinnest sheet in a single shear application. Bearing strength of particular sheet used must also be checked.

A fatigue life comparison of a well designed riveted joint to several adhesive bonded joints is shown in the section on bonding in Figure 143. It appears, at least from this standpoint, better performance would be expected from a bonded joint; however, considering all the parameters (cost, reliability or quality control, production schedules, etc.), the automatic riveting concept could prove most worthy.

Electric Welding: Electric welding is often used in aircraft construction. It is the only welding method used for joining structural corrosion-resistant steel; and has been generally adopted for most aluminum alloys. Six basic resistance welding processes are commonly used with aluminum: spot, seam welding to make lag joints, upset and flash-welding for butt joining, percussion welding to attach studs to surfaces.

These processes are rapid and economically justified for high volume production. With proper material preparation consistent weld quality may be achieved automatically by the welding equipment. This technique is independent of operator skill; and one machine may be used to weld a range of thicknesses and sizes

Spotwelding: Used primarily in shear applications; however, it is not recommended in the following areas:

(1) attachment of flanges to shear webs

(2) attachment of spar caps or shear web flanges to wing skin

(3) attachment of ribs to spars or shear webs

(4) at truss panel points in spars or ribs

(5) at junction points of stringers or stiffeners with ribs, unless a stop rivet is used

(6) at ends of stringers or stiffeners, unless a stop rivet is used

(7) on each side of a joggle, or wherever there is a possibility of a tension load component, unless a stop rivet is used

(8) splices exposed to the airstream should be so designed that flow of the airstream would not tend to pry it apart

Anodically treated surfaces cannot be spotwelded; consequently the faying surfaces of a spotwelded seam must be left unprotected prior to welding. The assembled parts are anodically treated or painted after welding. For this reason there is some doubt about the advisability of spotwelding aluminum alloys, other than 5052 or clad materials, if the assemblies are subject to

severe corrosion. It is possible to spotweld through wet zinc-chromate primer applied to the faying surfaces.

A French aircraft company, has recently developed a series of light aircraft, using spotwelding quite extensively. This company set out to incorporate mass-production techniques, and in so doing reduced costs accordingly. The number of parts is reduced by using certain components in several applications. Standard joining techniques are employed in fabricating major subassemblies (wing section, forward fuselage section, aft fuselage section, etc.) These are mated on the final assembly jig as in an automobile assembly line.

Normal riveting is limited only to primary joints; whereas all the remaining connections are spotwelded with automatic welding machines. These machines are programmed with perforated tape to perform the complete welding operation; consequently the operator stands by and only takes over in the event of any malfunctioning.

Fuselage welding is performed in two stages. By using this fabrication technique, the main structural elements of the fuselage are welded by machine in about ten hours.

The fuselage consists of a forward section and tail cone joined by a riveted skin splice. The longerons also extend out from the rear section, and are spliced with rivets to the longerons of the forward section. This constitutes an all riveted primary joint. Figure 137.

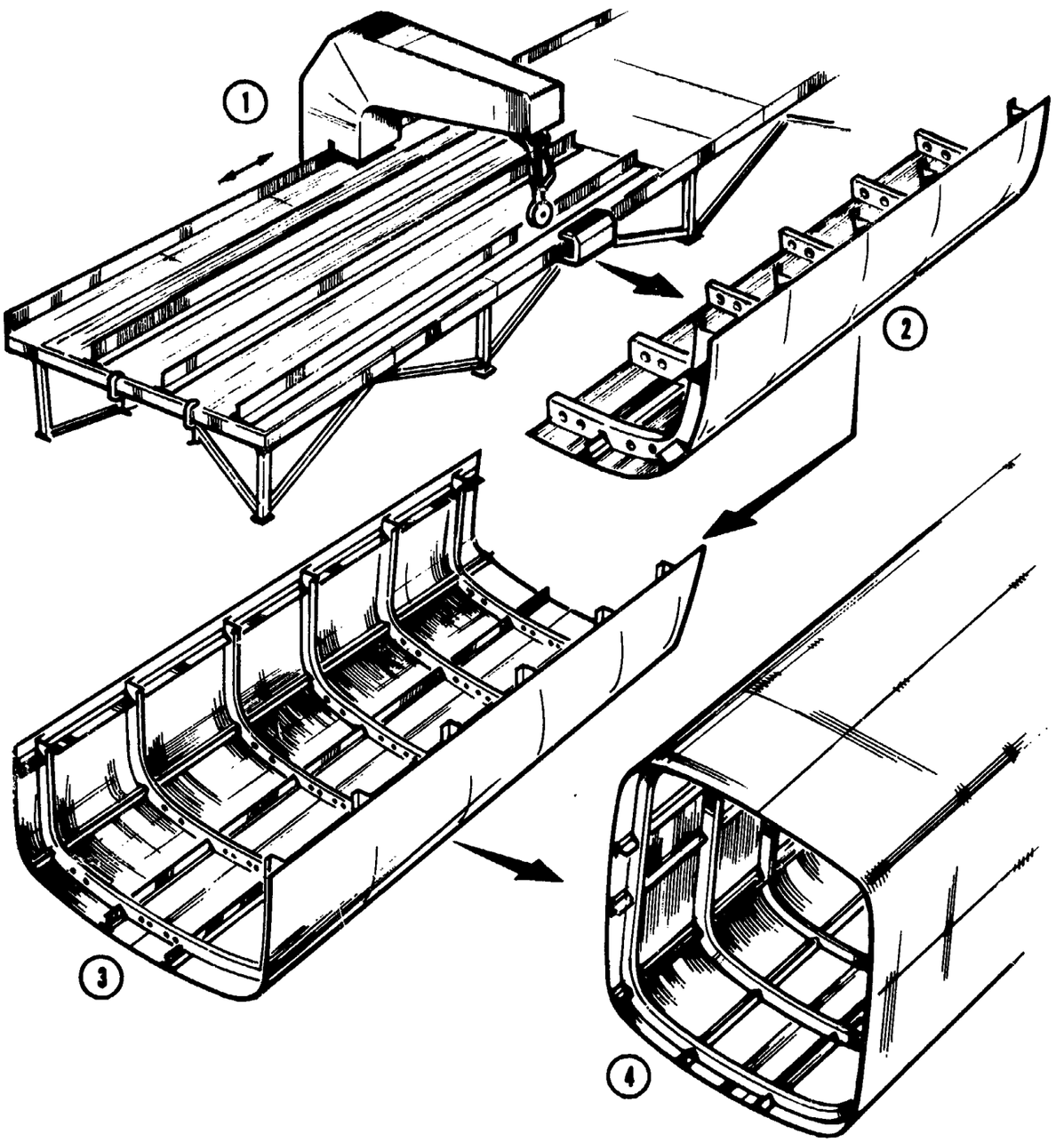
Fabrication of the wing is performed in a very similar manner whereby riveting is used only on the wing spars, ribs to stiffeners, stiffener to spar cap attachments, all these considered as primary joints.

The allerons and flaps have identical profile. The skin is formed over the contour and spotwelded to the ribs and bent-up sheet metal longeron. (Ref.Fig.138) The trailing edge is constructed with beaded sheet metal skins spotwelded to the ribs, the longeron and at the trailing edge. This process applies to all movable surfaces on the aircraft.

Design-Allowable Strengths of Resistance Spotweids: The strength of a spotwelded joint is governed by the shear strength of the individual spots, and the effect of the spotwelds on the tensile strength of the basic sheet. Therefore, both the shear strength of the spotweld, and the tension efficiency of the spotwelded sheet, must be considered in determining the strength of a spotwelded joint.

The allowable ultimate shear strengths of single spotwelds are given in Table XXV. Values are reproduced from MIL-HDBK-5. The allowable strength of a spotweld between two sheets of different material or thickness is the lower of the allowables for the individual sheets, as determined from the tables.

CURRENT LIGHT AIRCRAFT SPOT WELDED FUSELAGE CONSTRUCTION



The longitudinal stiffeners are first welded to the skins. The transverse members are then welded to the panel which is sufficiently flexible to be fitted into the second stage jig without any shaping.

Figure 137

CURRENT LIGHT AIRCRAFT SPOT WELDED FLAP CONSTRUCTION

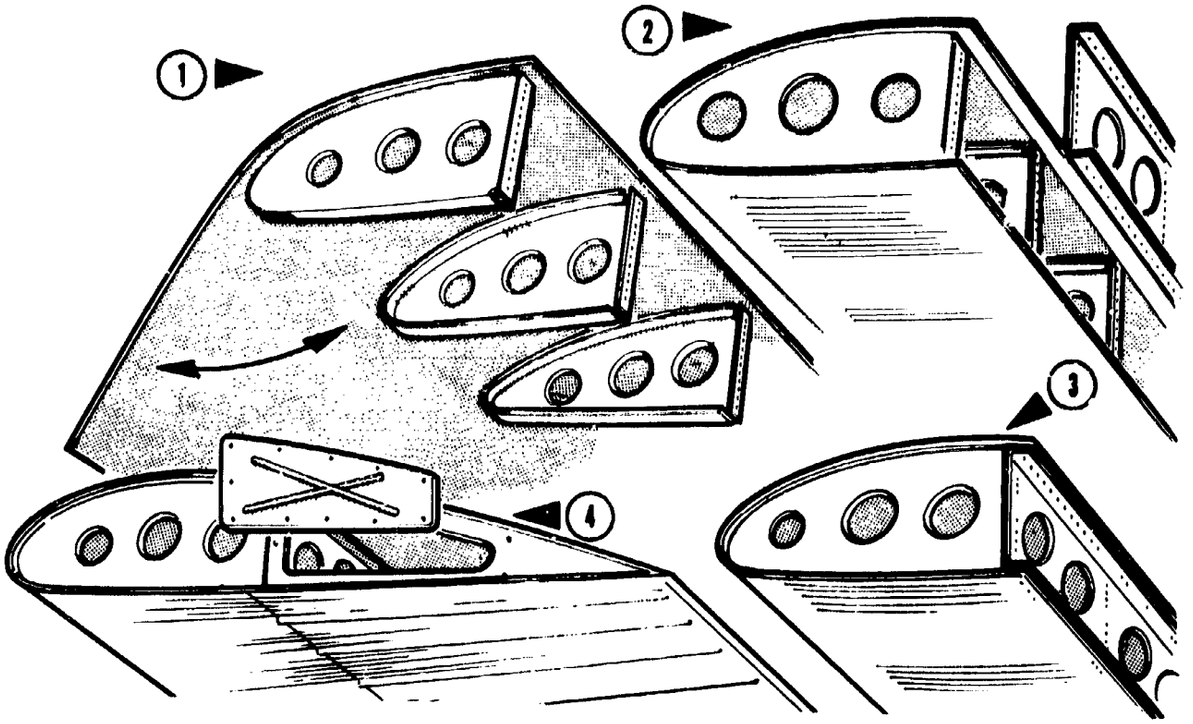


Figure 138

TABLE XXV

ALLOWABLE ULTIMATE SHEAR STRENGTHS OF SINGLE SPOTWELDS (ALUMINUM ALLOYS)
(Pounds per Spotweld)

Sheet Thickness (inches)	Aluminum Alloys, Clad or Bare Ultimate Tensile Strength of Material - psi			
	Below 19,500	19,500-27,999	28,000-55,999	56,000 & Above
	3003-0	3003-H14 5052-0	6061-T4 6061-T6	2024-All Tempers 7075-T6 7178-T6
0.012	16	24	52	60
0.016	40	56	80	88
0.020	64	80	108	112
0.025	88	116	140	148
0.032	132	168	188	208
0.040	180	240	248	276
0.050	236	320	344	372

Due to the anticipated light loadings involved with this type of aircraft, the joint strengths would be based primarily on the shear strengths of the spotwelds.

Seam welding: Identical to spotwelding, except for the use of power-driven rollers as electrodes. A continuous airtight weld can be obtained at the rate of two to seven feet per minute by this method.

Some advantages of electric resistance spot and seam welding:

(1) Spotwelding is faster than riveting because no layout and drilling of holes are necessary. Numerous spotwelds can also be made in the time required to insert and head one rivet.

(2) Spot and seam welding do not add weight to the structure.

(3) Seam-welded watertight joints do not require the insertion of tape and a sealing compound. Weight and expense are saved.

(4) The drag of rivet heads is eliminated on exterior surfaces.

Butt welding: Butt welding is applicable to almost all metals. The work to be welded is clamped in large copper jaws also serving as electrodes. One of the jaws is movable. At the proper time, pressure is applied to the movable jaw to bring the work in contact. When the electric current is applied after the parts are pressed together it is called upset butt welding. In flash welding the edges are brought close enough together to start arcing, and when they reach fusion temperature, the current is turned off and pressure is applied. All wrought alloys of solid cross-section up to about 0.5 square inch in cross-sectional area can be upset butt welded. Square-cut abutting surfaces, free of lubricant, are required for optimum welding results. Shearing or sawing the ends just before welding is adequate preparation,

Arc welding: Arc welding is based on the heat generated in an electric arc. Variations in this process are metallic arc welding, carbon arc welding, atomic-hydrogen welding, inert-arc welding (heliarc), and multiarc welding.

Arc welding to a limited extent has been used for many years in aircraft fabrication. Probably the flexibility and general all-around good results obtained with gas welding retarded its extensive use; however, in recent years, its use is increasing rapidly as its economics and advantages become more apparent. In arc welding, the applied heat is more concentrated, resulting in a quicker welding with less expansion and warping as compared to gas welding. This makes it possible to hold closer tolerances on parts requiring machining after welding. An allowance of 1/16 inch is usually sufficient for most assemblies.

By using the heliarc (inert-arc) welding process, satisfactory welds may be made with aluminum, and if argon is used for a shielding gas, no flux is

required. Dispensing with flux is a definite advantage because flux removal from aluminum welded joints is extremely important to avoid corrosion. Many types of welded joints cannot be made when using welding methods requiring fluxing. Corrosion-resisting steel as thin as 0.010 inch can be welded by this process. Steel, copper, and many alloys can be readily welded by this process.

Parent material weld allowables: Allowable ultimate tensile stress in alloy steels for material adjacent to the weld, when structure is welded after heat treatment, is shown in Table XXVI.

TABLE XXVI

ALLOWABLE ULTIMATE TENSILE STRESSES NEAR FUSION WELDS IN 4130, 4140, 4340, OR 8630 STEELS

Section thickness 1/4 inch or Less	
Type of Joint	F_{tu} (ksi)
tapered joints of 30° or less	90
all others	80

For alloy steel members subjected to bending, the allowable modulus of rupture when welded after heat treatment should not exceed the F_b equivalent to that for steel having a F_{tu} = 90,000 psi.

Strength of Weld Metal:(Welding Rods). Table XXVII indicates allowable weld metal strengths for various steels. These are based on 85 percent of respective minimum tensile ultimate test values.

TABLE XXVII

WELD METAL STRENGTHS FOR WELDED JOINTS (Welding Rods)

Material	Heat Treatment After Welding	F_{su} ksi	F_{tu} ksi
Carbon and alloy steels	none	32	51
Alloy steels	none	32	51
Alloy steels	stress relieved	43	72
Alloy steels	stress relieved	50	85
Steels	quench & temper	60	100
4130	125 ksi	63	105
4140	150 ksi	75	125
4340	180 ksi	90	150

Welding Considerations: There are many general considerations all designers should be familiar with in designing welded joints. The following apply particularly to arc welding.

(1) Straight tension welds should be avoided because of their weakening effect. When a weld must be in tension, a fishmouth joint or finger-patch should be used to increase the length of the weld and to put part of it in shear.

(2) A weld should never be made all around a tube in the same plane. A fishmouth weld should be made. This situation arises frequently when attaching an end fitting to a strut.

(3) Two welds should not be placed close together in thin material. Cracks will result because of the lack of metal to absorb shrinkage stresses.

(4) Welds should not be made on both sides of a thin sheet.

(5) Welds should not be made along bends, or cracks will develop in service.

(6) Welded reinforcements should never end abruptly. The sudden change of section will result in failures by cracking when in service.

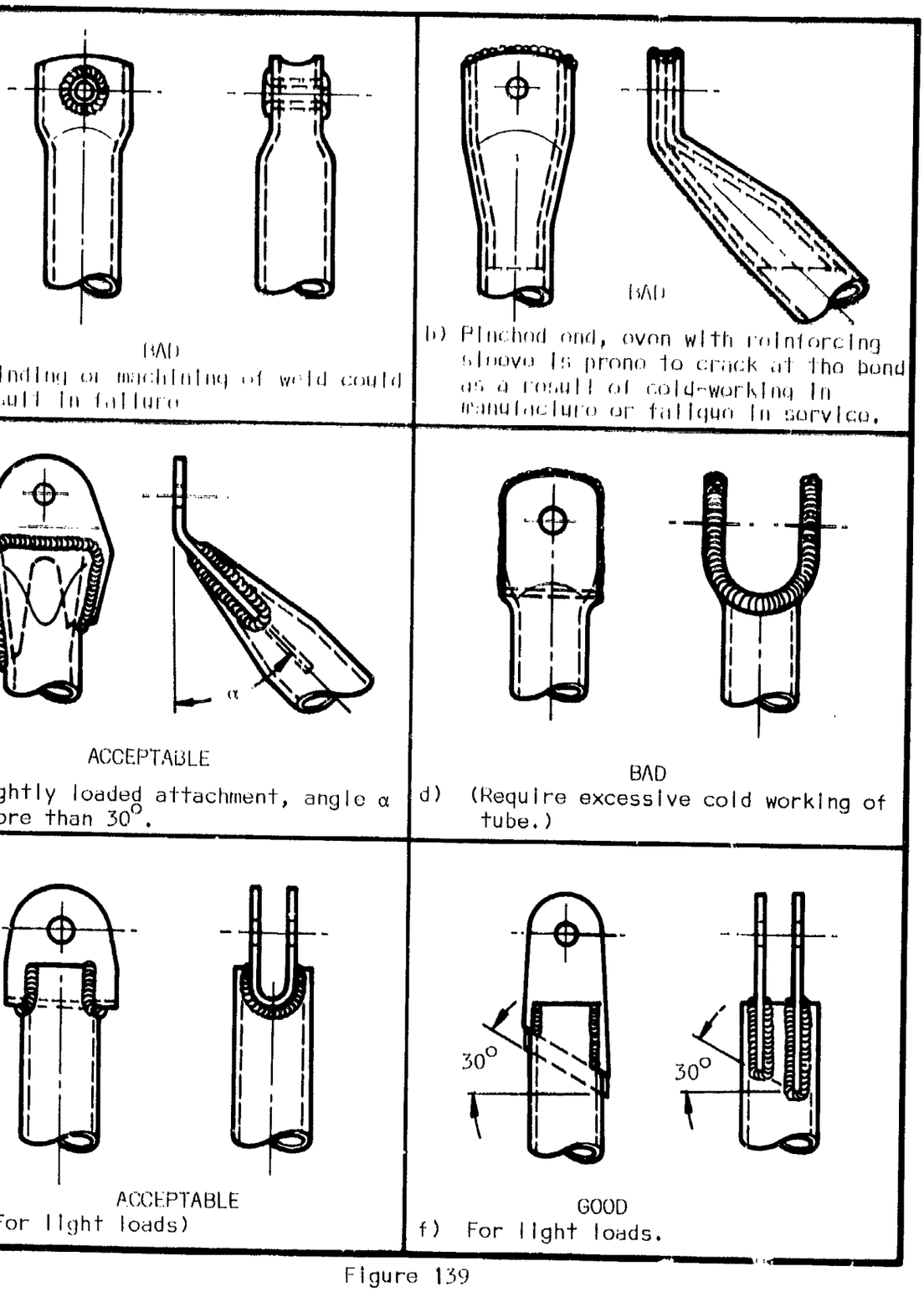
(7) Aircraft bolts should never be welded in place unless they are made of weldable material and are going to be welded to a similar metal. Furthermore, welding will destroy the heat-treated condition of the bolt. This has to be considered in the design/analysis. The same comments are valid for aircraft nuts. However, when required, tack welding in three places is usually all that is necessary to position them.

(8) When possible, welded parts should be normalized or heat treated after completion, to refine the grain and relieve internal stresses caused by shrinkage.

If welded parts are not normalized they could develop cracks in service, particularly if subjected to vibrational stresses. This is because weld material is cast metal lacking the strength, ductility, or shock resistance of wrought metal. The internal stresses are also seeking to adjust themselves. Sharp bends or corners, or rapid changes of section in the vicinity of welds are especially liable to cracking.

In the design of tubular joints, care should be taken to make all welds accessible. Figure 139 illustrates industry accepted design practices. These configurations provide proper stress distributions through the joints and should be followed as much as possible.

DESIGN PRACTICES FOR WELDED TUBULAR JOINTS



BAD

a) Grinding or machining of weld could result in failure

BAD

b) Pinched end, even with reinforcing sleeve is prone to crack at the bend as a result of cold-working in manufacture or fatigue in service.

ACCEPTABLE

c) Lightly loaded attachment, angle α not more than 30°.

BAD

d) (Require excessive cold working of tube.)

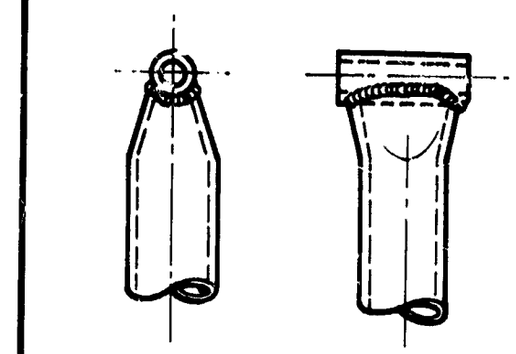
ACCEPTABLE

e) (For light loads)

GOOD

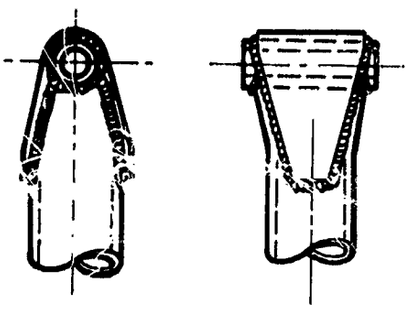
f) For light loads.

Figure 139



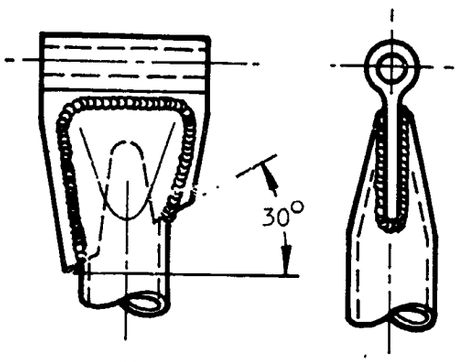
LIGHT LOADS

g) (Not very strong in compression due to crushing under spacer tube).



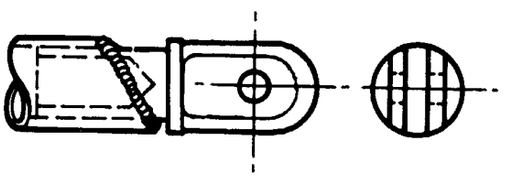
LIGHT LOADS

h) (This is an improvement on "g" Provide enough material on bushing to avoid machining of weld).



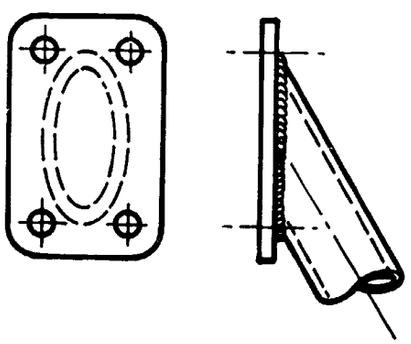
HEAVY LOADS

i) Stagger termination of welds at opposite sides of tube.

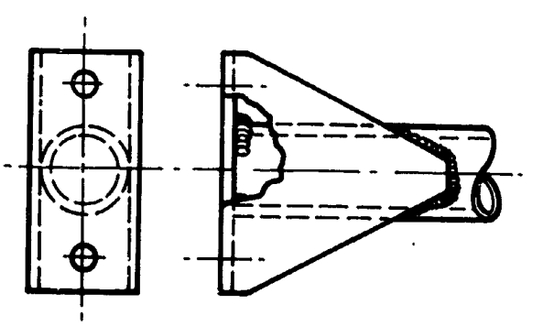


ACCEPTABLE

j) Welding of standard clevis

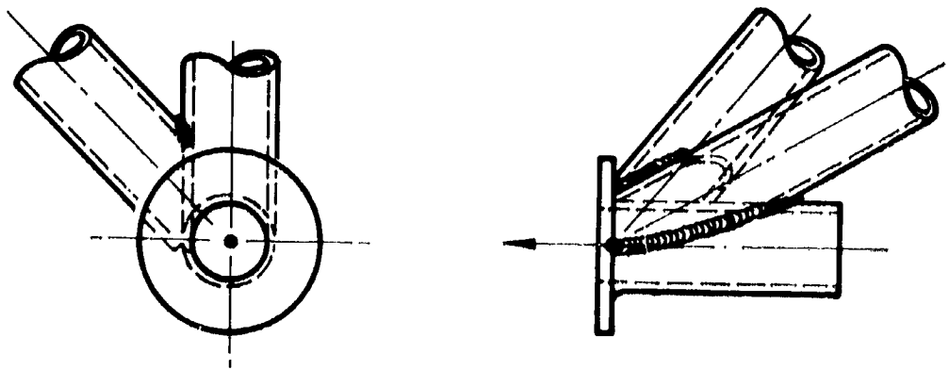


k) Satisfactory for a fixed end attachment



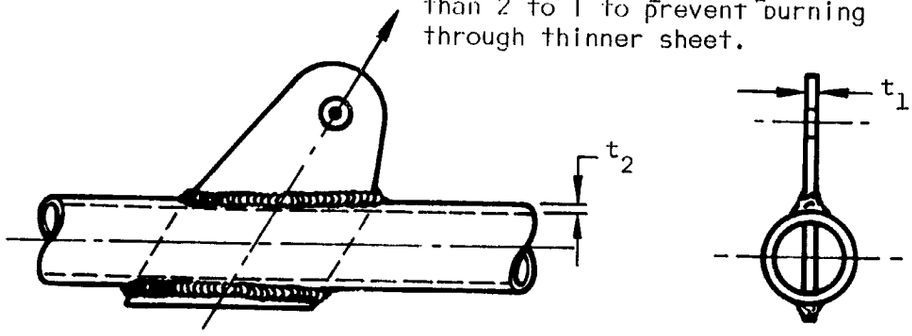
l) Satisfactory for a fixed end attachment

Figure 139-Continued.



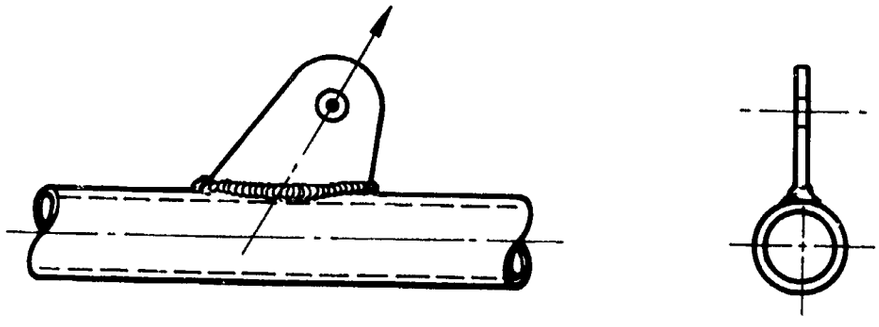
m) Minimize eccentricity between tube center lines and loads.

Note: applicable to any weldment: Keep thickness ratio between two welded parts (t_1 and t_2) less than 2 to 1 to prevent burning through thinner sheet.



HEAVY LOADS

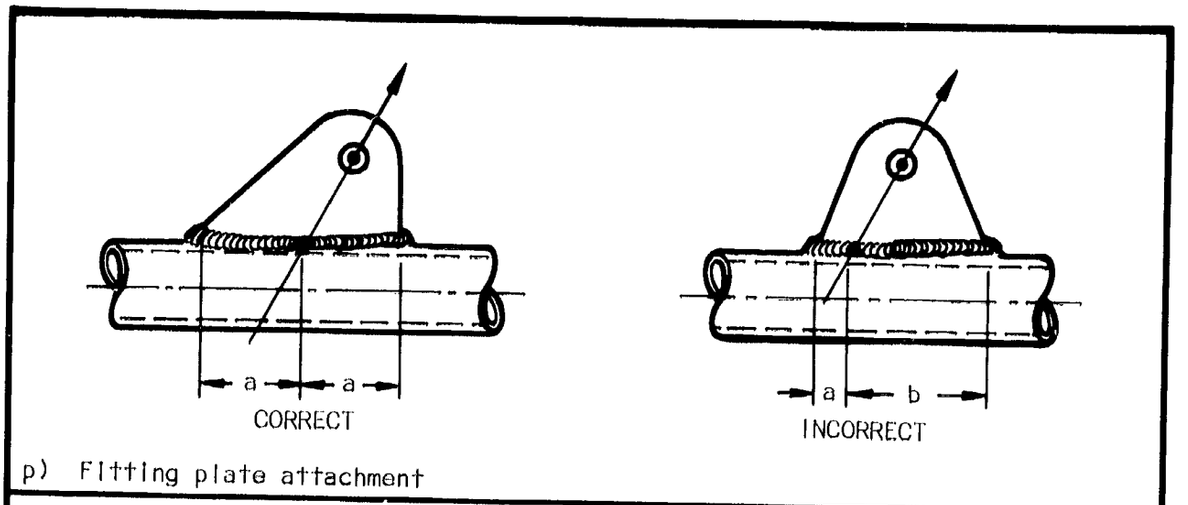
n) Fitting plate attachment.



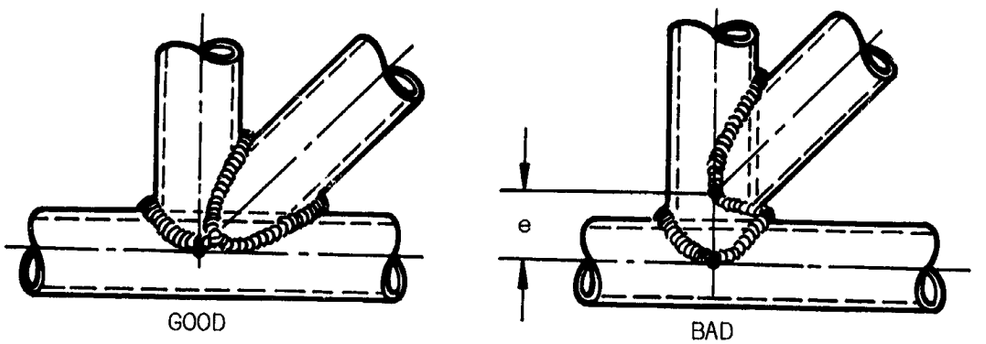
LIGHT LOADS

o) Fitting plate attachment.

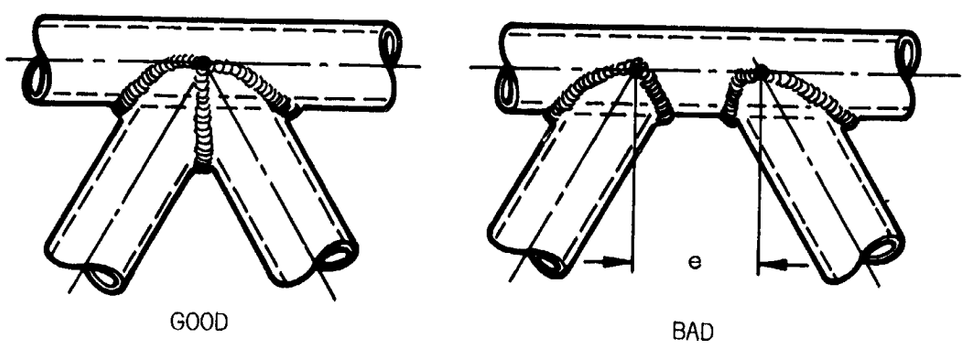
Figure 139-Continued.



p) Fitting plate attachment



q) Tube Cluster - (Keep eccentricities to minimum)



r) Tube Cluster - (Keep eccentricities to minimum)

Figure 139 -Continued.

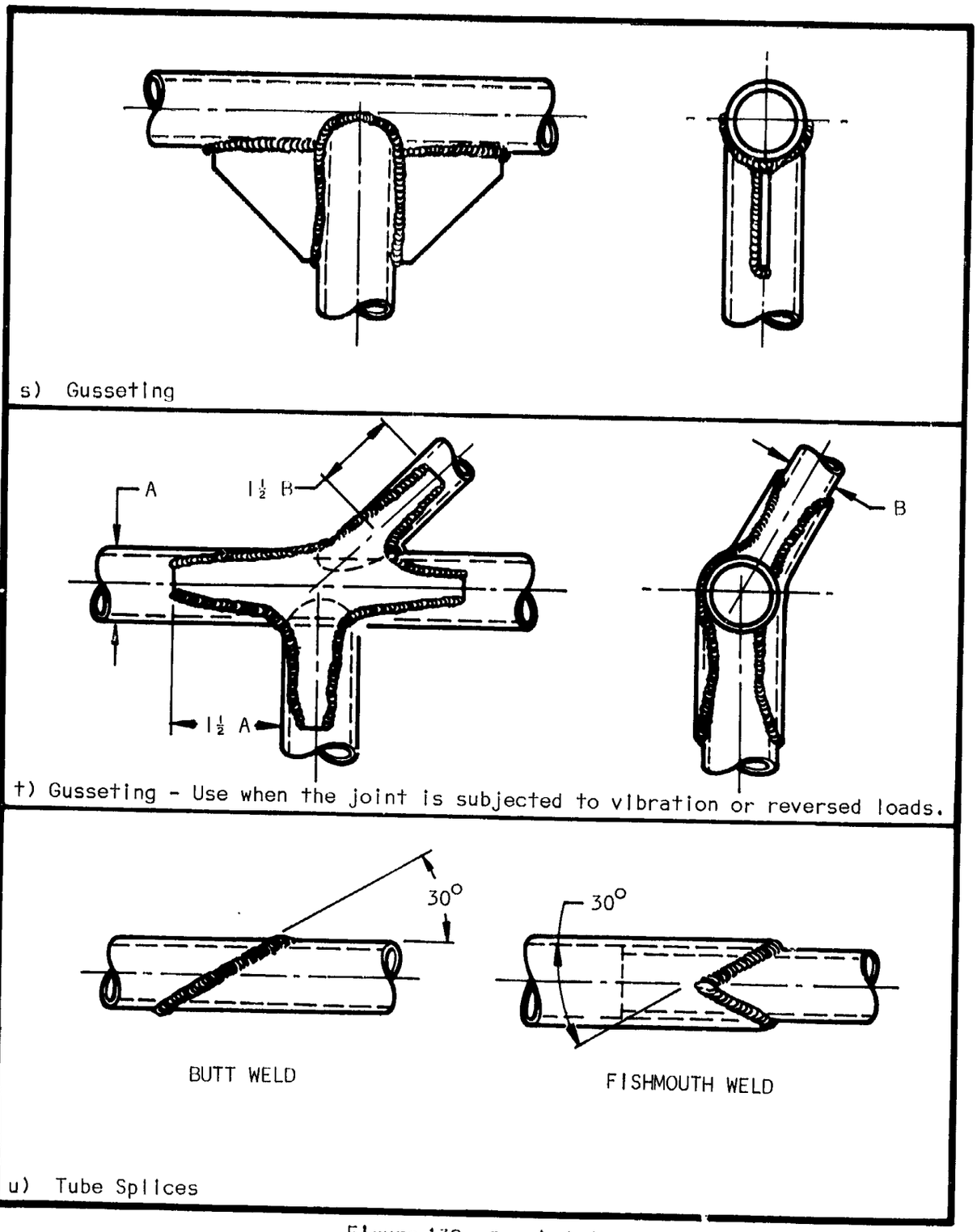


Figure 139 -Concluded.

Brazing: Brazing is a method of metal joining, using a filler metal having a melting temperature less than the parent material being joined. Brazing is primarily used for joining assemblies for use at normal atmospheric or slightly elevated temperatures because the usual brazing alloys are compositions which soften readily at relatively moderate temperatures. Brazing is distinguished from soldering by the melting point of the filler metal (filler metal for soldering has a much lower melting point), and differs from welding in that no substantial amount of the base metal is melted. Thus, the temperatures for brazing are intermediate between those for welding and soldering. The strength and corrosion resistance characteristics of a brazed assembly also generally fall between those of welded and soldered assemblies.

Brazing aluminum: Nonheat-treatable wrought alloys brazed most successfully are the 1xxx and 3xxx series, and the low-magnesium 5xxx series. Alloys containing a higher magnesium content are more difficult to braze by the usual flux methods, because of poor wetting by filler metal and excessive penetration. Filler metals are available that melt below the melting temperature of all commercial-wrought nonheat-treatable alloys.

Of the heat-treatable alloys, those most commonly brazed are the 6xxx series. The 2xxx series may be brazed quite satisfactorily; however, the 7xxx series is low melting and, therefore, not normally brazeable, with the exception of 7075 and x7005.

Material Combinations - Aluminum

(1) It is desirable from a production standpoint to design assemblies in their entirety from 2xxx or 3xxx alloys, or combinations of these two materials.

(2) Combinations of alloys (2xxx to 61xx, 2xxx to 53xx, etc.) are difficult to braze and should be avoided.

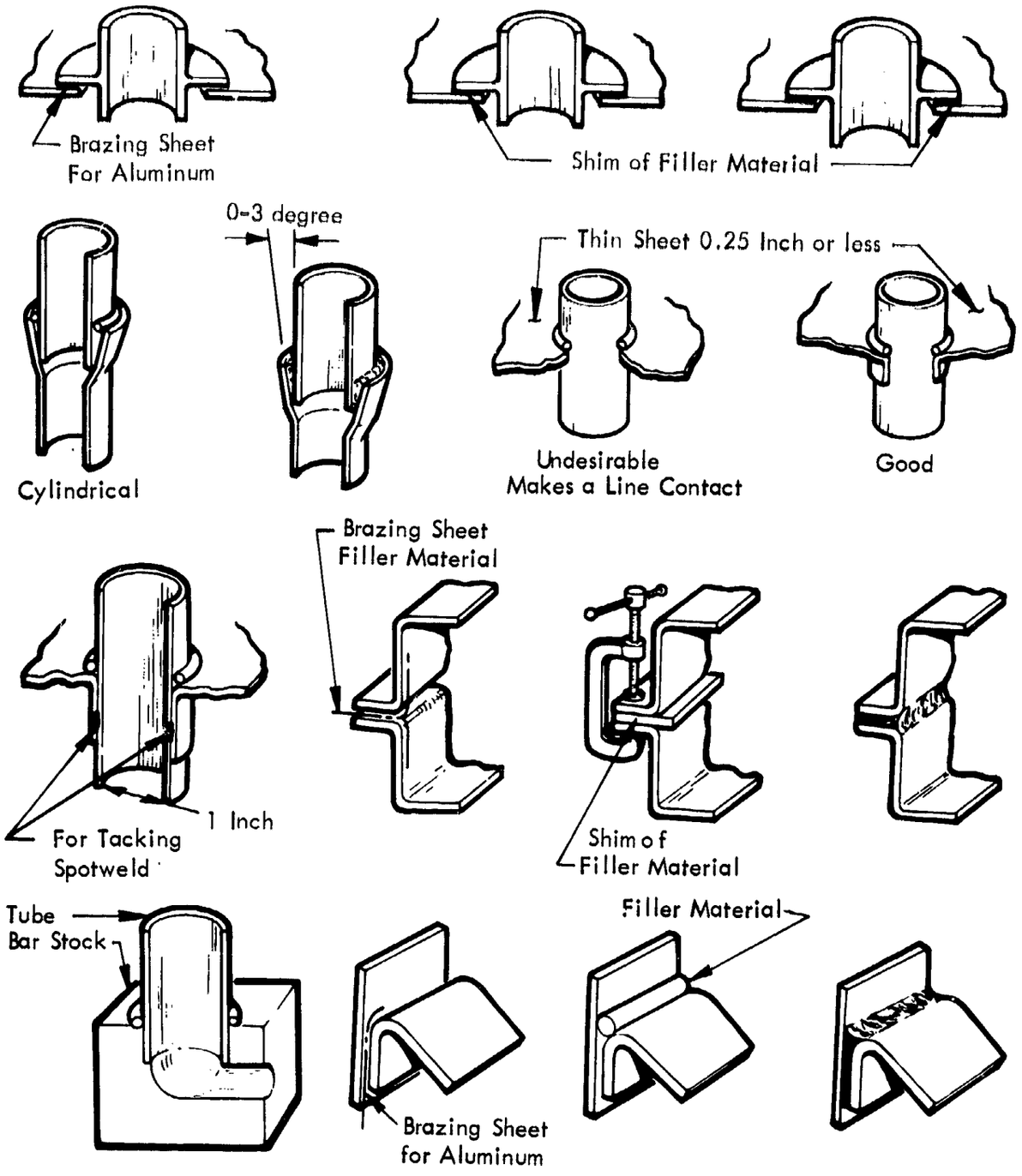
(3) Combinations of 61xx or 53xx to 61xx are satisfactory.

(4) Brazing sheets must be used in combination with 2xxx or 3xxx alloys only.

Brazing sheets should be used where a large number of joints are necessary in flat or formed sections of sheet; or possibly for ducts, tanks, or other assemblies where it would be difficult to secure wire or other forms of filler material adjacent to the joints. This material would also be used in an area requiring brazing in a position other than one allowing gravity flow of the filler material. Typical examples of brazed joints are shown in Figure 140.

Brazing steel: Joining steel parts into single units may be done by brazing with copper or silver alloys.

TYPICAL EXAMPLES OF BRAZING



Duct and Tank Applications

Figure 140

When copper alloys are used, brazing is performed within a furnace (copper furnace brazing), having a controlled heat of 2050°F. This is above the melting point of copper (1985°F); therefore this may be accomplished by induction, torch, resistance, furnace, or dip methods.

The selection of the brazing method depends upon the materials involved, the shape and size of the parts, whether heat treatment after brazing is required, the number of parts, etc.

Materials for brazing steel: Most steels may be brazed by either method; however, corrosion-resistant steel may not be copper-furnace brazed. Only the stabilized grades of 18-8 stainless steel (321 and 347) can be silver brazed as the temperatures involved impair the corrosion resistance of the unstabilized grades (302 and 303). The physical properties of heat-treated and cold-worked materials are reduced by the temperatures required for brazing.

Heat treatment may be performed on copper-furnace-brazed assemblies; however, due to the low melting point of the silver alloys, it is not possible to heat treat steel assemblies after silver brazing has been performed.

Fusion welding after brazing is normally prohibited within three inches of a brazed joint.

The same general design guide illustrated for various joints in Figure 73 should also be used for steel materials.

Allowable stresses: F_{su} = allowable ultimate shear stress for the brazed area = 15000 psi (this applies to all conditions of heat treatment for all applicable materials).

Because of decarburation occurring during brazing, the strength of the parent material in most cases is reduced as follows:

TABLE XXVIII
EFFECT OF BRAZING ON ALLOWABLE STRENGTH

Material	Allowable Strength
heat-treated material including normalized used in as-brazed condition	mechanical properties of normalized material
heat-treated material (including normalized) reheat-treated during or after brazing	mechanical properties corresponding to heat treatment performed

Advantages of brazing:

(1) parts too thin to weld may often be brazed.

(2) heavy sections may be joined to thin sheets.

(3) warpage and distortion are reduced.

(4) brazed joints are vacuum tight.

Disadvantages of brazing:

(1) assemblies made of 2xxx and 3xxx aluminum alloys are fully annealed during brazing, and cannot be restored to the original hardness; steels must be heat treated again to obtain original strengths.

(2) series 53xx and 61xx aluminum alloys must be heat treated and artificially aged after brazing to obtain the condition required.

(3) brazed assemblies cannot be put into the furnace for a second brazing unless there is a filler material with a lower melting point than used in the previous brazing.

(4) resistance to corrosion of aluminum alloys generally is not impaired by brazing; however, if flux is not completely removed, the residue will cause corrosion (interdendritic attack on the fillets, and intergranular attack on the base metal); if flux is not removed, it causes rapid pitting in the presence of moisture.

(5) when two aluminum alloys are brazed together, exposure to salt water or some other electrolyte may result in attack on the more anodic part; this condition is aggravated if the anodic part is relatively small compared to the other piece.

(6) furnace brazing causes a certain amount of diffusion of a clad surface reducing its corrosion resistance; Brazing Sheet No. 100 must be used for such applications (filler metal on one side and a special alclad alloy on the other side).

Applications of brazing:

(1) Controls and mechanisms for:

(a) accessories.

(b) electrical system.

(c) fuel and oil system.

(d) heating, ventilating, and de-icing systems.

(e) power plant controls.

(f) hydraulic equipment.

(2) Supports and attachments for:

(a) accessories, instruments, radio, etc.

(b) antenna masts and housings.

(c) pitot masts.

(d) landing gear doors or entrance doors.

(3) Miscellaneous.

(a) landing gear up-lock systems.

(b) handles (assist, door, pump, seat adjustment, etc.)

Bonding: Many times, adhesives are called the modern tool for joining assemblies; however, the only modern aspect is that bonding agents have been greatly improved. There is much historical precedent associated with this technique back to the era when wood aircraft structure was first glued together. The old Mosquito bomber of the early 1940's used plywood wings bonded with wood glue.

Although much research was conducted prior to 1940, the initial successful adhesives were not developed until the early 1940's. A group of phenolic resin-synthetic rubber hybrids were developed by one United States automobile manufactuer which maintained high strength over a wide range of temperatures. About this same time an adhesive manufacturing company in England was experiencing success with an adhesive formulation based on a phenolic resin-polyvinyl combination.

The American developed adhesives were single component systems which could be easily applied with simple tools (brush, roller, etc.), whereas the British system was a more sophisticated two-part system. With this process, it was necessary first to apply a liquied phenolic resin to the adherends,followed by a layer of powder over the liquid film. The powder, a polyvinyl formal, developed the necessary toughness or elasticity in the bonded joint, while the phenolic resin provided the proper adhesion characteristics.

Due to the apparent simplicity in applying the single-component system, further development of these adhesives were more closely followed in the United States and abroad.

Coincidental with the development of these newer adhesives, the airplane was playing a major role in the fighting of World War II. The aircraft industry was, therefore, desperately in search of unique manufacturing techniques to save weight or provide smoother airfoil surfaces. This urgency led to the immediate acceptance of adhesive bonding for use in aircraft structure. In the United States, the government approved the single component adhesive system as an aircraft structural bonding agent while England began utilizing the double component system for joining metal to wood in the De Havilland Hornet.

Within a few years, vinyl-phenolic bonded-sandwich structures became more predominant for use in wing panels and fuselage sections of the B-57 and Matador missile. By the mid 1950's, structural adhesive bonding was used extensively in the manufacturing of the B-58. Since then, new epoxy adhesive systems have been used more consistently and more daringly. Bonding of aluminum to itself, and to other metals and non-metals, has become common practice. Because of the great potential in weight reduction, the major technical effort to develop reliable adhesive bonding data has been restricted to aluminum alloys used in aircraft such as bare and alclad 2020-T6, 2024-T3, T6, T86, and 7075-T6.

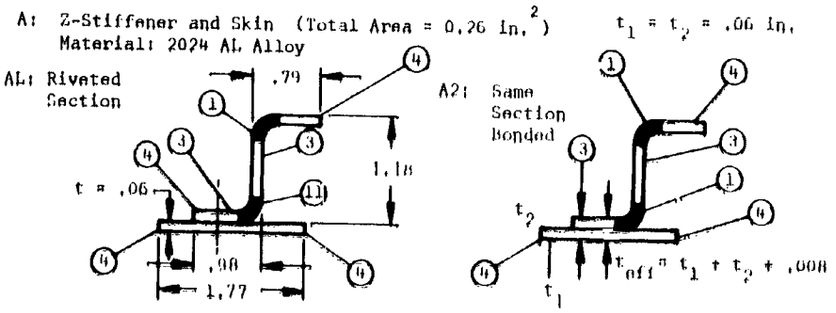
A dramatic example in present-day application of adhesive bonding is the supersonic F-111 fighter-bomber. Most of the entire exterior skin is an adhesive-bonded honeycomb-sandwich structure. Another prime example of complex bonded structures being made today is associated with helicopter rotor blades. The Bell Helicopter (model UH-1D) uses an adhesive to bond an aluminum honeycomb core and doublers to the main spar, a brass nose bar, and a stainless-steel leading edge. This 22-foot long all-bonded assembly is cured at 120 psi and 350 degrees F.

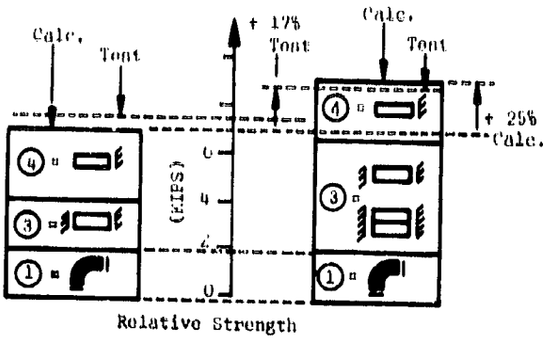
It is apparent that adhesive bonding has a definite place in the aircraft industry. The crippling strength of compression panels is significantly improved due to the integral stiffening effect of the bonded laminates (ref. Fig.141).

The fatigue strength of compression panels is increased thru the use of good bonded design. Figure 142 compares three configurations and reveals that the one with insufficient skin width to stringer bond is inferior to the riveted configuration beyond 10^4 load cycles thus demonstrating the importance of proper bonded design.

Fatigue strength comparisons of Redux bonded single and double lap joints with a riveted joint are made in Figure 143. Here again, the superiority of well designed bonded joints is evident. Results of box beam fatigue tests involving riveted, bonded, and integrally stiffened construction are presented in Figure 144. The advantage gained by using scarf joints in lieu of lap joints is shown in Figure 145 where the S-N curves for both configurations are plotted.

COMPARISON OF CRIPPLING STRENGTH OF BONDED AND RIVETED BUILT-UP COMPRESSION ELEMENTS

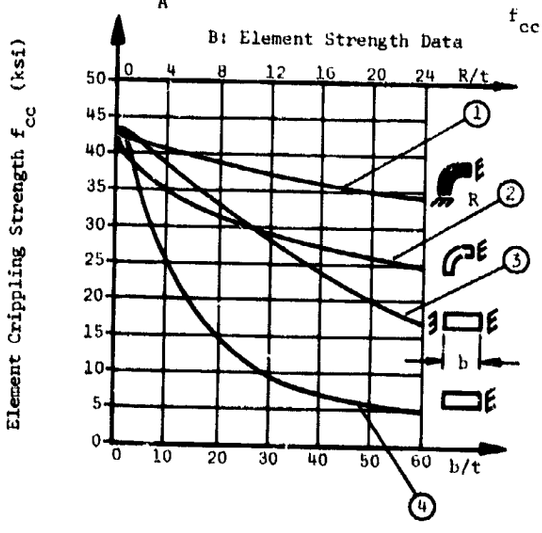




Calculation of Crippling Strength

$$f_{cc} = \frac{\sum_{1}^{n} a \cdot (f_{cc})}{A}$$

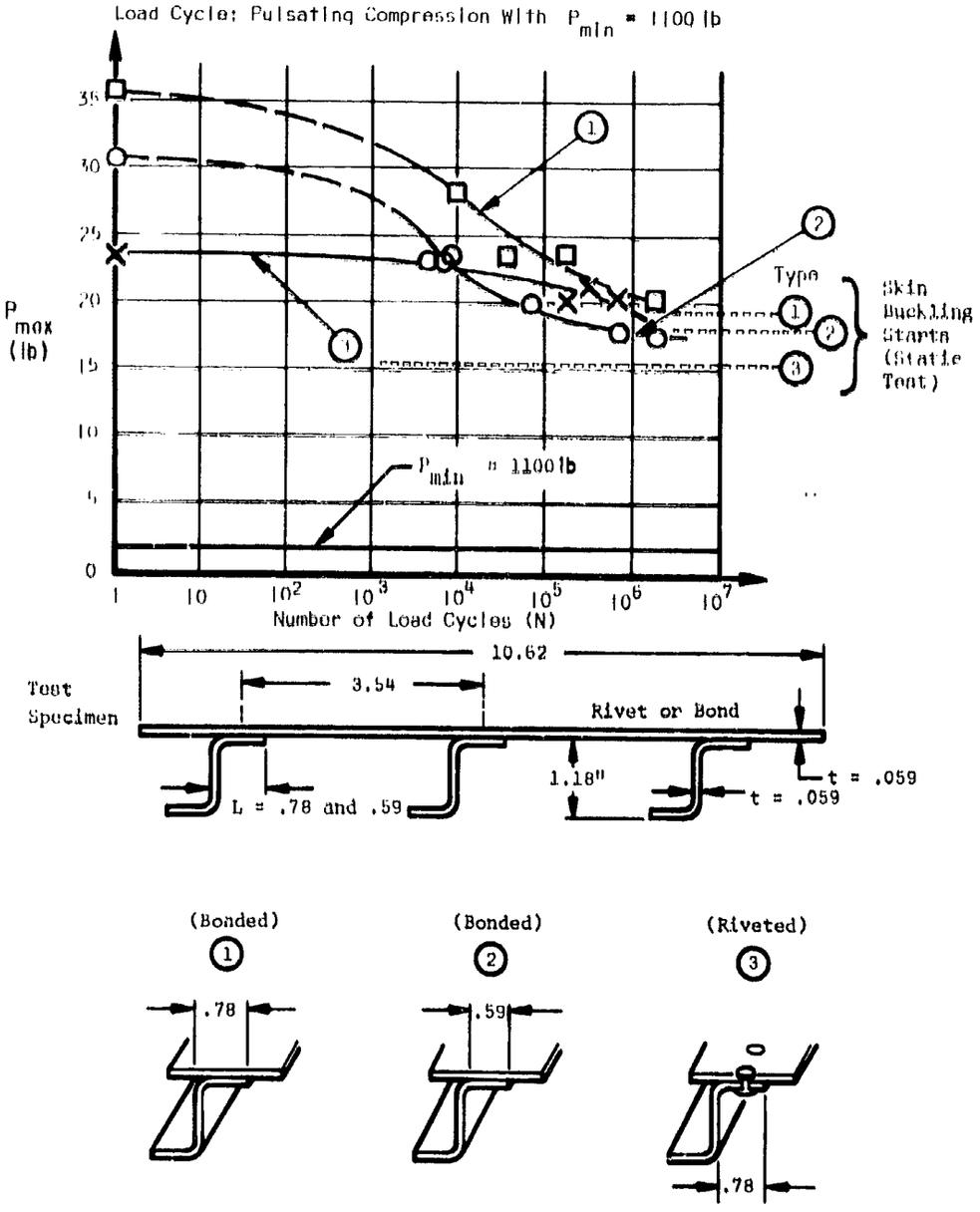
Where: a = Area of individual elements
A = Total area of section
f_{cc} = Crippling stress of elements according to above curves.



Data Extracted from Article Written by L. Jungstrom; Design Aspects of Bonded Structures; Bonded Aircraft Structures Published by C.I.B.A. (A.R.L.) Limited; 1957

Figure 141

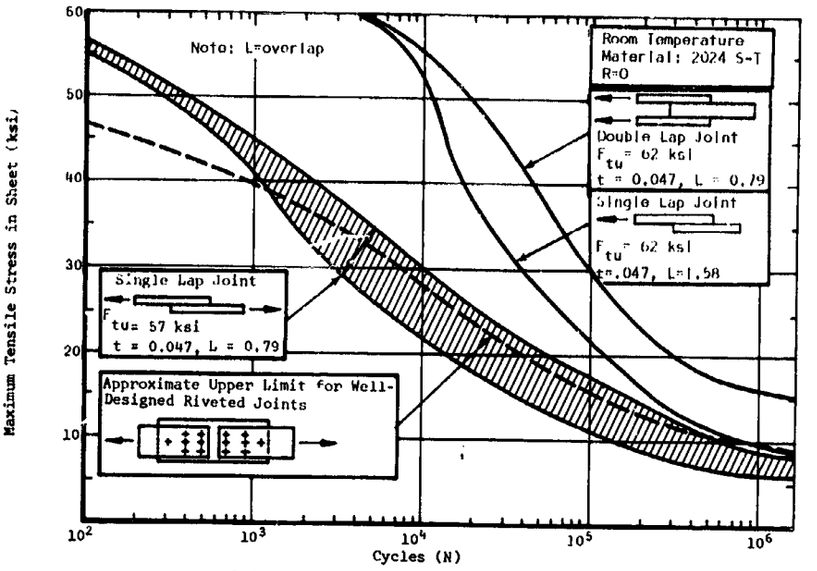
EFFECT OF WIDTH OF SKIN TO STRINGER BOND ON
FATIGUE STRENGTH OF COMPRESSION PANELS



Data Extracted from Article Written by O.L. Jungstrom;
Design Aspects of Bonded Structures; Bonded Aircraft
Structures Published by C.I.B.A. (A.R.L.) Limited 1957

Figure 142

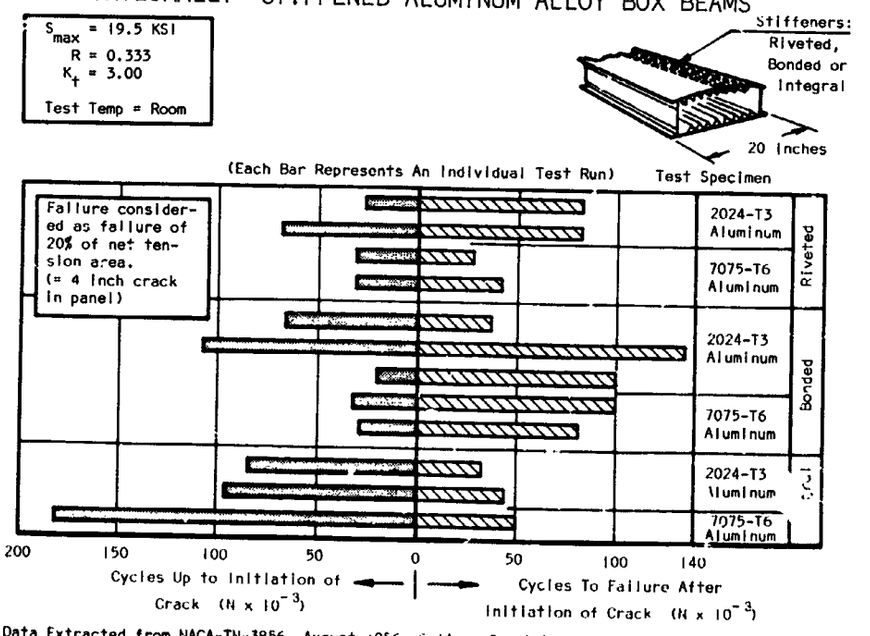
COMPARISON OF FATIGUE STRENGTH OF BONDED
SINGLE- AND DOUBLE-LAP JOINTS WITH A RIVETED JOINT



Data taken from: FFA Report HU-226 and FFA Mudd. No 30

Figure 143

COMPARISON OF RIVETED, BONDED, AND
INTEGRALLY- STIFFENED ALUMINUM ALLOY BOX BEAMS



Data Extracted from NACA-TN-3856, August 1956; Fatigue Crack Propagation In Aluminum-Alloy Box Beams

Figure 144

COMPARISON OF FATIGUE STRENGTH OF A SIMPLE LAP JOINT AND A SCARF JOINT

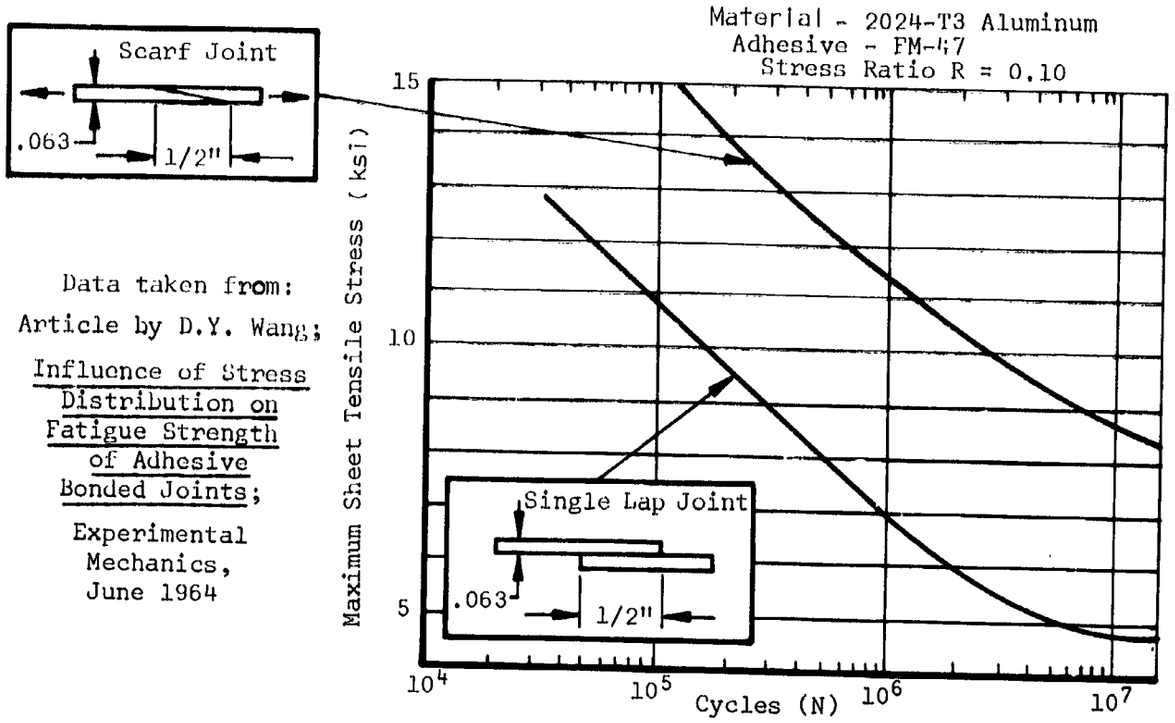


Figure 145

Higher strength-to-weight ratios are possible with sandwich materials. Often it is the only way to join thin-gage sheets; the adhesive bond can double as a seal; dissimilar metals can be fastened without corrosion effects and irregular shapes or complex sections can be fastened comparatively easily. Helicopters, for example, because of vibration, require the damping provisions provided by the nitrile rubber-epoxy adhesive system. Table XXIX lists the many advantages as well as the limitations occurring through the use of bonded structures.

General design and production philosophy for bonded structures:

(1) Know the materials (test data).

(2) Structures should be properly designed for the use of adhesives.

(3) Use appropriate prebond treatments, tightly written instructions, and permit no deviations.

(4) Insist that the recommended process or specifications be rigidly adheared to when:

(a) Applying and curing the adhesive.

(b) Handling, fitting, and jigging of the parts.

(5) Train personnel to understand the importance of good workmanship and its influence on joint strength and life.

(6) Set up a quality-control system to maintain a high standard of reliability. Destructive test specimens should be frequently processed concurrently with production bonds.

Initial strength of a joint does not constitute a good reliable bond which will satisfy its intended service life. The adherend surface preparation is an important prerequisite in the permanence of joints subjected to simultaneous stress and adverse environment. Joints made with poorly prepared adherends may exhibit the same initial breaking strength as those made with adherends having undergone an elaborate chemical cleaning process. The bonds made with the minimum surface treatment, however, will prove inferior with respect to permanence. Elaborate metal-cleaning procedures might be alleviated by using a pre-priming operation incorporated in the material production line at the mill. This method is already used by a honeycomb panel manufacturer in the United States. A primer is applied to both surfaces of sanwich facing material, accomplishing the following:

(1) provides proper substrate for primary honeycomb bonding

(2) maintains clean surface for a later secondary bond if necessary

(3) primer acts as an additional corrosion-resistant barrier to all exposed surfaces of the adherend whether or not a secondary bond is made

This process could easily be incorporated as an additional step at the mill; however, the basic material cost could increase as much as 20 percent.

Repairs for bonded construction: Repairs to damaged panels and surfaces might be necessary either during production or after they are in service for some time. Consequently, effective repair methods must be developed to maintain the original contour, insure structural integrity, and prevent damage propagation.

Repairability requires: (1) the damaged part, dependent upon the extent of the damages, must be removable, if necessary, by some means that will leave the remaining parts undamaged; (2) the damaged part must be capable of being repaired, using mechanical fasteners, adhesive bonding, or a combination of both, without loss of properties to the remaining bonds.

Quite often repairs are made with materials differing from the material of the damaged structure. Therefore, a repair adhesive must be capable of

satisfactorily bonding a variety of materials, preferably under the same conditions of temperature and pressure. Another requirement for any repair adhesive must be that it displays an apparent forgiveness for less efficient cleaning methods in the field as compared to those used in the initial manufacture of the part. Regardless of whether the damaged assembly was made with a combined riveting and bonding technique, or by bonding alone, a repair can usually be made by using follow-up pressure-type mechanical fasteners. Another means of pressure application would be fabricated-in-place vacuum-bag blankets with portable vacuum pumps.

The following summarizes the main requirements of a repair adhesive:

(1) Since ovens, autoclaves, and special equipment will not be available at most field facilities, the repair adhesive must satisfactorily cure at near room temperature.

(2) It must also be capable of easy application within the temperature range of 40 to 100 degrees F.

(3) It must give good bond strength initially and after environmental exposure, for materials cleaned by methods not yielding the best possible surfaces for bonding.

(4) The effects of repeated cure on the original bond must not affect its integrity.

(5) It must withstand exposure to cleaning fluids used in service operations.

(6) It should have a good shelf life (at least 3 months), remain acceptable through a wide range of storage conditions, have at least 2 hours, and preferably 10 hours, of open assembly time.

TABLE XXIX

ADVANTAGES AND LIMITATIONS OF BONDING

DESIGN FACTOR	ADHESIVE BONDING ADVANTAGES	LIMITATIONS
Aerodynamic Smoothness	Smooth exterior contours greatly improved.	
Cost	Savings achieved through bonding of large assemblies which have been properly designed for bonding or by weight savings.	Special tools and facilities are required for contoured parts.
Corrosion of Dissimilar Material Joints	Versatility of joining dissimilar materials is greatly improved. Corrosion in faying surfaces is reduced. Metals may be readily joined to non-metallics.	Differential coefficient of expansion must be considered due to the build-up of residual stresses.
Stress Concentration	More uniform distribution of stress through a bonded joint along entire length. Greatly reduces stress concentration.	Residual stresses may be induced during heat cure.
Fatigue Resistance	Great improvement--10 to 1 over rivets. Reduces crack propagation.	
Static Strength	Adhesives exhibit high strengths when stressed in shear. The more efficient adhesives either approach or surpass the sheet metal strength at an L/t ratio between 20 and 30. L = Lap length; t = adherend thickness.	Production adhesives are generally limited to 350°F.
Design Factor Weight and Size	Reduction of weight and size may be obtained. Greater capability for joining thin or brittle materials. In properly designed bonded structures, the following weight savings could be achieved over riveted structures: (1) Compression members: up to 25 percent (2) Tension members: 10 to 15 percent (3) Tension members designed by fatigue criteria: up to 20 percent (4) Some miscellaneous weight may be saved by eliminating the necessary local reinforcements usually required with conventional fasteners. NOTE: A typical overall weight savings for civil aircraft is 3 to 6 percent of the total structure weight	
Production	Many details may be eliminated which simplifies the overall design. Large areas may be bonded in a single operation.	A close tolerance between mating parts is essential. Special skills and personnel training are usually required.
Inspection	Non-destructive test techniques are available to insure good reliability.	Extensive quality control must be exercised, since the strength level of bonded joints may not be fully determined through non-destructive testing.
Sealing	Internal fuel cells and pressurized cabins are automatically sealed when bonded.	Bacteria growth in fuel may attack the adhesive. Components may require additional protective coating in these areas.
Electrical Insulation	Excellent.	Jumpers are mandatory for electrical continuity.
Miscellaneous	Compared to welding, thermal damage to parent metals is greatly reduced. Field repair is easily performed.	Proper surface preparation is mandatory for good quality bonds. Work areas for bonding must maintain a high standard of cleanliness.
Experience	Adhesives have been successfully used on military and commercial aircraft for over 10 years.	

PHASE II - APPLICATION OF MATERIALS AND CONCEPTS

In this section, several appropriate and previously listed potential materials will be applied to a conceptual, but typical, light airplane. These same material selections and applications would be applicable for other airplanes of similar structural loading magnitudes and manufacturing quantities; but the light airplane designer is not restricted to these same selections. The following discussions will make apparent the inter-relationship of such considerations as performance and configuration specifications, weight, cost, production rate, and manufacturing method.

Airplane Configuration

Study Guidelines.- The Mission Analysis Division of NASA, established the guidelines for the design of a typical General Aviation type airplane to be used on the Application Phase of this study. The airplane is a single-engine, four-place configuration and is referred herein as the "Far Term Airplane". The guidelines are listed in Table XXX and Appendix M.

TABLE XXX

FAR TERM AIRPLANE GUIDELINES

Accommodations	
Passengers and crew	4
Baggage	200 lbs.
Cabin volume	112 ft^3.
Propulsion	
Maximum power	250 hp
Maximum weight	380 lbs

Performance	
Endurance	4 hrs. + 30 minutes
$V_{maximum}$	152 knots @ S.L.
V_{cruise}	130 knots @ 5000 ft.
V_{stall}	48 knots @ S.L.
Takeoff distance/50 ft.	1000 ft.
Minimum rate of climb	1000 ft. per minute
Service ceiling	14,000 ft.

Design Justifications.- Figure 146 illustrates the airplane which satisfies the contract guidelines. Table XXXI lists the dimensions and general data.

Certain major parameters were determined by an optimization technique developed for the study. These were the wing loading, power loading and gross weight, and hence wing area and installed power.

The wing has a tapered planform with no sweep at the quarter-chord. The aspect ratio of seven, typical of most current four-place light airplane wings, has evolved as the optimum trade-off between weight, structural integrity, and performance. The 63 series airfoil wing provides an appreciable amount of

THREE-VIEW OF FAR TERM LIGHT AIRPLANE

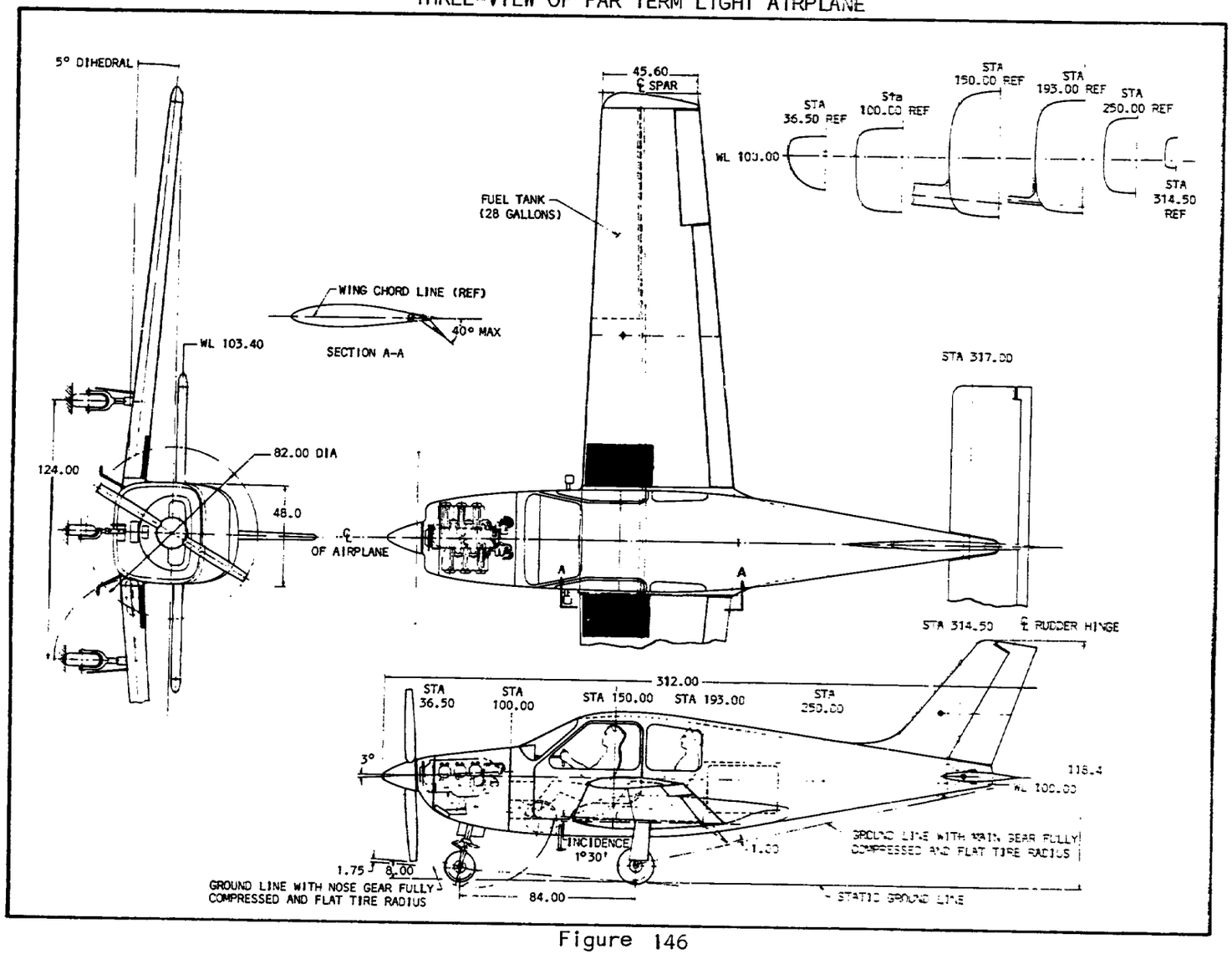


Figure 146

TABLE XXXI

FAR TERM AIRPLANE GENERAL DATA

Gross weight	(W)	2850 lbs.
Power	(P)	250 BHP
Wing		
Area	(S)	180 $ft.^2$
Span	(b)	35.5 ft.
Aspect ratio	(AR)	7.0
Taper ratio	(λ)	.6
Root chord	(c_r)	6.338 ft.
Tip chord	(c_t)	3.803 ft.
Mean aerodyn.chord	(MAC)	5.173 ft.
Sweep @ c/4	(Λ)	0^0
Dihedral	(Γ)	5^0
Airfoil		NACA 63_2-A215
Center of gravity travel		10%–30% MAC

Vertical tail		
Area	(S)	18.25 $ft.^2$
Height	(b)	5.06 ft.
Aspect ratio	(AR)	1.4
Taper ratio	(λ)	.5
Root chord	(c_r)	57.5 in.
Tip chord	(c_t)	29.0 in.
Mean aerodyn.chord	(MAC)	54.7 in.
Sweep	(Λ)	35^0
Airfoil		NACA 0009
Horizontal tail		
Area	(S)	40 $ft.^2$
Span	(b)	12.65 ft.
Aspect ratio	(AR)	4.0
Taper ratio	(λ)	1.0
Chord (constant	(c)	3.16 ft.
Sweep	(Λ)	0^0
Airfoil		NACA 0012

laminar flow if care is taken in manufacturing a smooth upper surface back to the main spar. Increasing the leading edge radius by about 20% prevents leading edge stall at high lift coefficients. A 70% of span, 25% of chord*, double slotted flap with fixed vane will provide a maximum lift coefficient of 2.3 for the wing. Maximum extension angle of the flaps is 40°. The ailerons are 25% of chord and 30% of span. They are similar to a plain sealed flap and are continuously piano-hinged on the upper skin. Aileron movement is 25° up and $12\frac{1}{2}^0$ down. A tapered wing (λ = .6) was selected because of its low weight, structural efficiency and slightly lower induced drag. Tapering also allows greater thickness near the root for gear retraction.

The wing has a single spar located at 40% of the chord, which is approximately the thickest portion of the airfoil section. The low wing was selected for crash worthiness, structural considerations and ideal main gear retraction arrangement.

The fuel is located entirely in integral wing leading edge tanks (28 gallons in each wing). The tanks will be at the outboard section of the wing as far as possible from the occupants, to reduce post-crash fire hazards. No fuel will be carried aft of the spar, to facilitate aileron and flap controls installation. A volume computation shows that the fuel tanks will extend approximately 100 inches inboard from the wing tips.

*25% of chord for entire flap set, 20% of chord for main flap.

The horizontal and vertical tail areas were designed to give acceptable tail volumes for this type of airplane. The horizontal tail is an all moving stabilator used for simplicity and control effectiveness. It has an adjustable anti-servo tab to provide control feel and trim.

The cabin volume is 112 cu. ft. (excluding baggage space). Minimum width is 3.67 ft. The contract guidelines were 112 cu. ft., and 3.50 ft. minimum width. The baggage space exceeds 16 cu. ft. and is arranged to accommodate four 9" x 21" x 31" suitcases. The cabin will have an access door on each side. The baggage compartment will have an access door on the right hand side only. Part of this door will form the wing root fillet.

The retractable landing gear was decided upon because a trade off study during the performance of this contract indicated it would result in a lower direct operating cost providing the utilization exceeds 150 hours per year. It allows more efficient performance with less power at all speeds. The main gear retracts inboard and after the main spar.

Weight and Balance Study.- Preliminary weight and balance estimations were based on Figure 146. The neutral point (stick fixed) was determined in appendix Q to be 35% mean aerodynamic chord (for a 90% tail efficiency factor). Using a 5% stability margin, the most aft C.G. is then located at 30% mean aerodynamic chord.

To limit the tail size and trim drag to reasonable values, the C.G. travel was limited to 20% M.A.C. which is representative of current light aircraft design. Weight and balance computations are in Appendix R.

Most contemporary four-place light airplanes have useful weights which are met by trading off passengers, fuel, and baggage. Very few can carry maximum passenger, fuel, and baggage load simultaneously. However, the Far Term airplane is designed to carry four 170 pound passengers, maximum fuel capacity, and 200 pounds of baggage simultaneously.

Application of Selected Materials and Structural Concepts

The material/concepts selected for the various airplane components are based primarily on the results of phase I of the Study, and are summarized in Tables XXI and XXII. Several additional factors influenced the final structural arrangements. On the wing components, for example, single spar construction over stringer-spar construction was chosen for two reasons: (1) The airfoil components loading intensities were of such low magnitudes that little if any advantage could be gained with the stringer-spar concept: (2) Concern over the possibility that the stringer configuration would tend to create ridges in the smooth airfoil sections and thus degrade the aerodynamic characteristics.

In selecting materials for the components, primary concern was given to the wing. The importance of structural integrity was paramount, therefore, continuous filament type composites were used for the main spar and wing skins.

The continuous fiber, cross lamination configurations give optimum fracture thoughness and fatigue strength because their inherent discontinuities tend to inhibit crack propagation between the filiaments. A review of Table XXI and XXII indicate graphite/epoxy and S-glass/epoxy to be the most promising candidates for this structure.

The empennage, while treated as primary structure, was nevertheless considered to have slightly lower requirements from the standpoint of fatigue and fracture toughness. For those reasons non-continuous glass, with thermosetting resins were used for structure. Three non-continuous filament composites were considered in Phase I: (1): 3/8" E-glass/nylon 6/10; (2): 1/2" E-glass/polyester and (3): 1" S-glass/epoxy. The 1" S-glass/epoxy is the most efficient strengthwise, and will be used in the design of the horizontal tail. It is a compression moldable material. The 1/2" E-glass/polyester material although not always more efficent than the 3/8" E-glass/nylon 6/10 exhibited higher stiffness characteristics and resistance to environmental conditions. It is also a compression moldable material and will be used for the design of the vertical tail.

The fuselage utilized both types of composites. The longerons and other moment reacting members were made with the continuous filament S-glass/epoxy material while the low load intensity fuselage shear panels incorporated non-continuous 1" S-glass/epoxy moldable material.

Material/concepts involving aluminum alloys were not incorporated in the fabrication of the main components. A review of the Phase I indicated the most promising composites exhibited superior structural efficiencies. In addition, the moldable reinforced plastics showed greater potential over the aluminum, from the standpoint of mass production processes which would offer greater fabrication cost savings.

Component Design.- This sub-section will discuss the design of the vertical tail, horizontal tail, wing, and the fuselage.

Vertical tail: Based on the three-view in Figure 146, the vertical tail has a total area (exposed) of 15.84 sq. ft. The fin area is 9.18 sq. ft., and the rudder area is 6.66 sq. ft. The design concept selected was based on a compression molded reinforced thermosetting plastic (i.e., 1/2" E-glass/polyester available in the industry in .025 thick prepreg sheets). See Figure 147 and 148. An alternate material, injection molded glass/nylon, will be discussed in a later section on cost an manufacturing considerations.

The four-piece stabilizer (Figure 147) consists of a R.H. skin, a L.H. skin, a spar, and a root closing rib. Early studies of the tail were based on the assumption that a grid pattern of internal stiffeners would be required to keep the panel sizes small in order to increase shear buckling allowables, but structural analysis indicated that "chordwise only" internal stiffeners would be adequate. As shown in Figues 147 and 148, the skin and stiffeners are integral, and the hinge fittings are integral with the spars.

VERTICAL STABILIZER, FAR TERM LIGHT AIRPLANE

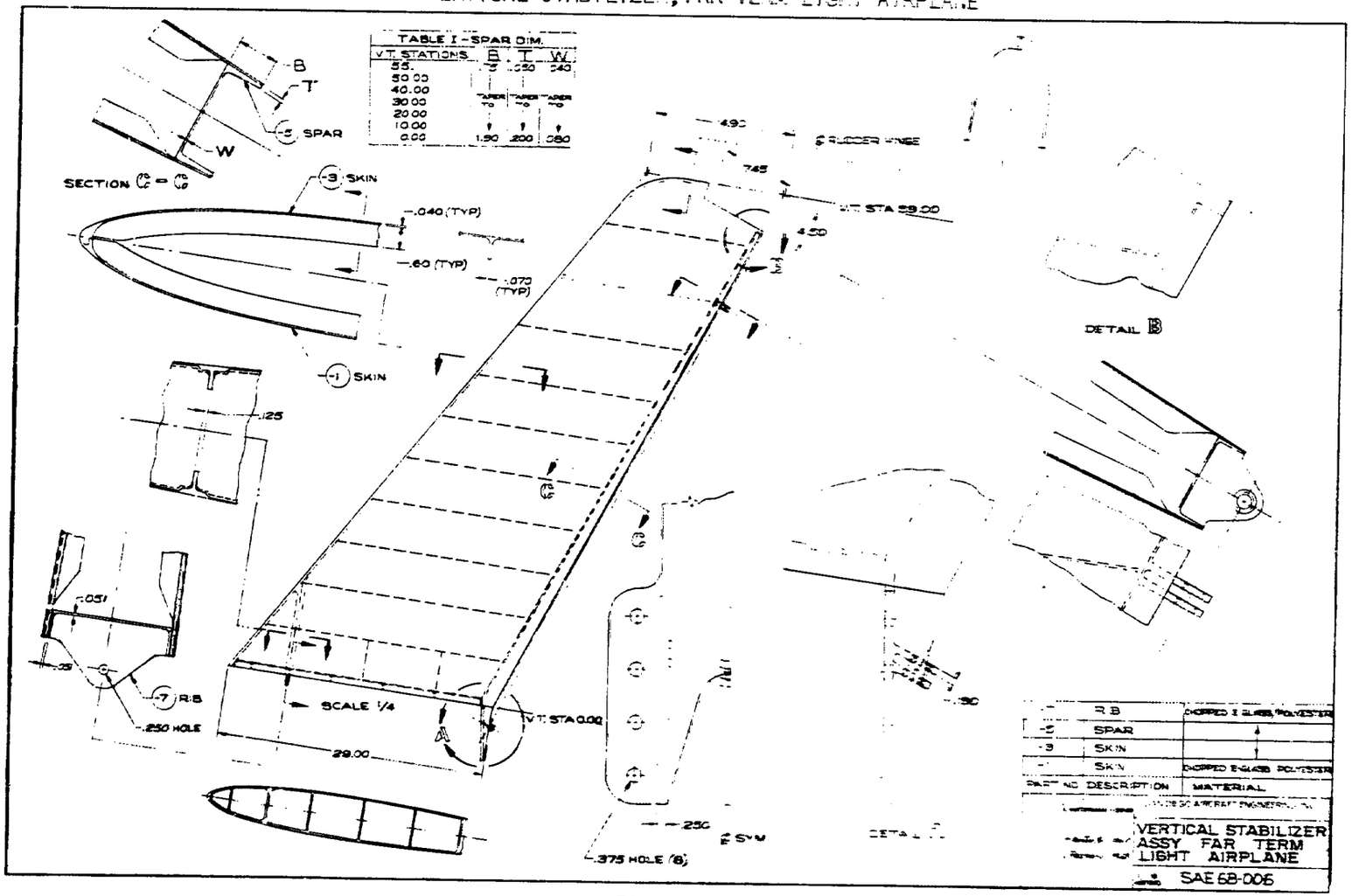


Figure 147

RUDDER, FAR TERM LIGHT AIRPLANE

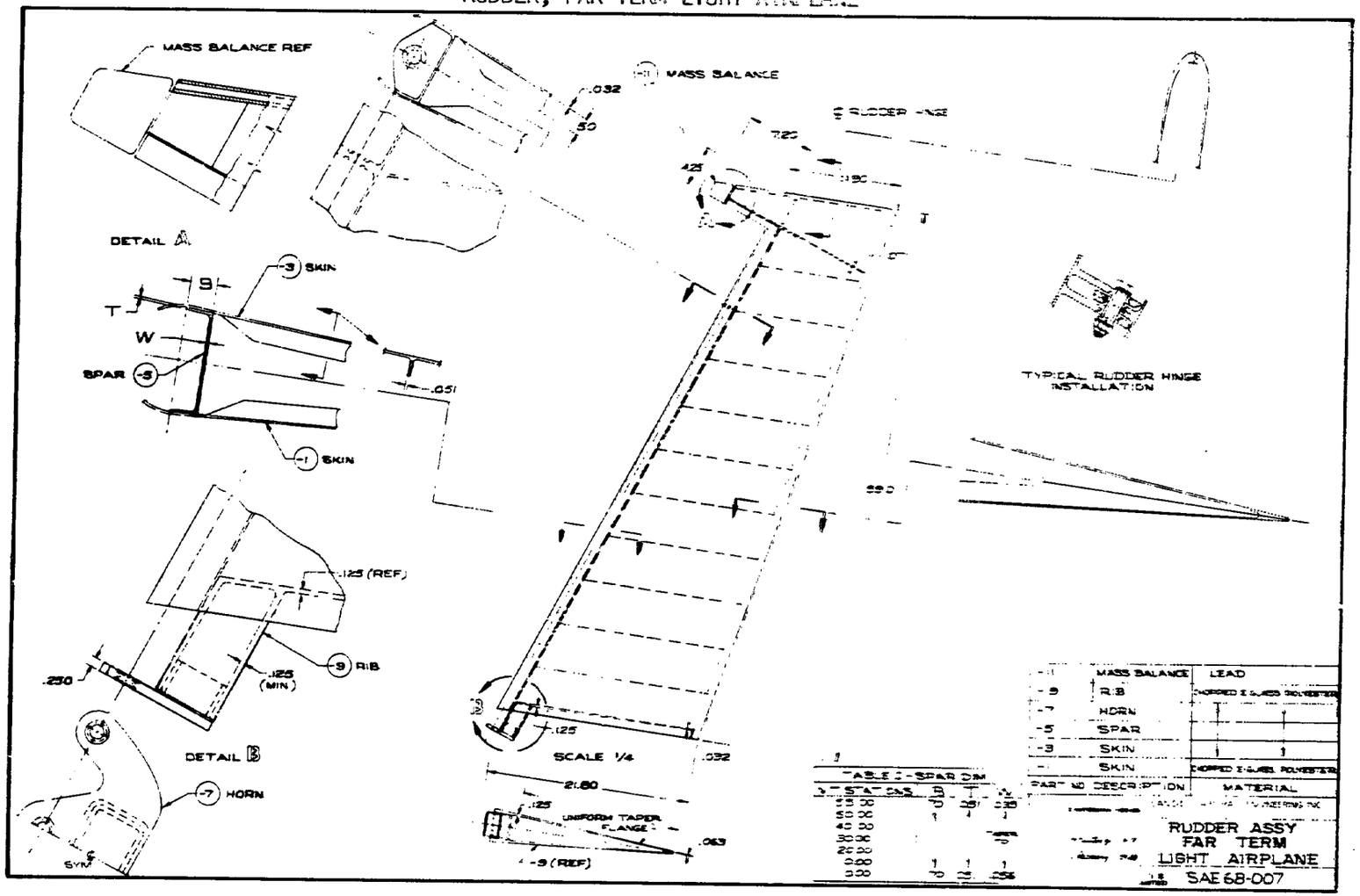


Figure 148

Part release is a basic consideration on the design of molded parts. Fortunately, a relatively small draft angle is required for plastics (1°); and possibly some short sections could be released from the mold without draft.

Due to the relatively low bearing allowables for reinforced plastics (20,000 psi), most of the bolted connections will be critical in bearing. Large diameter bolts will be required. Some weight could be saved if hollow bolts were used. Most bolt holes will be cored, so no drilling will be required after molding. A minimum of two-diameter edge distance is used for all bolts. Molded-in-place inerts will be used at all hinge lugs. Vertical loads will be reacted at the bottom hinge only, which also reacts the rudder control horn loads.

The six-piece rudder is of similar construction (Figure 148) to the stabilizer or fin. The skins are reinforced with internal chordwise stiffeners, as on the fin. An attempt was made to reduce the number of parts by integrating the spar with the root rib, but part extraction, as on the fin, becomes a problem unless a complex mold is used. The lead mass balance will be bonded to the skins and upper arm. Due to the tapered shape, the mass balance is also mechanically locked in place.

The vertical fin and the rudder are entirely bonded. Adequate bonding surfaces are provided for on their respective peripheries. The leading edge of the fin has a tongue-and-groove design which insures alignment, and does not expose thin overlaps which might peel off. Also, the build up of material at the leading edge provides additional protection for erosion or hail damage. If necessary, a pressure-sensitive tape could be laid up over the leading edge.

Spar flanges, rib flanges, and skin stiffeners heights were designed considering the flow capability of the material into deep crevices. Industry sources have indicated that both glass/polyester prepreg and Nylon 6-10 will adequately fill these thin, deep grooves in the mold. An attempt was made to design the root rib and the spar in one piece, but it was found that this method resulted in locking of the part in the mold. Otherwise, the mold would have to be more complicated to permit ejection.

Horizontal tail: The horizontal tail is a single-slab flying tail (stabilizer), hinged at the 25% point of its constant chord.

Referring to Figure 149, the structural concept for the stabilizer is based on an all-bonded construction of glass-reinforced plastic components. These components are compression molded from a prepreg 1 in. S-glass/epoxy composite. The stabilizer is made up of the following molded plastic componnents:

(1) Two each of two nearly oposite skins
(2) One main spar
(3) One trailing edge spar
(4) Two identical leading edge ribs

(5) One torque box
(6) Two identical anti-servo tab skins
(7) Two identical anti-servo tab closing channels
(8) One anti-servo tab control bracket
(9) Two identical anti-servo tab mass balance fairings

The remaining components are two identical mass-balance weights for the anti-servo tab, and the main stabilizer mass balance.

The skins are designed such that the upper right and left skins are interchangeable with the lower left and right skins, respectively. Each skin has integrally molded chordwise skin stiffeners and a tongue or groove in its leading and outboard edges. This wedge shaped tongue-and-groove design was recommended by a molder in preference to the full radii type specified on the vertical stabilizer. The wedge-shaped tongue-and-groove insures alignment and does not leave thin overlaps which might peel off. Also the extra material at the leading edge provides additional resistance to erosion and hail damage. If necessary, a pressure sensitive tape could be applied to the leading edge.

The main spar, molded all in one piece, has an I-beam cross section, the web thickness and height of which are constant. The cap width and thickness are tapered outboard. The upper and lower caps of the I-beam meet one another via an elliptical contour at each end of the spar. The center section of the spar caps have thin extensions which act as closures to the torque box. Also integrally molded on the spar are two sets of clevis hinge fittings and a boss with a cored hole for the main mass balance arm. Due to the low bearing allowables for reinforced plastics (20,000 psi), the clevis hinge fittings have molded-in inserts, sized for large diameter (possibly hollow) bolts (i.e., 3/8). A standard minimum edge distance of two diameters is specified for clevis hinge fitting holes. Each clevis hinge fitting is designed to mate with a set of three lugs on the fuselage.

The torque box consists of a pair of identical ribs, integrally connected with a channel. This so-called torque box becomes a true torque box when it is mated and bonded to the spar, between the spar cap extensions. These extensions are bonded to the ribs and to the interconnecting channel on the so-called torque box. Considerable effort was expended to eliminate load path discontinuities and to maintain efficient bonding joints. The interconnecting channel on the so-called torque box has a boss with a cored hole, which aligns with a similar hole in the spar web. These respective holes support the main stabilator mass balance arm. Manufacturing considerations and cost analyses of this part will likely dictate breaking this part into two separate (but identical) ribs and a shallow box with a hole in it. As it is now, it will require two massive cores normal to the direction of mold pressure application.

The trailing edge spar is molded full span in one piece, with eight sets of five-lug piano hinges molded integrally into its otherwise constant I-beam cross section. This I-beam cross section is closed on both ends to provide a continuous bonding interface with the skins. The aft ends of the torque box ribs nest into the front side of the trailing edge spar.

HORIZONTAL STABILIZER, FAR TERM LIGHT AIRPLANE

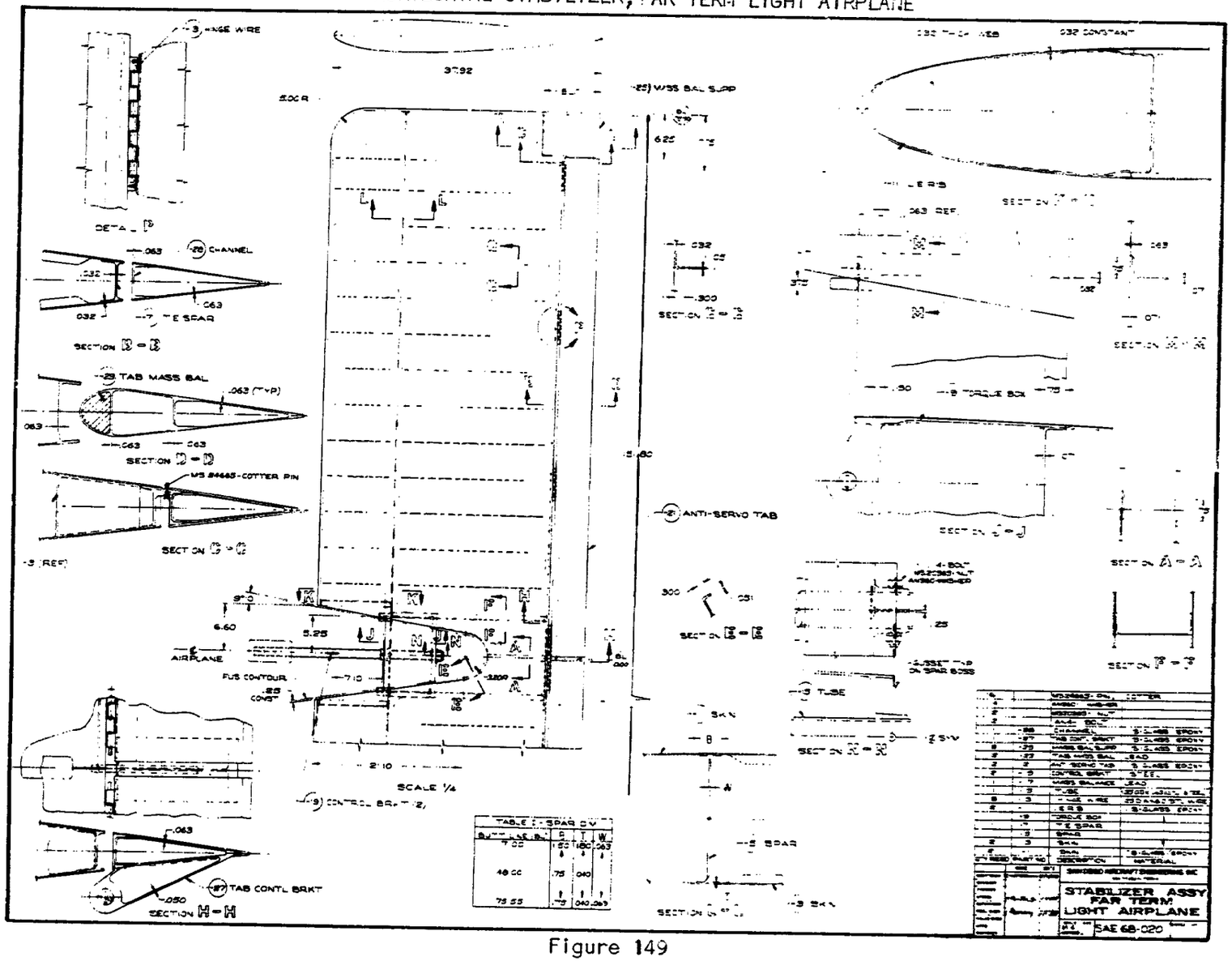


Figure 149

Mating with the eight sets of piano hinges on the aft spar is an anti-servo tab. The inboard end of the right hand and left hand portions of each tab is mated to one of the two male extensions on a single anti-servo tab control bracket. The lever arm on this control bracket has a No. 10(3/16 I.D.) insert integrally molded in. The right hand and left hand portions of the anti-servo tab each consist of a skin, a closing channel and a mass balance fairing, which are respectively interchangeable, one side for another. Each identical one-piece skin has a constant deep "V" cross section. Each identical closing channel has a constant cross section except for four sets of five-lug piano hinges, which mate with those on the trailing edge spar. An attempt was made to make the anti-servo tab a one-piece extrusion of glass/nylon (rather than a channel + skin). This was subsequently discarded due to the inadequate torsional stiffness of this material. An identical and interchangeable mass balance fairing closes off both outboard ends of the anti-servo tab. Identical lead weights are bonded into a cavity in each mass balance fairing.

A single leading edge rib is nested and bonded to the forward side of the main spar, immediately outboard of each clevis fitting on the spar. These two ribs are identical.

Table XXXII tabulates weights and unit weights for the primary empennage components.

TABLE XXXII
FAR TERM LIGHT AIRPLANE EMPENNAGE WEIGHTS

	Area (ft^2)	VERT. FIN 9.18	RUDDER 6.66	STAB. 40.00
Injection molding Nylon 6/10 (.051 lb./cu. in.)	Weight (lb)	14.44	9.35	NA
	Unit weight ($\frac{lb}{ft^2}$)	1.58	1.4	
Compression molding Chopped E-glass/ polyester (.070 lb./cu. in.)	Weight	13.13	8.5	NA
	Unit weight	1.43	1.28	
Compression molding 1" S-glass/epoxy (.062 lb./cu.in.)	Weight	11.63	7.5	36.06
	Unit weight	1.27	1.13	0.90
Contemporary sheet metal light airplane	Unit weight	1.47	1.10	1.07

Wing: The wing has outboard leading edge wet fuel tanks and the main landing gear, mounted aft of the single spar, retracts inboard and slightly aft. See Figures 150 and 151. The wing has a single spar located at the 40% chord. It has an open-side-aft channel cross-section. The channel's height, cap thickness, and web thickness taper outboard, and the cap width remains constant. The spar is compression molded from high modulus graphite filament reinforced epoxy prepreg. The spar web is made up of prepreg epoxy/graphite tapes in a multi-layer, multi-direction pattern. The spar caps are also made up of the same (or similar) epoxy/graphite tapes, with 72% of the graphite running spanwise and the remainder at $\pm 45^0$. There will be a comparable constructed auxiliary spar between the main landing gear support rib and the root rib for reacting a part of the main landing gear loads. The main landing gear support fittings will be glass-reinforced plastic with metal bushings for bearing loads. One is mounted between the main spar and the above-mentioned auxiliary spar on each wing half. See Figure 152.

Each wing half is attached to the fuselage with two bolts through the spar web and into a fuselage frame, and one bolt each at the front and rear of the wing root closing rib. The main spar on each wing half, extends to the fuselage centerline, at which point they are joined by 18 to 20-in. splice plates nested to the outside and inside surfaces of each spar cap, and by a 4-in. wide splice plate on each side of the web.

The two aft closing members on each wing half are: a zee-section along the aileron interface and a channel along the flap interface (See Figure 151). Each wing half has five sets of ribs (leading edge + aft), plus two additional leading edge ribs. They are located at: (1) the root (see Figures 150 and 151, section D-D); (2) the landing gear interface (see Figures 150 and 152 section C-C); (3) the inboard end of the fuel tank at WS 105.6 (wet bulkhead); (4) midway in the fuel tank, or between the aileron and flap; and (5) the tip (see Figures 150 and 151, section A-A), which is a wet bulkhead. The two additional leading edge ribs quarter the fuel tank. The first four ribs also provide integral hinge supports for the flap (see Figure 151, section D-D).

The skin consists of three details for each wing half (i.e., a leading edge skin from the top spar cap to the bottom spar cap, an upper aft skin, and a lower aft skin, each of which extend from root to tip). All of these skins are made from compression molded multi-directional graphite/epoxy prepreg tapes and have no integral stiffeners. The initial wing design specified separate "T"-section chordwise skin stiffeners, which will be bonded to the inner skin surfaces.

The aileron on each wing half consists of an upper and lower integrally stiffened skin. The skin stiffeners are spaced five inches apart for a total of 18 per aileron. The forward closing web is integral with the upper skin, as are the piano-hinge lugs. See Figure 151, section K-K. There is a closing rib at each end of the aileron. The aileron would be mass balanced at the outboard end with the weight traveling up and down within the wing tip fairing.

WING PLANFORM, FAR TERM LIGHT AIRPLANE

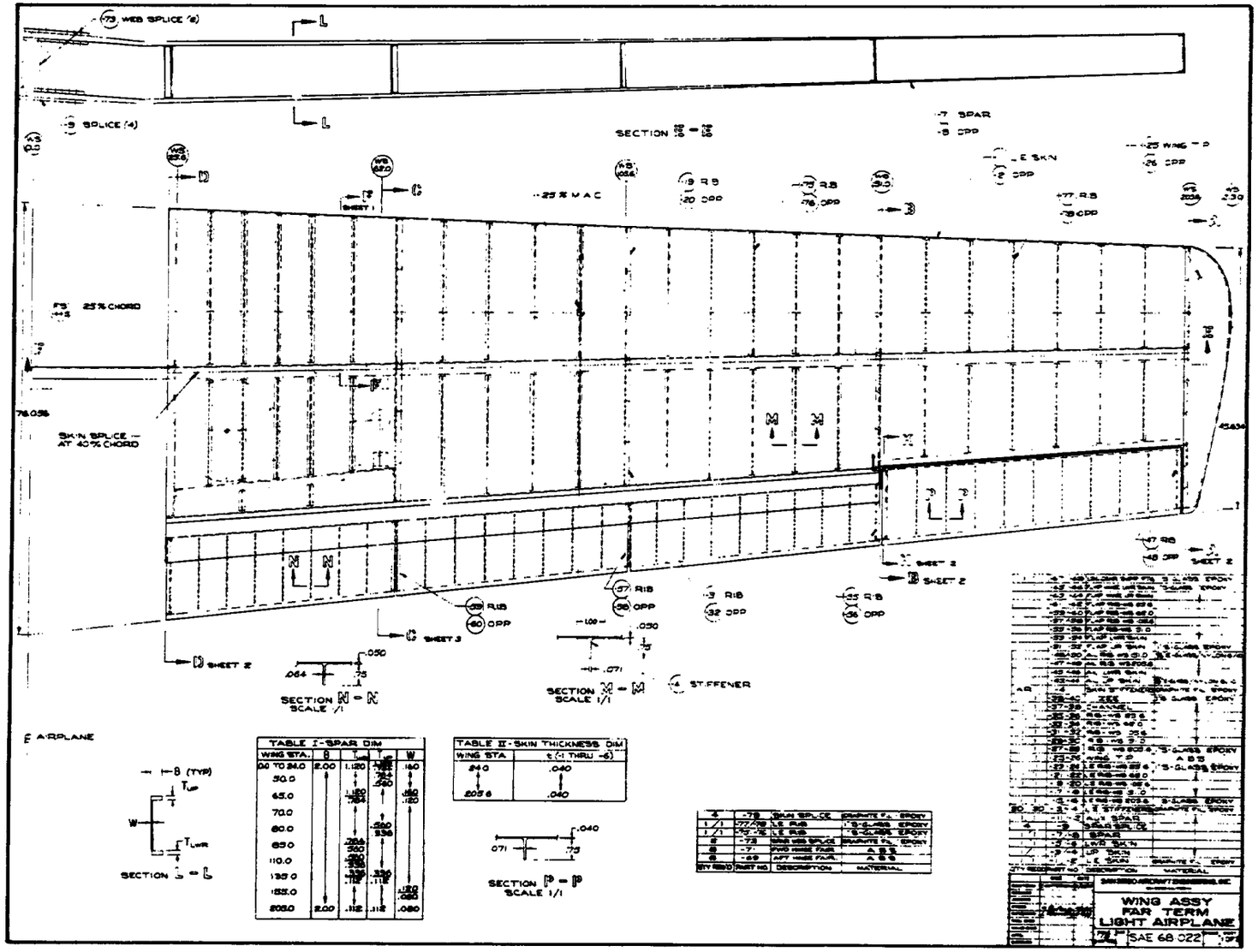


TABLE I - SPAR DIM

WING STA.	B	T_{upr}	T_{LWR}	W
00 TO 24.0	2.00	1.120	.784	.160
30.0		.980	.700	.140
65.0		.840	.560	.120
70.0				
80.0			.560	
85.0		.784	.336	
110.0		.560		
135.0		.336	.336	
155.0		.112	.112	.160
205.0	2.00	.112	.112	.080

TABLE II - SKIN THICKNESS DIM

WING STA.	t (-1 THRU -6)
24.0	.040
205.6	.040

BOM			
-4	-78	SKIN SPLICE	GRAPHITE F.L. EPOXY
1/1	-77/-78	LE RIB	5-CLASS EPOXY
1/1	-76/-78	LE RIB	5-CLASS EPOXY
-5	-78	WEB WEB SPLICE	GRAPHITE F.L. EPOXY
-6	-77	AFT HINGE FAIR.	A 8 S
-6	-69	AFT HINGE FAIR.	A 8 S

QTY REQ'D	PART NO.	DESCRIPTION	MATERIAL

Figure 150

WING SECTIONS, FAR TERM LIGHT AIRPLANE

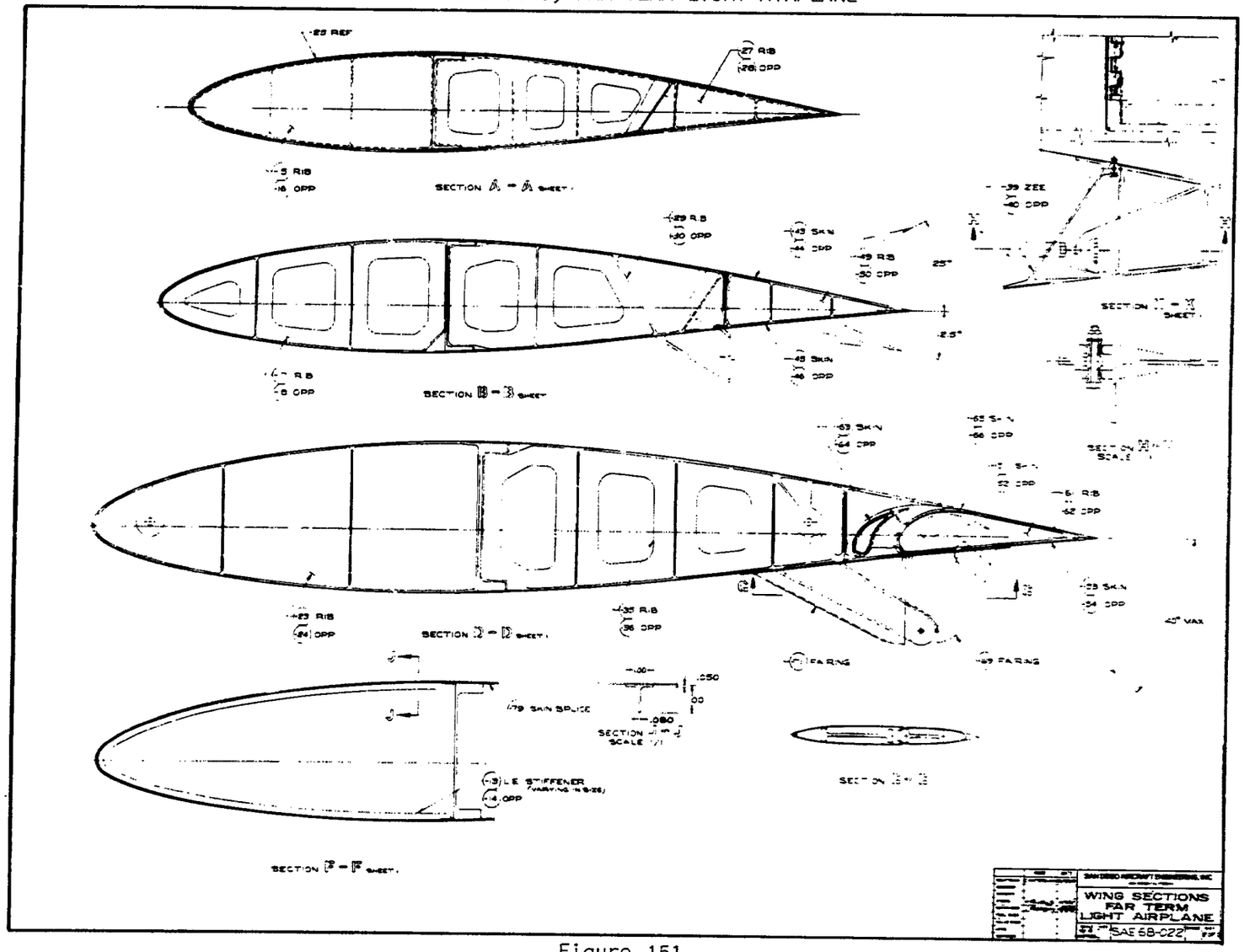


Figure 151

WING/LANDING GEAR INTERFACE, FAR TERM LIGHT AIRPLANE

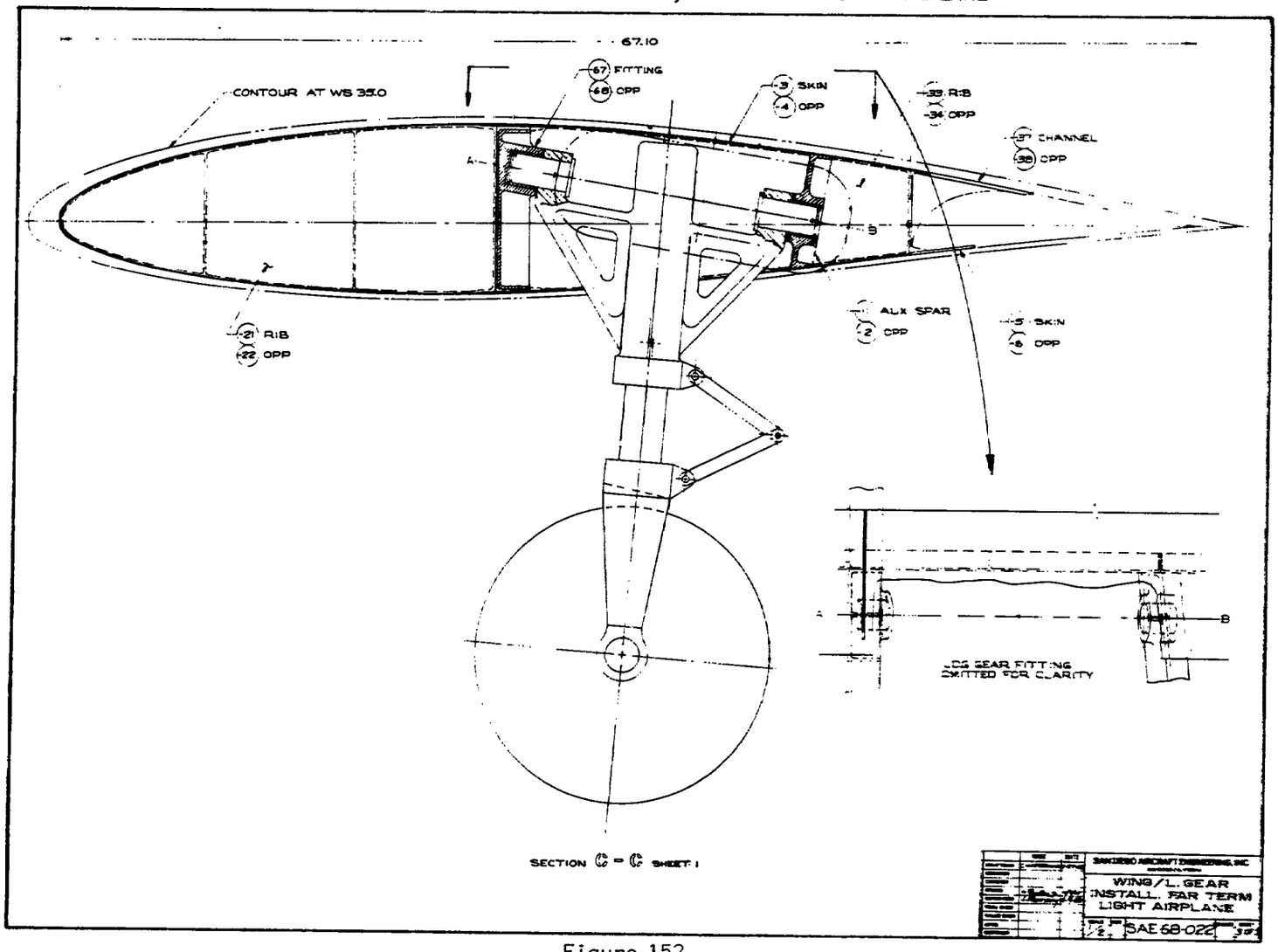


Figure 152

The flap on each wing half is divided into three segments connected and closed off with four hinge arm-ribs (see Figure 151, section D-D). Each flap segment consists of an upper and a lower, integrally stiffened, skin with a tongue-and-groove leading edge configuration. Each vane segment consists of an upper and a lower (unstiffened) skin with a similar leading edge joint.

Nonstructural tip fairings and hinge fairings are of hot-formed thermoplastic. See Figures 150 and 151.

Referring again to Figures 150, 151, and 152, the material selection and the type of molding considered for each of the 202 machine molded, reinforced plastic components are as follows: The spars, spar splices and skins (-7, -11, -9, -73, -1, -3, & -5) are made of compression molded high modulus graphite filament/epoxy; the ailerons (-43 thru -49) are made of injection molded E-glass/nylon; the tip fairings (-25) and the flap hinge fairings (-69 & -71) are made of hot-formed ABS; and the remainder of the components are made of compression molded S-glass/epoxy.

All of the above components are then appropriately prepared for bonding, fixtured and secondary bonded to form a right hand and a left hand wing half; which are subsequently attached to one another and to the fuselage with mechanical fasteners.

Two alternate wing construction concepts (designated II and III) were considered as possible weight and/or cost savers. Referring to Figure 153, Configuration II replaces the graphite channel section spar with an S-glass rectangular rigid urethane (foam core) section. Also, the graphite skins are replaced with S-glass skins. The resultant weight saving in the spar is exceeded by the weight penalty in the skins. See Table XXXIII. Configuration III is the same as II, except graphite is used in place of the S-glass. This concept (i.e., III) amounts to a 10% saving in total wing weight and, as will be discussed later, a 5% saving in wing cost. Both graphite wing construction concepts represent significant weight (and cost) savings over conventional sheet aluminum construction, (if the cost of graphite can be reduced to $1.00 or $2.00 per pound).

Fuselage: The fuselage is conventional in size and shape. The overall dimensions include a maximum width of 48 inches, maximum height of 60 inches, and a length of 232.5 inches (firewall station 100.00 to aft tip of stringer fairing). There are two passenger doors, one baggage compartment door, two side windows, and a one-piece windshield. The fuselage design is only preliminary since neither loads nor stress analyses have been performed to size the various components.

Referring to Figure 154, the structural concept for the thirty-three piece fuselage is based on all bonded construction of glass reinforced plastic components. The firewall is stainless steel.

Skins and frames are compression molded from a prepreg one-inch S-glass/epoxy composite. The longerons and channels are bag-molded from continuous-filament S-glass/epoxy prepreg tapes. The stringer fairings are molded from one-inch E-glass/polyester composite prepreg.

TABLE XXXIII
WING WEIGHTS (POUNDS)

ITEM	FAR TERM LIGHT AIRPLANE			CONTEMPORARY AIRPLANE
	CONFIG. I	CONFIG. II	CONFIG. III	ALUMINUM WING
	Graphite Constr.	S-Glass Constr. Foam Core Spar	Graphite Constr. Foam Core Spar	
Skins	77.3	110.6	77.3	106.0
Spars	92.6	82.6	65.1	85.0
Ribs	26.9	26.9	26.9	26.0
Stringers				7.0
Skin stiffener	16.5	16.5	16.5	
Skin splices	8.3	11.9	8.3	
Tip	1.5	1.5	1.5	1.5
Total	222.3	250.0	195.6	227.5

WING SPAR CONFIGURATIONS

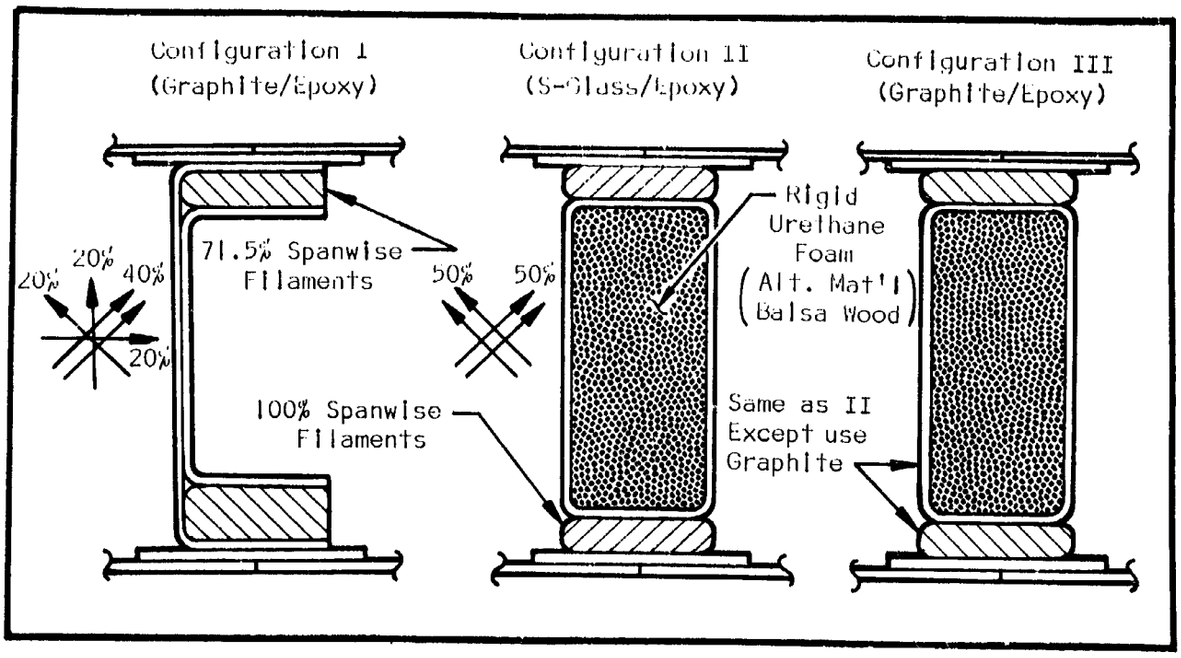


Figure 155

FUSELAGE, FAR TERM LIGHT AIRPLANE

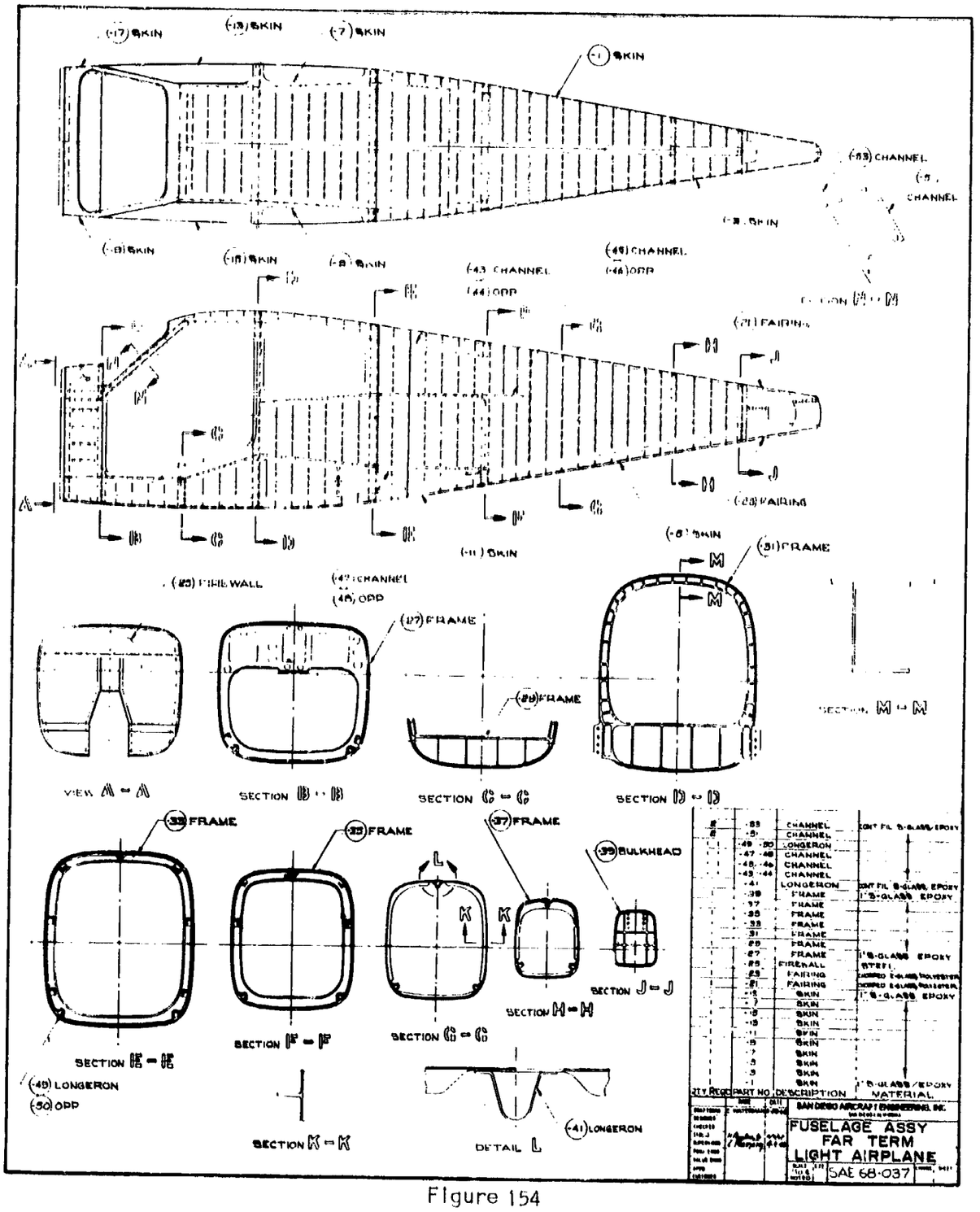


Figure 154

Component Technical Analysis.- The preliminary loads and stress analyses for the Far Term airplane were developed and performed using conventional methods generally accepted by the aircraft industry today. The material/concepts chosen for the various components are based primarily upon the phase I part of the Study.

Several additional factors influenced the final structural arrangements on airfoil components. For example, single-spar construction over stringer-spar construction was chosen for two reasons: (1) The airfoil component loading intensities were of such low magnitudes that little, if any, advantage could be gained with the stringer-spar concept; (2) concern existed over the possibility that the stringer configuration would tend to create ridges in the smooth airfoil section and thus degrade the aerodynamic characteristics of the smooth wing.

In selecting materials for the various components, primary consideration was given to the wing. The importance of structural integrity was paramount for this component; therefore, continuous-type filament composites were used for the main spar and wing skins. The continuous-fiber, cross-lamination configurations give optimum fracture toughness and fatigue strength because their inherent discontinuities tend to inhibit crack propagation between the filaments.

The empennage, while treated as primary structure, was nevertheless considered to have slightly lower priority from the standpoint of fatigue and fracture toughness. For these reasons non-continuous glass with thermosetting resins was used for structure.

The fuselage utilized both types of composites. The longerons and other moment reacting members were made with the continuous filament material, while the low load intensity fuselage shear panels incorporated non-continuous glass-reinforced plastic.

The selection of adhesives to be used for the secondary bonding of structural elements such as spars to skin and stiffeners to skin is not covered in this report. However, it is recommended that an ambient temperature-cure type adhesive be used, where needed, in order to minimize secondary stresses between elements due to differential thermal expansion effects.

The material allowables for the continuous filament composites are presented in two forms. First, the material allowables for the non-continuous filament composites are listed in Table XXXIV. The 3/8" E-Glass/Nylon 6/10 properties were obtained from reference 25 . The 1" S-Glass/Epoxy allowables resulted from data in reference 26 . Where, in particular cases, the material properties were not furnished by the manufacturers, the values were estimated using reference 14 or other means.

Second, plots of the allowables as a function of percent of unidirectional fibers (remainder at $\pm 45^{\circ}$). Graphite/Epoxy and S-Glass/Epoxy allowables in this form are shown in Figures 155 and 156, respectively. The second form assumes all fibers in one direction with the allowable given as a function of load angle to fiber. Graphite/Epoxy and S-Glass/Epoxy allowables in this form

are included in Figures 157 and 158, respectively. Composite allowable values given in reference 16 were used to generate the curves in Figures 156 thru 158.

It should be recognized at this time that some of the values presented in the Material Allowables section are considered average or typical. This is due mainly to the fact that these materials have just recently been developed and are constantly being improved. Further development of these composites should eventually result in complete test programs for the determination of design mechanical properties similar to those established in reference 7 for metallic materials.

For the purposes of this study the available material allowables are considered adequate for the following reasons:

(1) Reduction factors were generally included with the allowable when calculating margins of safety.

(2) A majority of the calculated margins of safety were over +0.20.

(3) Projected material allowables 15 years from now should be well above the values presently used in light of the accelerating state of the art improvement being made.

TABLE XXXIV

COMPOSITE ALLOWABLES - NON-CONTINUOUS FILAMENT

Composite	F_{tu} ksi	F_{cu} ksi	F_{bu} ksi	F_{su} ksi	F_{bru} ksi	E_t psi/10^6	E_c psi/10^6	E_f psi/10^6	G psi/10^6	ω lb/in^3
3/8" E-Glass Nylon 6/10	20	18	32					1.2	(3) .391	.048
Chopped E-Glass Polyester	20.1	25.5	31.5	(1) 9.2	(1) 19.7	(1) 1.18	(1) 1.37	1.99	(3) .655	.070
1" S-Glass Epoxy	45	61	85	8	(2) 22	8.5	7.8	7.1	(3) 2.38	.060

Notes: (1) Use glass fiber/polyester mat properties per ref. 14
(2) 1.1 F_{bru} of Chopped E-Glass/Polyester
(3) Shear Modulus, $G = \frac{E_{eff}}{2(1+\mu)}$; $E_{eff} = .75E$

CONTINUOUS FILAMENT GRAPHITE/EPOXY ALLOWABLES
VS % OF UNIDIRECTIONAL FIBERS
(Remainder at ±45°)

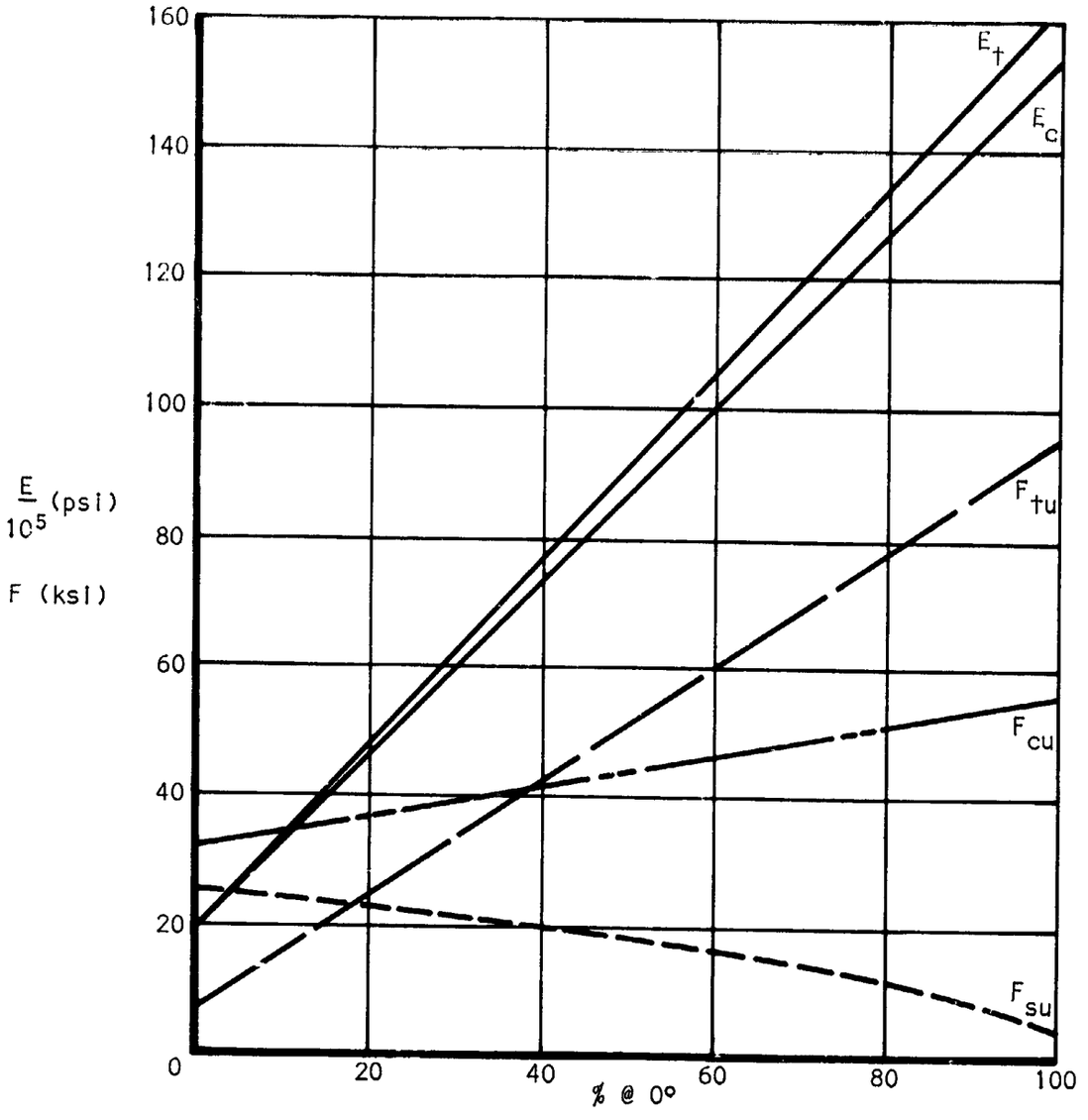


Figure 155

CONTINUOUS FILAMENT S-GLASS/EPOXY ALLOWABLES
VS % OF UNIDIRECTIONAL FIBERS
(Remainder at ±45°)

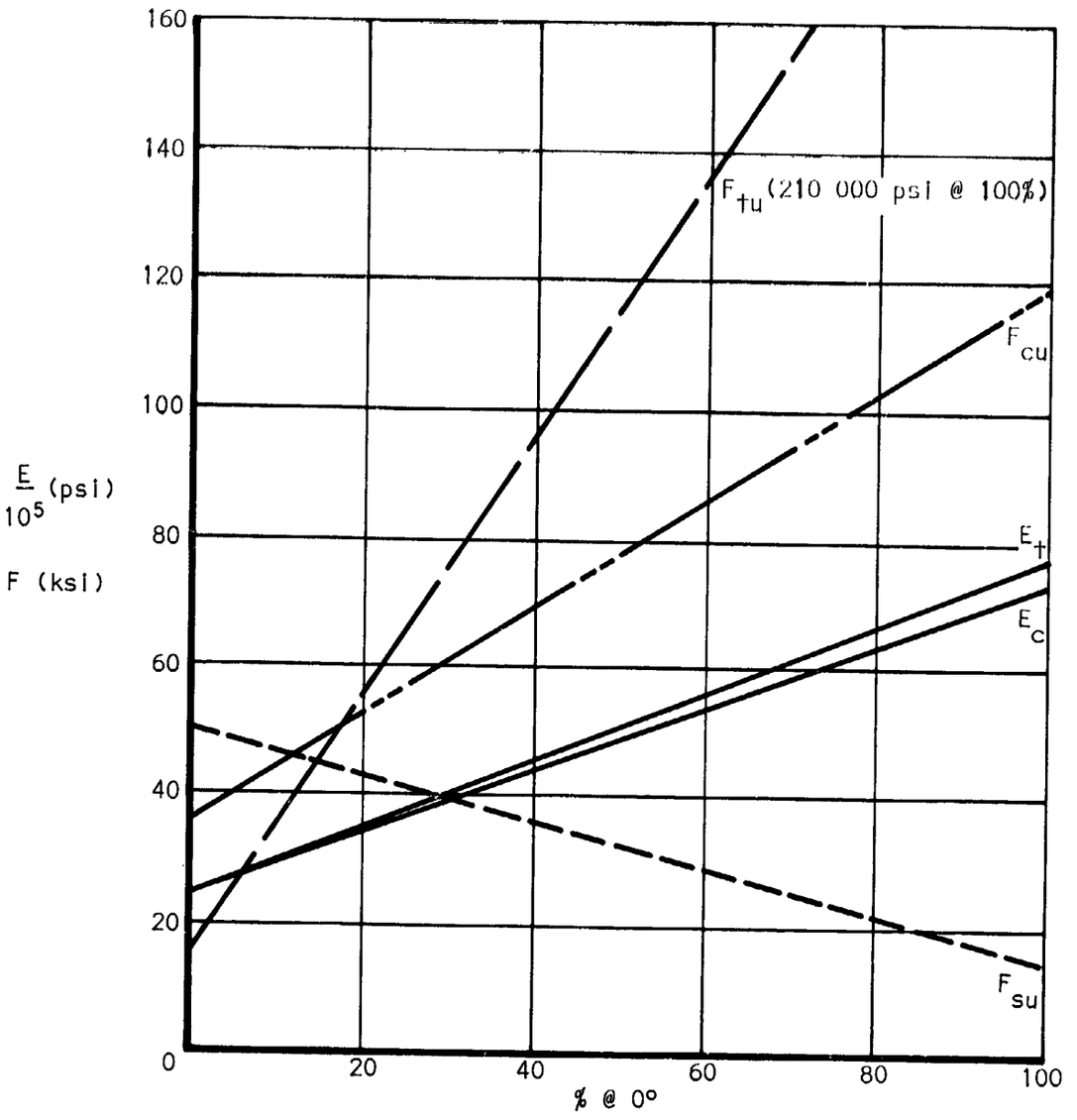


Figure 156

CONTINUOUS FILAMENT GRAPHITE/EPOXY ALLOWABLES
VS LOAD ANGLE TO FIBER

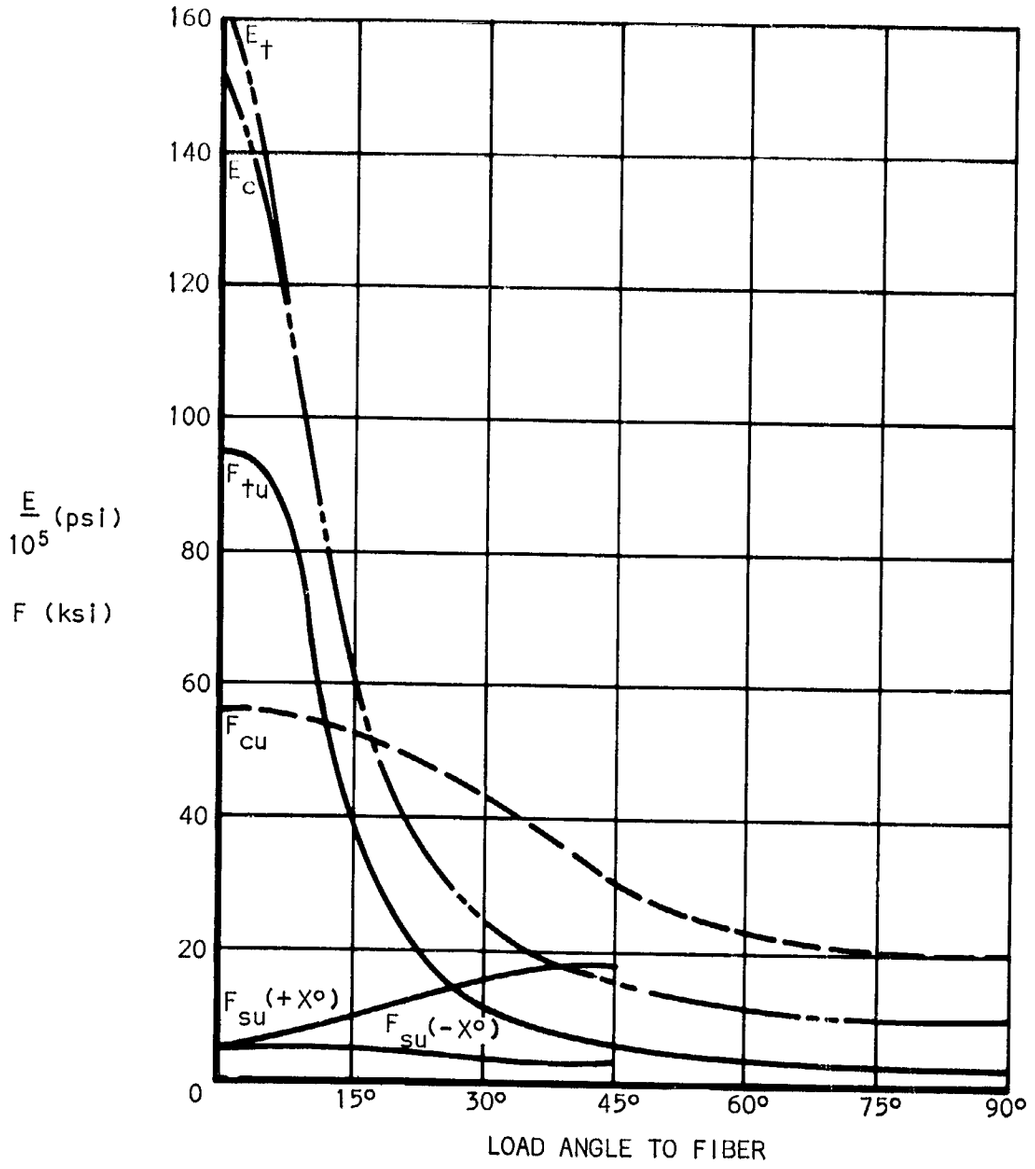
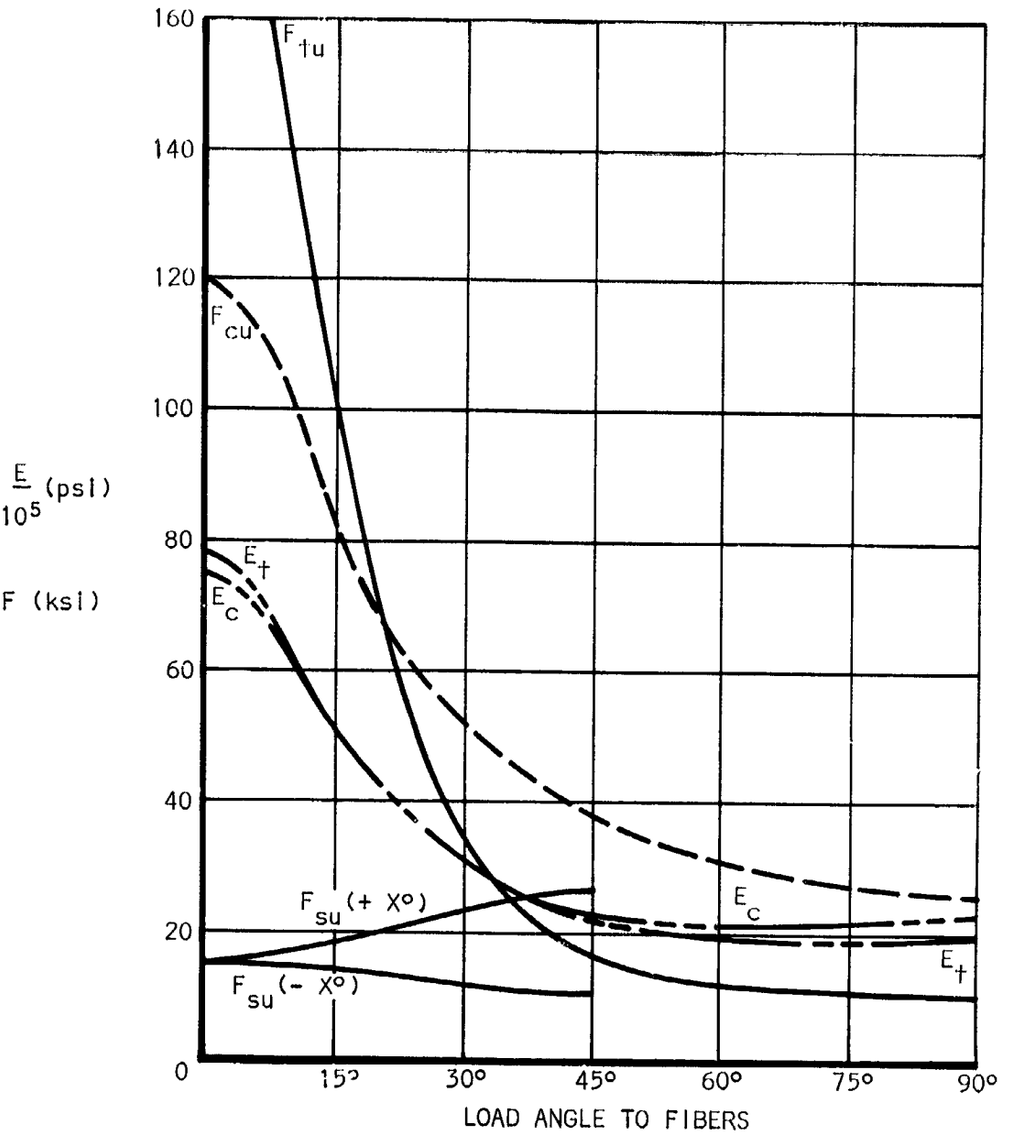


Figure 157

CONTINUOUS FILAMENT S-GLASS/EPOXY ALLOWABLES
VS LOAD ANGLE TO FIBERS



Figuro 158

Wing geometry.-

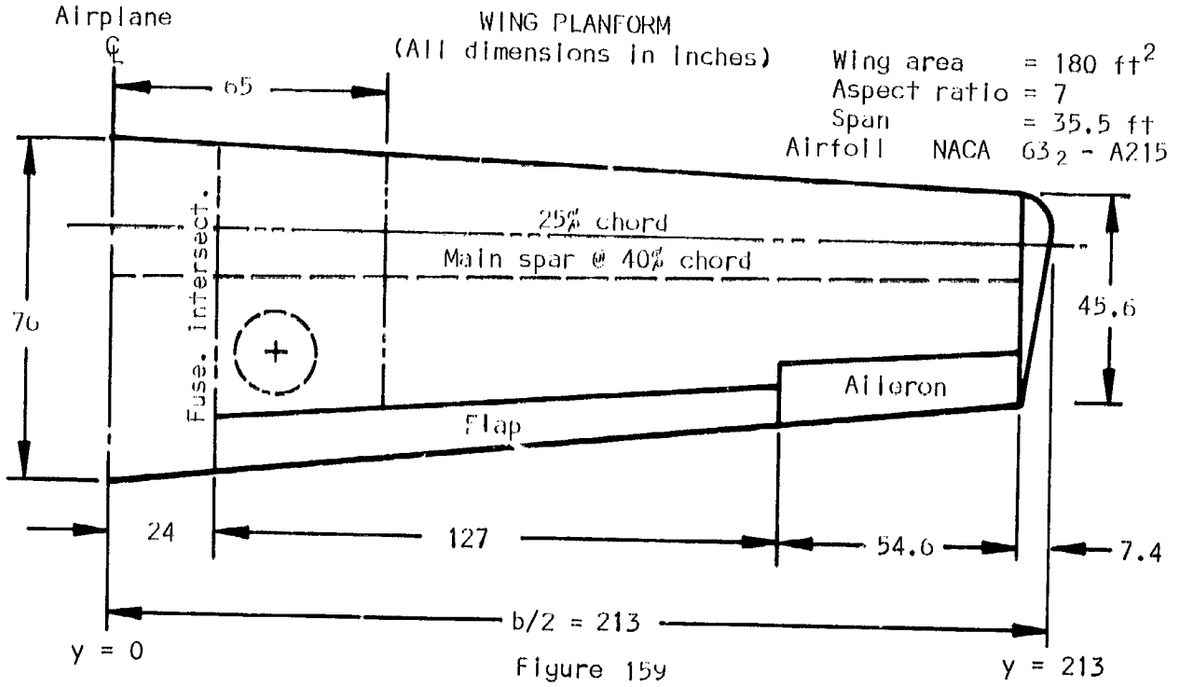


Figure 159

Wing loads criteria.-

Min. design airspeeds (FAR part 23, Appendix A):

Flap speed, $V_{F\ min}$ = 102 mph

Maneuver speed, $V_{A\ min}$ = 140 mph

Cruise speed, $V_{c\ min}$ = 160 mph

Dive speed, $V_{D\ min}$ = 222 mph

Limit flight load factors and average wing load $\bar{w}$: (FAR part 23, Appendix A)

$\frac{W}{S} = \frac{3000}{180}$ = 16.5 psf limit

Limit n_1 = 3.8g positive

Limit $\bar{w} = n_1 (\frac{W}{S})$ = 3.8(16.5) = 62.8 psf

Ult $\bar{w}$ = 94.2 psf = .654 psi

Item	Normal category
Flaps up	3.8
	-1.9
	3.8
	-1.9
Flaps down	1.9
	0

Inertia relief factor, J_n:

Assume that the inertia distribution is similar to the airloading

$$J_n = \frac{W_g - W_w}{W_g} = \frac{3000-317}{3000} = .90$$

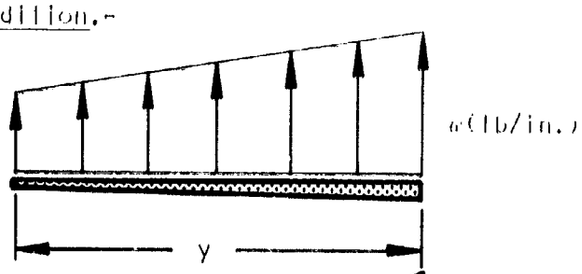
Where W_g Aircraft gross weight = 3000 lbs.

W_w (Wing + contents) 317 lbs.

Wing design, symmetrical flight condition.-

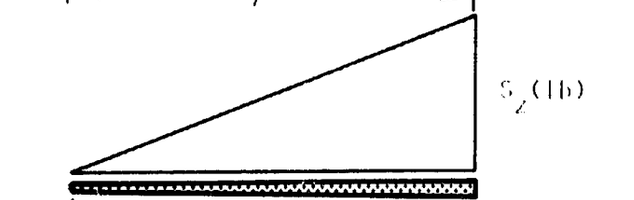
WING RUNING LOAD:

$\omega = \bar{w} \; c \; J_n$



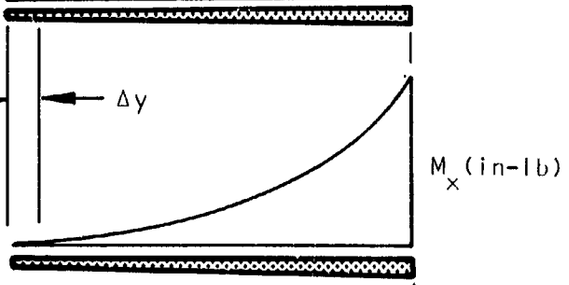
WING BEAM SHEAR:

$S_z = \Sigma \; \omega \; \Delta y$



WING BEAM MOMENT:

$M_x = \Sigma \; S_z \; \Delta y$



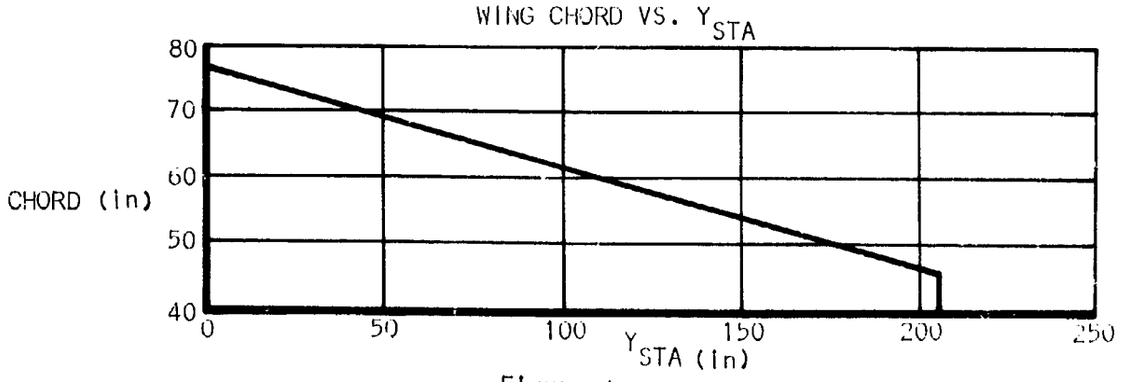
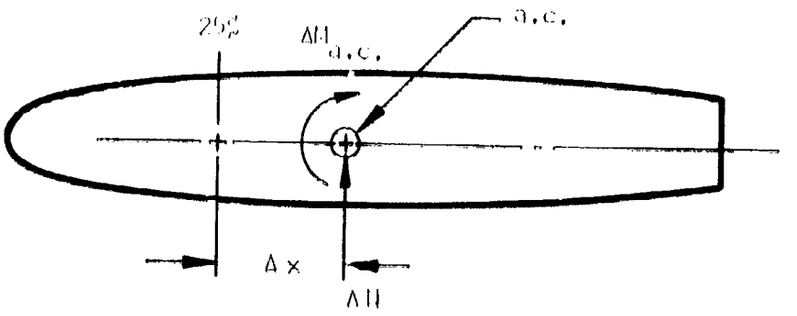


Figure 160

Wing torque @ 25% chord:

(1) Use $C_M = -.03$ based on 63_2215 airfoil; reference 6, page 527.

(2) For the maximum torque conditions the slight contribution from the drag component, ΔD, is neglected.



$$\Delta M_{y_{.25c}} = \Delta M_{ac} - \Delta x\, \Delta N$$

$$= C_M\, \omega \Delta y c - .017c(\omega \Delta y)$$

$$= \omega c \Delta y\, (C_M - .017)$$

$$M_{y_{.25c}} = \Sigma \omega c (C_M - .017)\, \Delta y, \quad C_M = -.03$$

$$= -.047\, \Sigma \omega c \Delta y$$

$$\Delta M_{ac} = C_M\, \omega \Delta y c$$

Where

$$\Delta x = X_{ac} - .25c, \quad X_{ac} = .267c$$

$$= .267c - .25c$$

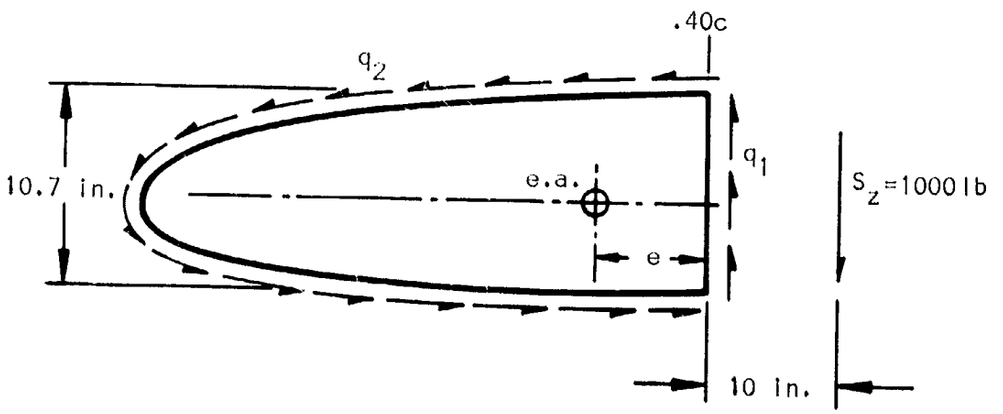
$$= .017c$$

$$\Delta N = \omega \Delta y$$

Wing torque @ Elastic Axis, (e.a.):

(1) For preliminary design purposes assume Elastic Axis outboard of wheel well to be at 40% chord.

(2) Determine e.a. inboard of wing Sta. 65 (thru wheel well).



@ Wing-fuselage intersection:

$\Sigma M_{@\ .40c}$

$q_2\ 2A = 10(1000)$ Where $2A = 2(455-205)$

$= 500\ in^2$ (Ref. Fig. 161)

$\therefore q_2 = \frac{10000}{500} = 20\ lb/in$

ΣS

$hq_1 = S_Z + hq_2$ $h = 10.7$ (Ref. Fig. 162)

$\therefore q_1 = \frac{1000 + 10.7(20)}{10.7} = 114\ lb/in$

$\text{Atwist} = \Sigma \frac{q \cdot L}{t} = \frac{q_1 h}{t_1} + \frac{q_2 L_2}{t_2} - \frac{q_3 h}{t_1} - \frac{q_3 L_2}{t_2} = 0$

Where q_3 is equal to shear flow necessary to restore cell to zero twist.

Assume: $t_1 = 2t_2$; $L_2 = 60.5$ in (scaled); $h = 10.7$ in (Ref. Fig. 162)

$$\text{Atwist} = \frac{114(10.7)}{2t_2} + \frac{20(60.5)}{t_2} - \frac{10.7(q_3)}{2t_2} - \frac{60.5(q_3)}{t_2} = 0$$

$$= 600 + 1210 - 5.35q_3 - 60.5q_3 = 0$$

$$q_3 = \frac{1810}{65.85} = 28\ lb/in$$

$\Sigma M_{@\ .40c}$ using adjusted shear flow:

$eS_z = q_2' 2A$ $q_2' = q_3 - q_2$

$= 28 - 20 = 8\ lb/in$

$e = \frac{8(500)}{1000} = 4\ in$

$c = 72.5$ in @ STA. 24, therefore: $e = \frac{4c}{72.5} = .055c$

$.40c - .055c = .345c$

In the load analysis the elastic axis of the wing inboard of the wheel well bulkhead at Sta. 65 will be assumed at 34.5%c.

From Sta. 213 to 65:

$My = My_{25\%} + S_z \Delta x_{e.a.}$, $\Delta x_{e.a.} = .40c - .25c = .15c$

$= My_{25\%} + .15c\ S_z$

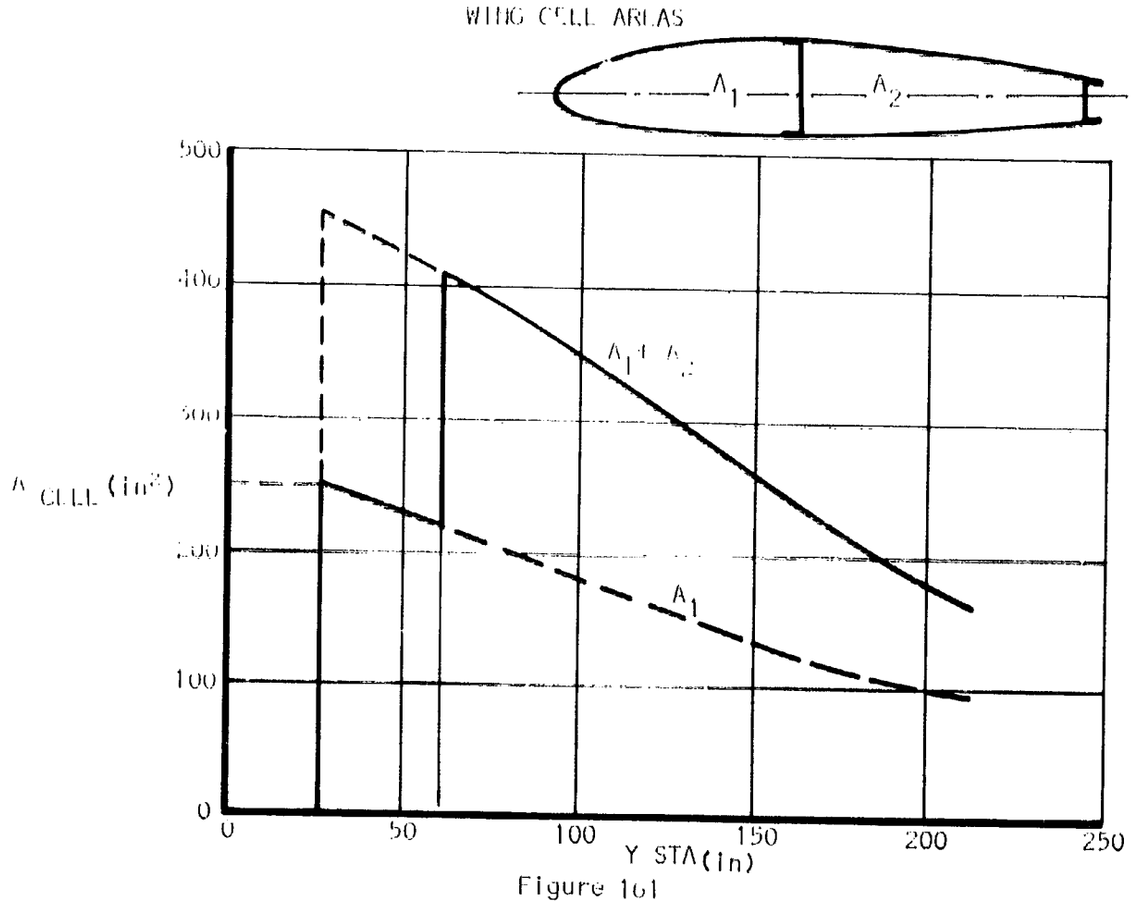


Figure 161

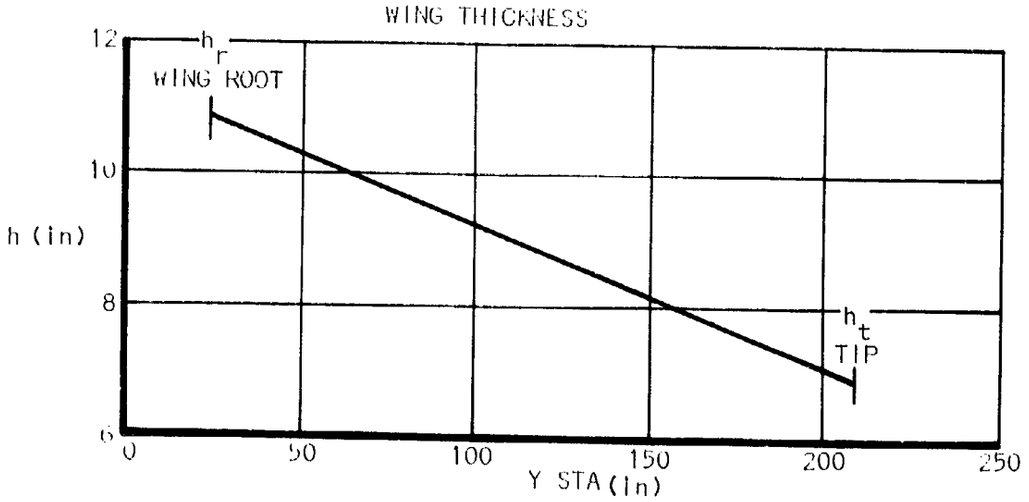
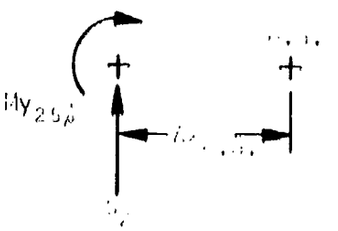


Figure 162

From Sta. 65 to 0:

$$\Delta x_{c.g.s.} = .345c - .25c$$
$$= .095c$$

$$My = My_{25\%} + .095c\ S_z$$



ULTIMATE SHEAR, MOMENT, AND TORQUE
SYMMETRICAL FLIGHT CONDITION

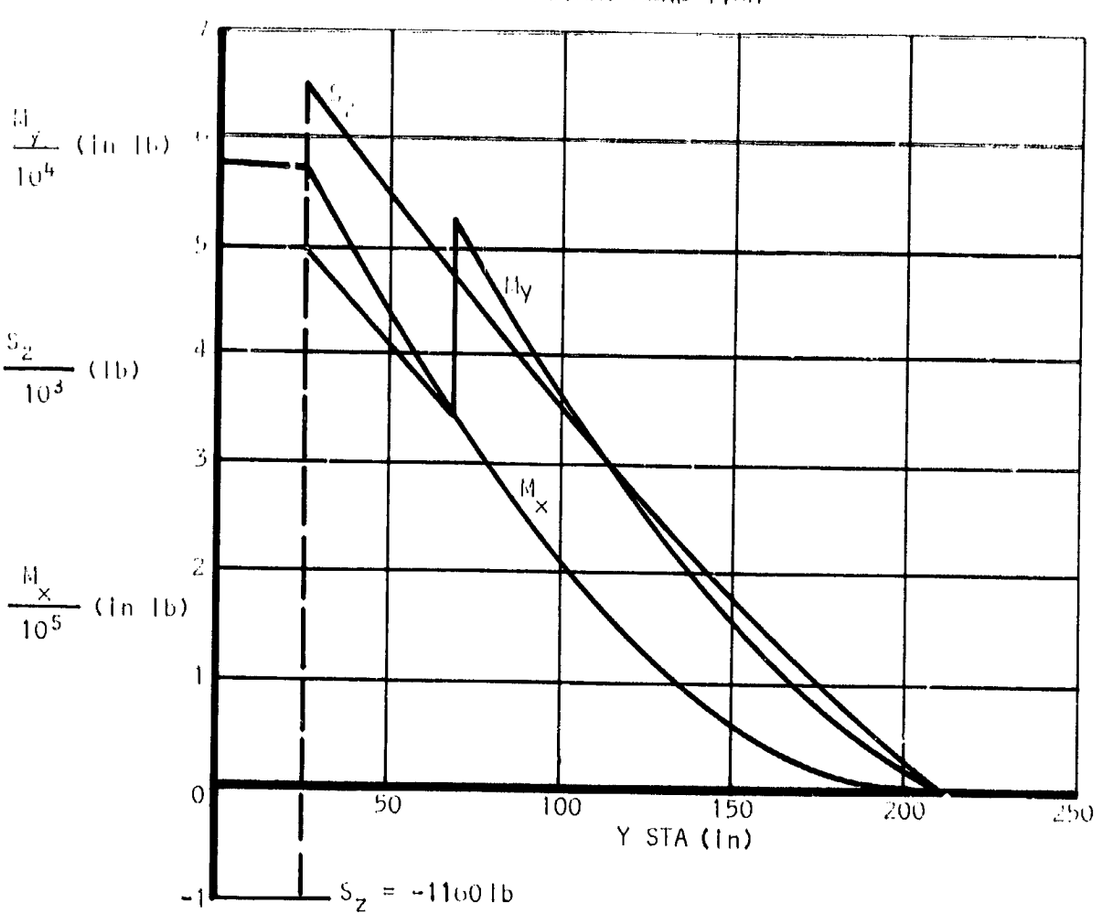


Figure 103

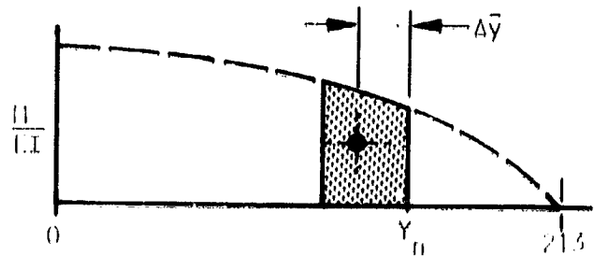
Wing deflections: Determine wing deflection at max. ult. sym. flight condition and at V_{flap}.

V_F = 102 mph Reference page 232

Limit load factor @ V_F, n_{flap} = 2.15g ref. V-n Dia. page 34

n_1 = 3.8g page 232

$\frac{n_{flap}}{n_1} = \frac{2.15}{3.8} = .566$



wing $\delta = \Sigma \frac{M \times \bar{y}}{EI} \Delta y$

where $\frac{M \times \Delta y}{EI} = A_n$

$\bar{y} = y_{ref} - y_n + \Delta\bar{y}$, where y_{ref} = Sta. at which deflection is desired

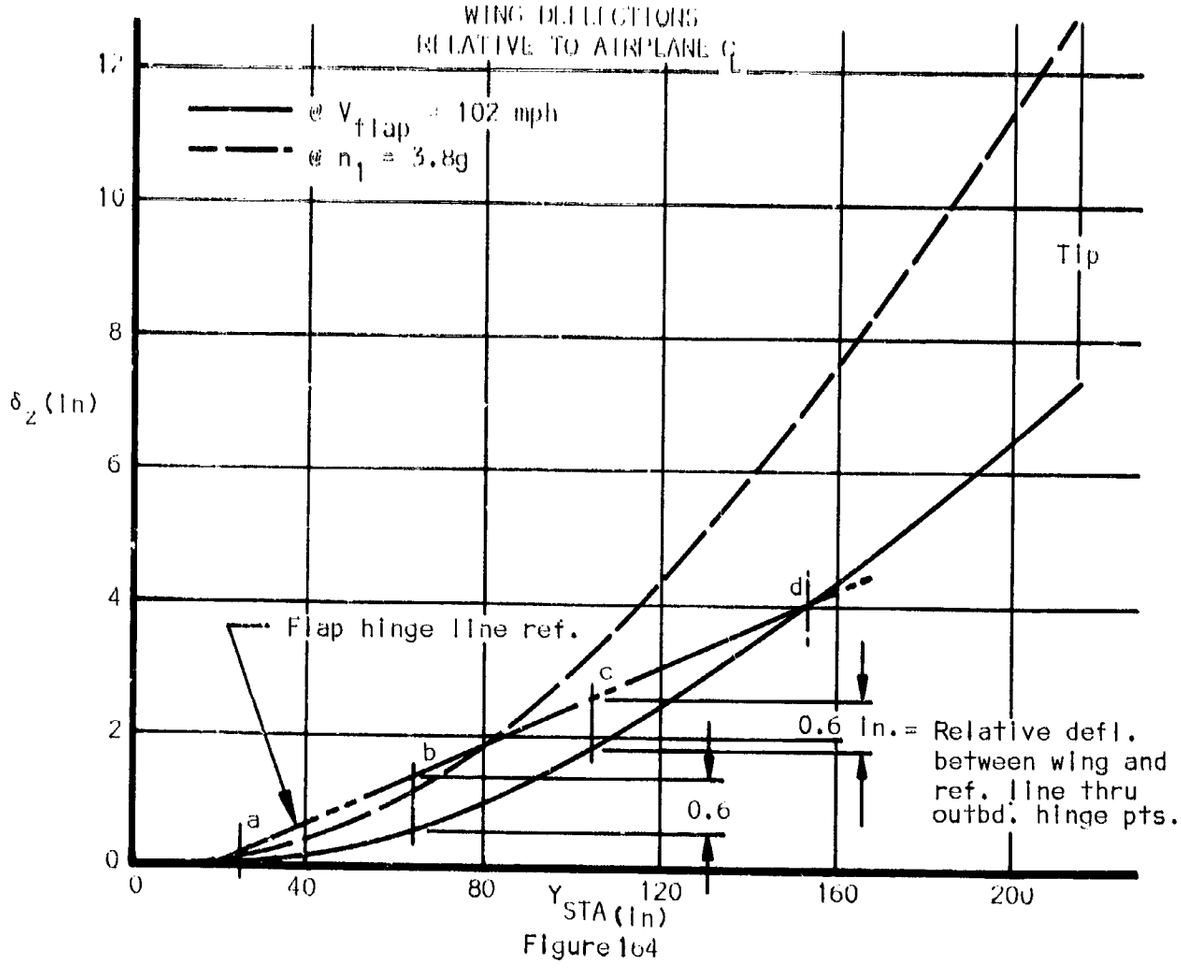


Figure 164

Design unsymmetrical flight condition.- The main spar carry-thru is designed for 100% of the sym. loading on one side and 70% on the other per FAR part 23, Appendix A.

UNSYMMETRICAL WING LOADING

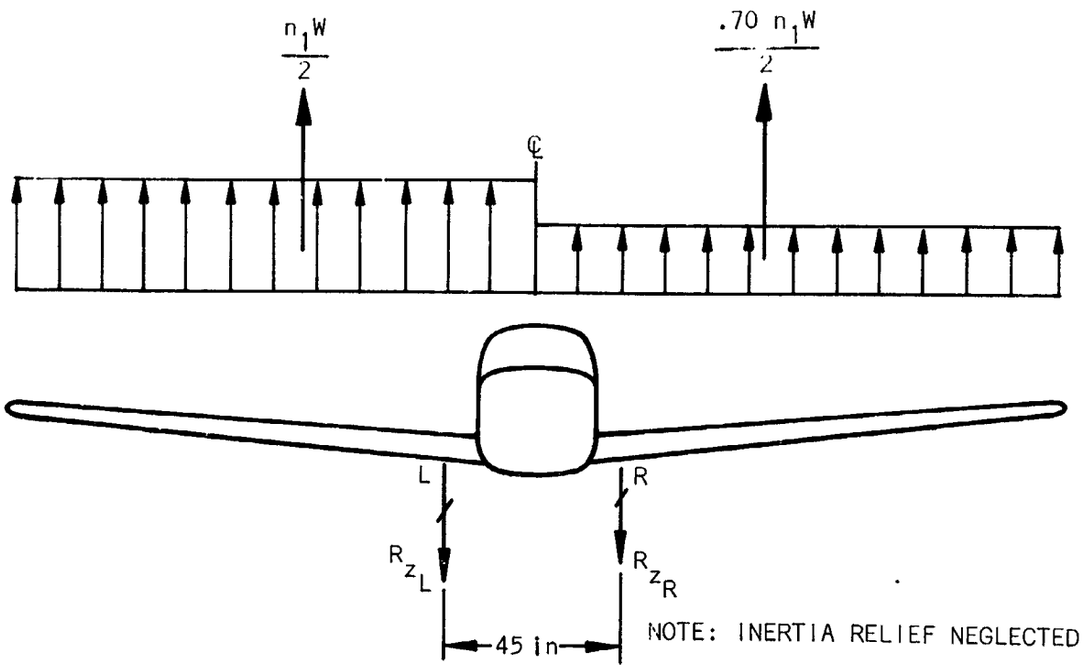


Figure 165

$\bar{y}$ = 97.5 (@MAC)

ult n_1 = 5.7
W = 3000 lb } Ref. pg. 232

$\frac{n_1 W}{2}$ = 8550 lb. , $\frac{.70 n_1 W}{2}$ = 5980 lb

ΣM@R

$$\frac{n_1 W}{2}(\bar{y} + 22.5) - 45R_{z_L} - \left(\frac{.70 n_1 W}{2}\right)(\bar{y} - 22.5) = 0$$

$$8550(120) - 45R_{z_L} - 5980(75) = 0$$

$$R_{z_L} = \frac{577000}{45} = 12800 \text{ lb.}$$

ΣS

$$R_{z_R} = \frac{n_1 W}{2} + \frac{.70\ n_1 W}{2} - R_{z_L}$$

$$= 8550 + 5980 - 12800$$

$$= 1730 \text{ lb}$$

Design landing conditions.-

Parameters:

Limit load factor

n = 3.0 g established
$ult.n$ = 4.5 g
W = 3000 lb. assume max gross wt. for landing config.
$L = \frac{\text{Lift}}{\text{wt.}}$
= .667 Ref. FAR part 23, para. 23.725(b)
V = Descent velocity
= 10 ft/sec ref. FAR part 23, para. 23.473(d)

LANDING LOADS GEOMETRY

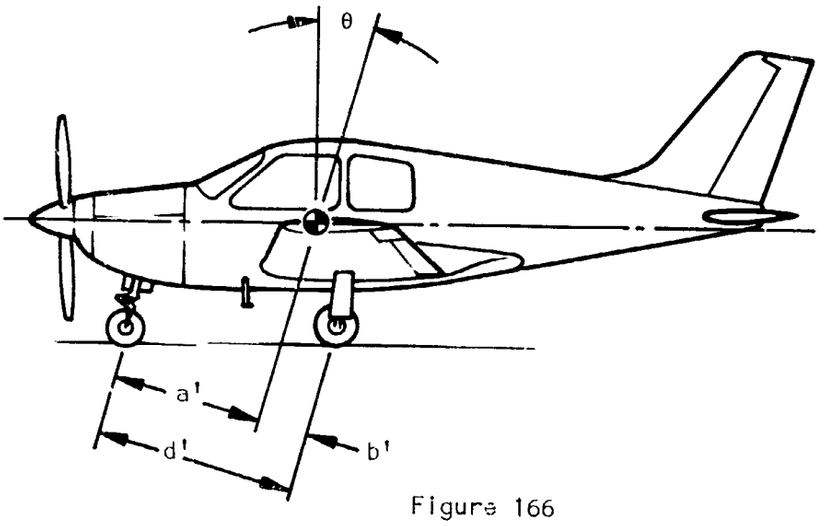


Figure 166

$K = \tan\theta = .25$ { FAR part 23 Appendix C

$a' = 57$ in
$b' = 19$ in
$d' = 76$ in
} Calc.

Basic conditions: Ref. FAR part 23, appendix C

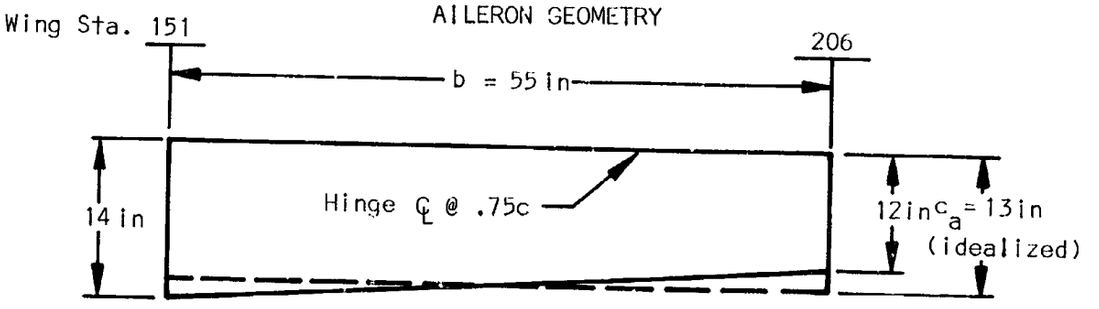
TABLE XXXV
ULTIMATE LANDING LOADS

Item		Level Landing 3 Point	Level Landing 2 point	Tail-Down Landing
Vert. Component @ c.g.		nW = 13500 lb	13500 lb	13500 lb
Fore & Aft Component @ c.g.		KnW = 3380 lb	3380 lb	0
Lateral Component @ c.g.		0	0	0
Main gear Both Wheels	V_r	$\frac{(n-L)Wa'}{d'}$ = 7870 lb	(n-L)W = 10500 lb	(n-L)W = 10500 lb
	D_r	$\frac{KnWa'}{d'}$ = 2535 lb	KnW = 3380 lb	0
Nose gear	V_f	$\frac{(n-L)Wb'}{d'}$ = 2620 lb	0	0
	D_f	$\frac{KnWb'}{d'}$ = 845 lb	0	0

Wing control surface loading conditions.-

Aileron loading : S_{ail} = 715 in^2

AILERON GEOMETRY



Aileron control @ Sta. 151
Aileron support - continuous piano hinge

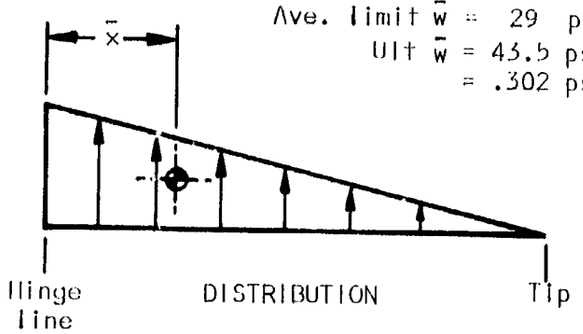
Figure 167

Control surface loading determined from FAR part 23, Appendix A

Ave. limit $\bar{w}$ = 29 psf for $\frac{n_1 W}{S}$ = 62.8 psf

Ult $\bar{w}$ = 43.5 psf

= .302 psi



$$\bar{x} = .33c_a = .33\ (13) = 4.29$$

Net ult. aileron loads:

$$P_{aileron} = \bar{w}\, S_{ail.} \quad , \quad S_{aileron} = 715\ in^2$$

$$= .302(715) = 216\ lb$$

$$\omega/in = c_a \bar{w} \quad , \quad c_a = 13\ lb/in\ , \text{page } 241$$

$$= 13(.302)$$

$$= 3.92\ lb/in$$

$$\max M_y' = b\omega\bar{x} = 55(3.92)(4.29) = 925\ in\text{-}lb$$

Aileron torsional wind-up:

$$\theta = \Sigma\left[\left(\frac{1}{2AG}\right)\left(\Sigma\,\frac{qL}{t}\right)\left(\Delta y\right)\right]_{206}^{151}$$

$$A = \frac{A_{151}+A_{206}}{2} = 23.5\ in^2$$

$$L = 28.8\ in.$$

$$\Delta y = 206-151 = 55\ in.$$

$$q = \left(\frac{M_y}{2}\right)\left(\frac{1}{2A}\right) = \frac{.925}{2(2)(23.5} = 9.8\ lb/in$$

Try 40% glass reinforced nylon 6/10

$$G = .391(10^6)psi \quad \text{Reference page 227}$$

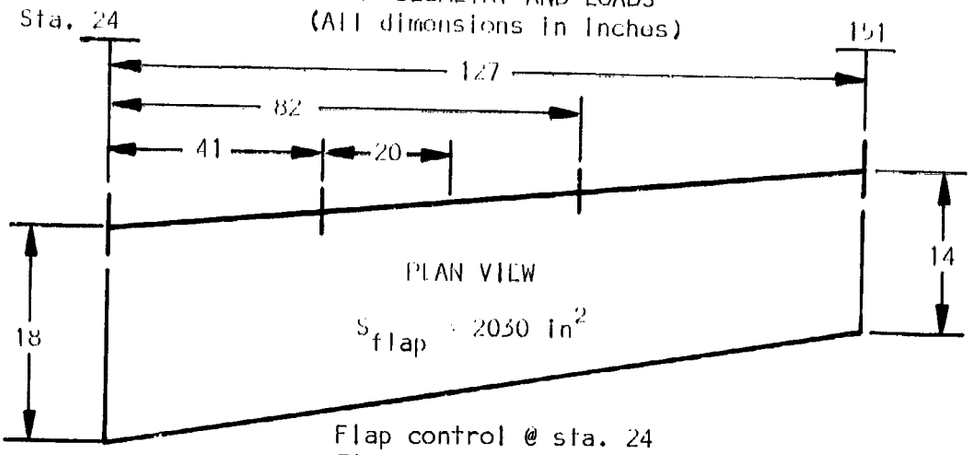
with t = .050

$$v = \left[\frac{1}{2(23.5)(.391)(10^6)}\right]\left[\frac{9.8(28.8)}{.050}\right]\left[55\right] = \frac{15500}{920000} = .0168 \text{ rad.}$$

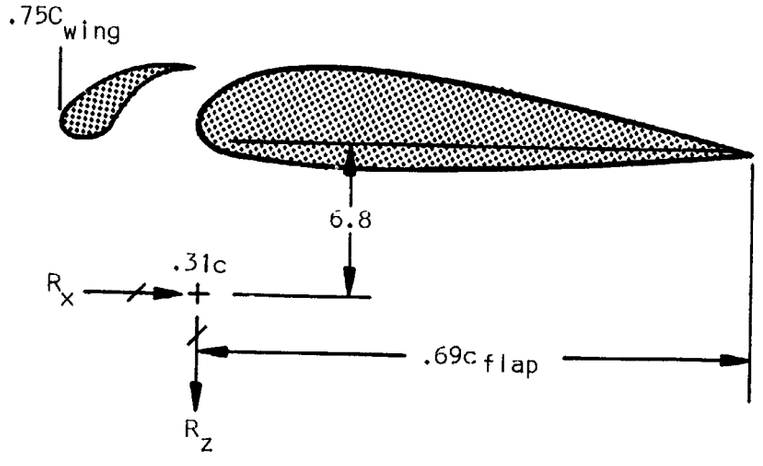
$= 1.0°$

Flap loading(primary) :

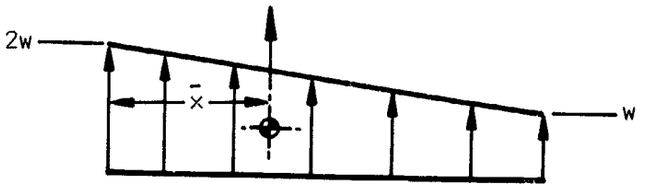
FLAP GEOMETRY AND LOADS
(All dimensions in inches)



Flap control @ sta. 24
Flap supports ~ 4



Load condition per FAR part 23, Appendix A



DISTRIBUTION
Figure 168

Ave. limit $\bar{w}$ = 40 psf for $\frac{n_1 W}{S}$ = 62.8 psf

Reference page 242

ult $\bar{w}$ = 60 psf = .417 psi

$\bar{w} = \frac{2w + w}{2} = 1.5w$, $w = \frac{\bar{w}}{1.5} = \frac{.417}{1.5} = .278$ psi

$2w = 2(.278) = .556$ psi

$\bar{x} = .444c_{flap}$, $\Delta\bar{x} = \bar{x} - x_{attach} = .444c - .31c = .134c$

Reference page 243

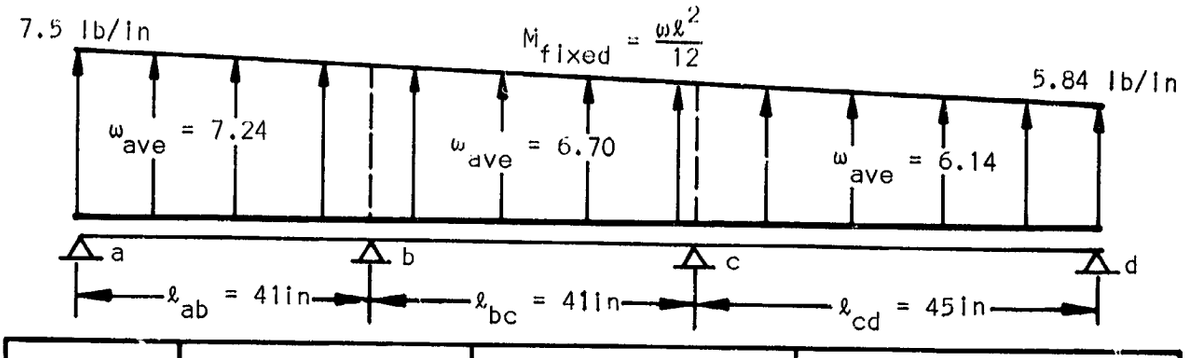
$\omega/in = \bar{w}c_{flap} = .417c_{flap}$

@ Sta. 24, $\omega = .417(18) = 7.5$ lb/in

@ Sta. 151, $\omega = .417(14) = 5.84$ lb/in

TABLE XXXVI

MOMENTS PER MOMENT DISTRIBUTION METHOD USING AVE. ω BETWEEN SUPPORTS.



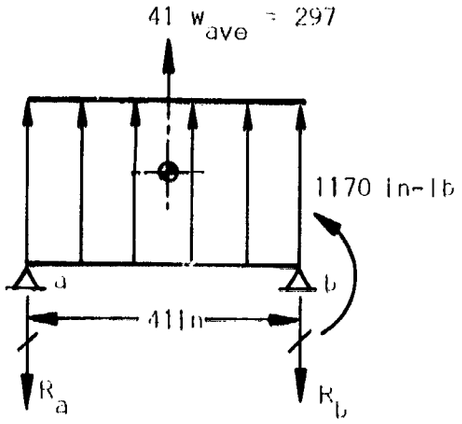
K	0	.50	.50	.52	.48	0
Fixed Moment	1015	1015	937	937	1035	1035
Balance	1015	-39	39	51	-47	-1035
Carry over	20	508	-26	-20	518	24
Balance	-20	-267	267	280	-258	-24
Carry over	134	10	-140	-134	12	129
Balance	-134	-75	75	76	-70	-129
Carry over	38	67	-38	-38	64	35
Balance	-38	-52	52	53	-49	-35
Carry over	26	19	-26	-26	17	24
Balance	-26	-22	22	22	-20	-24
Net Moment	0	1170	1163	1202	1203	0

K: Distribution factor

Support reactions due to airloads:

ΣM @ b (left side)

$$R_{z_a} = \frac{20.5(297) - 1170}{41} = 120 \text{ lb}$$



ΣM @ c (left side)

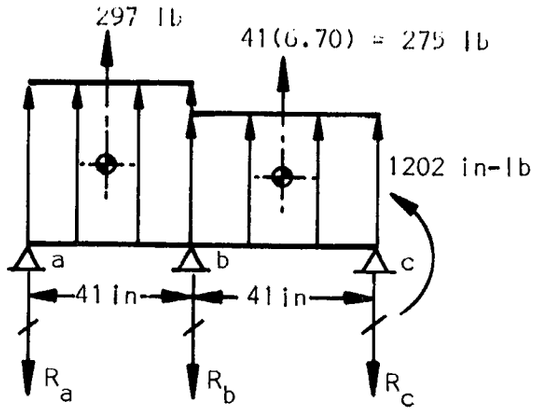
$$R_{z_b} = \frac{61.5(297) + 20.5(275) - 82(120) - 1202}{41}$$

$$R_{z_b} = 313 \text{ lb}$$

ΣM @ c (right side)

$$R_{z_d} = \frac{22.5(276) - 1202}{45} = 111 \text{ lb.}$$

$$R_{z_d} = 111 \text{ lb}$$



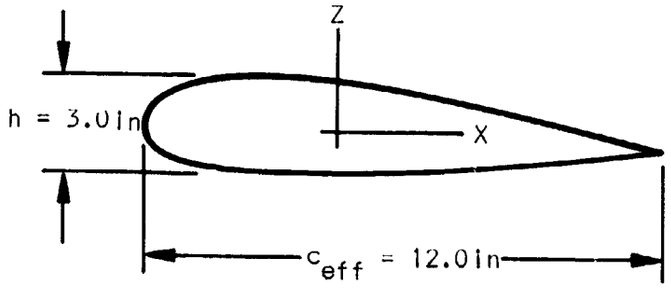
$$R_{z_c} = \Sigma w_{ave} \Delta y - R_{z_a} - R_{z_b} - R_{z_d}$$

$$R_{z_c} = 297 + 276 + 275 - 120 - 313 - 111$$

$$R_{z_c} = 304 \text{ lb}$$

Flap loading (secondary):

The secondary loads generated at the wing-flap hinge line due to wing deflections are based on the following criteria:



1) Flap $I_x = 0.75\ in^4$ } estimated
   Flap $I_z = 9.00\ in^4$

2) Flaps set at 40°

3) Wing deflections for $V_{flap} = 102$ mph given in Fig. 164

Using the criteria with the moment distribution method yields the following ultimate loads, critical at support b

$R_{x_b} = 590$ lb (aft)

$R_{z_b} = 59$ lb (dwn)

$M_{x_b} = 2020$ in-lb (comp. upper surface)

$M_{z_b} = 20300$ in-lb (comp. lead. edge)

Net ult. flap loads:

The resultant flap loading, critical at support b, is presented in Table XXXVII

TABLE XXXVII
NET ULTIMATE FLAP LOADING

LOAD	DUE TO AIRLOADS	SECONDARY	NET
R_{x_b}	0	590 lb	590 lb (aft)
R_{z_b}	313 lb	59 lb	372 lb (dwn)
M_{x_b}	1170 in-lb	2020 in-lb	3190 in-lb compression upper surface
M_{z_b}	0	20300 in-lb	20300 in-lb compression lead. edge

Flap torsional wind-up:

Determine torsional wind-up assuming flap hinge attachments at .31c.

$$M_y = \sum_{151}^{24} \omega\ \Delta\bar{x}\ \Delta y \qquad (\omega \text{ from page } 244)$$

From sta.151 to 106

ω_{ave} = 6.14 lb/in, $\Delta\bar{x}$ = .134 (14.5) = 1.94, Δy = 45 in.

$\omega_{ave}\ \Delta\bar{x}\ \Delta y$ = 6.14 (1.94)(45) = 535 in-lb

From sta. 106 to 65

ω_{ave} = 6.70 lb/in, $\Delta\bar{x}$ = .134(16) = 2.15, Δy = 41 in.

$\omega_{ave}\ \Delta\bar{x}\ \Delta y$ = 6.70(2.15)(41) = 592 in-lb

From sta. 65 to 24

ω_{ave} = 7.24 lb/in, $\Delta\bar{x}$ = .134(17.5) = 2.35, Δy = 41 in.

$\omega_{ave}\ \Delta\bar{x}\ \Delta y$ = 7.24(2.35)(41) = 697 in-lb.

$$M_y = 535 + 592 + 697 = 1824 \text{ in-lb}$$

$$\theta = \Sigma \left[\left(\frac{1}{2AG} \right) \left(\Sigma \frac{qL}{t} \right) (\Delta y) \right]_{151}^{24}$$

where:

$$A = \frac{A_{151} + A_{24}}{2} = 21.8 \text{ in}^2$$

$$L = \frac{L_{151} + L_{24}}{2} = 30.8 \text{ in}$$

$$q = \left(\frac{M_y}{2} \right) \left(\frac{1}{2A} \right) = \frac{1824}{2(2)(21.8)} = 21 \text{ lb/in}$$

Δy = 151 - 24 = 127 in

Use 1" S-glass/epoxy material

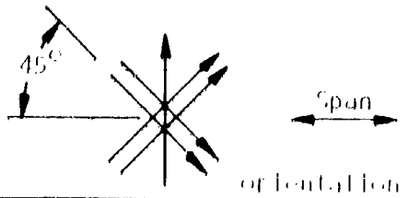
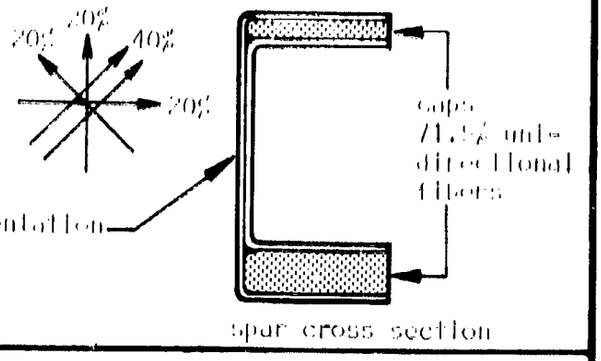
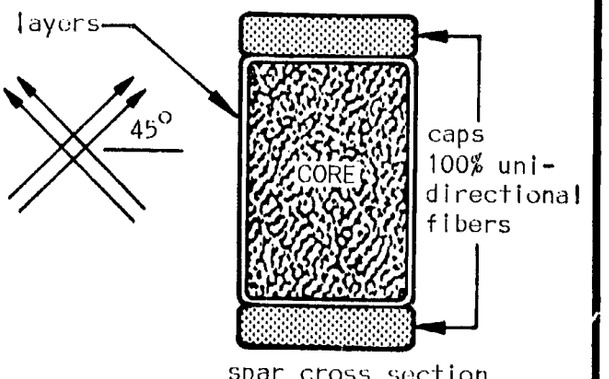
$G = 2.38(10^6)$ psi Reference page 227

with t = .040

$$\theta = \left[\frac{1}{2(21.8)(2.38)(10^6)} \right] \left[\frac{21(30.8)}{.040} \right] [127] = \frac{82\ 200}{4\ 160\ 000} = .0198 \text{ rad.} = 1.1^\circ$$

Wing material/concepts.- Three different material/concepts were considered for the wing. The wing skin and main spar were taken as the variables while the ailerons, flaps, chordwise skin stiffeners, trailing edge spar, auxiliary spar, and wing ribs were held similar for all three material/concept configurations.

TAB - XXXVIII
WING MATERIAL CONCEPTS

Config.	
I	WING SKIN Graphite/epoxy 5-layer laminate  MAIN SPAR Graphite/epoxy Multi-layer constant width caps with variable thickness web 
II	WING SKIN S-glass/epoxy 5-layer laminate  MAIN SPAR S-glass/epoxy Multi-layer constant width caps and constant thickness web around rigid foam or balsa wood core. 
III	Same as Material/Concept II except graphite/epoxy used in place of S-glass/epoxy.

Wing, Material/Concept I.-

Stress analysis of skins, and stiffeners;

Assumptions:

(1) Shear resistance at limit load.
(2) Maintain minimum skin t_{sk} = .040 in. (5 layers).

Material:

Skin - continuous filament Graphite/Epoxy
Stiffeners - 1" S-Glass/Epoxy

Ultimate skin shear stress:

$$q_t = \frac{M_y}{2A}$$

$$f_s = \frac{q_t}{t_{sk}}$$

Ref. Table XXXIX

TABLE XXXIX - ULTIMATE WING SKIN SHEAR STRESS

Wing sta.	M_y in-lb	2A in^2	q_T lb/in	f_s psi
	Fig.163	Fig.161	Fig.169	Fig.172
213	0	-	-	-
185	6270	416	15	375
165	11780	480	25	625
145	18000	540	33	825
125	25500	610	42	1050
105	33700	674	50	1250
85	43000	740	58	1450
65	53800	820	66	1650
	33800	440	77	1930
45	41700	480	87	2180
24	49800	500	100	2500

Ultimate skin shear flow vs. wing station is plotted in Figure 169 for the maximum flight condition.

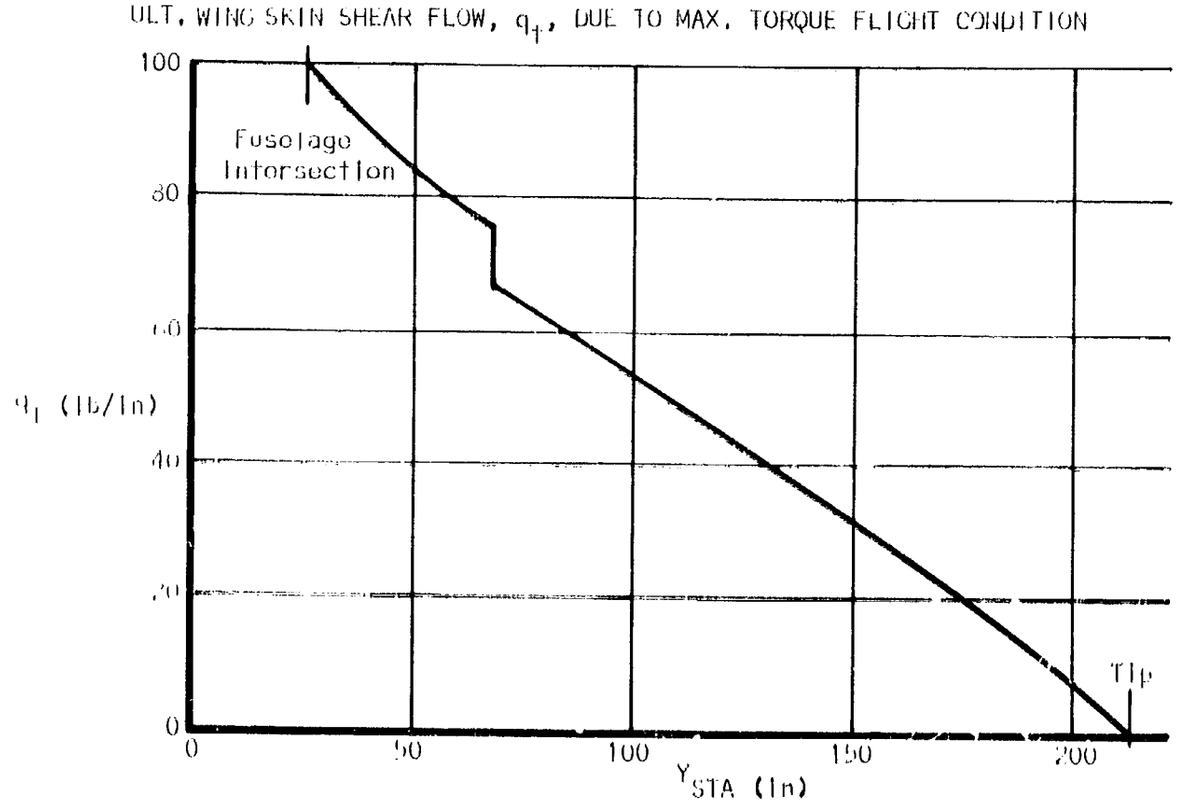


Figure 169

Determine shear buckling allowables, τ_{cr}, for wing skin panels (assume all sides fixed):

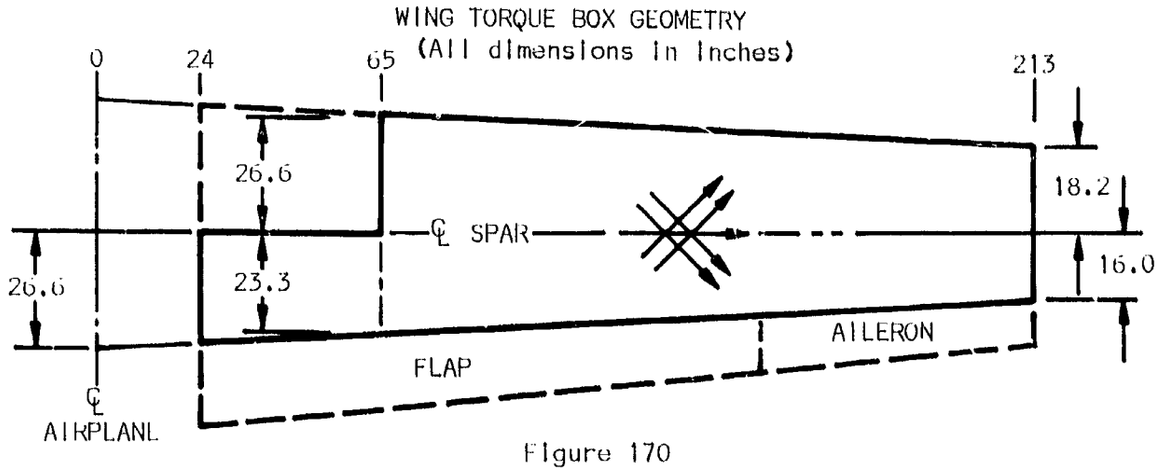
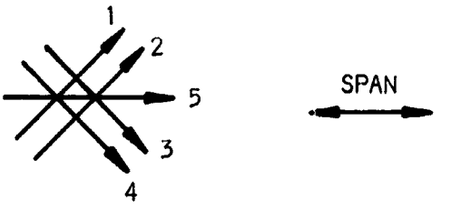


Figure 170

$$\tau_{cr} = \frac{K_s \bar{E}_c t_{sk}^2}{b_{sk}^2}$$

Find $\bar{E}_c$

$$\bar{E} = \frac{\Sigma En}{\Sigma Layers}$$



$$5\bar{E}_c = E_1 + E_2 + E_3 + E_4 + E_5$$

$E_1 = E_2 = 15.4(10^6)$ psi
$E_3 = E_4 = 1.00(10^6)$ psi
$E_5 = 1.48(10^6)$ psi
} Reference Figure 157

$$\bar{E}_c = \frac{[2(15.4) + 2(1.00) + 1.48)]\,[10^6]}{5}$$

$$= 6.86(10^6) \text{ psi}$$

(Stations 24 to 65) with 6-inch stiffener spacing

$$K_s = 9.0 \text{ for } \frac{b}{a} = \frac{6.0}{23.3} = .258 \qquad \text{Ref. Figure 171}$$

$$\tau_{cr} = \frac{K_s \bar{E}_c t_{sk}^2}{b_{sk}^2}, \qquad \bar{E}_c = 6.86\ (10^6) \text{ psi}, \quad t_{sk} = .040 \text{ in.}$$

$$= \frac{9.0(6.86)\ (10^6)\ (.040)^2}{(6.0)^2} = 2750 \text{ psi}$$

Station 65,(outboard) with 8-inch stiffener spacing

$$K_s = 9.2 \text{ for } \frac{b}{a} = \frac{8.0}{26.6} = .30 \qquad \text{Ref. Figure 171}$$

$$\tau_{cr} = \frac{9.2(6.86)\ (10^6)\ (.040)^2}{(8.0)^2} = 1580 \text{ psi}$$

(Station 213) with 8-inch stiffener spacing

$$K_s = 10.0 \text{ for } \frac{b}{a} = \frac{8.0}{18.2} = .44 \qquad \text{Ref. Figure 171}$$

$$\tau_{cr} = \frac{10.0(6.86)\ (10^6)\ (.040)^2}{(8.0)^2} = 1720 \text{ psi}$$

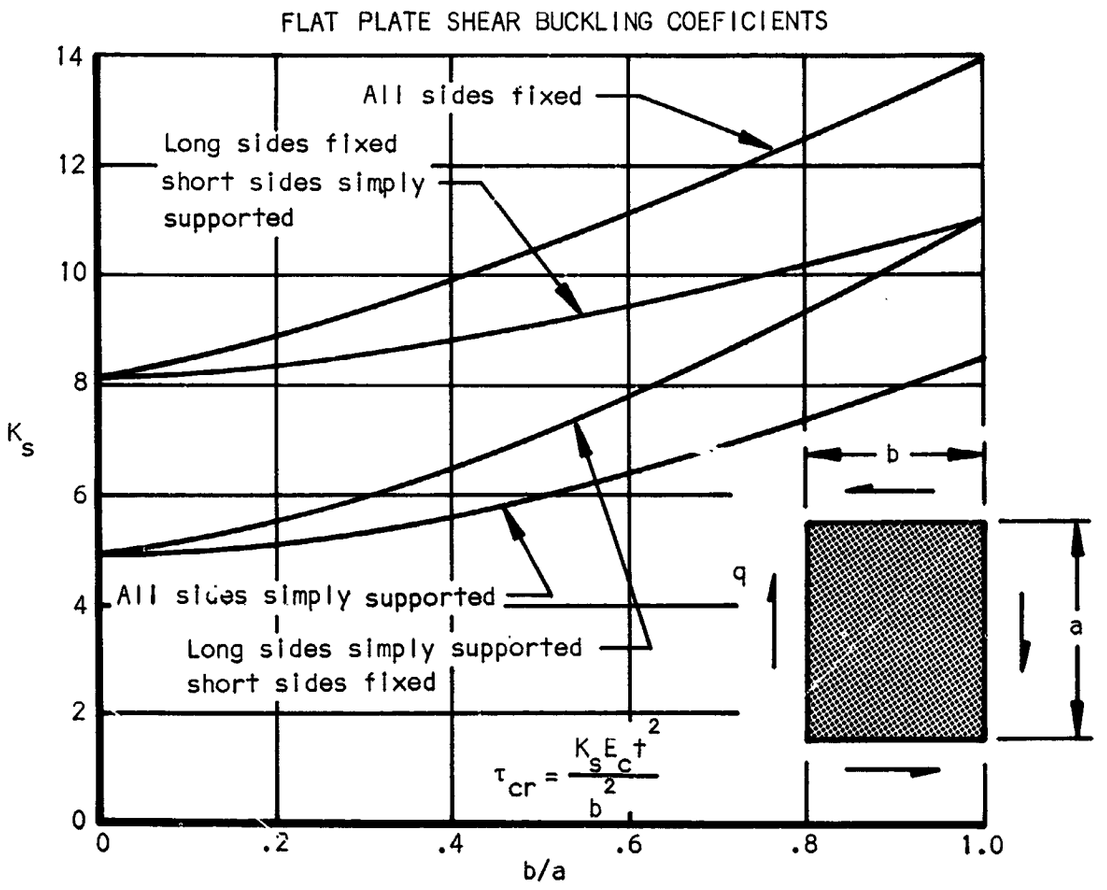


Figure 171

Comparison of actual ultimate skin shear stress with requirement of $\tau_{cr} \geq .667\ f_{s_{ult}}$, reference Figure 172, indicates that the wing is shear resistant for the maximum ultimate torque condition.

(Station 65 critical)

Limit f_s = 1050 psi

τ_{cr} = 1580 psi

Ref. Figure 172

$$\text{Buckling M.S.} = \frac{\tau_{cr}}{f_s} - 1 = \frac{1580}{1050} - 1 = \underline{\underline{+ 0.50}}$$

ULT. WING SKIN SHEAR STRESS VS SHEAR BUCKLING ALLOWABLE

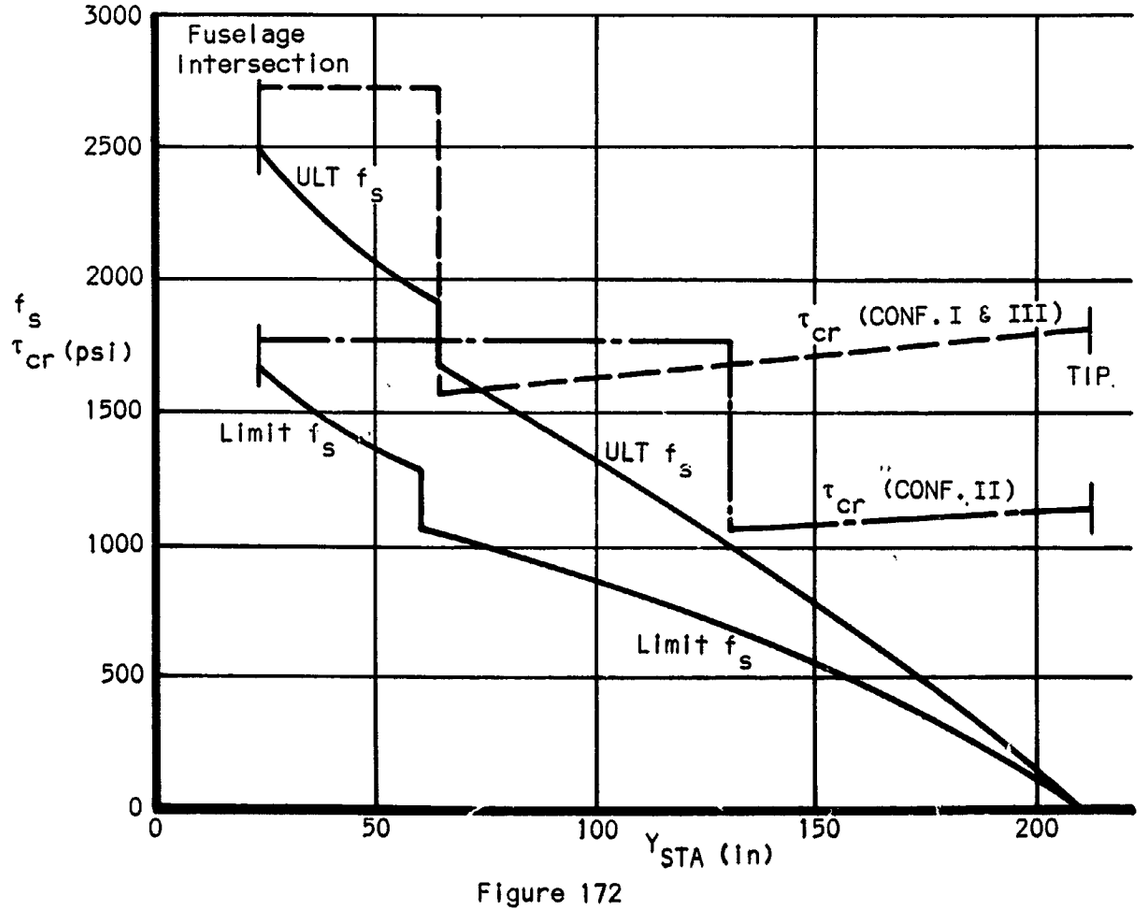


Figure 172

Wing skin stiffeners: Made of non-continuous 1" S-Glass/Epoxy material and analyzed using pressure distribution data from reference 6 . The distribution as shown in Figure 173 is for two different airfoils @ C_L = 1.00. To obtain an idealized normal chordwise pressure distribution for the NACA 63_2-215 airfoil, used in this study, the curves in Figure 173 were averaged. The resulting distribution is presented in Figure 174.

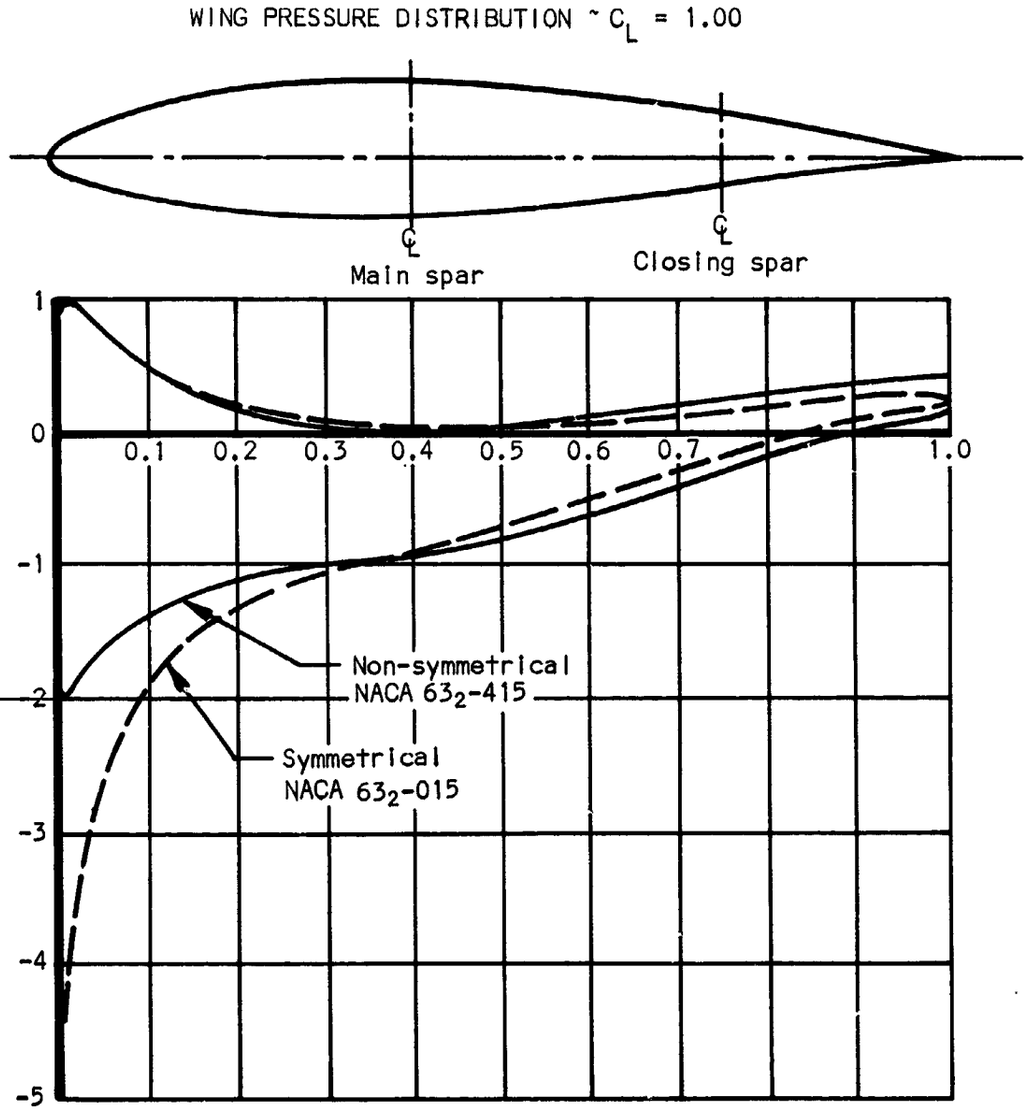


Figure 173

NACA 63_2- 215 AIRFOIL

IDEALIZED NORMAL CHORDWISE PRESSURE DISTRIBUTION

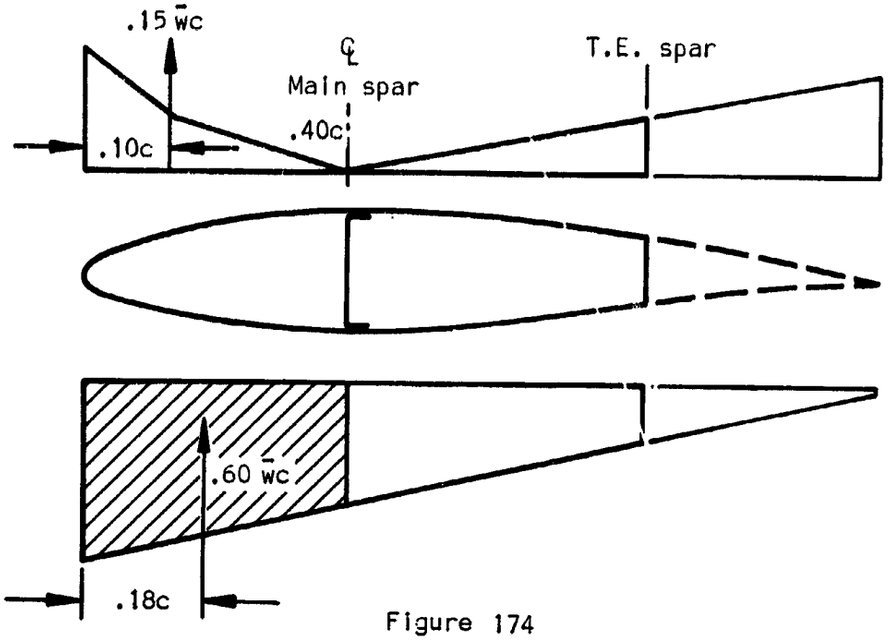


Figure 174

(Critical stiffeners between leading edge and main spar - lower surface @ station 24)

Use .20c in calculating stiffener moment.

$$M_{stiff.} = \frac{W\ell}{8} = \frac{.60\bar{w}c \times \overset{6\text{-in.}}{\text{spacing}} \times .40c}{8}$$

$$= .18\bar{w}c^2 = .18(.654)(5260)$$

$$= 620 \text{ in-lb}$$

Where $\bar{w} = .654$ psi p. 232

$c^2 = (72.5)^2$

$= 5260 \text{ in}^2$

Assume composite section with 2.50 in. of skin effective.

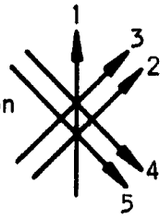
$$f_{b_{element}} = \frac{M_x \, y \, n}{I_{x_{tr}}}$$

Where n = effectiveness factor $= \frac{\bar{E}_{skin}}{\bar{E}_{stiff.}}$

$\bar{E}$ = equivalent E

SKIN FIBER ORIENTATION

$\bar{E}$ is in direction of stiffener



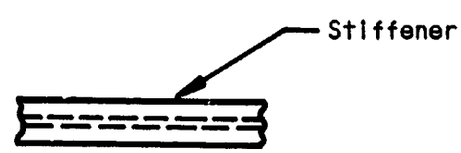


Figure 175

$$\Sigma N_{layers}\ \bar{E} = N_1E_1 + \ldots + N_nE_n$$

Where (Ref. Fig 157):

$$E_1 = 1.00(10^6)\ \text{psi}$$

$$E_2 \text{ thru } E_5 = 1.484(10^6)\ \text{psi}$$

$$\frac{5\bar{E}}{10^6} = 1.0 + 4(1.484)$$

$\bar{E}_{skin} = 1.39(10^6)$ psi; $\bar{E}_{stiff.} = 7.8(10^6)$ psi Ref. Table XXXIV

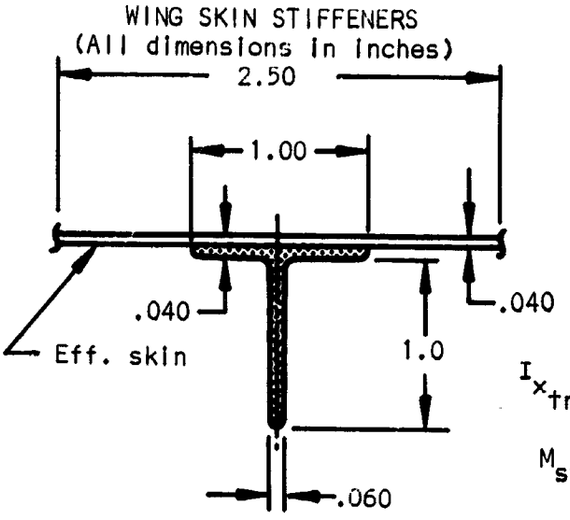


Figure 176

$$n = \frac{\bar{E}_{skin}}{\bar{E}_{stiff.}} = \frac{1.39(10^6)}{7.8\ (10^6)} = .178$$

skin $A_{tr} = nA$; stiff. $A_{tr} = A$

$$\bar{y} = \frac{\Sigma A_{tr}y}{\Sigma A_{tr}} = .32 \text{ in.}$$

$$I_{x_{tr}} = \Sigma A_{tr}y^2 + \Sigma\ I_o - (\bar{y})^2(\Sigma A_{tr}) = .01324\ \text{in}^4$$

$M_{stiff.} = 620$ in-lb Ref. page 255

$$\text{stiff. } f_b = \frac{M\ y}{I_{x_{tr}}} = \frac{620(.76)}{.01324} = 35600 \text{ psi}$$

(outstanding leg critical)

Using 1" S-Glass/Epoxy: $F_{tu} = 45000$ psi Ref. Table XXXIV

$$\text{Stiff. bend. M.S.} = \frac{F_{tu}}{f_b} - 1 = \frac{45000}{35600} - 1 = \underline{+0.26}$$

Leading edge: Check leading edge for ability to support stiffeners and beam loads to wing bulkheads.

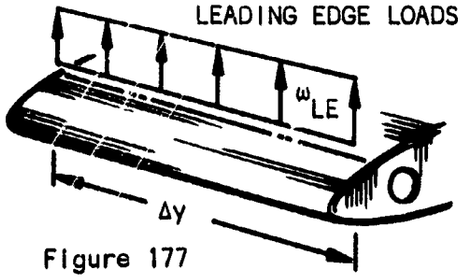


Figure 177

$$\omega_{LE} = \omega_{\text{lower surf.}} + \omega_{\text{upper surf.}}$$

$$\omega_{\text{lower surface}} = \frac{.40c - .18c}{.40c}(.60\bar{w}c) = .330\bar{w}c$$

$$\omega_{\text{upper surface}} = \frac{.40c - .10c}{.40c}(.15\bar{w}c) = .750\bar{w}c$$

$\omega_{LE} = .330\bar{w}c + .750\bar{w}c = 1.080\bar{w}c$, Ref. page 256

And $\bar{w} = .654$ psi $\therefore \omega_{LE} = .706c$

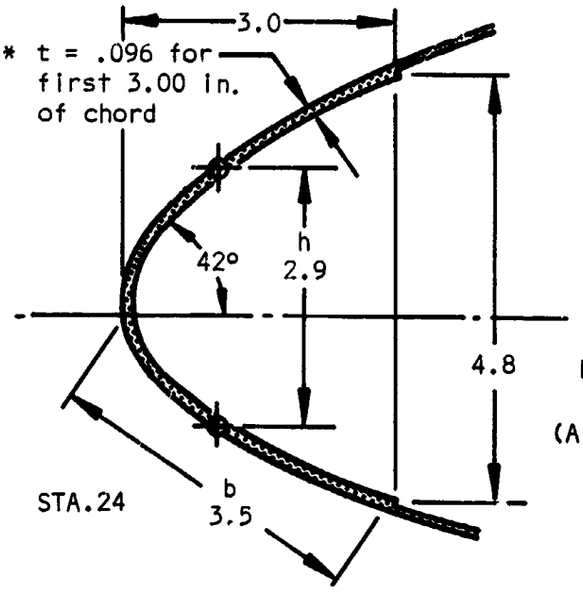
$$M_{max} = \frac{\omega_{LE}(\Delta y)^2}{8} = \frac{.706c(\Delta y)^2}{8} = .0882c\ (\Delta y)^2$$

Bending critical between wing stations 24 and 65

$$M_{max} = .0882(69.5)\ (41)^2 = 10300 \text{ in-lb}$$

Where $\begin{cases} c = 69.5 \text{ in} \\ \Delta y = 41 \text{ in} \end{cases}$

Assume moment reacted as couple between upper and lower cap centroids.



$$P_c = \frac{M_{max}}{h}$$

$h = 2.9$ in. Ref.Fig. 178

$$P_c = \frac{10300}{2.9} = 3550 \text{ lb.}$$

LEADING EDGE GEOMETRY
Figure 178
(All dimensions in inches)

* For Wing/Material Concepts II and III, t = .080 in.

The tension and compression stresses in the critical laminates will be based on the following basic combination of fiber orientation (Ref. p. 255).

LEADING EDGE FIBER ORIENTATION

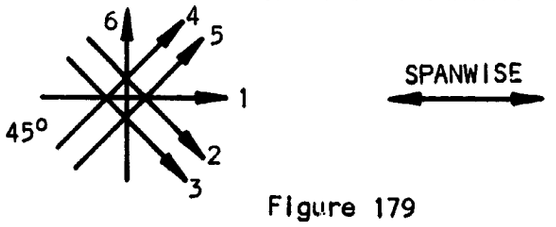


Figure 179

The critical layer is No. 1 since it is unidirectional with the applied couple force, therefore:

$$f_1 = \frac{P_c}{A_1 + A_2\left(\frac{E_2}{E_1}\right) + A_3\left(\frac{E_3}{E_1}\right) + A_4\left(\frac{E_4}{E_1}\right) + A_5\left(\frac{E_5}{E_1}\right) + A_6\left(\frac{E_6}{E_1}\right)}$$

All A's are equal, therefore $A_1 = \frac{tb}{6}$ and:

$$f_t = f_c = \left(\frac{6}{tb}\right)\left(\frac{P_c}{1 + \frac{E_2}{E_1} + \frac{E_3}{E_1} + \frac{E_4}{E_1} + \frac{E_5}{E_1} + \frac{E_6}{E_1}}\right)$$

$$f_t = f_c = \left(\frac{6}{tb}\right)\left(\frac{P_c}{1 + 4(.0914) + .0615}\right)$$

$$= \frac{6\,P_c}{1.428tb} = \frac{4.2\,P_c}{tb} = \frac{4.2(3550)}{.096(3.5)} = 44350\text{psi}$$

Where

$E_1 = 16\ 250\ 000$ psi

$E_2 = E_3 = E_4 = E_5 = 1\ 484\ 000$ psi

$E_6 = 1\ 000\ 000$ psi

$\frac{E_2}{E_1} = \frac{1\ 484\ 000}{16\ 250\ 000} = .0914$

$\frac{E_6}{E_1} = \frac{1\ 000\ 000}{16\ 250\ 000} = .0615$

$F_{cu} = 56500$ psi ; $K_c = 0.80$ (stability)

Compression critical M.S. $= \frac{F_{uN}}{f_c} - 1 = \frac{.80(56500)}{44350} - 1 = +\underline{0.02}$

Stress analysis of main spar:

Assumptions:

(1) Maintain constant 2.00 in. cap width for bonding purposes.
(2) Use a 71.5 percent unidirectional fiber configuration for the cap. This is an estimation as to the optimum arrangement for maintaining adequate shear resistance through the thickness of the spar cap.
(3) Make spar web shear resistant at limit load.

Material:

Continuous filament Graphite/Epoxy spar web: The following combination of fiber directions is assumed for the web remembering that the positive (up) shear condition is twice the negative shear condition. Therefore, twice as many $+45^\circ$ layers are needed as -45° layers for shear resistance.

SPAR WEB FIBER ORIENTATION

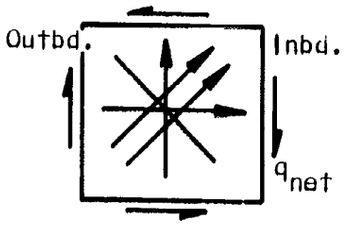


Figure 180

$$\tau_{cr} = \frac{K_s \bar{E}_c t_w^2}{h_w^2} \geq \text{limit } f_s$$

$$= \frac{4.8(6.16)(10^6)t_w^2}{h_w^2}$$

$$= \frac{29.6(10^6)t_w^2}{h_w^2}$$

Where:

$K_s = 4.8$ for $\frac{a}{b} = \infty$

$E_c = 15.4(10^6)$ psi

$\bar{E}_c = \frac{2E_c}{5} = \frac{2(15.4)(10^6)}{5}$

$= 6.16\ (10^6)$ psi

(Assuming 2 out of 5 layers effective in +45° direction.)

Also,

$$\tau_{cr} = \frac{q_{net}}{t_w} = \frac{29.6(10^6)t_w^2}{h_w^2}$$

And,

$S_{web} = S_z - S_r$

S_r = shear relief due to taper

$$= 2\left(\frac{M_x}{h_f}\right) \tan\theta$$

$$\tan\theta \left(\frac{h_r - h_t}{2}\right)\frac{2}{b} = .0107$$

$$S_r = 0.0214\ \frac{M_x}{h_f}$$

Therefore,

$$S_{web} = S_z - .0214\ \frac{M_x}{h_f}$$

The required spar web thickness vs. wing station is presented in Figure 183

Where:

$$t_w = \left(\frac{q_{net}\ h_w^2}{29.6(10^6)}\right)^{1/3}$$

$$q_{net} = \frac{S_{web}}{h_w} + q_t$$

$h_w = .90h$ (Ref. Figure 162

q_t, (Ref. Figure 169

$h_r = 11.35$, $h_t = 6.80$ } Ref. Figure 162

$b = 426$ Ref. Figure 159

M_x Ref. Figure 163

$h_f = .95h$ Ref. Figure 162

SPAR WEB GEOMETRY

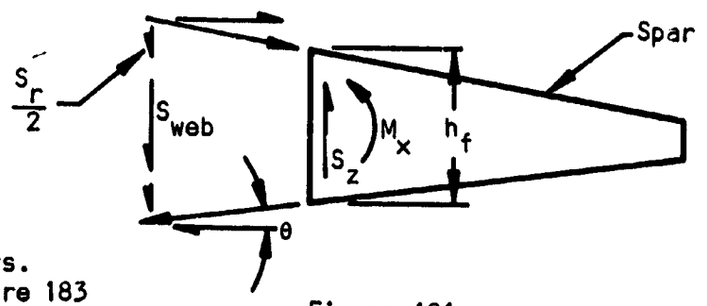


Figure 181

WING SPAR WEB, NET ULTIMATE SHEAR FLOW

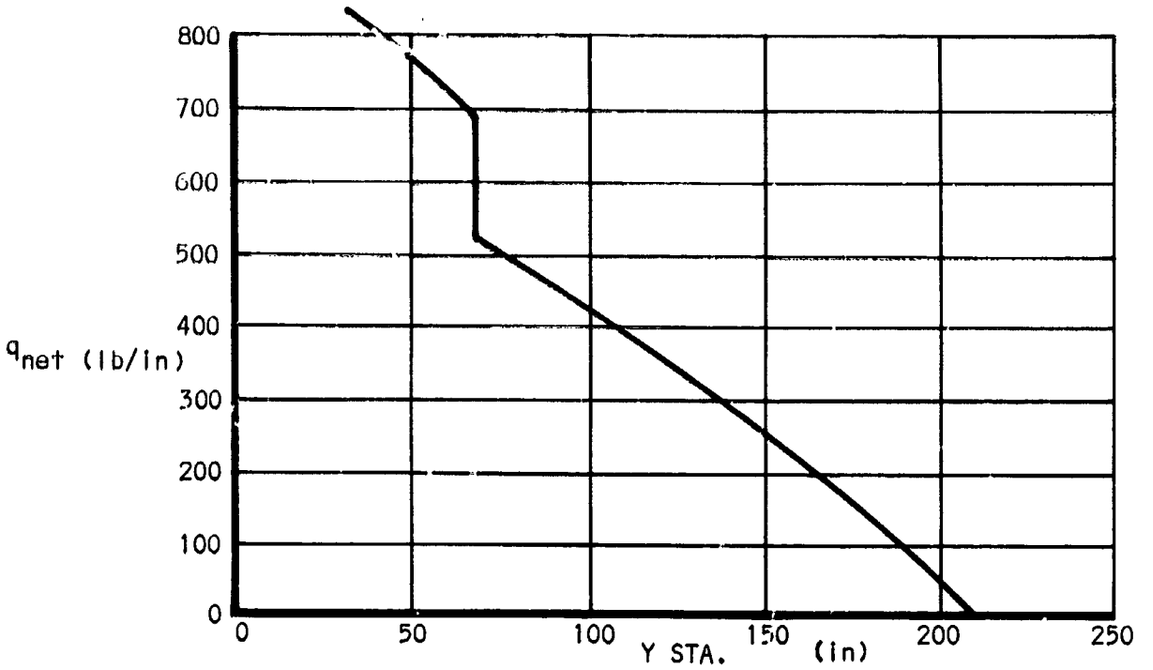


Figure 182

WING SPAR WEB THICKNESS- MATERIAL/CONCEPT I

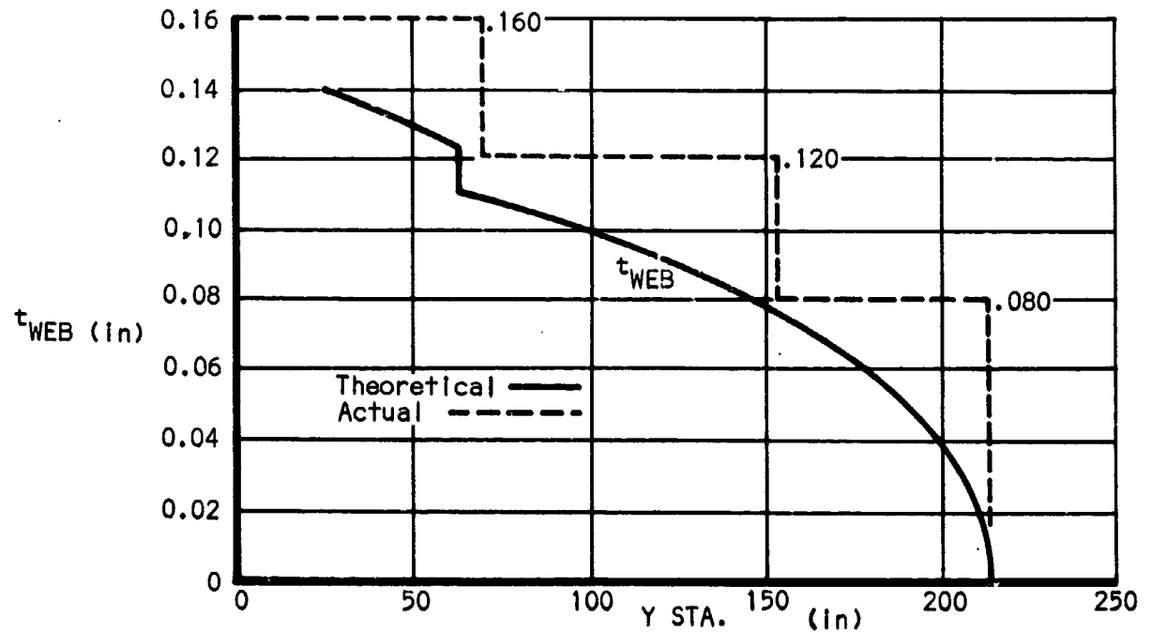


Figure 183

Spar flange (composite section): During spar bending a portion of the wing skin laminate and the wrap-around layers of the spar web together with the spar web are all effective. In the following analysis they will be treated as composite elements using the basic flange cap as the base material.

$$f_{b_{element}} = \frac{M_x\, y\, n}{I_{x_{tr}}} \qquad n = \text{effectiveness factor} = \frac{\bar{E}_{element}}{\bar{E}_{base\ material}}$$

$\bar{E}$ = equivalent E for each element = $\dfrac{N_1E_1 + \ldots + N_nE_n}{\Sigma N}$, N = layers in each direction

$I_{x_{tr}} = \Sigma A_{tr}y^2 + \Sigma I_{o_{tr}}$, assuming equal flanges top and bottom.

Skin element (assume 5.00 in. eff. width)

$$\frac{\bar{E}}{10^6} = \frac{4E_1 + E_5}{5} = \frac{4(1.484) + 1.00}{5}$$

$\bar{E} = 1.39(10^6)$ psi

E_1 thru $E_4 = 1.484(10^6)$ psi
$E_5 = 1.00(10^6)$ psi
} Ref. Figure 157

SKIN ELEMENT FIBER ORIENTATION

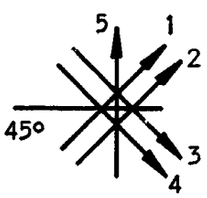


Figure 184

For the cap element,

$\bar{E} = 12.2(10^6)$ psi Ref. Figure 155 (For 71.5% unidirectional fibers)

For the web element,

SPAR WEB ELEMENT FIBER ORIENTATION

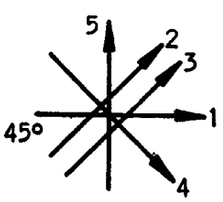


Figure 185

$$\frac{\bar{E}}{10^6} = \frac{E_1 + 3E_2 + E_5}{5}$$

$$= \frac{16.25 + 3(1.484) + 1.00}{5}$$

$\bar{E} = 4.34(10^6)$ psi

For the skin splice element

$$\frac{\bar{E}}{10^6} = \frac{2E_1 + 4E_3 + 2E_7}{8}$$

$$= \frac{2(16.25) + 4(1.484) + 2(1.00)}{8}$$

$$\bar{E} = 4.93(10^6) \text{ psi}$$

SKIN SPLICE FIBER ORIENTATION

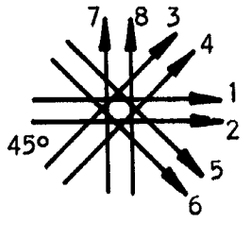


Figure 186

TABLE XL - EFFECTIVENESS FACTORS, n

Element	$\bar{E}$	n
Skin	$1.39(10^6)$	.114
Splice	$4.93(10^6)$	.404
Web	$4.34(10^6)$	.356
Cap	$12.2\ (10^6)$	1.000

$$n = \frac{\bar{E}_{element}}{\bar{E}_{cap}}$$

cap = base material

$$A_{tr} = An$$

COMPOSITE SECTION @ STA. 24
(All dimensions in inches)

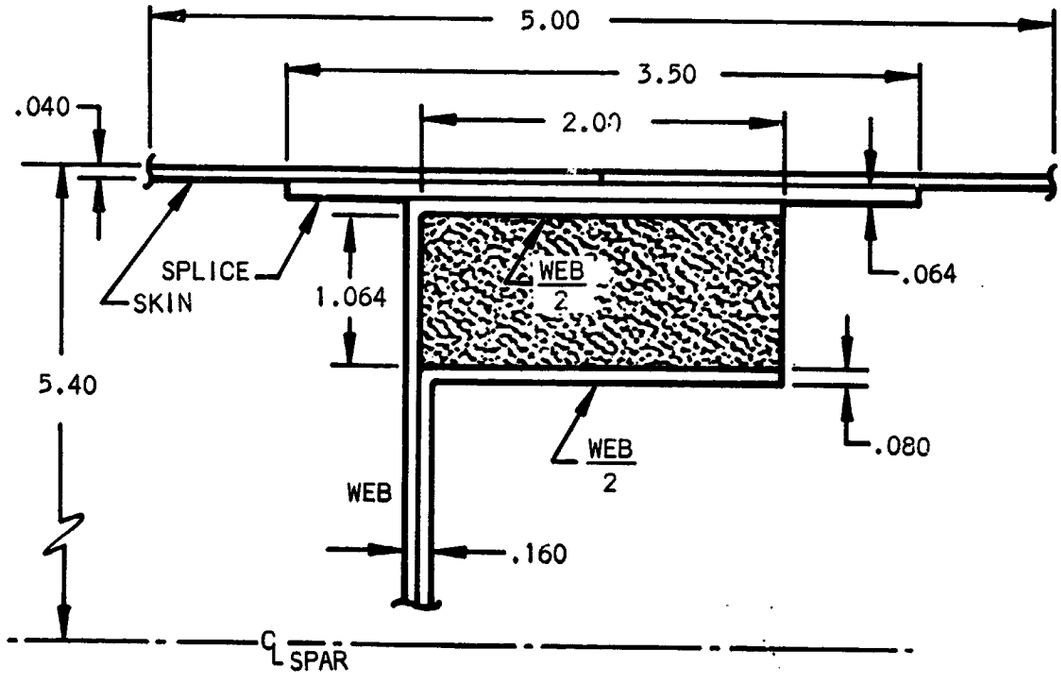


Figure 187

$I_{x_{tr}} = 110.288 \text{ in}^4$

Check bending stress, Reference Figure 187 and Table XL for y and n, respectively.

$$f_b = \frac{M_x \, y \, n}{I_{x_{tr}}} = \frac{568000 \, y \, n}{110.288} = 5150 \, y \, n$$

TABLE XLI - MAIN SPAR MARGINS OF SAFETY

Element	f_b	$K_t F_{tu}$	$K_c F_{cu}$	M.S. Tension	M.S. Comp.
Effective skin	3150	3850	24000	+ 0.22	+ High
Skin Splice	11100	16800	29600	+ 0.52	+ High
Web	9700	14000	28800	+ 0.43	+ High
Cap	26800	49000	39200	+ 0.83	+ 0.46

Notes:

(1) $M.S. = \frac{KF}{f_b} - 1$ for ten., $K_t = 0.70$ fatigue factor

for comp., $K_c = 0.80$ stability factor

(2) F_{tu} and F_{cu} obtained from Figures 155 and 157 by using the element E as a reference ordinate.

Shear stress @ spar $\mathcal{L}$

$$f_s = \frac{V \, Q_{tr}}{I_{x_{tr}} b} = \frac{V \, \Sigma(A_{tr} y)}{I_{x_{tr}} b}$$

$$= \frac{847(11.8990)}{.160(110.288)} = 5700 \text{ psi}$$

$V = q_{net} \, h_w = 874(9.70) = 8470$ lb.

$h_w = .90h$, Ref. Figures 162 and 182

$\Sigma A_{tr} y = 11.8990 \text{ in}^3$

$b = .160$ in Ref. Figure 183

Use rule of mixtures to determine F_{su}

$$F_{su_{web}} = \frac{\Sigma F_{su_n} \, tn}{\Sigma t_n}$$ Where n = individual layer

$F_{su_1} = F_{su_4} = 5200$ psi

$F_{su_2} = F_{su_3} = 17800$ psi

$F_{su_5} = 2800$ psi

Figure 157

COMPOSITE SECTION STA 24
FIBER ORIENTATION

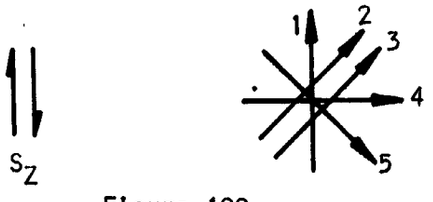


Figure 188

$$F_{su_{web}} = \frac{2(5200) + 2(17800) + 2800}{5} = 9760 \text{ psi}$$

$$\text{web M.S.} = \frac{F_{su}}{f_s} - 1 = \frac{9760}{5700} - 1 = +\underline{0.72}$$

Spar cap thicknesses were determined at wing stations 75 and 125 maintaining similar margins of safety to those calculated at station 24.

The resulting required spar cap thicknesses versus wing station are shown in Figure 189, along with the actual thicknesses ultimately used in the design. Since the spar was generally tension critical, the compression flange thickness was decreased in order to save weight. The reduction in moment of inertia was offset by the reduction in distance from the neutral axis to tension flange, thereby positive margins were maintained in tension.

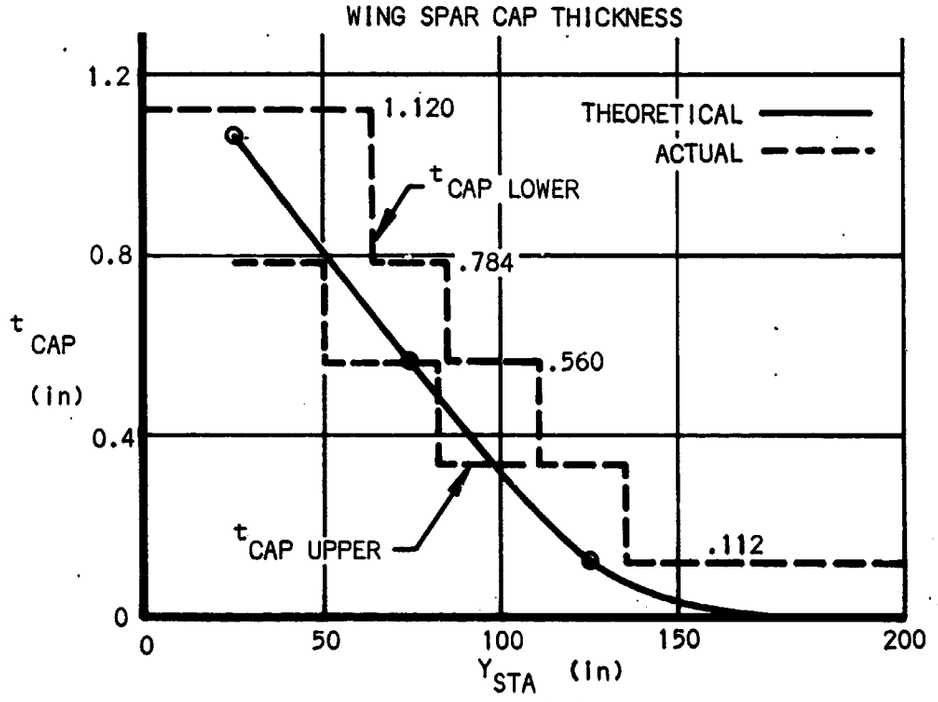


Figure 189

Stress Analysis Closing Spar:

Material:

Non-continuous filament 1" S-Glass/Epoxy.

CLOSING SPAR GEOMETRY

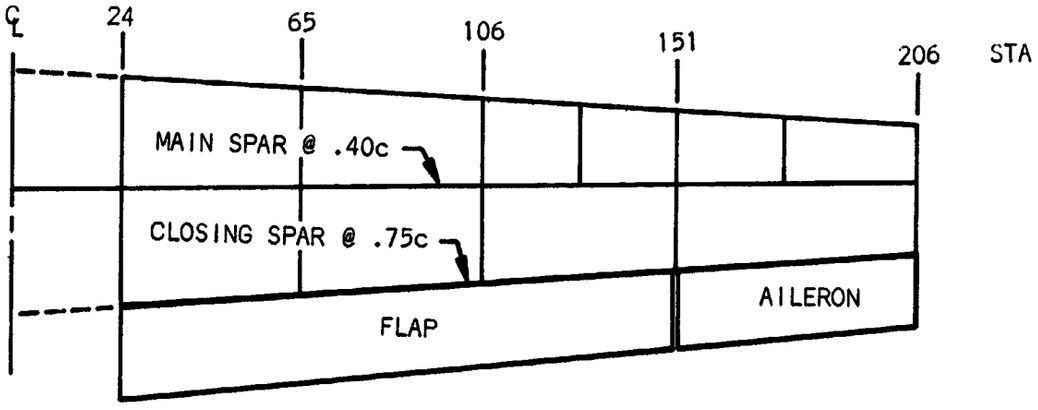


Figure 190

Closing spar flange: The flange is critical inboard of station 151 for basic airloads plus wing-flap deflection secondary loading.

M_{x_b} = 3190 in-lb., Ref. Table XXXVII

$$P_c = \frac{M_{x_b}}{h_f} = \frac{3190}{4.7} = 680 \text{ lb.}$$

$$f_t = f_c = \frac{P_c}{bt} = \frac{680}{1.0(.063)} = 10800 \text{ psi}$$

F_{tu} = 45000 psi
F_{cu} = 61000 psi
} Ref. p. 227

K_c = .80
K_t = .70
} Ref. p. 263

EFFECTIVE SECTION
CLOSING SPAR
(All dimensions in inches)

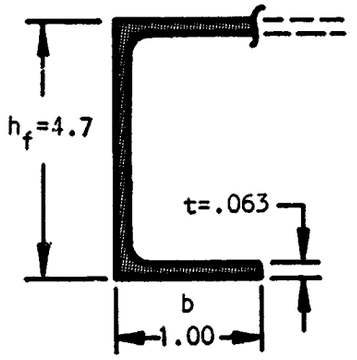


Figure 191

$$\text{Tension critical M.S.} = \frac{K_t F_{tu}}{f_t} - 1 = \frac{.70(45000)}{10800} - 1 = \underline{+ 1.91}$$

Closing spar web: Web gage determined to be .051 by inspection.

Wing - Fuselage Main Attachment, stress analysis:

Unsymmetrical flight condition critical:

S_{z_L} = 12800 lb (Ref. p.239; $S_{z_L} = R_{z_L}$)

$S/bolt = \frac{12800}{4} = 3200$ lb.

The attachment is critical for bearing where it is assumed that the fuselage bulkhead made of 1" S-Glass and the Graphite/Epoxy spar web have equivalent bearing allowables.

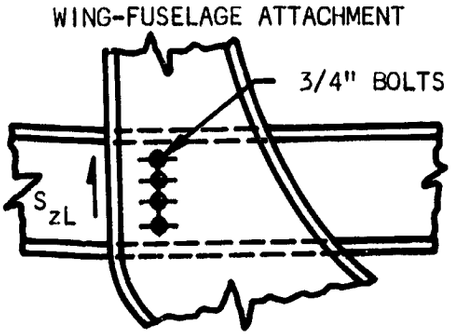


Figure 192

In order to determine required t, use K_{br} = 2.0; F_{bru} = 22000 psi (Ref. p. 227)

$$\frac{F_{bru}}{K_{br}} = \frac{S}{Dt_{req}}$$

$$t_{req} = \frac{SK_{br}}{F_{bru}\,D} = \frac{3200\,(2.0)}{22000(.75)} = 0.388 \text{ in.}$$

Main Spar Splice, stress analysis:

Flanges; Symmetrical flight condition critical

P_c = 57500 lb.

F_{bru} = 22000 psi

$P_{allow} = Dt\,F_{bru}$

= 625(1.00)(22000)

= 13750 lb/bolt

Use 7 bolts to maintain a margin of safety of over + 0.50.

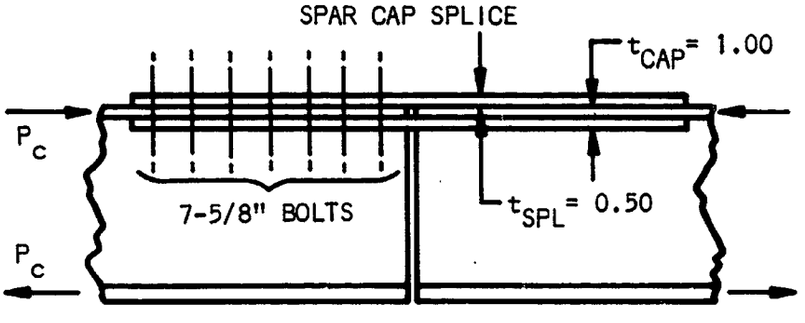


Figure 193

$$M.S. = \frac{\Sigma P_{allow}}{P_c} - 1$$

$$= \frac{7(13750)}{57500} - 1 = +\underline{0.68}$$

Web; Unsymmetrical flight condition critical:

$S_{z_{Q_L}}$ = 4300 lb ; Use 1/2" dia. bolts

(Critical bolt loads)

$$P_z = \frac{S_z}{4} = \frac{4300}{4} = 1075 \text{ lb.}$$

$$P_y = \frac{Mz}{\Sigma z^2} = \frac{4300(1.0)(4.0)}{2[(4)^2 + (1.33)^2]}$$

$$= 1075 \text{ lb}$$

$$P_r = \left(P_z^2 + P_y^2\right)^{1/2} = 1180 \text{ lb.}$$

(Bearing critical) (F_{bru} = 22000 psi)

$$f_{br} = \frac{P_r}{Dt} = \frac{1180}{.50(.160)} = 14750 \text{ psi ;}$$

$$M.S. = \frac{F_{bru}}{f_{br}} - 1 = \frac{22000}{14750} - 1 = \underline{+0.49}$$

SPAR WEB SPLICE
(All dimensions in inches)

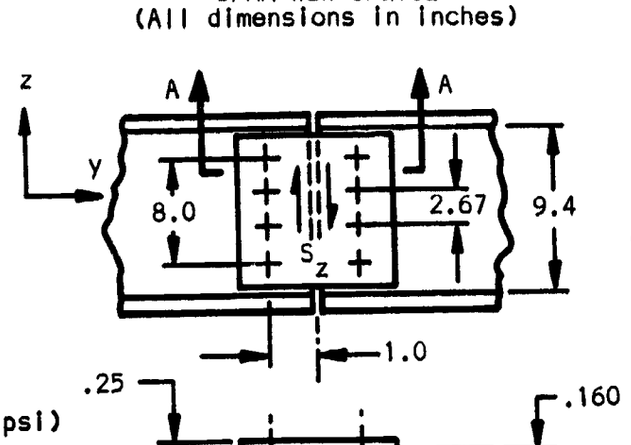


Figure 194

Wing, Material/Concept II.-

Stress analysis of skins and stiffeners:

Assumptions: (1) Shear resistance at limit load.
(2) Maintain minimum skin t_{sk} = .040 in (5 layers).

Material: Skins - continuous filament S-Glass/Epoxy.
Stiffeners - 1" S-Glass/Epoxy.

Ultimate skin shear stress: same as Material/Concept I (Ref. page 249)

Shear buckling allowables

$$\tau_{cr} = \frac{K_s \bar{E} t_{sk}^2}{b_{sk}^2}$$

$$5\bar{E}_c = E_1 + E_2 + E_3 + E_4 + E_5$$

$$E_1 = E_2 = 7.6(10^6) \text{ psi}$$

$$E_3 = E_4 = 2.2(10^6) \text{ psi}$$

$$E_5 = 2.27(10^6) \text{ psi}$$

$$\bar{E}_c = \frac{[2(7.6) + 2(2.2) + 2.27][10^6]}{5} = 4.37(10^6) \text{ psi}$$

SKIN FIBER ORIENTATION

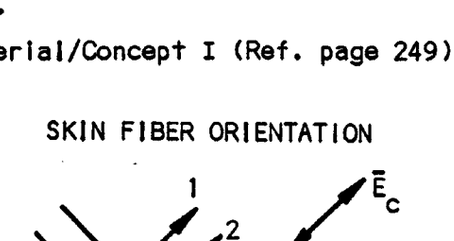


Figure 195

The τ_{cr} vs. wing station was calculated in similar fashion to the material/concept I procedure on page 250 except for the change in $\bar{E}_c$. Reference Figure 172 for a plot of the values.

Figure 172 indicates that the wing is shear resistant for the maximum limit torque condition.

(Sta. 24 critical)

limit f_s = 1670 psi

τ_{cr} = 1750 psi

Ref. Figure 172

$$\text{Buckling M.S.} = \frac{\tau_{cr}}{f_s} - 1$$

$$= \frac{1750}{1670} - 1 = + \underline{0.05}$$

Wing skin stiffeners: Same as Material/Concept I.

Leading edge: Assumed effective section on page 257.

$$f_1 = \frac{P_c}{4A_1 + 6A_5\left(\frac{E_5}{E_1}\right)} \; ; \; A_1 = \frac{tb}{10} \; , \; A_1 = A_5 \; ;$$

Therefore:

$$f_t = f_c = \left(\frac{10}{tb}\right)\left[\frac{P_c}{4 + 6\left(\frac{E_5}{E_1}\right)}\right]$$

$$f_t = f_c = \left(\frac{10}{.080(3.5)}\right)\left[\frac{3550}{4 + \left(6\,\frac{2.2}{7.8}\right)\left(\frac{10^6}{10^6}\right)}\right]$$

= 22300 psi

Compression critical M.S

$$= \frac{120000}{22300} - 1 = + \text{high}$$

LEADING EDGE FIBER ORIENTATION

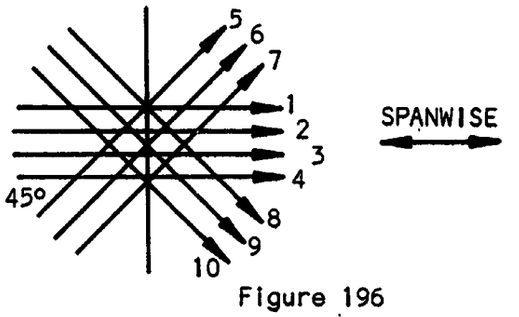


Figure 196

t = 0.080 in. ; E_1 = 7.8(10⁶) psi

b = 3.4 in. ; P_c = 3550 lb (Ref. p. 257)

E_5 = 2.2(10⁶)psi

F_{cu} = 120 000 psi

K_c = .80 stability factor

Stress analysis of main spar:

Assumptions:

(1) Maintain constant 2.00 in. cap width for bonding purposes.
(2) Use a 100% unidirectional fiber configuration for the cap.
(3) Form spar web around a 2.5 lb/ft³ rigid urethane foam block to maintain its shear resistance and also to provide for an adequate flange to web shear transfer area.

Spar flange and web (composite section): The spar flange will be analyzed as a composite section following the methods, on pages 261 thru 264, used for the Material/Concept I member. (Material: Continuous filament S-Glass/Epoxy).

Skin element, (assume 5.00 in. effective width):

E_1 thru E_4 = 2.20(10^6) psi
E_5 = 7.80(10^6) psi
} Ref. Fig. 158

$$\frac{5\bar{E}}{10^6} = 4E_1 + E_5 = 4(2.20) + 7.80$$

$$\bar{E} = 3.32(10^6) \text{ psi}$$

SKIN FIBER ORIENTATION

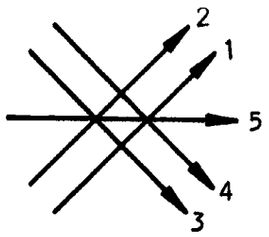


Figure 197

Skin splice element:

E_1 thru E_4 = 2.2(10^6) psi
E_5 & E_6 = 1.95(10^6) psi
E_7 & E_8 = 7.8(10^6) psi
} Ref. Fig. 158

SKIN SPLICE FIBER ORIENTATION

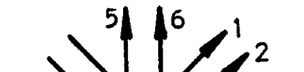


Figure 198

$$\frac{8\bar{E}}{10^6} = 4E_1 + 2E_5 + 2E_7 = 4(2.20) + 2(1.95) + 2(7.8)$$

$$\bar{E} = 3.54(10^6) \text{ psi}$$

Cap element: 100% unidirectional

$\bar{E}$ = 7.8(10^6) psi Ref. Fig.158

WEB FIBER ORIENTATION

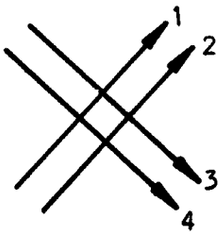


Figure 199

Web element:

E_1 thru E_4 = 2.20(10^6) psi

TABLE XLII - EFFECTIVENESS FACTORS, n

Element	$\bar{E}$	n
Skin	3.32(10^6)	.426
Splice	3.54(10^6)	.454
Web	2.20(10^6)	.282
Cap	7.80(10^6)	1.000

$$n = \frac{\bar{E}_{element}}{\bar{E}_{cap}}$$

$\Sigma A_{tr} y = 5.318 \text{ in}^3$; $I_{x_{tr}} = 56.360 \text{ in}^4$

COMPOSITE SECTION @ STA 24
(All dimensions in inches)

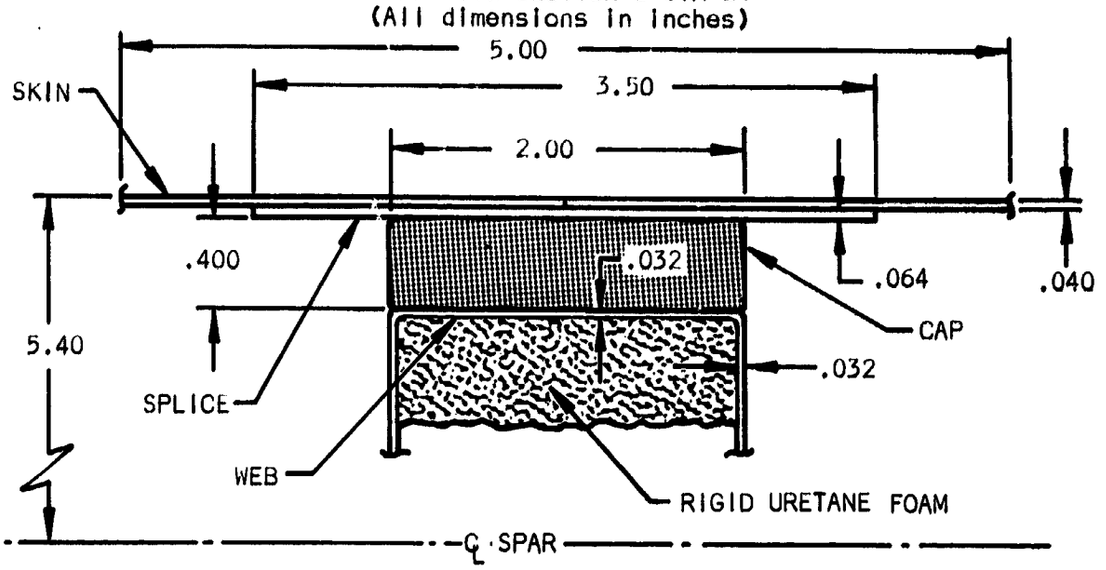


Figure 200

Check bending stress:

$$f_b = \frac{M_x\ y\ n}{I_{x_{tr}}} = \frac{568\ 000\ y\ n}{56.360} = 10100\ y\ n \qquad M_x = 568\ 000\ \text{in-lb}$$

TABLE XLIII - MAIN SPAR MARGINS OF SAFETY

Element	f_b	$K_t F_{tu}$	$K_c F_{cu}$	M. S. Tension	M. S. Comp.
Effective skin	23100	27300	44800	+ 0.18	+ 0.95
Skin Splice	24300	31500	47200	+ 0.30	+ 0.94
Cap	53500	147000	96000	+ 1.75	+ 0.80

Ref. notes on p. 263

Shear stress @ spar ℄ :

$$f_s = \frac{V\ \Sigma(A_{tr}y)}{I_{x_{tr}}\ b} = \frac{8470(5.318)}{56.360(.064)} = 12500\ \text{psi}$$

Where:

$\Sigma A_{tr}y = 5.318\ \text{in}^3$

$b = .064$ in

$V = q_{net}h_w = 8470$ lb.

$F_{su} = 50000$ psi

$$\text{Web M.S.} = \frac{50000}{12500} - 1 = \underline{+\ \text{high}}$$

The resulting main spar cap and web thicknesses for the Material/Concept II configuration are presented in figure 201 and 202.

WING SPAR CAP THICKNESS-MATERIAL/CONCEPT II

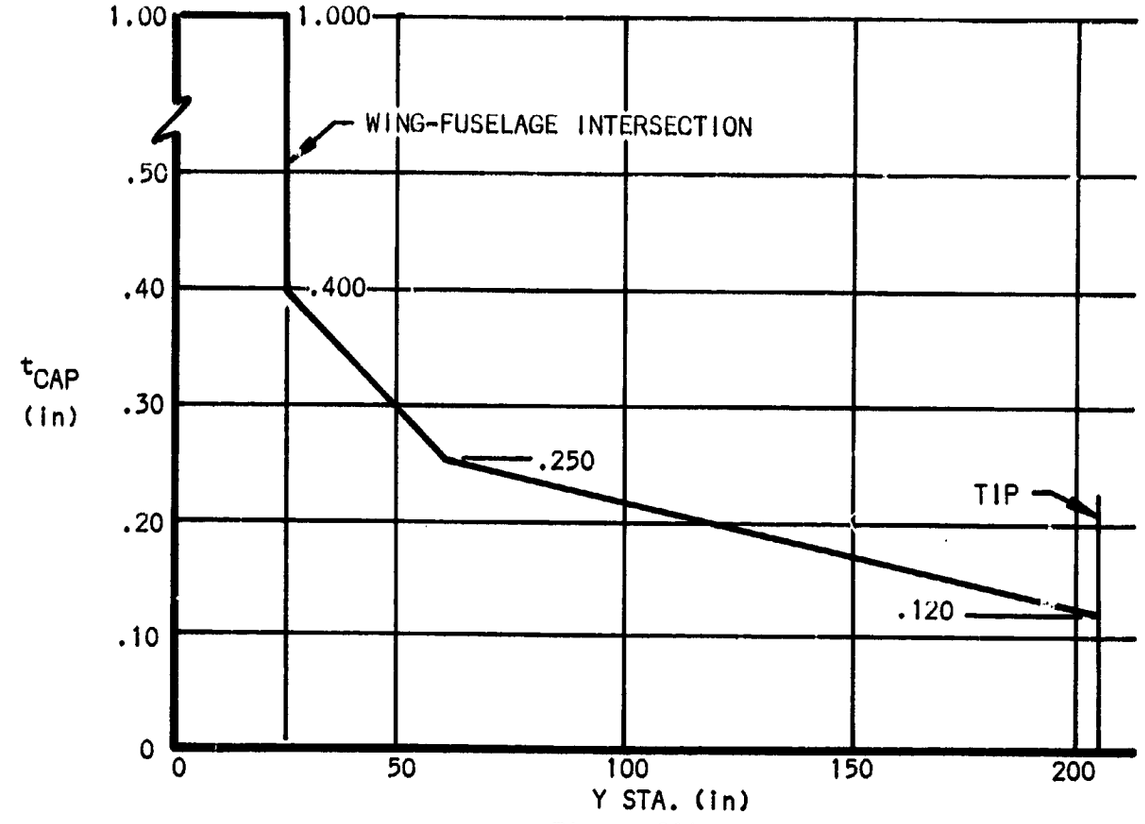


Figure 201

WING SPAR WEB THICKNESS-MATERIAL/CONCEPT II

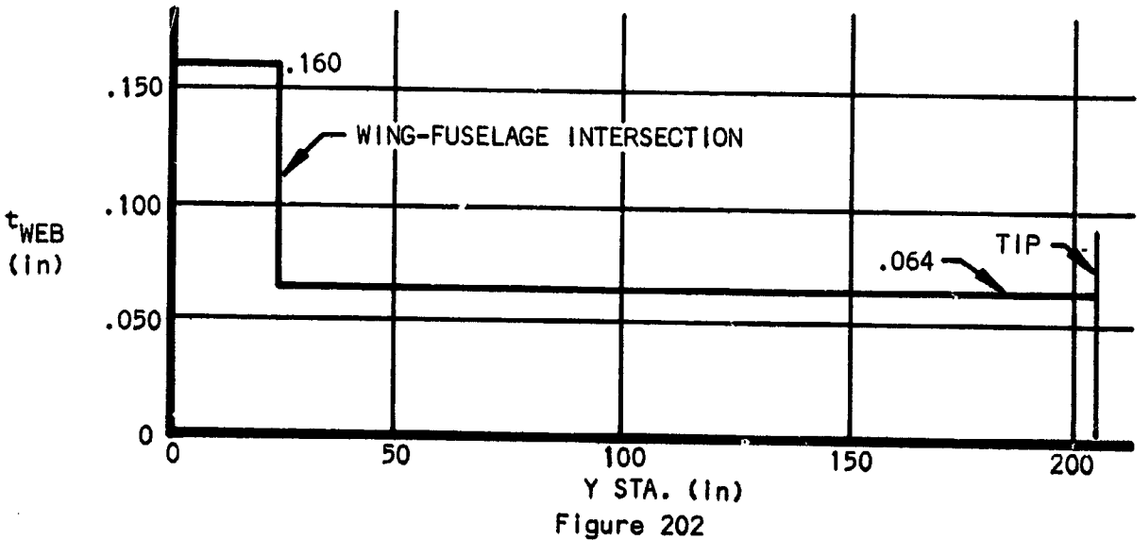


Figure 202

Wing Material/Concept III.-

Stress analysis of skins and stiffeners:

Assumptions: Same as Material/Concept I (Ref. p. 249)

Material: Skins - continuous filament Graphite/Epoxy
Stiffeners - 1" S-Glass/Epoxy

Ultimate skin shear stress: Same as Material/Concept I (Ref. p.249)

Shear buckling allowables: Same as Material/Concept I (Ref. Figure 172)

Wing skin stiffeners: Same as Material/Concept I (Ref. p. 254)

Leading edge: Assumed effective section on page 257 .

$$f_t = f_c = \frac{10}{tb} \frac{P_c}{4 + 6\frac{E_5}{E_1}}$$

$$= \frac{10}{.080(3.5)} \frac{3550}{4 + 6\frac{1.484}{15.4}\frac{10^6}{10^6}}$$

= 27800 psi

LEADING EDGE FIBER ORIENTATION

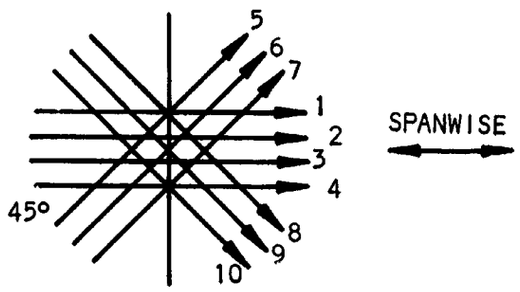


Figure 203

t = 0.080 in
b = 3.5 in Ref. p. 257

F_{cu} = 56500 psi

E_1 = 15.4 (10^6) psi
E_5 = 1.484 (10^6) psi Ref. Fig. 157
P_c = 3550 lb. Ref. p. 257

K_c = 0.80 assumed stability factor

$$\text{Comp. M.S.} = \frac{K_c F_{cu}}{f_c} - 1 = \frac{.8(56500)}{27800} - 1 = +\underline{0.62}$$

Stress analysis of main spar:

Assumptions: Same as Material/Concept II (Ref. page 268)

Material: Continuous filament Graphite/Epoxy.

Spar flange and web (composite section): The spar flange will be analyzed as a composite section following the methods, on pages 261 thru 264, used for the Material/Concept I member.

Skin element (assume 5.00 in. effective width):

E_1 thru E_4 = 1.484(10^6) psi

E_5 = 16.25(10^6) psi

$\frac{5\bar{E}}{10^6}$ = 4(1.484) + 1625

Where

$\bar{E}$ = 4.44(10^6) psi

SKIN FIBER ORIENTATION

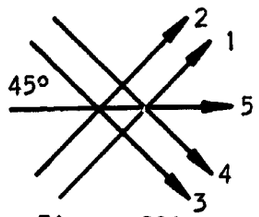


Figure 204

Skin splice element: Same as Material/Concept I.

$\bar{E}$ = 4.93(10^6) psi

Web element:

E_1 thru E_4 = 2.12(10^6) psi

WEB FIBER ORIENTATION

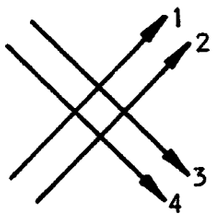


Figure 205

Cap element: 100% unidirectional

$\bar{E}$ = 16.25(10^6) psi

COMPOSITE SECTION @ STA. 24
(All dimensions in inches)

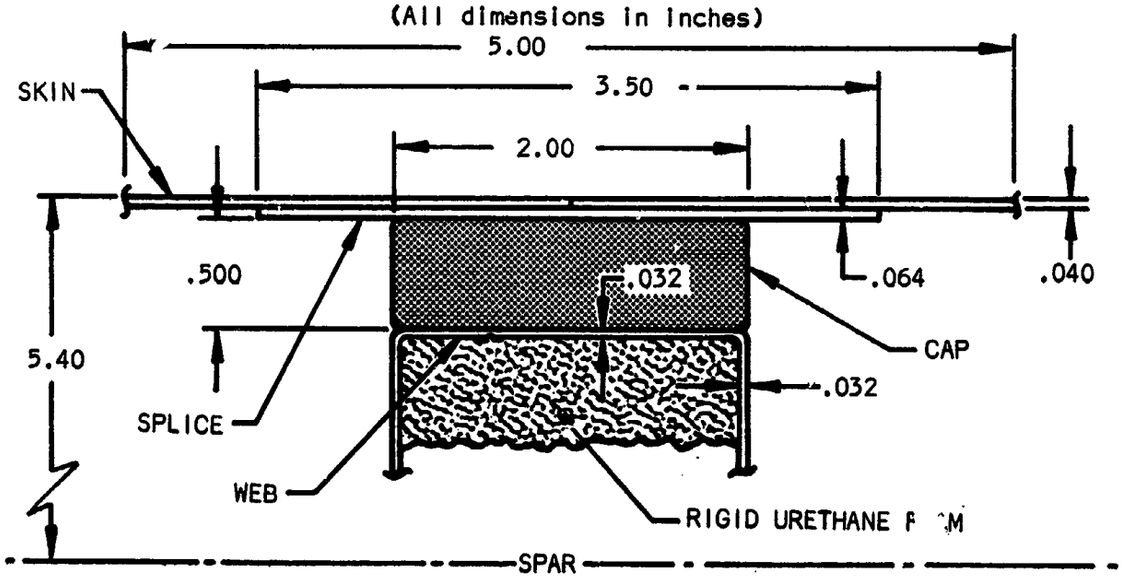


Figure 206

TABLE XLIV - EFFECTIVENESS FACTORS, n

Element	$\bar{E}$	n
Skin	$4.44(10^6)$	.273
Splice	$4.93(10^6)$	.303
Web	$2.12(10^6)$	.130
Cap	$16.25(10^6)$	1.000

(Reference Figure 206).

$$n = \frac{\bar{E}_{element}}{\bar{E}_{cap}}$$

cap = base material

$\Sigma A_{tr} y = 6.126$ in^3

$I_{x_{tr}} = 62.322$ in^4

$M_x = 568000$ in-lb.

$$f_b = \frac{M_x \, y \, n}{I_{x_{tr}}} = \frac{568000 \, y \, n}{62.322} = 9130 \, y \, n$$

TABLE XLV - MAIN SPAR MARGINS OF SAFETY

Element	f_b	$K_t F_{tu}$	$K_c F_{cu}$	M. S. Tension	M. S. Comp.
Effective skin	13400	17500	40000	+ 0.31	+ 1.98
Skin splice	14700	20700	40800	+ 0.41	+ 1.78
Cap	45800	67000	45800	+ 0.46	+ 0.00

Ref. notes on page 263.

Shear stress @ spar $\mathcal{Q}$

$$f_s = \frac{V \, \Sigma(A_{tr} y)}{I_{x_{tr}} \, b} = \frac{8470(6.126)}{62.322(.064)}$$

$= 13000$ psi

$F_{su} = 24800$ psi

$$\text{Web M.S.} = \frac{F_{su}}{f_s} - 1 = \frac{24800}{13000} - 1 = \underline{+0.91}$$

Where:

$\Sigma A_{tr} y = 6.126$ in^3

$b = 2(.032) = .064$ in.

$V = q_{net} h_w = 8470$ lb

The resulting main spar cap and web thicknesses for the material/concept III configuration are presented in Figures 207 and 208.

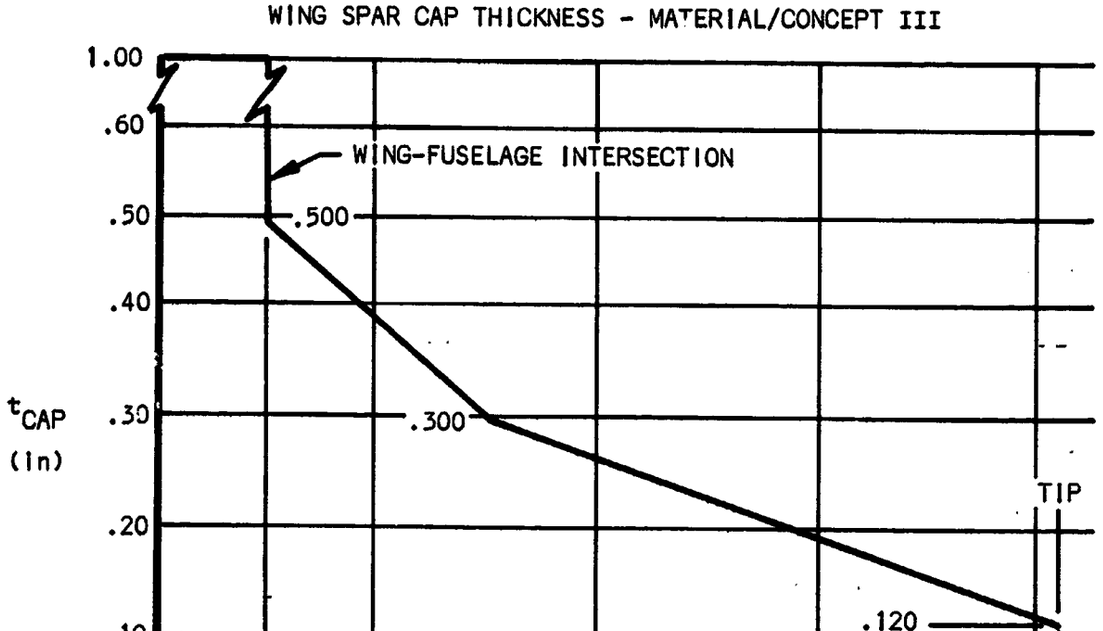


Figure 207

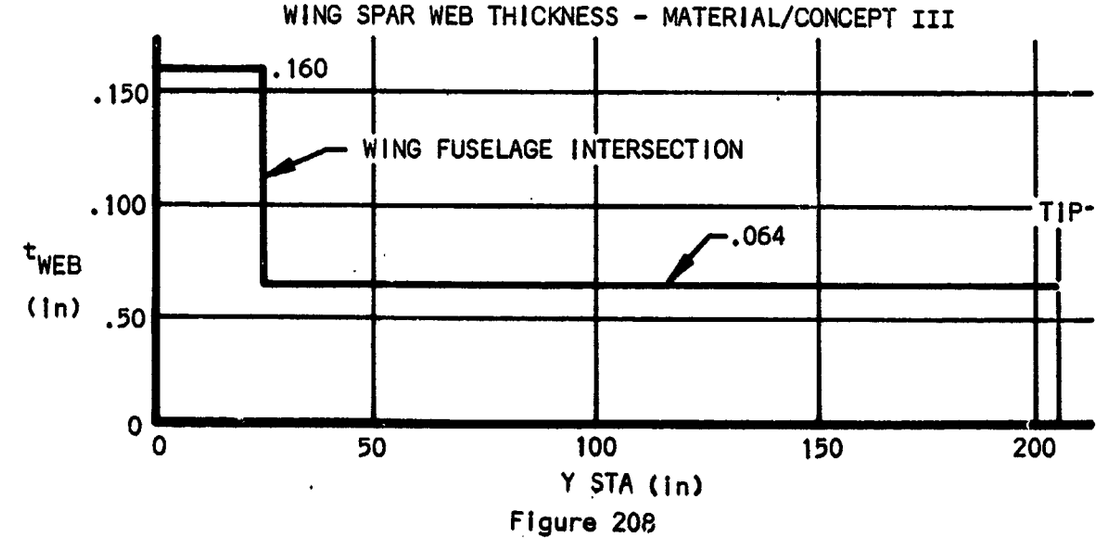


Figure 208

TABLE XLVI - WING MARGIN OF SAFETY SUMMARY

Item	Material	Type of Loading	Stress Level	Allowable (psi)	Factors	M.S.
Material/concept I						
Wing Skin	Graphite	Shear	1050	τ_{cr} = 1580	-	+0.50
Skin Stiff.	1" S-Glass	Bend.	35600	F_{tu} = 45000	-	+0.26
Lead. Edge	Graphite	Bend.	44350	F_{cu} = 56500	0.80	+0.02
Cap-Spar Flg.	Graphite	Bend.	26800	F_{cu} = 49000	0.80	+0.46
Eff.Skin-Spar Flg.	Graphite	Bend	3150	F_{tu} = 5520	0.70	+0.22
Web-Spar	Graphite	Shear	5700	F_{su} = 9760	-	+0.72
Closing Spar	1" S-Glass	Bend	10900	F_{tu} = 45000	0.70	+1.91
Flange Splice	Graphite	Bearing	13100	F_{bru} = 22000	-	+0.68
Web Splice	Graphite	Bearing	14750	F_{bru} = 22000	-	+0.49
Material/concept II						
Wing Skin	S-Glass	Shear	1670	τ_{cr} = 1670	-	+0.05
Lead. Edge	S-Glass	Bend	22300	F_{cu} =120000	0.80	+High
Cap-Spar Flg.	S-Glass	Bend	53500	F_{cu} =120000	0.80	+0.80
Eff.Skin-Spar Flg.	S-Glass	Bend	23100	F_{tu} = 39000	0.70	+0.18
Web-Spar	S-Glass	Shear	12500	F_{su} = 50000	-	+High
Material/concept III						
Cap-Spar Flg.	Graphite	Bend	45800	F_{cu} = 56500	0.80	0.00
Eff.Skin-Spar Flg.	Graphite	Bend	13400	F_{tu} = 25000	0.70	+0.31
Web-Spar	Graphite	Shear	13000	F_{su} = 24800	-	+0.91
Lead Edge	Graphite	Bend	27500	F_{cu} = 56500	0.80	+0.62

Note: Items not repeated in succeeding material/concepts are common to the preceding configuration.

Horizontal tail stress analysis.-

Geometry:

HORIZONTAL TAIL PLANFORM
(All dimensions in inches)

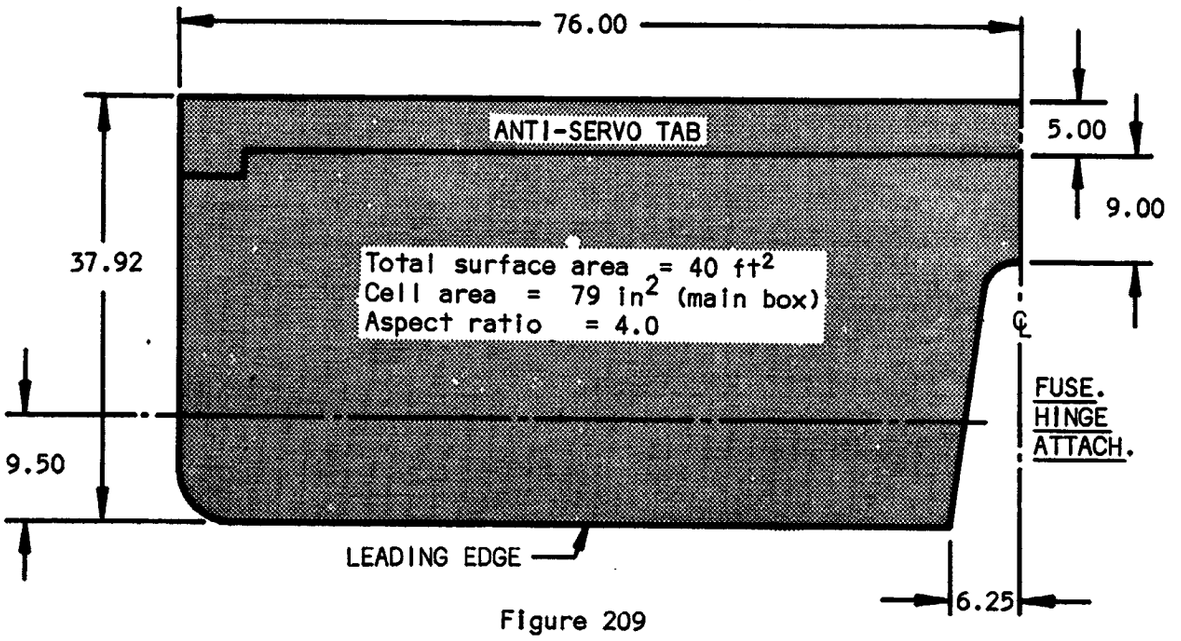


Figure 209

Loads criteria: Based on FAR. part 23, Appendix A.

Wing loading: $n_1 \frac{W}{S} = 62.8$ lb/ft^2 ref. pg. 232

Average tail loading: $\bar{w} = .400$ lb/in^2 ult.

Desing maneuver/gust condition: Critical for beam shear and moment.

Running load, ω:

$\omega = \bar{w}\, c$, = 15.2 lb/in $\quad c = 37.92$ in

$\bar{w} = .400$ lb/in^2

Beam shear, S_z:

$S_z = \Sigma w \Delta y$

Beam moments, M_x:

$M_x = \Sigma S_z \Delta y$

HORIZONTAL TAIL ULTIMATE SHEAR AND MOMENT,@ 25% CHORD, MANEUVER/GUST CONDITION

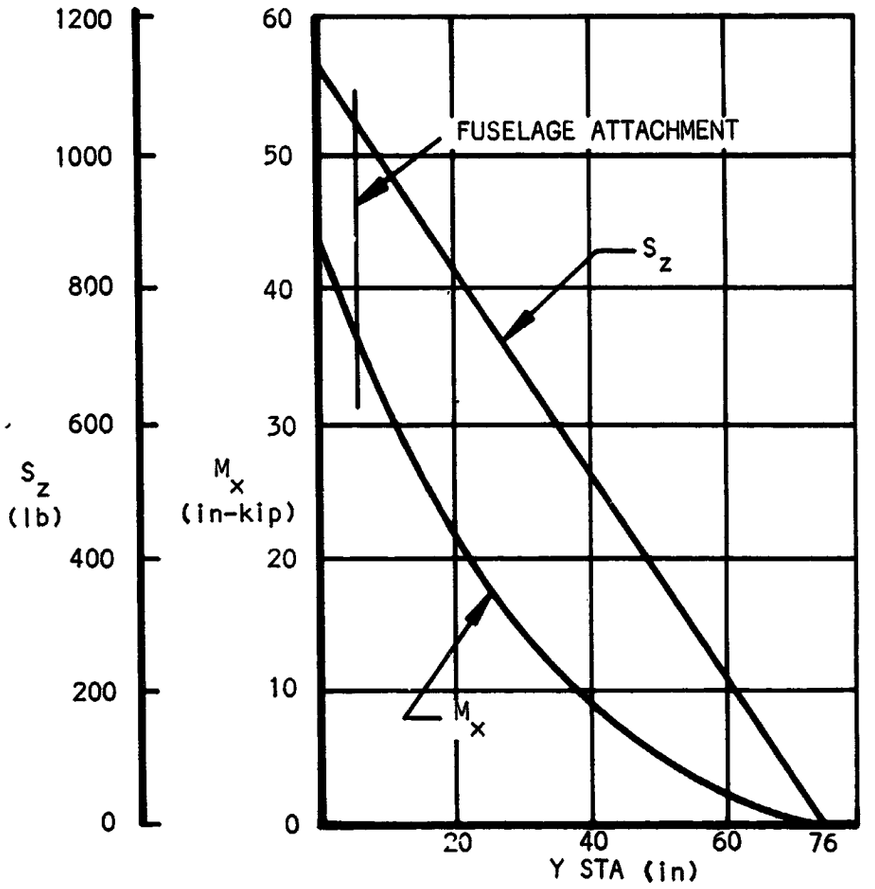


Figure 210

Anti-servo tab loading condition: Critical for tab and also for torque on the horizontal tail.

LOADING DISTRIBUTION ON ANTI-SERVO TAB

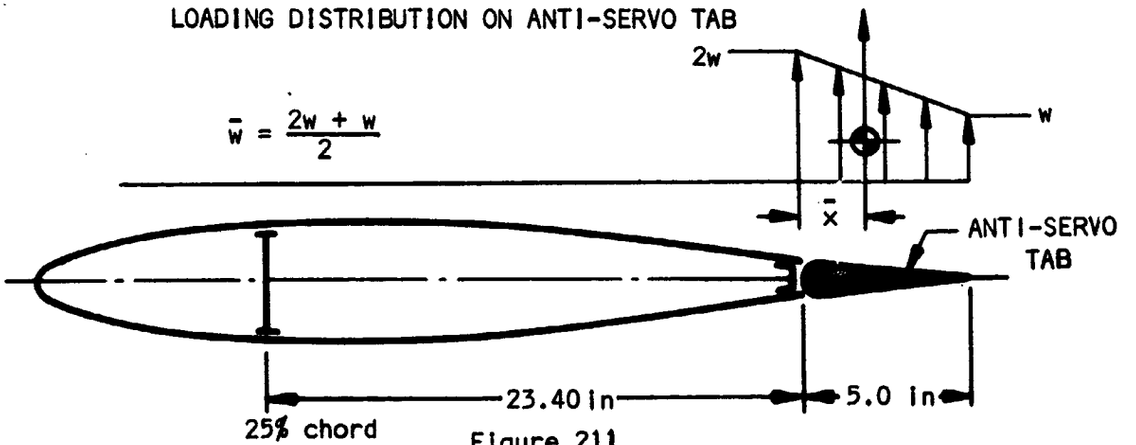


Figure 211

Average tab loading: Reference FAR Part 23, Appendix A, Table 2

$\bar{w}$ = 49 lb/ft^2 limit Where $w = \frac{\bar{w}}{1.5}$ Ref. Figure 211

= .51 lb/in^2 ult.

Running load, $\omega = 5\bar{w} = 5(.51) = 2.55$ lb/in

Beam shear, $S_z = \Sigma\omega\Delta y = \omega\ell = 2.55(76) = 194$ lb/side = 388 lb/total

Torque, M_y:

@ servo tab hinge line

$M_{y_{st}} = \Sigma\omega\bar{x}\,\Delta y, = 76\ (2.55)(2.22) = 430$ in-lb/side, $\bar{x} = .444(5.0) = 2.22$ in.

@ 25% of horizontal tail chord

$M_y = \Sigma\omega(\bar{x} + 23.40)(\Delta y) = (2.55)(25.62)(76) = 4960$ in-lb/side

= 9920 in-lb/total

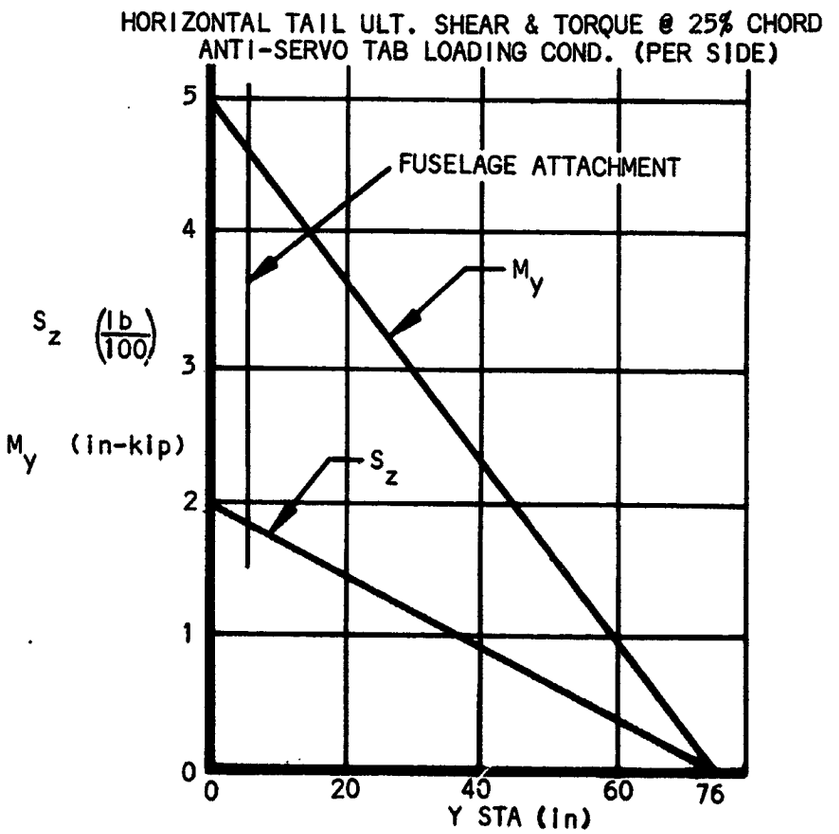
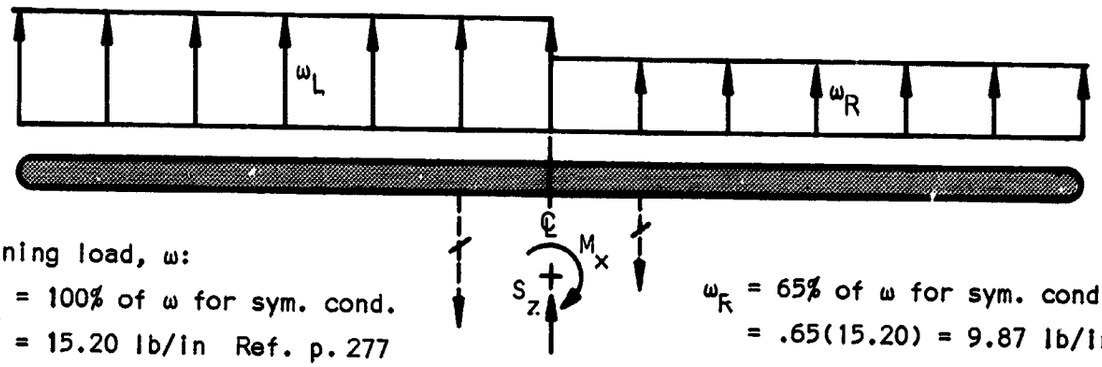


Figure 212

Unsymmetrical flight condition: Critical for horizontal tail-fuselage attachments. Distribution based on FAR Part 23, Appendix A, Table II.

HORIZONTAL TAIL UNSYMMETRICAL LOAD DISTRIBUTION



Running load, ω:

ω_L = 100% of ω for sym. cond.
= 15.20 lb/in Ref. p. 277

ω_R = 65% of ω for sym. cond.
= .65(15.20) = 9.87 lb/in

VIEW LOOKING FORWARD

Figure 213

Summation of loads at ℄ aircraft:

$$S_z = \Sigma w_L \, \Delta y + w_r \, \Delta y = 15.20(76) + 9.87\,(76) = 1880 \text{ lb total}$$

$$M_x = \sum_{o}^{\ell} S_{z_L} \, y - \sum_{o}^{\ell} S_{z_R} \, \Delta y = \frac{1140(76)}{2} - \frac{740(76)}{2} = 15300 \text{ lb-in}$$

Horizontal tail material/concept.- The single spar, chordwise skin stiffener concept using non-continuous 1" S glass/epoxy, in all cases, was the configuration used for the horizontal tail.

Stress analysis, skins and stiffeners:

Assumptions: (1) Shear resistance at limit load.
(2) Minimum skin t_{sk} = .032 in.

Ultimate skin shear stress: Anti-servo tab loading condition critical.

HORIZONTAL TAIL TORQUE BOX SHEAR FLOW

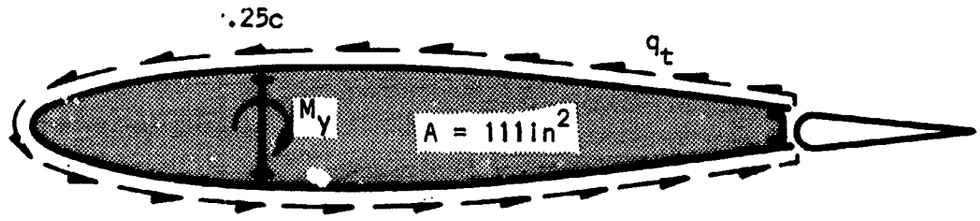


Figure 214

@ Fuselage Attachment:

$$q_t = \frac{T}{2A} = \frac{M_y}{2A} = \frac{4600}{2(111)} = 21 \text{ lb/in}, \quad M_y = 4600 \text{ in-lb} \quad \text{Ref. Fig. 212}$$

$$\text{ult. } f_s = \frac{q_t}{t_{sk}} = \frac{21}{.032} = 657 \text{ psi} ; \quad \text{Limit } f_s = 438 \text{ psi}$$

Shear buckling allowable, τ_{cr}: using 5.00 in. stiffener spacing and simply supported panels:

$$\tau_{cr} = \frac{K_s \bar{E}_c t_{sk}^2}{b_{sk}^2}$$

Where: Typical panel size 5.00 by 23.4

$$\frac{b}{a} = \frac{5}{23.4} = .214 \qquad K_s = 5.1$$

$\bar{E}_c$ = effective modulus

$$= .75 E_c = .75(7.8)(10^6)$$

$$= 5.85(10^6) \text{ psi}$$

$$\tau_{cr} = \frac{5.1(5.85)(10^6)(.032)^2}{(5)^2}$$

$$= 1220 \text{ psi}$$

Comparison of ultimate skin shear stress with the buckling allowable shows the component to be shear resistant at ultimate load.

$$\text{Limit } f_s = 438 \text{ psi}$$

$$\text{Buckling M.S.} = \frac{\tau_{cr}}{f_s} - 1 = \frac{1220}{438} - 1 = \underline{\underline{+1.78}}$$

Skin stiffeners: Critical between main spar and closing spar for maneuver/gust condition. Assume 80% of total normal airload on tail reacted by skin stiffeners on top surface.

HORIZONTAL TAIL SKIN STIFFENER LOADING

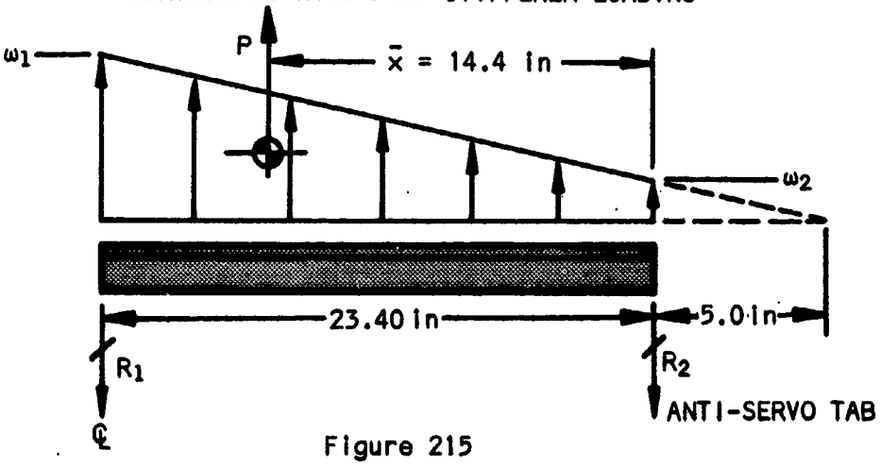


Figure 215

$\omega_1 = .80\bar{w} \times \text{spacing} = .80\ (.400)(5.0)$

$= 1.60$ lb/in.

Where:

$\bar{w} = .400$ lb/in^2 ref. p. 277

5.00 in. spacing

$\omega_2 =$

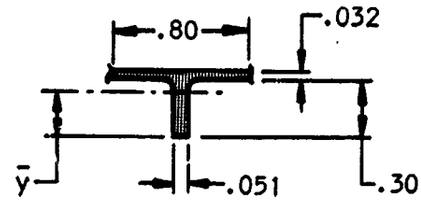
$\omega_2 = 5\ \frac{W_1}{28.40} = 5\ \frac{1.60}{28.40} = .282$ lb/in

$P = \frac{\omega_1 + \omega_2}{2}\ (23.40) = \frac{1.60 + .282}{2}\ (23.40) = 22.00$ lb.

$R_1 = \frac{P\bar{x}}{23.40} = \frac{22.00(14.4)}{23.40} = 13.60$ lb

$R_2 = P - R_1 = 22.00 - 13.60 = 8.40$ lb

$M_{max} = 65$ in-lb



(All dimensions in inches)

Stiffener section, assumming .80 in. of skin is effective in bending.

Stiffener $f_b = \frac{M\bar{y}}{I_{xx}} = \frac{65(.256)}{.000353} = 47100$ psi

$\bar{y} = .256$ in.

$I_{xx} = .000353$

Bending M.S. $= \frac{F_{bu}\ K_c}{f_b} - 1 = \frac{61000(.80)}{47100} - 1$

$= + \underline{\underline{0.04}}$

$F_{cu} = 61000$ psi (Ref. Table XXXIV)

$K_c = .80$ stability factor

Stress analysis, Main spar:

Assumptions:

(1) Maintain a flange width, b, to flange thickness, t, ratio of 4.0 (max). However hold b to a minimum of 0.75 in. for bonding purposes.

(2) Use I-Beam configuration.

(3) React moment as couple between top and bottom flange.

(4) Make spar web shear resistant

(5) Make spar web compression resistant to 50 psi bonding pressure required to bond skins to main spar.

Spar flange: Maneuver/gust condition critical.

max $M_x = 37500$ in-lb @ sta. 5 Ref. Figure 210

couple $P_c = \frac{M_x}{h_f} = \frac{37500}{4.4} = 8530$ lb

$f_t = f_c = \frac{P_c}{A_{eff.}}$

$A_{eff} = A_{flg} + A_{skin}$

$= 1.50(.180) + 1.50(.032)$

$= .318$ in.^{2}

$f_t = f_c = \frac{8530}{.318} = 26800$ psi

Tension critical

Tension M.S. $= \frac{tu}{f_t} \frac{K_t}{} - 1$

$F_{tu} = 45000$ psi Ref. Table XXXIV

$K_t = .80$ fatigue factor(assumed)

Tension M.S. $= \frac{45000(.80)}{26800} - 1 = +\underline{0.34}$

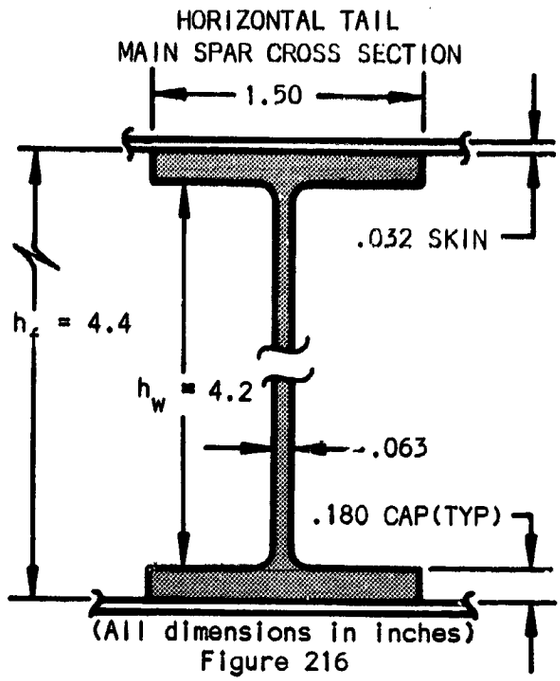


Figure 216

Stress analysis, Spar web: Critical for shear buckling, due to maneuver/gust condition, outboard of sta. 5.0.

$\tau_{cr} = \frac{K_s \bar{E}_c t^2}{h_w^2}$

$\tau_{cr} = \frac{4.8(5.85)(10^6)(.063)^2}{(4.2)^2} = 6300$ psi

$f_s = \frac{S_z}{A_{web}} = \frac{1140}{.265} = 4300$ psi

Shear buckling M.S. $= \frac{\tau_{cr}}{f_s} - 1$

$= \frac{6300}{4300} - 1 = + \underline{0.46}$

Where:

$K_s = 4.8$ for simply supported web with no intermediate stiffeners, ref. figure 171

$\bar{E}_c = .75\ E_c = 5.85(10^6)$ psi

$S_z = 1140$ lb Ref. Figure 210

$A_{web} = h_w\ t_w = 4.2\ (.063)$

$= .265$ in^2

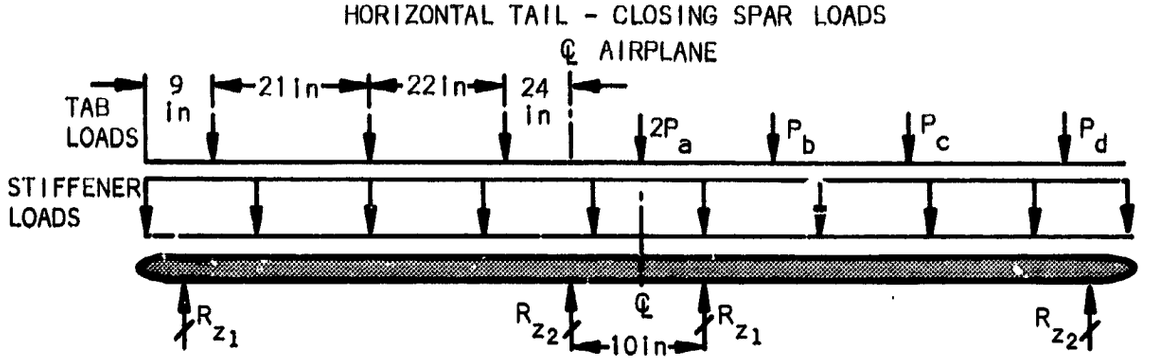
A check of the spar web for the 50 psi limit bonding pressure condition indicated that the .063 in thick web should be maintained throughout.

Stress analysis, closing spar: Reacts the anti-servo tab loading plus chordwise skin stiffener loading.

Tab loads:

$P_a = 31$ lb , $P_b = 58$ lb $P_c = 50$ lb , $P_d = 55$ lb

HORIZONTAL TAIL - CLOSING SPAR LOADS



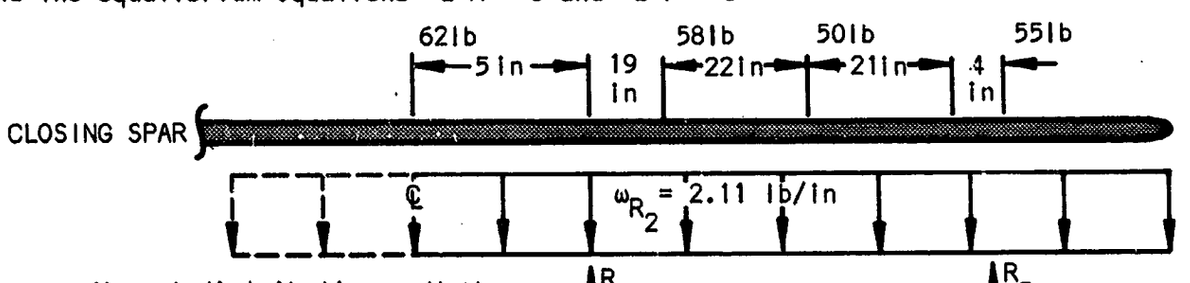
VIEW LOOKING FORWARD

Figure 217

Stiffener loads:

$$\omega_{R_2} = \frac{R_2}{.80 \times \text{spacing}} = \frac{8.40}{.80(5.00)} = 2.11 \text{ lb/in}$$

Beam shear and moment: Determined using the moment distribution method and the equalibrium equations $\Sigma M = 0$ and $\Sigma F = 0$



Moment distribution method

Operation	← 10		66 →	← 5
I	Const. →			
R		.868	.132	1.0
FEM		-95	-1633	-1669	-26
1		-1340	198	1643	
	670	670	-822	-99	
2		-1300	192	99	
	650	650	-50	-96	
3		-610	90	96	
Net moment		-2025	-2025	-26	-26

Reactions:

ΣM @ R_{z1}

$$R_{z2} = \frac{62(55)+41(50)+19(58)+2.11(71)^2(.5)-2025}{66} = 150 \text{ lb}$$

$\Sigma F = 0$

$R_{z1} = 76(2.11)+31+58+50+55-150 = 204$ lb

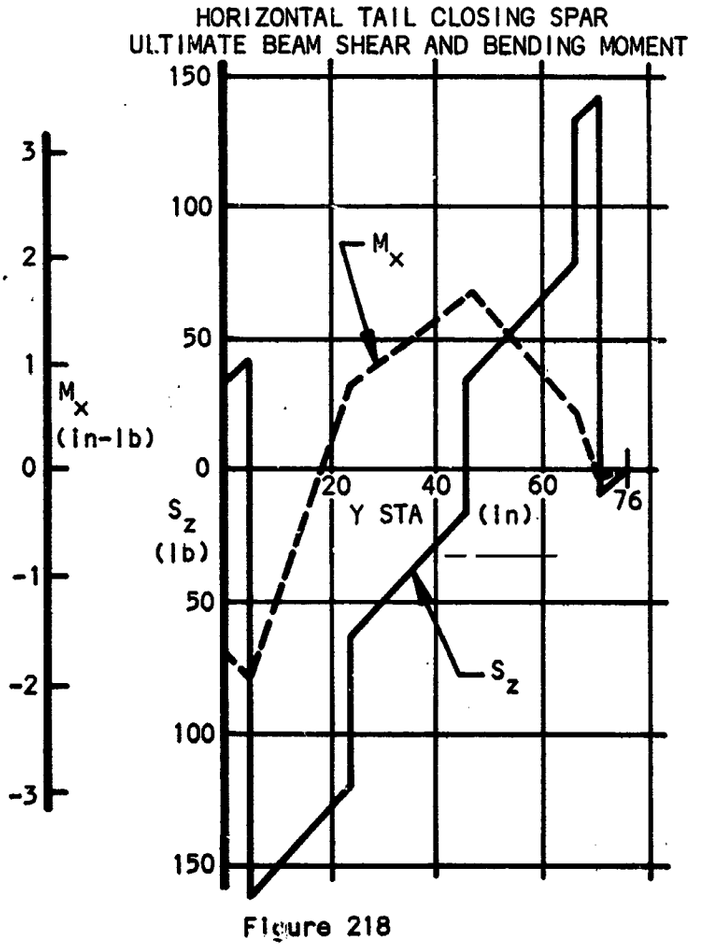


Figure 218

Closing spar flange: critical at inboard support:

$M_x = 2025$ in-lb Ref. Figure 218

$$\text{couple } P_c = \frac{M_x}{h_f} = \frac{2025}{1.3} = 1550 \text{ lb}$$

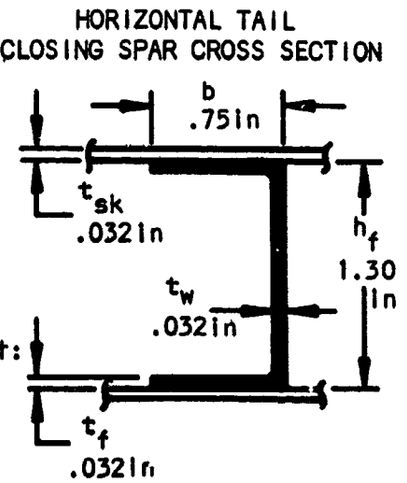


Figure 219

$$f_t = f_c = \frac{P_c}{A_{eff.}} \quad ; A_{eff.} = A_{flg} + A_{skin} = .75(.032 + .032) = .048 \text{ in}^2$$

Tension critical:

$$f_t = \frac{1550}{.048} = 32300 \text{ psi}$$

Where:

F_{tu} = 45000 psi Ref. Table XXXIV

K_t = .80 Fatigue factor (assumed)

$$\text{Tension M.S.} = \frac{F_{tu}K_t}{f_t} - 1 = \frac{45000(.80)}{32300} - 1 = \underline{+0.12}$$

Closing spar web: Make shear resistant

$$\tau_{cr} = \frac{K_s \bar{E}_c t_w^2}{h_a^2}$$

$$\tau_{cr} = \frac{4.8(5.85)(10^6)(.032)^2}{(1.2)^2}$$

$$= 20000 \text{ psi (not critical}$$

$$f_s = \frac{S_z}{A_u} = \frac{162}{.0384} = 4220 \text{ psi}$$

$$\text{Shear M.S.} = \frac{F_{su}}{f_s} - 1 = \frac{8000}{4220} - 1 = \underline{+0.90}$$

Where:

K_s = 4.8 for simply supported web no intermediate stiffeners, Ref. Figure

$\bar{E}_c = 5.85(10^6)$ psi Ref. p. 283

h_w = 1.2 in

max S_z = 162 lb. @ inboard support

$A_u = 1.2(.032) = .0384 \text{ in}^2$

F_{su} = 8000 psi Ref. Table XXXIV

Stress analysis, fuselage attachment:

Critical condition: unsymmetrical maneuver/gust + servo tab loading.

HORIZONTAL TAIL- FUSELAGE HINGE LOADS

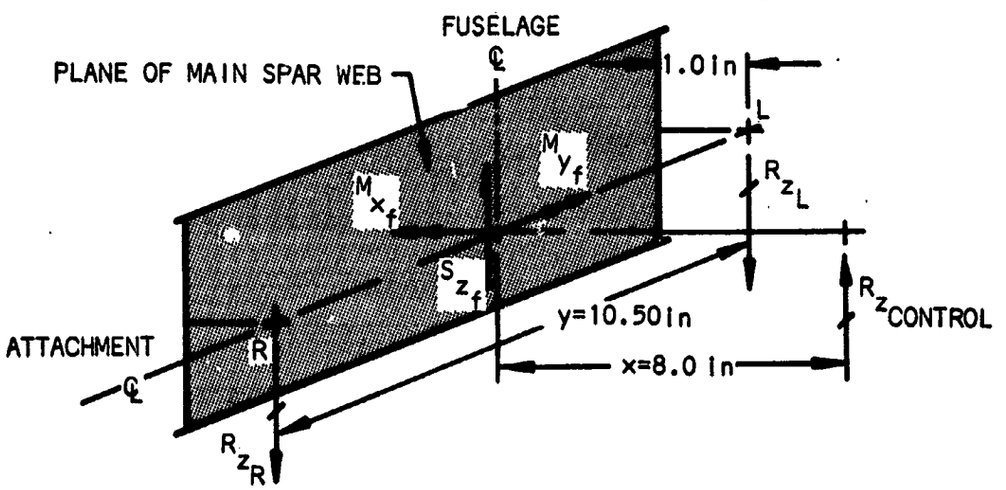


Figure 220

@ Fuselage $\mathbb{C}$;

$$S_z = S_{z_{\text{unsym. flight}}} + S_{z_{\text{anti-servo tab}}}$$

$$= 1880 + 388 = 2268 \text{ lb (Ref. page 279 and 280)}$$

$$M_x = M_{x_{\text{unsym. flight}}} = 15300 \text{ in-lb. (Ref. page 280)}$$

$$M_y = M_{y_{\text{anti-servo tab}}} = 9920 \text{ in-lb (Ref. page 279)}$$

Net attachment lug loads:

$$R_{z_{\text{control}}} = \frac{M_{y_f}}{x} = \frac{9920}{8.0} = 1240 \text{ lb}$$

$$R_{z_R} = \frac{S_z}{2} + \frac{M_x}{y} + \frac{R_{z_{\text{cont.}}}}{2} =$$

$$\frac{2268}{2} + \frac{15300}{10.5} + \frac{1240}{2}$$

$$= 1134 + 1460 + 620 = 3214 \text{ lb.}$$

$$R_{z_L} = 1134 - 1460 + 620 = 294 \text{ lb.}$$

Lug bearing critical (multi-lug):

$$f_{br} = \frac{R_{z_R}}{D_1 t},$$

3 fuse. lugs,
t = .25 in/lug
2 spar lugs,
t = .375 in/lug
Σ t = .75 in/side

$$f_{br} = \frac{3214}{.500(.75)} = 8570 \text{ psi}$$

F_{bru} = 22000 psi Ref. Table XXXIV

HORIZONTAL TAIL
MAIN SPAR LUG
(All dimensions in inches)

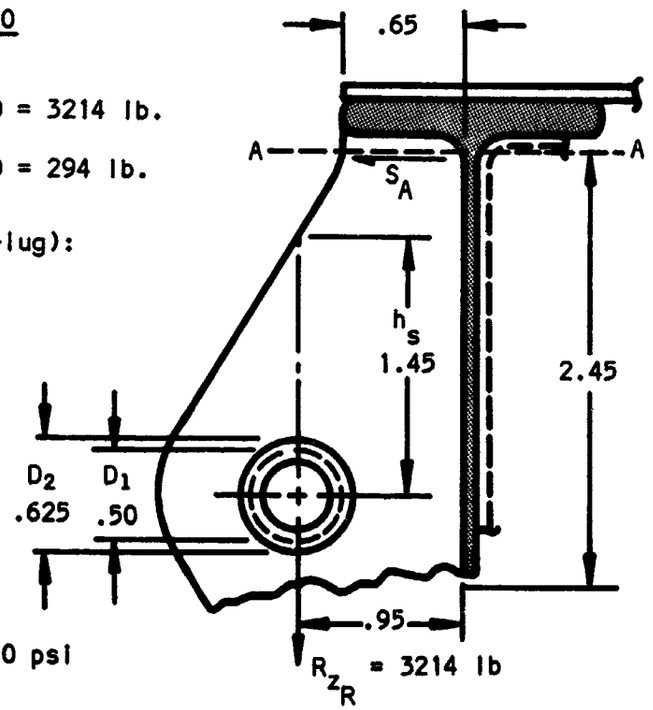


Figure 221

Bearing M.S. = $\frac{F_{bru} K_{br}}{f_{br}} - 1 = \frac{22000(0.5)}{8570} - 1 = \underline{+0.28}$; K_{br} = 0.5 assumed

Stress analysis, Anti-servo tab:

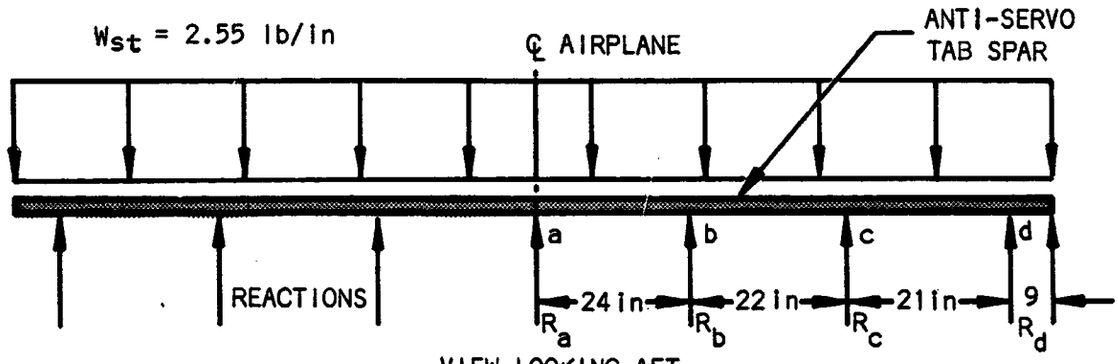
Assumptions:

(1) Shear resistant skin
(2) Limit tab wind up between tip end fuselage to approx. 2 degrees.

Spar: The leading edge of the tab served as the spar for carrying shear and moment. It also provided the lugs for the attachment to the closing spar of the horizontal tail.

The shear, moment and lug reactions were determined thru the use of the moment distribution method and the equilibrium equations.

HORIZONTAL TAIL ANTI-SERVO TAB SPAR LOADS



VIEW LOOKING AFT

Figure 222

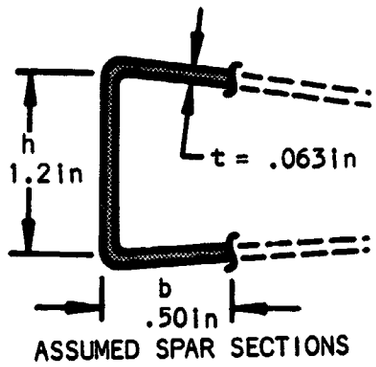
max M = -126 in-lb; max S = 33 lb

R_a = 31 lb , R_c = 50 lb.

R_b = 58 lb , R_d = 55 lb.

$$f_b = \frac{M}{hbt} = \frac{126}{1.2(.80)(.063)} = 3340 \text{ psi}$$

$$f_s = \frac{S_z}{ht} = \frac{33}{1.2(.063)} = 436 \text{ psi}$$



ASSUMED SPAR SECTIONS

The above calculated stresses give high margins of safety.

Anti-servo tab torsional windup: Anti-servo tab condition critical (Ref. page 278) Distribution shown below.

ANTI-SERVO TAB CHORDWISE LOAD DISTRIBUTION

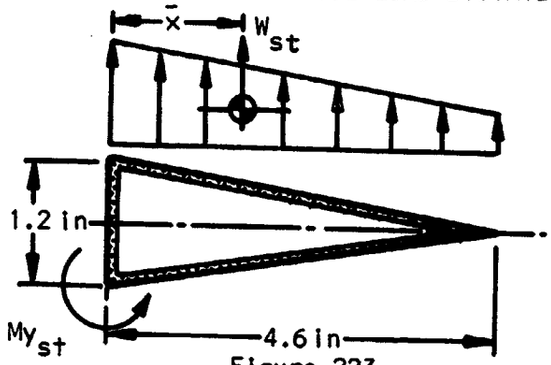


Figure 223

$$\theta_{tip} = \Sigma\left[\left(\frac{1}{2AG}\right)\left(\Sigma\frac{qL}{t}\right)\left(\Delta y\right)\right]_{o}^{y=76}$$

$$\theta_{tip} = \left[\frac{L}{(2A)^2(Gt)}\right]\left[\Sigma\, w_{st}\,\bar{x}y\Delta y\right]_{o}^{y=76}$$

$$= \left[\frac{10.4}{(5.52)^2(2.38)(.063)}\right]\left[\frac{5.66(76)^2}{2}\right]$$

$$= .0369 \text{ radius} = 2.12^{\circ}$$

Where:

$q = \frac{T}{2A}$

$T = W_{st}\,\bar{x}\,y$

$L = 1.2 + 2(4.6) = 10.4$ in.

$G = 2.38(10^6)$ psi Ref. Table XXXIV

$2A = 2\left(\frac{1.2}{2}\right)4.6 = 5.52$ in^2

TABLE XLVII - HORIZONTAL TAIL MARGIN OF SAFETY SUMMARY

	Item	Material	Type of loading	Stress level	Allowable (psi)	Factors	M.S.
Basic Tail	Skin	1"S-Glass	Shear	438	τ_{cr} = 1220	---	+1.78
	Skin Stiff.		Bending	47100	F_{cu} = 61000	0.80	+0.04
	Spar flange		Bending	26800	F_{tu} = 45000	0.80	+0.34
	Spar web		Shear	4300	τ_{cr} = 6300	---	+0.46
	Closing spar flange		Bending	32300	F_{tu} = 45000	0.80	+0.12
	Closing spar web		Shear	4220	F_{su} = 8000	---	+0.90
	Fuse. attach. lugs	1"S-Glass	Bearing	8570	F_{bru} = 22000	0.50	+0.28
Tab	Flange	1"S-Glass	Bending	3340	F_{tu} = 45000	0.80	+high
	Web	1"S-Glass	Shear	436	F_{su} = 8000	---	+high

Vertical tail stress analysis.- For simplification of loads determination, the tail was divided into panels, A thru F.

VERTICAL TAIL GEOMETRY

(All dimensions in inches)

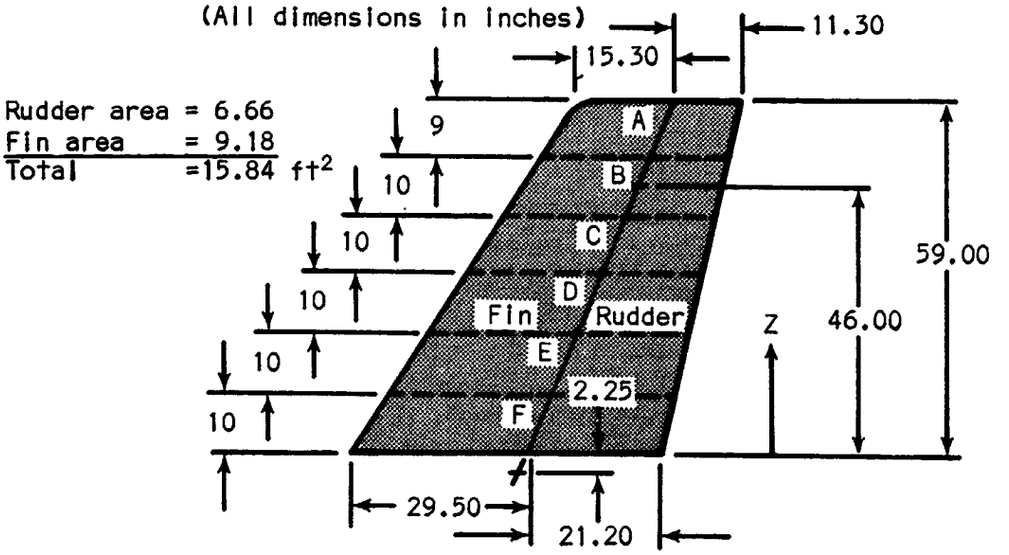


Figure 224

Effective Aspect Ratio

Reference 8, p.325

$$AR_e = \frac{1.55b_v^2}{S_v} = \frac{1.55(4.92)}{15.84} = 4.82 \; ; \quad c_{ave} = c_{tip} + \left[\frac{(59-z)(c_{root} - c_{tip})}{59}\right]$$

Fin

$$c_{ave} = 15.30 + \frac{(59 - z)(29.50 - 15.30)}{59} = 15.30 + (59 - z)(.241)$$

Rudder

$$c_{ave} = 11.30 + (59 - z)(.168)$$

TABLE XLVIII VERTICAL TAIL PANEL DIMENSIONS

Panel	z	59-z	.241(59-z)	c_{ave} Fin	.168(59-z)	c_{ave} Rudder
A	54.50	4.5	1.085	16.38	.76	12.06
B	45.0	14.0	3.38	18.68	2.35	13.65
C	35.0	24.0	5.78	21.08	4.03	15.33
D	25.0	34.0	8.20	23.50	5.71	17.01
E	25.0	44.0	10.60	25.90	7.40	18.70
F	5.0	54.0	13.00	28.30	9.08	20.38

Vertical tail loads criteria: Based on FAR Part 23, Appendix A.

Wing loading, $n_1 \frac{W}{S}$ =62.8 lb/ft^2 Ref. p. 232

Vertical tail design flight condition (fin): The gust load condition as required by FAR Part 23, paragraph 23.443 for a 30 ft/sec. nominal intensity gust at V_c (V_c = 150 mph) was determined critical.

From FAR Part 23, Appendix B, Figure 5: loading, Figure 8: distribution.

For $\frac{W}{S_v} = \frac{2977}{15.84}$ and AR_e = 3.00 (baseline), $\bar{w}_{3.00}$ = 34

For actual AR_e = 4.82

$$\bar{w} = \bar{w}_{3.00}\left[\frac{5\ AR}{3(AR + 2)}\right]$$

$$= 34\left[\frac{5(4.82)}{3(4.82 + 2)}\right]$$

= 40 lb/ft^2 limit ave.

$$P_{total}(ult) = \bar{w}\ S_v\ 1.5 = 40(15.84)1.5$$

= 950 lb

VERTICAL TAIL CHORDWISE LOAD DISTRIBUTION

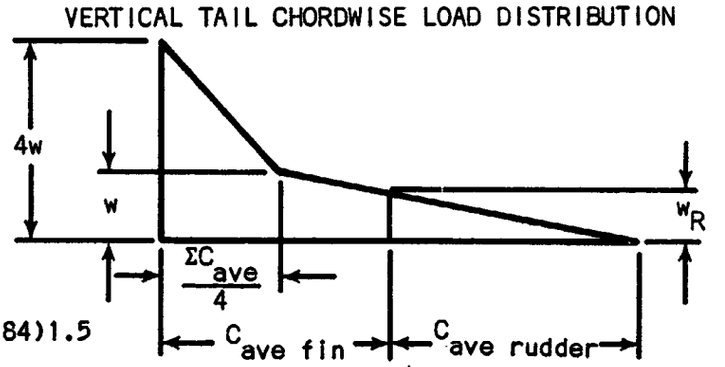


Figure 225

Distribution:

$$w = \frac{P_{total}}{144\ S_v} = \frac{950}{144(15.84)}$$

= 0.418 lb/in^2 ult.

$$w_r = \frac{c_{ave_{rudder}}}{.75\ \Sigma\ c_{ave}}\ (w)$$

Rudder hinge loads:

$$w_{tip} = \frac{w_r\ c_{ave_{rudder}}}{2}$$

Therefore,

$$w_{tip} = \frac{\left[c_{ave_{rudder}}\right]^2}{1.5\ \Sigma\ c_{ave}}\ w$$

RUDDER LOADS SPANWISE DISTRIBUTION

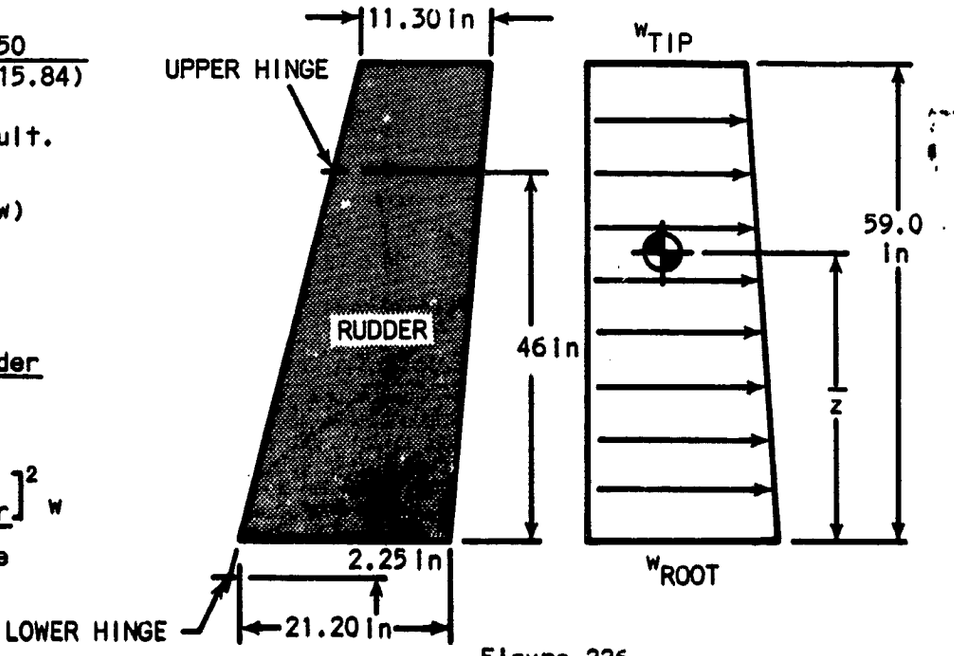


Figure 226

$$w_{tip} = \frac{(11.30)^2(.418)}{1.5(15.30+11.30)} = 1.34 \text{ lb/in.};$$

$$w_{root} = \frac{(21.20)^2(.418)}{1.5(29.80+21.20)} = 2.47 \text{ lb/in}$$

$$P_{y_u} = \frac{28.85\left(\frac{1.34+2.47}{2}\right)(59)}{48.25} = 67 \text{ lb.};$$

$$P_{y_\ell} = 112 - 67 = 45 \text{ lb}$$

Running load: $w = \bar{w}\, c_{ave}$

where: P_{y_u} = upper rudder hinge load.

Beam shear: $S_y + \Sigma\, w\, \Delta z + P_{y_u}$;

Beam moment: $M_x = \Sigma\, S_y\, \Delta y$

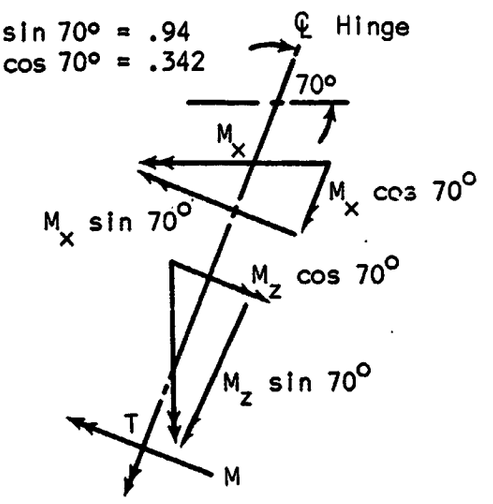
Torque about hinge line: $M_z = \Sigma\, w\, \bar{x}\, \Delta z$

where $\bar{x} = .68\, c_{ave}$.

Resolution of loads @ hinge line:

$$M = M_x \sin 70^\circ - M_z \cos 70^\circ$$
$$= .94\, M_x - .342\, M_z$$

$$T = M_x \cos 70^\circ + M_z \sin 70^\circ$$
$$= .342\, M_x + .94\, M_z$$



VERTICAL TAIL-FIN GUST LOAD CONDITION
SHEAR, TORQUE AND BENDING

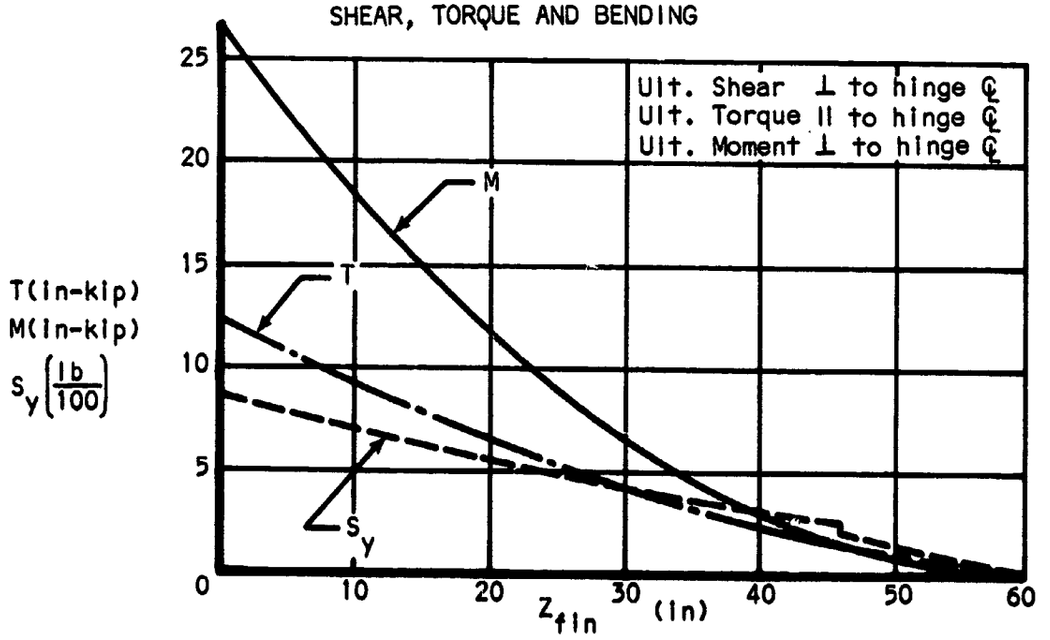


Figure 227

Design flight condition (rudder): The maneuver condition generated by sudden maximum rudder displacement is critical per FAR Part 23, Appendix B. At this time the airplane is in unaccelerated flight with zero yaw.

From FAR Part 23, Appendix B: Figure 1 curve A: loading; Figure 7: distribution

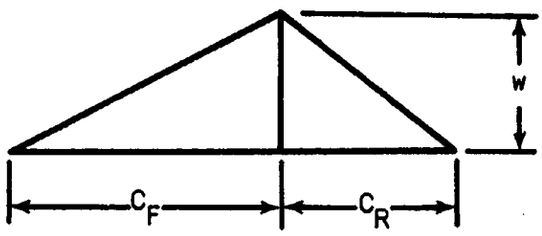
Wing loading: $\frac{W}{S} = \frac{2977}{180} = 16.5$; $K_{\bar{w}} = 39$

Tail load: $\bar{w} = K_{\bar{w}} \left(\frac{n}{4.4}\right) = 39 \left(\frac{3.8}{4.4}\right) = 33.7$ lb/ft^2 limit ave.; n = 3.8

Distribution; $w = 2\bar{w} = \frac{2(33.7)}{144}$

= 0.468 lb/in^2 limit

= 0.702 lb/in^2 ult.



Rudder hinge loads:

$w_{tip} = \frac{w\, c_{tip}}{2} = \frac{.702(11.30)}{2} = 3.97$ lb/in

$\bar{z} = .449(59) = 26.5$ in.

$w_{root} = \frac{w\, c_{tip}}{2} = \frac{.702(21.20)}{2} = 7.45$ lb/in.

Note: For spanwise load distribution see Figure 226.

Σ M @ lower hinge

$$P_{y_u} = \frac{(\bar{z} + 2.25)\left(\frac{w_{tip} + w_{root}}{2}\right)(59)}{(46 + 2.25)} = \frac{28.75\left(\frac{3.97 + 7.45}{2}\right)(59)}{48.25} = 201 \text{ lb}$$

$$P_{y_\ell} = \Sigma P_y - P_{y_u} = 337 - 201 = 136 \text{ lb}$$

Beam shear, moment and torque: The shear, moment and torque on the rudder were determined using the same general equations on page 292 as were used for the fin portion of the vertical tail. The resulting diagrams are presented in Figure 228.

Stress analysis of fin skins and stiffeners:

Assumptions:

(1) Shear resistance at limit load
(2) Minimum skin t_{sk} = .040 in.

Ultimate skin shear stress: Gust condition critical. Torque, parallel to and about the main spar.

VERTICAL TAIL-RUDDER ULT. SHEAR, MOMENT AND TORQUE
(Maneuver cond. critical taken ⊥ and ∥ @ hinge)

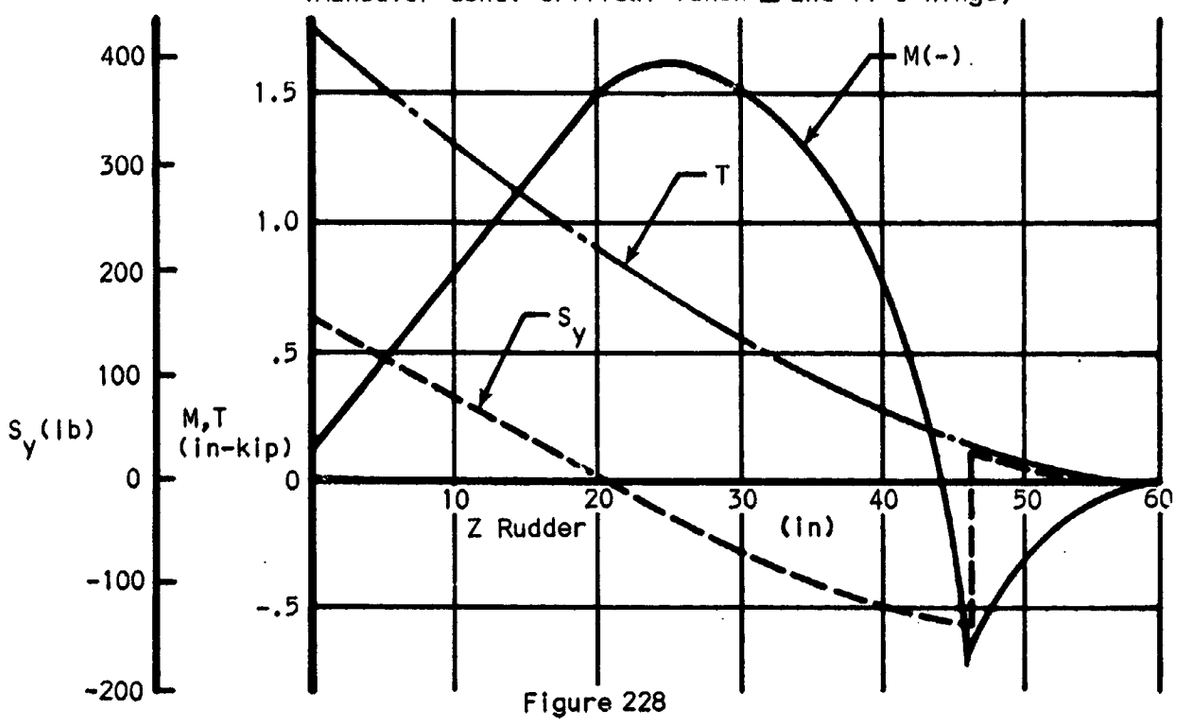


Figure 228

SHEAR FLOW IN FIN TORQUE BOX

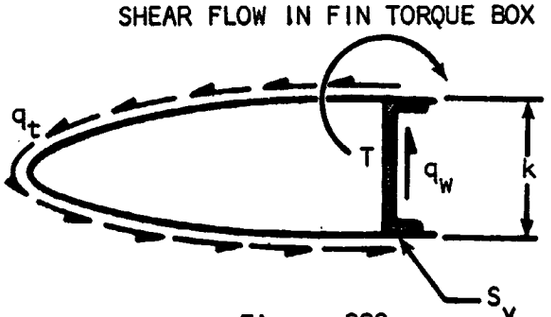


Figure 229

Skin $q_t = \frac{T}{2A}$

where:

T = torque, given in Figure 228

A = fin cell area, given in Figure 230

Skin $f_s = \frac{q_t}{t}$. The resulting skin shear stresses are shown in Figure 231

Shear buckling allowable:

$$\tau_{cr} = \frac{K_s \bar{E}_c \tau^2_{sk}}{b^2_{sk}}$$

$\tau_{cr} = 1.49(10^6)$ psi

Where:

K_s Based on simply supported panel.

$\bar{E}_c$ = effective modulus = $.75E_c$
= $.75\ (1.99)(10^6)$

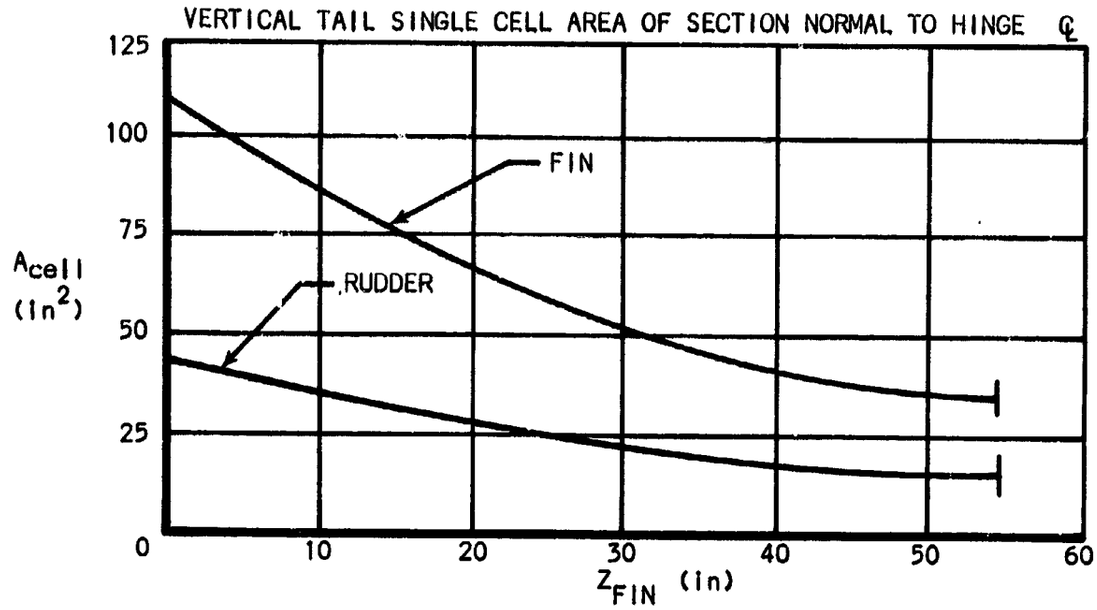


Figure 230

A comparison of skin shear stress versus buckling allowable in Figure 231 shows the vertical tail to be shear resistant at limit load.

@ root:

limit f_s = 715 psi ; τ_{cr} = 750 psi ; Buckling M.S. = $\frac{\tau_{cr}}{f_s} - 1 = \frac{750}{715} - 1 = +0.05$

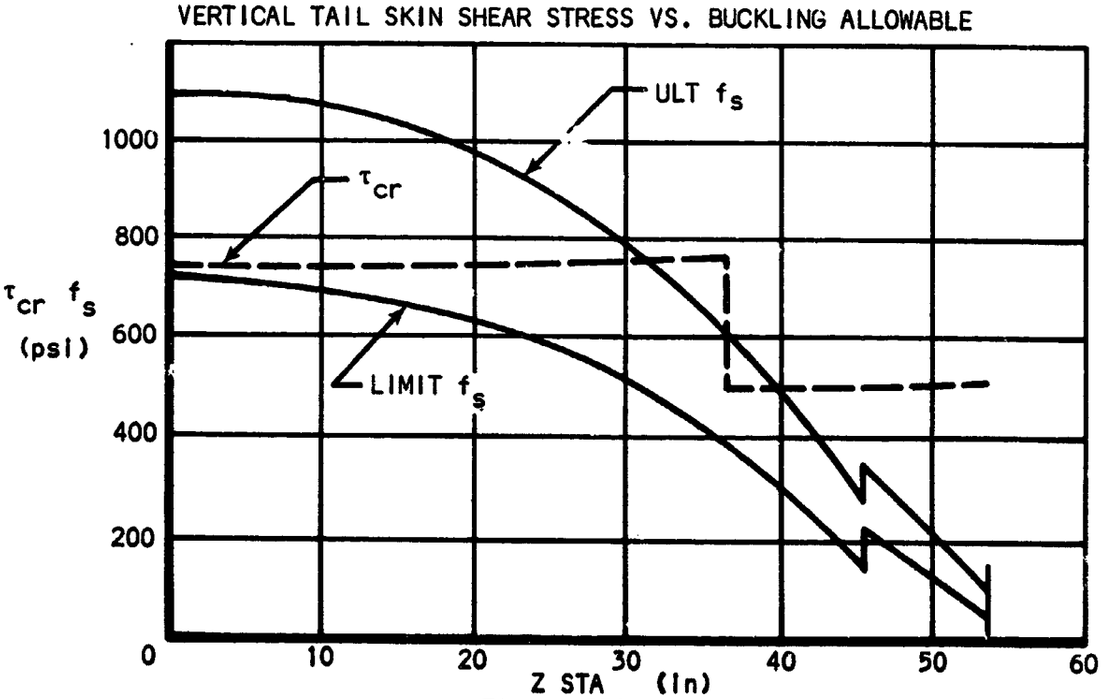


Figure 231

Skin stiffeners: First stiffener (shown below) above fuselage attachment is critical for gust load condition.

C_{ave} = 26 in.

w = .418 lb/in^2

w_x = .748 lb/in^2

P_{y_n} = 83 lb

w_r = .235 lb/in^2

Maximum moment based on distribution shown in Figure 232.

M_{max} = 187 in-lb assumes 80% of normal loading on tail acts on one surface.

LOADING DISTRIBUTION ON FIN STIFFENER

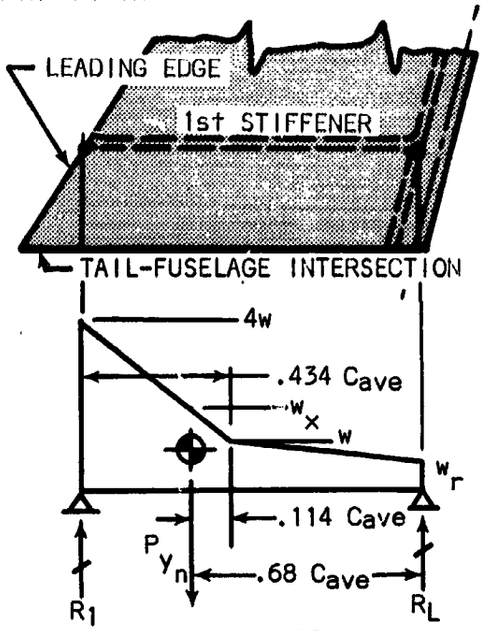


Figure 232

Section properties: Figure 233

$\bar{y}$ = .457 in.

I_{xx} = .0034 in^4

$$f_b = \frac{M\bar{y}}{I_{xx}} = \frac{187(.457)}{.0034} = 25100 \text{ psi}$$

F_{bu} = 31500 psi Ref. Table XXXIV

K_c = .80 stability factor (assumed)

$$\text{Bending M.S.} = \frac{F_{bu}\,K_c}{f_b} - 1$$

$$= \frac{31500(.80)}{25100} - 1 = \underline{+0.00}$$

FIN STIFFENER CROSS-SECTION

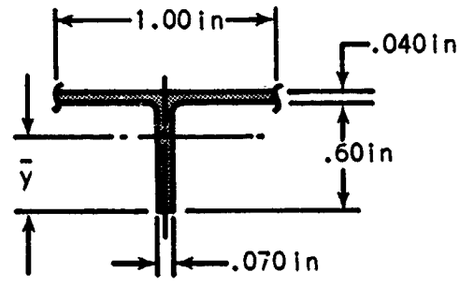


Figure 233

Stress analysis, Main spar:

Assumptions:

(1) Maintain a flange width, b, to flange thickness, t, ratio of 8.0 (maximum). However, hold b to a minimum of 0.75 in. for bonding purposes.
(2) Use channel configuration.
(3) React moment as couple between top and bottom flange.
(4) Make spar web shear resistant for limit load.

Spar flange: Gust condition critical

Maximum M @ root = 26800 in-lb Ref. Figure 227

$$f_t = f_c = \frac{P_c}{A_{flg}}$$

$$P_c = \frac{M}{h} = \frac{26800}{3.75} = 7150 \text{ lb}$$

$$A_{flg} = bt_f = 1.90(.240) = .456 \text{ in.}^2$$

$$f_b = \frac{7150}{.456} = 15650 \text{ psi}$$

Tension critical

F_{tu} = 20100 psi

K_t = .80 fatigue factor (assumed)

$$\text{Tension M.S.} = \frac{F_{tu} K_t}{f_t} - 1$$

$$= \frac{20100(.80)}{15650} - 1 = +0.03$$

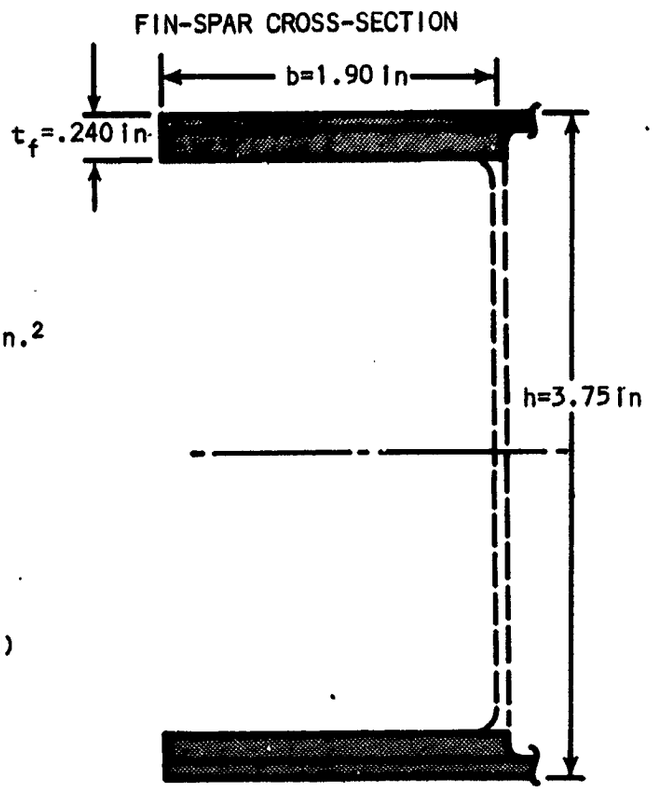


Figure 234

Spar web: Critical for shear buckling due to gust condition.

The web thicknesses were determined by first constructing a family of allowable shear buckling curves based on the formula used for the horizontal tail (ref. page 283). Next, the ultimate shear stresses were calculated for a number of possible thicknesses using the net shear flow. These stresses were plotted as a family of curves in the same figure as the allowables (Figure 235). The spar web gages were thus chosen on the basis that

$$f_{s_{limit}} \leq \tau_{cr}$$

Station 11 critical , Ref. Figure 235

$$f_{s_{limit}} = \frac{f_{s_{ult}}}{1.5} = \frac{2500}{1.5} = 1670 \text{ psi} , \qquad \tau_{cr} = 2500 \text{ psi}$$

$$\text{Buckling M.S.} = \frac{\tau_{cr}}{f_s} - 1 = \frac{2500}{1670} - 1 = \underline{+0.50}$$

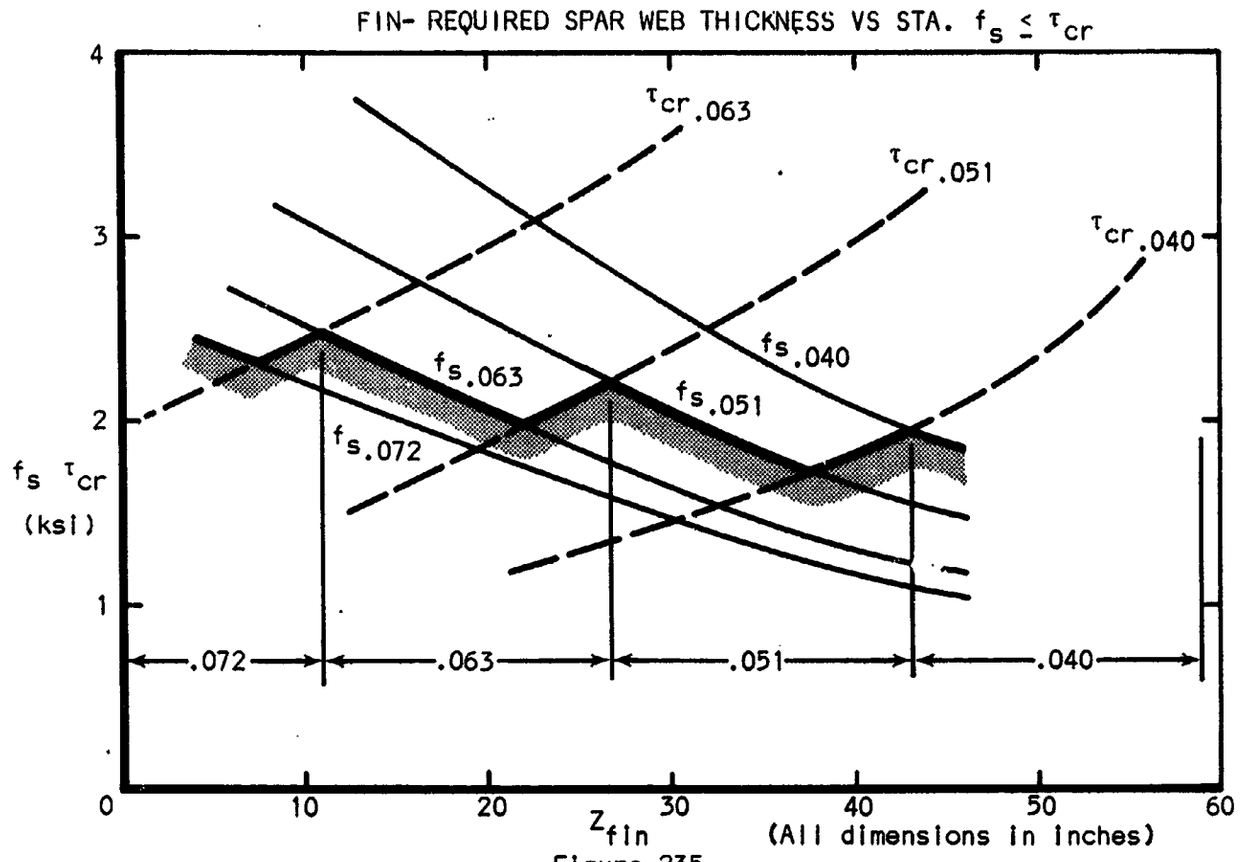


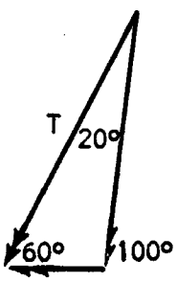
Figure 235

Fuselage attachment:

Critical condition: Gust load condition (ref. Figure 227).—A resolution of forces is necessary since the main spar is not parallel or perpendicular to the attachment planes.

Resolution of forces @ fin-fuselage interface

$$T' = T\left(\frac{\sin 60^\circ}{\sin 100^\circ}\right) - M\left(\frac{\sin 27^\circ}{\sin 82^\circ}\right) = .833\ T - .459\ M$$

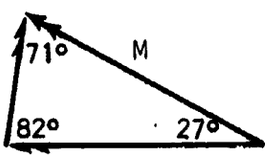


$$M' = M\left(\frac{\sin 71^\circ}{\sin 82^\circ}\right) + T\left(\frac{\sin 20^\circ}{\sin 100^\circ}\right) = .954\ M + .349\ T$$

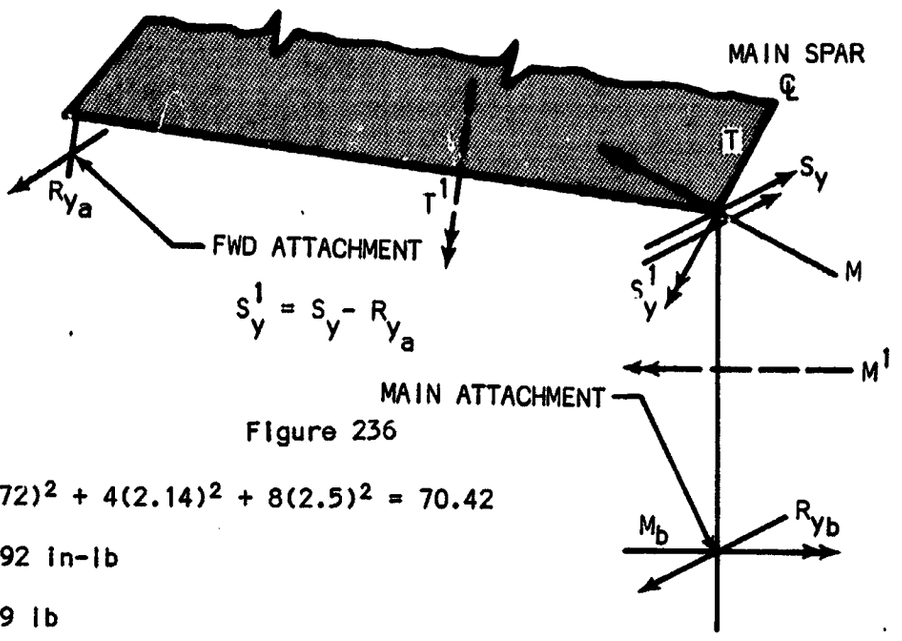
$$S_y' = S_y - R_{y_a}$$

Net attachment loads:

$$\text{Bolt } S_y = \frac{M_b\, z}{\Sigma z^2 + \Sigma y^2} + \frac{R_{y_b}}{8}$$



FIN-FUSELAGE ATTACHMENT LOADS



$S_y^1 = S_y - R_{y_a}$

Figure 236

$\Sigma z^2 + \Sigma y^2 = 4(.72)^2 + 4(2.14)^2 + 8(2.5)^2 = 70.42$

$M_b = 32592$ in-lb

$R_{y_b} = 1019$ lb

$S_y = \frac{32592(2.14)}{70.42} + \frac{1019}{8} = 1117$ lb

$S_z = \frac{32592(2.50)}{70.42} = 1158$ lb

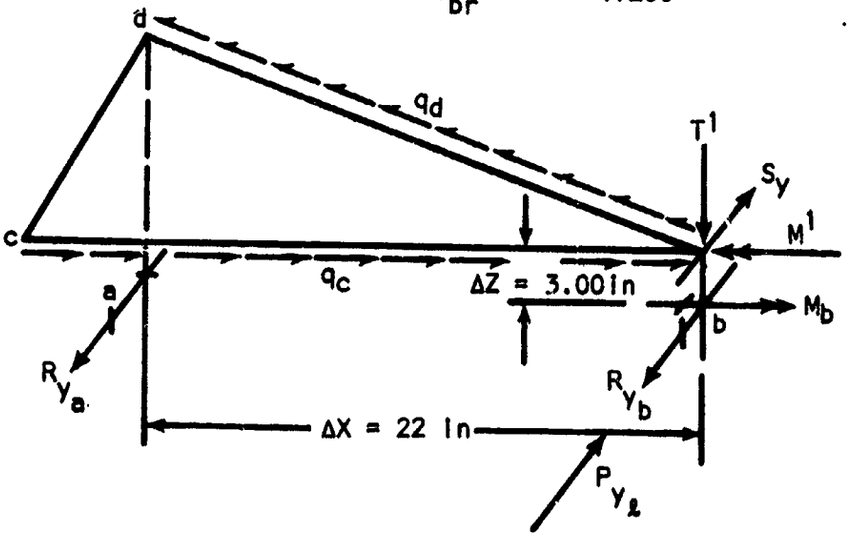
Main attachment, bearing critical: Check 3/8" bolt bearing in .25 thickness

$f_{br} = \frac{S_r}{Dt} = \frac{1610}{.375(.25)} = 17200$ psi , Where: $S_r = (S_y^2 + S_z^2)^{\frac{1}{2}} = 1610$ lb

$F_{bru} = 19700$ psi , Bearing M.S. $= \frac{F_{bru}}{f_{br}} - 1 = \frac{19700}{17200} - 1 = \underline{+0.15}$

$q_d = \frac{T}{2A_d} = \frac{T}{212}$

$q_c = \frac{T'}{2A_c} = \frac{T'}{260}$

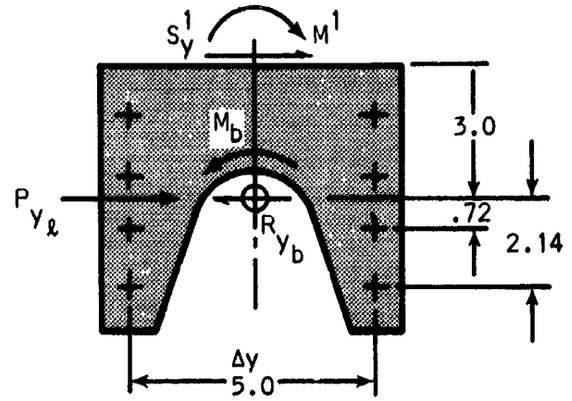


$$R_{y_a} = \frac{T'}{\Delta x} = \frac{T'}{22}$$

$$M_b = M' + \Delta z\, S'_y = M' + 3\, S'_y$$

$$R_{y_b} = S'_y + P_{y_\ell}$$

FIN MAIN SPAR, ATTACHMENT TO FUSELAGE



(All dimensions in inches)

Figure 237

Stress analysis of rudder: The rudder is critical for the maneuver condition described on page 293. The net loads are included in Figure 228. The stress analysis was performed in a similar manner to the fin portion of the vertical tail. A margin of safety summary for the rudder is found on Table XLIX.

TABLE XLIX - VERTICAL TAIL MARGIN OF SAFETY

	Item	Material	Type of loading	Stress level	Allowable (psi)	Factors	M.S.
Fin	Skin	Chopped E-Glass/ Epoxy	Buckling	715	τ_{cr} = 750	---	+0.05
	Skin stiffeners		Bending	25100	F_{bu} = 31500	0.80	+0.00
	Spar flange		Bending	15650	F_{tu} = 20100	0.80	+0.03
	Spar web		Buckling	1670	τ_{cr} = 2500	---	+0.50
	Spar attach. - fuse		Bearing	17200	F_{bru} = 19700	---	+0.15
	Fwd. attach. - fuse		Bearing	9000	F_{bru} = 19700	---	+1.19
	Rudder attach. - upper		Tearout	2580	F_{su} = 9200	---	+1.50
Rudder	Skin	Chopped E-Glass/ Epoxy	Buckling	438	τ_{cr} = 458	---	+0.05
	Skin stiffeners		Bending	21100	F_{bu} = 31500	0.80	+0.20
	Spar flange		Bending	9150	F_{tu} = 20100	0.80	+0.76
	Spar web		Buckling	1125	τ_{cr} = 2000	---	+0.67
	Lwr. attach.		Bearing	3880	F_{bru} = 19700	0.50	+1.54

Component Cost and Manufacturing Considerations.- The cost analyses discussed in this sub-section are limited to just two of the four primary structural components. These, the vertical stabilizer and the wing, are structurally the least and most demanding, respectively. In any event, thse two analyses demonstrate the magnitude of the potential savings associated with machine molded/high production rate construction concepts. Manufacturing considerations for all four (vertical tail, horizontal tail, wing, and fuselage) primary structural components will be discussed briefly.

Vertical tail: The vertical stabilizer, with its minimum structural requirements, is a feasible application for both compression molded thermosetting (reinforced) plastic and injection molded (reinforced) thermoplastic.

Compression molding of prepreg sheet molding thermosetting composites, such as E-glass/polyester, is considerably slower than injection molding. It does offer, though, a good possibility of achieving the required thin skins. This is possible due to the partial distribution of prepreg material, normally preheated, in the dies before the dies are closed. This means the material has a shorter distance to travel to the die extremities. Also, the material "setting" time is slower and the material has considerably more time to flow, since it "sets" or cures by chemical reaction rather than by "freezing" as with thermoplastics.

Compression molding, using prepreg sheet molding compound, does not lend itself to mass production as well as injection molding, due to its slower "set" time, hand loading requirements and supporting activity requirements such as precutting and preheating of the sheet molding compound. It is far superior though to the normal hand lay up procedures normally associated with reinforced thermosets.

Compression molding of the vertical tail, using E-glass/polyester would require only 1000 psi (approximately) and 300°F. The precut and preheated prepreg material is loaded (presently by hand) into the heated die halves, after which the die halves are slowly mated.

A hydraulic press of at least 450-ton capacity will be required to mold each vertical stabilizer skin. Closing and opening speed should be adjustable and variable within each cycle (i.e., the press should have a high speed initial closing rate to first die mate, followed by an adjustable final closing rate). This action should be semi-automatic. Such a press is estimated to cost $11-$12 per hour to operate.

The dies, most probably fabricated from aluminum, are estimated to cost from $10,000 to $24,000. These estimates are based on todays tool fabrication costs. It would be very difficult to predict whether such costs will be higher or lower in fifteen years. Compression molding die costs are higher than injection molding die costs since many more dies are required to produce parts at an equal rate. This will become evident in the following cost consideration discussions.

Coring is not as readily achieved with compression molding as with injection molding. This is due to the possibility of very high local pressure differentials that can exist between opposite sides of a core during distribution of the more viscous resin, as the dies are closing.

Table L

INDUSTRY ESTIMATES OF VERTICAL STABILIZER TOOLING COSTS (DOLLARS)

MOLDER OR MOLD MAKER	R. H. SKIN	L. H. SKIN	SPAR	RIB	BONDING FIXTURE
Injection					
A	←	60,000	→		—
B	50,000	50,000	—	—	—
C	50,000	50,000	—	—	—
D	←	16,000	→		(600)
E	←	100,000	→		—
E	←	(30-36,000)	→		—
For analyses purposes, use	24,000	24,000	—	—	1500
Compression					
F	10-12,000	10-12,000	—	—	—
G	24,000	24,000	5000	4000	3000-(1500)
E	24,000	24,000	5000	4000	3000
H	←	65-70,000	→		15,000
J	—	—	1800	3000	—
For analyses purposes, use	24,000	24,000	5000	4000	2000

NOTES: 1) ( ) = Est. for Aluminum Tooling

2) Molders A,B,C....are located in the Los Angeles - San Diego area.

The design of vertical stabilizers constructed of the above materials differs only in that the injection molded nylon stabilizer is about 10% heavier (due to its lesser strength/stiffness) and the nylon stabilizer can be molded in two pieces rather than four, due to its superior moldability. See Figure 238.

The injection molded stabilizer can be molded as a left-hand skin/rib and a right-hand skin/spar. The compression molded stabilizer possibly could be molded into the same two components, but would more likely be molded into a separate left hand skin, right hand skin, spar, and a rib, as shown earlier in Figure 147. Earlier attempts at two-piece construction, with the bond line all in a single plane, were abandoned due to inherent structrual/weight penalties, i.e., using the tongue-and-groove joint on a split spar and split rib. Figure 238 illustrates the tongue-and-groove joint on the leading edge only.

TWO-PIECE CONCEPT VERTICAL STABILIZER

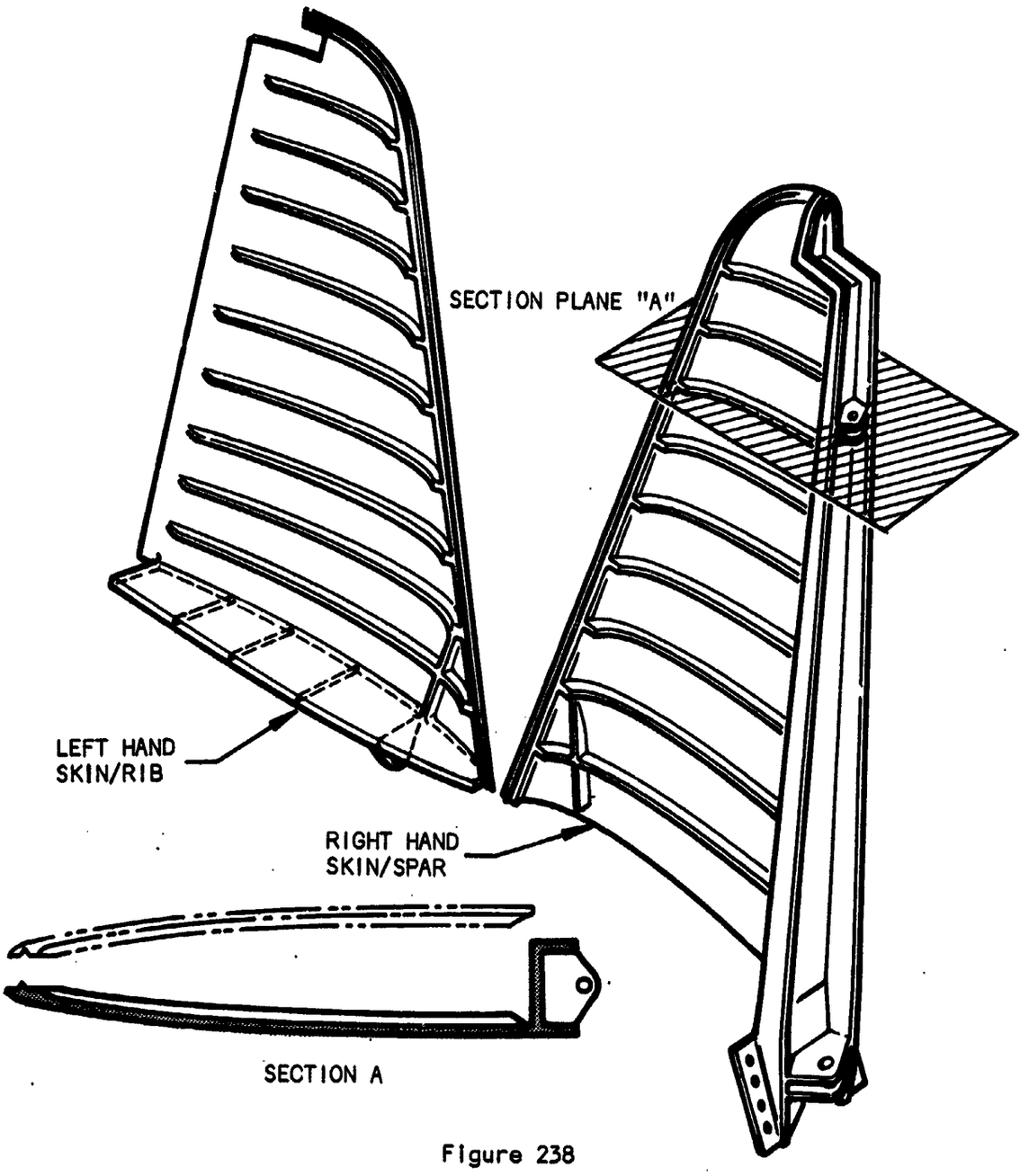


Figure 238

Section plane A, identical in nature on both components, taken from Figure 238, is illustrated in Figure 239, with the method that would be employed in molding both parts (i.e., the right hand skin/rib and the left hand skin/spar). This molding die arrangement is applicable particularly to injection molding but could possible also be applicable to compression molding. No movable cores are required, except to hold the molded in place metallic inserts in the clevis fittings on the spar. The skin/spar or skin/rib at first glance might appear to be trapped in the female mold, but it can readily be stripped from the die by using a lateral mode of extraction. In the worst case, die segment B in Figure 239 might have to be stripped from the part after the part is removed from the female die half. This two-piece concept is not at all unusual for injection molding. Die segment B would be retracted automatically as would all the other cores for the fastening and hinge fitting holes.

VERTICAL STABILIZER MOLDING DIE ARRANGEMENT
(For injection and possible compression molding)

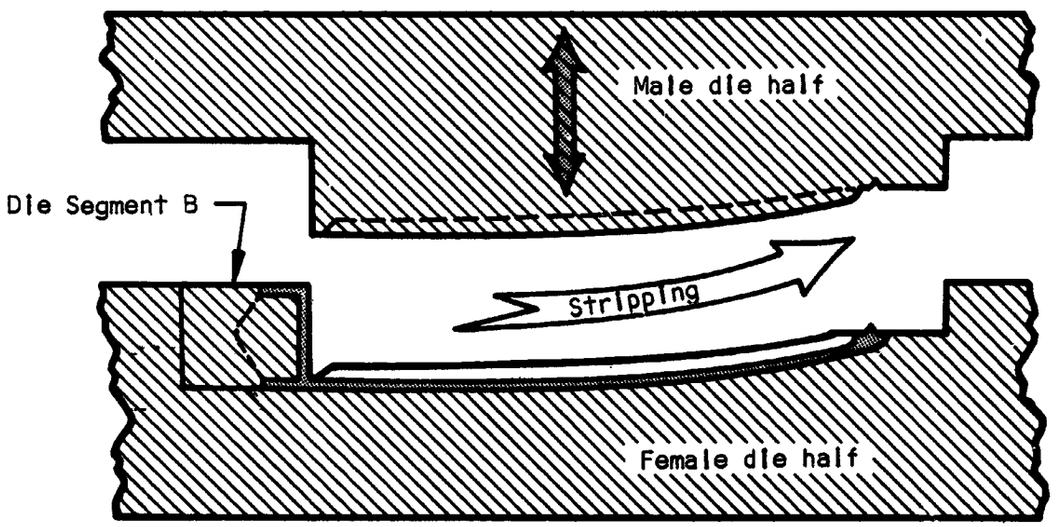


Figure 239

The rudder, of similar configuration, can also be constructed using this skin/spar + skin/rib concept.

This two-piece construction eliminates the otherwise required separate tooling costs and separate molding time costs for both the spar and the root rib. Additionally, the amount of trimming, inspection, bonding prep, actual bonding, and joint clean-up are reduced.

Additional discussions with injection molders reveal optimism concerning the feasibility of molding large thin skin components. It is quite reasonable to assume that the thin skins would be readily achievable in fifteen years, and are probably achievable today. The United States is lagging Europe and Japan, where the world's largest molding machines are built, in injection molding capability.

More and more injection molders in the United States are beginning to use aluminum dies. They are significantly cheaper and steel inserts can be used in high wear areas. Also, the higher thermal conductivity of aluminum provides for reduced cycle time, i.e., higher production rates.

An injection molded vertical stabilizer, according to molders, would require little or no clean-up after molding. The part could be submarine gated, so it would be removed from the dies, free of any gate projections. Any clean-up that would be required could be accomplished by the molding machine operator. The vertical stabilizer would be molded at a rate, conservatively estimated at 30 parts per hour, and more likely at 60 parts per hour.

Bonding of the stabilizer components, whether injection molded nylon or compression molded E-glass/polyester, would be accomplished in a fixture with provision for heating to accelerate curing of the adhesive. The surfaces to be bonded would require light sanding before application of the adhesive. Should the components be made of nylon, bonding will require considerably more attention. Nylon, and particularly glass reinforced nylon, is difficult to bond. It would require a special etch* of the surfaces to be bonded.

Table LI summarizes all the cost analyses performed on the vertical stabilizer. It is significant to note that one injection molding machine, operating two shifts per day, can produce both components of the nylon vertical tail in 100,000 units per year quantities, while it requires twenty compression molders, operating three shifts per day, to mold the four glass/polyester components in like quantities. Production rate for injection molding, estimated at 60 pieces per hour, is a liberal estimate of today's capability, but a conservative estimate of molding rates fifteen years from now. The four-per-hour production rate for compression molded glass/polyester is possibly attainable today and will surely be routine fifteen years from now. Estimates of fabrication sequences and times associated with both the injection molded and the compression molded vertical stabilizer are detailed in Table LII.

*e.g., calcium chloride-ethanol

Table LI

COST ANALYSIS TO PRODUCE 100,000 VERTICAL STABILIZERS PER YEAR

	INJECTION MOLDING	COMPRESSION MOLDING
PIECES PER ASSY	2	4
CYCLE TIME/PIECE	$\frac{1 \text{ min}}{80\% \text{ eff}}$ = 1.25 min	$\frac{15 \text{ min}}{80\% \text{ eff}}$ = 18.75 min
TOTAL TIME FOR 100,000 ASSEMBLIES	$\frac{1.25 \text{ min} \times 100{,}000 \text{ assy} \times 2 \text{ pcs/assy}}{60 \text{ min}}$ = 4160 hrs	$\frac{18.75 \text{ min} \times 100{,}000 \text{ assy} \times 4 \text{ pcs/assy}}{60 \text{ min}}$ = 125,000 hrs
FABRICATION COSTS	**INJECTION MOLDING**	**COMPRESSION MOLDING**
Raw Materials	(14.3 lbs/assy) X (.65 $/lb) X 100,000 assy = $929,500	(14.3 lbs/assy) X (.60 $/lb) X 100,000 = $858,000
Tooling		
Prepreg cutters	Not required	1 @ $ 1,500.00 = $ 1,500.00
Die sets	1 @ $48,000.00 = $48,000.00	5 @ 57,000.00 = 285,000.00
Trim tools	Not required	1 @ 3,000.00 = 3,000.00
Bonding fixtures	20 @ $ 1,500.00 = $30,000.00	20 @ 2,000.00 = 40,000.00
	$78,000.00	$329,500.00
Molding		
Machine charge	$\frac{\$7000}{\text{mo}} \times \frac{12 \text{ mo}}{*2080 \text{ hrs} \times 3 \text{ shifts}}$ = $13.50/hr	Estimated = $ .56/hr
Labor & overhead	10.00/hr	10.00/hr
	$23.50/hr	$10.56/hr
	4160 hrs X $23.50/hr = $97,760	125,000 hrs X $10.56/hr = $1,320,000
Auxiliary Operations	$\frac{9.35 \text{ min}}{\text{assy}} \times \frac{100{,}000 \text{ assy}}{80\% \text{ eff}} \times \frac{1 \text{ hr}}{60 \text{ min}}$ = 19,500 hrs	$\frac{16.23 \text{ min}}{\text{assy}} \times \frac{100{,}000 \text{ assy}}{80\% \text{ eff}} \times \frac{1 \text{ hr}}{60 \text{ min}}$ = 33,812 hrs
	19,500 hrs X $10/hr = $195,000	33,812 hrs X $10/hr = $338,120
SUMMARY		
Raw Materials	$ 929,500	$ 858,000
Tooling	78,000	329,500
Molding	97,760	1,320,000
Auxiliary Operations	195,000	338,120
	$1,300,260	$2,845,620
UNIT COST	$\frac{\$1{,}300{,}260}{100{,}000 \text{ assy}}$ = $13.00/assy	$\frac{\$2{,}845{,}620}{100{,}000}$ = $28.45/assy

Note: *Total available working hours per year for one shift:
8 hrs X 5 days X 52 weeks = 2080 hrs

Table LII

FABRICATION SEQUENCES AND ESTIMATED TIMES
(for vertical stabilizer)

SEQUENCE		TIME (min.)
	Compression Molding	
1)	Die cut SMC* to spec. shapes	
	a) Skins (10 pcs @ 20/min)	.50
	b) Spar (10 pcs @ 20/min)	.50
	c) Rib (5 pcs @ 10/min)	.50
2)	Preheat SMC blanks	1.00
3)	Load & cure in press (part of molding charge)	-
4)	Degrease	.33
5)	Cool (no charge)	-
6)	Trim flash (4 parts @ .30 ea)	1.20
7)	Inspect "	1.20
8)	Bonding preparation (4 parts)	1.20
9)	Load all four parts in fixture	.30
10)	Apply adhesive	.60
11)	Close fixture & cure	6.45
12)	Remove from fixture	.15
13)	Inspect	1.20
14)	Dress joints	1.00
15)	Stock or convey to assembly area	.10
		16.23
*sheet molding compound		
	Injection Molding	
1)	Inspect (after molding)	.90
2)	Place skin/spar and skin/rib in bonding fixture	.10
3)	Prepare mating surfaces for bonding	.30
4)	Apply adhesive	.30
5)	Close fixture	.05
6)	Cure adhesive	6.55
7)	Open fixture & remove bonded fin	.15
8)	Dress bonded joints & inspect	1.00
		9.35

End result of the analyses indicates that the vertical stabilizer, manufactured at the rate of 100,000 units per year, can be produced at a manufacturer's cost of: (1) $13.00 when injection molded of glass/nylon 6-10, or (2) $28.45 when compression molded of glass/polyester. These costs are significantly competitive with conventional sheetmetal construction as indicated in Figure 240. Of prime significance is the indication that both injection molded and compression molded vertical stabilizers can be manufactured at a lower cost than conventional sheetmetal, even at current quantities. E.g., compare the following price-quantity relationships for the three types of construction.

	Current Quantities (i.e., 1000/Yr)	High Production Quantities (i.e., 100,000/Yr)	Production Rate Break-even Point With Sheetmetal (Units/Yr)
Sheetmetal	$110	$34	*
Compression molded	88	28	620
Injection molded	61	13	360

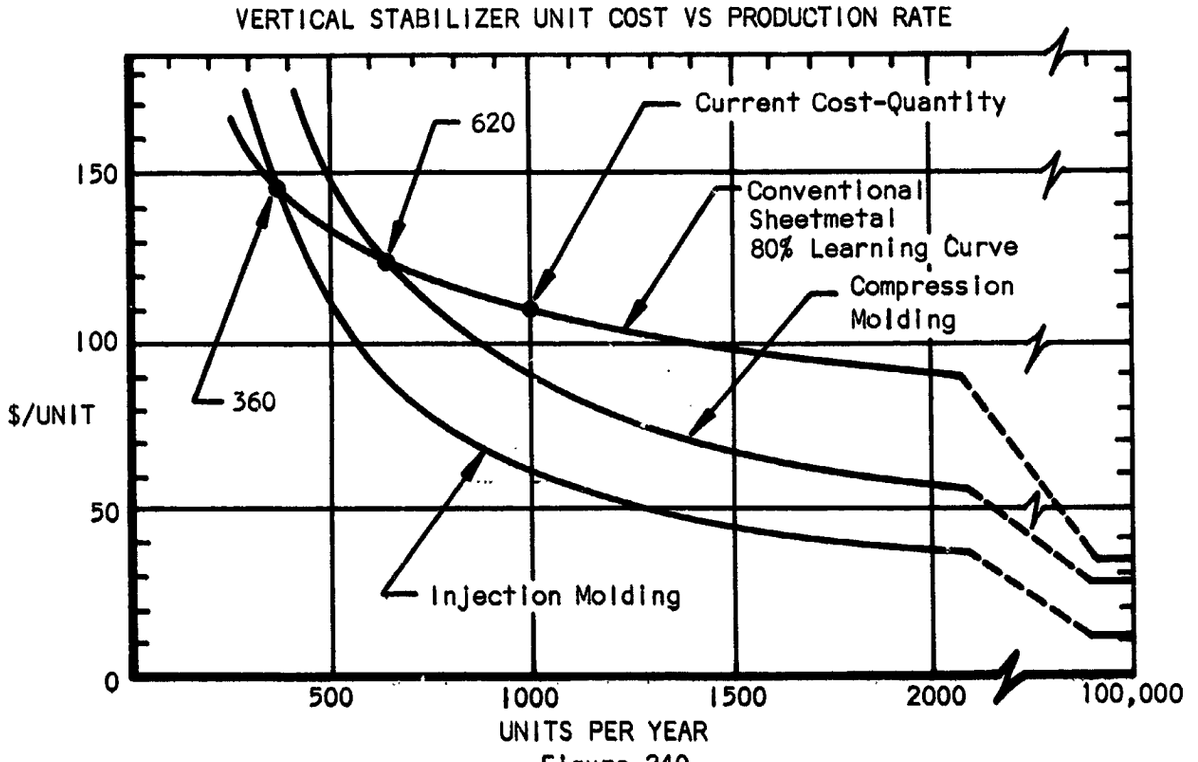


Figure 240

* The reader should be aware that the "learning curve" is a function of cumulative quantities, which were assumed to have occured within one year; for comparison with the yearly production rates of the molded units.

Referring to Figure 240, conventional sheetmetal construction unit cost is less than that for compression molded and injection molded construction only at production rates less than 620 and 360 units per year, respectively.

Horizontal tail: This portion of the airplane, being more heavily loaded than the vertical stabilizer, requires the use of an epoxy/glass composite. Neither chopped E-glass/polyester nor injection molded nylon 6-10 is structurally adequate for most of the horizontal tail components. Therefore, most if not all of the ten different reinforced plastic horizontal tail components will be compression molded from an epoxy/glass composite.

Referring to Figure 241, components (-11, -25, & -27) might later be proven to be more economically produced from injection molded nylon 6-10. The skin quarter-panels, i.e., top or bottom on either side (-1 or -3), will require a molding press capacity of approximately 1500 tons (for compression molding). This is easily within today's readily available capacity.

The main spar (-5) will require 400 to 500 tons for molding, but a larger tonnage capacity press might have to be used to provide large enough platens. The spar, as molded, is only 4.5 in. wide, but is over 151 in. long. Alternate approaches might be to build extensions for the platens outside the main platen area, or to mold the spar in two presses set side by side.

The trailing edge spar, and the anti-servo tab channel and skin (-7, -28, & -21, respectively), also being of outsize lengths, will each require either excess press capacity (tonnage), or two or more presses set side by side.

The torque box (-9), if it is made in one piece as indicated, will require a large core on each side to form the pans on each side. As mentioned earlier, this part might be easier and cheaper to fabricate if it were separated into two identical ribs and a shallow box.

Wing: The wing, being the most demanding of all the primary structural components, requires the use of at least S-glass/epoxy, and preferably high modulus graphite/epoxy. For the purpose of this study, the wing components were assumed, in general, to be fabricated in a manner similar to the vertical tail. I.e., die costs, in general, were estimated on a projected area basis, proportionate to the vertical tail die costs. This is valid for dies of comparable depth and complexity. Most of the wing components are no larger than the horizontal tail components. Exceptions to this are the spar and the skins. Molding presses of more than adequate capacity are available today, even for components as large as the spar and skins. Dies for the spar could possibly be made in segments due to their out-size length requirements. The spar could be molded in one big press or in a series of presses set side by side.

For outsize, but simple, components such as the wing skins (with no integral stiffeners) a new castable ceramic mold material offers significant

HORIZONTAL TAIL, EXPLODED VIEW

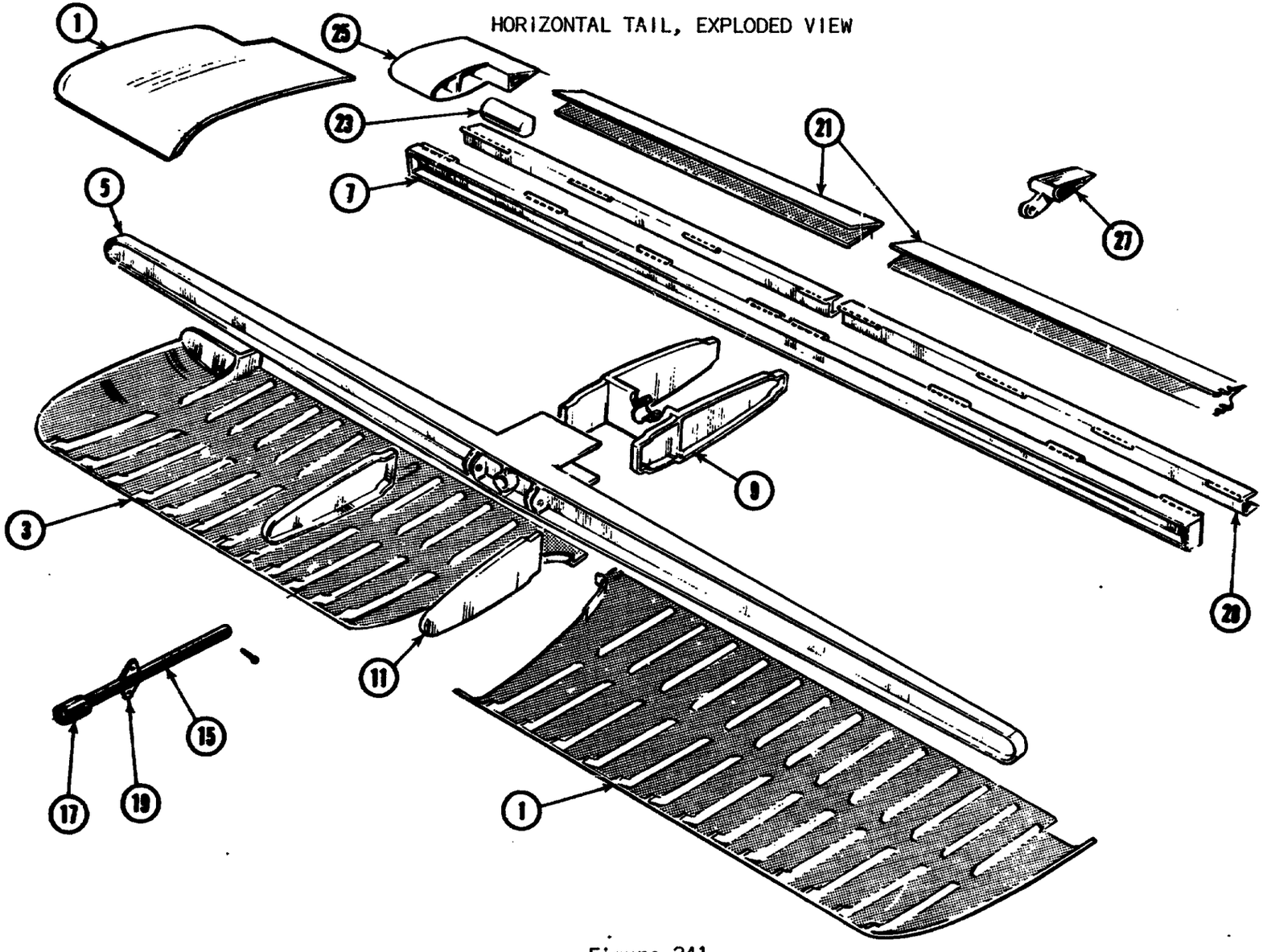


Figure 241

WING, EXPLODED VIEW

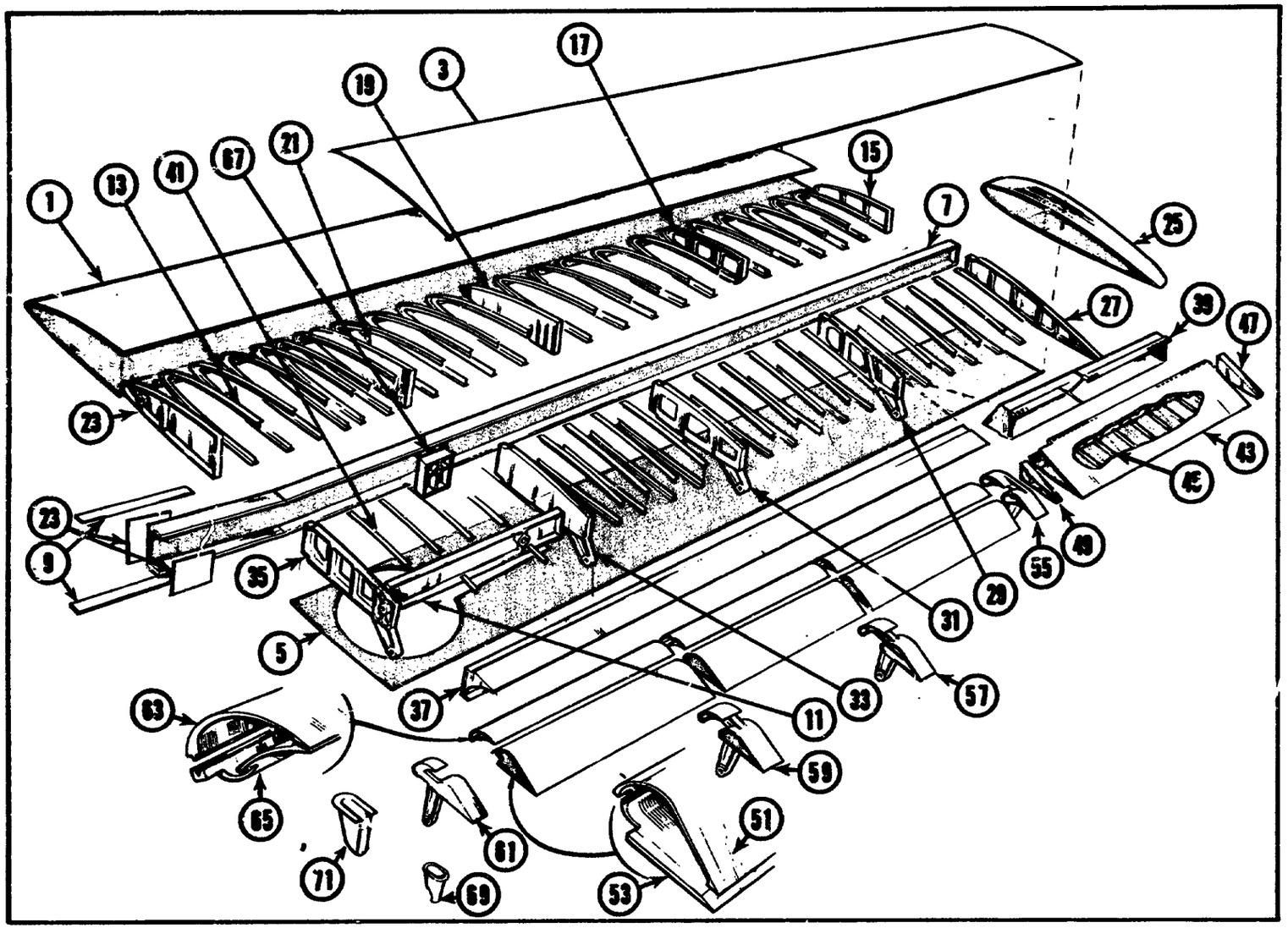


Figure 242

cost savings. It is not recommended for applications such as shapes with stand-up ribs or where cores are required. Such molds are normally fabricated with a two-inch thickness of the ceramic material backed up with foamed fused silica blocks. The bonded-on foam blocks are cut smooth and flat and mounting studs are then potted into the foam. No internal reinforcing is employed. Another advantage is the ability to cast-in-place all the necessary electric heaters or steam lines. The basic cost of this ceramic material is $1100/ton (i.e., $0.55/lb). It has a density of 120 lb/ft^3.

These molds can be fabricated in matched sets (male and female) and are completely adequate for the 1000 psi compression molding requirements. Die cost for the wing skins was based on the use of matched sets of the above ceramic molds. Using only a female mold and a pressure bag reduces total wing manufacturing cost by a maximum of 3%. Since the (bagged) inner skin surface is not as reproducible as with matched molds, the 3% is well spent, to minimize bonding preparation for the skin stiffeners.

As with the vertical and horizontal tail, the wing is assumed to be assembled by secondary bonding in appropriate jigs and fixtures.

The first cost analysis, based on the tapered wing illustrated in Figure 242, assumed that each component* would be machine molded individually in a press of appropriate capacity. This first analysis considered both the 30-minute cure time for current epoxies and an estimated cure time of 15 minutes for future epoxies. Referring to Figure 243, bars (1) thru (5) represent the above described wing. Bar (1), for single-cavity molding and 30-minute epoxy cure time, has a molding cost which is 54.2% of the total wing manufacturing cost. Therefore the savings in bar (2) are large when the production rate is doubled, by halving the current 30-minute cure time.

Subsequent analyses of the wing based on the use of multi-cavity dies, took advantage of the potential savings attainable with higher production rates. Since factory time is not practically available below $10 per hour, the minimum size molding press considered was 650-ton capacity, which cost about $12 per hour to operate. It turned out that platen area, not component projected area/pressure requirements, determined the number of cavities per die or the number of die modules. It was first assumed that only a constant chord constant thickness wing, with its many identical parts, could take advantage of multi-cavity molding. I.e., it would be impractical to attempt to mold dissimilar or unidentical components on the same stroke of the press. This would be true due to the slight difference in molding requirements between unidentical components. It turns out that the no-two-parts-alike tapered wing can also take advantage of multi-cavity tooling, when the associated quantities are on the order of 100,000 units per year, as in these analyses.

Referring again to Figure 243, bars (3) and (4) represent the same wing as bars (1) and (2), respectively, except for the use of multi-cavity tooling.

---

*There are no two components alike in the tapered wing.

FAR TERM LIGHT AIRPLANE WING UNIT MANUFACTURING COSTS
(for 100 000 units/year production rate, except ⑨)

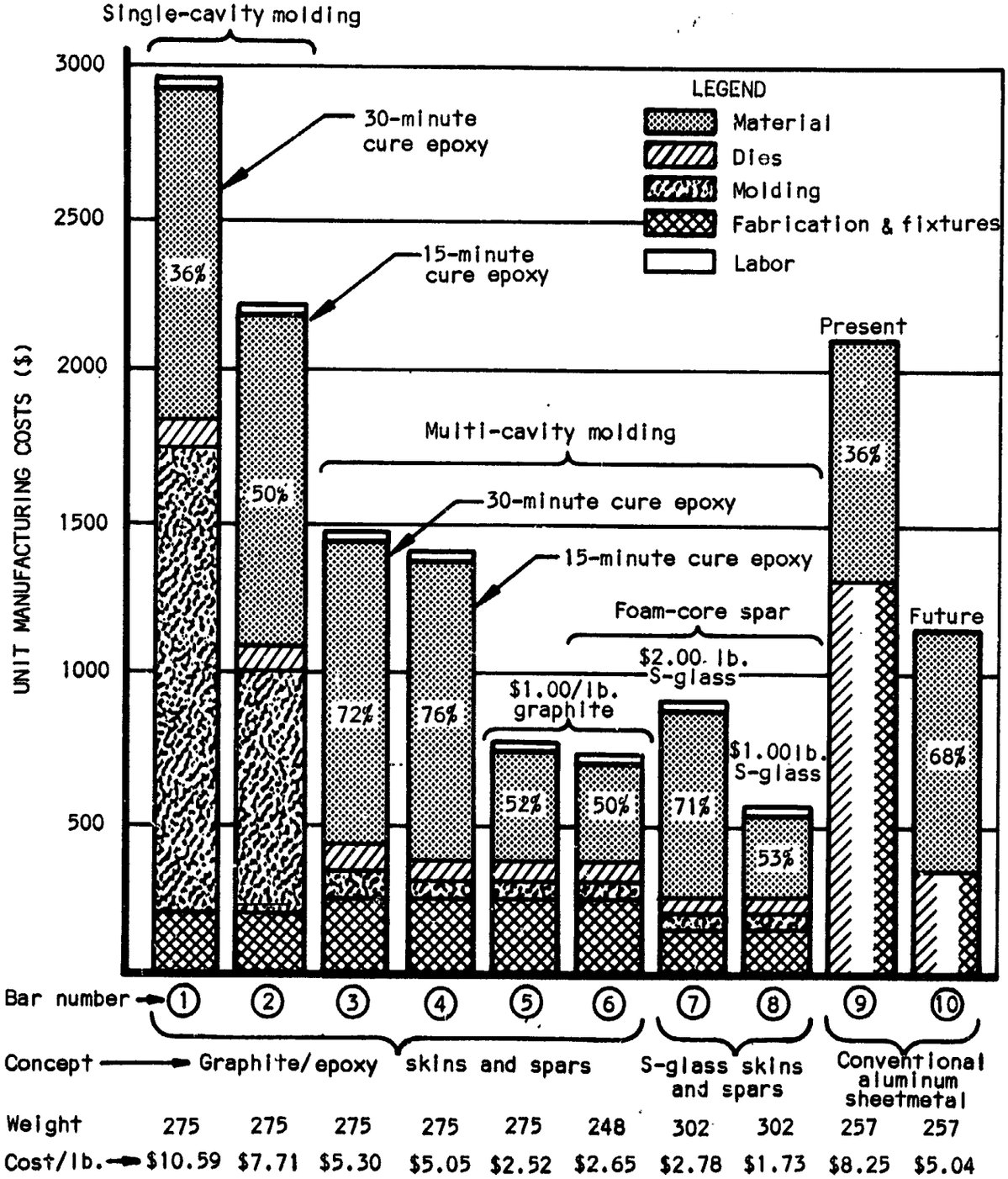


Figure 243

Multi-cavity molding appears to offer a significant reduction in unit manufacturing cost; i.e., about 35%, for the 15-minute cure wings.

Examination of bar (4) makes apparent the high (76%) portion of the wing unit cost represented by the raw material. Most (82%) of the raw material in bar (4) is for graphite/epoxy at $5.00 per pound. Obviously, the unit manufacturing cost of the wing is a significant function of the cost of graphite.

Industry sources have estimated the cost of graphite in fifteen years, ranging from $1.00/lb. to $100.00/lb. Bar (5) optimistically charts wing unit manufacturing cost for the same wing as bar (4), using $1.00/lb. rather than $5.00/lb. graphite. Figure 244 plots the cost of the multi-cavity molded, 15-minute epoxy cure wing as a function of the cost of graphite up to $10.00 per pound.

Bar (6) in Figure 243 plots a wing comparable in cost to bar (5) which which has a foam-core spar, offering a significant (10%) weight reduction over the wings considered in bars (1) through (5).

For comparison, a wing which replaces the graphite/epoxy components with S-glass/epoxy components is plotted as bar (7). Its cost also is a significant function of the cost of the S-glass/epoxy (i.e, $2.00 per pound). Some savings in fabrication are realized by molding the many skin stiffeners integral with the skins. This is accomplished by first partially curing the unidirectional filament skins and then integrally molding the chopped fiber stiffeners to the skins, final curing them together.

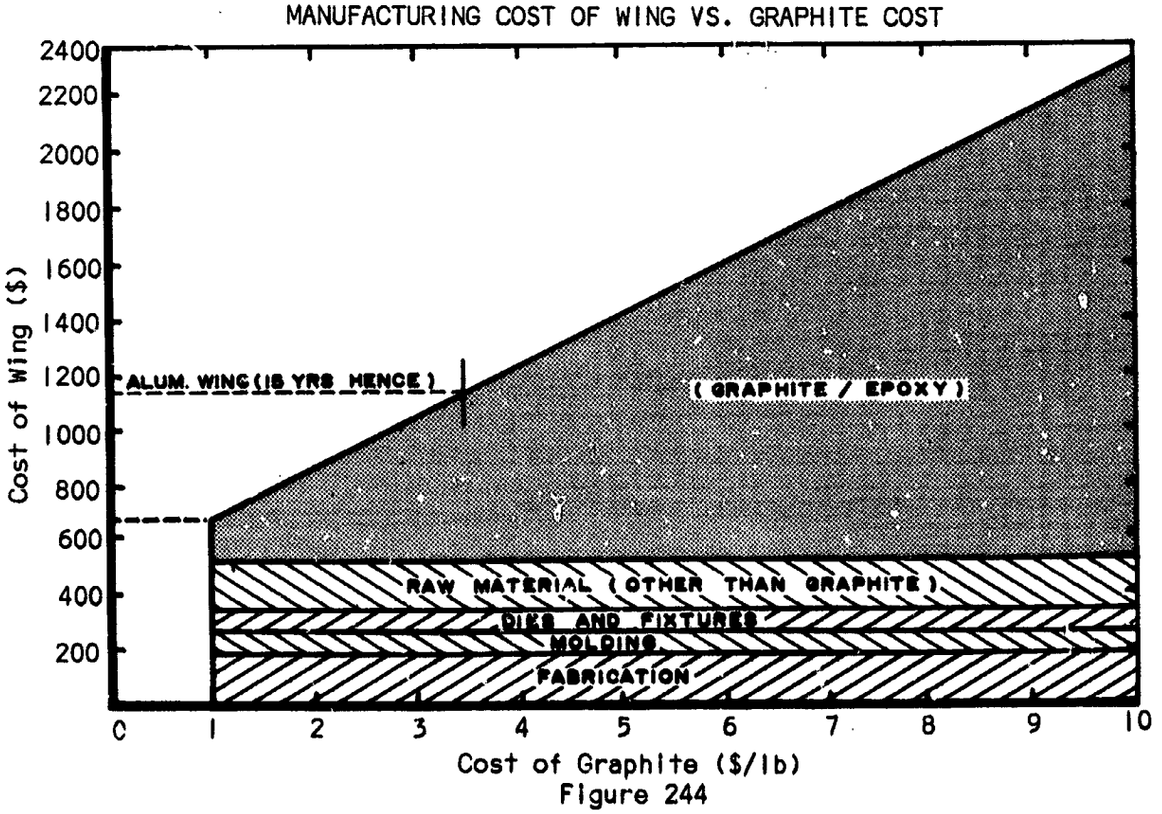


Figure 244

FUSELAGE, EXPLODED VIEW

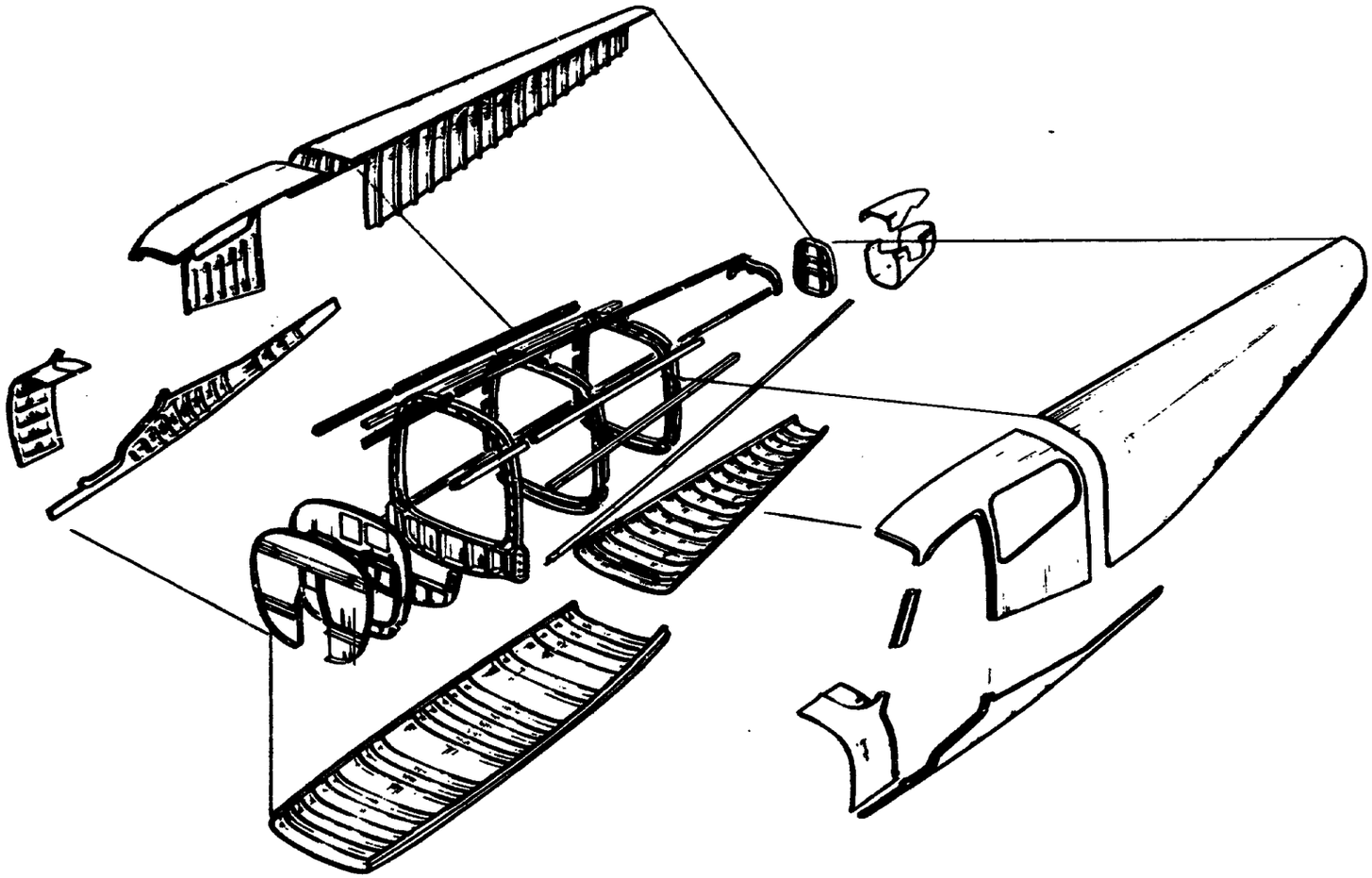


Figure 245

It is only fair to assume that S-glass could eventually be procured at a cost equally as low as graphite. Therefore, in Figure 243, bar (8) indicates a low unit manufacturing cost of approximately $521.00 for an S-glass wing using $1.00/lb. S-glass.

Referring to Figure 243, the foam-core graphite wing [ref. bar (6)] then appears to have the lowest weight with a very low unit cost; but the S-glass wing [ref., bar (8)] has the lowest unit cost and a significantly lower specific unit cost of $1.73 per pound.

Bars (9) and (10) plot the wing unit manufacturing cost of a conventional sheetmetal (aluminum) wing. Bar (9) is based on current production quantities and bar (10) represents reduction in cost due to high production rates and the classic 80% learning curve.

Fuselage: All the fuselage (see Figure 245) components except the stainless steel firewall and the channels and longerons are large, but conventional, compression moldings. All the previous discussions of compression molding consideration associated with the tail and wing, are equally applicable to the fuselage components. The channels and longerons, having constant cross-sections, can readily and economically be bag molded over male dies. Even with the specification of continuous and unidirectional filaments for the channels and longerons, there is a possibility that each might be molded in a continuous lay up and cure operation. Like the vertical and horizontal stabilizers and the wing, the fuselage would be an all-bonded assembly.

In conclusion, it can be said that the most significant reductions in light airplane unit manufacturing cost will be the result of high (mass) production methods and processes. E.g., machine molding and forming of primary components, all-bonded assembly, numerically controlled spot welding and riveting, prepriming (at the mill) of aluminum sheets (for bonding), automatic nondestructive inspection of bonded joints, etc. Less tangible, but significant, savings are realized with the elimination of corrosion on plastic components.

The various components of the Far Term airplane were not specifically designed for the minimum number of parts. The more simple components (fin, rudder, stabilizer) approached the minimum number of parts due to material/concept and molding compatability. On the other hand, further cost reductions might be achieved if a detailed minimum parts study was done for each component. The complex structures such as the wing and fuselage would benefit the most from such a study.

Although this study has concentrated heavily on the utilization of plastic materials, aluminum will remain a prime candidate for light airplane structure in the future. Aluminum is exceptionally machinable, formable, and joinable. Its use will continue with the greater use of mass production techniques mentioned above. Greater use of 6061 T6 and 5086-H32 aluminum alloys will likely occur with resultant savings in material cost. No one group of materials, metallic or nonmetallic, will be used universally. It will still remain for the designer to weigh the pros and cons of each material for each individual application. See Appendix S for an estimated consummer price breakdown of the Far Term airplane.

CONCLUSIONS

General

This study investigated every aspect of light airplane and helicopter design, manufacturing methods, and materials in use or of potential use as structural and non-structural components. Significant conclusions drawn from the investigation now follow.

Present helicopter construction is not different from typical light airplane construction but helicopter designers use more of the sophisticated techniques common in military aircraft and commercial transports, such as bonding and chemical milling, because weight savings are more important in a helicopter than in a light airplane.

Typical light airplane structure consists of relatively large sheet metal panels 0.025 to 0.032 inch thick, whereas helicopter fuselages have smaller panels 0.020, 0.016 and even 0.012 inch thick, supported by many very lightweight formers and stiffeners. These lighter but more elaborate constructions, coupled with lower production rates,are conducive to higher airframe costs. The average helicopter cost is $30.00 per pound of empty weight, compared to $10.00 per pound of empty weight for light airplanes.

Very consistent data was obtained on the cost of aircraft structure. Two different approaches were used to obtain this information. Results from both methods were in good agreement.

(1) A grass-roots system based on parts catalogs and list prices.

(2) Manufacturers' data.

Because of the lower rate of helicopter production (586 helicopters versus 15,747 airplanes manufactured in 1966 - a ratio of 1 to 27), and assuming this ratio remains more or less constant, in fifteen years the light helicopter industry may be manufacturing 3,700 units per year, still below the present production rate of the light airplane industry. Consequently the mass production techniques visualized for producing 100,000 light airplanes may not be justified for light helicopter manufacturing.

Helicopter manufacturers stated:

> "Helicopter airframe costs could be reduced right now, just by using heavier gages which would reduce the number of parts required, and would also add stiffness. At the present time, we spend many hours just matching door and door frames which are too elastic and have a tendency to deform."

There is no doubt, after comparing hundereds of different materials, and discussing the study with leading light airplane and helicopter manufacturers in the United States, that aluminum sheet metal airframe is here to stay. Aluminum is a very readily machinable, formable, and joinable material. It is one of the most economical; and manufacturing processes, techniques, and equipment are at hand. On that basis, it would be unwise to deviate much from

this. A new material would mean new tooling, a learning period, etc.

Modern light airplanes and helicopters are made almost exclusively of 2024-T3 aluminum alloy. The study indicates some relatively new alloys, such as 6061-T6 and 5086-H32, can replace most of the skin material with resultant cost savings. Some manufacturers are aware of this. 6061-T6 is used in some models by leading aircraft manufacturers. Wooden construction is obsolete for mass produced airplanes.

Riveting is still the easiest, cheapest, and most inspectable way of joining two pieces of metal. Two women with an air gun, a bucking bar, and two hours of training can install perfectly acceptable rivets at a rate of 20 per minute; and, when the nature of the assembly permits it, automatic riveting machines can drill and squeeze rivets at the rate of 30 per minute with one operator.

Automatic spotwelding of aluminum sheet metal deserves a very careful look. The light aircraft industry is looking to structural bonding with great hopes. The idea is well proven: it works with military and commercial airplanes. Modern helicpter blades would not be feasible without metal bonding. Light aircraft manufacturers are beginning to use it.

The pre-priming of aluminum sheets at the mill might solve, economically, one of the biggest problems of bonding surface preparation. New fast-curing low-pressure adhesives are eagerly awaited by most light aircraft manufacturers. Automated, fully-reliable quality-control devices will make bonding more attractive. Human handling should be reduced as much as possible. At present, quality depends too much on the individual handling of each assembly. The advantage of the extensive use of bonding might be emphasized mainly on weight savings, (3 to 6 percent of structural weight). Fatigue life improvement due to bonding is a well known fact, but of little concern to the light aircraft manufacturer.

The use of fiberglass prepreg laminates and ultraviolet curing seems the most promising technique for lightly-loaded or non-structural parts. This concept has been proven in the mass production of drones. Just recently, several light airplanes made of glass reinforced laminates have reached the flight testing stage in the United States and Germany. They could be considered Near Term designs, and if the manufacturing costs would be comparable to the sheet metal counterparts, they might lead the way to a revolution in light aircraft production.

Considering the raw material cost for a typical four-place airplane is only $ 765.00 (4.5 percent of consumer price), there is no doubt but that the only possibility for a radical improvement in price for a Far Term airplane will be in the reduction of airframe labor cost, rather than reduction of material costs.

In an opinion canvass of leading aircraft manufacturers, they were all in

agreement that at the present, hand layup fiberglass construction is not cheaper than sheet metal construction. To this, can be added the fact that the basic raw material - fiberglass fabric (E-Glass) @ $2.00 per pound at present, is three times more expensive than aluminum sheet metal. This makes the success of the all-fiberglass hand layup airplane very doubtful for the near term.

The Far-Term airframe should be an injection or compression molded article, using a thermoplastic or perhaps a thermosetting material. The production of airplane parts by molding is not only feasible, but probable; the materials are existent; molding techniques and limitations are well known.

Nylon matrixes, reinforced with chopped glass could be used for injection molding components twice the size of a briefcase. The structural efficiency number for shear buckling is 23 compared with 22 for aluminum sheet. The price of reinforced nylons is $1.64 per pound today, but in fifteen years it may be as low as 65 cents a pound. The time required to mold a part is measured in seconds, at the most, one minute.

Glass-fiber-reinforced epoxy systems with a shear buckling index of 33, cost $4.00/lb at the present and it is forcast to be only $2.00 in fifteen years. Graphite-fiber-reinforced plastics, still in the development stage, are estimated by the industry to be commercially available in fifteen years for as low as $2.00 per pound.

Analysis of the effect of mass production, revealed that the institution of automotive-type manufacturing methods could reduce the price of typical and representative light airplane by approximately 48 percent. By using existing aircraft manufacturing methods (plus normal evolution) and the classic 80% (constant) learning experience, the price of this representative airplane could theoretically be reduced by approximately 23 percent on the 100,000th unit.

The cost analysis of an all plastic Far Term airplane, shown in Appendix S, and the comparative analysis of a conventional sheet metal aircraft with equivalent requirements, shown in Appendix T, indicates the obvious advantage of reduced labor. The reader should bear in mind that this illustration of cost analysis is based on several more-or-less arbitrary assumptions and statistics. Even with present day technologies, cost analysis is a mixture of art and science, often times tempered by personal experience.

Recommendations for Future R&D Programs

As a result of this study, various areas are identified where additional research will enhance the possibility of a safer and more useful light aircraft. Some of the recommendations follow directly from the investigations performed during the study, while others are those suggested by various people within the industry. The recommendations are divided into two categories. Those indicated by the study and relate to structural materials and concepts, and those beneficial to other design areas of future light aircraft. No attempt was made to rank the various recommendations.

Category I.- Structural Materials and Concepts.

(1) Fatigue characteristics of panels as related to panel size, rivet spacing, and material thickness.
(2) Fatigue characteristics of typical repairs on aircraft. For example oversize holes, patches or splices on spar caps.
(3) Materials for landing gear springs.
(4) Stress corrosion in regard to protection and corrective action.
(5) A structural adhesive which will cure at room temperature with high T peel strength (75 lbs/in), high shear strength (4500 psi), curing at 10 psi (vacuum bag) in 10 minutes, one phase, rolled on curtain coating, lack of sensitivity to surface contamination.
(6) An extruded helicopter blade, which combines heavy sections at the leading edge and very thin sections at the trailing edge.
(7) Data on fatigue of bonded structures.
(8) Test data on creep and fatigue of plain laminate and sandwich panels with representative fiber orientation. Test laminates to obtain F_{tu} vs ϕ for various fiber patterns. Also combined loading to confirm biaxial strength criteria.
(9) Mechanical properties of laminates as function of resin and void content.
(10) Develop aluminum sheet metal with prime coat ready for bonding without any further surface preparation except solvent cleaning. The coating should provide also corrosion resistance. The coating should be applied at the mill for low cost.
(11) Specifications for raw materials, resins reinforcements for composites. Standardize test methods, specimens.
(12) Tests for determining crack propagation characteristics of various fiber orientated composite laminates.
(13) Establish design criteria for plastic structural components: Maximum and minimum temperatures, humidity, hail stone, sand and dust errosion.
(14) Test data on non-continuous glass reinforced laminates (mechanical properties, and environment limitations or degradation).
(15) Test data on compression allowables of laminate plates and flange members for varying width/thickness ratios and also for different fiber orientations.
(16) Tests for determining attachment allowables in laminate composites varying fiber orientations, thickness and edge distance.
(17) Tests for determining effect of stress concentrations in composite laminates under static and sudden loading conditions. Vary thickness and fiber orientation. Also include bolted attachment configurations.

Category II.- Other Design areas.

Power Plant.-

(1) Cooling drag, optimum air inlets and exhaust designs for horizontal opposed power plants.
(2) Methods of reducing propeller noise.
(3) Design parameters of small diameter, multi-blade propellers in shrouded ducts.
(4) Development of ultra-low pitch blade settings for ground roll braking.
(5) Simple CO detectors and CO elimination
(6) Improved fuel injection equipment (mass and flow sensing).
(7) Engine mounts, with lower frequency having less damping for better isolation in operating range.

Systems.-

(1) Improved braking methods.
(2) Improved flotation of tricycle gears on soft fields.
(3) Survey of landing loads, accelerations, sink speeds, etc. to determine if a more realistic design criteria is required.
(4) Oxigen systems for high altitude unpressurized aircrafts.
(5) De-icing of inlets, leading edges and control surfaces.
(6) Simple, inexpensive air conditioning system.
(7) A simple fuel system design, which would bleed fuel from wing tanks simultaneously to eliminate "fuel management", as required with present systems.
(8) More experimental data on crashworthiness of light airplanes and revised design requirements.
(9) More VGH data for fatigue evaluation of light airplanes. Perhaps FAR 23 should be subdivided according to type of operation (commercial survey, training etc.) or perhaps another subdivision should be made at 6000 lbs gross weight.

Manufacturing.-

(1) Automated plexiglass forming.
(2) A core material for hollow laminated parts, which can be easily removed,(for instance water soluble).
(3) A better bagging material for laminate fabrication than the presently used PVA ,(should be reusable).
(4) Establish processing techniques for Ultra Violet curing of plastics.
(5) An improved casting process to yield thinner walls and greater precission in the manufacturing of piston engine cylinders.
(6) Develop manufacturing techniques, tools, and establish design criteria for compression and injection molding of very large glass reinforced moldings and laminates.

Aerodynamics.-

(1) Control surfaces hinge moments experimental data.
(2) Additional basic data on laminar flow airfoils including effects of various types of moveable surfaces.
(3) Effects of different leading edge shapes on laminar flow airfoils.
(4) Improved effectiveness of vertical tails.
(5) T-tail characteristics.
(6) Nacelle shapes and locations for pusher engine installations. Also effects of wing and flaps on propeller.
(7) Flight path control with flap and power modulation.
(8) Simple methods of stability augmentation.
(9) Data regarding spoilers and vortex generators.
(10) Additional data on stall and section characteristics at low Reynolds numbers.
(11) Minimizing pitch changes with gear, flap and power changes by changing vertical placement of horizontal tails (full scale wind tunnel tests).
(12) Variable stability for production airplanes, heavy in cruise and light in low-speed flight.
(13) Means of getting usable C.G. ranges of 10 to 40% MAC. with reflexed airfoils, upward floating ailerons or flaps.
(14) Drag reduction of tricycle landing gear.
(15) Improvement in handling qualities at 1.1 Vs in landing approaches.
(16) Use of canard surfaces for supplemental longitudinal control.
(17) Practical methods of eliminating adverse yaw in low-speed airplanes.
(18) Summary of NASA-NACA data applicable to stability and control design for personal airplanes.
(19) Stabilator design for minimum pitch change with power and flaps.
(20) Improvement of spiral stability with upward floating ailerons.
(21) Condensed bibliography listing significant reports and summary reports from the beginning of NACA.
(22) Bibliography of STOL and high lift reports.
(23) Up-dating of many reports regarding airfoil data and structural data to take advantage of present state of the art.
(24) A method of automatic flight control from take-off to landing as applied to general aviation.
(25) Span load distribution for wing tips or various planforms and various section shapes

APPENDIX A
ACCIDENTS, RATES
U. S. GENERAL AVIATION
1938-1966

Year	Accidents		Fatalities	Hours* Flown (000)	Plane-Miles* Flown (000)	Accident Rates			
						100,000 Hours		Million Plane-Miles	
	Total	Fatal				Total	Fatal	Total	Fatal
1938.....	1,861	176	274	1,478	129,359	125.9	11.9	14.3	1.3
1939.....	2,222	203	315	1,922	177,868	115.6	10.5	12.4	1.1
1940.....	3,471	232	359	3,200	264,000	108.4	7.2	13.1	0.8
1941.....	4,252	217	312	4,460	346,303	95.3	4.8	12.2	0.6
1942.....	3,324	143	220	3,786	293,593	87.7	3.7	11.3	0.4
1943.....	3,871	167	257	NA	NA	NA	NA	NA	NA
1944.....	3,343	169	257	NA	NA	NA	NA	NA	NA
1945.....	4,652	322	508	NA	NA	NA	NA	NA	NA
1946.....	7,618	690	1,009	9,788	874,740	77.8	7.0	8.7	0.7
1947.....	9,253	882	1,352	16,334	1,502,402	56.6	5.3	6.1	0.5
1948.....	7,850	850	1,384	15,130	1,469,540	51.8	5.6	5.3	0.5
1949.....	5,459	562	896	11,031	1,128,992	49.4	5.0	4.8	0.4
1950.....	4,505	499	871	9,650	1,061,500	46.6	5.1	4.2	0.4
1951.....	3,824	441	750	8,451	975,480	45.2	5.2	3.9	0.4
1952.....	3,657	401	691	8,186	972,055	44.6	4.8	3.7	0.4
1953.....	3,232	387	635	8,527	1,045,346	37.9	4.5	3.0	0.3
1954.....	3,381	393	684	8,963	1,119,295	37.7	4.3	3.0	0.3
1955.....	3,343	384	619	9,500	1,216,000	35.1	4.0	2.7	0.3
1956.....	3,474	356	669	10,200	1,315,000	34.0	3.4	2.6	0.2
1957.....	4,200	438	800	10,938	1,426,285	38.4	4.0	2.9	0.3
1958.....	4,584	384	717	12,579	1,660,109	36.4	3.1	2.8	0.2
1959.....	4,576	450	823	12,903	1,716,019	35.5	3.5	2.7	0.3
1960.....	4,793	429	787	13,121	1,768,704	36.5	3.3	2.7	0.2
1961.....	4,625	426	761	13,602	1,857,946	34.0	3.1	2.5	0.2
1962.....	4,840	430	857	14,500	1,964,586	33.4	3.0	2.5	0.2
1963.....	4,690	482	893	15,106	2,048,574	31.0	3.2	2.3	0.2
1964.....	5,069	526	1,083	15,738	2,180,818	32.2	3.3	2.3	0.2
1965 (Prelim.)	5,250**	516	1,018	16,733	2,562,380	31.4	3.1	2.0	0.2
1966 (Prelim.)	5,425**	538	1,069	17,456**	2,697,018**	31.2	3.1	2.0	0.2

* Source FAA
** Estimated by CAB

APPENDIX B

GENERAL AVIATION ACCIDENTS,
CASUALTIES AND DAMAGE FOR 1963 (TYPICAL)

		Small single engine fixed wing	Rotorcraft	All other	Total
Accidents	Total	4069	183	438	4690
	%	87%	4%	9%	100%
	Fatal	401	15	66	482
	Serious	255	18	22	295
	Minor/None	3413	150	350	3913
Casualties	Fatalities	727	20	146	893
	Serious injury	384	28	50	462
	Minor/No injury	6079	263	994	7336
	Total Aboard	7176	307	1185	8668
Damage	Destroyed	952	106	39	1097
	Substantial	3076	330	144	3550
	Minor/None	41	2	0	43
Fire after impact	Fatal	109	20	5	134
	Non Fatal	85	20	11	116

APPENDIX C
ACCIDENTS PER ELIGIBLE AIRCRAFT BY STATE FOR 1965

State or other areas	Total eligible aircraft	Air carrier	General aviation						
			Fixed-wing multi-engine	Fixed-wing 1-engine 4-place and over	Rotor-craft	All other	Total eligible gen. av. aircraft	Total accidents	Accidents per 100 aircraft
Total.....	97,741	2,299	11,977	49,789	1,503	32,173	95,442	5,196	5.45
United States..	97,459	2,283	11,902	49,653	1,492	32,129	95,176	5,062	5.3
Alabama.....	1,201	0	167	638	5	391	1,201	89	7.4
Alaska.....	1,702	102	64	725	50	761	1,600	147	9.2
Arizona.....	1,462	1	159	768	27	507	1,461	105	7.2
Arkansas.....	1,397	0	195	601	7	594	1,397	78	5.6
California.....	13,108	172	1,352	6,961	320	4,303	12,936	629	4.9
Colorado.....	1,458	47	147	791	15	458	1,411	110	7.8
Connecticut.....	694	2	86	338	16	252	692	44	6.4
Delaware.....	320	6	76	143	1	94	314	16	5.1
District of Columbia	599	45	192	295	18	49	554	3	.54
Florida.....	3,630	137	636	1,779	69	1,009	3,493	221	6.3
Georgia.....	1,676	122	223	761	6	564	1,554	111	7.1
Hawaii.....	169	23	36	44	4	62	146	17	11.6
Idaho.....	929	0	64	497	20	348	929	48	5.2
Illinois.....	4,482	282	594	2,395	31	1,180	4,200	156	3.7
Indiana.....	2,560	25	378	1,460	38	659	2,535	116	4.6
Iowa.....	1,911	0	158	1,130	9	614	1,911	73	3.8
Kansas.....	2,782	0	329	1,678	8	767	2,782	110	4.0
Kentucky.....	704	1	107	391	7	198	703	47	6.7
Louisiana.....	1,530	0	195	602	[illegible]	628	1,530	109	7.1
Maine.....	438	0	31	179	4	224	438	18	4.1
Maryland.....	952	0	109	486	19	338	952	79	8.3
Massachusetts.....	1,253	23	151	638	25	416	1,230	74	6.0
Michigan.....	3,744	39	445	2,028	21	1,211	3,705	145	3.9
Minnesota.....	2,540	105	185	1,152	17	1,081	2,395	115	4.8
Mississippi.....	1,111	0	125	448	10	528	1,111	68	6.1
Missouri.....	2,472	231	297	1,254	15	675	2,241	132	5.9
Montana.....	1,199	2	74	613	13	497	1,197	73	6.1
Nebraska.....	1,363	1	118	696	18	530	1,362	64	4.7
Nevada.....	736	29	121	373	34	179	707	54	7.6
New Hampshire.....	263	0	30	131	0	102	263	19	7.2
New Jersey.....	2,074	21	254	1,110	29	660	2,053	111	5.4
New Mexico.....	1,089	0	143	701	3	242	1,089	87	8.0
New York.....	4,368	599	636	1,765	65	1,303	3,769	184	4.9
North Carolina.....	1,660	43	188	847	17	565	1,617	79	4.9
North Dakota.....	764	0	25	297	3	439	764	51	6.7
Ohio.....	4,148	1	661	2,211	33	1,242	4,147	182	4.4
Oklahoma.....	2,132	3	287	1,084	43	715	2,129	102	4.8
Oregon.....	1,925	1	211	1,109	46	558	1,924	86	4.5
Pennsylvania.....	3,048	0	495	1,516	72	965	3,048	144	4.7
Rhode Island.....	134	0	16	65	7	46	134	7	5.2
South Carolina.....	692	0	88	369	12	223	692	39	5.6
South Dakota.....	775	0	37	347	1	390	775	43	5.5
Tennessee.....	1,266	29	221	638	4	374	1,237	56	4.5
Texas.....	7,971	152	1,137	4,023	118	2,541	7,819	407	5.2
Utah.....	583	1	49	369	8	156	582	52	8.9
Vermont.....	172	0	18	88	0	66	172	15	8.7
Virginia.....	1,244	1	123	665	18	437	1,243	72	5.8
Washington.....	2,213	36	113	1,137	56	871	2,177	127	5.8
West Virginia.....	448	1	66	216	7	158	447	25	5.6
Wisconsin.....	1,834	0	226	824	13	771	1,834	72	3.9
Wyoming.....	534	0	64	277	5	188	534	57	10.7
Outside U.S....	282	16	75	136	11	44	266	87	32.7
Puerto Rico.....	197	15	48	94	10	30	182	--	--
Virgin Islands.....	23	0	15	8	0	0	23	--	--
Other countries.....	62	1	12	34	1	14	61	--	--

APPENDIX D
TYPE OF ACCIDENT VS PHASE OF OPERATION FOR SMALL FIXED-WING AIRCRAFT IN 1963 & 1964

Type of Accident	Phase of operation							
	Static	Taxi	Takeoff	In-flight	Landing	Unknown	Total small fixed wing	Total - all operations
1963								
Ground/waterloop, swerve	0	31	132	0	441	1	605	608
Wheels-up landing	0	0	4	0	242	0	246	251
Gear collapsed	1	19	22	0	157	0	199	202
Gear retracted	4	9	32	0	175	0	220	225
Hard landing	0	1	2	0	287	0	290	334
Nose over/down	6	118	17	0	131	1	273	274
Airframe failure-in flight	0	0	1	47	3	1	52	57
-on ground	0	0	1	0	2	0	3	5
Engine tearaway	0	0	0	1	0	0	1	1
Stall, spin, spiral	0	1	140	181	83	2	407	416
Total of above	11	179	351	229	1521	5	2296	2373
All other	68	141	383	769	782	32	2175	2394
1964								
Ground/waterloop, swerve	1	38	138	0	496	0	673	
Wheels-up landing	0	0	5	0	316	0	321	
Gear collapsed	1	28	30	0	128	0	187	
Gear retracted	3	13	38	0	119	0	173	
Hard landing	0	0	2	0	417	0	419	
Nose over/down	6	98	26	0	117	1	248	
Airframe failure-in flight	0	0	1	30	0	0	31	
-on ground	0	0	0	0	4	0	4	
Engine tearaway	0	0	1	2	0	0	3	
Stall	0	0	178	93	62	3	336	
Spin	0	0	7	26	4	2	39	
Spiral	0	0	8	10	2	0	20	
Mush	0	0	11	9	5	0	25	
Total of above	11	177	445	170	1670	6	2479	
All other	84	147	343	860	836	21	2448	

APPENDIX E

TYPE OF ACCIDENT VS KIND OF FLYING FOR SMALL FIXED-WING AIRCRAFT IN 1963 AND 1964

Year	Type of Accident	Instructional				Non-Commerical					Commercial							Miscelaneous								
		Dual	Solo	Other	Total	Pleasure	Business	Corporate	Other	Total	Areial Application	Fire control	Pipe line patrol	Air taxi passenger	Air taxi cargo	Other	Total	Test	Demonstration	Ferry	Towing glider	Hunting	Other	Total	Grand total-small Fixed-wing	Grand total all operations
1963	Ground/waterloop, swerve	22	43	42	107	274	84	5	62	425	24	0	1	13	7	2	47	4	3	5	0	2	12	26	605	608
	Wheels-up landing	11	0	1	12	98	80	10	15	203	0	0	0	11	2	0	13	6	5	5	0	0	2	18	246	251
	Gear collapsed	4	4	5	13	91	49	6	5	151	8	0	0	10	1	0	19	7	1	3	0	2	3	16	199	202
	Gear retracted	9	0	5	14	78	82	10	9	179	0	0	0	12	0	1	13	5	5	4	0	0	0	14	220	225
	Hard landing	21	31	16	68	135	34	4	36	209	1	0	0	0	0	0	1	1	4	5	0	0	2	12	290	334
	Nose over/down	9	8	20	37	132	53	3	18	204	11	0	0	2	4	2	19	0	1	5	1	1	5	13	273	274
	Airframe failure-in flight	1	0	0	1	28	15	2	1	46	2	0	0	0	0	1	3	1	0	0	0	0	1	2	52	57
	-on ground	0	0	0	0	3	0	0	0	3	0	0	0	0	0	0	0	0	0	0	0	0	0	0	3	5
	Engine tearaway	0	0	0	0	0	0	0	0	0	0	0	0	0	0	0	0	0	0	0	0	0	1	1	1	1
	Stall, spin, spiral	19	15	5	39	204	34	0	12	250	75	0	2	6	0	2	85	5	1	0	0	10	17	33	407	416
	Total of above				291					1670							200							135	2296	2373
	All other				165					1574							307							129	2175	2394
1964	Ground/waterloop, swerve	29	75	20	124	272	104	6	102	484	25	0	1	13	1	0	40	3	1	12	1	0	8	25	673	
	Wheels-up landing	25	2	2	29	133	104	12	13	262	0	0	0	7	1	0	8	2	5	11	0	0	4	22	321	
	Gear collapsed	6	3	6	15	82	52	3	9	146	8	0	0	5	2	0	15	3	1	3	0	2	2	11	187	
	Gear retracted	15	0	2	17	72	53	4	7	136	0	0	0	4	2	0	6	2	5	7	0	0	0	14	173	
	Hard landing	33	59	13	105	200	40	3	58	301	0	0	0	1	1	0	2	2	0	4	0	0	5	11	419	
	Nose over/down	6	10	8	24	112	47	2	27	188	5	0	1	9	4	2	21	0	1	7	0	2	5	15	248	
	Airframe failure-in flight	0	1	0	1	15	7	1	2	25	1	0	0	2	0	0	3	0	0	0	0	0	1	2	31	
	-on ground	0	0	0	0	2	2	0	0	4	0	0	0	0	0	0	0	0	0	0	0	0	0	0	4	
	Engine tearaway	0	0	0	0	0	0	0	0	0	1	0	0	1	0	0	2	0	0	0	0	0	1	1	3	
	Stall,spin,spiral,mush	16	5	3	24	196	58	2	19	275	71	2	1	5	0	7	86	6	6	8	0	5	10	35	420	
	Total of above				339					1821							183							136	2479	
	All other				199					1641							324							127	2448	

APPENDIX I

TYPE OF ACCIDENT VS KIND OF FLYING FOR
HELICOPTERS IN 1963 AND 1964

Type of accident \ Year	1963	1964	1965
Hard landing	42	43	31
Roll over	6	13	13
Collision with ground/water			
Controlled	9	17	18
Uncontrolled	7	15	12
Collision with objects	38	50	49
Stall, spin, spiral, mush	7	19	20
Airframe failure			
In flight	5	1	3
On ground	1	3	3
Engine failure	44	59	52
Rotor failure		15	16
Sub-total	159	235	227
All other	24	23	12
Grand total	183	258	239
Active helicopters	1171	1306	1503
Hours flown	387,000	447,000	450,000
Accident rate - per vehicle	.156	.198	.159
- per 100,000 hours	47.3	57.7	53.11

Data from CAB Bureau of Safety Reports: BOSR 5-4-5
BOSR 7-5

APPENDIX G

ANALYSIS, IN-FLIGHT AIRFRAME FAILURE IN U.S. GENERAL AVIATION, 1965

DOCKET NUMBER	CAUSE: Inadequate Inspection & Maintenance	Inadequate Design	Inadequate Material	WEATHER: Gust	WEATHER: Turbulence	WEATHER: Loss of Control Disorientation	WEATHER: Ice, Sn etc.	Collision (e.g., Bird)	General Lack of Proficiency	Horseplay	Foolishness	Lack of Respect for Nature	LOCATION: Wing	Fuselage	Vertical	Horizontal	Powerplant	Propeller	Landing Gear	Controls	Systems	Total Aircraft	CASUALTY: Fatal	Serious	Minor	AIRCRAFT*
2-0109						X							S	S			S					DI	4		1	Beech A-35
2-0437									X													S		1	1	Cessna 320
2-0448	X																			*		DA	2			Navion G
2-0687						X						X	DA									DI	1			Beech 35
2-0729										X			DA													Mooney M-18C
2-0815			X																M			SA			1	Piper PA-16
2-0928					X																	DI			2	Cessna 182
2-1096	X			X	X								DA										2	1		Kranich 1B Glider
2-1192			X										DA													Bell 47-G2
2-1334				X										S								DI		1	4	Beech SNB-5
2-1346	X												*									DI			2	Beech J-50
2-1373						X	X															DA	4			Beech 23
2-1516								X					DA									DA	1			Aero Comndr 560-F
2-1648															DA	DA						DI	2			Beech N-35
2-1760						X	X					X										S			4	Beech 35-B-33A
2-1855					X	X	X					X											1			Cessna 195A
2-1904					?	X	X					X	DA									DI	1			Navion NAV-4
2-1909					?	X	X					X										DA	4			Piper PA-24
2-1918						X						X	DA									DI	1			Schweizer SGS126B
2-1925						X	X					X	DA		DA	DA						DA	2			Beech P-35
2-1930			X										DA									DI	1			Beech 35
2-1933	X																			*SA		DI	1			Boeing A75N 1
2-1978						X	X					X	DA		DA	DA						DA	1			Beech H-35
2-2005					X	X						X				DA						DI	4			Cessna 310B
2-2007						X							DA									DA	2			Beech 35
2-2114									X	X												SADI	2			Piper PA-12
2-2156								?							DA	DA						DI			1	Campbell CH47G-2
2-2159						X	X					X					*S					DA	1			Ryan Navion B
2-2160	X	?	?																			DA	2			Boeing A75N1
2-2238		?	?		X															S		SI		1		Aeronca 11AC
2-2249										X					DA	DA						DI	1			Bellanca 14-13
2-2255			X										DA										3			Hiller UH-12E4
2-2259			X										DA									DI	3			Cessna 195B
2-2265	X														DA	DA			SI			SI		1	2	Bell 47H-1
2-2266	X		X										DA									DI		1		Snow S2C
2-2296	X									X			DA									DI	1	1		Piper J-4
2-2298	X												DA			DA						DI	3			Beech B-35
2-2342						?	X					X	DA		DA	DA						DA	1			Piper PA-24
2-2356									X				UA						*			DI	2			Aero Comndr 680F (P)
2-2397						?	X					X	DA		DA	DA							2			Piper PA-24
2-2398			X			X	X						DA							*SA		DI	4			Piper PA-24
2-2400						X	X					X	DA		DA	DA						DI	3			Bellanca 14-19-2
2-2412						X	X					X	DA									DI	2			Beech B-35
2-2446						X	X					X	DA									DI	3			Mooney M-20C
2-2445						X	X					X			SA	DA						DI	4			Beech 95-55
2-2466			X			X						X								*			1			Piper PA-22
2-2477						?							DA		SA	SA							4			Mooney M20A
2-2485					X							X	DA									DI	2			Piper PA-23
2-2508		X											DA									DI	5			Navion G
2-2512	?					X															*	DA	2			Aero Comndr 680F (P)
2-2514						X						X	DA			DA	DA					DI	3			Piper PA-24-250
2-2516	X					X							DA									DI	4			Piper PA-22
2-2528						X						X	DA			DA	DA					DI	3			Beech 35
2-2529			X			X						X	DA				DA						2			Bellanca 14-13
3-0124	X							X						M											1	Globe-Swift GC-1B
3-0548									X				DA									DI			1	Pratt-Read PRG-1
3-1024	X		X													SI										Piper PA-18
3-1629									X							SA										Cessna 140
3-1861									X													SA				Piper PA-24-250
QUANTITY	13	1	7	1	2	5	0	2	5	3	0	20														
%	22	1.7	11.8	1.7	3.4	8.5	-	3.4	8.5	5.1	-	34														

LEGEND: D = destroyed; S = substantial; M = minor; A = in air; I = at impact; * = cause assoc. with...

* Tabulated from CAB Summary Reports of Accidents

APPENDIX H
OPERATING COST ANALYSIS

	MODEL	Cessna 140	Cessna 150	Cessna 172	Cessna 175	Cessna 182	Cessna 206	Cessna 210	Cessna 310	Piper PA12	Piper PA18	Piper PA20	Piper PA22	Piper PA23	Piper PA30	Piper PA32	Piper PA24-260	Piper PA28-140	Piper PA28-180	Beech Queen Air 65	Beech Queen Air 90D	Beech U-55	Beech M-35	Champ, 7ECA	Mooney Mark 21	Exp Sr. Aero Sport	T-Craft BC65	Piazenny PL-1
DIRECT $/HR	Fuel: X gal/hr x 39¢/gal	1.96	1.84	2.76	4.31	4.03	7.00	5.40	14.00	3.25	2.75	3.04	2.55	13.00	6.75	6.75	3.33	3.25	4.20	17.00	18.00	4.18	2.42	2.39	4.57	3.40	1.32	2.34
	Oil: X $/qt ÷ Y hr/qt *	.32	.18	.29	1.30	.25	.30	.20	.60	.22	.05	.10	.21	1.00	.40	.50	.04	.05	.05	1.20	1.20	.09	.09	.32	.29	.30	.08	.12
	Inspections & maintenance including 25 & 100 hr. insp. parts & normal maintenance of airframe eng.	.66	1.38	1.70	3.32	2.45	2.00	4.25	3.50	2.00	.75	1.50	.66	—	2.60	1.25	1.50	.85	.88	6.00	6.00	1.59	3.89	2.00	3.00	1.10	.25	1.12
	Engine & prop overhaul (as recommended by mfg'r	.50	.82	1.72	—	1.86	1.50	2.50	4.00	1.00	1.35	.50	.30	2.50		2.00	2.30	.91	1.12	6.00	6.00	2.00	2.90	.10	.60	—	.20	.84
	Total Direct operating costs	3.44	4.22	6.47	8.93	8.49	10.80	12.35	22.10	6.47	4.90	5.14	3.72	16.50	9.75	10.05	7.17	5.06	6.25	30.20	31.20	7.77	9.30	4.81	8.46	4.80	1.85	4.52
INDIRECT $/YR	Hangar rent or tie-down	55	250	330	—	—	400	—	600	120	185	120	135	—	575	185	180	185	180	240	240	480		—	420	420	120	360
	Insurance (pub liability, psgr liability/seat, hull)	20	495	381	1300	680	1400	1140	1500	60	902	186	297	—	985	1575	712	1131	1287	3600	3600	540	360	595	855	—	225	150
	Depreciation	20	1000	1600	—	>750	1500	6400	4000	200	667	100	21	—	—	4000	3900	1935	3000	10900	12000	—	3900	—	—	—	—	—
	Method	—	—	—	—	—	—	—	—	—	—	—	—	—	—	—	—	—	—	—	—	—	—	—	—	—	—	—
	Over how many years	5	6	6	—	—	7	—	7	10	6	—	5	—	—	6	—	6	6	10	10	—	—	—	—	—	—	—
	Salvage value?	—	1000	2000	—	—	4000	—	10000	800	—	—	—	—	—	—	—	—	—	15%	15%	—	—	—	—	—	—	—
	Taxes	10	95	99	75	225	250	300	400	18	55	12	53	—	365	233	225	125	143	—	—	110	—	52	167	56	—	20
	Interest	—	410	529	400	900	1200	1200	2400	180	185	—	287	—	1200	852	1500	570	665	3%	3%	360	—	200	530	—	—	—
	Total indirect cost	100	2000	2939	810	5555	4750	9040	8900	578	1974	318	773	—	3126	6645	4236	3846	6275	14060	17340	1470	4236	847	1972	476	345	530
	Anual utilization (hrs)	100	500	425	—	750	500	400	500	200	500	100	180	250	500	300	600	950	500	500	500	250	600	500	500	150	200	200
SEAT MILE $	Direct hourly costs	3.44	4.20	6.47	—	8.49	10.80	12.35	22.10	6.47	4.90	5.14	3.72	16.50	9.75	10.05	7.17	5.06	6.25	30.20	31.20	7.77	9.30	4.81	8.46	4.80	1.85	4.52
	Indirect hourly costs	1.00	4.00	6.91	—	7.50	9.50	22.60	17.80	2.89	3.94	3.18	4.29		6.25	22.15	7.06	4.05	10.55	28.15	37.80	5.86	7.06	2.82	3.94	3.17	1.73	2.65
	Total hourly costs	4.44	8.20	13.47	—	15.89	20.30	34.95	39.90	9.36	8.84	8.32	8.01	29.41	16.00	32.20	14.23	9.11	17.80	58.35	69.00	13.65	16.36	7.63	12.40	7.97	3.58	7.17
	Cost per mile (@ mph block speed)	@ 90 .049	@100 .082	@115 .117	—	@160 .099	@140 .145	@160 .218	@180 .222	@110 .085	@100 .088	@115 .073	@100 .08	@190 .162	@188 .085	@150 .215	@142 .10	@98.3 .09	@125 132	@200 .291	@200 .345	@160 .085	@148 .110	@100 .078	@160 .078	@120 .066	@75 .043	@100 .072
	Number of seats	2	2	4	4	4	4-6	4-6	4-6	2	2	4	4	4-5	4-6	6	4	2	4	7-9	8	4	4	2	4	2	2	2
	Cost per seat mile	.025	.041	.029	—	.025	.036	.054	.037	.024	.044	.018	.022	.040	.021	.036	.025	.045	.066	.036	.043	.021	.037	.038	.020	.033	.024	.036
	Total no. aircraft	1	70	31	3	7	1	1	3	1	2	2	6	7	1	4	4	11	6	1	2	3	2	26	2	1	1	1

* Cost of oil @ 45¢/qt.

APPENDIX J

VEHICLE PRICE PER lb OF USEFUL LOAD

VEHICLE	PRICE	GROSS WEIGHT	EMPTY WEIGHT	USEFUL LOAD	$/USEFUL LOAD	CRUISE SPEED
	$	lb	lb	lb	$/lb	mph
Maule M-4 Jetasen	10,396	2100	1190	910	11.44	150
M-4 Rocket	13,986	2100	1190	910	15.40	165
Mooney Master	14,995	2500	1475	1025	15.36	138
Mark 21	18,250	2575	1525	1050	19.18	152
Mustang	33,950	3680	2380	1300	26.10	230
Piper Super Cub	9,280	1750	930	820	11.30	115
Cherokee 140	8,500	2150	1201	949	8.96	133
C180	12,900	2400	1230	1170	11.00	143
235B	15,900	2900	1410	1490	10.65	156
Six	21,500	3400	1738	1662	12.93	168
Comanche B	24,990	3600	2207	1393	17.90	194
Navajo	89,500	6200	3603	2597	34.40	210
Aero Commander 100	8,500	2250	1280	970	8.77	128
200	29,500	3000	1940	1060	27.80	214
Alon A2 Ercoupe	7,975	1450	930	520	15.30	124
Beech Baron B55	63,950	5100	3036	2064	31.00	225
Bonanza V35	32,500	3400	1941	1459	22.25	203
Musketeer Sport III	12,500	2200	1325	875	14.30	131
Bellanca 260C	22,950	3000	1850	1150	20.00	196
Cessna 150	6,995	1600	975	625	11.20	120
172	10,950	2300	1275	1025	10.70	130
182	17,150	2300	1560	1240	13.80	159
210	27,975	3400	1960	1440	20.80	192
Hughes 500	78,800	2400	1040	1360	58.00	143
Brantley 305	59,500	2900	1840	1060	56.10	110
Corvair	2,150			800	2.69	50
Chevrolet II	2,200			880	2.50	55
Chevelle 6	2,275			880	2.59	55
Chevrolet V-8	3,000			1100	2.72	60
Cadillac	5,000			1320	3.79	70

NOTE: Useful load includes all persons on board, fuel, oil and baggage.

	FIXED GEAR AIRPLANE (A_f)		RETRACTABLE GEAR AIRPLANE (A_r)	
Consumer price	$ 23 995.00		$ 25 975.00	
Direct operating costs (hrly)				
Fuel (15.8 gph @ 43¢/gal)	$ 6.79		$ 6.79	
Oil (3/4 pt/hr @ 60¢/qt)	.23		.23	
Inspection and maintenance	1.75		1.75	
Engine and prop overhaul	3.83		3.83	
Total direct operating costs	$ 12.60		$ 12.60/hr	
Indirect operating costs (yrly)				
Hangar rent ($40/mo)	$ 480.00	$ 480.00	$ 480.00	$ 480.00
Insurance	1008.00	1008.00	1183.00	1183.00
Depreciation	(12%) 2880.00	(5%) 1200.00	(12%) 3110.00	(5%) 1300.00
Tax ($7.7/1000 valuation)	185.00	185.00	200.00	200.00
Interest (80% x 23995 x 5.5%) for A_f	1056.00	Paid off		
(80% x 25975 x 4.75%) for A_r			989.00	Paid off
Total indirect operating costs	$ 5609.00	$ 2873.00	$ 5962.00/yr	$ 3163.00
Cruise speed	163 mph		190 mph	
Cost per mile	$ 0.0773		$ 0.0664	

Break even point

A_r A_f

$0.0664d + 5962 = 0.0773d + 5609$

$-5609 = .0664d$

$353 = .0109d$

$d = 32{,}400$ miles/yr

(For first five years)

Break even point

A_r A_f

$0.0664d + 3163 = .0773d + 2873$

$+2873 \quad .0664d$

$290 = .0109d$

$d = 26{,}600$ miles/yr

(After fifth year)

	FIXED GEAR AIRPLANE (B_f)		RETRACTABLE GEAR AIRPLANE (B_r)	
Consumer price	$ 14 995.00		$ 16 595.00	
Direct operating costs (hrly)				
Fuel (8 gph @ 43¢/gal)	$ 3.44		$ 3.78	
Oil	.14		.14	
Inspection and maintenance	1.20		2.85	
Engine and prop overhaul	1.25			
Total direct operating costs	$ 6.03/hr		$ 6.77/hr	
Indirect operating costs (yrly)				
Hangar rent ($40/mo)	$ 480.00	$ 480.00	$ 480.00	$ 480.00
Insurance	624.00	624.00	759.00	759.00
Depreciation	(12%) 1800.00	(5%) 750.00	(12%) 1991.00	(5%) 830.00
Tax ($7.70/1000 valuation)	116.00	116.00	128.00	128.00
Interest (80% x 14995 x 5.5%) for B_f	660.00	Paid off		
(80% x 16595 x 5.5%) for B_r			730.00	Paid off
Total indirect operating costs	$ 3680.00/yr	$ 1970.00	$ 4088.00/yr	$ 2197.00
Cruise speed	139 mph		178 mph	
Cost per mile $\frac{\$6.03/hr}{139\ mph}$ =	$ 0.0434/mile		$ 0.038 /mile	

Break even point

B_r B_f

$.0380d + 4088 = .0434d + 3680$

$-3680 \quad -.0380d$

$408 = .0054d$

$d = 75{,}600$ miles/yr

(For first five years)

Break even point

B_r B_f

$.038d + 2197 = .0434d + 1970$

$d = 42{,}000$ miles/yr

(After fifth year)

	FIXED GEAR AIRPLANE (C_f)		RETRACTABLE GEAR AIRPLANE (C_r)	
Consumer price	$ 13 900.00		$ 15 900.00	
Direct operation costs (hrly)				
Fuel (10 gph @ 43¢/gal)	$ 4.30			
Oil (@ 60¢/qt	.14		$ 4.05	
Inspection and maintenance	1.20		.14	
Engine and prop overhaul	1.25		1.60	
Total direct operating costs	$ 6.89/hr		1.26	
			$ 7.05/hr	
Indirect operating costs (yrly)				
Hangar rent ($40/mo)	$ 480.00	$ 480.00		
Insurance (8% x 13900)	650.00	650.00	$ 480.00	$ 480.00
Depreciation	(12%) 1668.00	(5%) 695.00	(12%) 768.00	(5%) 768.00
Tax ($7.70/1000 valuation)	107.00	107.00	1908.00	795.00
Interest (80% x 13900 x 5.5%) for C_f	612.00	Paid off	122.00	122.00
(80% x 15900 x 5.5%) for C_r			700.00	Paid off
Total indirect operating costs	$ 3517.00/yr	$ 1932.00	$ 3978.00/yr	$ 2165.00
Cruise speed	143 mph		162 mph	
Cost per mile $6.89/143 mph =	$ 0.0482/mile		$ 0.0435/mile	

Break even point

C_r C_f

$0.0435d + 3978 = 0.0482d + 3517$

$d = 98200$ miles/yr

(For first five years)

Break even point

C_r C_f

$0.0435d + 2165.00 = 0.0482d + 1932$

$d = 49600$ miles/yr

(After fifth year)

APPENDIX L

TYPICAL OPERATING COSTS FOR RECIPROCATING AND TURBO-PROP AIRPLANES

Data for figure 67	Turbo-prop engine	Reciprocating engine
Consumer price	$29,500	$17,000
Direct operating costs (hrly)		
Fuel	17.78 GPH @.25¢ 4.45	11.25 GPH @.43¢ 4.84
Oil	.2 qt/hr @.90¢ .18	3/4 pt/hr @.60¢ .22
Inspection & maint.	1.75	1.75
Engine & prop. overhaul	4.50	3.83
Total direct operating costs	$10.88	$10.64
Cruise speed	150 mph	150 mph
Cost per mile	$.0725/mi	$.071/mi
Indirect operating cost (yrly)		
Hanger rent ($40/mo)	480	480
Insurance (4% + $215)	1395	895
Depreciation (5%, 40% residual)	3540	2040
Tax ($7.70/$1000 value)	227	131
Interest 80% x I.R.	I.R.= 4.75% 1121	I.R.= 5.5% 748
Total indirect operating costs	$6763/yr	$4294/yr

APPENDIX M

AIRCRAFT GUIDELINES

General

The conceptual aircraft used in the design studies of Phase II must satisfy the requirements in this Appendix. Since this is a structural design study these requirements are meant to be of a general nature and not those of an optimum aircraft. A specific configuration has not been included since the various structural approaches may dictate different configurations.

Performance - Fixed Wing

The minimum performance with a pilot and three passengers (170 lbs. each), 200 lbs. of baggage, and enough fuel and oil for take-off, landing, and four hours normal cruise plus 30 minutes reserve will be:

(1) Maximum speed at rated rpm at sea level not less than 152 knots.
(2) Normal cruise at 5,000 feet not less than 130 knots.
(3) Minimum rate of climb at sea level not less than 1,000 feet per min.
(4) Service ceiling not less than 14,000 feet.
(5) The stall speed at sea level not greater than 48 knots.
(6) The takeoff distance over 50 feet will not be greater than 1,000 ft.

Performance - Helicopter

The minimum performance with a pilot and three passengers (170 lbs. each), 200 lbs. of baggage, and enough fuel and oil for take-off, landing, and three hours normal cruise plus 15 minutes reserve will be:

(1) Maximum speed at rated rpm at sea level not less than 150 knots.
(2) Normal cruise at sea level not less than 87 knots.
(3) Minimum rate of climb at sea level not less than 1,200 feet per min.
(4) Service ceiling not less than 14,000 feet.
(5) Hover in ground effect not less than 8,000 feet.
(6) Hover out of ground effect not less than 5,000 feet.

Propulsion

(1) Engines will be of the reciprocating or turbine type developing not more than 250 bhp total and weighing not more than 380 pounds total.
(2) Propellers may be either fixed or variable pitch.

Dimensions and Areas

(1) The cabin must accommodate four persons and have an internal volume (excluding baggage space) greater than 112 ft^3 with a width not less than 3.5 feet.
(2) The baggage volume must not be less than 16 ft^3 and accommodate four 9" x 21" x 31" suitcases.

Miscellaneous

(1) The landing gear may be either fixed or retractable tricycle type.
(2) The weight of fixed equipment will be 220 lbs.

APPENDIX N

PARAMETRIC STUDY OF FACTORS AFFECTING MAXIMUM SPEED

The following methods were used in determining the effects of various parameters on maximum speed. Each of the parametric variations were reduced to a change in equivalent parasite area, $f = D/q$. Since at maximum speed the induced drag represents only about 10% of the total drag, it has been considered to be invariable with dynamic pressure within the region of investigation. This will not introduce a significant error for this type of comparative study.

The formula for the slope of the velocity curve was obtained by differentiating the power equation:

$$KP = D \cdot V = q\, f \cdot V = \tfrac{1}{2} \rho\, f \cdot V^3$$

Assuming a constant power available,

$$V^3 d\, f + 3\, V^2 f\, dv = 0$$

$$\frac{dv}{df} = -\frac{1}{3}\,\frac{V}{f}$$

For the purpose of this analysis, variations of the following base configuration were considered.

$W = 2800$ lb.
$S = 175$ ft^2
$AR = 7$
$P = 250$ bhp
$V_{max} = 152$ kts

Effect of wing area.- Wing area affects both the parasite drag and the induced drag. For this study, both will be summed in terms of equivalent parasite area so that they can be presented as a Δf.

$$f_w = C_{D_o}\, S_e + K_1\, C_L^2\, S$$

$$= C_{D_o}\, S_e + \frac{K_1\, W^2}{q^2 S}$$

$$= .0075\,(S-20) + \frac{.055 \cdot 2800}{(78.5)^2\, S} \qquad \text{(152 K. @ S.L.)}$$

$$= .0075\,(S-20) + 70.0/S$$

S	.0075(S-20)	70/S	f_w	Δf
ft^2	ft^2	ft^2	ft^2	ft^2
145	.937	.483	1.420	-.142
155	1.012	.451	1.463	-.099
165	1.087	.424	1.511	-.051
175	1.162	.400	1.562	0
185	1.237	.378	1.615	.053
195	1.310	.359	1.669	.107

Effect of aspect ratio.- The aspect ratio of the wing influences the induced drag. This will be equated to an equivalent parasite area.

$$f_i = C_{D_i} S = K_1 C_L^2 S \qquad K_1 \text{ From Fig. 246 (total airplane)}$$

$$= \frac{K_1 W^2}{q^2 S} = \frac{2800^2 K_1}{(7.85)^2(175)} = 7.28 K_1 \ ft^2$$

A	K_1	f_i, ft^2	Δf, ft^2
5	.0738	.537	.137
6	.0626	.456	.056
7	.0550	.400	0
8	.0488	.355	-.045
9	.0442	.322	-.078
10	.0414	.301	-.099

Effect of wing thickness ratio: Wing thickness ratio (t/c) affects the minimum drag coefficient. For this study we will use the formula from Ref. 10, Page 2. Note that this only gives a relative comparison and not the actual value used for the basic wing.

$$Cd_o = .016 (t/c) + .00410$$

$$f = Cd_o S_e \qquad S_e = 155 \ ft^2$$

(t/c)	.016 (t/c)	Cd_o	$f_1 ft^2$	$\Delta f_1 \ ft^2$
.09	.00144	.00554	.859	-.074
.12	.00192	.00602	.933	0
.15	.00240	.00650	1.007	.074
.18	.00288	.00698	1.082	.149

Effect of gross weight.- The effect of gross weight is obtained from the change in induced drag.

$$f_i = C_{D_i} S ; \qquad C_{D_i} = K_1 C_L^2 \qquad \begin{cases} K_1 = .055 \text{ (Fig. 246)} \\ C_L = W/qS \end{cases}$$

$$f_i = \frac{K_1 W^2}{q^2 S} = \frac{.055 W^2}{(78.5)175} = \frac{W^2}{(19.6)10^6} \qquad (q = 78.5 \text{ lb/ft}^2 \text{ @ 152 kts, S.L.})$$

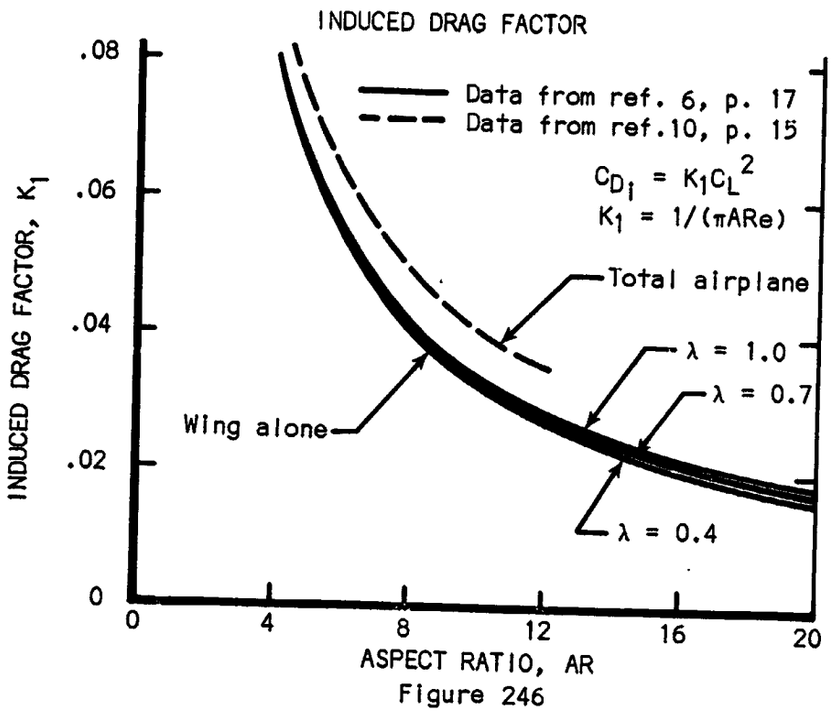


Figure 246

W, lb	f_i, ft^2	Δf, ft^2
1600	.131	-.269
1800	.165	-.235
2000	.204	-.196
2200	.247	-.153
2400	.294	-.106
2600	.345	-.055
2800	.400	0
3000	.459	.059
3200	.522	.122
3400	.590	.190
3600	.661	.261

Effect of fuselage frontal area.- Fuselage drag was calculated by the methods in Ref. 10. For a fineness ratio of 5, the fuselage drag coefficient, based on frontal area is $C_{D_\pi} = .0573$

A_π, ft^2	f, ft^2	Δf, ft^2
16	.916	-.230
18	1.030	-.116
20	1.146	0
22	1.260	.114
24	1.375	.229
26	1.490	.344
28	1.609	.463

Effect of laminar flow on maximum speed.- To determine the effect of laminar flow on the maximum speed of the base airplane, the change in equivalent parasite area is found, as the transition point moves from the leading edge to 0.6 chord. The arbitrarily assumed transition point for the base airplane is at 0.2 chord (probably optimistic).

$$f = 2 C_{f_{av}} K_t S_e$$

K_t = 1.165 (Thickness correction factor for 12% airfoil, Ref.11, Page 17.)

S_e = 155 ft^2 (exposed wing area)

$$f = 361 \cdot C_{f_{av}} \quad ft^2$$

$(X/C)_t$	$C_{f_{av}}$	f, ft^2	Δf, ft^2
0	.00328	1.184	.152
.10	.00312	1.126	.094
.20	.00286	1.032	0
.30	.00260	.940	-.092
.40	.00232	.837	-.195
.50	.00203	.733	-.299
.60	.00173	.624	-.408

Extent of laminar flow on wing and its effect on wing drag.- To determine the drag variation with laminar flow over a portion of the wing, the laminar skin friction coefficient, $C_{f_{lam}}$, was plotted along the chord from the leading edge to 0.6 chord. To obtain the average skin friction coefficient for the section the laminar and turbulent coefficients were weighted according to the amount of surface area each covered.

$$C_{f_{av}} = C_{f_{lam}} (X/C)_T + C_{f_{turb}} [1 - (X/C)_T]$$

The turbulent skin friction coefficient for a Reynolds number of 6×10^6 is found to be .00328 from Ref. 12, Fig. 4.1.5.1-13.

Transition Pt. $(X/C)_t$	$C_{f_{lam}}$	$C_{f_{turb}}$	$C_{f_{av}}$
0	---	.00328	.00328
.10	.00173	↓	.00312
.20	.00121		.00286
.30	.00100		.00260
.40	.00087		.00232
.50	.00077		.00203
.60	.00070		.00173

These results are plotted in Fig. 247.

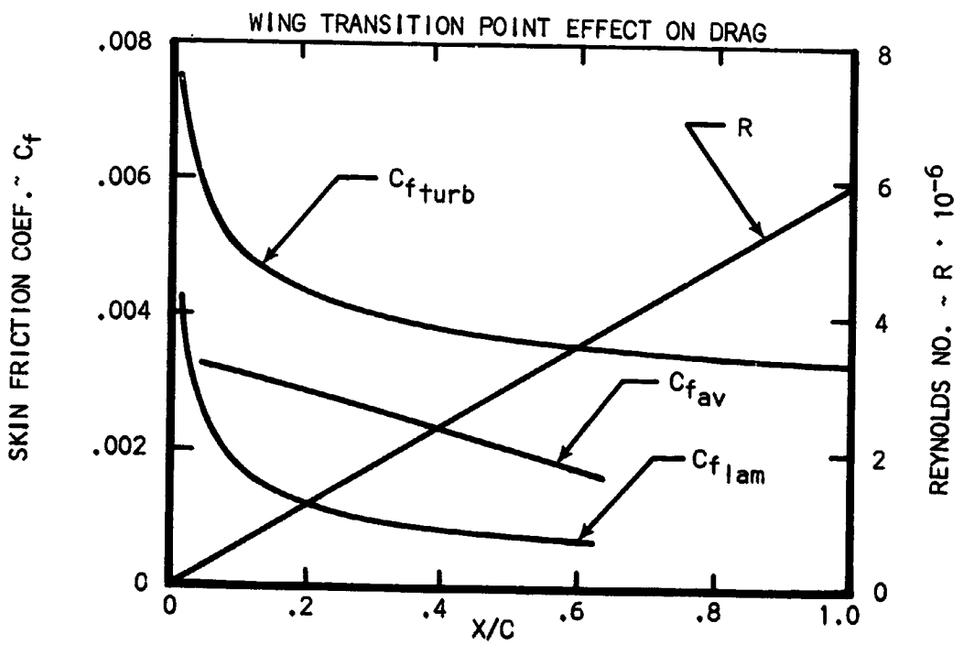


Figure 247

Landing gear drag:

Data for estimating the landing gear drag comes from Ref 13. The following values were selected:

Main gear - Spring leaf type

No fairing $C_{D_*} = .38$

With wheel fairing $C_{D_*} = .25$

(C_{D_*} based on wheel frontal area)

Wheel frontal area $A_f = .766\ ft^2$

Parasite area: No fairing $f = (2.0)(.766)(.38) = .582\ ft^2$

With fairing $f = (2.0)(.766)(.25) = .383\ ft^2$

Nose gear - Single strut

No fairing $C_{D_*} = .70$

With wheel fairing $C_{D_*} = .40$

Wheel frontal area $A_f = .703\ ft^2$

Parasite area: No firing $f = (.70)(.703) = .492\ ft^2$

With fairing $f = (.40)(.703) = .281\ ft^2$

Total parasite area No fairing $f = 1.074\ ft^2$

With wheel fairing $f = .664\ ft^2$

Effect of fixed landing gear on maximum speed. - The loss in maximum speed with a fixed gear can be estimated using the following formula:

$$\Delta V = \frac{f_{gear}}{\frac{df}{dV}} \qquad \frac{df}{dV} = -3\frac{f_o}{V_o} = (-3)(3.6)/152 = -.071$$

Without wheel fairings:

$f_{gear} = 1.074\ ft^2$

$\Delta V = 1.074/-.071$

$= -15.1$ knots

With wheel fairings:

$f_{gear} = .664\ ft^2$

$\Delta V = .664/-.071$

$= -9.4$ knots

APPENDIX P

PARASITE DRAG OF CURRENT AIRPLANES

As an aid in evaluation of current four-place airplanes, the following method was used to determine their equivalent parasite drag area. Starting with the basic power-required formula:

$$P_r = qfV + K_1 C_L^2 q S V = \frac{\rho f V^3}{2} + \frac{2 K_1 W^2}{\rho S V} \qquad \text{(ft.lb/sec)}$$

Equating the power available with the power required,

$$P_r = P_{av} n_p (550) = \frac{\rho f V^3}{2} + \frac{2 K_1 W^2}{\rho S V} \qquad \text{(ft.lb/sec)}$$

Essentially, there are two unknowns, f and n_p, so solving the equation for n_p as a function of f yields:

$$n_p = \left(\frac{\rho V^3}{1100 P_{av}}\right) f + \left(\frac{W^2}{275 \rho V S P_{av}}\right) K_1$$

The quantities inside the brackets can be determined from performance data and specifications, (K_1 the induced drag factor is a function of aspect ratio as shown in Figure 246, appendix N).

The next step is to plot n_p versus f at various flight conditions. Although the propulsive efficiency is not a known quantity, it is a fair assumption that, for propeller installations in this category, it will have a peak value of about 0.85. Where $n_p = 0.85$ intersects the n_p versus f curves at the minimum value of f (Since f is constant for a given configuration) a vertical line through this point will intersect the other curves at points prepresenting actual solutions to the above equation. It must be noted that each n_p versus f curve is a line of possible solutions to the equation for a given flight condition, but the actual solution is a single point at the actual parasite area, f.

These plots for several current airplanes are shown in Figures 248 through 253. The resulting parasite drag areas are tabulated here:

TABLE LIII- EQUIVALENT PARASITE AREAS FOR SEVERAL CURRENT AIRPLANES

Make and Model	Landing Gear	Parasite Area
CESSNA 172	Fixed	6.20 ft^2
CESSNA SKYHAWK	Fixed	6.10 ft^2
CESSNA 182	Fixed	5.65 ft^2
CESSNA SKYLANE	Fixed	5.35 ft^2
PIPER CHEROKEE "C"	Fixed	6.00 ft^2
PIPER CHEROKEE "C"	Fixed with fairings	5.[illegible] ft^2
CESSNA 210 CENTURION	Retractable	4.[illegible] ft^2
PIPER COMANCHE "260"	Retractable	4.1[illegible] ft^2
BEECHCRAFT DEBONAIR	Retractable	3.45 ft^2
PIPER CHEROKEE ARROW	Retractable	4.10 ft^2

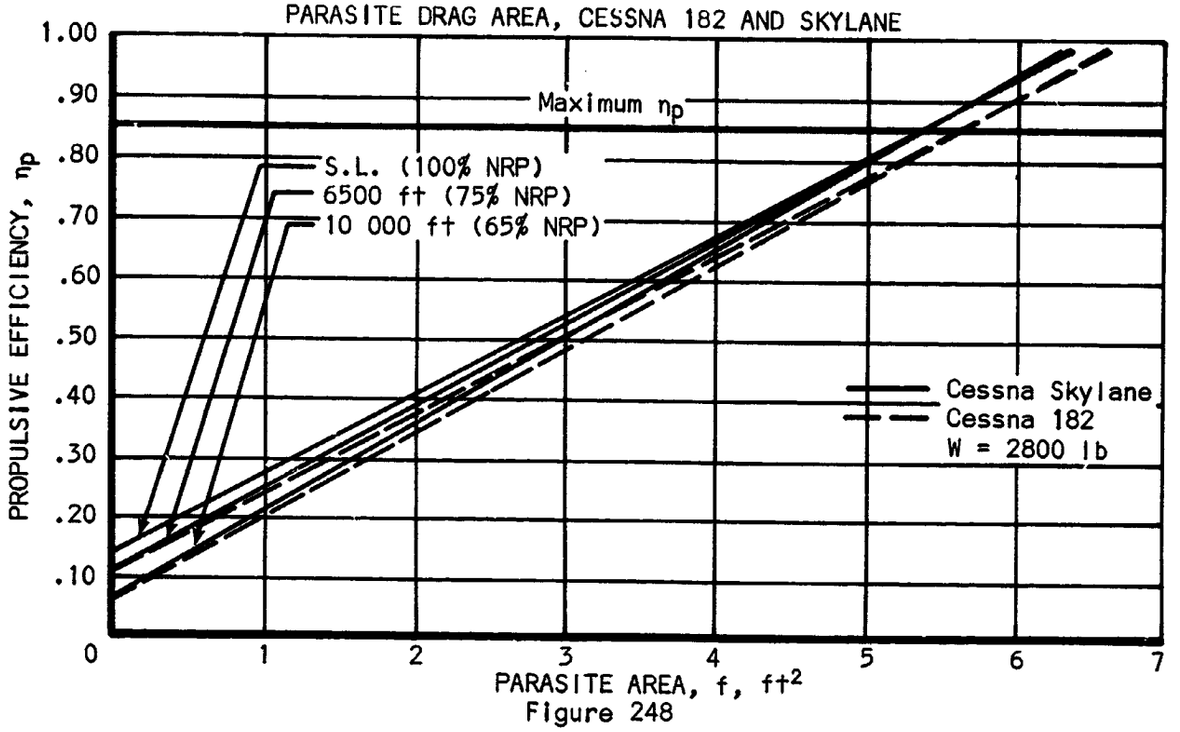


Figure 248

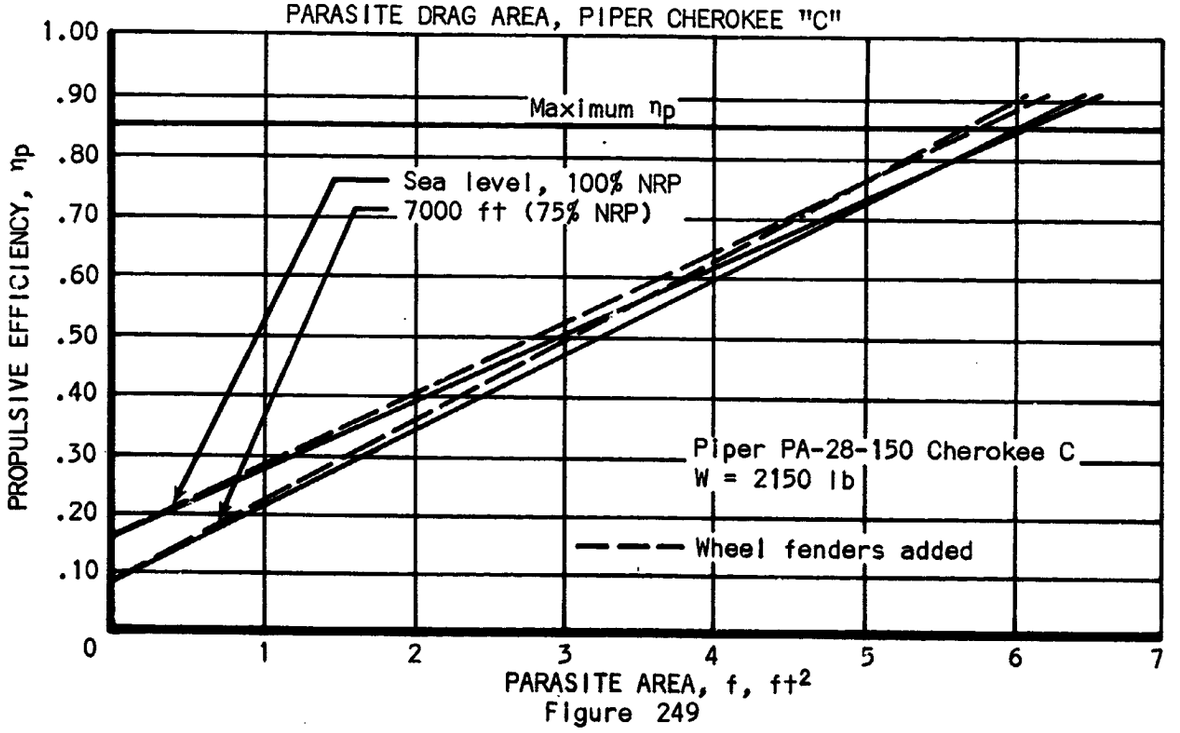


Figure 249

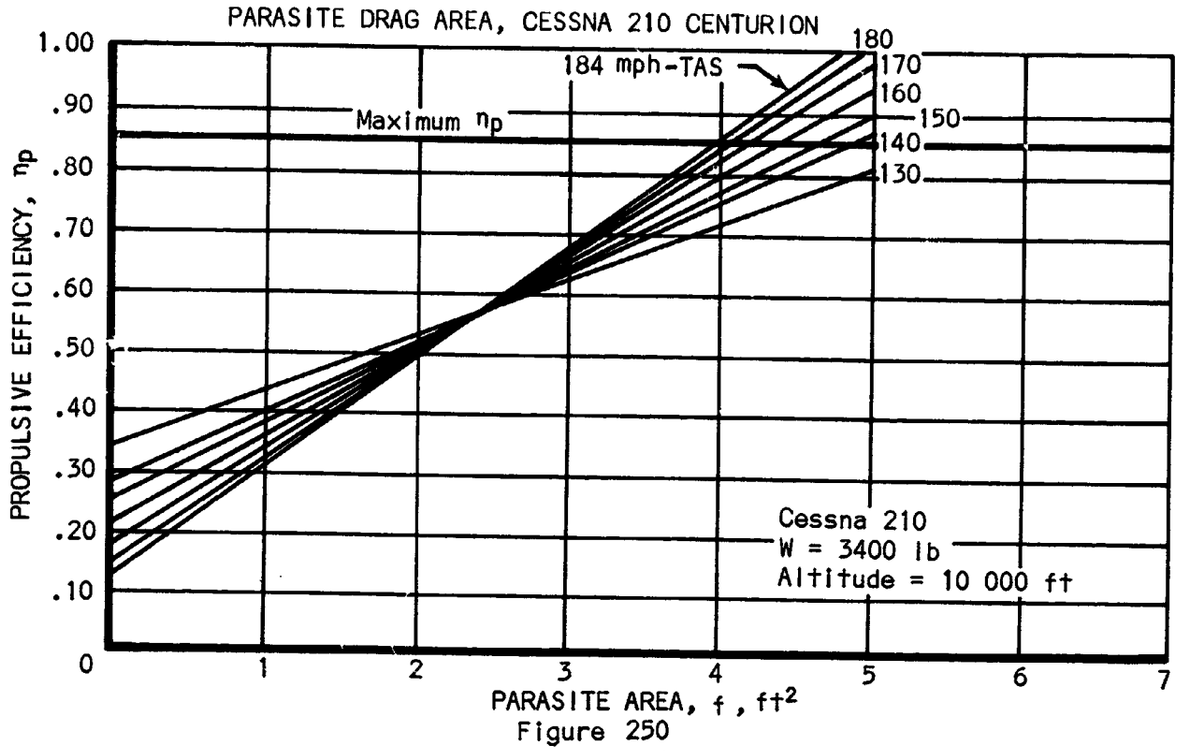


Figure 250

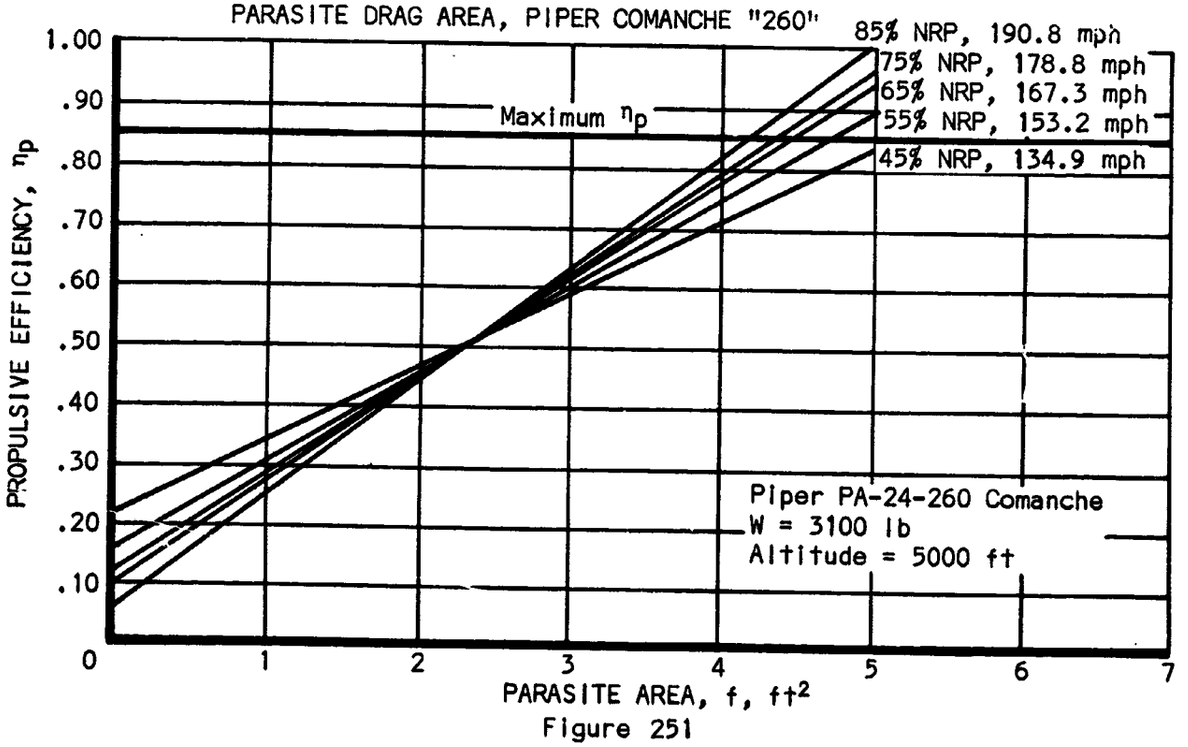


Figure 251

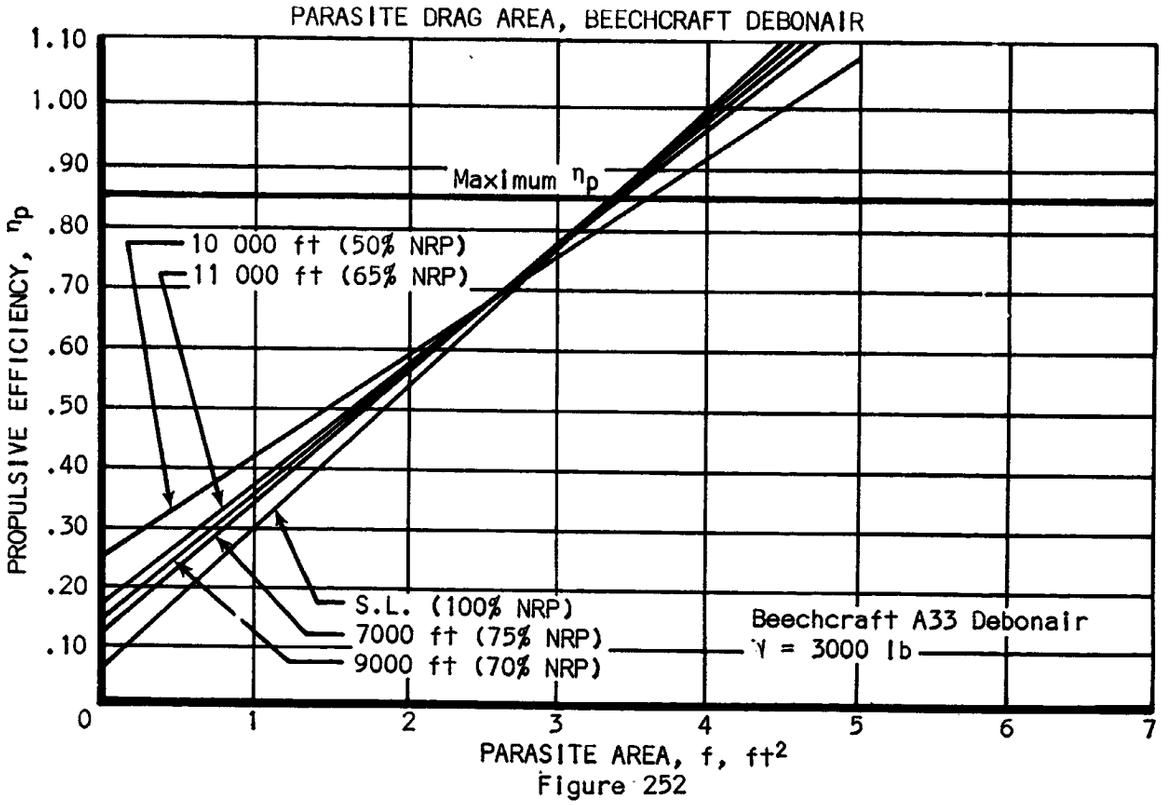


Figure 252

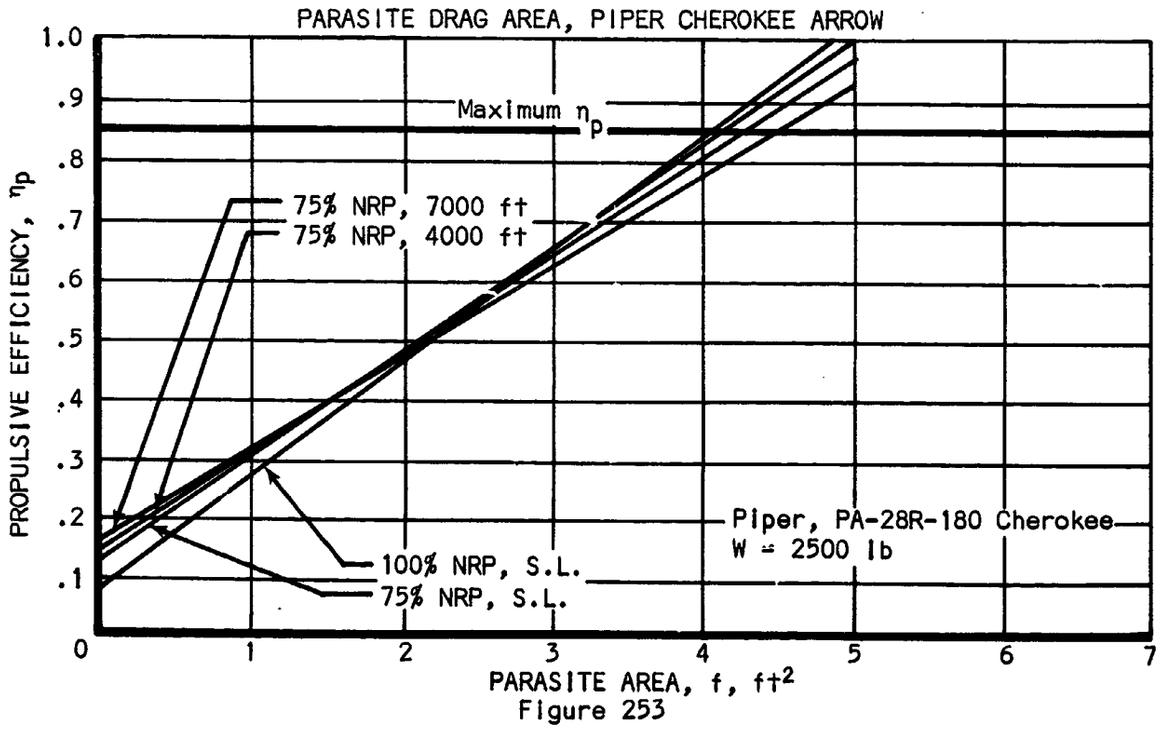


Figure 253

APPENDIX Q

STATIC STABILITY COMPUTATIONS

Finding Neutral Point

$$\left(\frac{dC_m}{dC_L}\right)_{n_p} = 0$$

$$\frac{dC_m}{dC_L} = \frac{Xa}{\bar{c}} + \left(\frac{dC_m}{dC_L}\right)_{fus} + \left(\frac{dC_m}{dC_L}\right)_{prop} - \frac{a_t}{a_w}\,\bar{V}_{n_t}\left(1 - \frac{d\varepsilon}{d\alpha}\right)\frac{q_t}{q_o}$$

Fuselage contribution

$$\left(\frac{dC_m}{dC_L}\right)_{fus} = \left(\frac{dM}{d\alpha}\right)\frac{1}{q\,S\bar{c}}\;\frac{1}{a_w} = \frac{(\text{Volume})}{28.7}\;\frac{(K_2 - K_1}{S\,\bar{c}\,a_w} \quad \text{(Ref. 8, Page 226)}$$

$$= \frac{257.5}{28.7}\;\frac{.85}{(180)(5.07)(.085)} = (9.0)\;\frac{.85}{77.2} = 0.10$$

Propeller Contribution

$$\left(\frac{dC_m}{dC_L}\right)_{prop} = .02\,\frac{\ell_p}{\bar{c}} = .02\,(1.5) = 0.03$$

Tail contribution

$$\left(\frac{dC_m}{dC_L}\right)_{tail} = -\frac{a_t}{a_w}\,\bar{V}_{n_t}\left(1 - \frac{d\varepsilon}{d\alpha}\right)\frac{q_t}{q_o}$$

$$= \left(-\frac{.057}{.085}\right)\left(\frac{40}{180}\right)\left(\frac{13.9}{5.07}\right)(.9)\,(1-.4)$$

$$= -.23$$

$$\frac{x_a}{\bar{c}} = .10 - .03 + .23 = +.10$$

$$N_p = \frac{x_{ac}}{\bar{c}} + \frac{x_a}{\bar{c}} = .25 + \frac{x_a}{\bar{c}} = .25 + .10 = .35\,\bar{c}$$

APPENDIX R

WEIGHT AND BALANCE CALCULATIONS (Far Term Airplane)

Balance Calculations (Reference point: Firewall)

Description	Weight (lb)	Horiz.Arm (in)	Horiz.Mom. (in-lbx1000)
Wing (180 ft^2)	302.0	53.1	16.036
Horiz. Tail (40 ft^2)	36	226.2	8.140
Vert. Tail (15.84 ft^2)	21.6	217	4.690
Fuselage	300	92	27.600
Main gear	116.2	55.9	6.500
Nose gear	49.8	-20.7	-1.030
Surface Controls	35.5	13	.462
Cowl	25	-22	-.550
Engine Mount	16	-7	-.112
Basic Engine	380	-24.6	-9.348
Air Induction	4	-31	-.124
Exhaust System	16	-16	-.256
Cooling System	5	-25	-.125
Fuel System	19	45.5	.860
Engine Controls	3.1	10	.031
Starting System	17	-38	-.646
Oil Cooler	5.5	-31.5	-.173
Prop Instl.	64	-47.5	-3.040
'nstruments & Nav. Fquipment	10.2	15	.153
Brake System	3.3	13	.043
Electrical Group			
Generator	16.2	-38	-.616
Battery	28	90	2.520
Battery Box	2.5	90	.225
Starter Contactor	1 1	-1	-.001
Battery Contactor	1.1	-1	-.001
Battery Cables	3.9	57	.222
Generator Regulator	1.7	1	.002
Switches, Reostats & Circuit Breakers	1.5	11	.017
Wiring	3	41	.123
Lights			
Navigation	.4	60	.024
Panel	.3	15	.004
Dome	.4	50	.020
Landing	2.4	31	.075
Front Seats 2	25	43.5	1.090
Rear Seat	23	77.8	1.790
Seat Belts (Front)	2	36	.072
Seat Belts (Rear)	2	71	.142
Furnishings	51.4	41	2.110
Air Conditioning	6	36	.216
Paint	7.9	93.0	.730
Total - Basic Airplane (Empty. Dry)	1609.0	Total = 57.87 in-lbx1000	

GROSS WEIGHT LOADING

Item	Weight (lb)	Horiz. Arm (in)	Horiz. Mom (in-lbx1000)
Empty weight	1609	---	57.87
Oil	22	-24	- .53
Fuel	340	42.5	14.45
Baggage	200	110.5	22.10
Pilot & Front Pass.	340	37.5	12.75
Rear Pass.	340	77.0	26.18
Total Loaded Airplane	2851		132.82

C.G. distance aft of firewall = $\frac{132.82(1000)}{2851}$ = 46.5 in. (Sta 146.5)

The leading Edge of M.A.C. is located at Sta. 129.0 (M.A.C. = 62 in.)

∴ 146.5 - 129.0 = 17.5 in. and in % of M.A.C. = $\frac{17.5 \times 100}{62}$ = 28.2

MAX AFT C.G. POSITION

Item	Weight (lb)	Horiz. Arm (in)	Horiz. Mom (in-lbx1000)
Empty weight	1609	---	57.87
Oil	22	-24	-.53
Baggage	200	110.5	22.10
Pilot	170	37.5	6.38
Rear Pass.	340	77.0	26.18
Total	2341		112.00

C.G. distance aft of firewall = $\frac{112.00\ (1000)}{2341}$ = 47.6 in. (Sta. 147.6)

∴ 147.6 - 129.0 = 18.6 in. and in % of M.A.C. = $\frac{18.6 \times 100}{62}$ = 30.0

FWD C.G. POSITION

Item	Weight (lb)	Horiz. Arm (in)	Horiz. Mom (in-lbx1000)
Empty weight	1609	---	57.87
Oil	22	-24	- .53
Pilot	170	37.5	6.38
Total	1801		63.72

C.G. distance aft of firewall = $\frac{63.72 \times 1000}{1801}$ = 35.4 in. (Sta 135.4)

∴ 135.4-129.0 = 6.4 in.; and in % of M.A.C. = $\frac{6.4 \times 100}{62}$ = 10.3

Maximum C.G. travel = 30.0 - 10.3 = 19.7%

FAR TERM AIRPLANE EMPTY WEIGHT BREAKDOWN (PISTON ENGINE)

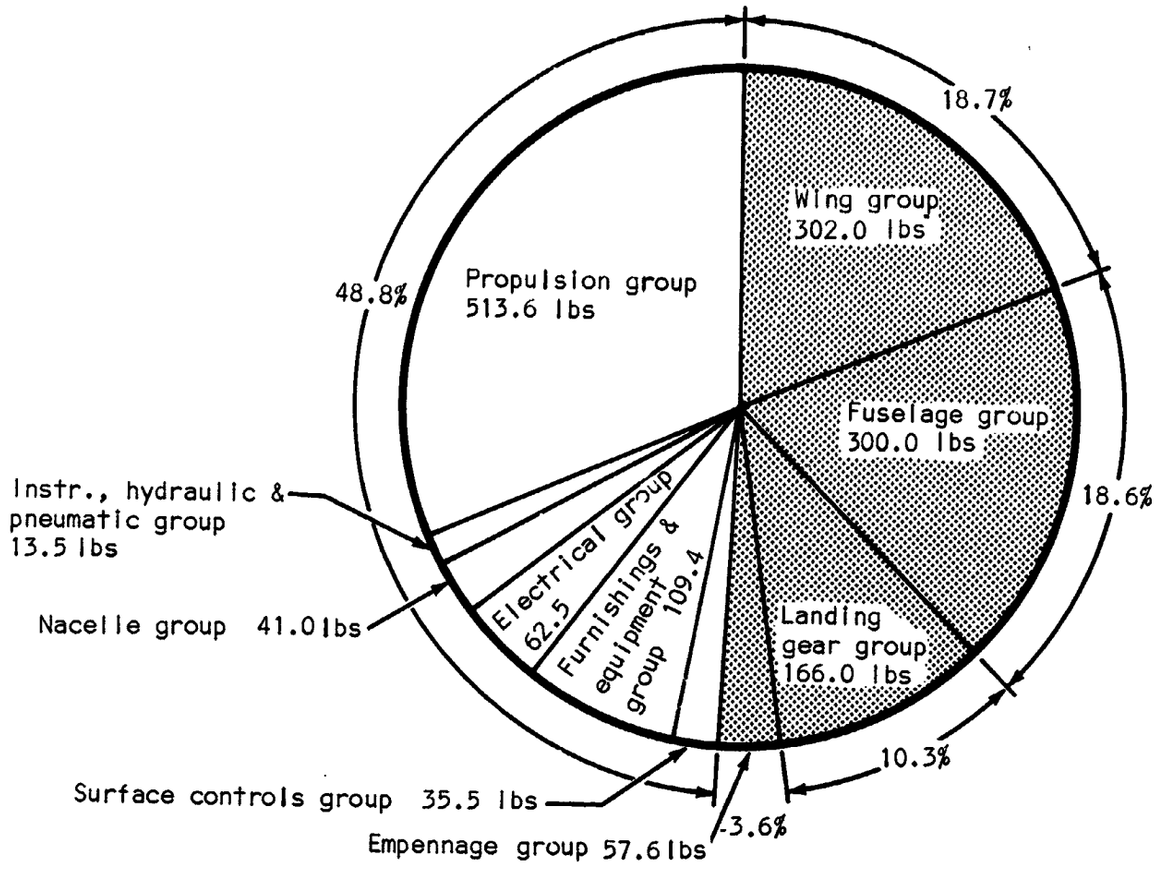


Figure 254

APPENDIX S

CONSUMER PRICE BREAKDOWN OF FAR TERM AIRPLANE (ESTIMATED)

An estimated total consumer price breakdown of the Far Term airplane has been determined by combining:

(1) the estimated costs of the primary structural components; i.e., the vertical tail, horizontal tail, wing and fuselage.

(2) the estimated cost of the remaining items such as burden, manufacturer and dealer markup, engine, hardware, etc., based in part on previous breakdowns of contemporary airplanes.

It is estimated that the reinforced plastic Far Term airplane of the 1980's, produced in six-figure quantities, will sell for approximately $10,973.00. A breakdown of this price is illustrated in the following pie chart.

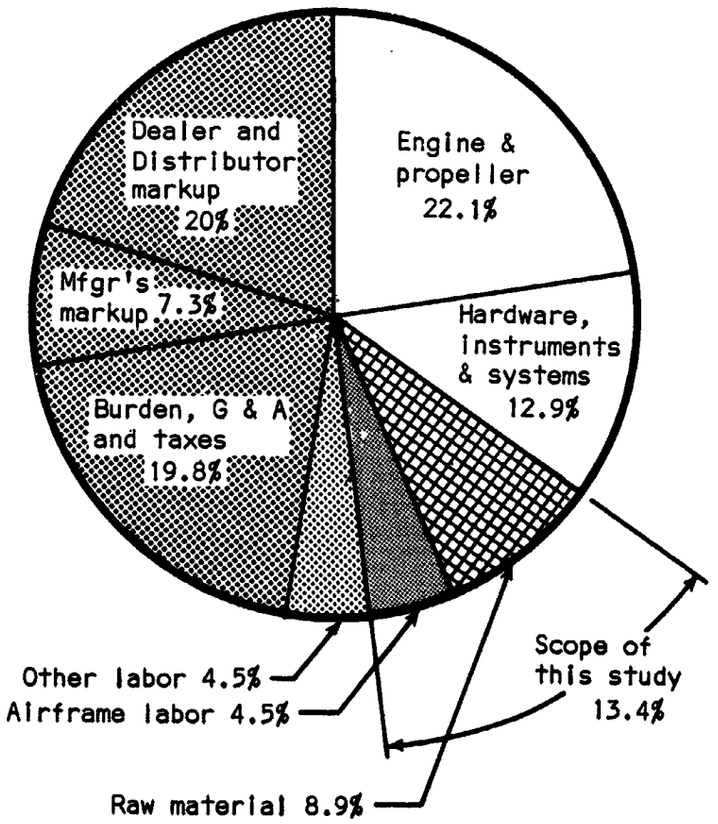


Figure 255

The following table breaks the consumer price down in further detail. Following the table is a list of assumptions upon which the pie chart and the table are based.

CONSUMER PRICE BREAKDOWN FOR THE FAR TERM AIRPLANE

	Item		Dollars	Percent Total
(1a)	Direct labor (structure)	$ 238.62	$ 734.62	6.7
(1b)	Direct labor (other)	496.00		
(2a)	Overhead (structure)	310.21	955.21	8.7
(2b)	Overhead (other)	645.00		
(3a)	Material (structure)	811.25	978.25	8.9
(3b)	Material (retractable L.G.,other)	167.00		
(4)	Molding time charge (not labor)		258.10	2.3
(5a)	Equipment (Engine & propeller)	2425.00	3842.00	35.1
(5b)	(L.G.,wheels, instruments, etc)	1417.00		
	Sub-total		$ 6768.18	61.7
(6)	Direct, sales, and G&A expenses		1211.92	11.0
(7)	Manufacturing cost		$ 7980.10	72.7
(8)	Factory profit (10% of Mfg. cost)		798.01	7.3
	Total dealer's cost		$ 8778.11	80.0
(9)	Distributor and dealer mark-up		2194.53	20.0
(10)	Total Estimated cost to consumer		$10972.64	100.0

AIRFRAME FABRICATION COST ANALYSIS

(11)	Airframe labor	$ 486.62
(12)	Airframe share of overhead	1434.64
(13)	Raw material	978.25
(14)	Molding time charge	258.10
(15)	Airframe fabrication cost	$ 3157.61

(16) AMPR weight is estimated to 1038 lbs.

(17) Unit airframe cost: $\frac{\$3157.61}{1038} = \$3.02/lb$

Direct labor - (structure)

$ .72	fin labor	4 plastic parts
.90	rudder labor	5 plastic parts
2.88	horiz.stab.labor	16 plastic parts
36.36	wing labor	202 plastic parts
5.76	fuselage labor	32 plastic parts
192.00	other labor	Estimated-other than plastic parts
$ 238.62	@ $2.70/hr. ave. wage = 89 hours	

fab. time estimated at 4 min/part

Direct labor - (other)

$ 1700.00	(total direct labor from Table XII)
-1360.00	(airframe labor from Table XII)
340.00	
+ 156.00	(10% Table XII $1560 est. for retractable L.G.)
$ 496.00	

Overhead (structure) -$ 310.21 = $238.62 x 130% from Table XII

Overhead (other) -$ 645 = $496 x 130%

Material (structure) -$

8.27	vertical fin	(13.13 lb x .63 $/lb)
5.36	rudder	(8.50 lb x .63 $/lb)
79.12	horiz. tail	(36.06 lb x 2.00 $/lb)
328.50	wing	(Fig. 243, bar ⑥; Fig. 244)
390.00	fuselage	(2.00 $/lb x 195 lb(primary structure)
$ 811.25		

Material (other) -$ 167.00 = $70 est. for retractable L.G. material + $97 est. for seats, upholstery, interiors, etc.

Molding (time charge) -$

13.20	vertical fin	$\frac{1{,}320{,}000\ \$}{100{,}000 \text{ units} \times 4 \text{ parts}} = 3.30\$/\text{part}$ Table LI
16.50	rudder	(3.30 $/part x 5 parts)
52.80	horiz. stab.	(3.30 $/part x 16 parts
70.00	wing	(estim. 202 parts, multicavity tooling)
105.60	fuselage	(3.30 $/part x 32 parts)
$ 258.10		

Equipment (Engine & propeller) -$ 2425.00 = 80%* x $\frac{250 \text{ HP}}{230 \text{ HP}}$ x 2795.00_{Table XII}$

Equipment (L.G., etc.) - $ 1417.00 = 1305_{Table XII}$ x 80% * (24.2%$_{Table XII}$ x 1560^{Δ})

Direct sales and G & A -$ 1211.92 = Overall burden - Mfg. overhead = (2.95 from p.99 x labor) - $955.21 = (2.95 x 734.62 - 955.21)

Distributor & dealer mark up -$ 2194.53 = dealer cost x 25% = 8778.11 x .25 (used 25% instead of 33% due to high volume sales, e.g. auto industry)

Airframe labor - $ 486.62 = 238.62 + ½ x 496 from page 352 (Airframe labor = Direct "structural labor" or + ½ of "Other labor")

Airframe share of overhead -$ 1434.64 = $\frac{\text{airframe labor}}{\text{all labor}}$ x (overhead + direct, sales, G & A expenses = $\frac{486.62}{734.62}$ x (955.21 + 1211.92)

---

* Assumed quantity-price improvement 15 years hence.
Δ Estimated price of retractable landing gear and other additional equipment, 15 years hence ($3000 x 52%). (52% = mass production factor as determined on page 102.

APPENDIX T

ESTIMATED COST OF CONVENTIONAL SHEETMETAL AIRPLANE AT 100,000TH UNIT

Today's sheetmetal airplane, comparable to the NASA guideline Far Term airplane on an empty weight basis, would cost $12.50/lb* x 1609 lb **, or $20,150.00.

Since 1956, one of the large light airplane manufacturers in the U.S. has produced a cumulative total of 25,000 airplanes, at an average present day price of $19,080. This is a line of airplanes which approximates the Far Term airplane and is fairly near the hypothetical $20,150.00 airplane.

From Table XII (page 97), direct labor amounts to 10% of the consumer price. In this case it would be 10% x $20,150.00 or $2015.00.

The labor cost on the 100,000th unit is determined using a constant (linear) 80% learning curve. It is very conservative to use a constant 80% since, according to the U.S. Airforce Project Rand Report R-291***, there is apparently a minimum below which the labor cannot be reduced. This leveling off of the labor cost apparently occurs not long after the 300th unit. The following values are points on a constant 80% curve.

Labor Cost	Quantity (cumulative)
2015	25,000
1612	50,000
1290	100,000

The consumer price of the 100,000th conventionally produced airplane can then be compared to the "Far Term" airplane as follows:

Item	Sheetmetal	"Far Term" (plastic)#
Labor	1290##	$ 734.62
Overhead @ 130%	1677	955.21
Material (structure)	906(765/17000 x 20150	811.25
Material (other)	167	167.00
Molding Time Charge		258.10
Engine, Propeller, L.G., etc.	3842	3842.00
	7882	6768.18
Direct, Sales, G&A###	2773	1211.92
Manufacturing Cost	10655	7980.10
Factory Profit @ 10%	1066	798.01
Dealer Cost	11721	8778.11
Dir. & Distr. Markup (25%)	2930	2194.53
Estimated Consumer Price	$14651	$10972.64

---

* See Figures 69 and 70 ** See page 349

*** U.S. Air Force Project Rand Reprt (R-291), July 1, 1956, Cost-Quantity Relationships in the Airframe Industry. See pages 95, 98, 99, 129-131, 136-139.

See page 352 ## Airframe labor = 80% total labor = $1032.

From page 99, overall burden (i.e. direct, sales, G&A) equals 2.95 x total direct labor less airframe labor = (2.95) (1290) - (.8) (1290) = $2773.

REFERENCES

1. A Summary of the Flight Safety Foundation, 19th Annual International Air Safety Seminar. November 15-18, 1966, Madrid, Spain.

2. Anon.: Statistical Abstract of the United States, 1967, page 355. United States Department of Commerce.

3. L. Pazmany: Light Airplane Design, 1963.

4. Anon.: Federal Aviation Regulations, Part 23, Airworthiness Standards, Normal, Utility and Acrobatic Category Airplanes.

5. Anon.: Material Selector Issue, MATERIALS ENGINEERING, mid-October 1966.

6. Abbott, I.H.; Van Doenhoff, A.E.: Theory of Wing Sections. Dover Publications, Inc. New York, 1959.

7. Anon.: MIL-HDBK-5A, Metallic Materials and Elements for Aerospace Vehicle Structures, Feb. 1967.

8. Perkins, C.D., and Hage, R.E.: Airplane Performance, Stability and Control. John Wiley, 1949.

9. Gessow, Alfred; Myers, Gary C.,Jr.: Aerodynamics of the Helicopter. The Macmillan Company, New York, 1952.

10. Sheridan, Hugo G.: Aircraft Preliminary Design Methods Used in the Weapon Systems Analysis Division. NAVWEPS Report No. R-5-62-13, June 1962.

11. Zeman, W., and Bonner, E.: A Survey of Subsonic and Supersonic Turbulent Skin - Friction Drag Estimation Procedures. North American Aviation Report NA-65-404.

12. USAF Stability and Control Datcom. Principal Investigators - Ellison, D.E.; Malthan, L.V. Prepared by: Douglas Aircraft Company for Air Force Flight Dynamics Laboratory, Wright Patterson Air Force Base, Ohio, Revised Edition November 1965.

13. Hoerner, S.F.: Fluid Dynamic Drag. published by the author, 1958.

14. Anon.: MIL-HDBK-17, Plastics for Flight Vehicles (Part I, Reinforced Plastics).

15. Anon.: Application of Glass Fiber Laminates in Aircraft. AC 20-21, Federal Aviation Agency, 1964.

16. Whinery, D., North American Aviation, Inc.; Fernandez, D.,Aerojet General Corporation: Manufacturing Methods for Plastic Airframe Structures By Filament Winding. Technical Report IR-9-371(V), August 1967. Air Force Materials Laboratory, WPAFB, Ohio.

17. Shanley, F.R.: Weight-Strength Analysis of Aircraft Structures. Dover Publications, Inc., New York, 1960.

18. Lyman, J.; Forest, J.; Porter, F.: Design and Analytical Study of Composite Structures. General Dynamics/Convair Division, Report GDC-ERR-AN-1077 Dec. 1966.

19. Bruhn, E. F.: Analysis and Design of Flight Vehicle Structures. Tri-State Offset Company, Cincinnati, Ohio, 1965.

20. Donely, Philip: An Assessment of Repeated Loads on General Aviation and Transport Aircraft. International Committee on Aircraft Fatigue - 5th symposium, Melbourne, Australia, May 1967.

21. Peters, R.W., and Dow, N.F.: Failure Characteristics of Pressurized Stiffened Cylinders. NACA TN 3851, 1956.

22. Williams, D., M.O.S.: A Constructional Method for Minimizing the Hazard of Catastrophic Failure in a Pressure Cabin. ARC Technical Report CP No. 286, 1956.

23. Grover, H.J.; Gordon, S.A.; and Jackson, L.R.: Fatigue of Metals and Structures. Batelle Memorial Institute. NAVWEPS 00-25-534, Revised ed., June 1, 1960.

24. Anon.: Lockheed Stress Manual.

25. Anon.: Catalog of Fortified Polymers. Liquid Nitrogen Processing Corporation.

26. Gamble, N.L.: Reinforced Plastics-Molded Aircraft Wheels of Epoxy Resin Reinforced with Noncontinuous Glass Filaments. Goodyear Aerospace Corporation, SPE Journal, January 1967.

27. Anon.: The Complete Automobile Pricing Manual. Automobile Pricing Publications, Inc., Burlingame, Calif. 1966.

28. Anon.: Materials and Design Engineering. Reinhold Publishing Company, New York, N.Y. Oct. 1964.

29. Huernberger, H.H.: Alcoa Green Letter on Alcoa Aluminum Alloy X7005.

30. Mehr, P.; Spuhler, E.; Mayer, L.: "Alcoa Alloy 7075-T73", Aluminum Company of America, Aug. 1965.

31. Frost, P.: Technical and Economic Status of Magnesium-Lithium Alloys. NASA SP-5028, Aug. 1965.

32. Anon.: Structural Technical Service and Development Data, Dec. 1, 1965. Metal Products Department, The Dow Chemical Company, Midland, Michigan.

33. Fisher, P.; Meredith, P.; and Thomas, P.: New High Strength Magnesium Casting Alloys for Aerospace Applications. SAE Aeronautics and Space Engineering and Manufacturing Meeting, Los Angeles, Calif., Oct. 1966. Paper No. 660656.

34. Fenn, R., Jr.; Crooks, D.; Brodie, R.; and Chinowsky, S.: Comparison of Lightweight Structural Materials: Be and Alloys of Be Mg, AL and Ti - SAE Aeronautics and Space Engineering and Manufacturing Meeting, Los Angeles, California, Oct. 1966. Paper No. 660652.

35. Anon.: Data from Fiberite Corporation, Winona, Minn.

36. Anon.: Owens-Corning Fiberglass Data Sheets TC-AL-64.

37. Anon.: Machine Design. Plastics Reference Issue, June 1966.

38. Anon.: "How About DAP for Large Parts?" Modern Plastics, Aug. 1967.

39. Anon.: U.S. Royalite and Royalex. United States Rubber Company Brochures.

40. Anon.: ABS Plastic Material Data. Marbon Chemical, Division of Borg - Warner Corp., Washington, West Virginia.

41. Anon.: Technical Data on High Performance Plastics. Chemical Materials Department, General Electric, Pittsfield, Massachusetts.

42. Anon.: Technical Information Bulletin, N-204. Textile Fibers Department, DuPont Company.

43. Anon.: ANC-18, Design of Wood Aircraft Structures, June 1951.

44. Anon.: Hexcel Data Sheet 3410, March 31, 1967. Hexcel Catalog.

45. Bethune, A., and Davis, R.: High-Efficiency Materials. Boeing Company, Space/Aeronautics R & D Issue, 1967.

46. Anon.: Duramics, Inc. 877 W. 16th Street, Newport Beach, California.

47. The International System of Units. NASA SP-7012.

48. Jewel, Jr., J.W.: Initial Report on Operational Experiences of General Aviation Aircraft. SAE. Paper No. 680203. Business Aircraft Meeting, Wichita, Kansas, April 1968.

SAN DIEGO AIRCRAFT ENGINEERING, INC.

Errata for NASA Report CR-73258

Gentlemen:

We have discovered an error in the NASA Report CR-73258, which you recently received. Please cut-out and paste in the following correction over a corresponding section at the bottom of page 354.

Direct, Sales, G&A###	2129
Manufacturing Cost	10011
Factory Profit @ 10%	1001
Dealer Cost	11012
Dir. & Distr. Markup (25%)	2753
Estimated Consumer Price	13765

* See Figures 69 and 70 ** See page 349
*** U.S. Air Force Project Rand Reprt (R-291), July 1, 1956, Cost-Quantity Relationships in the Airframe Industry. See pages 95, 98, 99, 129-131, 136-139.
See page 352 ## Airframe labor = 80% total labor = $1032.
From page 99, (direct + sales + G&A) = 2.95 x direct labor - overhead = (2.95)(1290) - 1677 = 2129.

Yours very truly,

L. Pazmany

Ladislao Pazmany
Chief Design Engineer